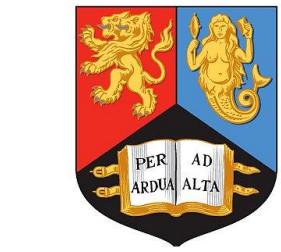

UNIVERSITY OF BIRMINGHAM

Visible-Light Photoredox-Catalysed Radical Cascade Reactions

by

Sifan Li

A thesis submitted to

The University of Birmingham

For the degree of

DOCTOR OF PHILOSOPHY

School of Chemistry

University of Birmingham

November 2022

Abstract

The research presented in this thesis details several novel radical cascade transformations under copper-catalysis or visible-light photoredox-catalysis.

The synthesis of [1,2]-annulated indoles from ene-ynamides *via* a radical triggered fragmentary cyclisation cascade under copper-catalysis or photoredox-catalysis is described. This reaction proceeds through a radical addition, radical cyclisation, desulfonylative aryl migration, and site-selective C(sp^2)-N cyclisation sequence. This work presents an example of a radical Smiles rearrangement process followed by aza-Nazarov type cyclisation, which enables the selective incorporation of the electron-rich aryl ring into the indole motif regardless of its original position.

The second part of thesis explores the synthesis of α-arylated carboxylic acids, esters, and amides from consecutive defluorination of α-trifluoromethyl alkenes in the presence of potassium alkyltrifluoroborates, water, and nitrogen/oxygen nucleophiles under organophotoredox-catalysed conditions. The utility of this method has been expanded through several product transformations. Mechanistic studies show that this metal-free reaction consists of a defluorinative alkylation, defluorinative hydroxylation, and defluorinative amination/hydroxylation cascade.

Finally, the modular synthesis of α-tertiary primary amines using α-aryl vinyl azides, redox-active *N*-(hydroxy)phthalimide ester, and cyanoarenes under visible-light conditions is

described. This strategy shows excellent functional group compatibility and allows the straightforward synthesis of 2,2-diaryl tetrahydroquinolines and 1,2-amino alcohols. The mechanistic studies support two parallel reductive photocatalytic cycles allowing for the denitrogenative alkylarylation of vinyl azides through decarboxylative radical addition followed by hetero-radical cross-coupling between α-amino alkyl radicals and aryl radical anions.

List of Publications

Published:

1. Li, S., Wang, Y., Wu, Z., Shi, W., Lei, Y., Davies, P. W., Shu, W., A Radical-Initiated Fragmentary Rearrangement Cascade of Ene-Ynamides to [1,2]-Annulated Indoles via Site-Selective Cyclization. *Org. Lett.* **2021**, *23*, 7209–7214. (This research is discussed in Chapter 2)

2. Li, S., Davies, P. W., Shu, W., Modular Synthesis of α-Arylated Carboxylic Acids, Esters and Amides *via* Photocatalyzed Triple C–F Bond Cleavage of Methyltrifluorides. *Chem. Sci.* **2022**, *13*, 6636–6641. (This research is discussed in Chapter 3)

3. Li, S., Shu, W., Recent Advances in Radical Enabled Selective $C_{sp}{}^3$–F Bond Activation of Multifluorinated Compounds. *Chem. Commun.* **2022**, *58*, 1066–1077. (This review is related to Chapter 3)

In Preparation:

1. Li, S., Du, H.-W., Davies, P. W., Shu, W., Synthesis of α-Tertiary Primary Amines and 1,2-Amino Alcohols from Vinyl Azides by Visible-Light Induced Denitrogenative Alkylarylation/Dialkylation. (This research is discussed in Chapter 4)

Acknowledgments

I would like to thank my supervisors Dr. Paul Davies and Prof. Wei Shu for offering me precious opportunity to undertake this research project, and for their guidance and support throughout my PhD studies.

I am very grateful to the Southern University of Science and Technology (China) for this joint PhD program and for their generous financial support.

I would like to thank all of the Davies group members for their continued support during the year in Birmingham. I would like to thank the Shu group members past and present for their enormous support and friendship. I would particular like to thank the radical sub-group members Yu, Yidan, Lin, Yufeng and Bihong for their useful advice. I would like to thank the staff of the analytical facilities in the University of Birmingham and Southern University of Science and Technology for their help.

I would like to thank my friends, especially Yahui, Yiyang, Na, Mingze and Bo for your friendship regardless of the distance. I could not have done this without all of you keeping my spirits up.

Lastly, I would like to thank my family for their endless love, unconditional support and encouragement.

Contents

List of Abbreviations

Å	Ångström
°C	degree Celsius
Ac	acetyl
acac	acetylacetonate
Ar	Aryl
aq.	aqueous
bpy	2,2'-bipyridine
Bn	benzyl
Boc	*tert*-butyloxycarbonyl
Bu	*n*-butyl
Bz	benzoyl
Cald	calculated
cat.	catalyst
Cy	cyclohexyl
d	doublet
Δ	heat
δ	chemical shift
DABCO	1,4-diazabicyclo[2.2.2]octane
DCE	1,2-dichloroethane

DCM	dichloromethane
DFT	density-functional theory
DMA	*N,N*-dimethylacetamide
DMF	*N,N*-dimethylformamide
DMAP	4-dimethylaminopyridine
DMSO	dimethylsulfoxide
DMEDA	*N,N'*-dimethylethylenediamine
DIPEA	*N,N*-diisopropylethylamine
d.r.	diastereomeric ratio
dtbpy	4,4'-di-*tert*-butyl-2,2'-bipyridine
equiv.	equivalent
ESI	electrospray ionisation
Et	ethyl
EWG	electron-withdrawing group
EnT	energy transfer
g	gram
h	hour(s)
HRMS	high-resolution mass spectrometry
i-	*iso-*
j	coupling constant

LED	light-emitting diode
m-	*meta*-
Me	methyl
µL	microliter(s)
NHPI	*N*-(hydroxy)phthalimides
NMR	nuclear magnetic resonance
Nu	nucleophile
o-	*ortho*-
p-	*para*-
PC	photocatalyst
ppy	2-phenylpyridine
Pr	propyl
r.t.	room temperature
SET	single electron transfer
TBAF	tetrabutylammonium fluoride
THF	tetrahydrofuran
TMS	trimethylsilyl
TLC	thin-layer chromatography

Chapter 1: Visible-Light Photoredox Catalysis

Radical reactivity offers a complementary strategy to traditional two-electron reactions in organic synthesis. One of the most rapidly expanding areas in radical chemistry is visible-light photoredox catalysis.[1] The quick adoption of photoredox catalysis by chemists aided the substantial developments of many previously inaccessible chemical transformations.[2-4]

The most commonly used photocatalysts in organic synthesis were originally developed for synthetic inorganic applications such as water splitting,[5] carbon dioxide reduction,[6] and new solar cell materials.[7] In 2008, near-simultaneous seminal reports from the MacMillan group,[8] the Yoon group,[9] and the Stephenson group[10] initiated the wide-spread use of photocatalysts in organic synthesis. Since then, many novel transformations based on the use of photoredox catalysis have been addressed.[2,3] Key to the fast development of photocatalysis in organic synthesis is the discovery of some metal-polypyridyl complexes and organic dyes that can show unique electronic properties in their excited states. Scheme 1 lists some commonly used photocatalysts in organic synthesis, including ruthenium and iridium polypyridyl complexes like $Ru(bpy)_3(PF_6)_2$ and *fac*-$Ir(ppy)_3$ (bpy = 2,2'-bipyridine; ppy = 2-phenylpyridine), organic photocatalysts like Mes-Acr-$MeClO_4$ and PTH (10-phenylphenothiazine).

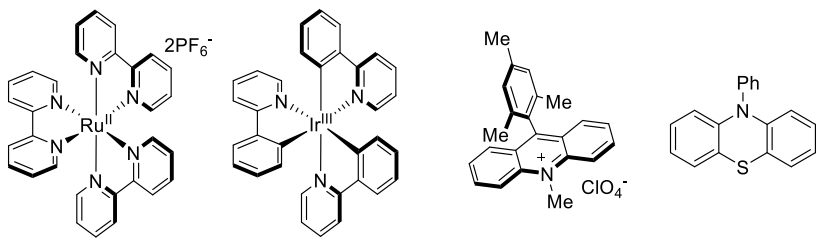

PC-1 $Ru(bpy)_3(PF_6)_2$ **PC-2** *fac*-$Ir(ppy)_3$ **PC-3** Mes-Acr-$MeClO_4$ **PC-4** PTH

Scheme 1: Selected examples of photocatalysts

Generally speaking, visible-light photocatalysis refers to the conversion of photon energy into chemical energy. The absorption of visible light (at a wavelength at which common molecules do not absorb) leads photocatalysts to an excited state, where they have unique electronic properties (Scheme 2).[11] For common metal-polypyridyl photocatalyst (PC) such as *fac*-Ir(ppy)$_3$, irradiation with visible light results a metal-to-ligand charge transfer (MLCT) event, in which an electron is promoted from a non-bonding metal-centred orbital to the π system of the ligand framework. Subsequent intersystem crossing (ISC) produces the excited state catalyst (*PC). At this stage, the excited state photocatalyst possesses both reducing and oxidising properties that provides a powerful tool for new chemical transformations. More specifically, the excited state photocatalyst can donate a high-energy electron from the π^* orbital (act as a reductant) or accept an electron to its low-energy metal centre (act as an oxidant). In addition, the oxidised or reduced state catalyst ($PC^{\bullet+}$ or $PC^{\bullet-}$) can undergo a second electron-transfer event to return to the original oxidation state, thus chemical reactions enabled by photoredox catalysis are redox neutral in nature, and the excited photocatalyst can be continuously generated during the reaction. More importantly, the rational design of photocatalyst through the modification of the ligand and the metal used can change the redox properties of the photocatalyst, thus expanding the applications of photoredox catalysis in organic transformations.[12]

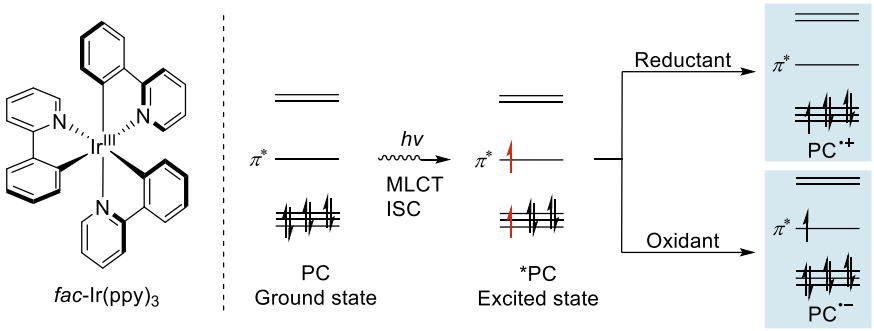

Scheme 2: Visible-light mediated excitation of photocatalyst

When a photocatalyst is sensitised to the excited state (*PC), one of the most important quenching processes of *PC is electron transfer (Scheme 3). This quenching process includes reductive and oxidative quenching cycles. For a reductive quenching cycle, the excited state catalyst *PC is reduced to its low oxidation state species $PC^{\bullet-}$ by a suitable reductive quencher (RQ), and the reduced state catalyst participates in another single-electron transfer (SET) event with an electron-acceptor (EA) to return to the original oxidation state PC. While in an oxidative quenching cycle, the oxidative quencher (OQ) oxidises the excited state catalyst to the high oxidation state species $PC^{\bullet+}$, and then $PC^{\bullet+}$ is reduced by an electron-donor (ED) to the ground state photocatalyst PC.

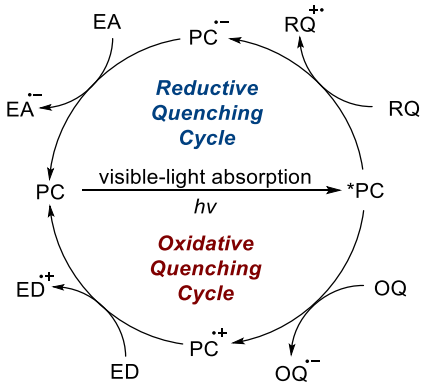

Scheme 3: Reductive and oxidative quenching cycles of photoredox catalysis

Another quenching process of the excited state photocatalyst is energy transfer (Scheme 4). Energy transfer in organic synthesis can be described as a two-electron exchange mechanism, which was first characterised by Dexter: absorption of visible light produces the triplet state catalyst PC^{3}*, and it donates one electron to the lowest unoccupied molecular orbital (LUMO) of the acceptor **5**, at the same time receiving one electron from the highest occupied molecular orbital (HOMO) of **5** to regenerate the ground state catalyst PC and form the excited state of the acceptor **6**, which can participate subsequent chemical transformations.[13]

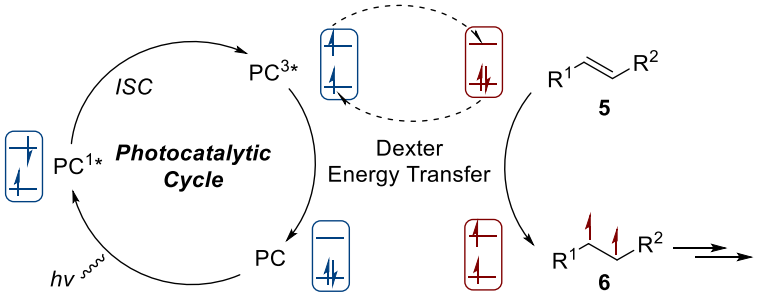

Scheme 4: General mechanism of energy transfer photocatalysis

The main theme behind my PhD research is the use of photoredox catalysis to generate reactive radical species through electron transfer process and their subsequent cascade reactions. In Chapter 2, radical species were generated through photoredox catalysis or copper catalysis, and a radical triggered cascade reaction of ene-ynamides to construct [1,2]-annulated indoles was described. Chapter 3 detailed the rapid synthesis of α-arylated carboxylic acids, esters, and amides through photoredox catalysed consecutive triple C–F bond cleavage of α-trifluoromethyl alkenes. The modular synthesis of α-tertiary primary

amines *via* visible-light mediated denitrogenative alkylarylation of vinyl azides with redox-active *N*-(hydroxy)phthalimide (NHPI) esters and cyanoarenes was discussed in Chapter 4.

These three radical-based transformations led to the discovery of a series of synthetically valuable *N*-heterocycles, carboxylic acids, esters, amides, and α-tertiary primary amines. The derivatisation of products has been realised, which expand the utility of these methodologies. The reaction mechanism of these transformations has also been investigated, providing more insights into these visible light mediated radical reactions.

Chapter 2: A Radical-Triggered Fragmentary Rearrangement Cascade of Ene-Ynamides to Construct [1,2]-Annulated Indoles

2.1 Introduction

2.1.1 Ynamides and Their Radical Reactivities

Ynamides **7** are a class of *N*-substituted alkyne compounds where the nitrogen atom bears an electron-withdrawing group (Scheme 5).[14] The types of nitrogen atom within the ynamide include: (1) vinylogous amides **8**; (2) imidazolidinones, oxazolidinones or lactams **9**, which can be chiral; (3) simple amides **10**, and sulfonamides **11**.

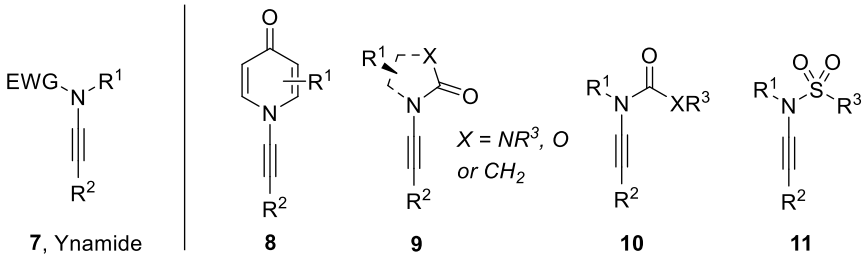

Scheme 5: Examples of ynamides

The first example of ynamide synthesis was reported more than 50 years ago. However, one major obstacle for the broader application of ynamides is due to the lack of a practical and efficient procedure for the preparation of ynamides. The emergence of alkynyliodonium chemistry provided a reliable method to the synthesis of this building block and helped the development of ynamide chemistry (Scheme 6).[15] Upon the nucleophilic addition of the deprotonated amide **12** to the β-carbon of the alkynyliodonium triflate **13**, an alkylidene carbene intermediate **15** is generated. Then a 1,2-migration process is proposed to happen to give the ynamide product **7**. In this methodology, the use of increased steric hindrance of the

amide such as α-branched amides result in less efficient nucleophilic addition, leading to lower yields.

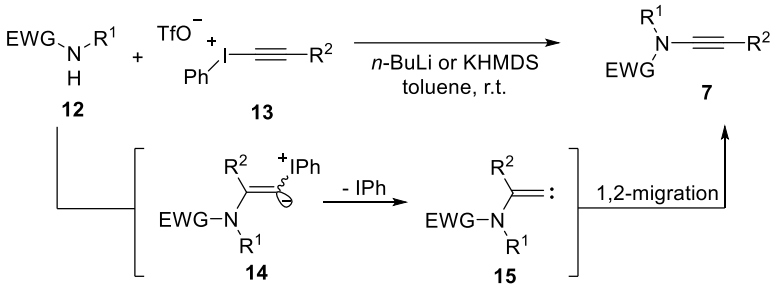

Scheme 6: Ynamide synthesis using alkynyliodonium salts

The discovery of metal-catalysed cross-coupling reactions provided versatile entry to ynamides. The most frequently used methods are listed in Scheme 7. Hsung and co-workers reported a practical copper-catalysed cross-coupling reaction of amides **12** with alkynyl bromides **16** using $CuSO_4 \cdot 5H_2O$ as catalyst, 1,10-phenanthroline as ligand, K_3PO_4 as base in toluene.[16] It is worth noting that this approach could be used for a large variety of substrates and the temperature could be as low as 60 °C, minimising ynamide decomposition. Evano and co-workers developed an approach to the synthesis of ynamides from amides **12** and 1,1-dibromo-1-alkenes **17**.[17] The use of copper(I) iodide and DMEDA (*N,N'*-dimethylethylenediamine) proved to be the optimal catalyst system, Cs_2CO_3 was the best base in this reaction. Stahl and co-workers documented the first copper-catalysed aerobic oxidative amidation of terminal alkynes in the presence of $CuCl_2$, pyridine, and Na_2CO_3.[18] The mechanism of the reaction involves sequential activation of the alkyne and amide in the presence of base, followed by reductive elimination and regeneration of copper(II) species

through oxidation. Although many ynamides can be isolated in good yields using this strategy, the major shortcoming of this method is the requirement of excess amount (5 equivalents) of amide in order to compete with the undesired formation of alkyne-alkyne homo-coupling product.

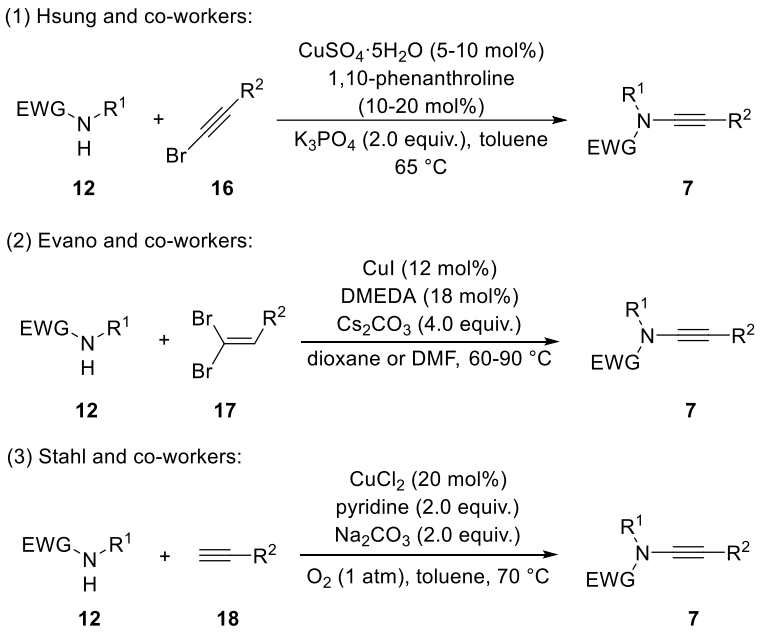

Scheme 7: Ynamide synthesis using amidative cross-coupling

The electron-donating ability of the nitrogen allows the regioselective addition of nucleophiles to the α-carbon position and electrophiles to the β-carbon of the ynamides (Scheme 8). Although ionic reactions of ynamides have been studied extensively, their radical reactivity remains less developed.[19]

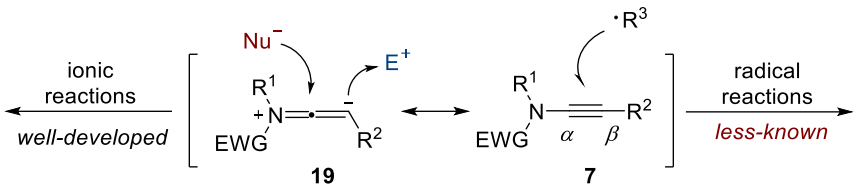

Scheme 8: Ionic and radical reactivity of ynamide

Ynamides are normally used as radical acceptors in free radical reactions, and their radical reactions can be classified by the radical addition on the α-position and β-position of the ynamides, leading to the formation of intermediate **20** and **21** respectively (Scheme 9). The following subsections detailed recent advances in the ynamide radical reactions classified by the radical addition sites on the ynamides.

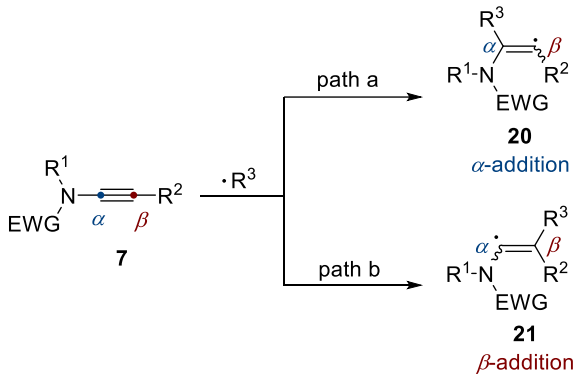

Scheme 9: General profile of α-and β-selective radical addition of ynamides

2.1.1.1 α-Selective radical addition of ynamides

Great progress has been made in the cyclisation of ynamides for the preparation of (hetero-)cyclic compounds over the past decades. Apart from ionic approaches, radical-mediated cyclisation of ynamides has received more attention in recent years. Intramolecular radical cyclisation of ynamides takes place on the α-position of the ynamide to form the

kinetically more favourable small ring (**23**) with cyclisation on the β-position (**24**) unfavoured (Scheme 10).[20]

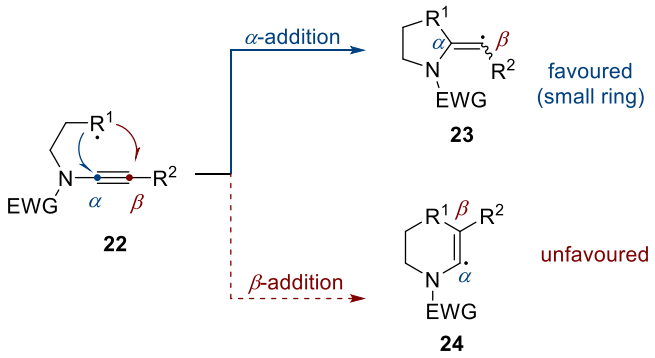

Scheme 10: Regioselective radical cyclisation of ynamides on the α-position

The first radical reaction of ynamides was reported by Malacria and co-workers in 2003.[21] Ynamides **25** were used to construct polycyclic product **26** through an intramolecular radical cascade reaction in the presence of *n*-Bu_3SnH and AIBN (azobisisobutyronitrile) at elevated temperature (Scheme 11). The generation of tin radical **27** led to halogen atom transfer (XAT) with ynamide **25** to give an aryl radical species **28**. Intramolecular radical cyclisation onto the α-carbon of the ynamide yielded a vinyl radical species **29**. The following 6-endo-cyclisation of the vinyl radical with the pendent carbon-carbon double bond led to the formation of intermediate **30**. Subsequent hydrogen atom transfer (HAT) with *n*-Bu_3SnH would generate another molecule of tin radical **27** and the polycyclic product **26**.

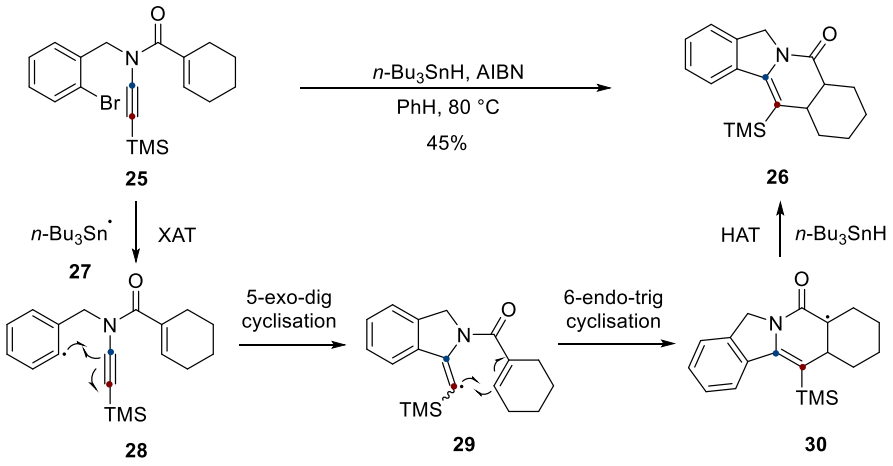

Scheme 11: AIBN-initiated radical cyclisation cascade of ynamides

The similar type of cyclisation reaction of ynamides can be achieved under photoredox-catalysed conditions. In 2018, the Evano group reported the development of copper-based photocatalysts and their applications to radical reactions (Scheme 12).[22] In the presence of a tertiary amine Cy_2N*i*-Bu, the photoexcited copper species *[Cu^{I}] was reduced to [Cu^{0}] complex. This copper(0) species then underwent single-electron transfer (SET) event with ynamide **31** to afford the radical anion species **33** and the ground state [Cu^{I}] complex. Elimination of the iodide in **31** gave an aryl radical species **34**, which participated in α-selective radical cyclisation followed by rearomatisation to give the product **32** in good yield.

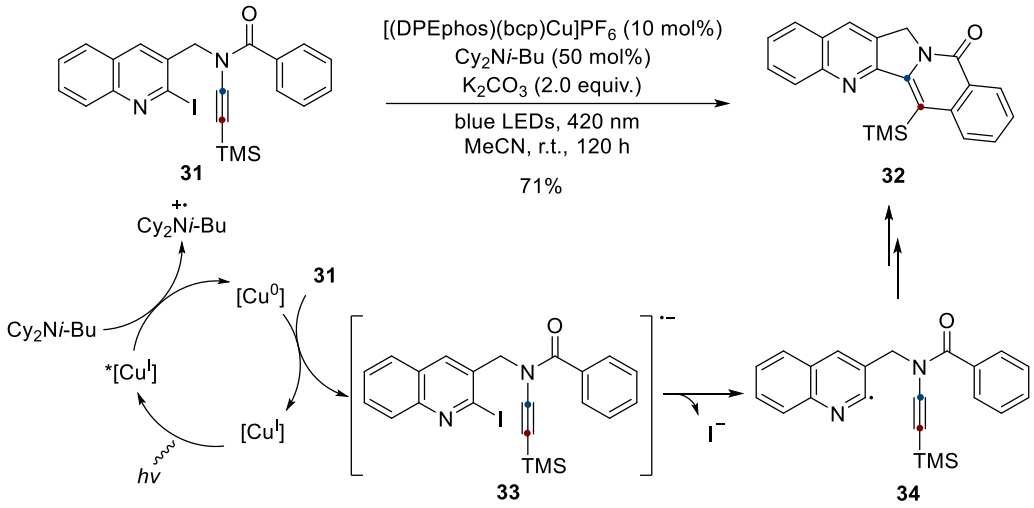

Scheme 12: Photoinduced radical domino cyclisation of ynamides

Another interesting example was reported by Gandon and Sahoo in 2019, which presented a sulfur-radical-triggered cyclisation of yne-tethered ynamide **35** to construct 4-thioaryl pyrrole **38** (Scheme 13).[23] The reaction started with the generation of thiyl radical species **39** from thiophenol **36** in the presence of *N*-hydroxyphthalimide **37**. It is worth noting that the reactivity of the alkyne moiety exceeded that of the ynamide, which lead to the selective thiyl-radical addition to the alkyne moiety to form the vinyl radical species **40**. Subsequent 5-exo-dig cyclisation resulted the radical intermediate **41**, which participated hydrogen-atom transfer with thiophenol **36** to give intermediate **42**. Finally, tautomerization of **42** generated the aromatic 4-thioaryl pyrrole product **38**.

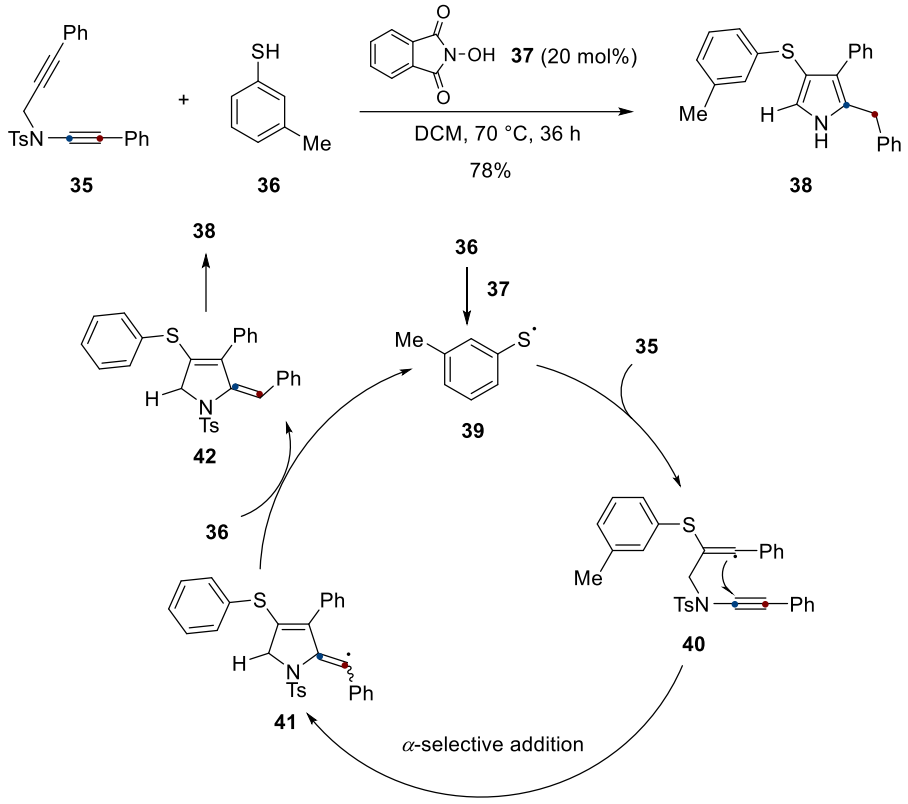

Scheme 13: Thiyl-radical-initiated regioselective cyclisation of yne-ynamides

Later, the same group applied this regioselective radical cyclisation strategy to other type of radical species (Scheme 14). An uncommon sulfur-to-selenium-to-carbon radical transfer process was employed which resulted a selenyl radical-mediated cyclisation of yne-ynamides to construct 4-selenyl-pyrroles **45**.[24]

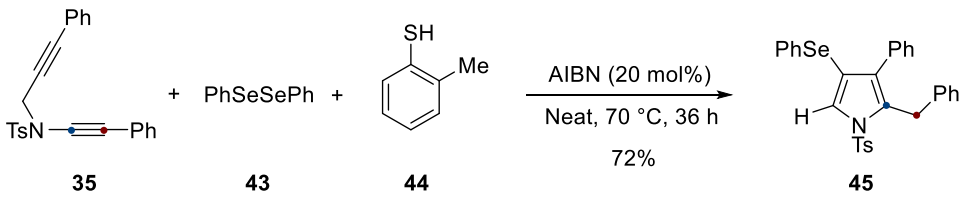

Scheme 14: Selenyl radical attack to alkyne

Ynamide radical cyclisation processes can also be combined with aryl migration strategies to construct novel heterocycles. In 2020, the Ye group reported a photoredox-catalysed regioselective radical coupling of ketyl-ynamides (**46**, **48**) to access 2-benzhydrylindoles **47** and 3-benzhydrylisoquinolines **49** (Scheme 15).[25] The reaction proceeded smoothly using $Ir(ppy)_2(dtbbpy)PF_6$ (dtbbpy = 4,4'-di-*tert*-butyl-2,2'-bipyridine) as photocatalyst, Hantzsch ester as reductant under irradiation of blue light in DMF or DCE. A variety of benzoyl ynamides transformed into corresponding *N*-heterocyclic products good yields through a radical triggered desulfonylated Smile rearrangement process.

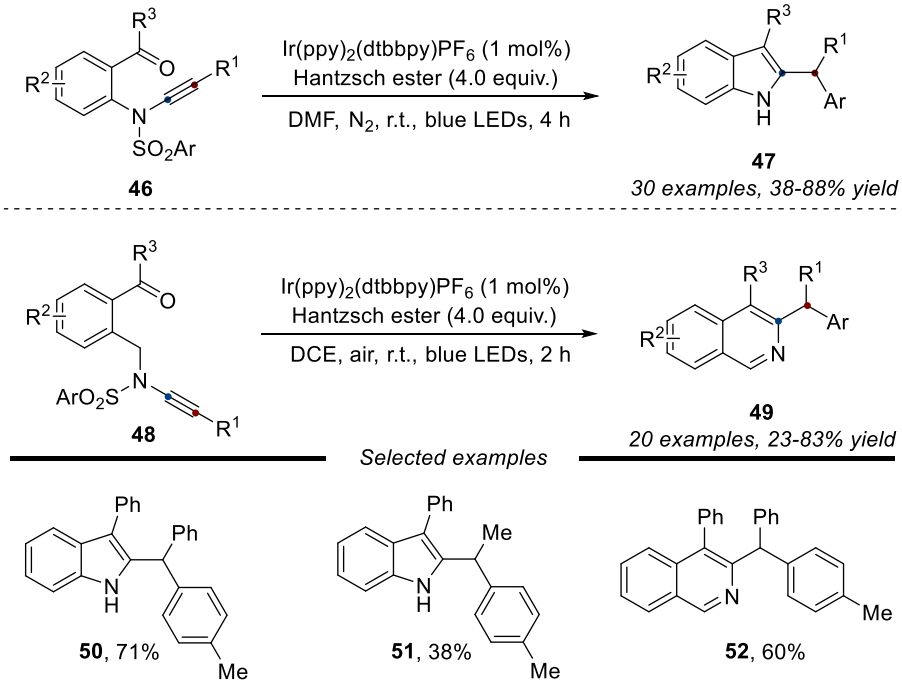

Scheme 15: Photoredox-catalysed regioselective coupling of ketyl-ynamides

The same group also demonstrated an intermolecular radical cyclisation/Smiles rearrangement of ynamide **53** using Togni's reagent **54** as external radical source, affording trifluoromethyl tetracyclic *N*-heterocycles **55** in 72% yield (Scheme 16).

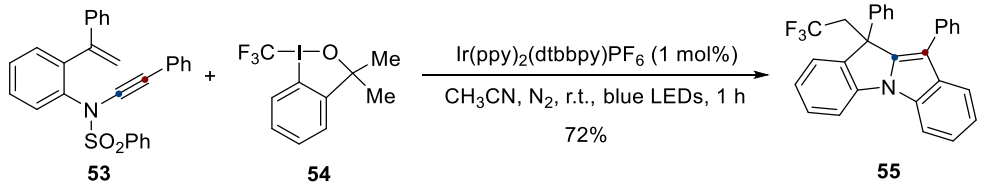

Scheme 16: External radical-initiated ynamide Smiles rearrangement

A different reaction pathway occurred when an alkyl sulfonyl protected benzoyl ynamide **56** was employed as substrate under similar reaction conditions (Scheme 17).[26] The reaction was postulated to undergo single-electron reduction of the ketone group in the ynamide **56** to generate a ketyl radical species **58** in the presence of photocatalyst and Hantzsch ester under blue light irradiation. Subsequent intramolecular cyclisation of **58** delivered vinyl radical species **59**, then a hydrogen atom transfer process with Hantzsch ester or its radical cation form occurred instead of Smiles rearrangement to give enamide **60**. Finally, the corresponding 2-hydroxymethylindoles **57** is obtained through acid-promoted 1,3-allylic alcohol transposition.

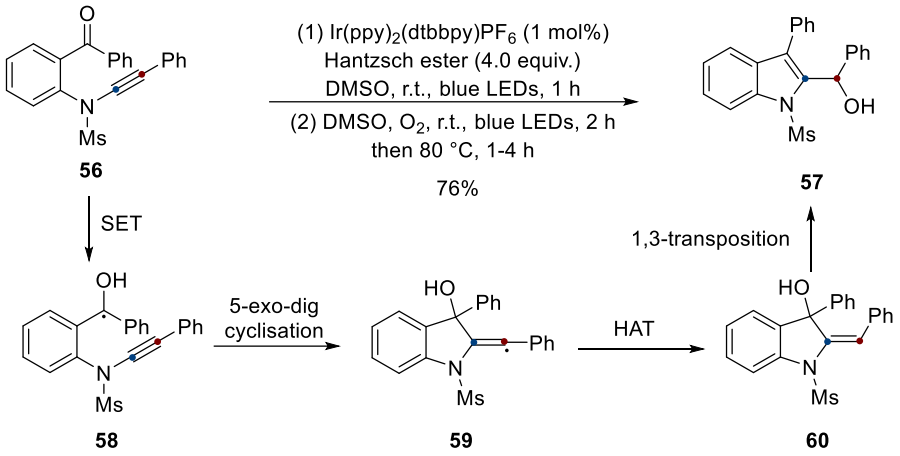

Scheme 17: Photoredox catalysed ketyl-ynamide coupling/1,3-allylic alcohol transposition

2.1.1.2 *β*-Selective radical addition of ynamides

Limited examples on the *β*-selective addition of ynamides using traditional two-electron approaches have been reported.[27] However, intermolecular radical addition of the carbon-carbon triple bond of ynamides tends to happen at the *β*-position of ynamides to form vinyl radical intermediates stabilised by adjacent nitrogen atom **21** (Scheme 18).

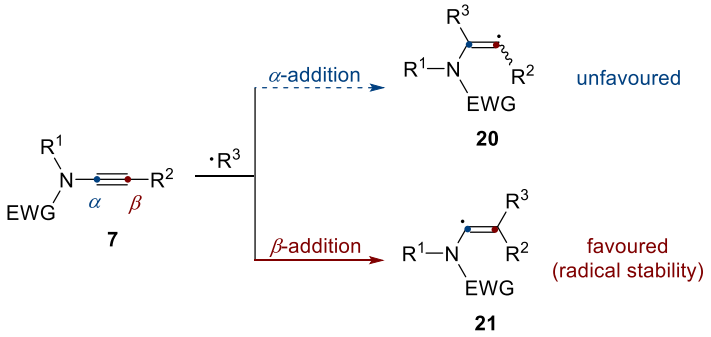

Scheme 18: Regioselective radical addition of ynamides on the *β*-position

In 2009, Yorimitsu, Oshima and co-workers demonstrated the regioselective intermolecular thiyl radical addition to ynamides (Scheme 19).[28] Triethylborane and O_2 were used as the

radical initiator. The reaction proceeded through the regioselective thiyl radical addition to the β-position of the ynamides **61** followed by hydrogen atom transfer, the resulting stereoselectivity for the *Z*-isomer **62** is due to the steric hindrance between the terminal substituent and the amide group.

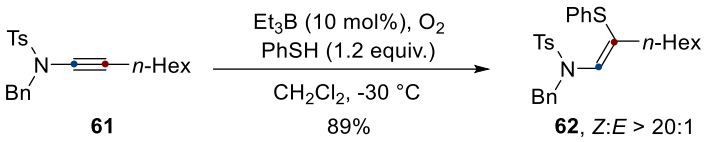

Scheme 19: Thiyl radical addition to the ynamides

In 2010, Castle and co-workers reported an example which enables the hydrothiolation of terminal ynamides **63** in a controllable fashion (Scheme 20).[29] The kinetically favoured *cis*-β-thioenamide **64** was obtained when 1.0 equivalent of thiol reagent was used in a short time. When excess amount of thiol and longer reaction time was employed, *cis*-β-thioenamide would convert to the thermodynamically favoured *trans* product **65** through a radical addition–β-thiyl radical elimination pathway.

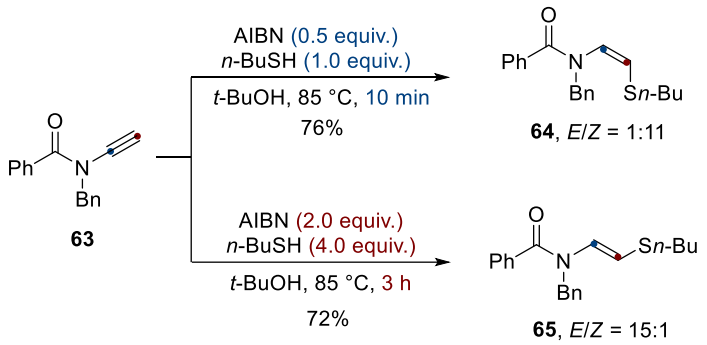

Scheme 20: Controlled radical hydrothiolation of terminal ynamides

In 2014, Pérez-Luna, Oestreich and co-workers reported radical silylzincation of terminal ynamides **66** to construct (*Z*)-α,β-disubstituted enamide **67** (Scheme 21).[30] In their proposed mechanism, oxidation of diethylzinc by oxygen led to the formation of ethyl radical **68**, which underwent HAT with $(Me_3Si)_3SiH$ to give silyl radical species **69**. The addition of **69** to ynamide **66** afforded (*Z*)-vinylic radical intermediate **70**, which would react with diethylzinc *via* homolytic substitution to give the alkenylzinc intermediate **71** and generate ethyl radical **68**. Finally, **71** underwent transmetallation with cyanocuprate followed by electrophilic substitution to furnish **67** in good yield with high regio- and stereoselectivity.

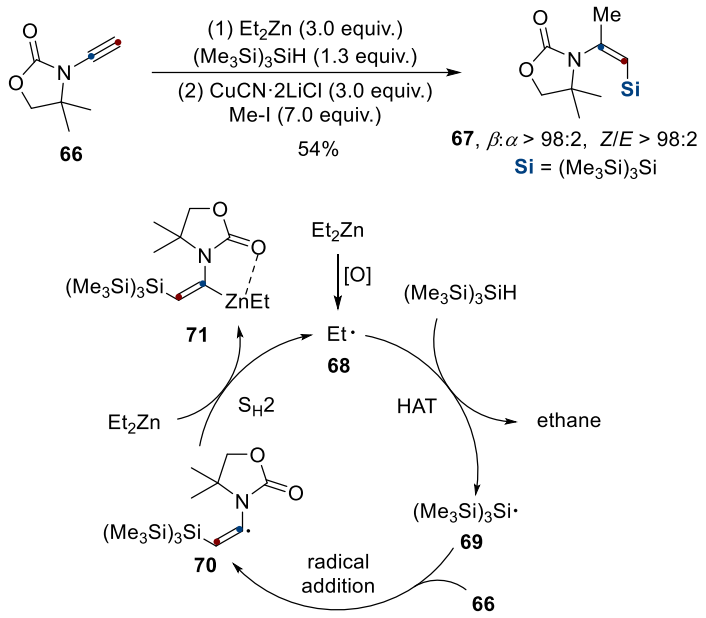

Scheme 21: Radical silylzincation of ynamides

The β-selective carbon-centred radical addition to ynamides has also been investigated. In 2019, the group of Ollivier and Fensterbank developed a photoredox catalysed trifluoromethylation of *N*-benzoyl ynamide **63** to construct isoindolinone **73**, using Togni's

reagent **72** as trifluoromethyl radical source, $Ir(ppy)_3$ as photocatalyst in acetonitrile under blue light irradiation (Scheme 22).[31]

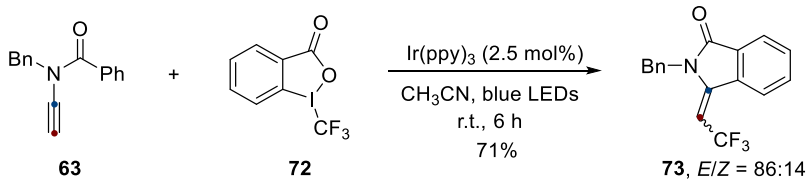

63 **72** **73**, *E*/*Z* = 86:14

Scheme 22: Trifluoromethyl radical triggered cyclisation of *N*-benzoyl ynamides

In 2020, Bertrand, Feray and co-workers reported the use of α-iodoacetate **75** as a bifunctional reagent in the presence of triethylborane for the intermolecular radical addition of ynamide **74** to construct α-iodo-enamide **76** (Scheme 23).[32] DFT calculations showed β-radical addition is clearly favoured over α-radical addition of the ynamides, which resulted the excellent regioselectivity. The selective formation of *E*-product was due to steric hindrance.

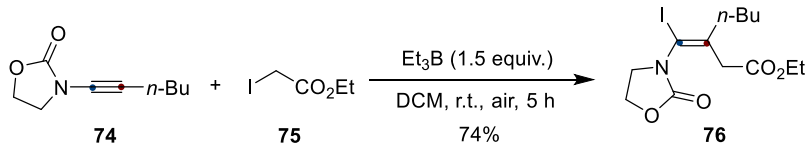

74 **75** **76**

Scheme 23: Radical carbo-iodination of ynamides

2.1.1.3 Summary

In this section, the preparation of ynamides as well as recent achievements made in the field of ynamides radical reactions have been discussed. A variety of previously unattainable transformations have been made in ynamides using radical approaches compared with ionic reactions. Although ynamides can serve as excellent radical acceptors at both α-carbon

position and β-position through intra- or intermolecular radical additions, the reaction type is mainly focusing on radical cyclisation reaction or simple alkyne 1,2-difunctionalisation. Further reaction development through the combination of photoredox catalysis with skeletal rearrangement processes would enrich the diversity of ynamide radical reactions.

2.1.2 The Smiles Rearrangement

The Smiles rearrangement is an intramolecular aryl migration reaction with the cleavage of a C−X single bond and the formation of a new C−X or C−C bond through nucleophilic *ipso* substitution (Scheme 24).[33,34] This rearrangement reaction can be used construct more challenging bond connections from easily prepared substrates, making it a powerful tool for (hetero)arene functionalization.

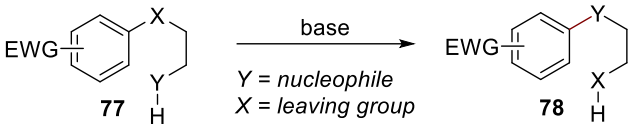

Scheme 24: Generalised Smiles rearrangement

The rearrangement process can be affected by several factors: the activation of the migrating aromatic ring, the nucleofugality of the leaving group, and the nucleophilicity of the entering group. Generally speaking, strongly electron-withdrawing groups such as nitro groups were primarily used to activate the aromatic ring. While the effects of the entering group (Y) and the leaving group (X) are intertwined. The mechanism of the Smiles rearrangement was proposed to proceed through an anionic sigma complex−the Meisenheimer intermediate **80**.[35]

The rate of the Smiles rearrangement was determined upon the collapse of the Meisenheimer intermediate through deprotonation at low base concentrations, while the formation of the Meisenheimer intermediate became rate-limiting at high base concentrations.

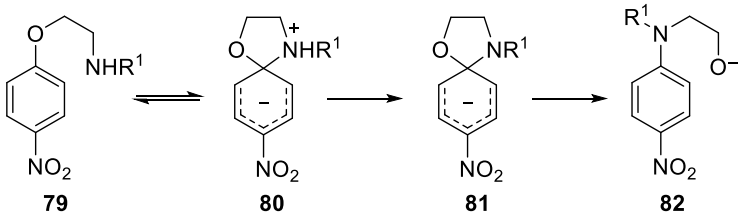

Scheme 25: The formation and collapse of the Meisenheimer intermediate

2.1.2.1 Two-electron Smiles rearrangement

The common Smiles rearrangement is an aromatic ring with electron-withdrawing groups migrates from one heteroatom to another to form a more stable anion. One major advance is the introduction of Smiles rearrangement into transition-metal catalysis for the construction of heterocyclic compounds. Snieckus and co-workers reported a copper-catalysed domino reaction incorporating Smiles rearrangement for the synthesis of tricyclic dibenzoxazepinones **85** from 2-iodobenzamides **83** and 2-bromophenols **84** (Scheme 26).[36] CuI and dbm (dibenzoylmethane) was the best catalyst system in this reaction, and no activation of the migrating aromatic ring was required. The authors proposed that this reaction was first underwent Ullmann coupling to give intermediate **86**, then a Smiles rearrangement was happened prior to a second Ullmann-type cyclisation to deliver intermediate **87**. Control

experiments showed that the final product **85** can be obtained from intermediate **87** through intramolecular cyclisation under base-assisted copper-free conditions.

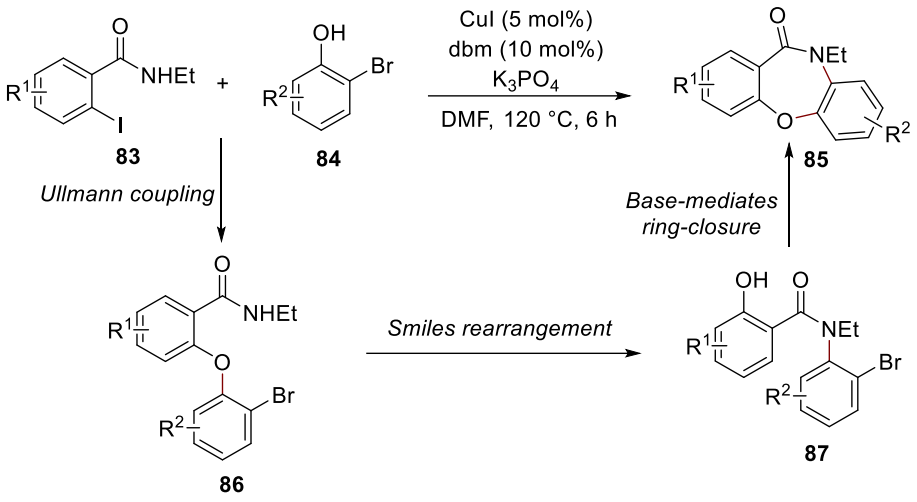

Scheme 26: Copper-catalysed domino synthesis of dibenzoxazepinones

One particular variation in Smiles rearrangement is the Truce-Smiles rearrangement. There are two important differences to the common Smiles rearrangement. The nucleophile is a carbanion rather than a heteroatom and the activation of the migrating aromatic ring is not required in the Truce-Smiles rearrangement. In 1958, Truce and co-workers reported the *n*-butyllithium-induced Smiles rearrangement of mesityl phenyl sulfone **88** to 2-benzyl-4,6-dimethylbenzenesulfinic acid **91** (Scheme 27).[37] In this reaction, *n*-butyllithium deprotonated a methyl group in the mesityl phenyl sulfone **88** to form intermediate **89**. This carbanion attacked the electron deficient *ipso*-carbon followed by the elimination of the sulfur species, which resulted in the rearranged sulfinic acid product **91** after protonation.

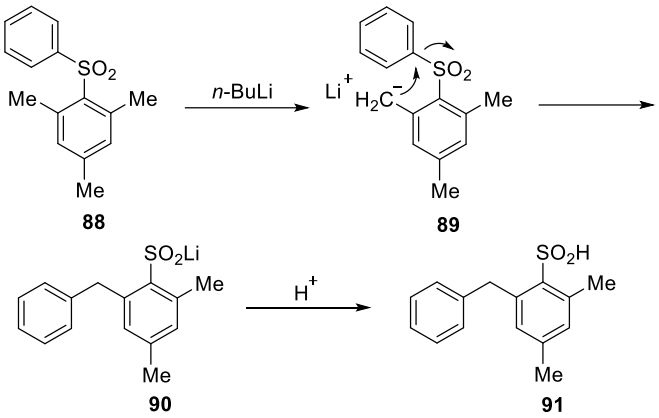

Scheme 27: The Truce-Smiles rearrangement

Greaney and co-workers reported the synthesis of biaryl compounds through aryne addition/Truce-Smiles rearrangement cascade under transition-metal free conditions (Scheme 28).[38] 2-Trimethylsilyl-(phenyl)triflate **92** was used as aryne precursor in the presence of fluoride. The addition of aryl sulfonamide **93** to aryne **95** delivered the intermediate **96**, which underwent a Truce-Smiles rearrangement with SO_2 extrusion to afford the biaryl product **94**. This protocol is effective for the preparation of sterically hindered tri and tetra-*ortho*-substituted biaryls, which may hard to access by traditional cross-coupling reactions.

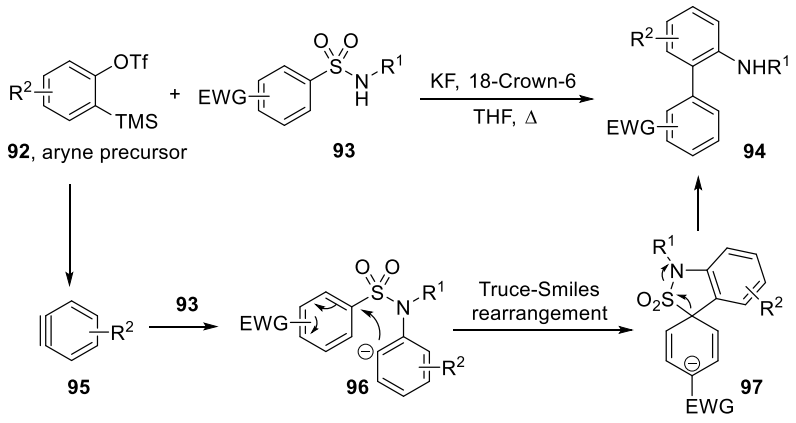

Scheme 28: A benzyne Truce-Smiles rearrangement

In 2017, the same group further applied the anionic addition/Smiles rearrangement/SO_2 extrusion cascade to the synthesis of tetrasubstituted enaminoates **100** using (hetero)aryl sulfonamides **98** and electron-deficient alkynes **99** (Scheme 29).[39] Primary aryl sulfonamides with electron-withdrawing groups and secondary *N*-alkyl sulfonamides were good substrates in this reaction. Secondary *N*-aryl sulfonamides (such as **103**) were less reactive because the decreased nucleophilicity prevented effective conjugate addition.

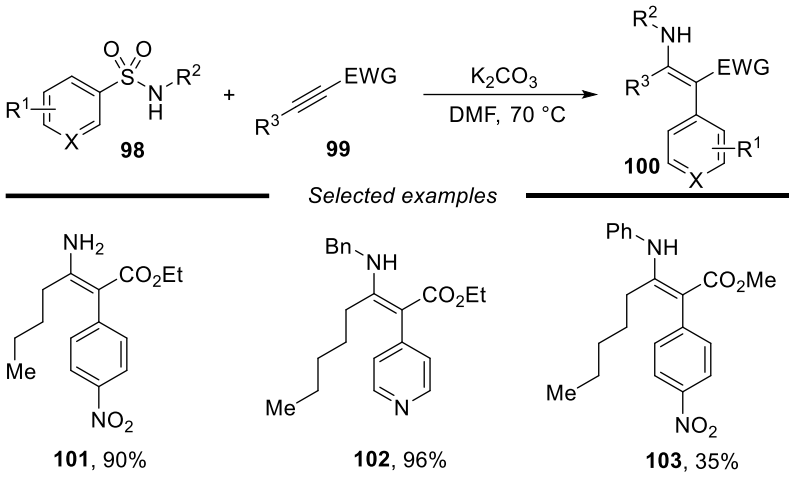

Scheme 29: Intermolecular aminoarylation of alkynes

2.1.2.2 Single-electron Smiles rearrangement

Smiles rearrangement reactions are normally two-electron processes, in recent years, many single-electron processes have also been demonstrated.[40] The use of aryl sulfonamide derivatives in radical Smiles rearrangements is a powerful way for aryl transfer through the extrusion of SO_2. In 1991, Pennell and Motherwell reported a radical Smiles rearrangement for the synthesis of biaryl products **106** from *N*-(2-iodophenyl)benzenesulfonamide **104** using

AIBN and Bu_3SnH as radical initiator (Scheme 30).[41] This transformation demonstrated that aryl radicals can be employed to trigger aromatic ring transposition.

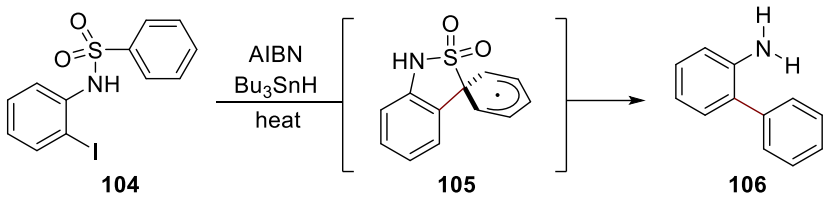

Scheme 30: Aryl radical triggered aryl migration strategy

In 2013, the Nevado group reported a copper-catalysed trifluoromethylation/aryl migration/desulfonylation cascade reaction of α,β-unsaturated tosyl amide **107** (Scheme 31).[42] This reaction started with radical conjugate addition to **107**. The resultant radical species **108** underwent Smiles rearrangement to deliver an amidyl radical **109**, which can participate hydrogen abstraction or cyclisation depending on the substitution pattern (R^1 = aryl or alkyl respectively). Later, the same group demonstrated that many other radical species could be introduced into this cascade reaction, and the amidyl radical can be trapped by intra- and intermolecular electrophiles to construct more complex multicyclic scaffolds.[43,44]

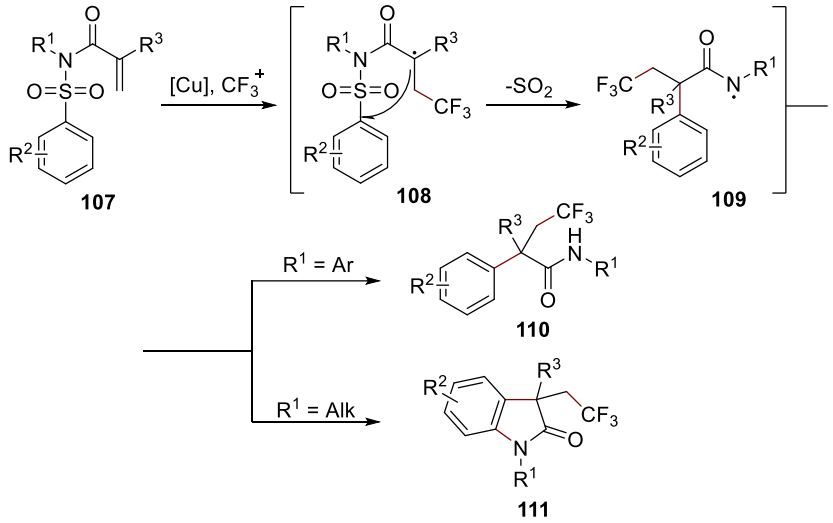

Scheme 31: Copper-catalysed radical cascade of conjugated tosyl amides

Recently, Nevado and co-workers reported an asymmetric radical sulfinyl Smiles rearrangement to access acyclic amides with an α-all-carbon quaternary stereocentre under visible-light photoredox catalysis (Scheme 32).[45] Enantioenriched *N*-arylsulfinyl acrylamides **112** were used as accepter with a wide range of radical sources **113** (including sulfonyl chlorides, perfluoroalkyl iodides and non-fluorinated alkyl halides) in the presence of photocatalyst *fac*-Ir(ppy)$_3$, base K_3PO_4 in acetonitrile and H_2O under light irradiation. A series of enantio-enriched amide products **114** were obtained in good yields and e.e values.

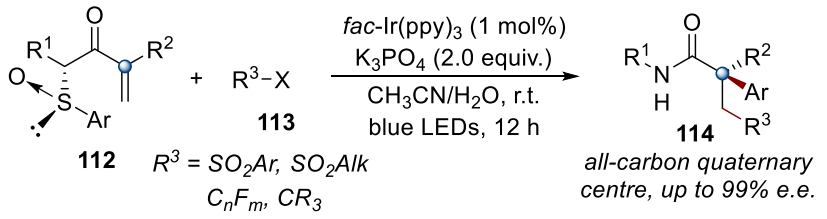

Scheme 32: Asymmetric radical sulfinyl Smiles rearrangement

The aforementioned cascade reactions initiated through radical addition to trigger Smiles rearrangement, Stephenson and co-workers developed a different strategy using arylsulfonylacetamides as bifunctional reagent to realise regioselective aminoarylation of styrenes (Scheme 33).[46] The reaction proceeded though single-electron oxidation of electron-rich alkenes **115** to form a radical cation intermediate **118**, which could be trapped by *N*-nucleophile **116** to provide a benzylic radical species **119**. Then a radical Truce-Smiles rearrangement happened to yield an amidyl radical **120** with the extrusion of SO_2. The product **117** was then formed after single-electron transfer and protonation processes. The high diastereoselectivity of this transformation was proposed to arise from either a kinetically favoured generation of the (*E*)-radical cation intermediate or a thermodynamic preference of radical intermediate **119** to adopt an *anti*-periplanar conformation between R^1 and R^2.

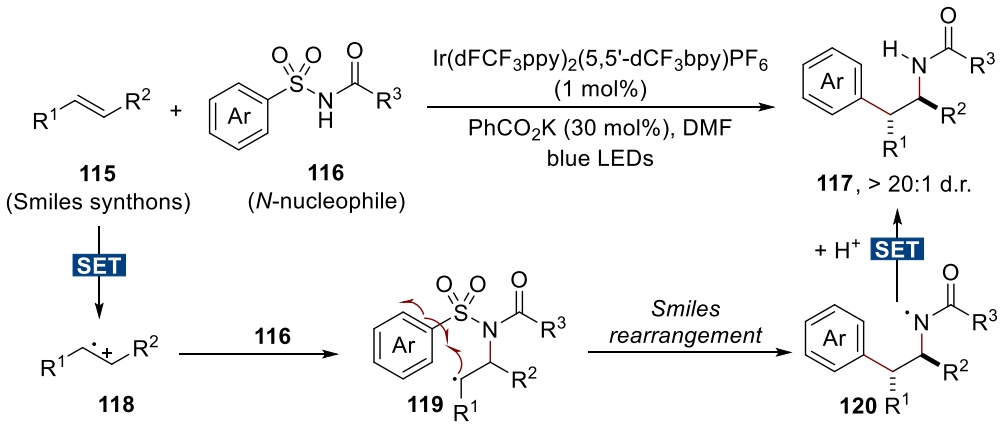

Scheme 33: Arylsulfonylacetamides as bifunctional reagents in Smiles rearrangement

2.1.2.3 Summary

The Smiles rearrangement in two- and one-electron systems provides a useful strategy for preparing aryl-containing scaffolds which are difficult to make by other methods. The radical Smiles rearrangement has grown significantly with the development of photoredox catalysis. The substrate scope has been greatly expanded through the introduction of various radical precursors under milder conditions. Smiles rearrangements in one-electron system are more widely applicable to the migrating aryl groups because the activation of aryl groups is not required. Aryl sulfonamide derivatives are easily available and have been greatly explored in radical desulfonylative aryl migration processes to construct nitrogen-, and aryl-containing molecules. Further developments focusing on the structural design of aryl sulfonamides to realise desulfonylative Smiles rearrangement to construct novel heterocyclic scaffolds is appealing.

2.2 Results and Discussion

2.2.1 Reaction Design and Optimisation

My first research project was aimed to combine the research interest in the Davies group and the Shu group: ynamide chemistry and radical chemistry. Our first attempt was inspired by Sahoo's work on the thiyl radical addition to alkyne-tethered ynamide, where a preferred addition of the thiyl radical to the alkyne rather than the ynamide was observed (see Scheme 13). Due the electron-donating ability of the nitrogen atom, I questioned if a reversed

reactivity could be achieved through the use of a more electrophilic radical species (such as trifluoromethyl radical). If possible, radical addition to the β-position of the ynamide **121** would produce a vinyl radical species **122**, which undergoes intermolecular cyclisation to give intermediate **123**. Further radical addition to the phenyl ring followed by re-aromatisation would lead to the formation of a trifluoromethyl-containing tricyclic product **124** (Scheme 34).

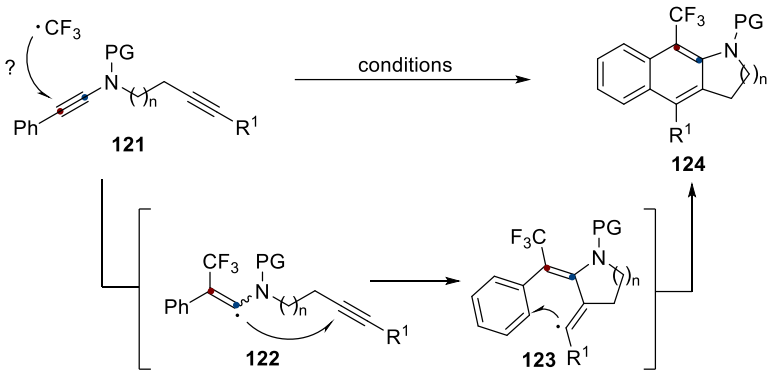

Scheme 34: Initial reaction proposal

To begin with, ynamides **125** was used as model substrate, Togni's reagent **72** was used as trifluoromethyl radical precursor, and the combination of copper catalyst $Cu(CH_3CN)_4PF_6$ with ligand 2,2'-bipyridine were used to serve as radical initiator (Scheme 35).[42] Preliminary results showed that the proposed tricyclic product **124** was not observed but compounds **126** and **127** (10% and 45% yields respectively) were formed when the reaction was conducted in acetonitrile at room temperature under N_2 atmosphere for 12 hours. Increasing the temperature to 40 °C led to slightly higher yields of both products, while **126** was not formed in the absence of the ligand. About 20% of **126** alongside 63% yield of **127** were obtained when the reaction was performed under blue light at room temperature.

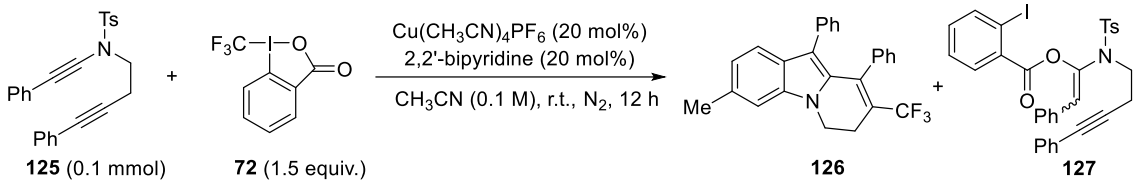

125 (0.1 mmol) **72** (1.5 equiv.) **126** **127**

Entry	Variations	Yield/%[a]	
		126	**127**
1	no variations	10	45
2	T = 40 °C	14	50
3	without 2,2'-bipyridine	n.d.	28
4	under blue LEDs	20	63

[a]Yields were determined by ^{1}H NMR spectroscopy of the crude reaction mixture using mesitylene as internal standard.

Scheme 35: Initial results of trifluoromethylation of ynamide 125

The formation of **127** was attributed to the carboxylate addition to the ynamide **125** when Togni's reagent **72** was used, a side-reaction which has been reported by Ollivier, Fensterbank and co-workers.[31] The structure of product **126** was confirmed by X-ray diffraction (Figure 1). The formation of this indole product **126** showed that trifluoromethyl radical addition still preferred to happen at the alkyne part of the ynamide, and a possible mechanistic pathway was proposed for the formation of this unexpected [1,2]-annulated indole product (Scheme 23).

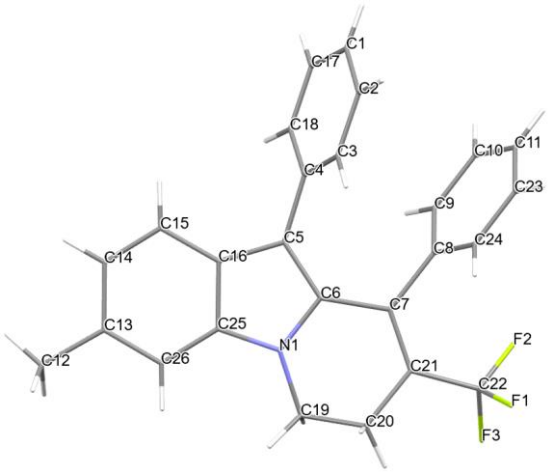

Figure 1: X-ray crystallography of 126. Crystallographic data solved by Dr. Xiaoyong Chang (SUSTech) and has been deposited at the Cambridge Crystallographic Data Centre, under deposition number CCDC 2175551

Initially, single-electron transfer between Togni's reagent **72** and copper(I) complex [Cu^{I}] generated [Cu^{II}] species and trifluoromethyl radical **128**. Selective radical addition to the alkyne part of the ynamide **125** generated a vinyl radical intermediate **129**.[23] Subsequent intramolecular 6-exo-dig cyclisation gave intermediate **130**, then a radical Smile rearrangement with the extrusion of SO_2 was postulated to happen to yield an intermediate **131** according to the studies reported by Nevado[42] and Zhang.[47] Further arylation process delivered the desired indole product **126** and regenerated the copper catalyst.

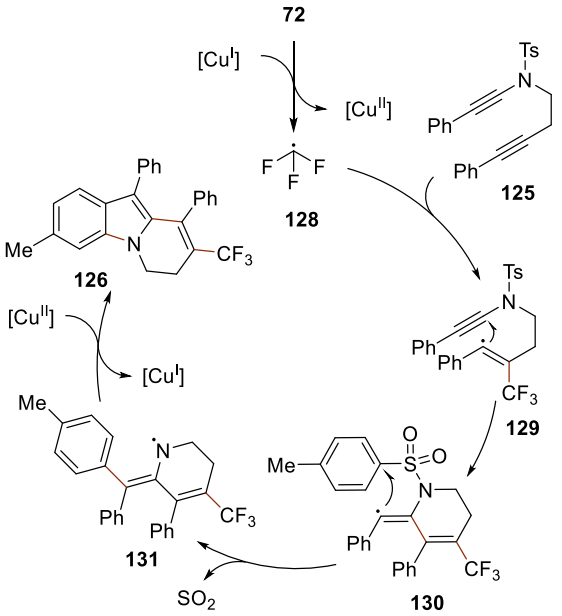

Scheme 36: Possible reaction pathway for the formation of product 126

Further optimisation studies based on ynamide **125** and Togni's reagent **72** did not provide higher yield of product **126** led to modify the structure of the ynamide and trifluoromethyl radical precursor used in this reaction (Scheme 37): (1) more reactive Togni's reagent **54** was used as trifluoromethyl radical precursor and also to avoid undesired carboxylate addition to the ynamide during the reaction; (2) ynamide **125** was changed to a less sterically hindered terminal ene-ynamide **132** to facilitate the intermolecular CF_3 radical addition step.

Further reaction optimisation under copper-catalysis led to the formation of **133** in 44% yield using **54** as trifluoromethyl radical precursor, CuCl as catalyst in acetonitrile at 60 °C. Visible-light photoredox catalysis was also employed for the optimisation, about 41% of the product was formed with 32% of the ynamide **132** recovered in the presence of photocatalyst *fac*-$Ir(ppy)_3$, $NaHCO_3$ in acetonitrile under blue light irradiation. Ynamide **132** was consumed

completely but the yield of the product did not improve when $NaHCO_3$ was not added. During the course of our study, Ye and co-workers reported a Smiles rearrangement of ynamide using photocatalysis (see Scheme 16),[25] our further optimisation studies were then based on copper-catalysis for differentiation. Finally, ynamide **134** was used as prototype substrate in our study: a tailored alkyl chain between the alkene and the nitrogen that would result more facile 5-exo-dig cyclisation, and a more stable tertiary alkyl radical species would be formed after the initial radical addition step.

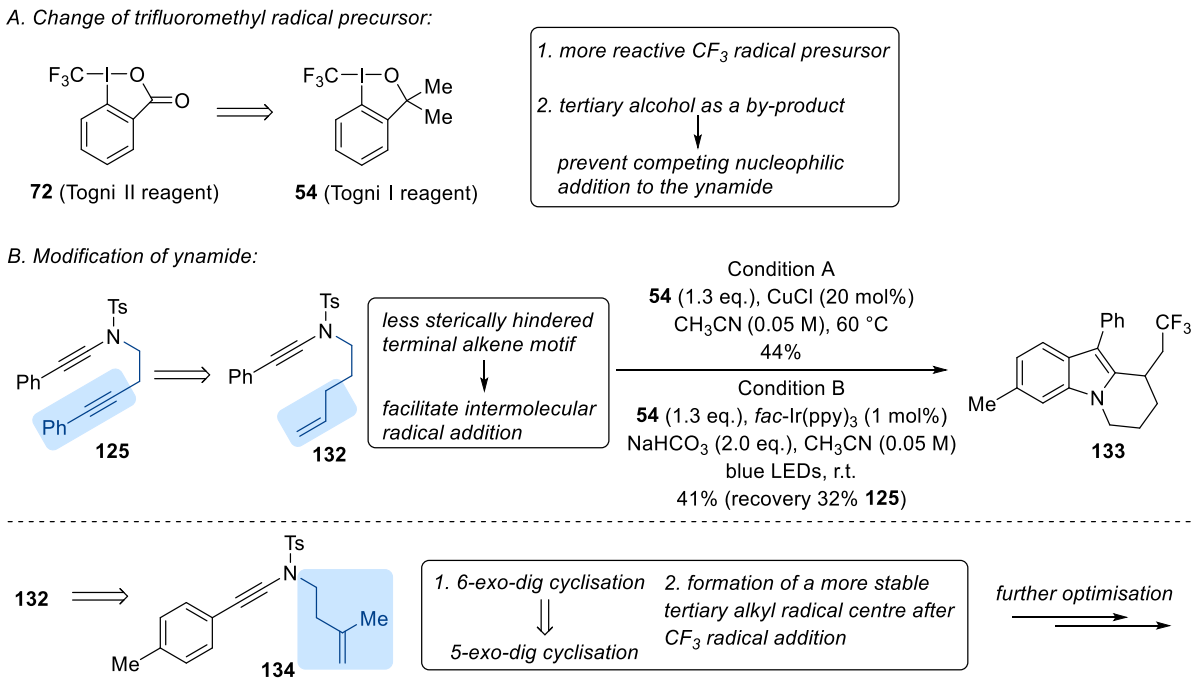

Scheme 37: Modification of the prototype ynamide and radical precursor

The synthesis of alkene-tethered ynamides **139** requires several steps: (1) the synthesis of Boc-protected alkene-tethered sulfonamide **137** through Mitsunobu reaction between Boc-protected sulfonamide **135** and alcohol **136**; (2) deprotection of Boc-protected sulfonamide

137 in hot DMSO; (3) preparation of ynamides **139** from sulfonamide **138** using alkynyliodonium chemistry or copper catalysed cross-coupling methods (Scheme 38).

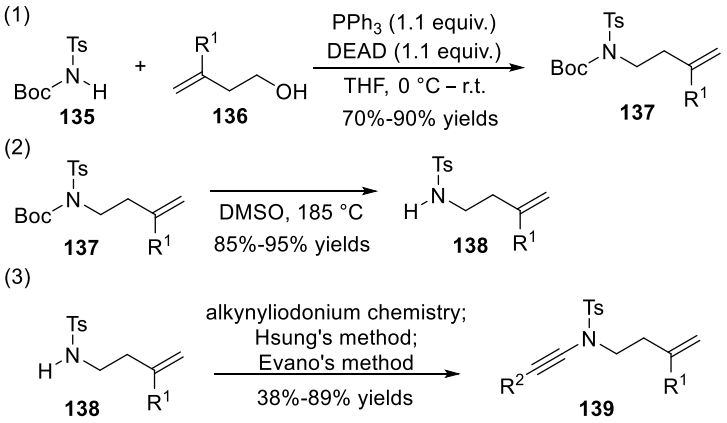

Scheme 38: Preparation of alkene-tethered ynamides

Early studies showed that ynamide **134** was normally consumed within two hours based on ^{1}H NMR spectroscopy when Togni's reagent **54** was used under copper catalysed conditions at 60 °C. A survey of several commercially available ligands with copper(I) chloride was tested as catalyst in this reaction (Table 1, entries 1-6). The use of *N,N'*-bidentate ligands such as bipyridines (**L1** and **L2**), 1,10-phenanthroline derivatives (**L3**–**L5**) successfully delivered the corresponding [1,2]-annulated indole product **140** in 43%–61% yields, while a tridentate ligand **L6** was not suitable in this reaction. A blank experiment revealed that ligand was not necessary in this reaction when copper(I) chloride was used as catalyst, the product **140** was obtained in 72% ^{1}H NMR yield and 63% isolated yield (Table 1, entry 7).

Other copper(I) complexes such as CuBr and CuI were also efficient catalysts in this reaction, albeit with slightly lower yields (Table 1, entries 8–9), while the use of copper(I) acetate only

led to 25% yield of the product, and no product was formed when $Cu(CH_3CN)_4PF_6$ was used without a ligand (Table 1, entries 10−11). Copper(II) complexes such as $Cu(OAc)_2$ and $Cu(OTf)_2$ failed to deliver the desired product **140** (Table 1, entries 12−13).

Table 1: Reaction screening for radical-triggered Smiles rearrangement of ynamides

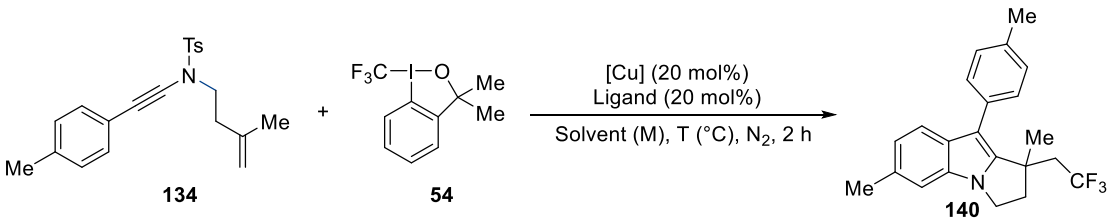

Entry	**134**:**54**	[Cu]	Ligand	Solvent (M)	T (°C)	Yield of **140** (%)[a]
1	1:1.2	CuCl	**L1**	CH_3CN (0.03)	60	43
2	1:1.2	CuCl	**L2**	CH_3CN (0.03)	60	61
3	1:1.2	CuCl	**L3**	CH_3CN (0.03)	60	52
4	1:1.2	CuCl	**L4**	CH_3CN (0.03)	60	51
5	1:1.2	CuCl	**L5**	CH_3CN (0.03)	60	43
6	1:1.2	CuCl	**L6**	CH_3CN (0.03)	60	n.d.
7	1:1.2	CuCl	No ligand	CH_3CN (0.03)	60	72 (63)
8	1:1.2	CuBr	No ligand	CH_3CN (0.03)	60	67
9	1:1.2	CuI	No ligand	CH_3CN (0.03)	60	67
10	1:1.2	CuOAc	No ligand	CH_3CN (0.03)	60	25
11	1:1.2	$Cu(CH_3CN)_4PF_6$	No ligand	CH_3CN (0.03)	60	n.d.
12	1:1.2	$Cu(OAc)_2$	No ligand	CH_3CN (0.03)	60	n.d.
13	1:1.2	$Cu(OTf)_2$	No ligand	CH_3CN (0.03)	60	n.d.
14	1:1.2	CuCl	No ligand	DCM (0.03)	60	47
15	1:1.2	CuCl	No ligand	THF (0.03)	60	n.d.
16	1:1.2	CuCl	No ligand	$PhCF_3$ (0.03)	60	38

17	1:1.2	CuCl	No ligand	Et_2O (0.03)	60	n.d.
18	1:1.2	CuCl	No ligand	MeOH (0.03)	60	n.d.
19	1:1.2	CuCl	No ligand	DMAc (0.03)	60	trace
20	1:1.2	CuCl	No ligand	CH_3CN (0.03)	r.t.	46
21	1:1.2	CuCl	No ligand	CH_3CN (0.03)	40	62
22	1:1.2	CuCl	No ligand	CH_3CN (0.03)	80	59
23	1:1.2	CuCl	No ligand	CH_3CN (0.10)	60	53
24	1:1.2	CuCl	No ligand	CH_3CN (0.05)	60	62
25	1:1.2	CuCl	No ligand	CH_3CN (0.02)	60	47
26	1:1	CuCl	No ligand	CH_3CN (0.03)	60	66
27	1:1.5	CuCl	No ligand	CH_3CN (0.03)	60	55

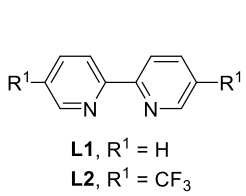

L1, R^1 = H
L2, R^1 = CF_3

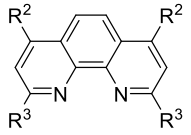

L3, R^2 = H, R^3 = H
L4, R^2 = H, R^3 = Me
L5, R^2 = Ph, R^3 = H

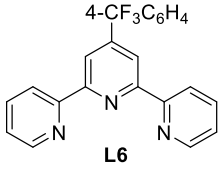

L6

[a]Reactions were performed on a 0.1 mmol scale; yields were determined by ^{1}H NMR spectroscopy of the crude reaction mixture using mesitylene as an internal standard, isolated yield was shown in parentheses. n.d. = not detected.

Next, a preliminary evaluation of different solvents showed that acetonitrile performed best under standard conditions, other solvents such as dichloromethane, tetrahydrofuran, (trifluoromethyl)benzene, diethyl ether and dimethylacetamide were not suitable for this transformation (Table 1, entries 14−19). Compromised yields were seen when the reactions were conducted at lower or higher temperatures (Table 1, entries 20−22). Higher or lower concentration of acetonitrile gave diminished yields of **140** (Table 1, entries 23−25). A

stoichiometry study revealed that 1 equivalent of ynamide **134** and 1.2 equivalents of Togni's reagent **54** worked best under reactions (Table 1, entries 26, 27). Thus far, the optimised reaction conditions were achieved for the reaction between ene-ynamide **134** and Togni's reagent **54**: using copper(I) chloride (20 mol%) as catalyst, and the acetonitrile (0.03 M) as a solvent at 60 °C under nitrogen atmosphere for 2 hours.

2.2.2 Scope of the Radical Triggered Smiles Rearrangement of Ynamides

With the optimised reaction conditions in hand, the generality of this approach was evaluated. First, the substitution patterns of the aryl groups on both the ethyl and sulfonamide regions of the ynamide was explored (Scheme 39). Ynamides with the same *para*-substituted aryl groups on the ethyl and sulfonamide regions worked well (**141**−**144**, 45%−71% yields). A scale-up reaction (6.0 mmol scale) was conducted for the gram-scale preparation of [1,2]-annulated indole **144**, which demonstrated the practicality and ready implementation of this protocol. The structure of **144** was also confirmed by X-ray diffraction (Figure 2).

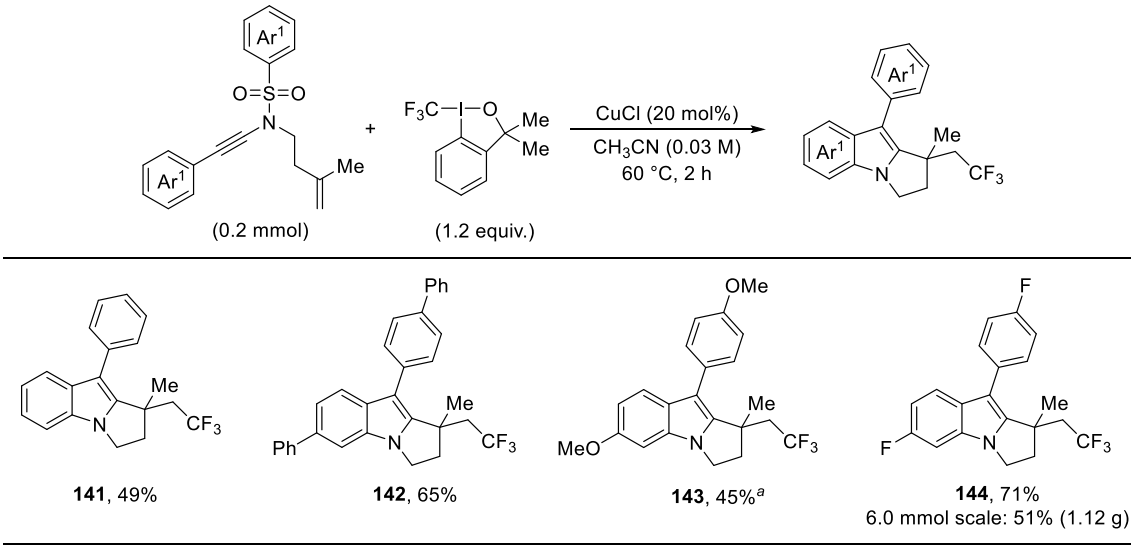

141, 49% **142**, 65% **143**, 45%[a] **144**, 71%
6.0 mmol scale: 51% (1.12 g)

*Reaction conditions: ynamide (0.2 mmol, 1.0 equiv.), Togni's reagent **54** (1.2 equiv.), CuCl (20 mol%), and CH_3CN (6.0 mL) in a Schlenk tube at 60 °C under N_2 atmosphere for 2 hours; isolated yields are reported.*

[a]Reaction was performed at room temperature.

Scheme 39: Substrate scope with identical aryl groups

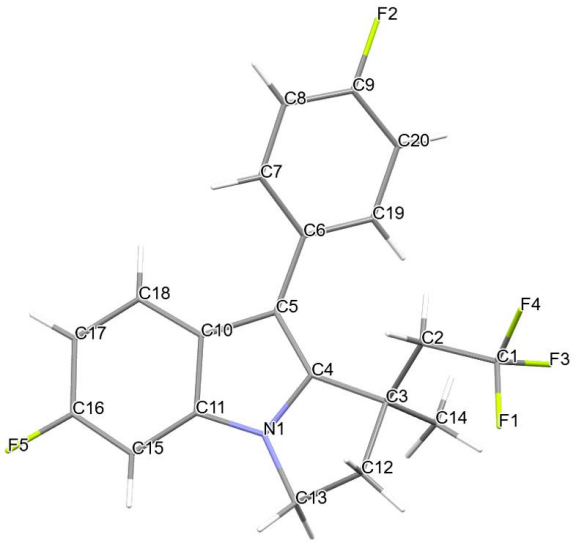

Figure 2: X-ray crystallography of indole product 144. Crystallographic data solved by Dr. Xiaoyong Chang (SUSTech) and has been deposited at the Cambridge Crystallographic Data Centre, under deposition number CCDC 2043670

A mixture of regioisomeric products were obtained when several ynamides with different aryl groups on the sulfonamide and alkyne parts were applied to the reactions, either aryl groups can be incorporate into the annulated indole motif (**145**–**150**, Scheme 40). For example, a substrate bearing electronically similar aryl substituents at the sulfonamide and alkyne group (*para*-methyl and *tert*-butyl phenyl groups respectively) delivered 1.0:1.0 mixture of isomers **145** and **146**. When a *meta*-methoxy phenyl group was placed at the alkyne part of the ynamide, the cyclisation step preferred to take place at the *para*-tolyl group from the

sulfonamide, resulting in the formation of **147** and **148** with a ratio of 2.8:1.0. Higher selectivity (**149**:**150** = 4.0:1.0) was observed upon replacing the *meta*-methoxy phenyl group with a *para*-fluoro phenyl substituent.

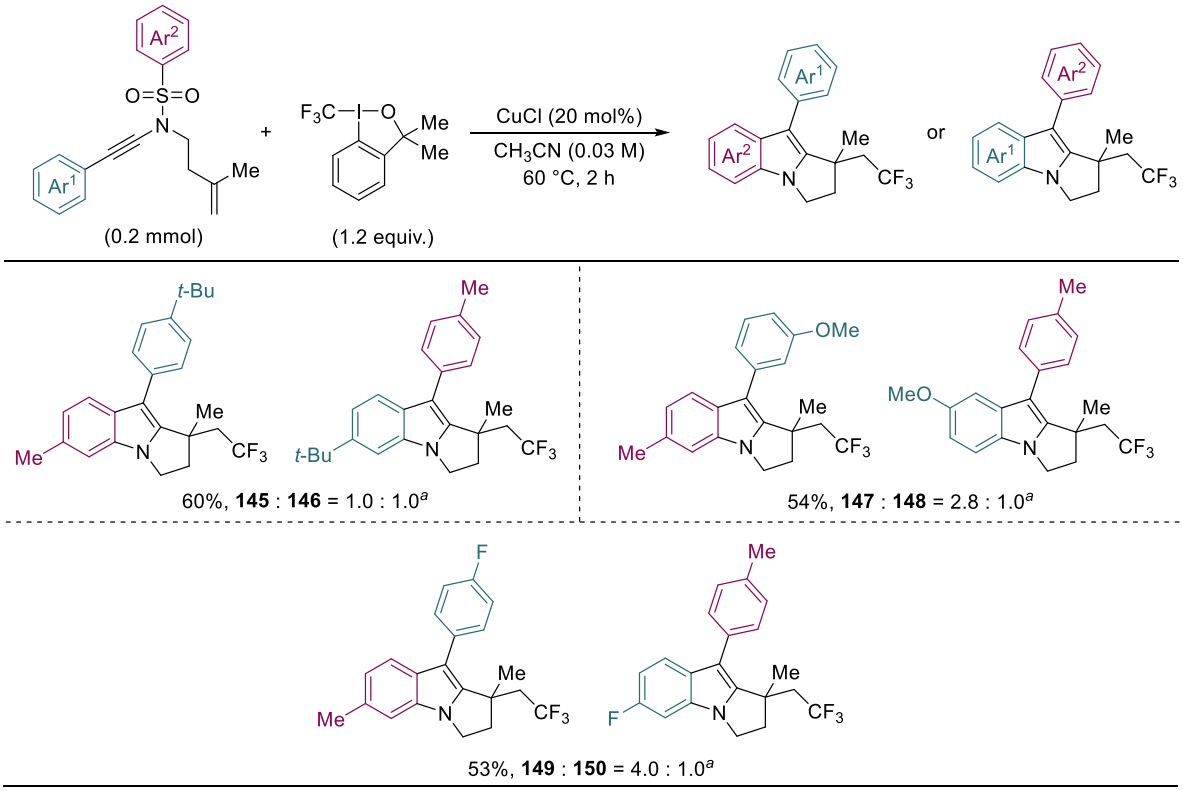

See Scheme 39 for reaction conditions. [a]Ratio were determined by ^{19}F NMR spectroscopy of the crude reaction mixture.

Scheme 40: Reaction scope and regioselectivity issues

Based on these results, the cyclisation step was proposed to be favoured at the more electron-rich aryl group, and a sole indole product might be obtained by exploiting electronic differences between the two aryl groups (Scheme 41).

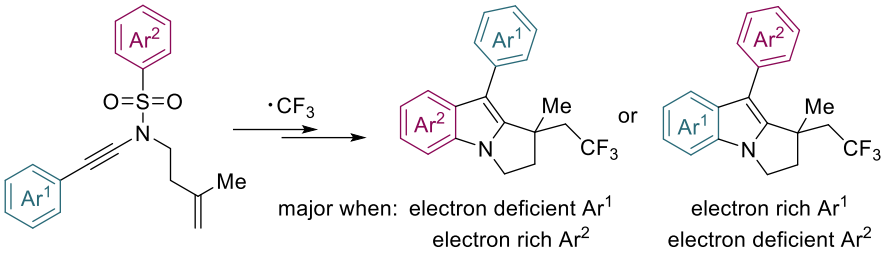

Scheme 41: Hypothesis for regioselective arylation step

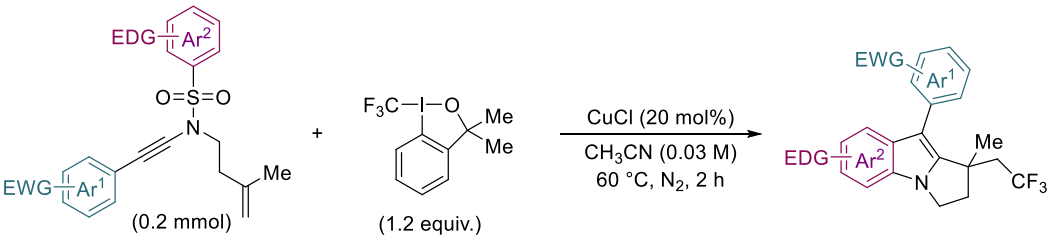

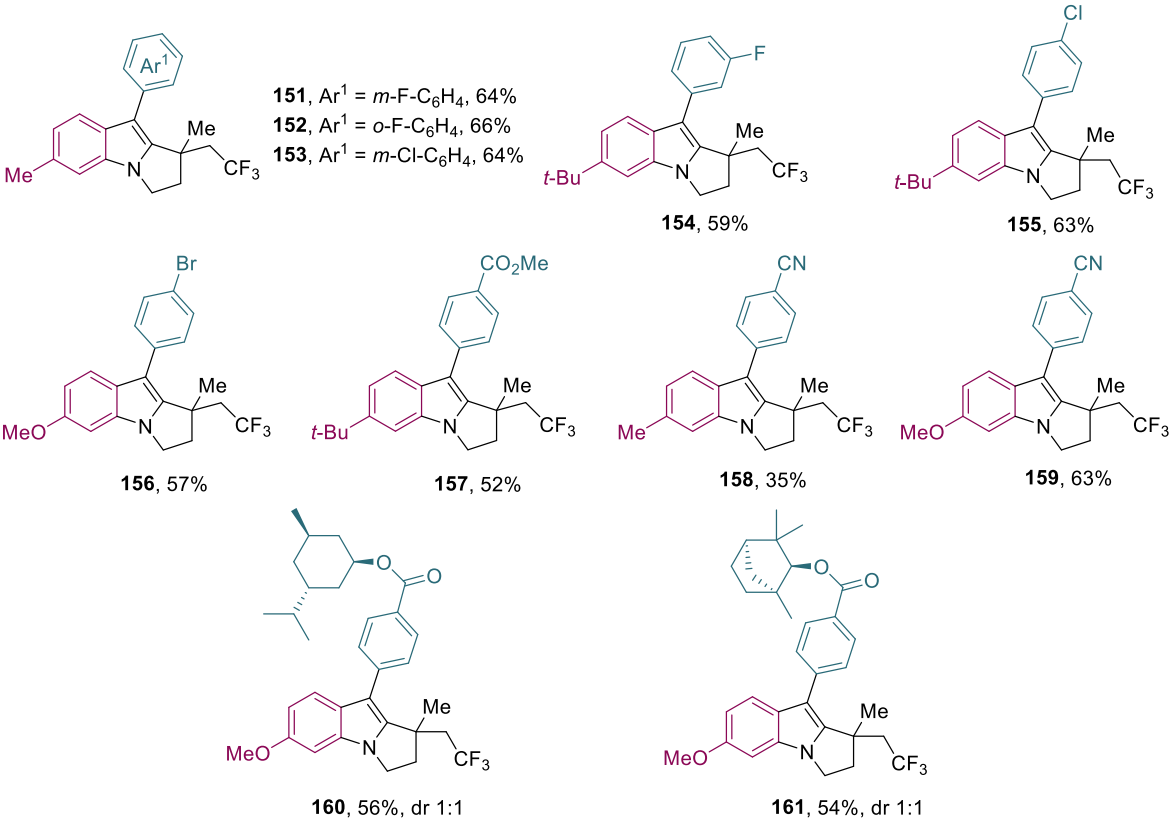

See Scheme 39 for reaction conditions, the other regioisomer was not observed based on ^{1}H NMR analysis.

Scheme 42: Substrates with Ar^2 embedded in the indole motif

The scope of this transformation was then further explored with consideration of the electronic properties between the two aryl groups within the ynamide. First, several ynamides with *para*-alkyl and *para*-methoxy substituents on the aryl sulfonamide and electron-deficient substituents on the aryl ethynyl portion were examined (Scheme 42). Exclusive formation of the [1,2]-annulated indole products resulting from the selective cyclisation onto the sulfonamide-derived aryl groups was observed. Functional groups on the aryl ethynyl part including halides (**151**−**156**), ester (**157**), nitrile (**158**, **159**) groups were well tolerated (35%−66% yields), and substrates derived from (−)-menthol and (+)-fenchol reacted smoothly under the reaction conditions (**160** and **161**, 56% and 54% yields respectively). The crystal structure of [1,2]-annulated indole **155** was shown in Figure 3.

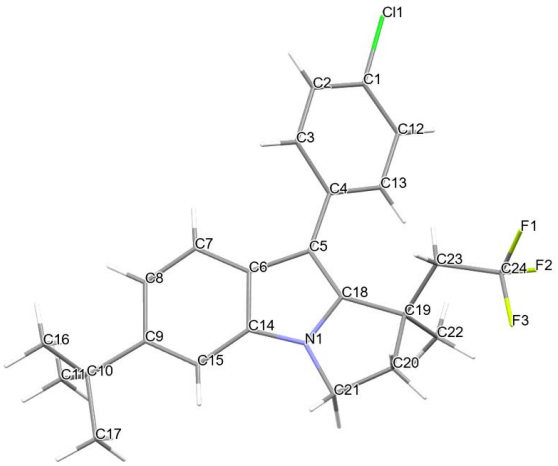

Figure 3: X-ray crystallography of indole product 155. Crystallographic data solved by Dr. Xiaoyong Chang (SUSTech) and has been deposited at the Cambridge Crystallographic Data Centre, under deposition number CCDC 2043671

A different skeletal construction of the indole motif can be achieved by inverting the electronic properties of the two aryl groups: ynamides bearing electron-donating substituents on the

aryl ethynyl moiety and electron-deficient aryl groups on the sulfonamide resulted the former aryl group incorporated into the [1,2]-annulated indoles (Scheme 43).

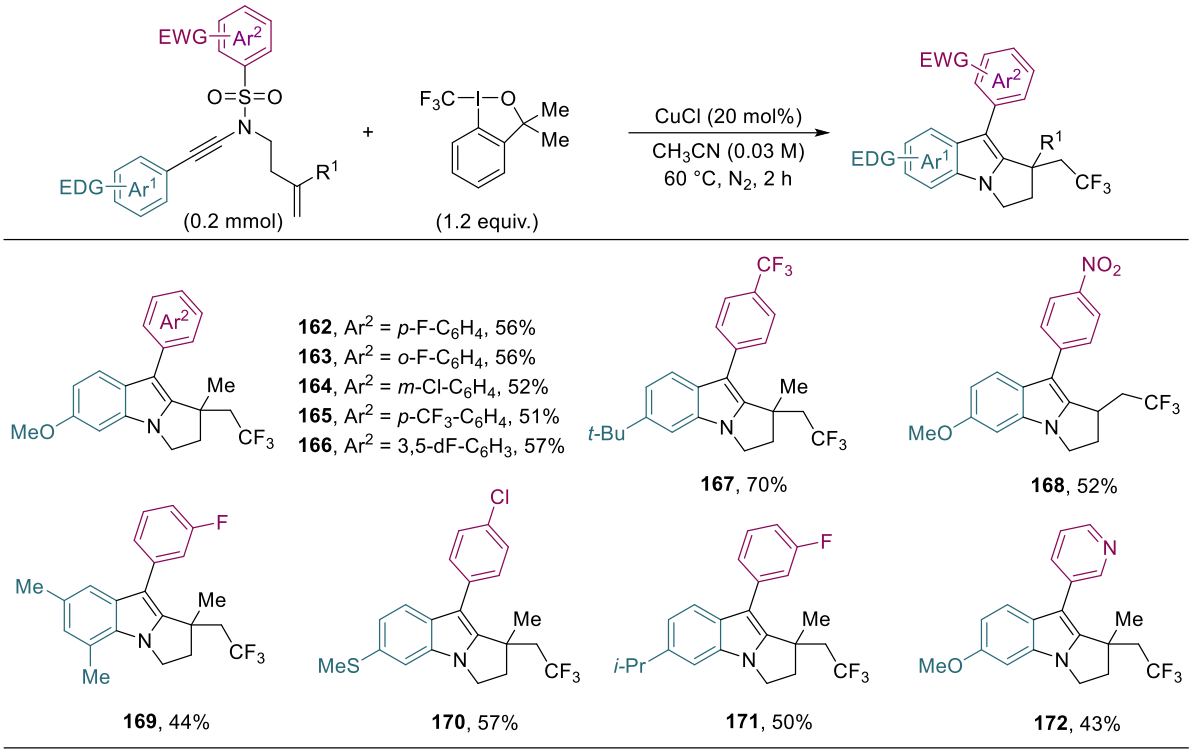

See Scheme 39 for reaction conditions, the other regioisomer was not observed based on ^{1}H NMR analysis.

Scheme 43: Substrates with Ar^1 embedded in the indole motif

Ynamides with aryl sulfonamides bearing *ortho*-, *meta*- and *para*-halogens, 3,5-difluoro, *para*-trifluoromethyl, and *para*-nitro groups were all effective under standard conditions, delivering corresponding indole products **162**–**168** in 51%–70% yields. Various electron-donating groups including *tert*-butyl, *iso*-propyl, methoxy, thioether groups on the aryl ethynyl parts worked well. In addition, a pyridine-containing substrate also worked in the reaction, providing product **172** in moderate yield. This type of skeletal assembly was further confirmed through the crystal structure of product **162** (Figure 4).

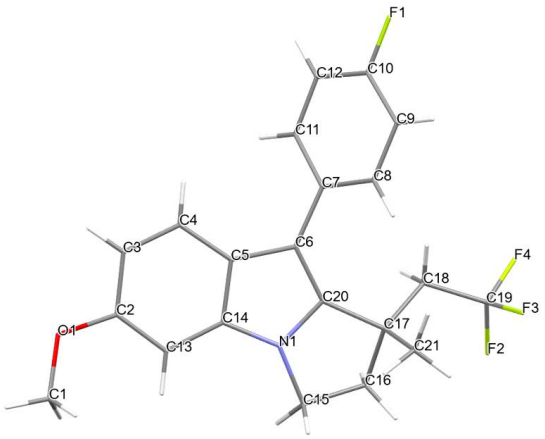

Figure 4: X-ray crystallography of indole product 162. Crystallographic data solved by Dr. Xiaoyong Chang (SUSTech) and has been deposited at the Cambridge Crystallographic Data Centre, under deposition number CCDC 2043669

Isomeric sets of ynamides **173**/**174** and **176**/**177** showed quite similar reaction efficiencies in this transformation (52%/58% yields, 62%/69% yields respectively), and delivered the same regioisomers **175** and **178** respectively, with the more electron-rich *para*-methoxy phenyl group fitted in the products regardless of its original connection (Scheme 44). Thus, starting materials can be designed and prepared based on the synthetic availability.

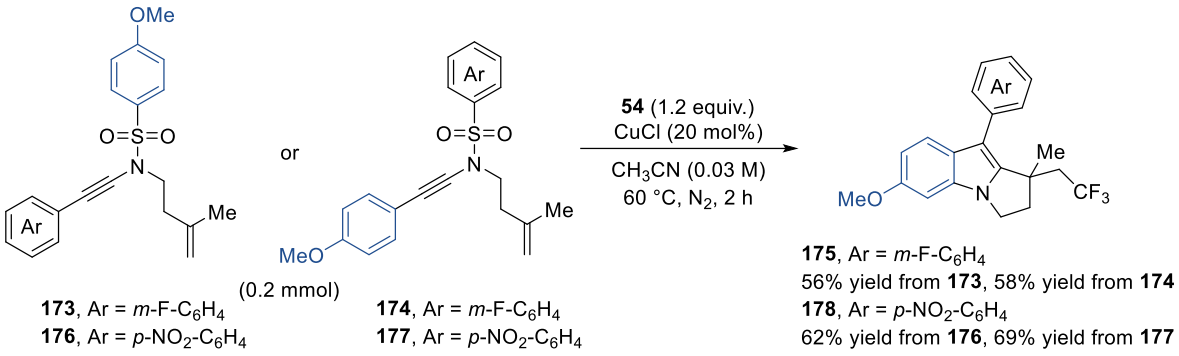

173, Ar = *m*-F-C_6H_4
176, Ar = *p*-NO_2-C_6H_4

174, Ar = *m*-F-C_6H_4
177, Ar = *p*-NO_2-C_6H_4

175, Ar = *m*-F-C_6H_4
56% yield from **173**, 58% yield from **174**
178, Ar = *p*-NO_2-C_6H_4
62% yield from **176**, 69% yield from **177**

See Scheme 39 for reaction conditions, the other regioisomer was not observed based on ^{1}H NMR analysis.

Scheme 44: Converging synthetic routes

Next, the length and structure of the alkyl chain tethered to the ynamides were modified, which led to the construction of more diverse [1,2]-annulated indole skeletons (Scheme 45). By increasing the alkyl chain length, pyrido [1,2-*a*]indoles and azepino-[1,2-*a*]indole (**179**–**181**) were obtained in good to moderate yields. Unbranched and *n*-butyl branched alkene groups were well tolerated, and the selective cyclisation step were observed in all cases.

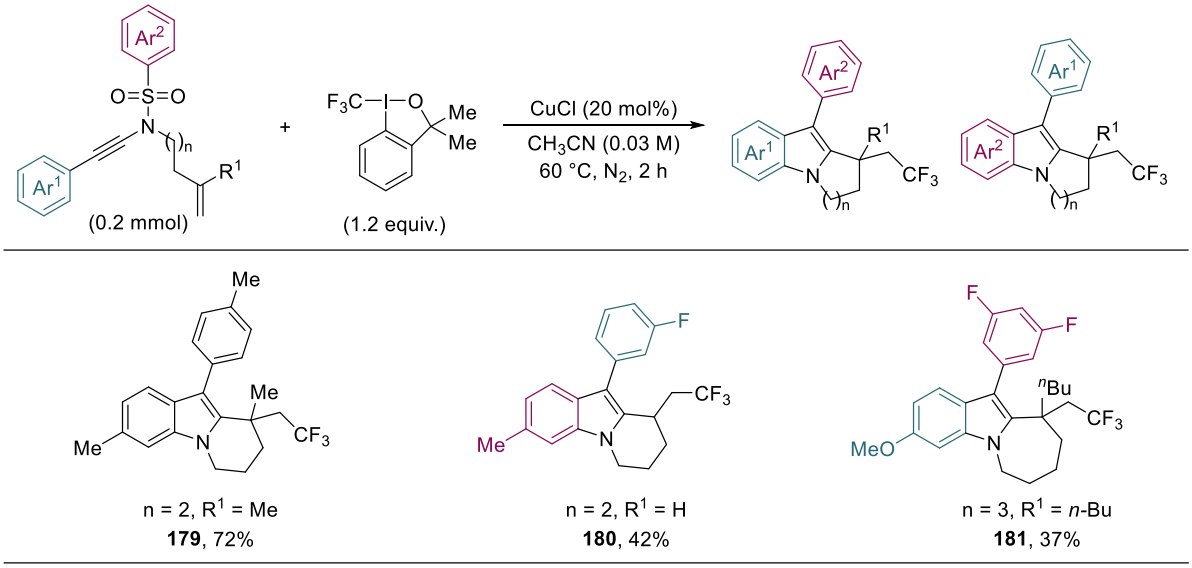

See Scheme 39 for reaction conditions, the other regioisomer was not observed based on ^{1}H NMR analysis.

Scheme 45: Rapid access to more diverse [1,2]-annulated indole motifs

Other electron-deficient radical precursors were also tried in this cascade reaction. Reactions conducted under the optimised copper-catalysed conditions failed to provide the desired product, possibly due to the insufficient generation of the corresponding radicals. The use of photoredox catalysis was tested to be an efficient way for the introduction of α,α-difluoroamidyl and α,α-difluorocarbonyl motifs into [1,2]-annulated indoles (Scheme 30, **182**–**184**, 44%–51% yields). Notably, the selective arylation step was retained under

photoredox catalysed conditions, affording single regioisomeric products **185** and **186** in 54% and 55% yields respectively.

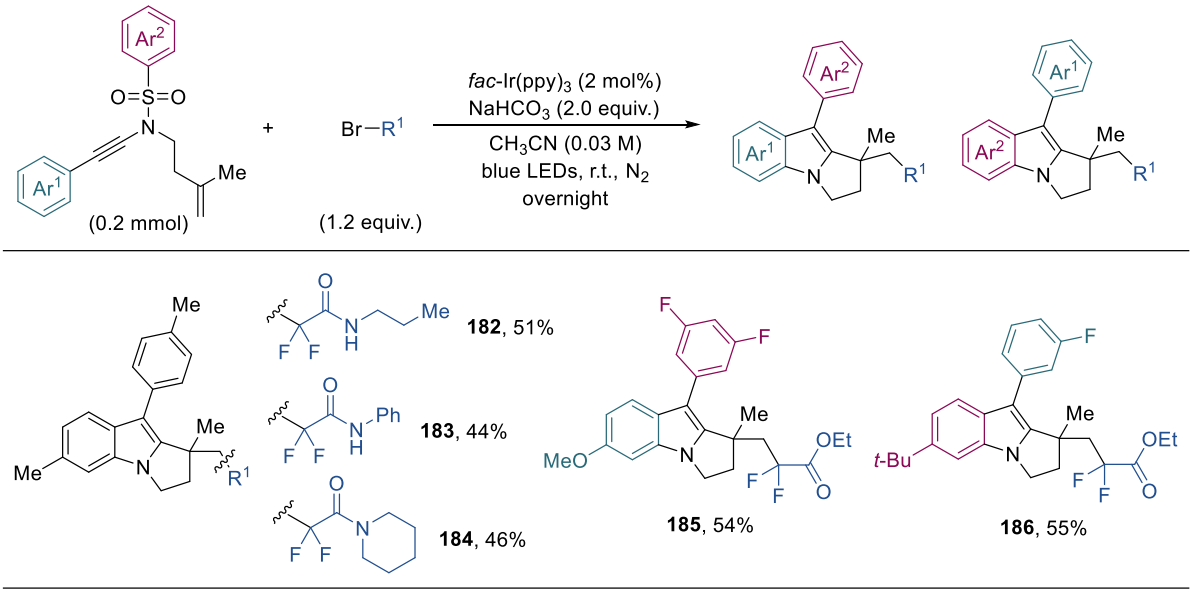

Reaction conditions: ynamide (0.2 mmol, 1.0 equiv.), corresponding radical precursors (1.2 equiv.), fac-Ir(ppy)$_3$ (2 mol%), NaHCO$_3$ (2.0 equiv.) in CH$_3$CN (6.0 mL), irradiated under blue LEDs at room temperature under N$_2$ atmosphere overnight; isolated yields are reported.

Scheme 46: Introducing other radical precursors under photoredox catalysed conditions

In addition, the reaction efficiency of a keto-ynamide **187** was also tested under the standard copper-catalysed conditions. However, fast decomposition of the ynamide was observed and no major product could be isolated, possibly due to the coordination of the carbonyl group to copper catalyst which led to catalyst deactivation (Scheme 47a). Applying this ynamide with Togni's reagent **54** to photoredox catalysed conditions led to the formation of the desired Smiles rearrangement product **188** in 51% yield. Interestingly, around 10% yield of **189** was also formed (Scheme 47b). The formation of **189** might result from the direct vinyl radical

addition to the *ortho*-position of the aryl sulfonamide instead of *ipso* substitution, after the initial trifluoromethyl radical addition, intramolecular cyclisation steps. The structure of both products was confirmed by X-ray diffraction (Figure 5, 6).

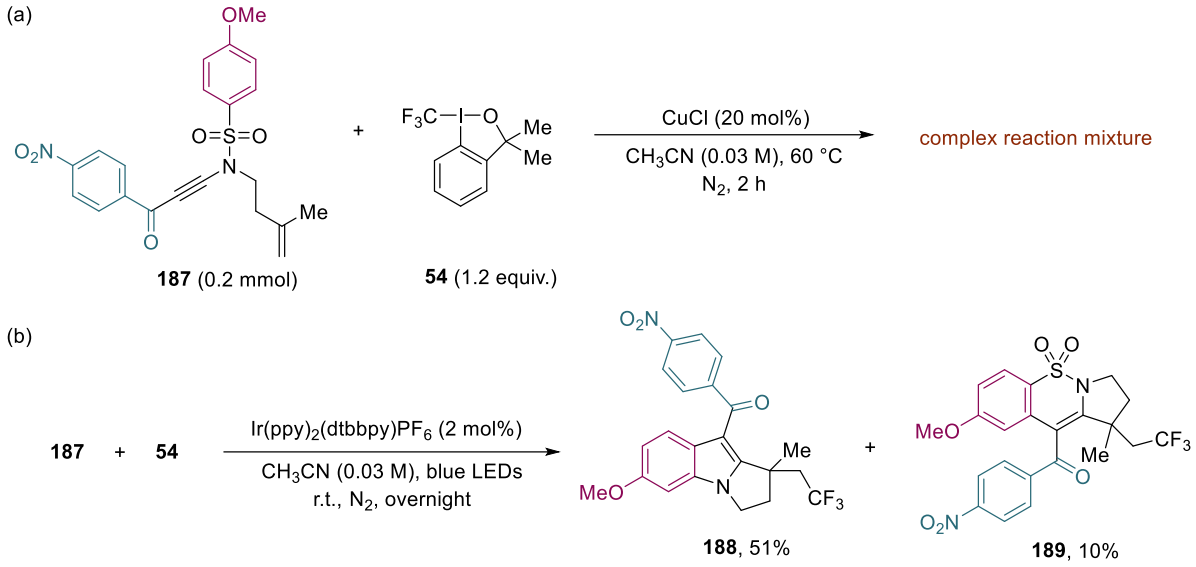

Scheme 47: Reaction of a keto-ynamide

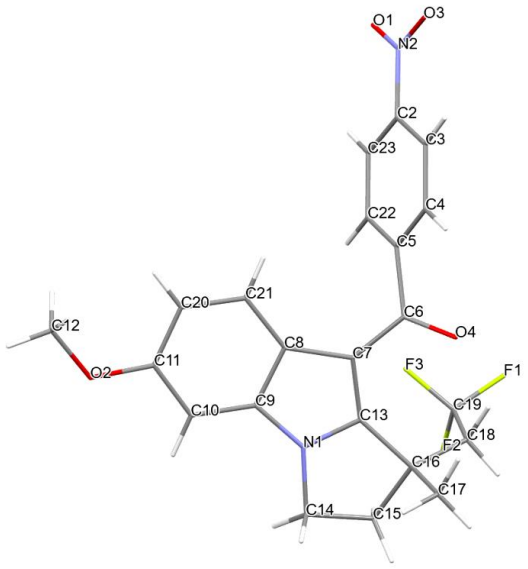

Figure 5: X-ray crystallography of the Smiles rearrangement product 188. Crystallographic data solved by Dr. Xiaoyong Chang (SUSTech) and has been deposited at the Cambridge Crystallographic Data Centre, under deposition number CCDC 2043672

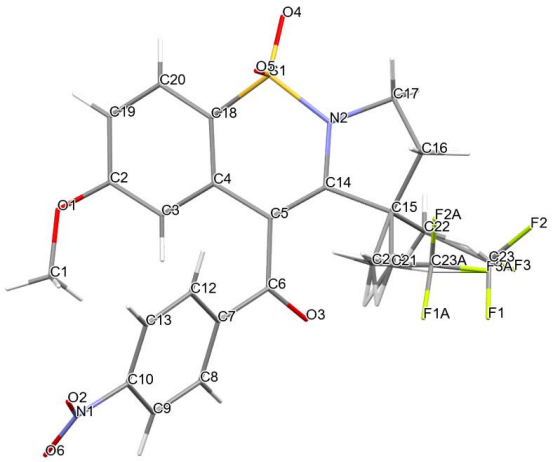

Figure 6: X-ray crystallography of the radical cyclisation product 189. Crystallographic data solved by Dr. Xiaoyong Chang (SUSTech) and has been deposited at the Cambridge Crystallographic Data Centre, under deposition number CCDC 2043674

2.2.3 Reaction Limitations and Unsuccessful Substrates

Although a series of ynamides were successfully converted into corresponding [1,2]-annulated indoles with good reaction efficiencies. A fine balance between the substitution pattern of the two aromatic groups needs to be achieved in order to get good reactivity and site-selectivity in the final arylation process. In addition, the choice of the two aryl groups in the ynamide remains empirical (Scheme 48). When substrates **134**–**136** with strong electron-deficient substituents but without strong electron-donating groups were used, low conversion of starting materials were observed even at longer reaction time. Possibly due to the insufficient oxidation of the nitrogen centred radical species into its cation form during the reaction (vide infra), resulting an unproductive reaction pathway. Substrate **193** with a thiophenyl group decomposed during the process, leading to the formation of complex reaction mixture. Furthermore, substrates with an alkyl ethynyl or a trimethylsilyl ethynyl moiety (**194**, **195**) were not suitable under the reaction conditions, possibly due to the instability of the forming vinyl radical intermediates during the reaction.

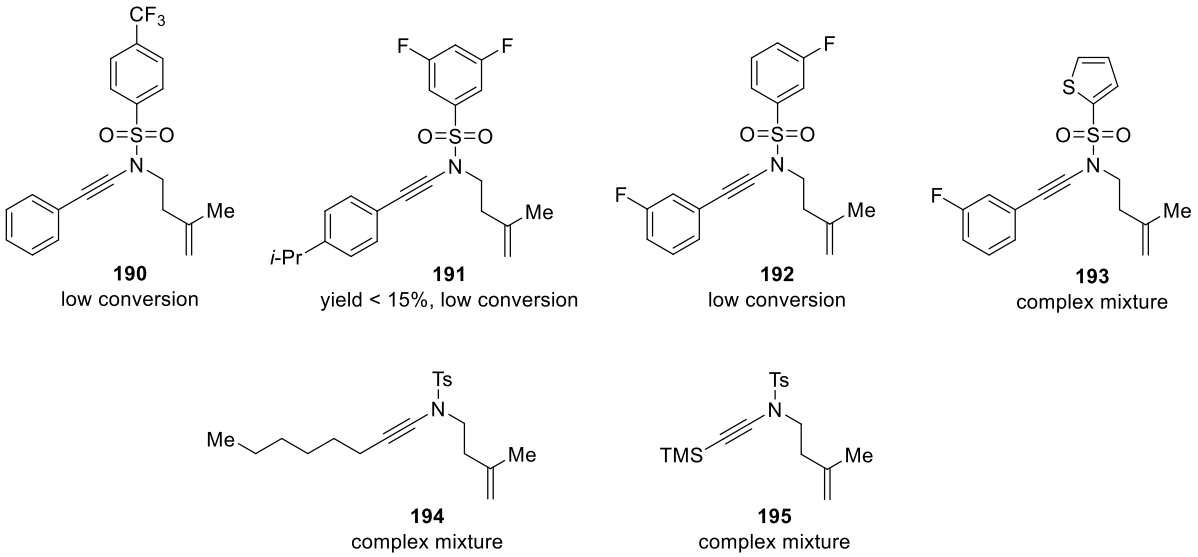

Scheme 48: Unsuccessful substrates

2.3 Mechanistic Studies

2.3.1 Radical Trapping Experiment

In order to gain more insights into the reaction mechanism, TEMPO ((2,2,6,6-tetramethylpiperdin-1-yl)oxyl) was added to the standard reaction (Scheme 49). The desired annulated indole product **140** was not formed, the CF_3–TEMPO adduct **196** was detected by ^{19}F NMR spectroscopy, with a signal at δ = -55.66 ppm. These results indicating the involvement of free radical species during the reaction.

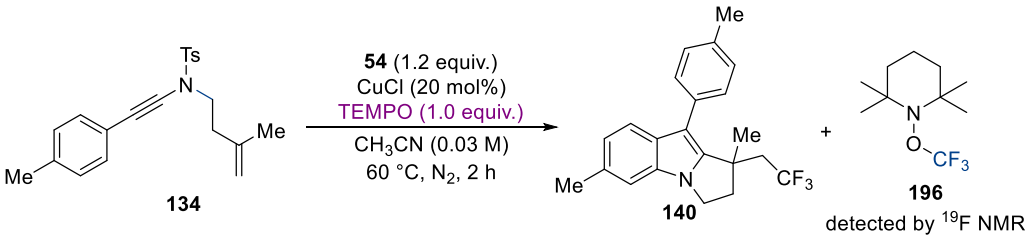

Scheme 49: Reaction with TEMPO

2.3.2 DFT Calculations Support Site-Selective Aza-Nazarov Cyclisation

There are two possible mechanistic pathways that would result the site-selective cyclisation in the indole formation step. As shown in Scheme 50, ynamide **197** with an electron-deficient aryl group on the sulfonamide and an electron-rich aryl ethynyl moiety was taken as an example.

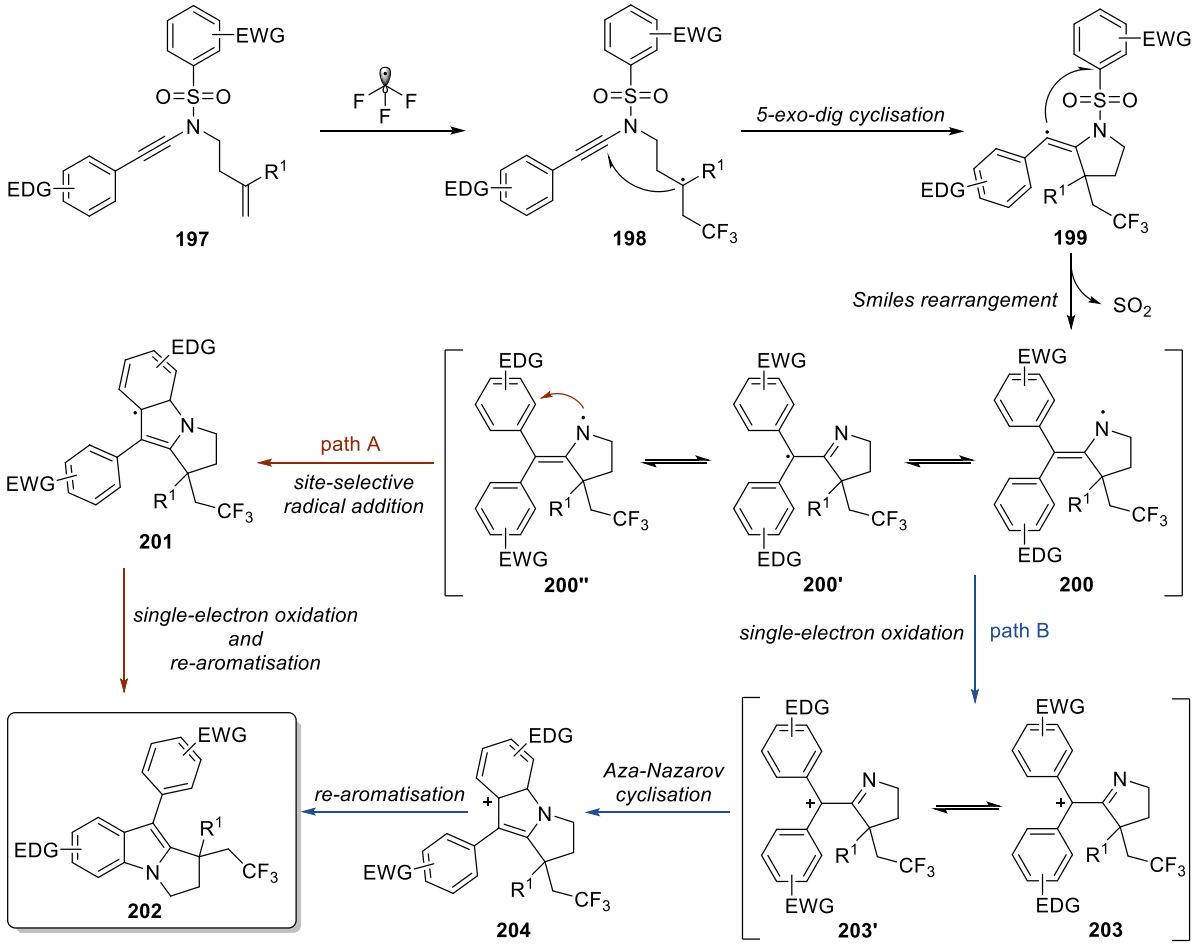

Scheme 50: Possible pathways for the formation of [1,2]-annulated indoles *via* site-selective cyclisation

The initial CF_3 radical addition to **197** resulted the alkyl radical intermediate **198**, which underwent intramolecular 5-exo-dig cyclisation to produce a vinyl radical intermediate **199**.

The desulfonylative Smiles rearrangement of **199** delivered a nitrogen-centred radical species **200** or its equivalents **200'**, **200''**. At this stage, this nitrogen-centred radical species might exhibit electrophilic properties that underwent site-selective radical addition to the *ortho*-position of the more electron-rich aryl group to produce **201**,[48] the following single-electron oxidation and re-aromatisation steps would then deliver the product **202** (path A). Another reaction pathway involved the single-electron oxidation of the nitrogen-centred radical species **200** by [Cu^{II}] species which led to the formation of the extended cation intermediates **203** or **203'** and regenerate the [Cu^{I}] species. Then an aza-Nazarov cyclisation happened through the 4π system incorporating the more electron-rich aryl group selectively to afford intermediate **204**. The desired product **202** was then be obtained upon deprotonation (path B). [49,50]

In order to determine whether the cation species was formed in the reaction, external nucleophile such as methanol was added into the reaction mixture with the aim to trap the cation species, but no adduct product was detected. Possibly a faster intramolecular cyclisation was happened rather than an intermolecular nucleophilic addition. Then density functional theory (DFT) calculations were performed to probe the excellent site-selectivity observed in the arylation step. The DFT calculations were performed by collaborators: Zibo Wu, Weiliang Shi and Yibo Lei from the Northwest University, China.

Two potential cyclisation pathways were considered using ynamide **205** as substrate: direct cyclisation of the N-centred radical formed by desulfonylative Smile rearrangement was compared with an aza-Nazarov type cyclisation of the cation generated on single-electron oxidation of the N-centred radical (Scheme 51). In principle, three sites are available for the C(sp^2)−N bond forming step, resulting in three regioisomeric products **151**, **151'** and **151''**. While the experimental results showed that [1,2]-annulated indole product **151** was formed exclusively, and the other two possible isomers were not observed. Thus, the formation of all the potential products by either potential way was investigated. First, the computed free-energy profile for the direct cyclisation of the N-centred radical showed that, starting from intermediate **A**, rotation of **A** to form **B** and **C** was slightly exergonic by 0.6 and 2.6 kcal/mol. A high barrier to cyclisation was observed (28.1−28.5 kcal/mol) with no substantial energy difference between the possible isomeric outcomes. By contrast, the computed free-energy profile of the aza-Nazarov type cyclisation pathway correlated well to the observed experimental outcome. Considerably lower barriers were seen compared to the radical cyclisation pathway and the formation of **151** was more kinetically favourable than its isomers ($\Delta G^{\ddagger}$ ~2.9-3.7 kcal/mmol).

Although the energy for the single-electron oxidation of the N-centred radical species to the cation intermediate and a complete computed reaction pathway remains to be validated, an aza-Nazarov type cyclisation instead of the direct N-centred radical cyclisation pathway was more likely to happen in the site-selective arylation step.

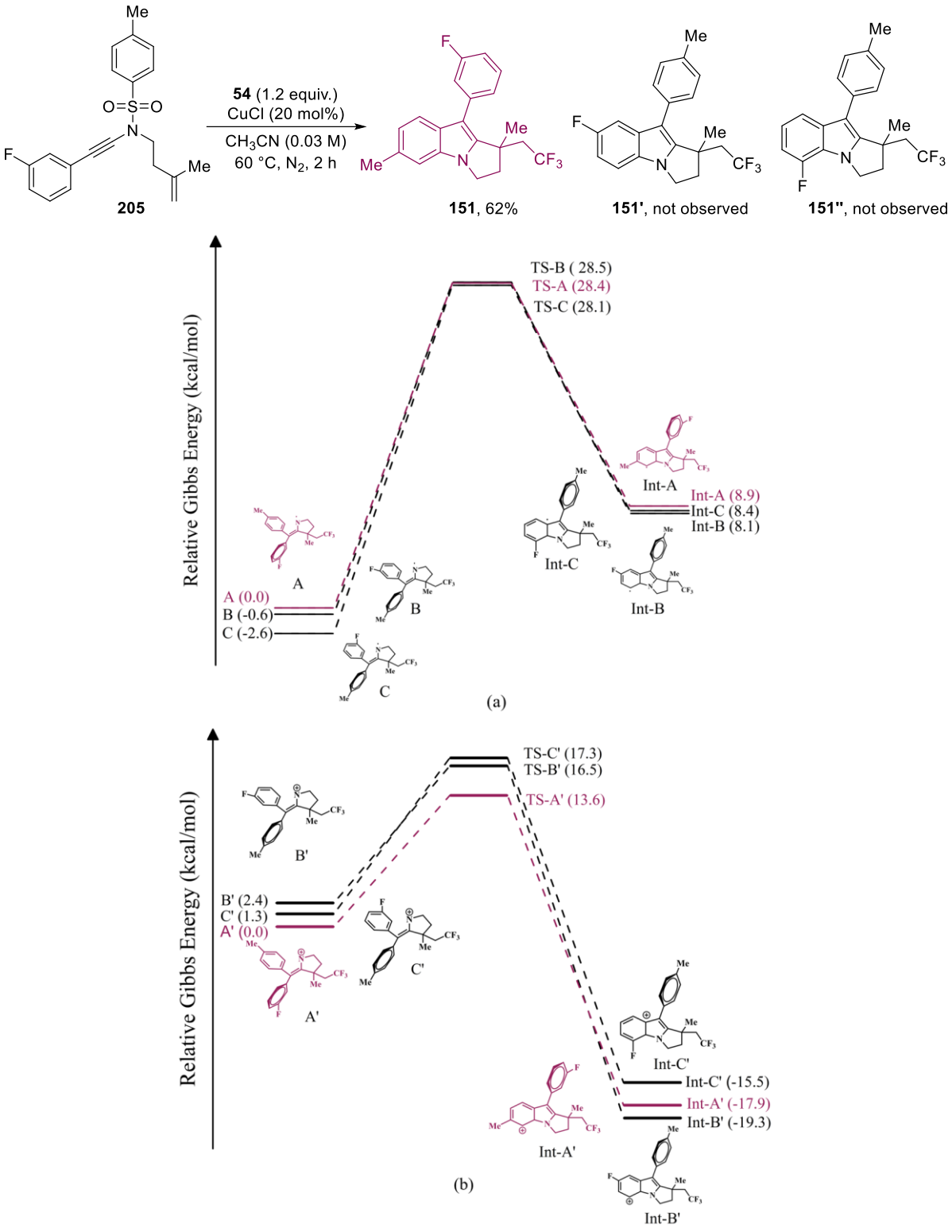

Scheme 51: Computed free-energy profiles using ynamide 205 as substrate. (a): N-centred radical cyclisation; (b): aza-Nazarov type cyclisation. DFT calculations were performed by Zibo Wu from the Northwest University, P. R. China.

2.4 Summary

In this chapter, a radical initiated fragmentary rearrangement cascade of alkene-tethered ynamides to construct [1,2]-annulated indoles was demonstrated. A variety of radical precursors could be employed to introduce electron-deficient fluorine-containing motifs into indoles under copper or photoredox catalysis. The reaction was successful with ynamides with various electron-rich and electron-deficient aryl groups on both sulfonamide and alkyne parts. By increasing the alkyl chain between the alkene and nitrogen, more diverse [1,2]-annulated indole skeletons such as pyrido[1,2-α]indole and azepino[1,2-α]indole could be accessed.

A site-selective C(sp^2)–N bond cyclisation was observed after a sequence of radical addition, intramolecular cyclisation, desulfonylative Smiles rearrangement, which enables the incorporation of electron-rich aryl group to the indole motif regardless of its original position. The DFT calculations revealed that the high selectivity was attributed to an aza-Nazarov cyclisation through a 4π electron system instead of the direct nitrogen radical addition to the aryl group.

Chapter 3: Photoredox Catalysed Triple C–F Bond Cleavage of α-Trifluoromethyl Alkenes to Access α-Arylated Carbonyl Compounds

3.1 Introduction

3.1.1 Defluorinative Functionalisation of α-Trifluoromethyl Alkenes

C–F bonds are thermodynamically strong and kinetically inert. The incorporation of fluorine can modulate the lipophilicity and metabolic stability of parent molecules.[51] These features make fluorine-containing molecules commonly found in biologically active molecules and have broad applications among pharmaceutical and agrochemical industries.[52,53] However, because of the lack of reactivity, organofluorocarbons are environmentally persistent and can lead to bioaccumulation. For example, highly toxic perfluorooctanoic acid derivatives used in surfactants and the production of fluorinated polymers have been found even in artic snow.[54] Selective replacement of fluorine in polyfluoroalkyl carbons with other functionalities under mild reaction conditions presents a challenging yet highly desirable goal.

α-Trifluoromethyl alkene derivatives (**206**) are useful synthetic intermediates in organic transformations for the preparation of partially fluorinated molecules (Scheme 52).[55] The electron-deficient property of α-trifluoromethyl alkenes gives their unique reactivities towards C–F bond activation. α-Trifluoromethyl alkenes can readily react by S_N2'-type reaction with nucleophiles adding to the γ-position carbon atom with respect to the fluorine substituent, along with β-fluoride elimination to yield *gem*-difluoroalkene products (**207**). After this stage, a second nucleophilic substitution can continue to occur at the α-carbon position followed by a second fluoride elimination to give mono-fluorinated alkenes (**153**, S_NV

process), while this process is normally an intramolecular reaction. Furthermore, the direct *ipso*-substitution of α-trifluoromethyl alkenes has also been reported.

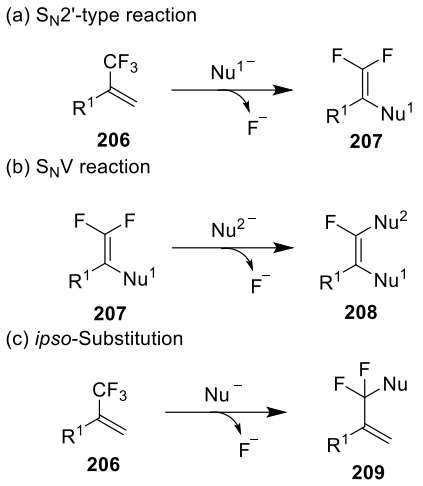

Scheme 52: General reaction profiles of α-trifluoromethyl alkenes

Traditional two-electron approaches for the defluorinative functionalisation of α-trifluoromethyl alkenes usually require strong base or harsh reaction conditions. For example, Rock and co-workers reported the addition of various organolithium reagents to α-trifluoromethyl alkenes (Scheme 53).[56] A variety of phenyl, alkenyl, phosphonate containing *gem*-difluoroalkenes could be prepared in good yields.

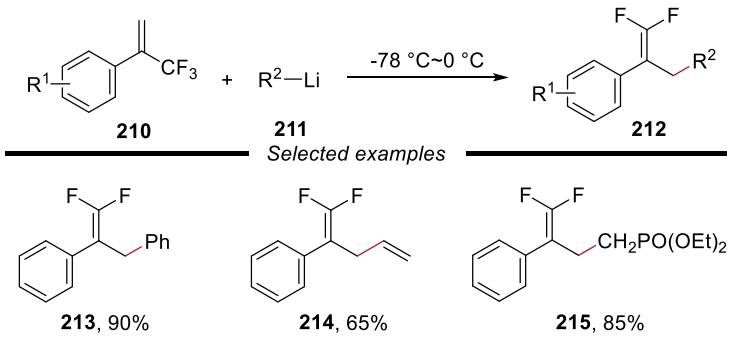

Scheme 53: α-Trifluoromethyl alkenes react with organolithium reagents

Photoredox-catalysis enabled selective manipulation of C – F bonds in α-trifluoromethyl alkenes provides promising one-electron strategy for the construction of fluorinated or non-fluorinated molecules under mild conditions.[57,58] The following sections discussed recent advances in the C–F bonds functionalisation of α-trifluoromethyl alkenes under photoredox conditions.

3.1.1.1 Photocatalysed mono-defluorination of α-trifluoromethyl alkenes

A general reaction mechanism for the photoredox-catalysed selective defluorination of α-trifluoromethyl alkenes to construct *gem*-difluoroalkene derivatives is illustrated in Scheme 54: the reaction is initiated through a single-electron transfer process between the excited photocatalyst $^*PC^n$ and a suitable radical precursor **216** to produce the reduced photocatalyst PC^{n-1} and radical species **219**, which undergo facile radical addition to the electron-deficient α-trifluoromethyl alkene **217** to give the alkyl radical intermediate **220**. Radical-polar crossover process occurs during which the radical intermediate **220** is further reduced by PC^{n-1} to afford the key sp^3-hybridized carbanion **221** and regenerate the ground-state photocatalyst. Finally, β-fluoride elimination take place to yield the *gem*-difluoroalkene product **218**.

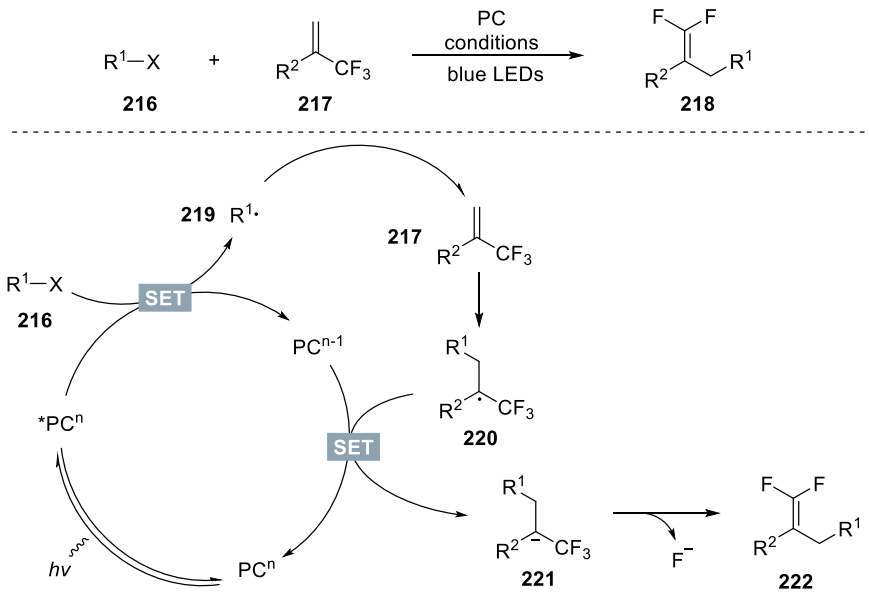

Scheme 54: A general mechanistic pathway of photoredox-catalysed *gem*-difluoroalkene formation from α-trifluoromethyl alkene

In 2016, Zhou and co-workers reported a photocatalytic decarboxylative/defluorinative functionalisation of α-trifluoromethyl alkenes (Table 2, entry 1).[59] α-Keto acids and α-amino acids were employed as acyl radical and α-amino alkyl radical precursors through photoredox catalysed decarboxylation process. The reaction proceeded in the presence of visible light, photocatalyst $Ir(dFCF_3ppy)_2(dtbbpy)PF_6$, and lithium hydroxide to deliver the desired γ,γ-difluoroallylic ketones or 1,1-difluorohomoallyl amines in good yields.

Shortly after, Molander group demonstrated the use of potassium alkyltrifluoroborates like **227** as alkyl radical precursors for the defluorinative functionalisation of α-trifluoromethyl alkenes (Table 2, entry 2).[60] Other kinds of radical precursors such as alkylbis(catecholato)

silicates and α-trimethylsilylamines were also employed for the construction of highly functionalised *gem*-difluoroalkene derivatives.

In a similar fashion, Shen, Loh and co-workers reported visible light-mediated trifluoromethylation of α-trifluoromethyl alkenes *via* C–F bond cleavage using CF_3SO_2Na as trifluoromethyl radical source in the presence of light and photocatalyst $Ir(dFCF_3ppy)_2(dtbbpy)PF_6$ in DMA (Table 2, entry 3).[61] A series of CF_3-containing *gem*-difluoroalkenes were obtained in good yields with excellent stereoselectivity.

In 2019, Yang and co-workers developed the defluoroalkylation of α-trifluoromethyl alkenes with strained cycloketone oxime **234** in the presence of photocatalyst $Ir(dFCF_3ppy)_2(dtbbpy)PF_6$, triphenylphosphine, and Na_2CO_3 in dichloromethane under blue light irradiation (Table 2, entry 4).[62] The generation of primary alkyl radical species **235** was resulted from a strain-relieved radical relocation process of the cycloketone oxime during the reaction.

The Zhou group reported the direct β-C–H *gem*-difluoroalkylation of aliphatic aldehyde and cyclic ketones through the combination of visible-light photocatalysis and organocatalysis (Table 2, entry 5).[63] According to their proposed mechanism, the condensation of aldehyde **237** with Cy_2NH (dicyclohexylamine) formed enamine, which was oxidised by the excited photocatalyst to give radical cation species. Deprotonation of the acidic β-C–H bond of the radical cation species in the presence of DABCO (1,4-diazabicyclo[2.2.2]octane) resulted the

Table 2: Photocatalysed mono-defluorination of α-trifluoromethyl alkenes

Entry	Representative substrates	Conditions	Radical species generated	Product	Contributor(s)
1	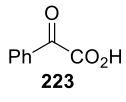 **223** 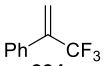 **224**	$Ir(dFCF_3ppy)_2(dtbbpy)PF_6$ (2 mol%) LiOH (2 equiv.), DMSO 5 W blue LEDs, r.t.	 **225**	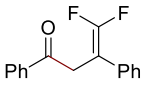 **226** 87%	Zhou, 2016
2	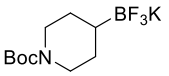 **227** 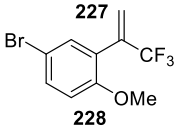 **228**	4CzIPN (5 mol%) DMSO blue LEDs, r.t.	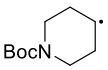 **229**	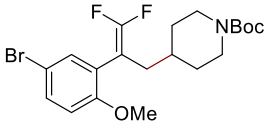 **230** 86%	Molander, 2017
3	CF_3SO_2Na **231** 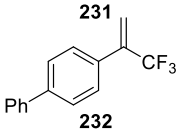 **232**	$Ir(dFCF_3ppy)_2(dtbbpy)PF_6$ (2 mol%) DMA blue LEDs, r.t.	 **128**	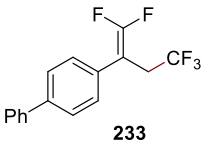 **233** 90%	Shen & Loh, 2018
4	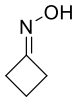 **234** 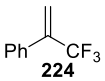 **224**	$Ir(dFCF_3ppy)_2(dtbbpy)PF_6$ (2 mol%) PPh_3 (3.6 equiv.) Na_2CO_3 (1.5 equiv.), DCM 30 W blue LEDs, r.t.	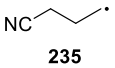 **235**	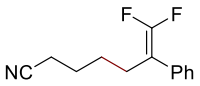 **236** 50%	Yang, 2019
5	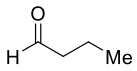 **237** 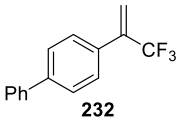 **232**	$Ir(dFCF_3ppy)_2(dtbbpy)PF_6$ (1 mol%) Cy_2NH (30 mol%) DABCO (1 equiv.) PTSA (30 mol%) DMF, blue LEDs, r.t.	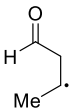 **238**	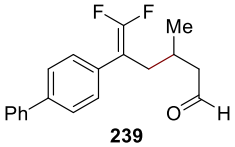 **239** 66%	Zhou, 2020
6	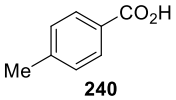 **240** 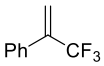 **224**	$Ir(dFCF_3ppy)_2(dtbbpy)PF_6$ (2 mol%) PPh_3 (1.5 equiv.) $NaHCO_3$ (1.2 equiv.) DMF, blue LEDs, r.t.	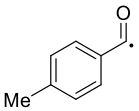 **241**	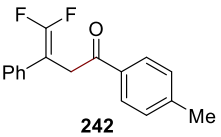 **242** 90%	Wang, 2020
7	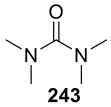 **243** 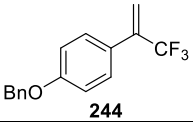 **244**	$Ir(dFCF_3ppy)_2(dtbbpy)PF_6$ (2 mol%) quinuclidine (20 mol%) $NaHCO_3$ (1 equiv.) MeCN, blue LEDs, r.t.	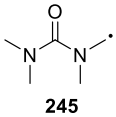 **245**	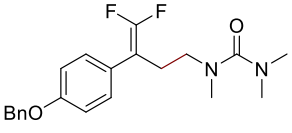 **246** 66%	Wang, 2021

formation of alkyl radical species **238**. Subsequent radical addition, radical polar crossover, and β-fluoride elimination processes delivered the desired product **239**.

In 2020, Wang and co-workers reported a photocatalysed deoxygenation/defluorination of α-trifluoromethyl alkenes with aromatic carboxylic acids such as **240** for the synthesis of γ,γ-difluoroalkylic ketones (Table 2, entry 6).[64] Aromatic carboxylic acids, triphenylphosphine were used with $NaHCO_3$ to generate acyl radical species **241** through a deoxygenation process in the presence of $Ir(dFCF_3ppy)_2(dtbbpy)PF_6$ under blue light irradiation.

Later, the same group described a protocol that combines photoredox catalysis and hydrogen atom transfer catalysis to achieve dehydrogenative difluoroalkylation of amides, ethers, and alkyl aldehydes (Table 2, entry 7).[65] The reaction proceeded using $Ir(dFCF_3ppy)_2(dtbbpy)PF_6$ as photocatalyst, quinuclidine as efficient hydrogen atom transfer catalyst, $NaHCO_3$ as base in acetonitrile under blue light irradiation.

In 2021, Martin and co-workers disclosed a visible-light mediated strategy that enabled site-selective difluoroalkylation of previously unactivated C–H bonds in amides (Scheme 55).[66] In their reaction, the site-selectivity was decided by the structure of the aliphatic amides **247** and the reaction conditions. In the presence of photocatalyst $Ir(dFCF_3ppy)_2(dtbbpy)PF_6$ and K_3PO_4 in toluene under blue light irradiation, proton-coupled electron-transfer process took place at the acidic trifluoromethyl-substituted amides leading to the formation of amidyl radical intermediate. 1,5-HAT process followed by radical addition/radical polar cross-over would

lead to the formation of the δ-C–H difluoroalkylation product **248**. While the formation of α-C–H difluoroalkylation product **249** under nickel catalysis and photoredox catalysis was mainly due to the binding of Ni(II) catalyst to the amide backbone.

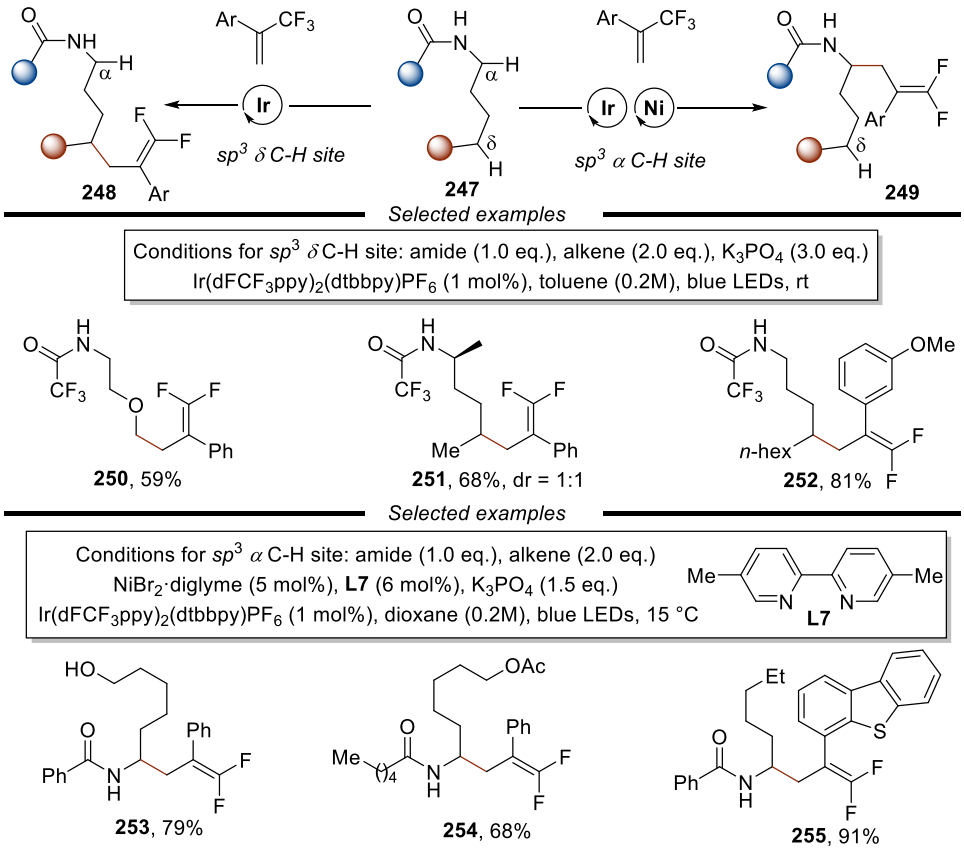

Scheme 55: Site-selective defluorinative C_{sp}^3–H alkylation of secondary amides

In addition to the generation of carbon centred radical species under photoredox conditions for the defluorinative functionalisation of α-trifluoromethyl alkenes, (NHC)-BH_3 complexes were also employed as NHC-boryl radical precursors for the formation of 1,1-difluoroalkene carbonyl mimics. In 2020, Yang and co-workers reported the photoredox-catalysed defluorinative borylation of α-trifluoromethyl alkenes **256** with (NHC)-BH_3 complex **257** in the

presence of photocatalyst $Ir(ppy)_2(dtbbpy)PF_6$ and K_2HPO_4 in THF under blue light irradiation.[67] The formation of NHC-boryl radical was resulted from direct single-electron oxidation of the (NHC)-BH_3 complex by the excited photocatalyst (Scheme 56a). In the same year, Wu's group independently reported a similar type of reaction (Scheme 56b),[68] while in their case, the generation of NHC-boryl radicals were facilitated by a kinetically favoured polarity-matched HAT process between a thiyl radical generated from **263** and (NHC)-BH_3 complex under photocatalysis.

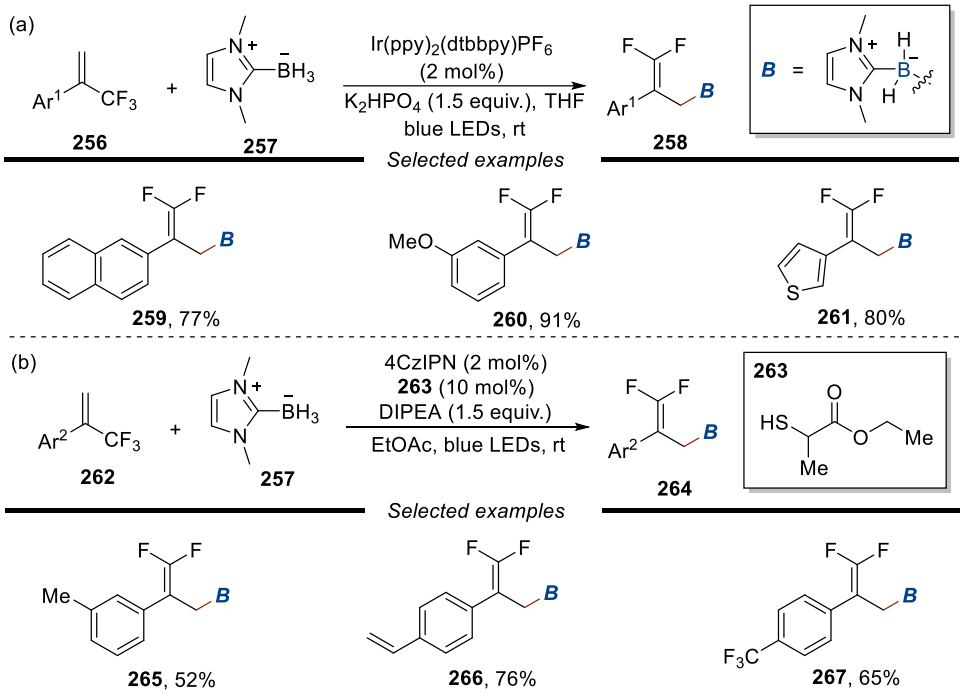

Scheme 56: Defluorinative borylation of α-trifluoromethyl alkenes

In 2020, Wang and co-workers developed a different strategy to achieve the defluorinative borylation of α-trifluoromethyl alkenes bearing electron-withdrawing groups using (NHC)-BH_3 complex (Scheme 57).[69] In their postulated reaction mechanism, the excited photocatalyst

reduced α-trifluoromethyl alkene **268** directly to give a radical anion species **270** and the oxidised photocatalyst, which underwent single-electron transfer with (NHC)-BH_3 complex **257** to deliver the ground-state photocatalyst $Ir(ppy)_3$ and NHC-boryl radical **271**. The radical anion **270** was highly stabilised that underwent hetero radical-radical cross-coupling with **271** to afford the intermediate **272**. β-Fluoride elimination of **272** yielded the desired borylated *gem*-difluoroalkene product **269**.

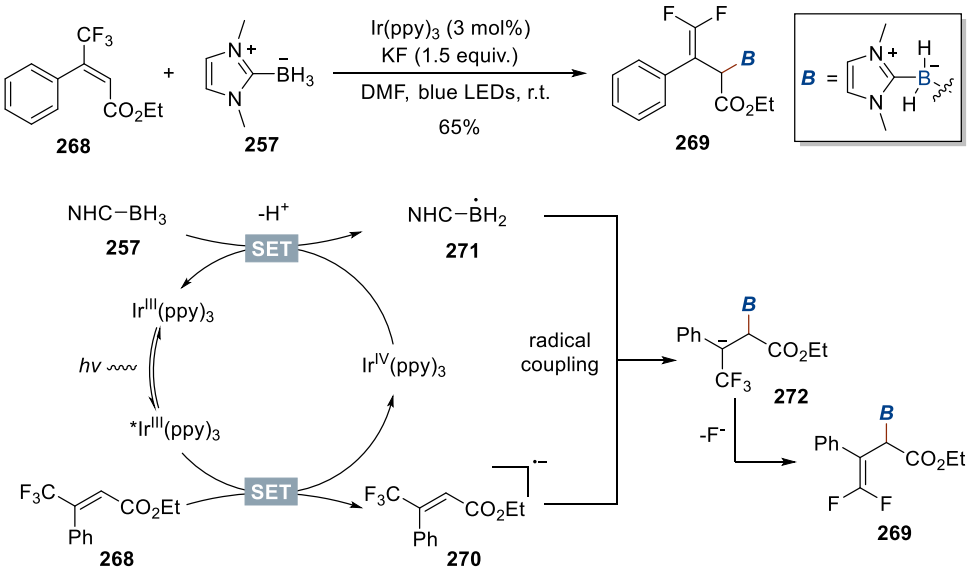

Scheme 57: Defluorinative borylation of α-trifluoromethyl alkenes with electron-withdrawing groups

3.1.1.2 Photocatalysed double C–F bond cleavage of α-trifluoromethyl alkenes

In addition to the mono-defluorinative functionalisation of α-trifluoromethyl alkenes for the construction of *gem*-difluoroalkenes, the *in situ* formed *gem*-difluoroalkene could undergo further defluorination process to provide mono-fluorinated compounds, this process is usually an intramolecular reaction.

In a seminal study published in 2017, Zhou and co-workers disclosed a visible-light mediated [3+3] annulation of tertiary amines **273** with α-trifluoromethyl alkenes **274** through two-fold unsymmetrical C(sp^3)–H functionalization and double C–F bond substitution.[70] Initially, a *gem*-difluoroalkene intermediate was formed through a sequence of radical generation/radical addition/radical-polar crossover/β-fluoride elimination. After this stage, they proposed that the tertiary amine motif in the *gem*-difluoroalkene was further oxidised by the excited photocatalyst to generated α-amino radical, which underwent intramolecular radical addition to the carbon-carbon double bond followed by second β-fluoride elimination to give the desired cyclic product **275**. Another possible pathway involved the intramolecular radical-radical cross-coupling between α-amino radical and fluoroalkenyl radical species under photoredox conditions.

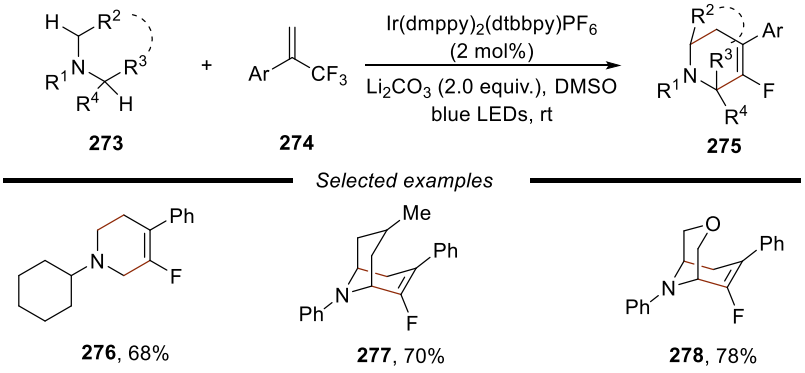

Scheme 58: Photocatalysed [3+3] annulation of tertiary amines with α-trifluoromethyl alkenes

Later, the same group developed a photoredox-catalysed decarboxylative/defluorinative [4+3] annulation of *O*-hydroxyphenylacetic acids **279** and α-trifluoromethyl alkenes **280** to access mono-fluorinated dihydrobenzoxepines **281** through two consecutive C–F bond cleavage in a

CF_3 group.[71] Initially, in the presence of Cs_2CO_3, the excited photocatalyst underwent single-electron oxidation of the deprotonated form of **279** to give benzylic radical species, subsequent radical addition, radical-polar crossover, and β-fluoride elimination processes afforded the intermediate **285**. Then a rapid intramolecular S_NV reaction happened to trigger a second fluoride elimination, delivering the mono-fluorinated heterocycles **281** in good yields.

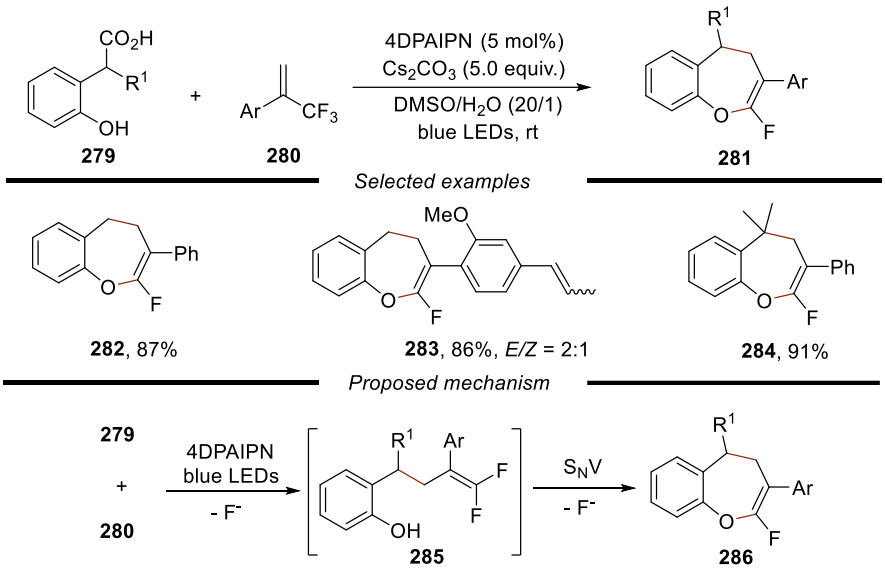

Scheme 59: Decarboxylative/defluorinative [4+3] annulation of *o*-hydroxyphenylacetic acids and α-trifluoromethyl alkenes

3.1.1.3 Summary

In contrast to traditional ionic approaches for the defluorinative functionalisation of α-trifluoromethyl alkenes, photoredox-catalysis enables the generation of radical species to occur under mild conditions, and reactions are usually redox-neutral. Although many types of radical species have been employed for the defluorination of α-trifluoromethyl alkenes, the final products are normally functionalised *gem*-difluoroalkenes. Multi-defluorinative

functionalisation of α-trifluoromethyl alkenes remains limited to the construction of mono-fluorinated cyclic products through intramolecular nucleophilic substitution of the *in situ* generated *gem*-difluoroalkenes. Methods focusing on the construction of structurally diverse molecules through multiple defluorination of α-trifluoromethyl alkenes will be of great interest.

3.1.2 Synthesis of α-Arylated Carboxylic Acids and Amides

α-Arylated carboxylic acids and amides are frequently observed substructures in biologically active molecules and drugs and therefore are of great interesting to the pharmaceutical industry (Scheme 60).[72] Great efforts have been devoted to the efficient synthesis of α-arylated carbonyl compounds.

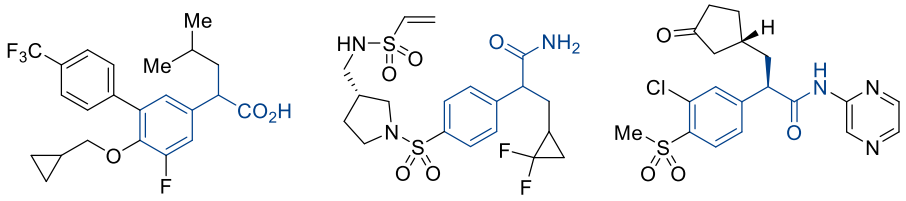

Scheme 60: Bio-active molecules displaying α-arylated carbonyl motifs

Pioneered by Buchwald and Hartwig, methods based on palladium-catalysed α-arylation of carbonyl compounds have been studied extensively.[73,74] In most cases, a metal enolate was formed during the reaction, and the general catalytic cycle for Pd-catalysed addition of enolates to aryl halides is presented in Scheme 61. Initially, oxidative addition of aryl halide **287** to Pd(0) complex **290** resulted the formation of arylpalladium(II) halide complex **291**. In

the presence of base, carbonyl compound **288** was deprotonated to form an enolate species, which underwent ligand substitution with coordinated halide to yield a palladium enolate complex **292** or **293**. Reductive elimination of **293** would deliver the arylation product **289**.

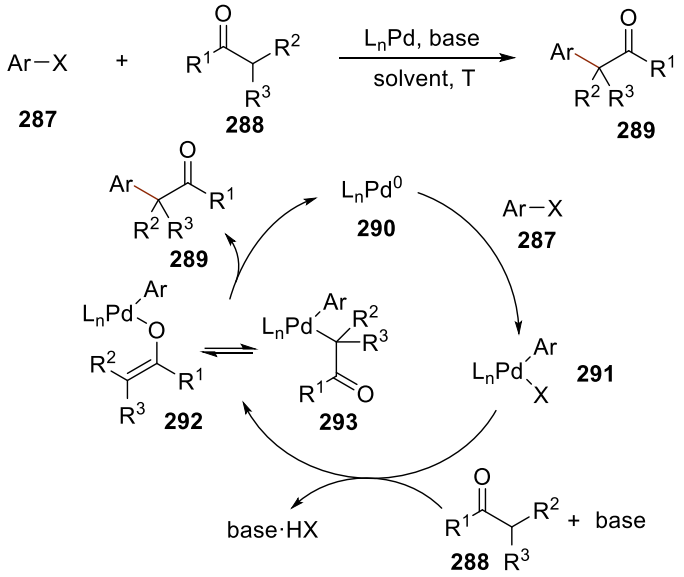

Scheme 61: General profile for Pd-catalysed α-arylation of carbonyl compounds

The most frequently used carbonyl compounds in the Pd-catalysed α-arylation reactions are esters.[75] However, examples using simple carbonyl derivatives such as aliphatic carboxylic acids and NH-containing amides remains rare. Mainly due to the strong coordination of carboxylates and amidates to transition metals;[76] the high pK_a value of α-CH bonds of carboxylates;[77] and the competing C–N coupling of the amidates.[78] To address these long-standing challenges, Hartwig and co-workers reported a one-pot two-step Pd-catalysed α-arylation of carboxylic acids **294** and secondary amides **295** with aryl halides using a traceless protecting strategy where disilyl protected acid and amide intermediates (**298**, **299**) were *in*

situ generated using TMSCl and base (Scheme 62).[79] This method showed good substituents compatibility and provided one-pot synthesis of several commercial Profen drugs. However, the reaction efficiency with primary amides was not demonstrated.

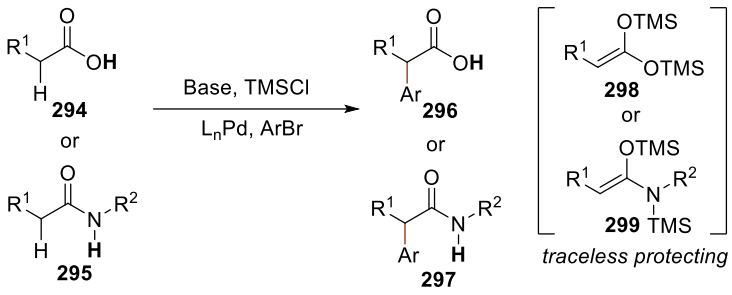

Scheme 62: α-Arylation of carboxylic acids and NH-containing amides

In 2020, Engle's group developed a palladium-catalysed α-selective hydroarylation of acrylates (Scheme 63). This report illustrated an analogous method to typical enolate α-arylation methodology for the synthesis of NH-containing α-arylated amides **302**.[80] Mechanistic showed that this transformation was enabled by the formation of a [Pd^{II}(Ar)(H)] intermediate, which underwent selective hydride insertion into the β-position of acrylates. While α,β-unsaturated carboxylic acids and primary amides were not suitable substrates in this method.

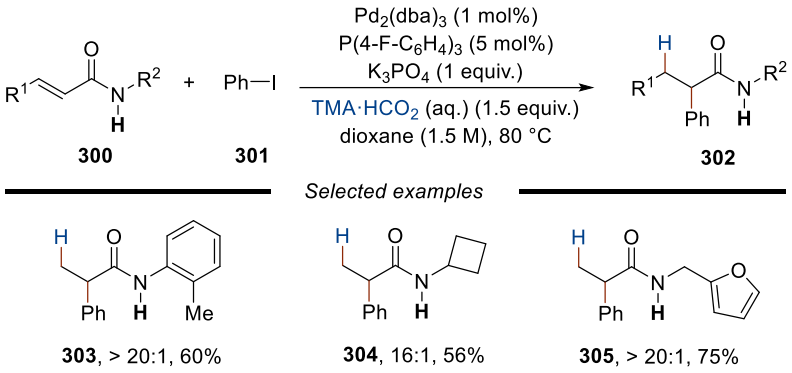

Scheme 63: Pd-catalysed α-hydroarylation of acrylamides

Alternatively, cross-coupling reactions from corresponding α-halo carbonyl derivatives **306** under nickel, copper, or palladium catalysis have also been demonstrated.[81] However, α-halo carbonyl electrophiles require multi-step synthesis and are not always stable, which limit their wider application.

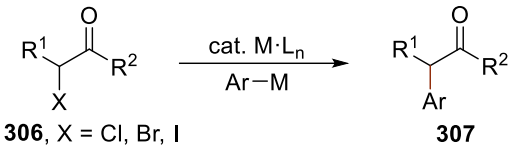

306, X = Cl, Br, I **307**

Scheme 64: Metal-catalysed cross-coupling of α-halo carbonyl compounds

Despite these advancements for the synthesis of α-arylated carbonyl compounds, a straightforward method providing rapid access to structural diverse α-arylated carboxylic acids, esters, and primary, secondary, and tertiary amides from easily available starting materials is desirable.

3.2 Results and Discussion

3.2.1 Reaction Design

The aim of this project was to achieve intermolecular consecutive defluorinative functionalisation of α-trifluoromethyl alkenes. *gem*-Difluoroalkene derivatives are normally formed after the mono-defluorination of α-trifluoromethyl alkenes, the possibility of applying *in situ* formed *gem*-difluoroalkenes to intermolecular defluorinative reaction under the same catalytic system was considered.

In 2019, Feng and co-workers reported a photoredox-coupled F-nucleophilic addition induced allylic alkylation of *gem*-difluorostyrenes (Scheme 65).[82] In this catalytic system, *gem*-difluorostyrenes **308** with electron-rich substituents were oxidised by the excited photocatalyst $*PC^n$ to form the reduced state photocatalyst PC^{n-1} and a radical cationic intermediate **311**. This intermediate was primed for nucleophilic addition by an external fluoride source with intramolecular electron regulation to give an α-CF_3-substituted benzylic radical intermediate **312**. Subsequent radical addition of **312** to radical acceptor **309** followed by β-fragmentation produced a benzenesulfonyl radical **314** and the product **310**. The photocatalyst PC^n was regenerated through the single-electron transfer between PC^{n-1} and the benzenesulfonyl radical **314**.

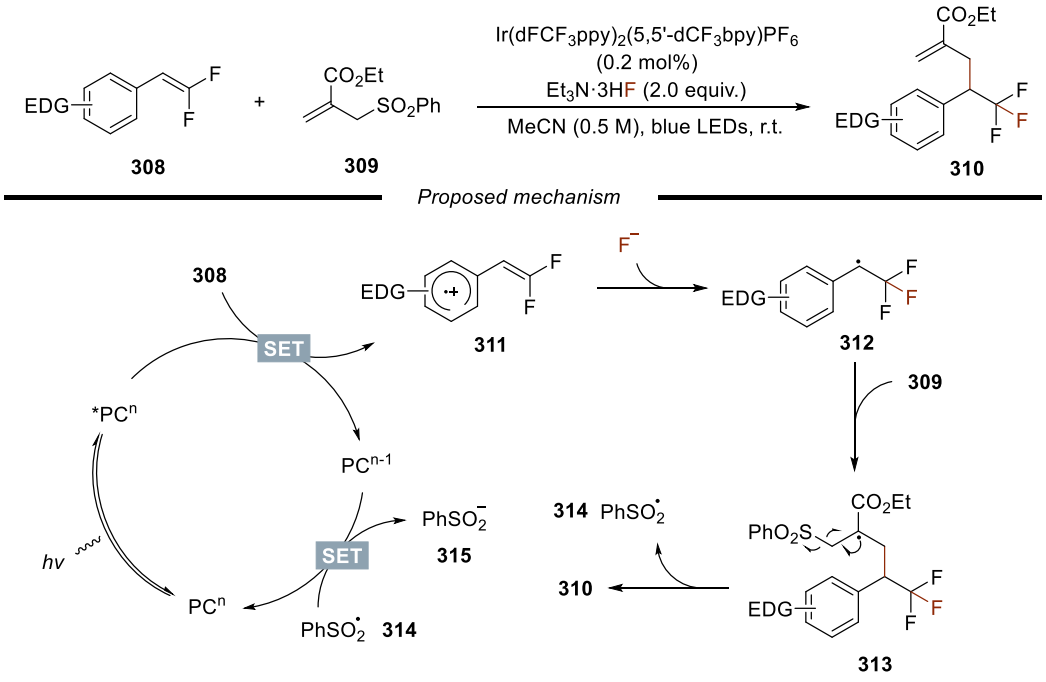

Scheme 65: Photoredox catalysed F-nucleophilic addition to *gem*-difluoroalkenes

Inspired by Feng's work, the oxidation of *in situ* generated *gem*-difluoroalkene **318** from α-trifluoromethyl alkenes by the excited photocatalyst $*PC^n$ was proposed to happen under suitable reaction conditions. In this case, the radical cation intermediate **319** could be trapped by external nucleophiles for further transformation (Scheme 66).

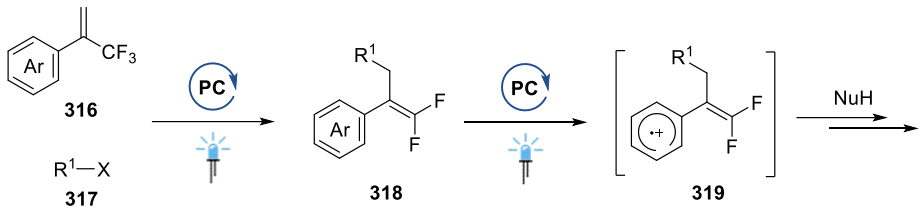

Scheme 66: Our reaction design

3.2.2 Reaction Optimizations for the Triple Defluorinative Formation of α-Arylated Carboxylic Acids

The Nicewicz group reported a series of studies involving acridinium photoredox catalysed anti-Markovnikov hydrofunctionalisation of alkenes.[83] A variety of compounds, such as triflamide, nitrogen-containing heteroaromatics, acids, alcohols, and even H_2O can be served as suitable nucleophiles to trap the alkene radical cation intermediates. At the early exploration of this project, water was chosen as potential nucleophile to test the feasibility of this proposal, α-trifluoromethyl alkene **232** was used as model substrate, and potassium cyclohexyltrifluoroborate **320** was used as alkyl radical precursor. Several photocatalysts with relatively high oxidative potentials were intentionally chose in order to ensure the single-electron oxidation of the *gem*-difluoroalkene intermediates (Scheme 67).

About 10% yield of α-arylated carboxylic acid **321** was formed when photocatalyst $Ir(dFCF_3ppy)_2(5,5'\text{-}dCF_3bpy)PF_6$ (**PC-5**, $E_{1/2}(*Ir^{III}/Ir^{II})$ = +1.65 V vs SCE in CH_3CN) was used in acetonitrile under the irradiation of blue light for 16 h. Increased yields were obtained when iridium-based photocatalyst was replaced with organic acridinium photocatalysts **PC-6** and **PC-7** possessing stronger oxidising abilities (26% and 53% yields respectively).

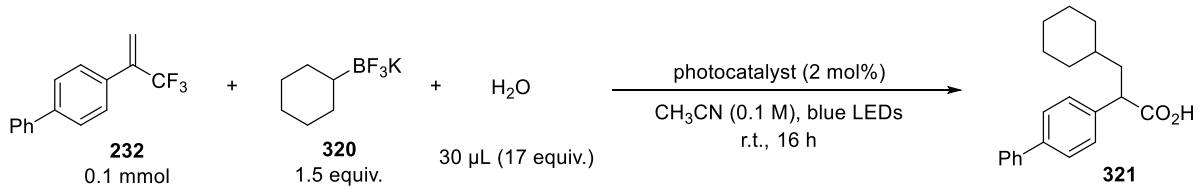

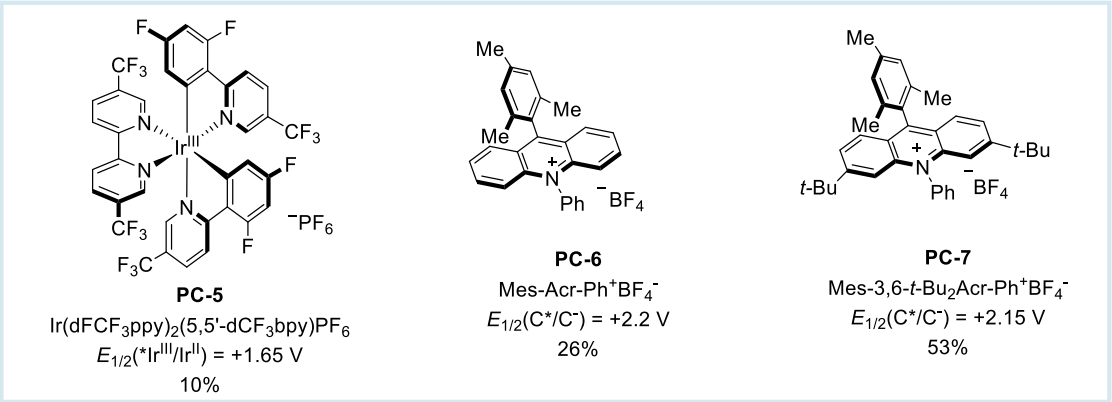

Scheme 67: Initial results of triple defluorination of α-trifluoromethyl alkenes

Further analysis of the ^1H NMR spectroscopy of the crude reaction mixture revealed that an acyl fluoride intermediate might be formed during the reaction (see Section 3.3.1). In order to convert the acyl fluoride intermediate into final carboxylic acid product, additional base-acid work-up procedure was carried out when the photoreaction was completed. A summary of the reaction optimisation details was listed on Table 3.

Compared with initial results, higher yields of **321** were seen for each cases when the base-acid work-up procedure was applied, and the acridinium photocatalyst **PC-7** gave the best result with 80% isolated yield of the carboxylic acid product (Table 3, entries 1–3). Compromised yields were obtained when H_2O was at lower or higher loading (Table 3, entries 4–8, 56%–86% yields). Other solvents like dichloromethane, diethyl ether, and toluene were less effective than acetonitrile, the product was not formed when 1,4-dioxane or dimethylformamide was used (Table 3, entries 9–13). Higher or lower concentration of the solvent led to decreased yields (Table 3, entries 14–15). Applying 1.2 equivalents of the radical precursor **320** into the reaction gave slightly lower yield (Table 3, entries 16). Control experiments verified the necessity of water, photocatalyst **PC-7**, and the blue light (Table 3, entries 17–15).

Table 3: Reaction optimisations of α-arylated carboxylic acid synthesis

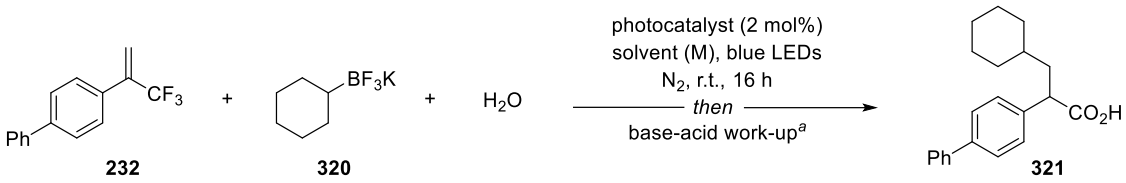

Entry	**232**:**320**	H_2O (µL)	Photocatalyst	Solvent (M)	Yield of **321** (%)[b]
1	1:1.5	30	**PC-5**	CH_3CN (0.1)	16
2	1:1.5	30	**PC-6**	CH_3CN (0.1)	44
3	1:1.5	30	**PC-7**	CH_3CN (0.1)	88 (80)
4	1:1.5	10	**PC-7**	CH_3CN (0.1)	56
5	1:1.5	50	**PC-7**	CH_3CN (0.1)	86
6	1:1.5	70	**PC-7**	CH_3CN (0.1)	84
7	1:1.5	100	**PC-7**	CH_3CN (0.1)	76
8	1:1.5	150	**PC-7**	CH_3CN (0.1)	60
9	1:1.5	30	**PC-7**	CH_2Cl_2 (0.1)	43
10	1:1.5	30	**PC-7**	Et_2O (0.1)	37
11	1:1.5	30	**PC-7**	1,4-Dioxane (0.1)	n.d.
12	1:1.5	30	**PC-7**	PhMe (0.1)	47
13	1:1.5	30	**PC-7**	DMF (0.1)	n.d.
14	1:1.5	30	**PC-7**	CH_3CN (0.2)	73
15	1:1.5	30	**PC-7**	CH_3CN (0.05)	58
16	1:1.2	30	**PC-7**	CH_3CN (0.1)	86
17	1:1.5	none	**PC-7**	CH_3CN (0.1)	n.d.
18	1:1.5	30	none	CH_3CN (0.1)	n.d.
19[c]	1:1.5	30	**PC-7**	CH_3CN (0.1)	n.d.

[a]Reactions were performed on 0.1 mmol scale; after the photoreaction was completed, the reaction mixture was added 1.0 mL of aqueous NaOH solution (0.2 M) and stirred for 5 minutes before the reaction mixture

was acidified by HCl solution (2 N). [b]Yields were determined by ^{1}H NMR spectroscopy of the crude reaction mixture using mesitylene as internal standard, isolated yield was shown in parentheses. [c]Reaction was performed in the dark. n.d. = not detected.

3.2.3 Substrate Scope for the Triple Defluorinative Formation of α-Arylated Carboxylic Acids and Esters

After obtaining the optimised reaction conditions, the substrate scope of the reaction was studied. During the investigation for the scope of α-trifluoromethyl alkenes, some substrates did not fully convert into corresponding carboxylic acids after 16 h, so the reaction time was extended to 48 h for full conversion unless otherwise stated (Scheme 68). α-Trifluoromethyl alkenes with *para*-substituted aryl groups (**322**–**327**) worked well in the reactions, delivering corresponding α-arylated carboxylic acids in 49%–84% yields. The functionalities include methoxy, *tert*-butyl, fluoride, trimethylsilyl and amide groups. Interestingly, a terminal ethyl-substituted α-arylated carboxylic acid **327** was obtained in 68% yield when an α-trifluoromethyl alkene with a 4-(trimethylsilyl)ethynylphenyl group was used. The loss of the trimethylsilyl-group was likely due to the release of fluoride anions during the reaction. Substituents on other positions like 3-methoxy, 3-allyloxy and 3,5-dimethyl groups were also tolerated (**328**–**330**, 55%–71% yields). α-Trifluoromethyl alkenes with fused aryl and heteroaryl groups were also suitable substrates in this transformation, delivering corresponding naphthyl (**331**), benzothiophenyl (**332**), dibenzofuranyl (**333**) and pyridinyl (**334**) substituted carboxylic acids in moderate to excellent yields (40%–90%). yield. In addition, the reaction efficiency of a cyclic alkene substrate was tested with primary alkyltrifluoroborate

336, affording a α,β-cyclic-α-arylated carboxylic acid **335** in 57% yield. The used of secondary or tertiary alkyl radical precursors with this cyclic alkene substrate resulted in low reaction efficiencies, probably due to increased steric hindrance. α-Trifluoromethyl alkenes with strong electron-withdrawing group (such as *para*-trifluoromethyl) substituted aryls were not suitable substrates in this reaction, only leading to the formation of corresponding *gem*-difluoroalkenes.

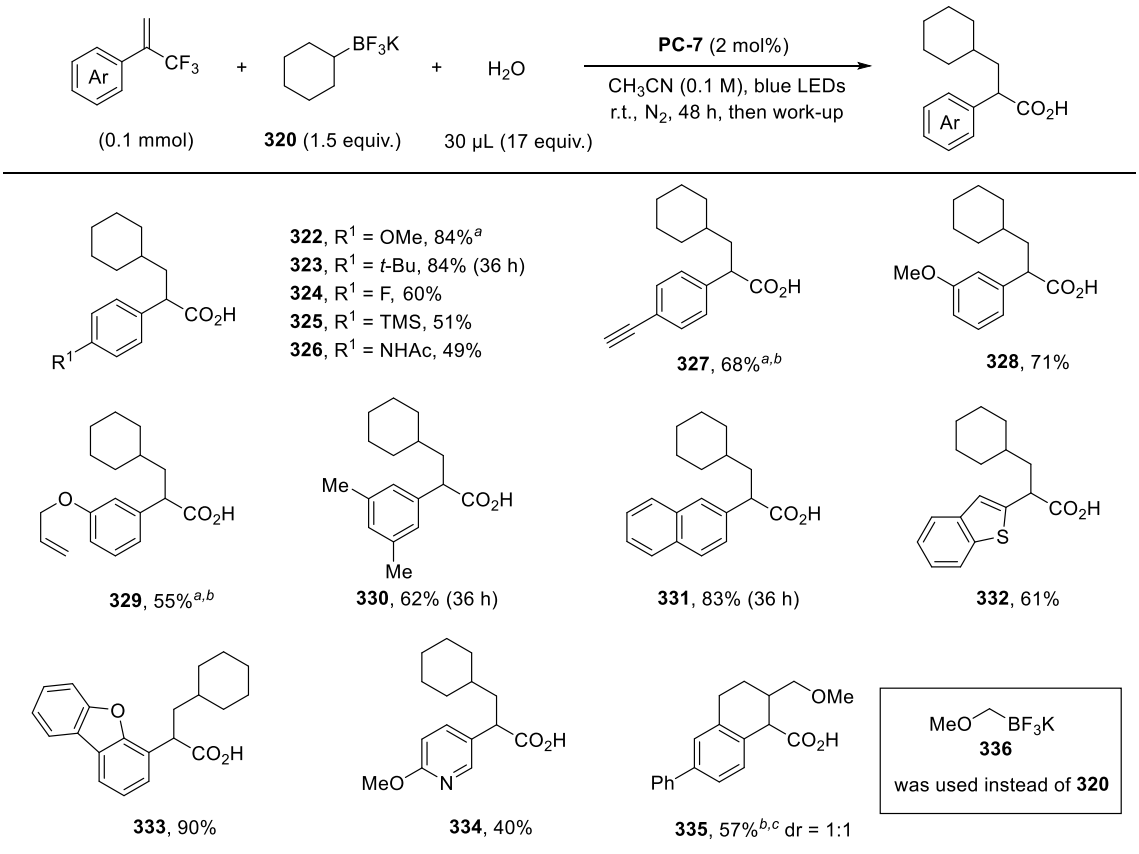

*Reaction conditions: α-trifluoromethyl alkene (0.1 mmol), alkyltrifluoroborate **320** (1.5 equiv.), H_2O (30 µL, 17 equiv.), **PC-7** (2 mol%) in CH_3CN (1.0 mL), irradiated at room temperature under N_2 atmosphere for 48 h, then NaOH/HCl work-up, isolated yields were reported. [a]50 µL of H_2O was used. [b]5 mol% of photocatalyst **PC-7** was used. [c]Reaction was run on 0.2 mmol scale.*

Scheme 68: Scope of α-trifluoromethyl alkenes

A variety of alkyltrifluoroborates were found to be suitable for this transformation (Scheme 69). Cyclic secondary alkyl groups including small and large rings (**337**, **338**), fluorinated alkyl group (**339**), heterocyclic alkyl groups (**340**, **341**), and acyclic alkyl group (**342**) were all incorporated into corresponding α-arylated carboxylic acids with good reaction efficiencies (44%–83% yields). Sterically hindered tertiary alkyl radical precursors were amenable to the coupling with good yields (**343**–**346**, 63%–82% yields). Ketone group was tolerated in this reaction, delivering **346** in 63% yield. Primary α-alkoxymethyltrifluoroborates were also employed to provide a series of γ-alkoxy acids in synthetic useful yields (**347**–**349**, 53%–61% yields).

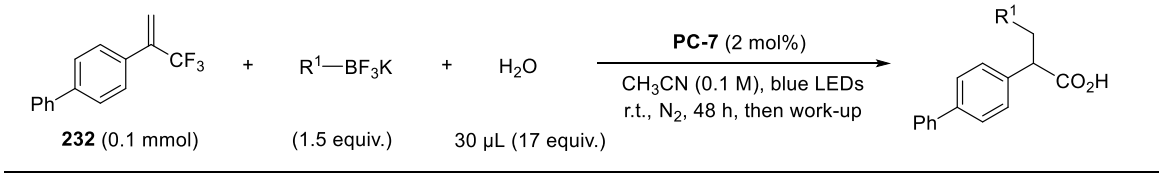

232 (0.1 mmol) (1.5 equiv.) 30 μL (17 equiv.)

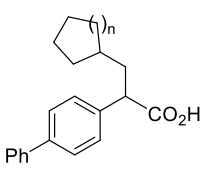

337, n = 1, 73%
338, n = 3, 57%

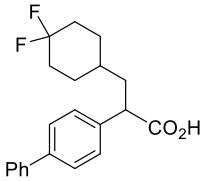

339, 80%

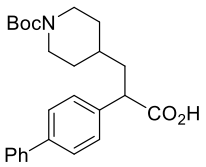

340, 44%[a]

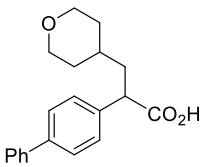

341, 83%

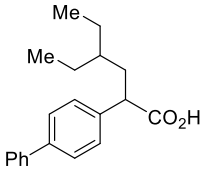

342, 78%

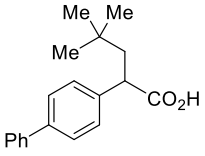

343, 75%[b,c]

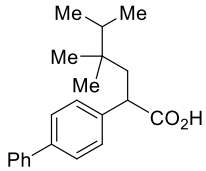

344, 82%[b,c]

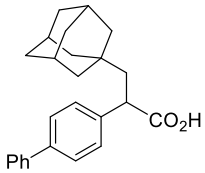

345, 68%

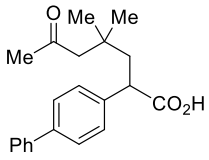

346, 63%[b,c]

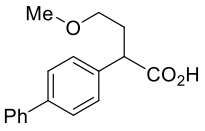

347, 57%

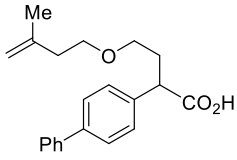

348, 53%

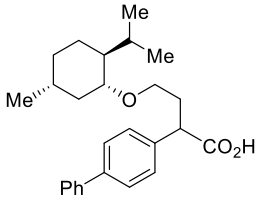

349, 61%[b,c] dr = 1:1

*Reaction conditions: α-trifluoromethyl alkene **232** (0.1 mmol), alkyltrifluoroborates (1.5 equiv.), H_2O (30 µL, 17 equiv.) and **PC-7** (2 mol%) in CH_3CN (0.1 M), irradiated under blue LEDs at room temperature under N_2 atmosphere for 48 h, then NaOH/HCl work-up, isolated yields were reported. [a]100 µL of H_2O was used. [b]50 µL of H_2O was used. [c]5 mol% of photocatalyst **PC-7** was used.*

Scheme 69: Scope of alkyltrifluoroborates

Next, the synthesis of α-arylated esters was studies by replacing H_2O with other *O*-nucleophiles such as aliphatic alcohols. Initial results showed that *gem*-difluoroalkenes were formed instead of α-arylated esters by simply replacing H_2O with aliphatic alcohols. The desired α-arylated esters were obtained in the presence of both H_2O and alcohols (Scheme 70). Although a mixture of α-arylated ester and corresponding α-arylated acid were formed under reactions, α-arylated esters could be isolated in decent yields by varying the amount of water and alcohol used in the reaction. For example, α-arylated esters **351** was obtained in 61% yield alongside small amount (< 5%) of corresponding carboxylic acid **343** by using 5.0 equivalents of methanol and 10 µL of H_2O. 58% Yield of **352** was formed when cyclohexanol was used as nucleophile.

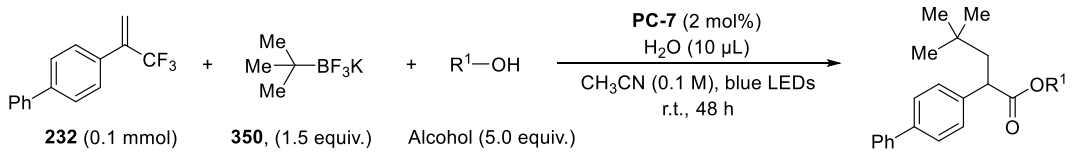

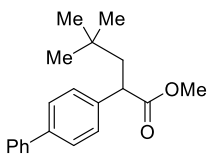

351, 61%

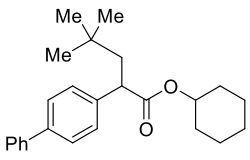

352, 58%

*Reaction conditions: α-trifluoromethyl alkene **232** (0.1 mmol), tert-butyltrifluoroborates **350** (1.5 equiv.), alcohol (5.0 equiv.), H_2O (10 µL) and **PC-7** (2 mol%) in CH_3CN (0.1 M), irradiated under blue LEDs at room temperature under N_2 atmosphere for 48 h.*

Scheme 70: Synthesis of esters *via* triple defluorination of α-trifluoromethyl alkenes

3.2.4 Synthesis of α-Arylated Amides *via* Triple Defluorination of α-Trifluoromethyl Alkenes

After the demonstration for the multicomponent synthesis of α-arylated esters by triple defluorinative functionalisation of α-trifluoromethyl alkenes. The synthesis of α-arylated amides with aliphatic amines as nucleophiles was investigated (Scheme 71). Cyclohexanamine **353** was employed as nucleophile to the reaction, and several photocatalysts with relatively high oxidative potentials were screened first. Initial results showed that the desired amide product **354** was not formed in all cases when 30 µL of H_2O was used in the reactions. When the amount of H_2O was increased to 50 µL, α-arylated amide **354** was formed in 59% yield in the presence of the acridinium photocatalyst **PC-7**. The successful obtaining of the amide product verified the feasibility of the reaction design, albeit the potential for the single electron oxidation of amine by the excited state photocatalyst.[84]

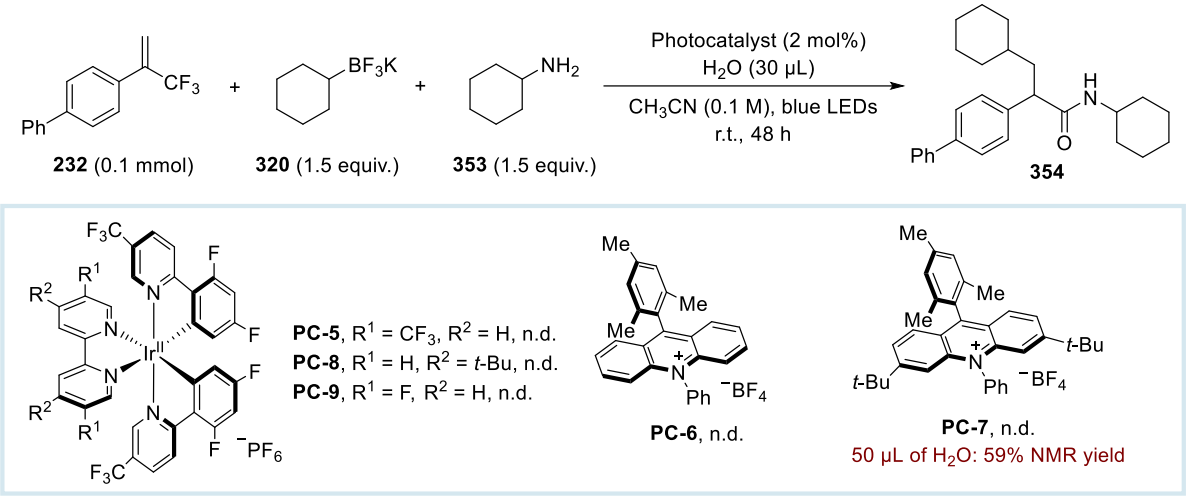

Scheme 71: Screening of photocatalysts for the modular synthesis of α-arylated amides

Optimisations of the amount of water used in the reactions was explored (Scheme 72). Low loading of H_2O in the reactions failed to deliver the product **354**. 72% yield of the α-arylated amide product was isolated when 100 µL H_2O was used, while further increasing the amount of water led to decreased yields. Next, different solvent concentrations were tested. The yields of the reaction decreased by 11% and 5% when the solvent concentration was 0.05 M and 0.2 M respectively (Scheme 73). The reaction was less effective when only 1.2 equivalents of radical precursor **320** was added. Thus far, the substrate scope for the modular synthesis of α-arylated amides *via* triple defluorination of α-trifluoromethyl alkenes was explored.

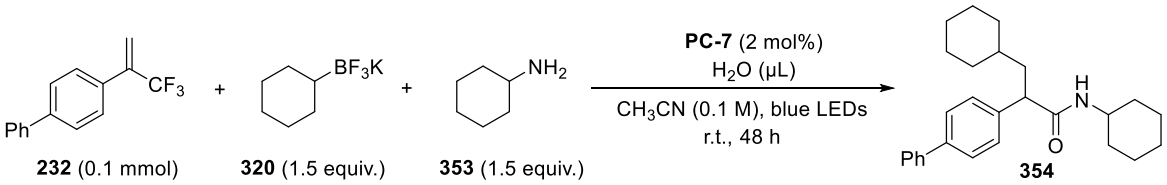

232 (0.1 mmol) **320** (1.5 equiv.) **353** (1.5 equiv.) **354**

Entry	Amount of H_2O (μL)	Yields of **354**[a]
1	10 μL	n.d.
2	30 μL	n.d.
3	50 μL	59%
4	100 μL	80% (72%)
5	150 μL	79%
6	200 μL	73%
7	250 μL	66%

[a]Yields were determined by ^{1}H NMR spectroscopy of the crude reaction mixture; isolated yield was shown in parentheses.

Scheme 72: Reactivity of various amount of H_2O to the α-arylated amide synthesis

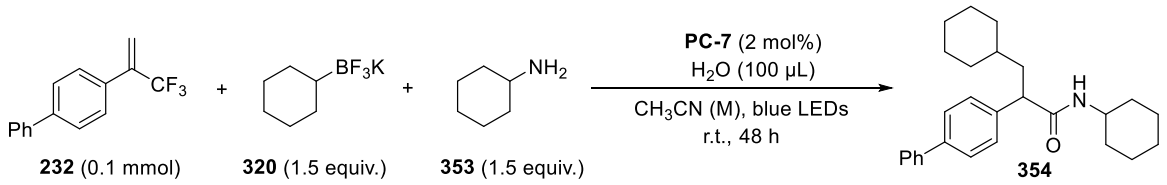

232 (0.1 mmol) **320** (1.5 equiv.) **353** (1.5 equiv.) **354**

Entry	Concentration of solvent	Yields of **354**[a]
1	0.05 M	69%
2	0.1 M	80% (72%)
3[b]	0.1 M	71%
4	0.2 M	75%

[a]Yields were determined by ^{1}H NMR spectroscopy of the crude reaction mixture; isolated yield was shown in parentheses. [b]1.2 equiv. of **320** was used.

Scheme 73: Screening of solvent concentrations

3.2.5 Substrate Scope for the Modular Synthesis of α-Arylated Amides

The optimised reaction conditions were successfully applied to the modular synthesis of α-arylated amides with broad range of alkyl amines and anilines (Scheme 74). Primary amines with a variety of functional groups and structural elements were compatible under reaction conditions. Alongside linear and branched alkyl substituents (**355**–**357**), allylic (**358**), propargyl (**359**) amines were tolerated. In addition, trifluoromethyl, phenyl, nitrile, and free hydroxy group containing alkyl amines delivered corresponding α-arylated amides in good yields (**360**–**363**, 56%–72% yields). Interestingly, a diamide product **364** was obtained in 75% yield when 1,2-diaminoethane was used as nucleophiles. Acyclic and cyclic secondary alkyl amines were also amenable to this multicomponent coupling reaction (**365**–**372**). Morpholine (**366**), azepane (**367**), piperidines bearing ketal (**369**), ester (**370**), free carboxylic acid (**371**) groups and a piperazine derivative (**372**) were successfully incorporated into corresponding amide motifs in 55%–83% yields. Anilines with electron-donating and electron-withdrawing groups were shown to be compatible in this reaction, affording **373**–**375** in 51%–75% yields.

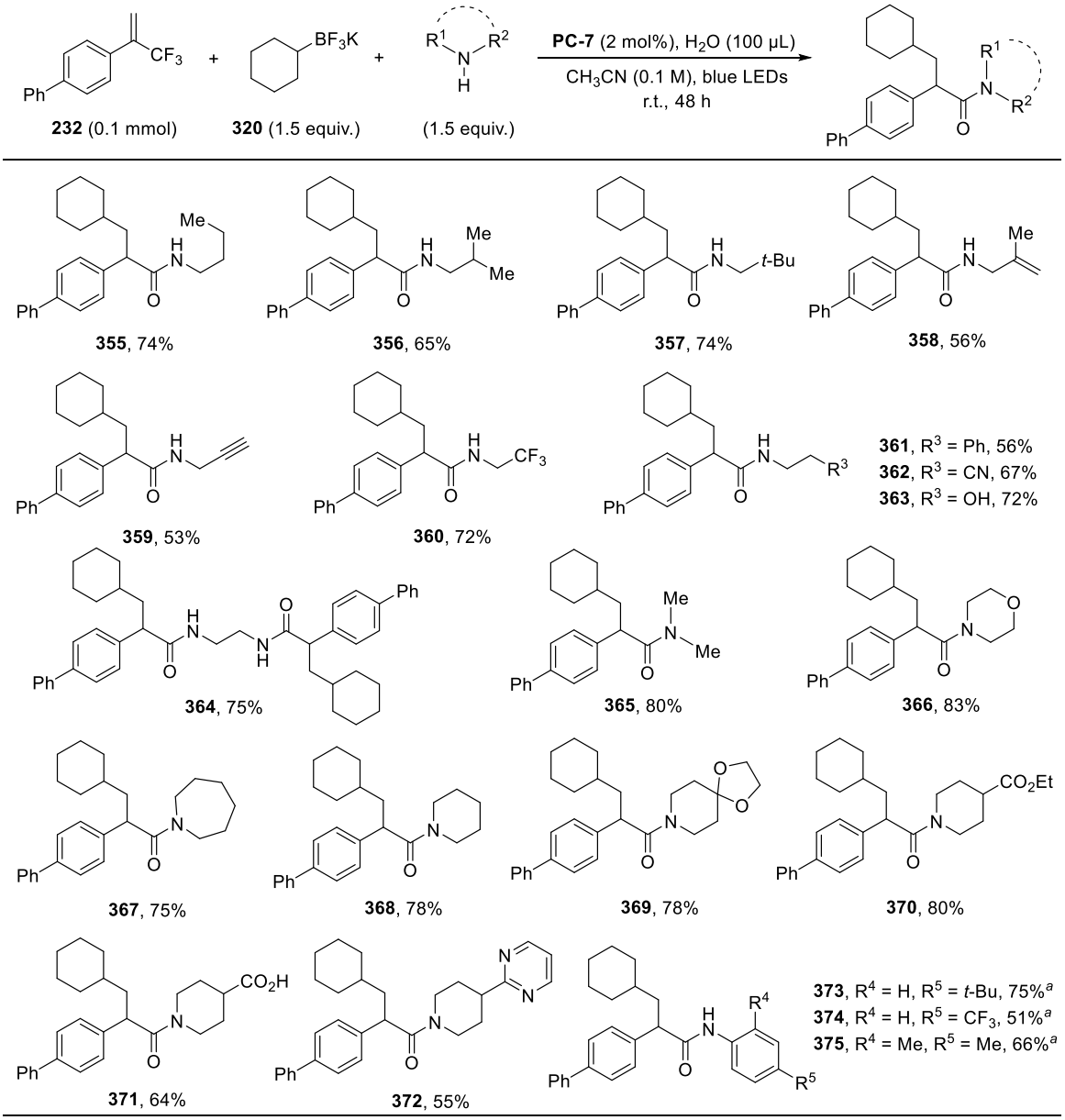

*Reaction conditions: α-trifluoromethyl alkene **232** (0.1 mmol), cyclohexyltrifluoroborate **320** (1.5 equiv.), amine (1.5 equiv.), H_2O (100 µL) and **PC-7** (2 mol%) in CH_3CN (0.1 M), irradiated at room temperature under N_2 atmosphere for 48 h, isolated yields were reported. [a]5 mol% of **PC-7** was used.*

Scheme 74: Scope of alkyl amines and anilines

Various potassium alkyltrifluoroborates can be used as coupling partners in the modular synthesis of α-arylated amides *via* triple defluorination of α-trifluoromethyl alkenes (Scheme

52). Primary, secondary, and tertiary alkyl radical precursors with silyl or ketone groups were well tolerated in the reactions, delivering corresponding amide products **376**–**379** in moderate to excellent yields. The trimethylsilyl group was eliminated when α-trifluoromethyl alkene with a 4-(trimethylsilyl)ethynylphenyl group was used in the reaction, delivering the desilylated α-arylated amide **380** in 43% yield. Natural occurring motifs such as estrone and (+)-dehydroabietylamine can also be incorporated into α-arylated amide products **381** and **382** in 67% and 62% yields respectively.

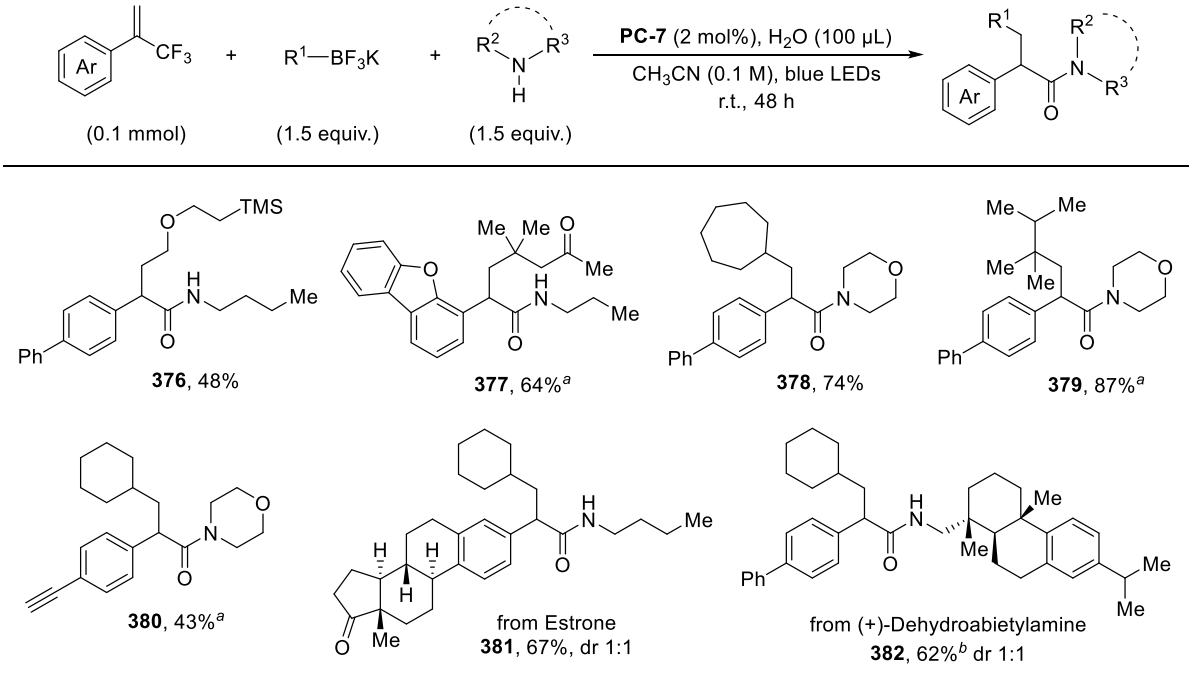

*Reaction conditions: α-trifluoromethyl alkene (0.1 mmol), alkyltrifluoroborate (1.5 equiv.), amine (1.5 equiv.), H_2O (100 μL) and **PC-7** (2 mol%) in CH_3CN (0.1 M), irradiated at room temperature under N_2 atmosphere for 48 h, isolated yields were reported. [a]5 mol% of **PC-7** was used. [b]CH_3CN : CH_2Cl_2 = 3:1.*

Scheme 75: Additional substrate scope for α-arylated amide synthesis

Next, the feasibility for the synthesis of α-arylated primary amides through the cleavage of three C–F bonds in α-trifluoromethyl alkenes was explored (Scheme 76). Several ammonium surrogates were screened, and ammonium acetate performed best under the reactions, delivering the primary amide **383** in 70% isolated yield. Other ammonium surrogates such as ammonium carbonate, ammonium hexafluorophosphate, and ammonium hydrogen carbonate were less efficient in the reactions (54%–75% yields). Only 35% of the amide product was formed when ammonium formate was used, and ammonium chloride was not suitable precursor for the synthesis of primary amide in this reaction.

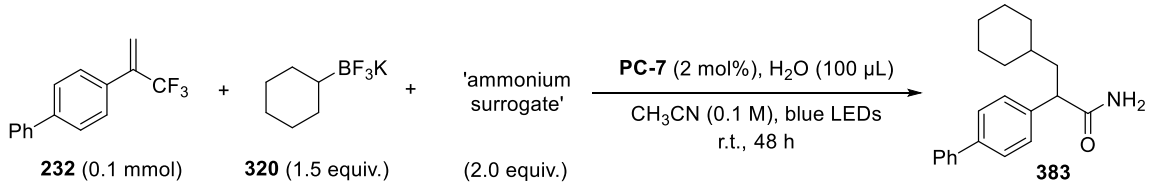

232 (0.1 mmol) **320** (1.5 equiv.) (2.0 equiv.) **383**

Entry	'ammonium surrogate'	Yields of **383**[a]
1	NH_4OAc	78% (70%)
2	$(NH_4)_2CO_3$	65%
3	$(NH_4)PF_6$	54%
4	$(NH_4)HCO_3$	75%
5	$(NH_4)CO_2H$	35%
6	NH_4Cl	n.d.

[a]Yields were determined by ^1H NMR spectroscopy of the crude reaction mixture; isolated yield was shown in parentheses.

Scheme 76: Screening of different ammonium surrogates

A series of α-arylated primary amides (**384**–**390**) with diverse substitution patterns were obtained in good yields (52%–75% yields). This protocol provides a rapid and modular access

to α-arylated primary amides, which would be difficult to achieve by traditional metal-catalysed α-arylation of carbonyl compounds (Scheme 77).

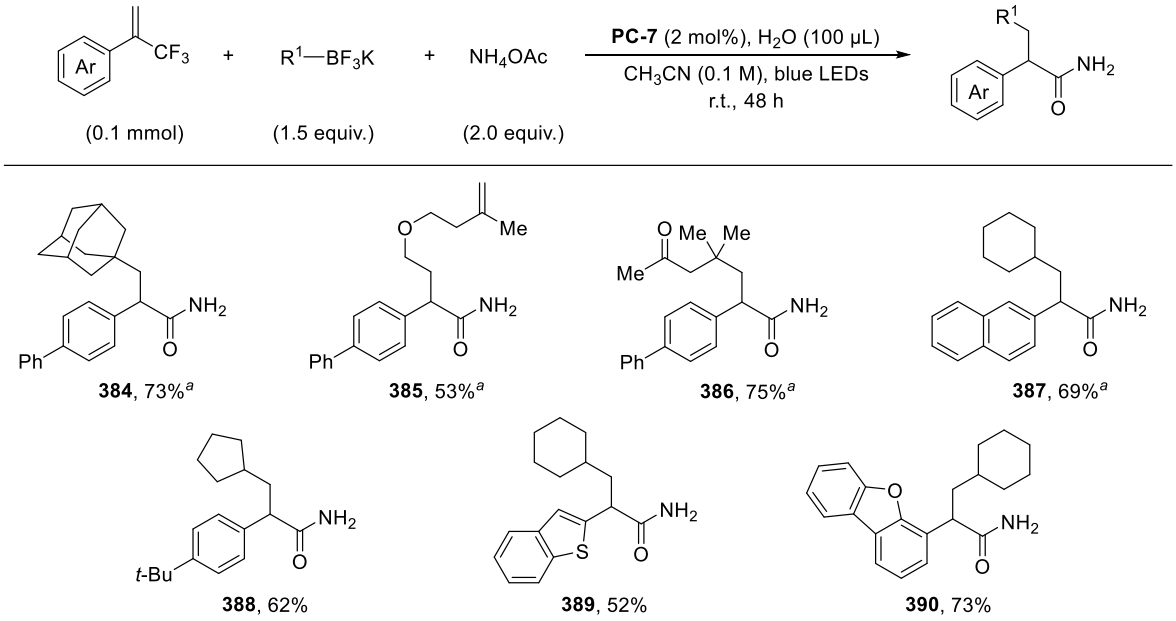

*Reaction conditions: α-trifluoromethyl alkene (0.1 mmol), alkyltrifluoroborate (1.5 equiv.), NH_4OAc (2.0 equiv.), H_2O (100 μL) and **PC-7** (2 mol%) in CH_3CN (0.1 M), irradiated at room temperature under N_2 atmosphere for 48 h, isolated yields were reported. [a]5 mol% of **PC-7** was used.*

Scheme 77: Substrate scope for α-arylated primary amides

3.2.6 Derivatisation of Products

Overall, this photoredox catalysed exhaustive defluorinative functionalisation of α-trifluoromethyl alkenes has enabled the synthesis of a series of α-arylated carbonyl derivatives, including carboxylic acids, esters, and primary, secondary, tertiary amides. The utility of this approach was demonstrated by the preparation of product **321** on a 2.0 mmol scale in 82% yield (Scheme 78a). α-Arylated carbonyl derivatives are important synthetic intermediates

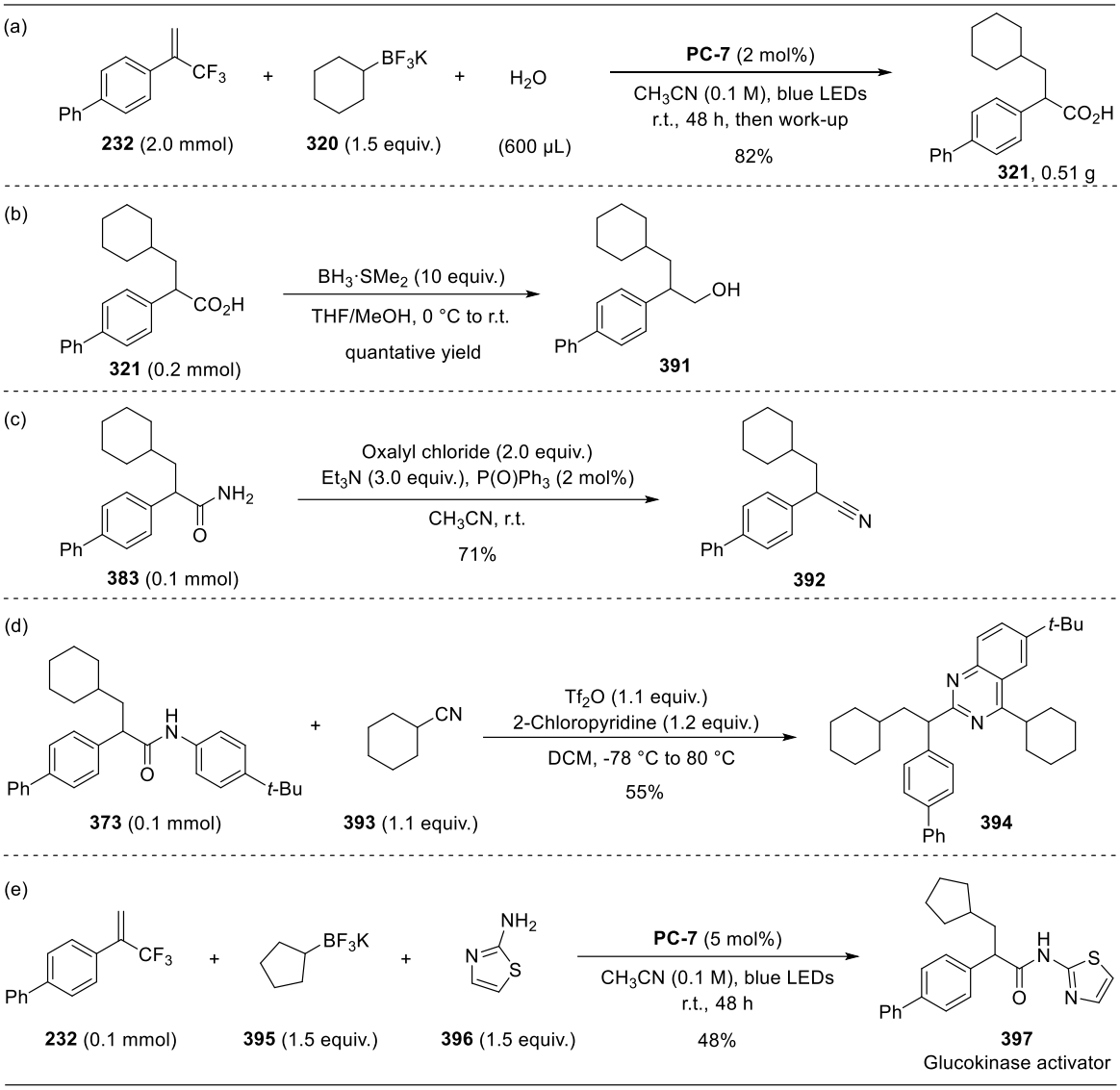

Scheme 78: Scale-up reaction and synthetic applications

that can be easily transformed into other motifs (Scheme 78b–e). For example, carboxylic acid **321** was reduced by borane to β-arylated alcohol **391** in quantitative yield. An α-arylated nitrile **392** was obtained in 71% yield from α-arylated primary amide **383** in the presence of oxalyl chloride, triethylamine, and triphenylphosphine oxide through an Appel-type dehydration process.[85] In addition, the reaction between α-arylated amide **373** and cyclohexane

carbonitrile **393** in the activation of trifluoromethansulfonic anhydride and 2-chloropyridine delivered a quinazoline derivative **394** in good yield. Furthermore, our photocatalytic approach can be used for the direct synthesis of a glucokinase activator **397** in moderate yield by employing α-trifluoromethyl alkene **232**, potassium cyclopentyltrifluoroborate **395** and thiazol-2-amine **396** under standard reaction conditions.

3.3 Mechanistic Studies

3.3.1 Control Experiments

Several control experiments were conducted to gain more insights into the reaction mechanism. The formation of carboxylic acid **321** was completely inhibited in the presence of TEMPO ((2,2,6,6-tetramethylpiperdin-1-yl)oxyl) (Scheme 79a). A ring-opening product **399** was obtained in 42% yield when the radical precursor **398** was used in the reaction (Scheme 79b). These results revealed that free radicals were likely involved in this transformation.

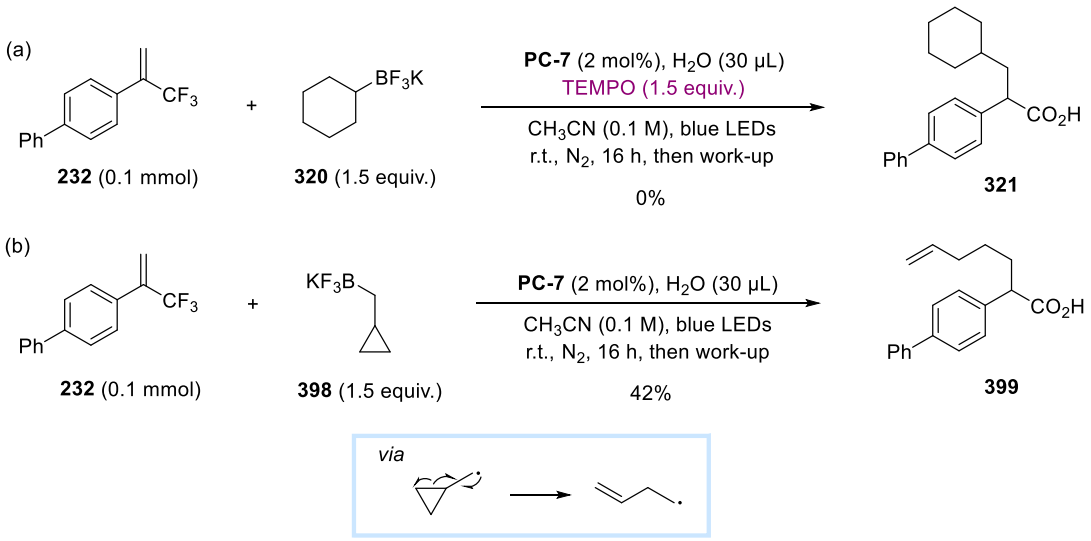

Scheme 79: Radical trapping experiments

In addition, when the reaction was conducted in the absence of H_2O, *gem*-difluoroalkene product **400** was obtained in 90% yield (Scheme 80a). Further applying **400** under standard reaction conditions, α-arylated carboxylic acid **321** was formed in good yield (Scheme 80b), indicating *gem*-difluoroalkene might be an intermediate in the reaction.

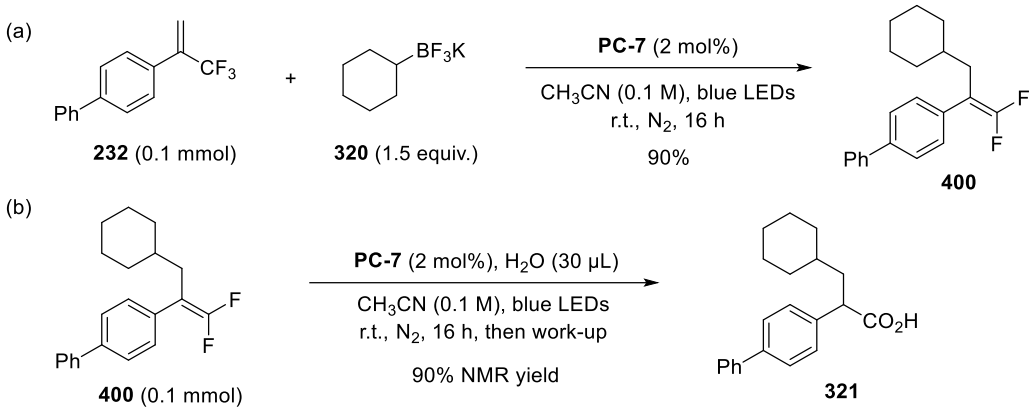

Scheme 80: Identifying *gem*-difluoroalkene as a possible intermediate

As discussed in the reaction optimisation section, α-arylated carboxylic acid **321** was formed in moderate yield when the reaction was performed without NaOH/HCl work-up procedure, and an increased yield was obtained after the work-up. The NMR spectroscopies of the reaction mixture before and after work-up procedure were analysed. As shown in Figure 7: before the base/acid work-up procedure was conducted, 53% of the product **321** was formed alongside 39% of a side-product according to the ^{1}H NMR spectroscopy. The side-product converted to **321** after the base/acid work-up procedure was performed (Figure 8).

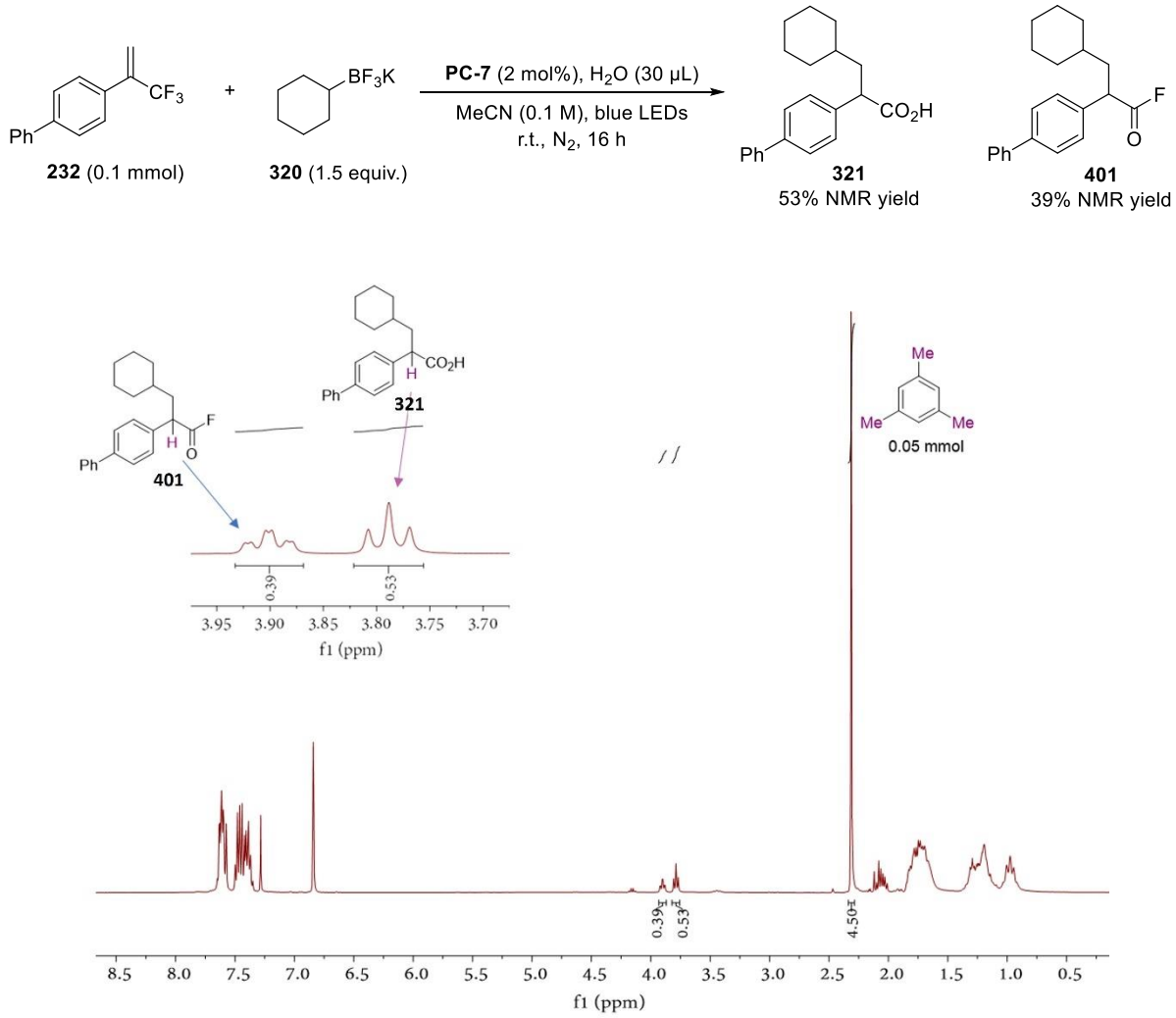

Figure 7: ^{1}H NMR spectroscopy of the crude reaction mixture before NaOH/HCl work-up procedure (mesitylene as an internal standard)

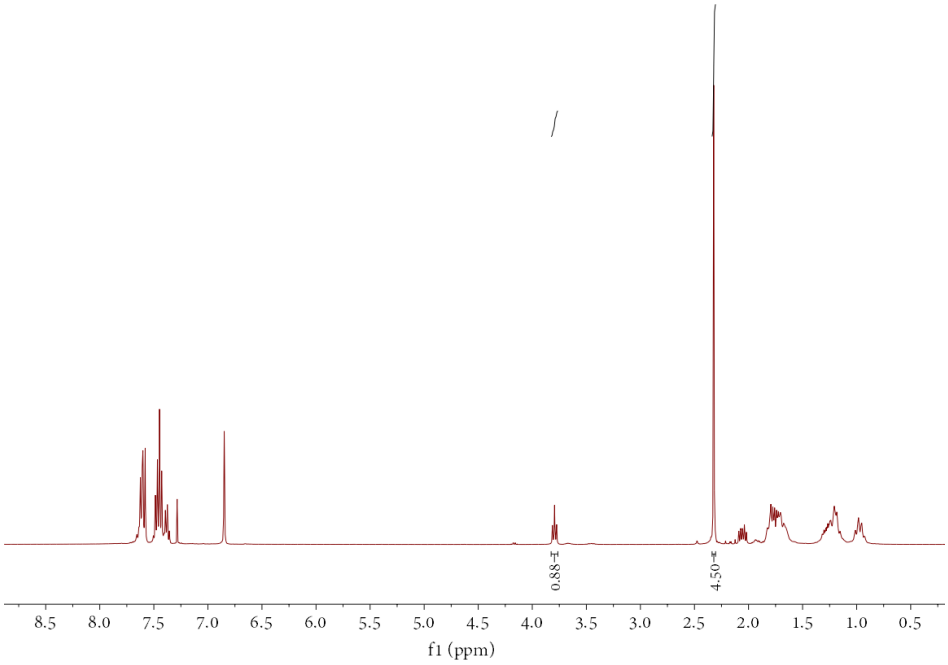

Figure 8: ^{1}H NMR spectroscopy of the crude reaction mixture after NaOH/HCl work-up procedure (mesitylene as an internal standard)

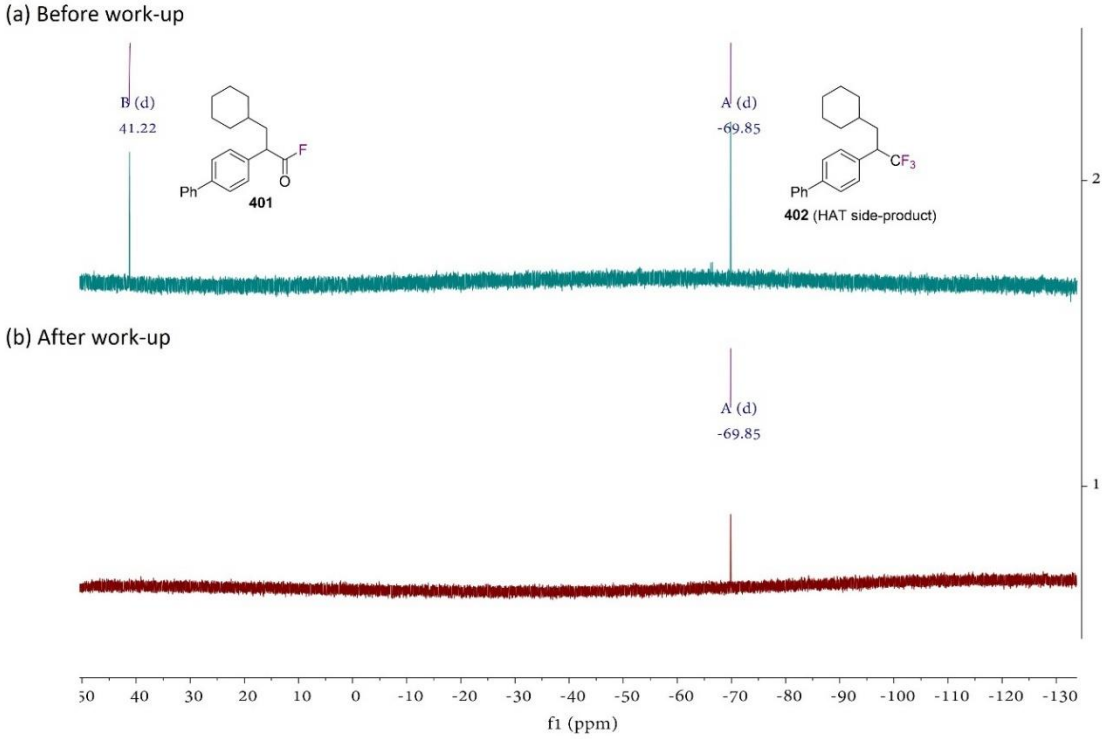

Figure 9: Comparison of the ^{19}F NMR spectroscopy of the crude reaction mixture

Two major signals (41.2 ppm and 69.9 ppm respectively) were shown in the ^{19}F NMR spectroscopy of the crude reaction mixture before work-up procedure (Figure 9a), while the signal at 41.2 ppm was not observed after performing the base-acid work-up (Figure 9b). Based on these results, this side-product was proposed to be an acyl fluoride species **401**, which reacted with NaOH to deliver the desired carboxylic acid product **321** after acidified by HCl solution.

The presence of the acyl fluoride species **401** was further confirmed by replacing NaOH aqueous solution to *n*-butylamine in the work-up procedure, which led to the formation of corresponding α-arylated amide **355** in 27% yield (Scheme 81).

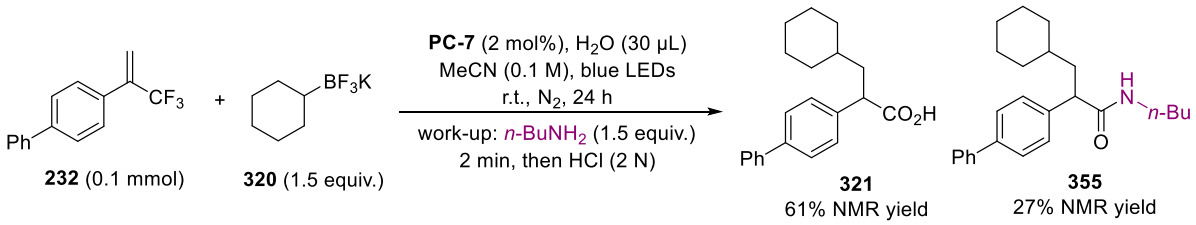

Scheme 81: Trapping acyl fluoride intermediate with *n*-butylamine

It has been reported that *gem*-difluoroalkene can be attacked by external *N*-nucleophiles to undergo fluoride-elimination to form enamine intermediates, which would be hydrolysed to give amide products.[86] However, when the reactions for the synthesis of amides **355** and **373** were conducted in the absence of H_2O, no products were formed but the *gem*-difluoroalkene **400** was obtained in 42% and 86% yields respectively (Scheme 82). These results indicating that H_2O was required for the defluorination of *gem*-difluoroalkene process.

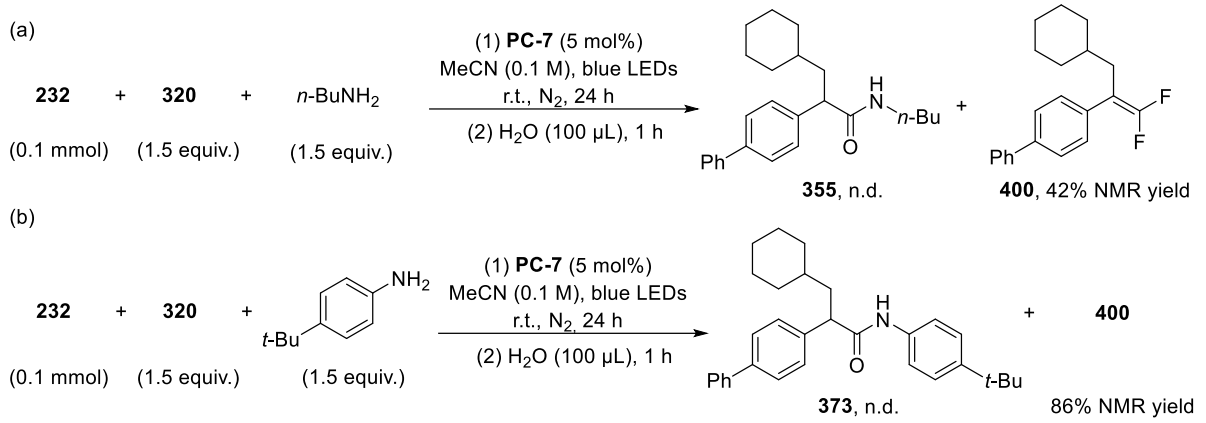

Scheme 82: Excluding a direct S_NV process

In summary, these control experiments supported the generation of alkyl radical species during the reaction, revealed that *gem*-difluoroalkene was an intermediate in this transformation that converted into acyl fluoride species and not subjected to a direct S_NV process.

3.3.2 Fluorescence Quenching Experiments

Furthermore, mechanistic investigations with a series of fluorescence quenching experiments using representative substrates were conducted: α-trifluoromethyl alkene **232**, potassium cyclohexyltrifluoroborate **320**, cyclohexylamine, ammonium acetate, and the reaction intermediate *gem*-difluoroalkene **400** (Figures 10–14). The Stern-Volmer plots for these quenching studies showed that *gem*-difluoroalkene **400** was the most effective quencher to the excited photocatalyst. Potassium cyclohexyltrifluoroborate **320** and α-trifluoromethyl alkene **232** were also suitable quenchers for the excited photocatalyst ***PC-7**.

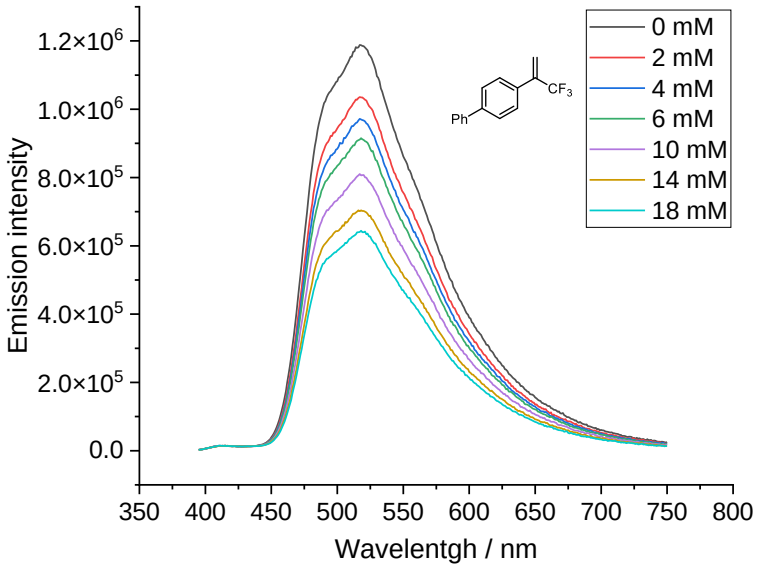

Figure 10: Stacked emission spectra of photocatalyst (PC-7) at different concentrations of α-trifluoromethyl alkene (232)

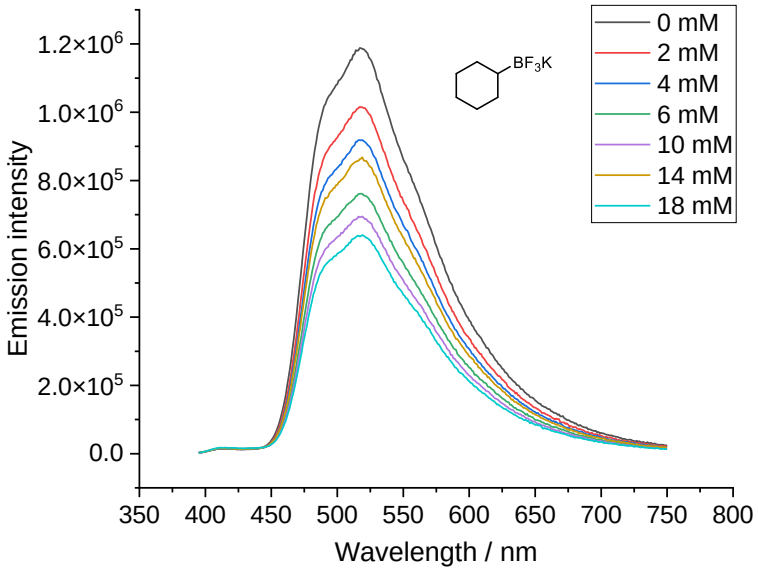

Figure 11: Stacked emission spectra of photocatalyst (PC-7) at different concentrations of potassium cyclohexyltrifluoroborate (320)

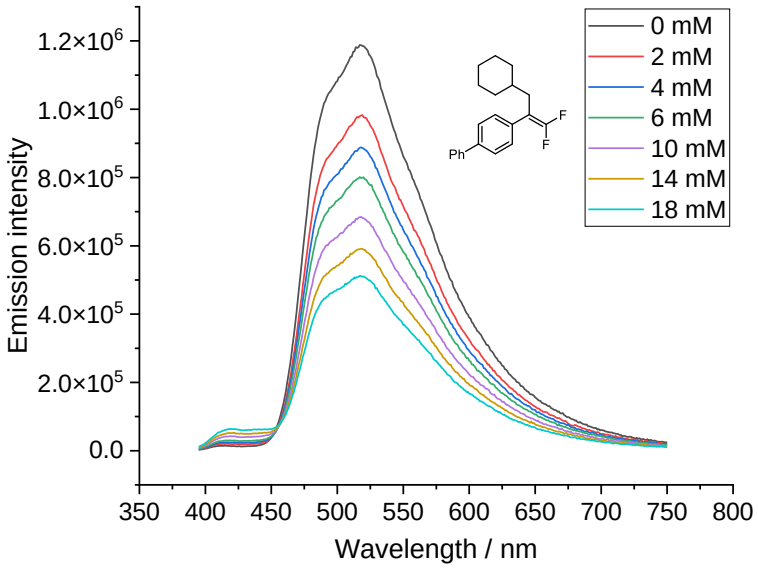

Figure 12: Stacked emission spectra of photocatalyst (PC-7) at different concentrations of *gem*-difluoroalkene (400)

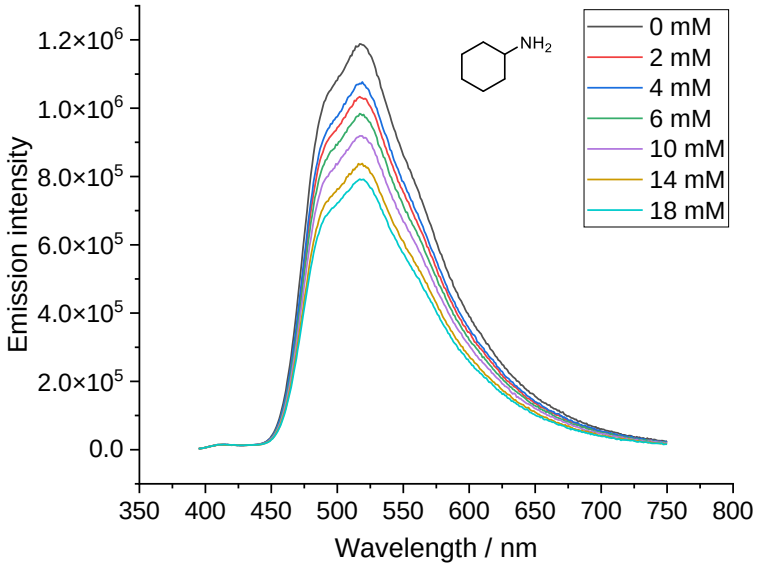

Figure 13: Stacked emission spectra of photocatalyst (PC-7) at different concentrations of cyclohexylamine

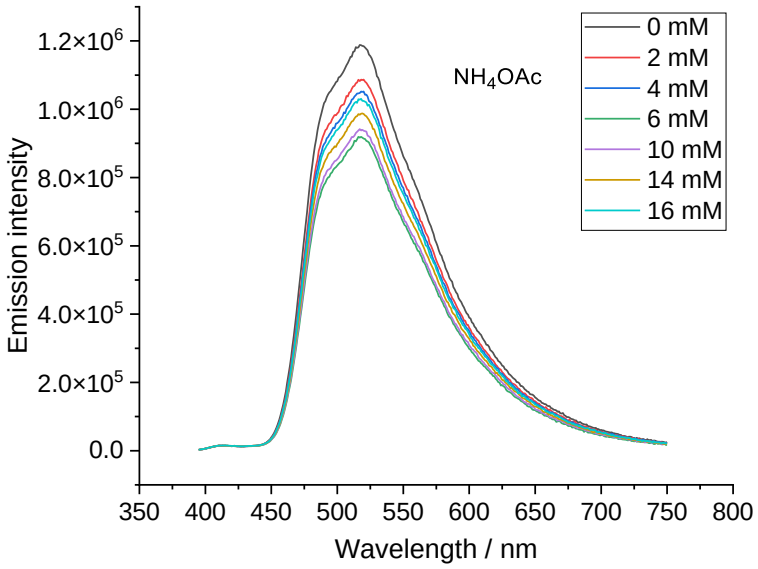

Figure 14: Stacked emission spectra of photocatalyst (PC-7) at different concentrations of ammonium acetate

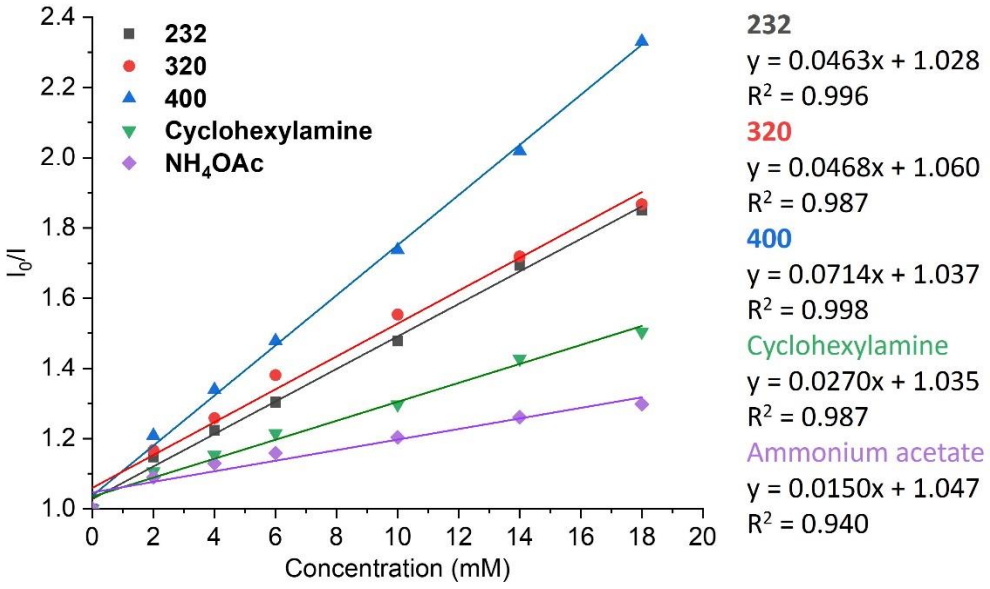

Figure 15: Stern-Volmer plot for the quenching experiments above

3.3.3 Proposed Mechanism

Based on the obtained experimental results, a possible mechanism was proposed in Scheme 83. Initially, under irradiation of blue light, acridinium photocatalyst **PC-7**^{n} was excited to its

excited state ***PC-7**^{n}. At this point, according to the Stern-Volmer fluorescence quenching studies, potassium alkyltrifluoroborate **403** was likely to be oxidised by ***PC-7**^{n} to form the reduced state photocatalyst **PC-7**$^{n-1}$ and alkyl radical species **404**. The radical addition of **404** to α-trifluoromethyl alkene **405** delivered a benzylic radical species **406**, which underwent single-electron transfer with **PC-7**$^{n-1}$ and subsequent β-fluoride elimination process to give *gem*-difluoroalkene intermediate **407** and regenerate the ground state photocatalyst **PC-7**^{n}. After this stage, a second single-electron oxidation of **407** by the excited state photocatalyst afforded a radical cation species **408** and the reduced state photocatalyst. α-Trifluoromethyl alkenes bearing strongly electron-withdrawing aryl substituents render this step inefficient. The radical cation intermediate **408** would be trapped by H_2O to give intermediate **409**. The SET process between **PC-7**$^{n-1}$ and **409** followed by the second β-fluoride elimination afforded the enol intermediate **410** or its tautomer acyl fluoride species **410'**, and the ground state photocatalyst **PC-7**. The desired α-arylated carbonyl compound **411** were then obtained through acyl substitution with *O*- or *N*-nucleophiles to facilitate the third C–F bond cleavage.

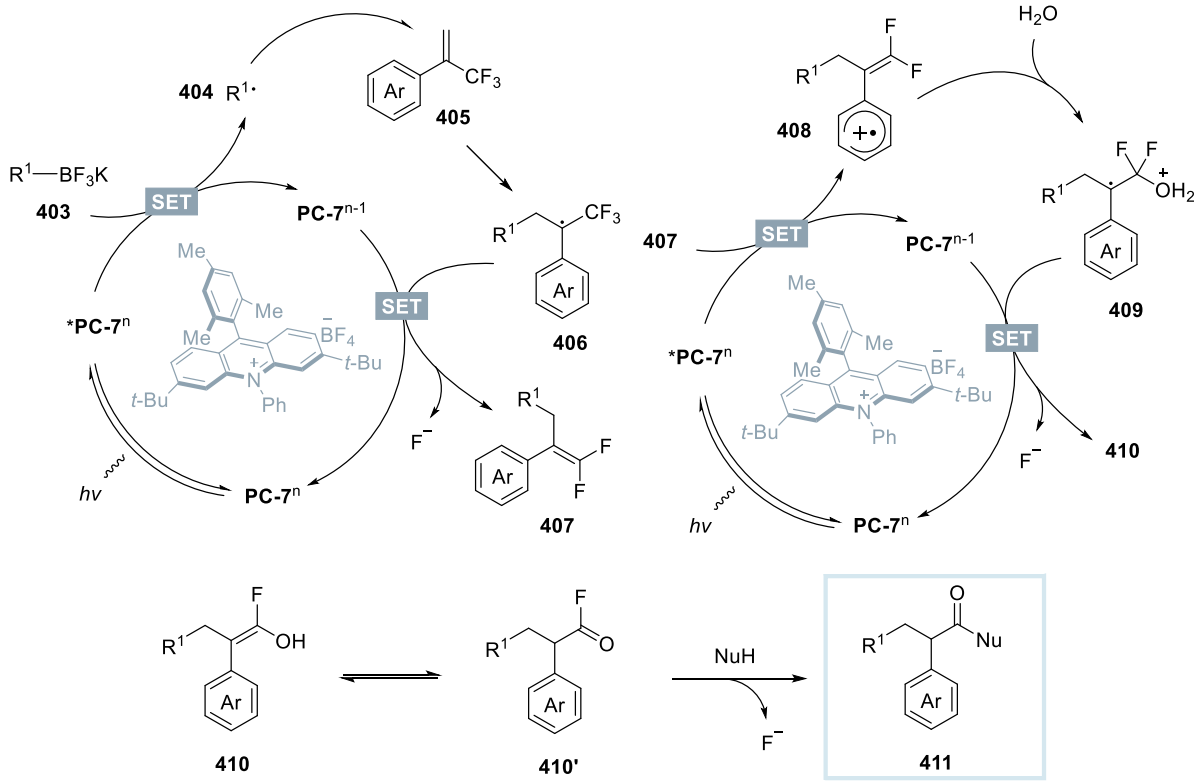

Scheme 83: Mechanistic proposal

3.4 Summary and Conclusions

The established photoredox catalysed defluorinative functionalisation of α-trifluoromethyl alkene enabled the modular synthesis of α-arylated carboxylic acids, esters, and amides with good reaction efficiencies. The reaction operated through consecutive cleavage of three C–F bonds, opening an avenue for converting methyltrifluorides into synthetically useful functionalities. This redox-neutral reaction exhibited broad substrate scope and excellent functional group compatibility, providing an alternative access to diverse α-arylated carbonyl compounds.

This work uses an organic acridinium photocatalyst for the efficient generation of alkyl radical species and the oxidation of *in situ* formed *gem*-difluoroalkenes under the same reaction conditions. Acyl fluorides species have been confirmed by control experiments and can undergo efficient intermolecular substitution with external nucleophiles, which means different types of carbonyl compounds can be accessed by simple alteration of nucleophiles.

Chapter 4: Visible-Light Induced Denitrogenative Alkylarylation of Vinyl Azides to Access α-Tertiary Primary Amines

4.1 Introduction

4.1.1 Recent Advances in the Synthesis of α-Tertiary Amines

Around half of the top-200 bestselling small-molecules drugs in 2018 are aliphatic amine derivatives, and nearly 25% of them are unprotected primary amines.[87] More specifically, primary amines with a fully substituted α-carbon show versatile physicochemical and biological properties that have broad applications in the pharmaceutical, agrochemical, and material sectors (Scheme 84).[88,89] As a consequence, great efforts have been devoted to the efficient synthesis of α-tertiary primary amine motifs. The following sections summarise recent developments in the synthesis of amines bearing α-tertiary centre sorted into two electron approaches and single electron approaches.

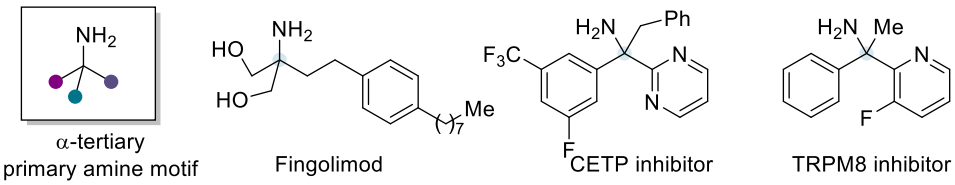

Scheme 84: Selected bio-active molecules displaying α-tertiary amine motif

4.1.1.1 Conventional Two-Electron Approach to α-Tertiary Amine Synthesis

Many methodologies for the synthesis of α-tertiary amine derivatives by the construction of C–N bond have been developed. For example, nucleophilic amination *via* Ritter-type reaction provides important approaches for the synthesis of α-tertiary amines. Baran and co-workers developed a copper-catalysed Ritter-type C–H amination of unactivated sp^3 carbons.[90] In this

reaction, solvent acetonitrile was the nitrogen source, F-TEDA-PF_6 was used as efficient HAT reagent with hydrocarbon substrate **412** as limiting reagent. The corresponding acetamide **413** was obtained in 90% yield under standard conditions. Metal-catalysed hydroaminations to access such amine motifs have also been reported. In 2015, the same group reported a Fe-catalysed hydroamination of alkenes with nitroarenes to access secondary amines with a fully substituted α-carbon centre (Scheme 85b).[91] Mechanistic studies showed that this reaction took place *via* initial reduction of the nitroarene to nitrosoarene, which combined with alkyl radicals derived from olefins. The cleavage of N–O bond would then deliver the desired amine product.

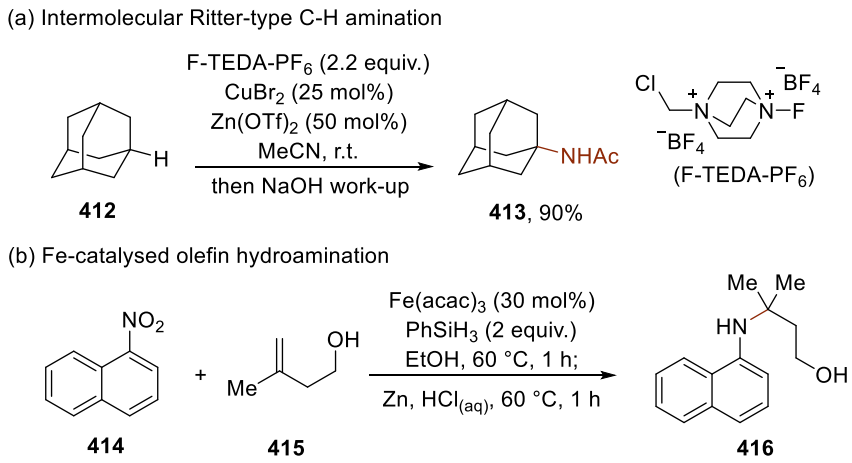

Scheme 85: Examples of α-tertiary amine synthesis *via* C–N bond formation

Methods focusing on the formation of C–C bond provide probably the most effective way to construct α-tertiary centre, which normally involve the addition of carbon-centred nucleophiles (such as organometallic reagents) to *N*-activated ketimine derivatives. Ellman and co-workers pioneered the methods of the addition of strong nucleophiles to *N-tert*-

butanesulfonyl imines **419** to construct primary amines **421** with fully substituted α-carbon (Scheme 86).[93] Although this is a powerful method, the synthesis of ketone-derived sulfinimides **419** requires the use of strong Lewis acids and heat. Limited examples of the addition of organometallic reagents to dialkyl imines to construct α-tertiary amines have been reported, possibly due to competitive α-deprotonation. Furthermore, this route to α-tertiary amines requires protection/deprotection steps, which is not atom economical.

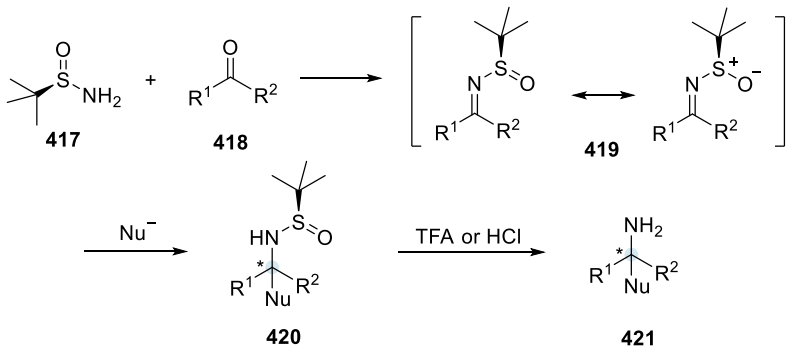

Scheme 86: General sequence for the synthesis of α-tertiary amines from *tert*-butanesulfinamide

The Dixon group developed a quinone-mediated synthetic method of α-tertiary amines from α-branched primary amines (Scheme 87).[94] In their one-pot multi-step protocol, reactive ketimine intermediates **424** were generated *in situ* through the reaction of amine **422** and quinone **423**, subsequent reaction with various nucleophiles such as organometallic reagents and TMSCN (trimethylsilyl cyanide) delivered intermediates **426** with quaternary centres. Finally, the I_2-mediated oxidation of **426** removed the quinone and afforded the α-tertiary amines **427**. Notably, intermediates **424** were successfully subjected into polarity-reversed

photoredox catalysis *via* nucleophilic α-amino alkyl radical intermediates. The synthesis of drug molecules by this strategy has also been demonstrated.

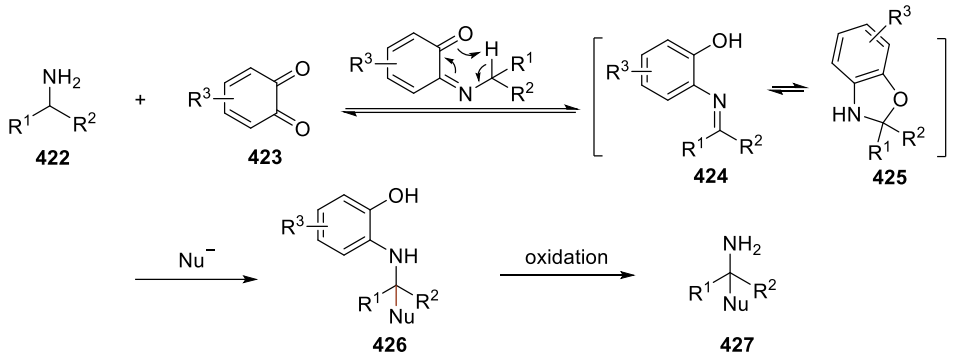

Scheme 87: Quinone-mediated synthesis of α-tertiary amines

4.1.1.2 Prior Art Synthesis of α-Tertiary Amines *via* Single-Electron Approach

Another important strategy for the synthesis of α-tertiary amines involves the reactions of α-amino radicals generated *via* photoredox catalysis or electrochemistry. There are two major methods for the generation of α-amino radicals: the direct α-hydrogen atom transfer of α-branched primary amines and single-electron reduction of ketimines.

In 2018, Schoenebeck and Rovis reported a hydrogen atom transfer (HAT) mediated α-alkylation of α-branched primary aliphatic amines **428** with electron-deficient alkenes **429** to construct γ-lactam products **430** (Scheme 88).[95] The high nucleophilicity of primary alkyl amines was dramatically diminished in the presence of CO_2 through the *in situ* formation of alkylammonium carbamate species, which allowed the selective functionalisation of less reactive α-C–H bond through a HAT process.

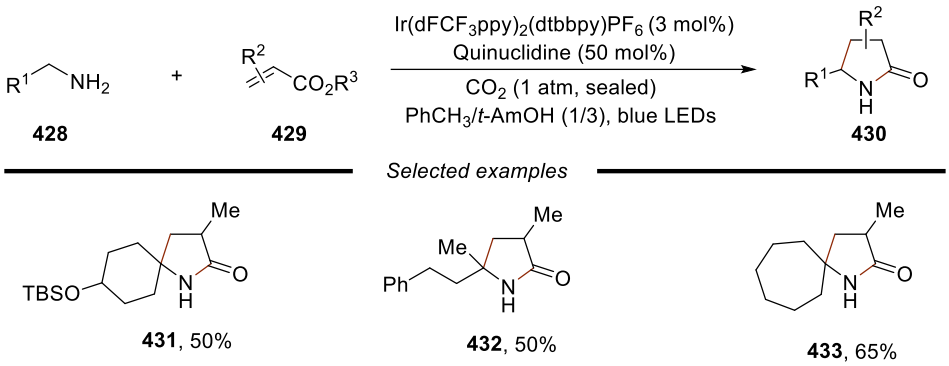

Scheme 88: α-Alkylation of primary amines enabled by CO_2 and electrostatics

In 2020, Cresswell and co-workers developed a practical photocatalytic strategy for the synthesis of α,α,α-trisubstituted primary amines **436** through the direct α-C–H bond functionalisation of primary amines **434** using $Bu_4N^+N_3^-$ (tetrabutylammonium azide) as an HAT catalyst (Scheme 89).[96] In the reaction mechanism, single-electron oxidation of azide ion by the excited photocatalyst $^*PC^n$ generated the azidyl radical $N_3\cdot$, which underwent HAT process from the relatively weak α-C–H bond of the primary amine to generate α-amino alkyl radical species **437**. The radical intermediate can undergo rapid addition to the acrylate acceptor **435** to deliver an α-carboxy stabilised radical **438**. Subsequent SET process between the reduced photocatalyst PC^{n-1} and radical **438** resulted the formation of corresponding enolate intermediate **439** and the ground state photocatalyst PC^n. The α-tertiary primary amine **436** was then formed from the proton transfer between **439** and HN_3, and the azide ion was regenerated at the same time.

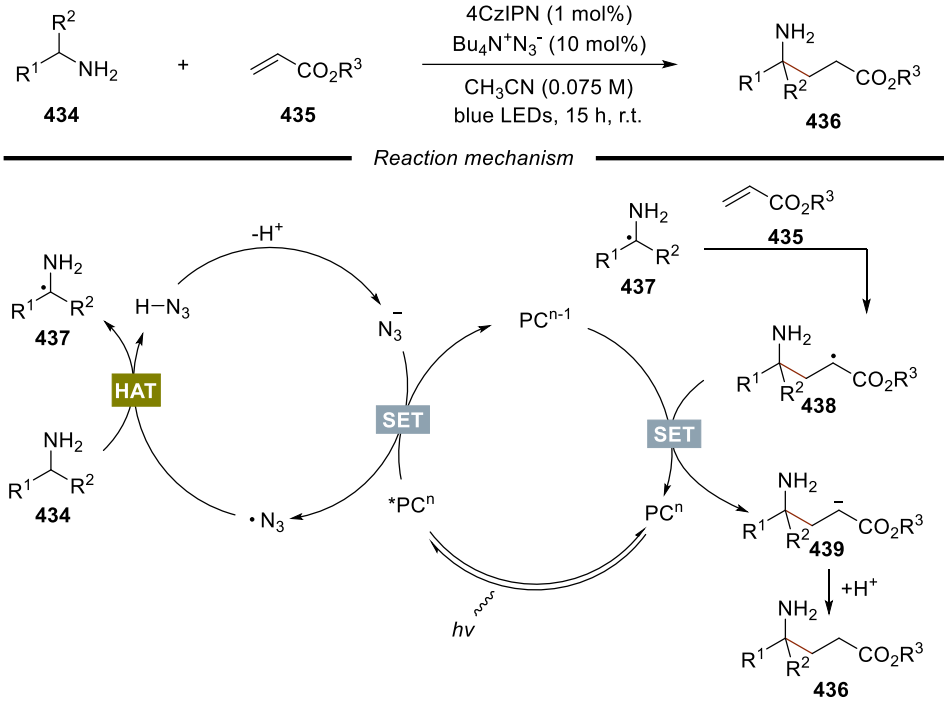

Scheme 89: Direct α-C–H alkylation of unmasked primary amines

Shortly after, the same group utilised the same strategy for the photocatalytic hydroaminoalkylation of styrenes with unprotected primary amines (Scheme 90).[97] A series of γ-arylamines were obtained in good yields in the presence of photocatalyst 3DPA2FBN, HAT catalyst $Bu_4N^+N_3^-$ (tetrabutylammonium azide) in DMF under the irradiation of blue light. Notably, a bio-active compound Fingolimod **442** was synthesised in 43% yield in single step from serinol **440** and 4-octylstyrene **47341**. In addition, the use of 2-bromostyrene **444** led to the formation of 2-bromo-substituted γ-arylamine **445**, which can be subjected to a palladium-catalysed intramolecular C–N bond formation, delivering a 1,2,3,4-tetrahydroquinoline product **446** in 65% yield.

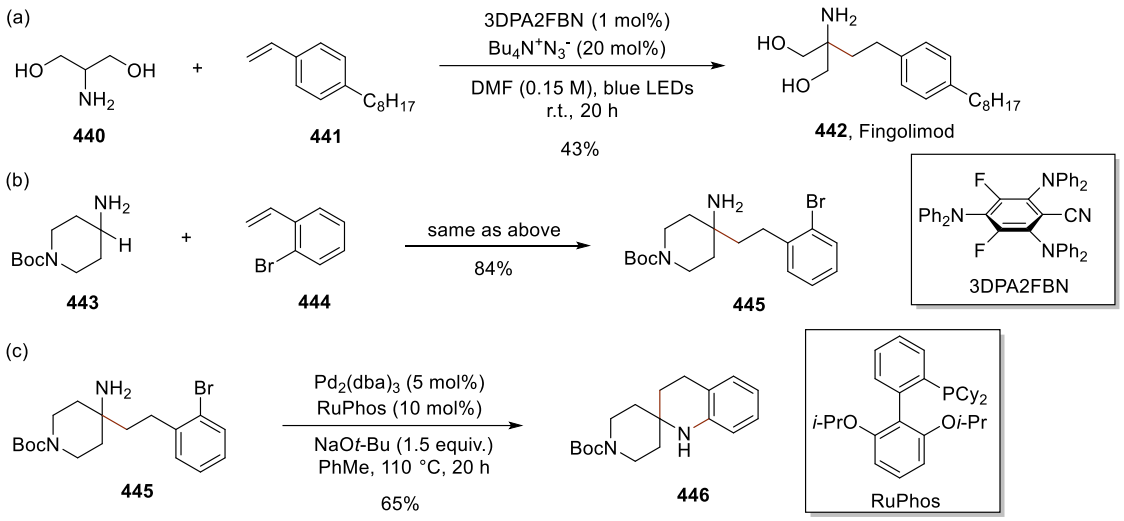

Scheme 90: Hydroaminoalkylation of styrenes and their applications

In 2022, Chiba and co-workers reported a photocatalytic method to the synthesis of α-tertiary primary amines from cyanoarenes and α-secondary benzylamines using polysulfide anions as photocatalyst (Scheme 91).[98] The key feature of this transformation is the dual role of polysulfide anions: first, the highly negative oxidation potential of the photoexcited polysulfide dianions (S_n^{2-}, n = 4 or 6) to ensure the single-electron reduction of cyanoarene **447** to its radical anion **450**; second, the catenated structure of polysulfide anion radicals ($S_n^{\cdot-}$, n =4 or 6) that was capable to undergo polarity-driven HAT at the α-amino benzylic C–H bond to generate benzylic radical species **451**. The hetero-radical coupling of **450** and **451** would then deliver the desired product **449**.

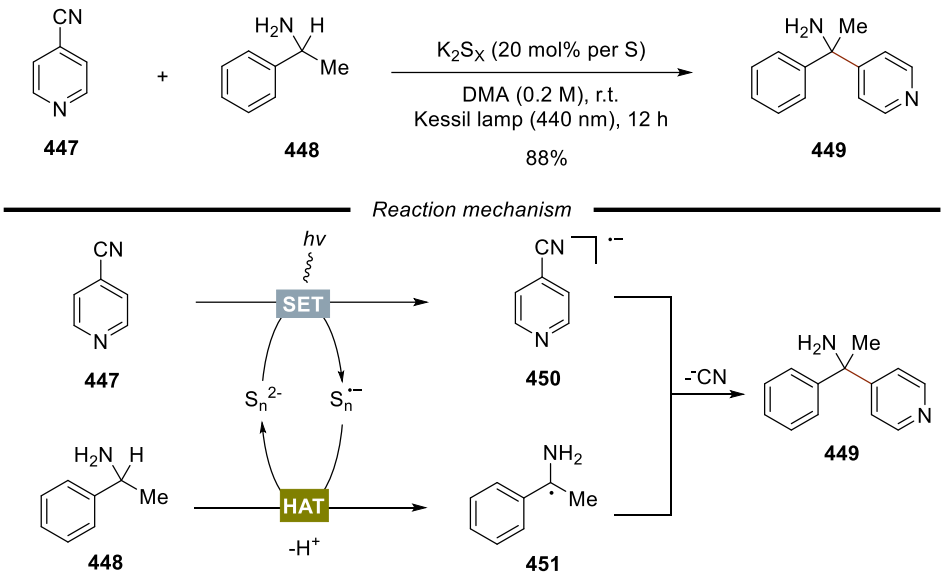

Scheme 91: Synthesis of α-tertiary amines by polysulfide anions photocatalysis

Another important strategy for the generation of α-amino alkyl radicals is through single-electron reduction of ketimines. In a 2020 review, Dixon and co-workers have summarised the synthesis of amine-containing molecules involving the manipulation of α-amino radicals through single-electron reduction of imine derivatives.[99] In here, representative examples for the synthesis of α-tertiary primary amines will be listed.

In 2019, Rovis and co-workers developed an electrochemical synthesis of α-tertiary primary amines from benchtop-stable iminium salts **452** and cyanoheteroarenes **453** *via* proton-coupled electron transfer (Scheme 92).[100] Under optimised conditions, in DMSO containing Et_4NCl using constant current of 5 mA and total charge (*C*) of 2 Faraday/mol using an undivided cell with Zn cathode and graphite anode, a series of sterically hindered primary and secondary amines **454** were obtained in moderate to excellent yields.

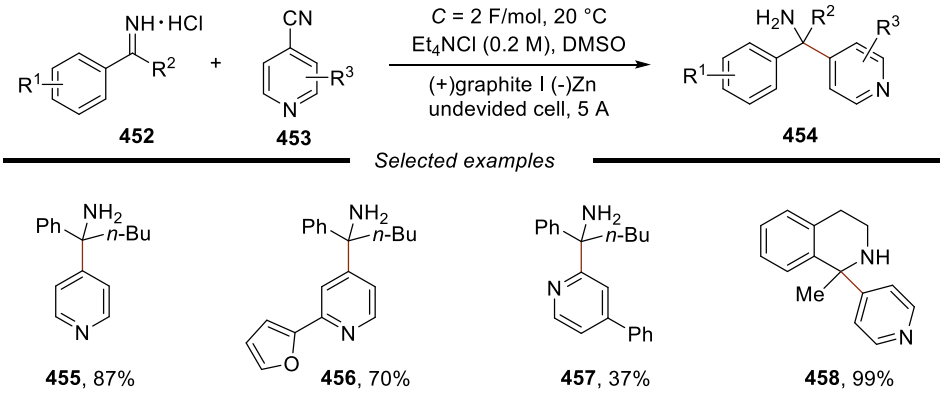

Scheme 92: Electrochemical synthesis of sterically hindered amines

Shortly after, the same group utilised photoredox catalysis to couple *o*-benzoyl oximes **459** and cyanoheteroarenes **453** to synthesise primary amines **454** with fully substituted α-carbons (Scheme 93).[101] In the reaction mechanism, the photocatalyst engaged in concurrent tandem catalysis by reacting with *O*-benzoyl oximes through energy transfer in the first catalytic cycle and a reductant toward the cyanoarene in the second catalytic cycle to realise the synthesis of primary amines *via* hetero-radical coupling.

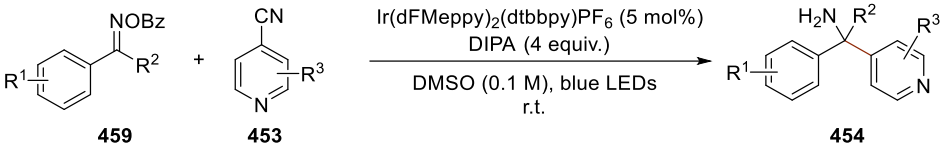

Scheme 93: Synthesis of hindered primary amines by concurrent tandem photoredox catalysis

In above examples, the generation of α-amino radicals was from pre-formed iminium ions or oximes. In 2018, Gilmore and co-workers reported a photocatalytic synthesis of hindered primary amines through the utilisation of α-amino radicals by the reduction of N–H imines generated *in situ* from ammonia and ketones (Scheme 94).[102] The first step of this

transformation is the formation of N–H imine **463** from trifluoroacetic acid promoted condensation between ketone and ammonia. At the same time, the excited photocatalyst can be reduced by external reductant Hantzsch ester to afford PC^{n-1}. The activated imine **463** was reduced by PC^{n-1} to give an unprotected α-amino radical **464** and regenerate the photocatalyst. Then second photoredox cycle reduced 4-cyanopyridine to a radical anion **465** that reacted with **464** to form the unprotected amine product **461** after the elimination of a cyanide anion.

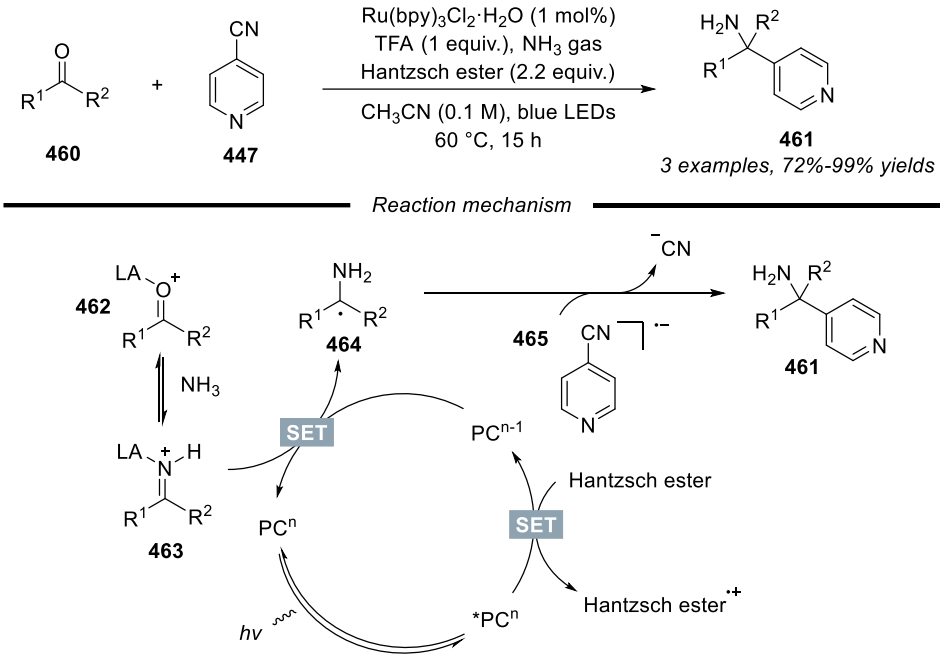

Scheme 94: Photoredox synthesis of primary amines using ammonia

In 2022, Gaunt and co-workers reported a stepwise, one-pot alkene hydroaminoalkylation to α-trialkyl primary amines under photocatalytic conditions (Scheme 95).[103] The reaction began with the condensation of benzylamine **466** and ketone **467** to afford imine intermediate **468**, which was used directly in the photoredox catalysis with acrylate **469** in the presence of

photocatalyst $Ir(dMeppy)_3$ in dichloromethane under blue light irradiation to deliver the aldimine motif **470**. The primary amine product **471** was obtained by treating **470** with hydrolytic work-up or hydrogenative work-up procedures.

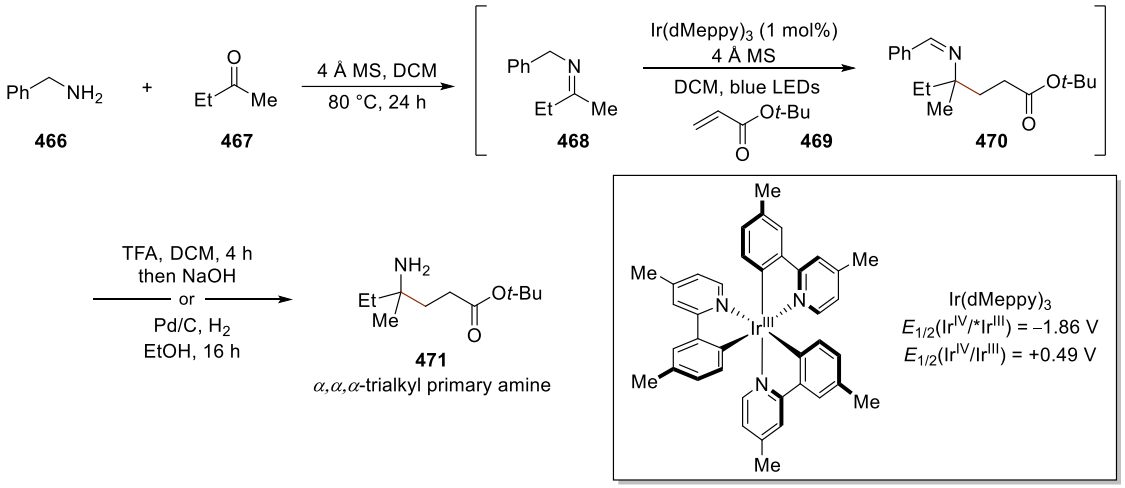

Scheme 95: Multicomponent photocatalytic synthesis of α-tertiary amines

In summary, the rapid adoption of photoredox catalysis enabled the synthesis of sterically hindered α-tertiary primary amines under mild conditions. A common feature of these approaches is the generation of α-amino alkyl radicals, which can be obtained through direct HAT process of amines, or through single-electron reduction of ketimines generated *in situ* or pre-formed, which might involve multistep synthesis. In this regard, identifying more straightforward access to structurally diverse α-tertiary primary amines from easily available materials is appealing.

4.1.2 Radical Reactivities of Vinyl Azides

Vinyl azides have been known for more than a century,[104] while limited applications of vinyl azides have been achieved due to their high explosivity, toxicity, reactivity, and inefficient synthesis (Scheme 96).[105] In recent years, multifaceted reactivities of vinyl azides have been found with the development of more convenient synthetic methods towards such motifs.[106]

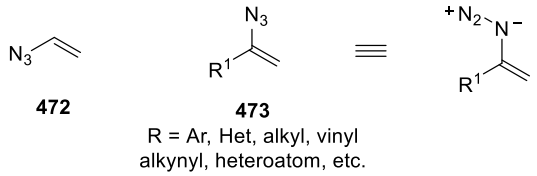

Scheme 96: Azidoethene and α-substituted vinyl azides

As a special sub-class of vinyl azides, α-substituted vinyl azides **473** exhibit unique reactivities towards various of transformations. This type of molecules can be prepared in the following ways (Scheme 97). The most exploited approaches to vinyl azides **473** are through the base-assisted elimination of hydrogen halides from vicinal haloazidoalkanes (such as **476**), which can be obtained from the treatment of NaN_3 to 1,2-dibromides **475**. Another synthetic approach to α-substituted vinyl azides is the Hassner method, which involves the reactions between alkenes **477** and iodine azide generated *in situ* from NaN_3 and iodine chloride to form vicinal azidoiodoalkane **478**. Subsequent KO*t*-Bu induced HI elimination of **478** would deliver the corresponding vinal azide **473**. In 2014, Bi and co-workers reported a hydroazidation of terminal alkynes to access to α-substituted vinyl azides by using Ag_2CO_3 as catalyst, $TMSN_3$ (azidotrimethylsilane) as azide source, in the presence of stoichiometric of H_2O in DMSO at

80 °C (Scheme 97c).[107,108] A wide range of terminal alkynes were efficiently transformed into corresponding vinyl azides, which are suitable for further transformations.

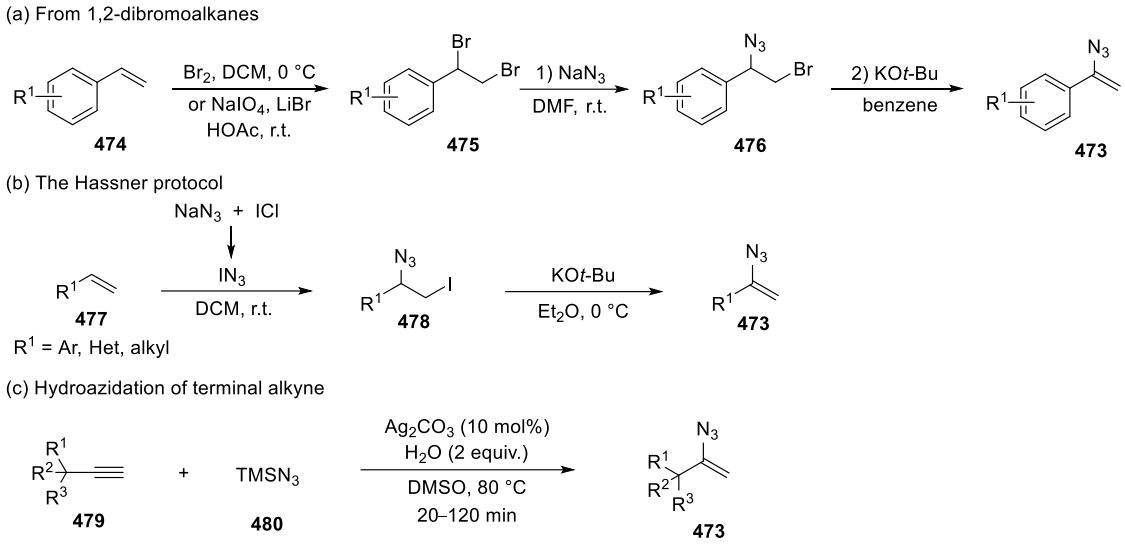

Scheme 97: Synthesis of α-substituted vinyl azides

In a 2017 review, Anderson, Bi and co-workers have summarised the reactions of vinyl azides as electrophiles/radical/nucleophile acceptors.[106] In this section, representative transformations where α-substituted vinyl azides acted as radical acceptors will be discussed.

α-Substituted vinyl azides, especially α-aryl vinyl azides, can participate in addition reactions with radicals to form benzylic radical species **482**. Facile denitrogenation of **482** leads to the formation of key iminyl radical intermediate **483**, which can be used for further transformations, such as hydrogen atom abstraction, dimerization, and cyclisation processes, depending on the reaction conditions and the structure of substrates (Scheme 98).

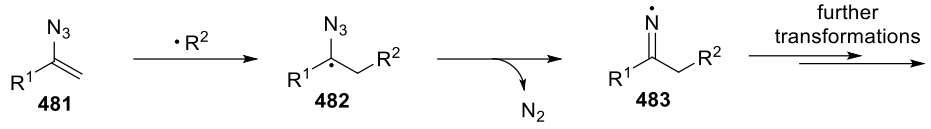

Scheme 98: General reaction profile of α-substituted vinyl azide as radical acceptor

4.1.2.1 Synthesis of β-Keto Products from Vinyl Azides

The first example of vinyl azides as radical acceptors was reported by the Suzuki group in 1975 (Scheme 99a).[109] Trialkylborane **484** was used to generate alkyl radicals under aerobic conditions. The addition of alkyl radicals to vinyl azides **485** followed by denitrogenation afforded iminoborane **486**, which underwent hydrolysis to form β-functionalised ketone product **487**. Heteroatom radicals such as thiyl radicals were also introduced by similar strategy to give β-keto sulfides **492**.[110]

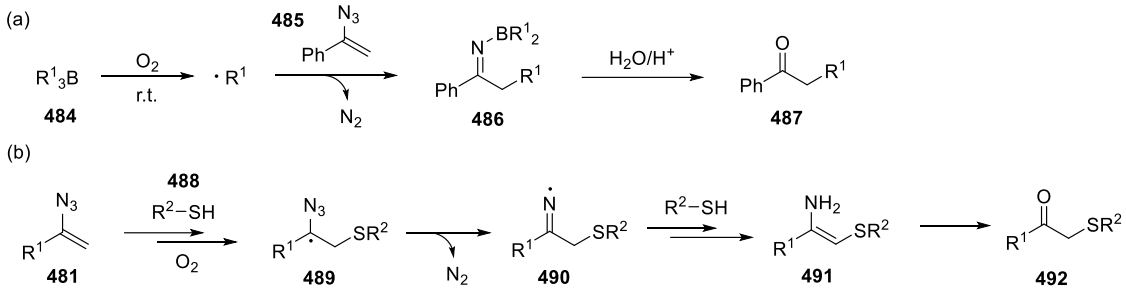

Scheme 99: Generation of iminyl radicals from vinyl azides

Early investigations on the radical addition to vinyl azides demonstrated the reaction pathway of iminyl radical formation–reduction–hydrolysis to ketones was feasible. In recent years, versatile radical species have been employed to this type of reaction with vinyl azides under mild conditions (Table 4). In 2017, a Mn^{III}-catalysed radical phosphorylation of vinyl azides to

access β-keto phosphines **495** was reported by Chen, Yu and co-workers.[111] Sulfonyl hydrazines, such as **496**, have been used as sulfonyl radical precursors with vinyl azides in the presence of KI, *tert*-butyl hydroperoxide to deliver β-keto sulfone **498**.[112]

Table 4: Synthesis of β-functionalised ketones from vinyl azides

Entry	Representative substrates	Conditions	Radical species generated	Product	Contributor(s)
1	**485**  **493** 	$Mn(acac)_3$ (20 mol%) NMP, 60 °C	 **494**	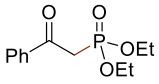 **495** 92%	Chen & Yu, 2017
2	**485**  **496** 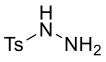	KI (40 mol%) TBHP (4 equiv.) DMSO, r.t.	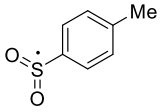 **497**	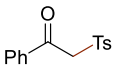 **498** 86%	Shao & Yu, 2017
3	**485**  **499** 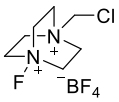	H_2O (2 equiv.) $MaHCO_3$ (2 equiv.) CH_3CN , r.t.	 **500**	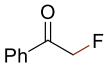 **501** 77%	Liu, 2016
4	**502** 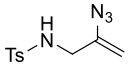 **231** CF_3SO_2Na	Mes-Acr-$MeClO_4$ (2.5 mol%) 1,4-dioxane (wet) blue LEDs, r.t.	 **128**	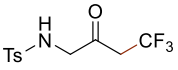 **503** 63%	Liu, 2017

The synthesis of α-fluoroketone derivatives **501** from vinyl azides and Selectfluor **499** has also been described by Liu group.[113] They proposed that the initial SET process between vinyl azide **485** and Selectfluor led to the formation of a radical cation species **500**. Subsequent fluorine atom transfer, H_2O addition, and elimination processes delivered the product **501**. Shortly

after, the same group exploited the synthesis of α-trifluoromethyl ketones from vinyl azides with the Langlois reagent (CF_3SONa) under organo-photoredox catalysis.[114]

In 2017, Nevado and co-workers developed a silver-catalysed diastereoselective synthesis of tricyclic ketones from vinyl azides and aliphatic carboxylic acids (Scheme 100).[115] The reaction started with the oxidative decarboxylation of aliphatic acid **504** in the presence of Ag_2CO_3 and $K_2S_2O_8$ to produce alkyl radical. The radical addition to vinyl azide **485** followed by denitrogenation delivered intermediate **506**, which underwent 1,5–H shift with the aliphatic C–H bond (*via* transition state **TS-507**) to yield a radical species **540**. Diastereoselective radical cyclisation happened (*via* transition state **TS-509**$_{syn}$) to give **510**. The desired ketone product **505** was produced after the oxidation and hydrolysis of **510**.

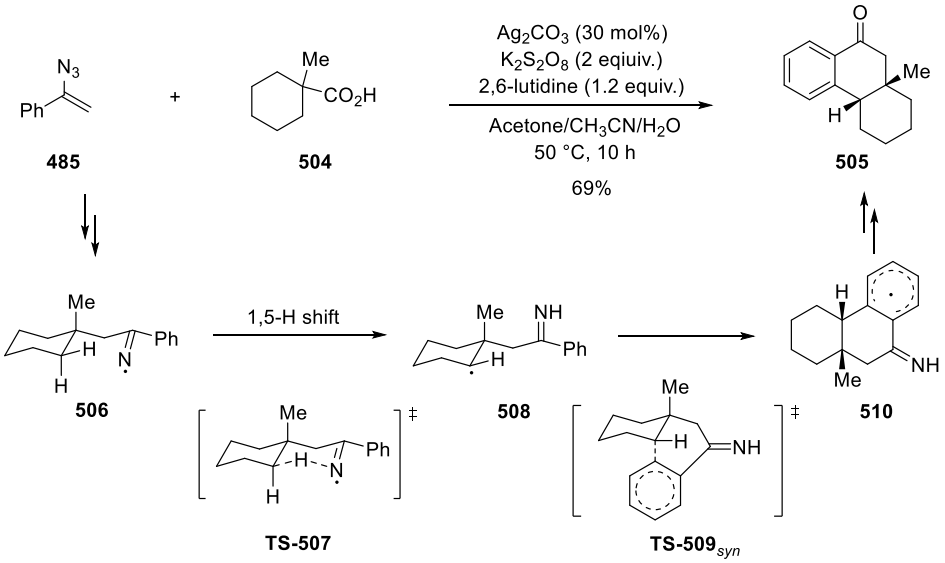

Scheme 100: Diastereoselective synthesis of elaborated ketones

4.1.2.2 Synthesis of Heterocyclic Product from Vinyl Azides

By rational design of the substrates, iminyl radicals generated from vinyl azides can also participate in cyclisation processes rather than HAT, leading to the formation of heterocyclic products. In 2011, Chiba and co-workers developed a Mn(III)-mediated formal [3+3]-annulation of vinyl azides and cyclopropanes to access azaheterocycles (Scheme 101).[116] The reaction proceeded through the oxidative fragmentation of cyclopropane **511** on reaction with Mn(III) to afford alkyl radical species **512**. Radical addition to the vinyl azide **485** followed by denitrogenation gave iminyl radical **513**, which was reduced by Mn(II) followed by cyclisation onto the ketone to afford intermediate **515**. Subsequent elimination and aromatization processes furnished the pyridine derivative **512** in good yield.

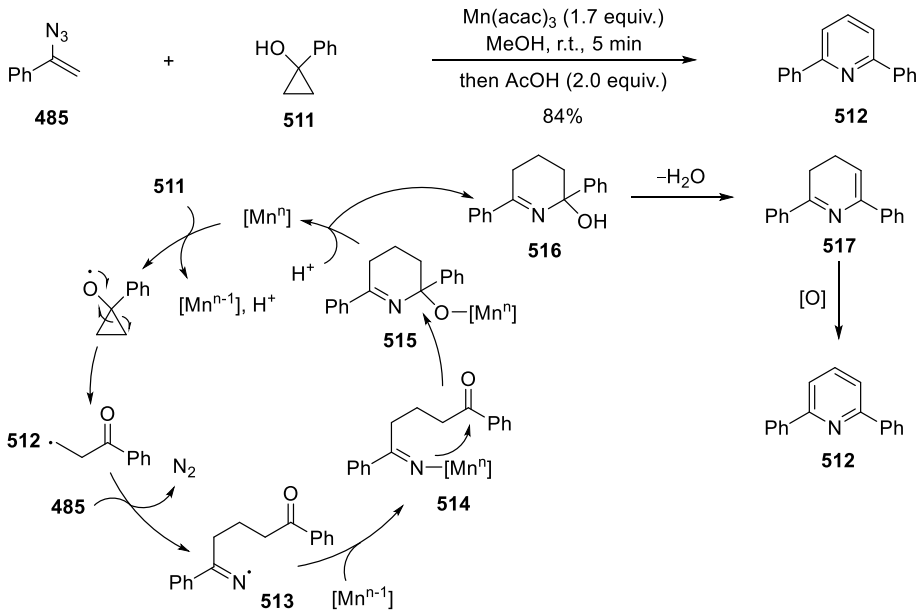

Scheme 101: Mn(III)-mediated formal [3+3]-annulation of vinyl azides and cyclopropanes

In 2015, Zhou and co-workers reported a visible-light induced radical reaction of vinyl azides **518** and α-carbonyl benzyl bromides **519** (Scheme 102).[117] A series of multi-substituted quinolines **520** were obtained in moderate to good yields in the presence of photocatalyst $Ir(ppy)_3$, K_2HPO_4, 18-crown-6 in acetonitrile/H_2O under blue light irradiation. The reaction proceeded through the generation of benzylic radical species from **519**, followed by radical addition to vinyl azides, denitrogenation, and radical cyclisation processes.

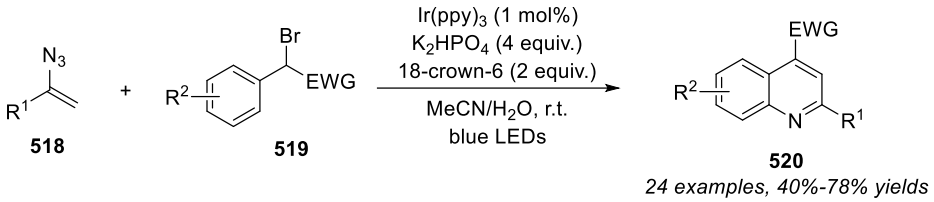

Scheme 102: Photocatalysed synthesis of quinolines from vinyl azides

4.1.2.3 Synthesis of Enamines from Vinyl Azides

Structurally, vinyl azides can be classified as *N*-diazoenamines, the cleavage of nitrogen molecule would be an ideal way to synthesise *N*-unprotected enamines. Although the sensitivity of enamines to hydrolysis made this methodology difficult to realise, it can be solved by introducing an electron-withdrawing group to the terminal of vinyl azides and stabilise the enamine.

In 2015, Bi and co-workers reported an efficient access to *N*-unprotected enamines **522** through a silver-catalysed intermolecular aminosulfonylation of terminal alkynes with sodium sulfinates and $TMSN_3$ (Scheme 103a).[118] The key process of this reaction was the generation

of sulfonyl radicals and their addition to the *in situ* formed vinyl azides. The enamine product was stabilised by the sulfonyl group, and can be used for various further transformations. Shortly after, the same group reported an electron-withdrawing-group-generable radical induced enamination of vinyl azides, which provided the synthesis of a series of β-functionalised *N*-unprotected enamines in good yields (Scheme 103b).[119] α-Ketonic acids, silver nitrite, and sodium sulfinates were employed in the reactions for the generation of benzoyl, nitro, and sulfonyl radicals respectively.

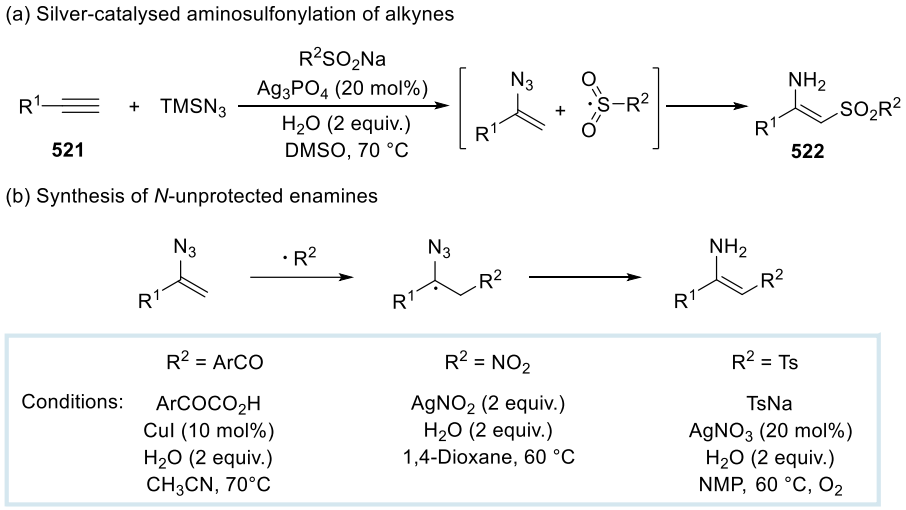

Scheme 103: Synthesis of *N*-unprotected enamines from vinyl azides

In summary, α-substituted vinyl azides (especially for α-aryl vinyl azides) have been proved to be excellent radical acceptors. The addition of a variety of radicals to vinyl azides provided a rapid and mild access to iminyl radicals that can be used for many transformations, such as C–H bond functionalisation, cyclisation, and difunctionalisation. With the advances in the radical

chemistry of vinyl azides, methodology developments focusing on transforming vinyl azides into new types of functionalities will broaden their applications in synthetic chemistry.

4.2 Results and Discussion

4.2.1 Reaction Design

The aim of this project was to explore whether sterically hindered α-tertiary amines could be accessed by using vinyl azides as primary amine precursors. As mentioned before, the key feature for the synthesis of sterically hindered amines under photoredox catalysis was the generation of α-amino alkyl radicals, which could be accessed by the single-electron reduction of ketimines. On other hand, iminyl radicals could be easily accessed from vinyl azides after the acceptance of external radicals and denitrogenation process. The possibility of single electron reduction of the imine intermediate formed from HAT process of iminyl radical to furnish corresponding α-amino alkyl radical was considered. If worked, it can participate further cross-coupling reactions to afford α-tertiary primary amine (Scheme 104).

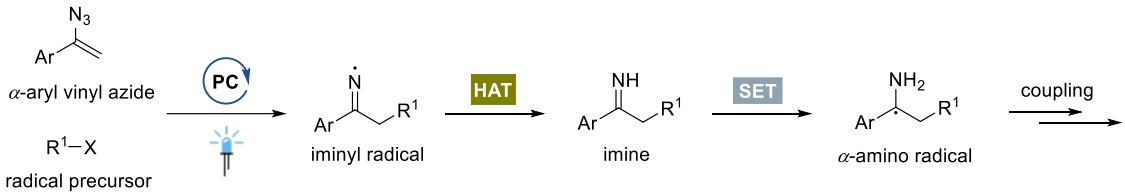

Scheme 104: Reaction design for the generation of α-amino radical from vinyl azide

4.2.2 Initial Results and Reaction Optimisation

After careful review of the literature precedents for the synthesis of α-trisubstituted primary amines (see section 4.1.1), the concurrent tandem photoredox catalysed amine synthesis reported by the Rovis group in 2020 was found to be similar to the proposed reaction design.[101] Therefore, their reaction conditions might be applied to the design route.

To begin with, *O*-benzoyl oxime was replaced with vinyl azide **523** and redox-active *N*-hydroxyphthalimide (NHPI) ester **524**, the remaining components 4-cyanopyridine **447**, photocatalyst **PC-10** $Ir(dFMeppy)_2(dtbbpy)PF_6$ and the reductant DIPA (diisopropylamine) were retained (Table 5, entry 1). However, the expected primary amine product **525** was not observed by simply applying their conditions to this reaction. Other reductants were then tested in the reaction (Table 5, entries 2−5), the product **525** was obtained in 27% NMR yield when DIPEA (*N,N*-diisopropylethylamine) was used, and the yields dramatically increased to 82% and 70% yields when Hantzsch ester **HE-1** and **HE-2** were used respectively.

With these promising results in hand, other reaction parameters with **HE-1** as reductant were screened. Other iridium-based photocatalysts were shown to be less effective than **PC-10** (Table 5, entries 6−8), organic photocatalyst such as **PC-12**, **PC-13** could also mediate this reaction (Table 5, entries 9, 10). A compromised yield of 65% was obtained when DMF was used as solvent, while other solvents such as acetonitrile, dichloromethane, and tetrahydrofuran were not suitable for this reaction, possibly due to the poor solubility of

reactants in these solvents (Table 5, entries 11−14). The reaction worked best when vinyl azide was the limiting reagent, with the use of 1.5 equivalents of **534**, 2.5 equivalents of **447** and 3.0 equivalents of **HE-1** (Table 5, entries 15−20). The reaction was effective under more concentrated conditions (0.2 M), but the yield decreased by 12% when the reaction was run at more dilute concentration (0.05 M) (Table 5, entries 21, 20). Control experiments verified the necessity of the reductant **HE-1** and blue light, while the reaction can also run in the absence of photocatalyst (72% yield). In addition, this transformation was sensitive to air, but can tolerate a small amount of H_2O.

Table 5: Reaction optimisation for multicomponent formation of α-tertiary primary amines

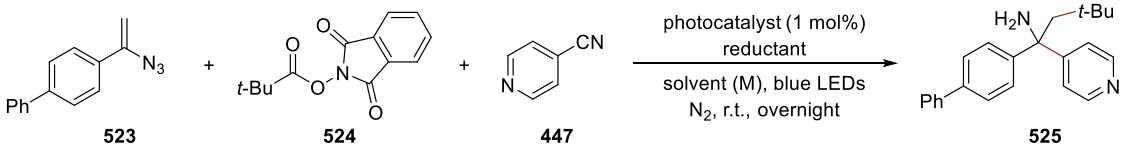

523 524 447 525

Entry	**523**:**524**:**447**	Photocatalyst	Reductant (equiv.)	Solvent (M)	Yield of **525** (%)[a]
1	1:1.5:2.5	**PC-10**	DIPA (3)	DMSO (0.1)	n.d.
2	1:1.5:2.5	**PC-10**	DIPEA (3)	DMSO (0.1)	27
3	1:1.5:2.5	**PC-10**	Et_3N (3)	DMSO (0.1)	n.d.
4	1:1.5:2.5	**PC-10**	**HE-1** (3)	DMSO (0.1)	82 (73)
5	1:1.5:2.5	**PC-10**	**HE-2** (3)	DMSO (0.1)	70
6	1:1.5:2.5	**PC-5**	**HE-1** (3)	DMSO (0.1)	70
7	1:1.5:2.5	**PC-8**	**HE-1** (3)	DMSO (0.1)	70
8	1:1.5:2.5	**PC-11**	**HE-1** (3)	DMSO (0.1)	63
9	1:1.5:2.5	**PC-12**	**HE-1** (3)	DMSO (0.1)	78

10	1:1.5:2.5	**PC-13**	**HE-1** (3)	DMSO (0.1)	67
11	1:1.5:2.5	**PC-10**	**HE-1** (3)	DMF (0.1)	65
12	1:1.5:2.5	**PC-10**	**HE-1** (3)	CH_3CN (0.1)	n.d.
13	1:1.5:2.5	**PC-10**	**HE-1** (3)	DCM (0.1)	n.d.
14	1:1.5:2.5	**PC-10**	**HE-1** (3)	THF (0.1)	n.d.
15	1:1.2:2.5	**PC-10**	**HE-1** (3)	DMSO (0.1)	80
16	1:2.0:2.5	**PC-10**	**HE-1** (3)	DMSO (0.1)	73
17	1:1.5:2.0	**PC-10**	**HE-1** (3)	DMSO (0.1)	78
18	1:1.5:3.0	**PC-10**	**HE-1** (3)	DMSO (0.1)	80
19	1:1.5:2.5	**PC-10**	**HE-1** (2.5)	DMSO (0.1)	75
20	1:1.5:2.5	**PC-10**	**HE-1** (3.5)	DMSO (0.1)	82
21	1:1.5:2.5	**PC-10**	**HE-1** (3)	DMSO (0.2)	81
22	1:1.5:2.5	**PC-10**	**HE-1** (3)	DMSO (0.05)	70
23	1:1.5:2.5	**PC-10**	none	DMSO (0.1)	n.d.
24	1:1.5:2.5	none	**HE-1** (3)	DMSO (0.1)	72
25[b]	1:1.5:2.5	**PC-10**	**HE-1** (3)	DMSO (0.1)	n.d.
26[c]	1:1.5:2.5	**PC-10**	**HE-1** (3)	DMSO (0.1)	n.d.
27[d]	1:1.5:2.5	**PC-10**	**HE-1** (3)	DMSO (0.1)	n.d.
28[e]	1:1.5:2.5	**PC-10**	**HE-1** (3)	DMSO (0.1)	81

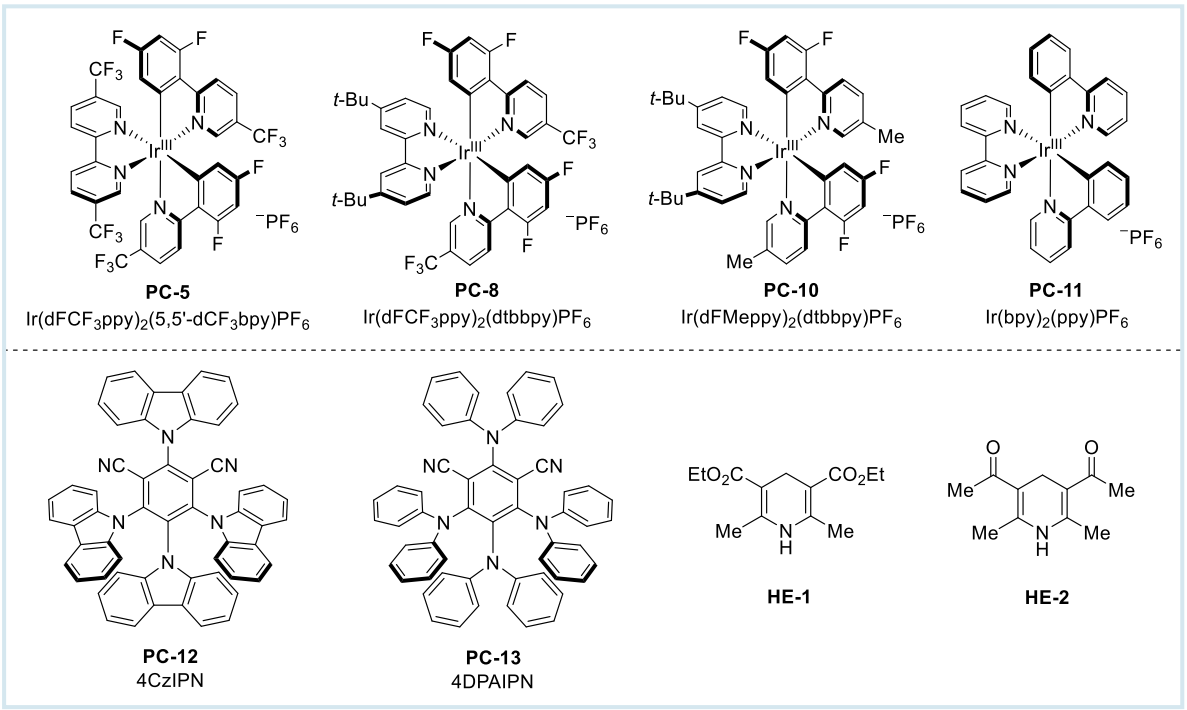

[a]Reactions were performed on 0.1 mmol scale; yields were determined by ^{1}H NMR spectroscopy of the crude reaction mixture using mesitylene as an internal standard, isolated yield was shown in parentheses. [b]Reaction was performed in the dark. [c]Reaction was performed in the dark at 60 °C for 4 h. [d]Reaction was performed under air. [e]3.0 equiv. of H_2O was added. n.d. = not detected.

4.2.3 Substrate Scope for the Synthesis of α-Tertiary Amines

After identifying the optimised reaction conditions for the synthesis of α,α,α-alkyldiaryl primary amines, the scope of NHPI esters was evaluated first. A wide range of alkyl carboxylic acids were converted into corresponding redox-active NHPI esters and reacted smoothly under the reaction conditions (Scheme 105). Primary (hetero)benzylic substrates with electron-donating groups such as *tert*-butyl, methylthio, methoxy groups; electron-withdrawing group such as trifluoromethyl group and halogen groups showed good reactivities in the reactions (**526**–**534**, 50%–70% yields). Other branched, linear primary alkyl

radical precursors bearing chloro (**534**), carbonyl (**536**) and *N*-heterocycle (**537**) groups were also good coupling partners. NHPI esters prepared from secondary carboxylic acids with different ring sizes worked well. Four, five and six-membered cyclic alkyl radical precursors with diverse functionalities such as esters, alkyl fluorides and ketones were well tolerated (**538**–**543**, 64%–73% yields). Tetrahydropyran (**544**), piperidine (**545**) motifs and acyclic secondary alkyl radical precursors (**546**) reacted smoothly in the reactions, delivering corresponding α-tertiary amines in 75%–84% yields. Tertiary carboxylic acids including bridged systems such as adamantane (**548**) and bicyclo[2,2,2]octane (**550**) participated in the amine synthesis with good reactivities. The structure of the α-tertiary amine product **548** was confirmed by X-ray diffraction (Figure 16). The preparation of amine product **550** on gram-scale (4.0 mmol scale) demonstrated the practically of this approach. In addition, redox-active NHPI ester can also be replaced with other radical precursors such as Togni's reagent **54** and diphenyliodonium triflate **553** for the introduction of trifluoromethyl and phenyl radicals into this system respectively, affording **551** and **552** in moderate yields.

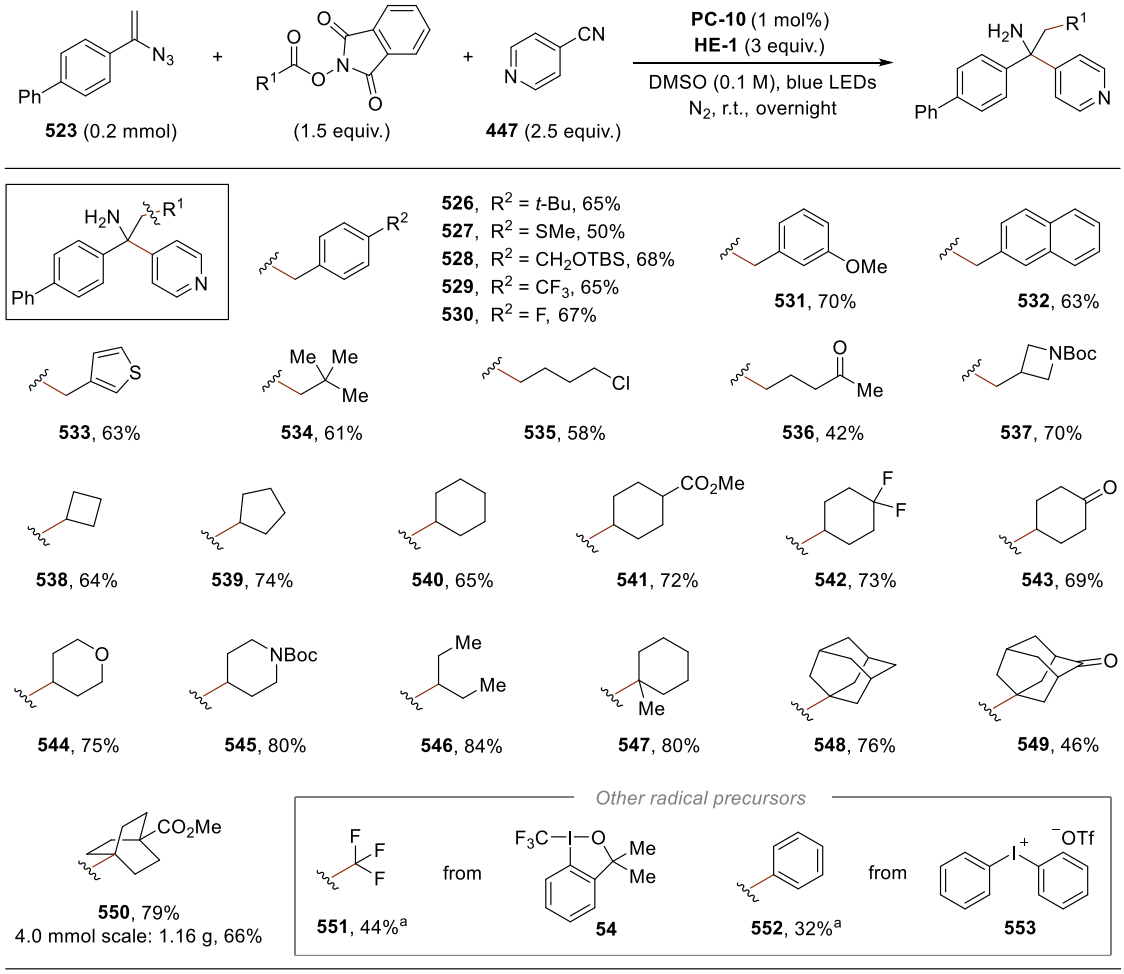

*Standard conditions: vinyl azide **523** (0.2 mmol), NHPI ester (1.5 equiv.), 4-cyanopyridine **447** (2.5 equiv.), photocatalyst **PC-10** (1 mol%) and Hantzsch ester **HE-1** (3 equiv.) in DMSO (0.1 M), irradiated under blue LEDs at room temperature under N_2 atmosphere overnight; isolated yields were reported. [a]Photocatalyst **PC-11** (1 mol%) was used.*

Scheme 105: Scope of NHPI esters and other radical precursors

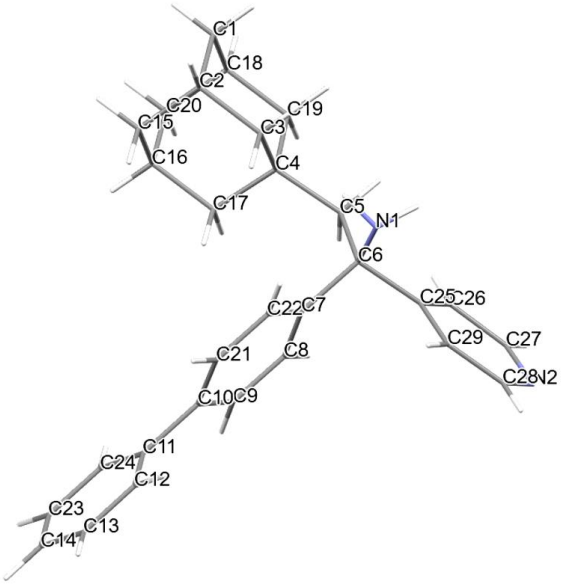

Figure 16: X-ray crystallography of amine product 548. Crystallographic data solved by Dr. Xiaoyong Chang (SUSTech) and has been deposited at the Cambridge Crystallographic Data Centre, under deposition number CCDC 2115824

Next, the scope of α-aryl vinyl azides was investigated (Scheme 106). *para*, *meta*, *ortho*-Substituted styrenyl vinyl azides with electron-donating groups such as methyl, *tert*-butyl, methoxy groups; electron-withdrawing groups such as trifluoromethyl, trifluoromethoxy groups worked well (**555**–**559**, 44%–78% yields). Vinyl azides with halogen substituents on the *meta* and *ortho* positions participated in the reaction with good reaction efficiencies (**560**–**562** and **566**, 67%–78% yields). An allyloxy group-containing vinyl azide was tolerated, delivering **564** in 58% yield. A free hydroxy group-containing vinyl azide substrate was also suitable coupling partner under standard conditions, delivering **565** in 61% yield. Fused aryl and heteroaryl including naphthyl (**569**), benzothiophenyl (**570**), dibenzofuranyl (**571**), indolyl (**572**) and thiophenyl (**573**) groups were all incorporated into corresponding α-tertiary amines in good yields (58%–65% yields).

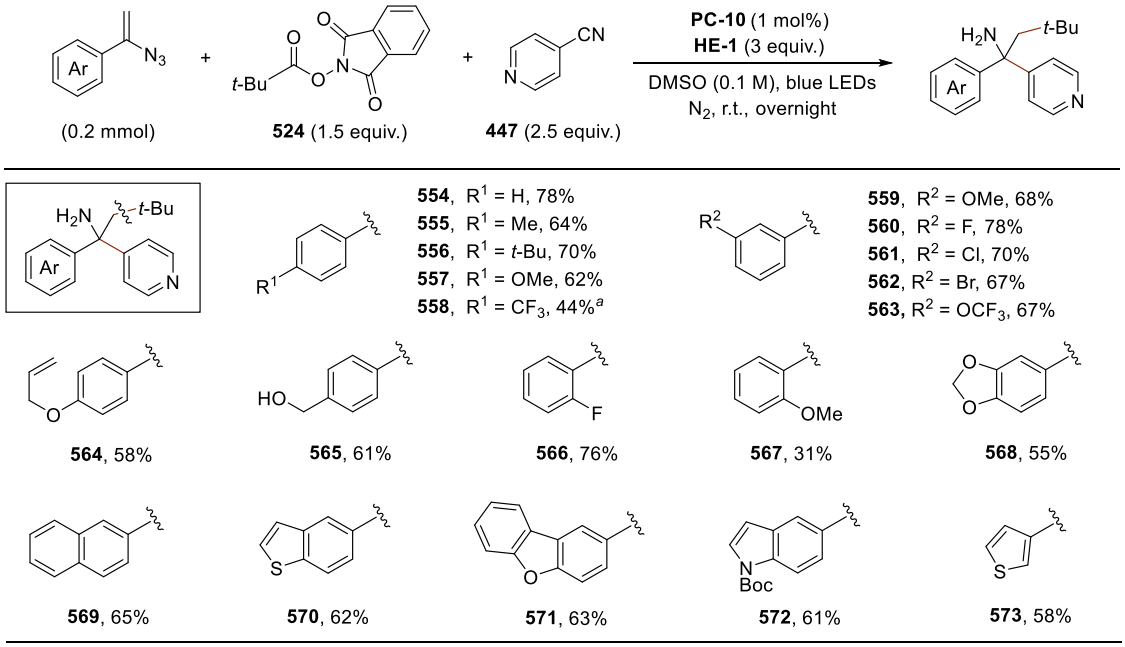

*Standard conditions: vinyl azide (0.2 mmol), NHPI ester **524** (1.5 equiv.), 4-cyanopyridine **447** (2.5 equiv.), photocatalyst **PC-10** (1 mol%) and Hantzsch ester **HE-1** (3 equiv.) in DMSO (0.1 M), irradiated under blue LEDs at room temperature under N_2 atmosphere overnight; isolated yields were reported. [a]Photocatalyst **PC-11** (1 mol%) was used.*

Scheme 106: Scope of α-aryl vinyl azides

The reactivities of different cyanoarenes was tested with vinyl azide **523** and NHPI ester **524** (Scheme 107). Photocatalyst **PC-11** was tested to show better reactivities in the reactions. 4-Cyanopyridines with different substituents like *tert*-butyl, cyclobutyl, cyclopentenyl, and dimethyl groups showed good reaction efficiencies in this transformation, affording products **574**–**577** with good yields (70%–74% yields). Quinoline and pyrimidine motifs were also introduced into corresponding α-tertiary amines (**579** and **580**) in moderate yields.

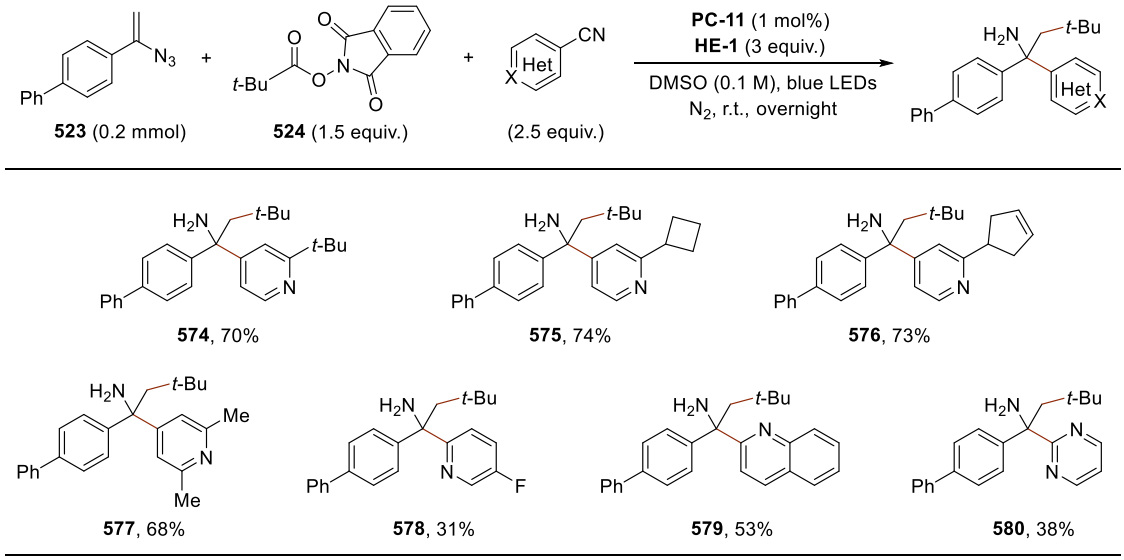

*Standard conditions: vinyl azide **523** (0.2 mmol), NHPI ester **524** (1.5 equiv.), cyanoarene (2.5 equiv.), photocatalyst **PC-11** (1 mol%) and Hantzsch ester **HE-1** (3 equiv.) in DMSO (0.1 M), irradiated under blue LEDs at room temperature under N_2 atmosphere overnight; isolated yields were reported.*

Scheme 107: Scope of cyanoarenes

4.2.4 Late-Stage Modification of Complex Molecules

After investigating the substrate scope of this method, the applicability of this approach through the late-stage functionalisation of complex molecules was explored (Scheme 108). Carboxylic acid groups are broadly occurring in natural products and drugs, this method provided a powerful method for converting aliphatic carboxylic acids into alkyl diarylamines with excellent chemoselectivity and functional group tolerance. NHPI esters prepared from stearic acid and linoleic acid were amendable to the synthesis of α-tertiary amines, delivering **581** in 71% yield, and **582** in 65% yield without olefin isomerization. Alkyl radical precursors derived from drug molecules such as gemfibrozil and gabapentin were good coupling partners in the reactions (**583** and **584**, 73% and 55% yield respectively). NHPI esters from naturally

occurring carboxylic like acids biotin and dehydrocholic acid readily participated in the coupling reactions, affording primary amines **585** (61% yield) and **586** (71% yield). Notably, three ketone groups in dehydrocholic acid motif remained intact under the reaction conditions, highlighting the good functional group compatibility of this method.

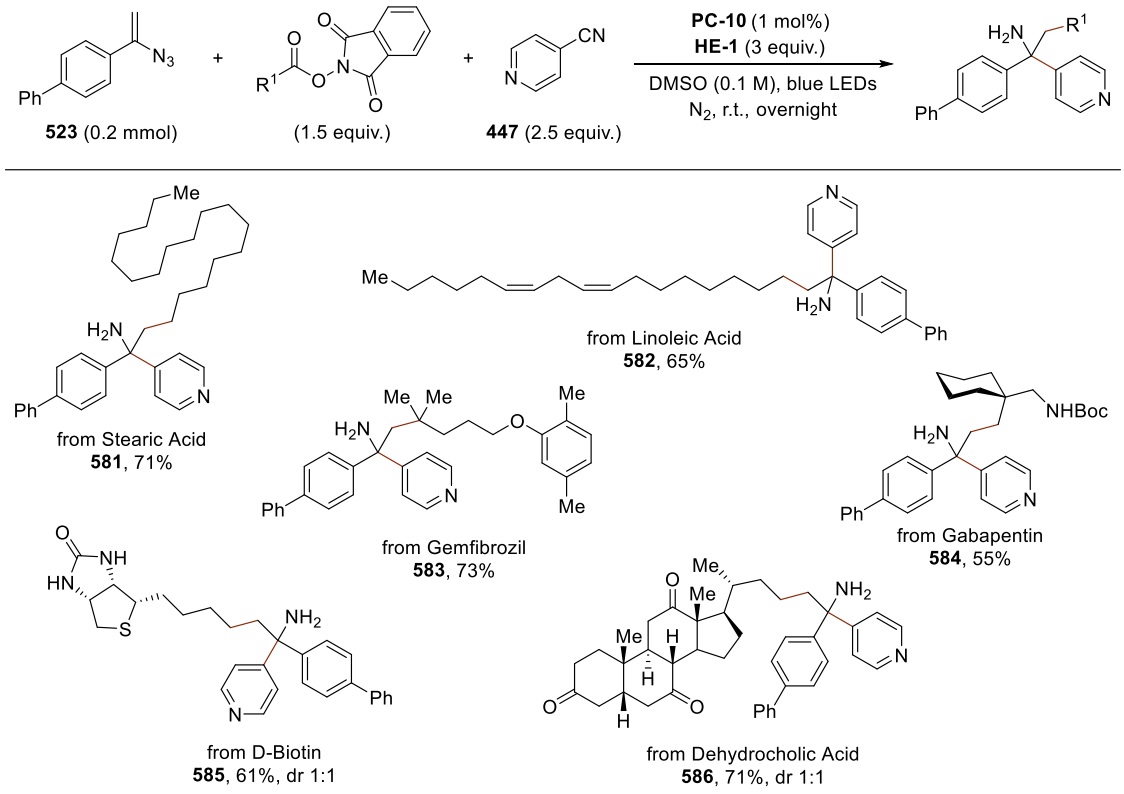

*Standard conditions: vinyl azide **523** (0.2 mmol), NHPI ester (1.5 equiv.), 4-cyanopyridine **447** (2.5 equiv.), photocatalyst **PC-10** (1 mol%) and Hantzsch ester **HE-1** (3 equiv.) in DMSO (0.1 M), irradiated under blue LEDs at room temperature under N_2 atmosphere overnight; diastereomeric ratio was determined by ^1H NMR spectroscopy of the crude reaction mixture; isolated yields were reported.*

Scheme 108: Late-stage functionalisation of natural products and drugs

4.2.5 Modular Synthesis of 2,2-Diaryl Tetrahydroquinolines

α-Tertiary primary amines obtained by this approach were also suitable for straightforward synthesis of 2,2-diarylated tetrahydroquinolines (THQs). Tetrahydroquinoline is an important heterocyclic motif that has been found in many complex molecules displaying interesting biological activities.[120]

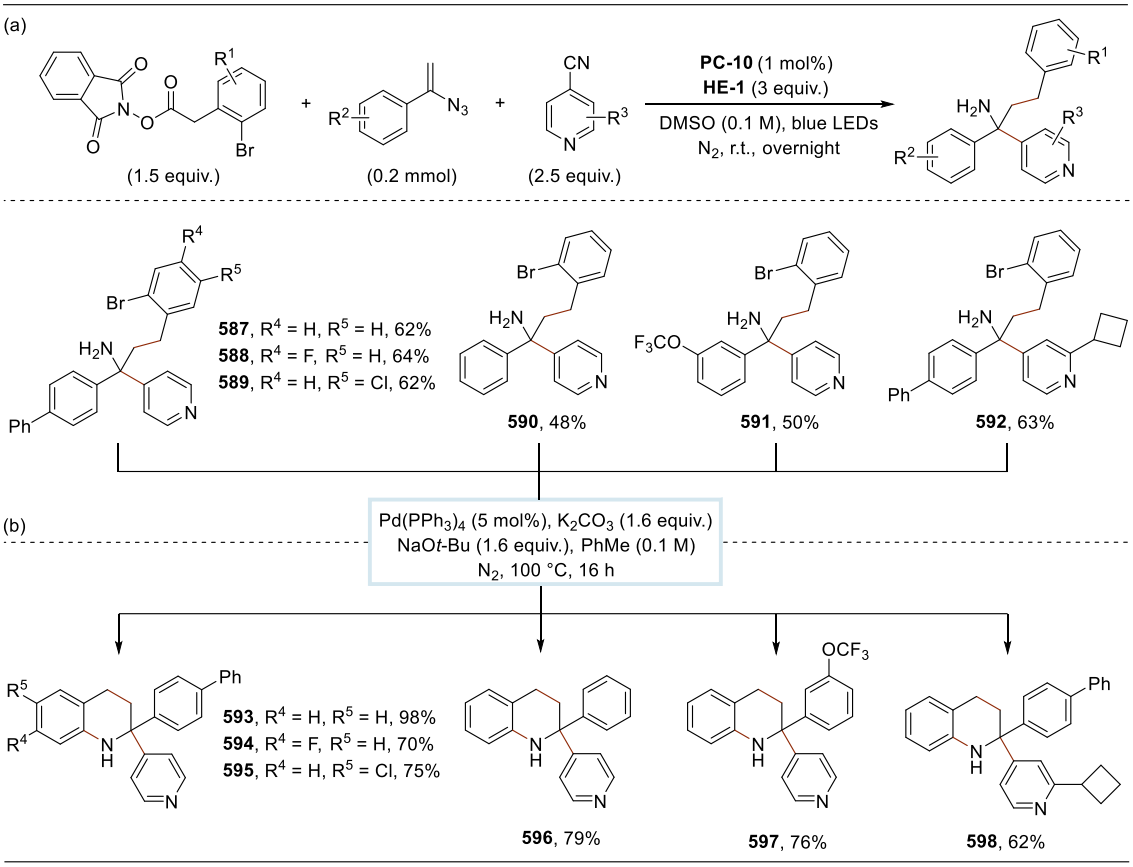

Standard conditions: (a) vinyl azide (0.2 mmol), NHPI ester (1.5 equiv.), cyanoarene (2.5 equiv.), photocatalyst ***PC-10*** *(1 mol%) and Hantzsch ester* ***HE-1*** *(3 equiv.) in DMSO (0.1 M), irradiated under blue LEDs at room temperature under N_2 atmosphere overnight; (b) α-tertiary amine (1 equiv.), K_2CO_3 (1.6 equiv.), NaOt-Bu (1.6 equiv.) and $Pd(PPh_3)_4$ (5 mol%) in toluene at 100 °C under N_2 atmosphere for 16 h; isolated yields were reported.*

Scheme 109: Modular synthesis of 2,2-diaryl tetrahydroquinolines

As shown in Scheme 109a, a series of 2-bromo-substituted γ-arylamines **587**–**592** were obtained in moderate to good yields by using NHPI esters derived from 2-bromo-substituted benzylic acids under standard reaction conditions. Then a palladium-catalysed intramolecular *N*-arylation of corresponding amine products provided an efficient access to class of 2,2-diary THQs (**593**–**598**, 62%–98% yields, Scheme 109b), presenting the potential of this approach to inspire rapid analogue evaluation in medicinal chemistry.

4.2.6 Direct Synthesis of 1,2-Amino Alcohols

The synthetic potential of this protocol was further expanded through the rapid access to a series of sterically hindered 1,2-amino alcohols. Aryl aldehydes have been reported to act as ketyl anion radical precursors under photoredox conditions.[121] The cross-coupling reactions between vinyl azides, redox-active esters, and aryl aldehydes were tested (Scheme 110).

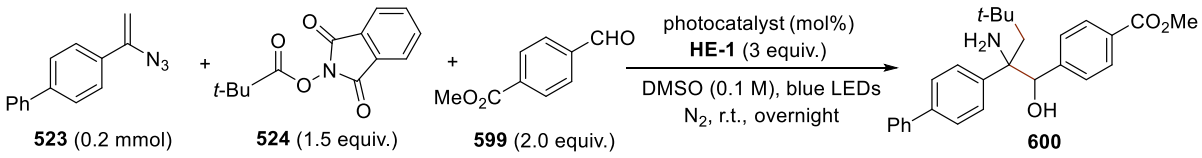

523 (0.2 mmol) **524** (1.5 equiv.) **599** (2.0 equiv.) **600**

Entry	Photocatalyst (mol%)	Yield of **600**[a]
1	**PC-10** (1)	62%, dr 1:1
2	**PC-14** (3)	82% (75%), dr 1:1
3	none	70%, dr 1:1

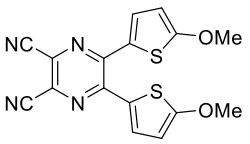

PC-14 (DPZ)

[a]*Yields and d.r. value were determined by ^{1}H NMR spectroscopy of the crude reaction mixture with mesitylene as internal standard, isolated yield was shown in parentheses.*

Scheme 110: Synthesis of 1,2-amino alcohols

By replacing 4-cyanopyridine **447** with methyl 4-formylbenzoate **599** under standard conditions, 1,2-amino alcohol **600** was formed in 62% yield with a diastereomeric ratio of 1:1 based on NMR spectroscopy analysis of the crude reaction mixture. The yield increased to 82% by using an organic photocatalyst **PC-14** (5,6-bis(5-methoxythiophen-2-yl)pyrazine-2,3-dicarbonitrile). This type of reaction was also efficient in the absence of photocatalyst, albeit with compromised yield.

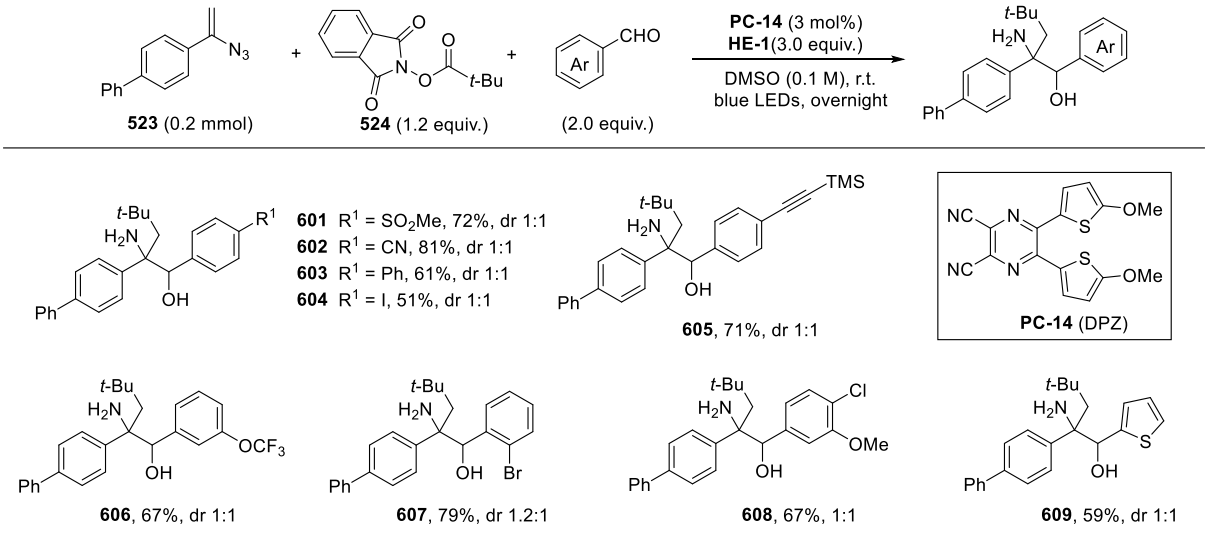

*Standard conditions: vinyl azide **523** (0.2 mmol), NHPI ester **524** (1.2 equiv.), aryl aldehyde (2.0 equiv.), photocatalyst **PC-14** (3 mol%) and Hantzsch ester **HE-1** (3.0 equiv.) in DMSO (0.1 M), irradiated under blue LEDs at room temperature under N_2 atmosphere overnight; diastereomeric ratio was determined by ^1H NMR spectroscopy analysis; isolated yields are reported.*

Scheme 111: Substrate scope of aryl aldehydes

Various aryl aldehydes were efficient coupling partners under the reaction conditions (Scheme 111). *para*-Substituted aryl aldehydes bearing functional groups such as sulfonyl, cyanide, iodide and alkynyl groups worked well, delivering corresponding product **601**−**605** in 51%−81%

yields. Aldehydes with trifluoromethoxy group and bromide at *meta* or *ortho* positions were also tolerated, as well as a 3,4-disubstituted substrate (**606**–**608**). Thiophene-2-carbaldehyde showed good reactivity in the reaction, affording product **609** in 59% yield.

4.3 Mechanistic Investigation

4.3.1 Control Experiments

Several experiments were conducted to gain more insights into the reaction mechanism. 2*H*-azirine was shown to be an important intermediate in vinyl azide chemistry.[122] In a control experiment (Scheme 112), when vinyl azide **523** and photocatalyst **PC-10** was reacted in DMSO under the irradiation of blue light, 2*H*-azirine **610** was obtained in 71% yield. However, the desired amine product **525** was not formed when 2*H*-azirine **610** was used instead of vinyl azide **523** under standard reaction conditions, which ruled out the 2*H*-azirine as an intermediate in this transformation.

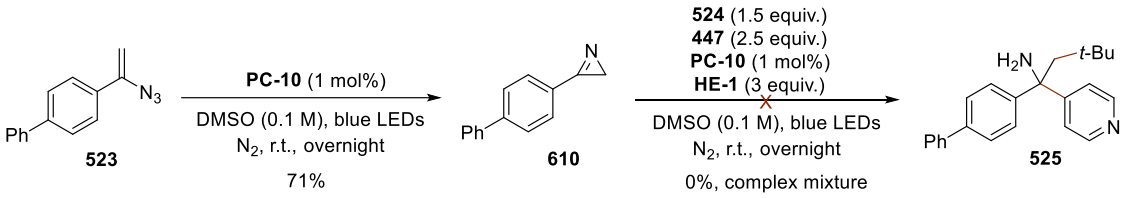

Scheme 112: Excluding 2*H*-azirine as an intermediate

When the reaction was conducted in the absence of cyanopyridine for 20 min, the ketimine intermediate **Int-611** was detected in 76% ^{1}H NMR yield, and the corresponding hydrolysed

ketone product **612** was isolated in 65% yield after column chromatography (Scheme 113). This result showed that ketimine is an intermediate in the reaction.

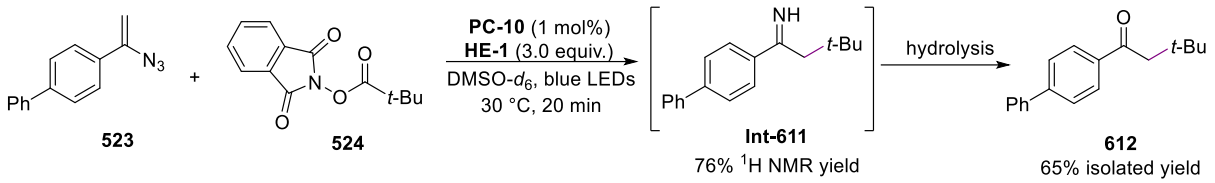

Scheme 113: Ketimine as an intermediate in the reaction

4.3.2 Radical Trapping Experiment

When the reaction was performed in the presence of 2.0 equivalents of TEMPO ((2,2,6,6-tetramethylpiperidin-1-yl)oxyl), the formation of α-tertiary amine product **525** was greatly depressed, and 5% yield of the TEMPO adduct **614** was isolated (Scheme 114a).

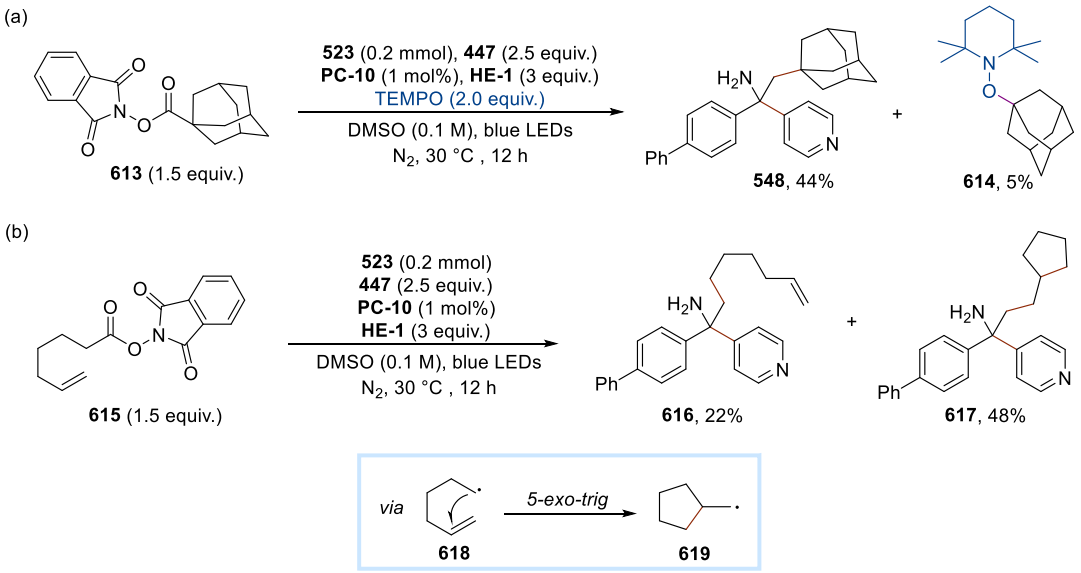

Scheme 114: Radical trapping experiments

When an alkene-bearing NHPI ester **615** was used as radical precursor with vinyl azide **523**, 4-cyanopyridine **447** under standard conditions, product **616** was obtained in 22% yield alongside 48% of the radical cyclisation product **617** (Scheme 114b). These results indicating the formation of alkyl radical species **618** and **619** under the reaction conditions.

4.3.3 Fluorescence Quenching Experiments

Mechanistic investigations with a series of fluorescence quenching experiments using prototype substrates were conducted (Figure 17−25). The results showed that the fluorescence of the excited photocatalyst ***PC-10** was greatly quenched by the Hantzsch ester **HE-1**, and **HE-1** itself showed an emission at 454 nm. The fluorescence quenching of the excited photocatalyst ***PC-6** by vinyl azide **523** was more likely to undergo an energy transfer process to form 2*H*-azirine.[117] NHPI ester **524** can quench the excited photocatalyst ***PC-10** at higher concentration, while no measurable fluorescence quenching was observed when 4-cyanopyridine **447** was used.

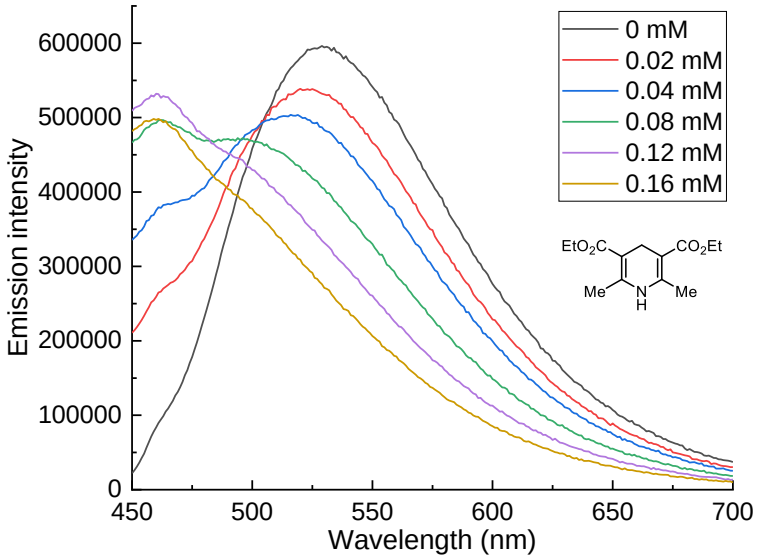

Figure 17: Stacked emission spectra of photocatalyst (PC-10) at different concentrations of Hantzsch ester (HE-1). Fluorescence intensity was integrated from 529 nm to 700 nm due to the overlapping with the emission of Hantzsch ester HE-1

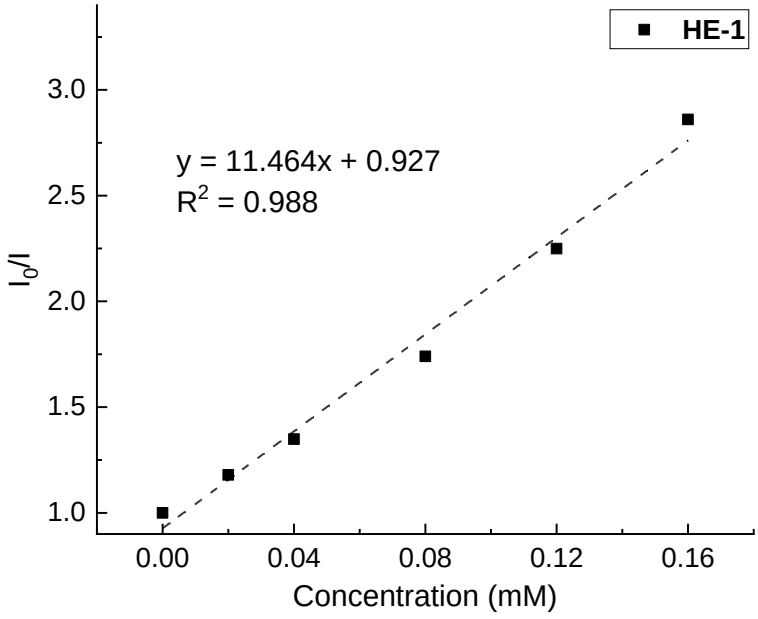

Figure 18: Stern-Volmer plot analysis derived from the data extracted from Figure 17

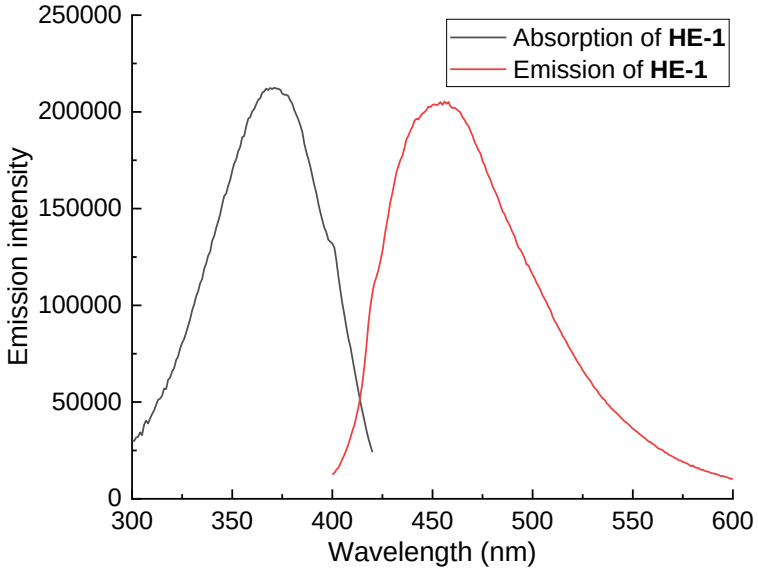

Figure 19: Absorption and emission spectra of Hanztsch ester HE-1. HE-1 was excited at 372 nm and the emission intensity was collected at 454 nm

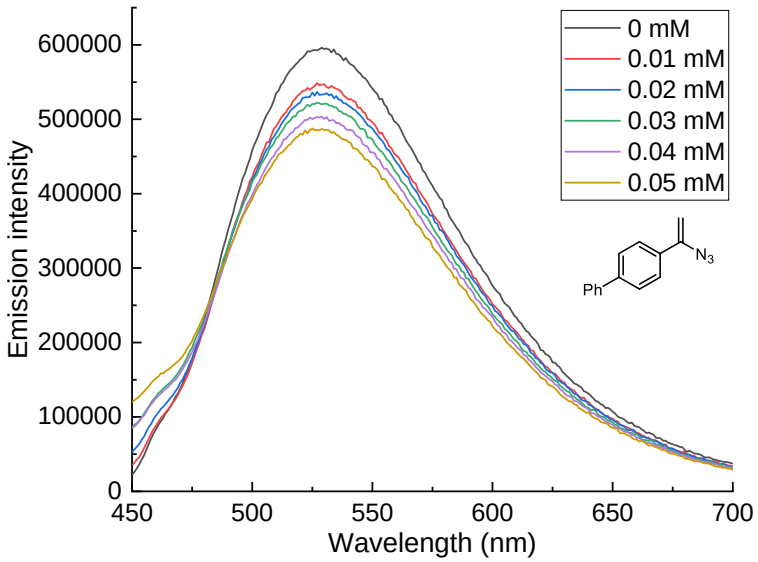

Figure 20: Stacked emission spectra of photocatalyst (PC-10) at different concentrations of vinyl azide 523

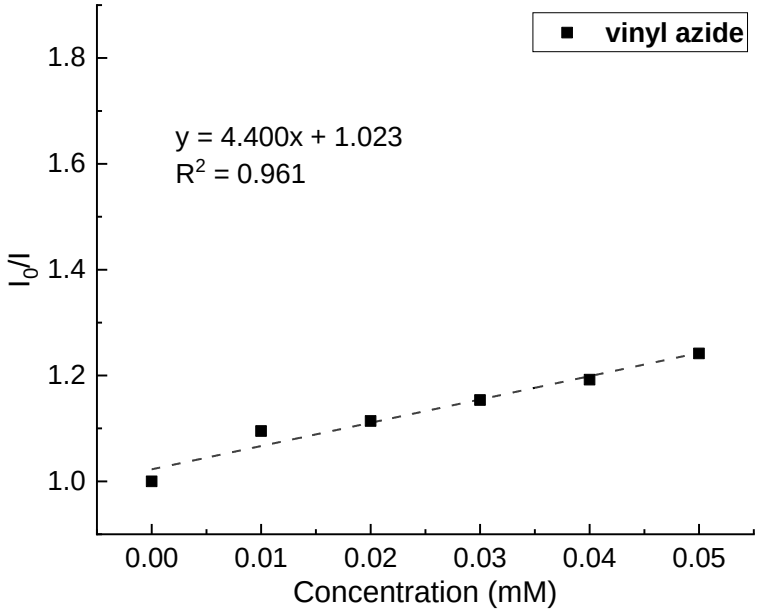

Figure 21: Stern-Volmer plot analysis derived from the data extracted from Figure 20

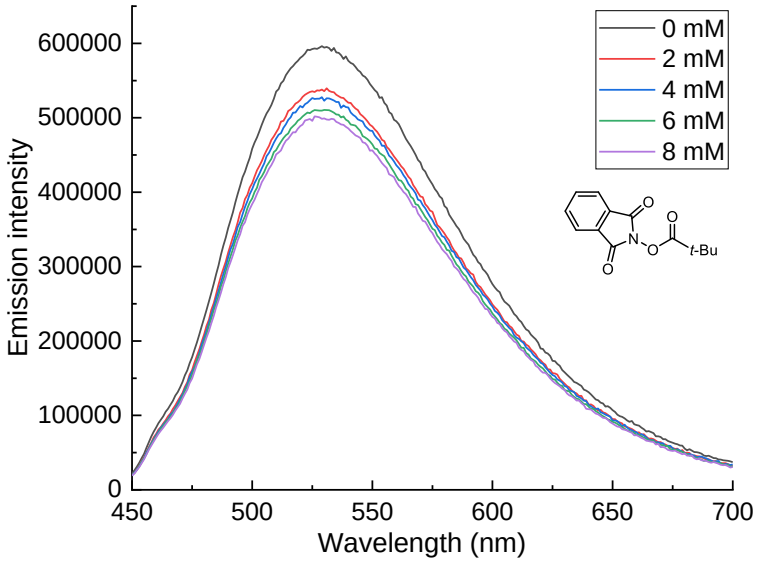

Figure 22: Stacked emission spectra of photocatalyst (PC-10) at different concentrations of NHPI ester 524

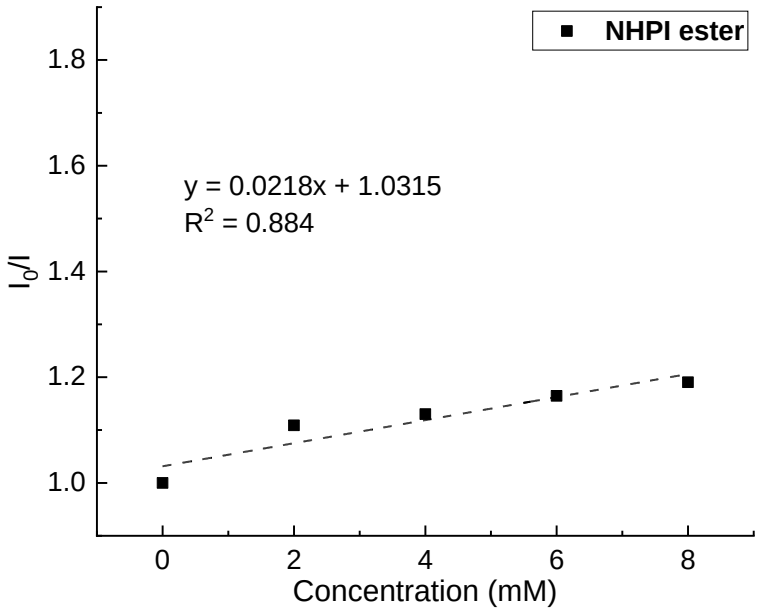

Figure 23: Stern-Volmer plot analysis derived from the data extracted from Figure 22

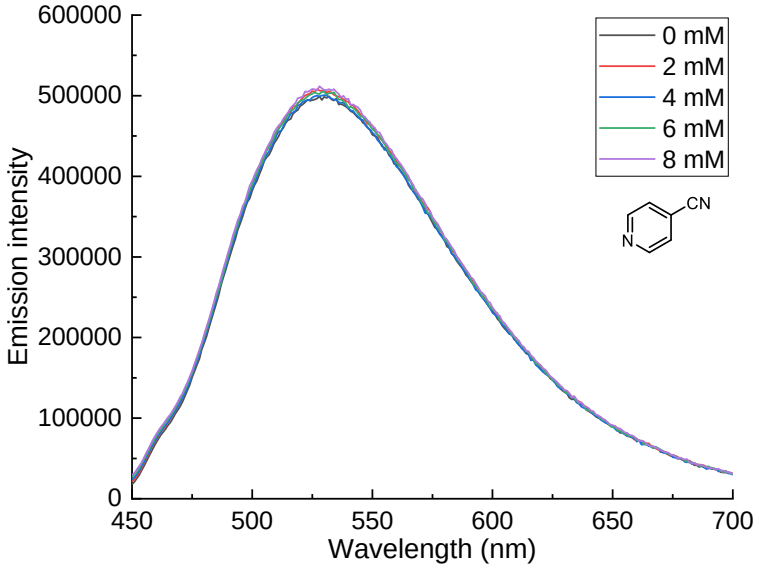

Figure 24: Stacked emission spectra of photocatalyst (PC-10) at different concentrations of 4-cyanopyridine 447

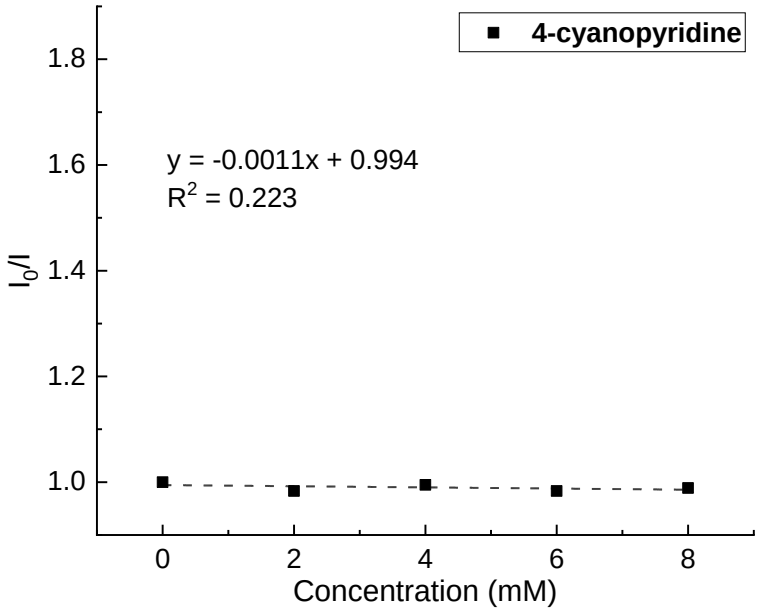

Figure 25: Stern-Volmer plot analysis derived from the data extracted from Figure 24

4.3.4 The Involvement of a Non-Catalytic Reaction Pathway

As I mentioned during the reaction optimisation studies that the prototype reaction was still efficient in the absence of any photocatalyst, and the α-tertiary amine product **525** was obtained in 72% NMR yield (see Section 4.2.2). Thus, a survey of representative examples using the conditions in the absence of photocatalyst (Conditions B) was conducted (Scheme 115). These results showed that although all the reactions were operative in the absence of photocatalyst, but consistently lower yields were obtained than those under the standard conditions (Conditions A). Then I speculated that there was a non-catalytic reaction pathway during the reaction. However, the reaction efficiency could be enhanced in the presence of a proper photocatalyst.

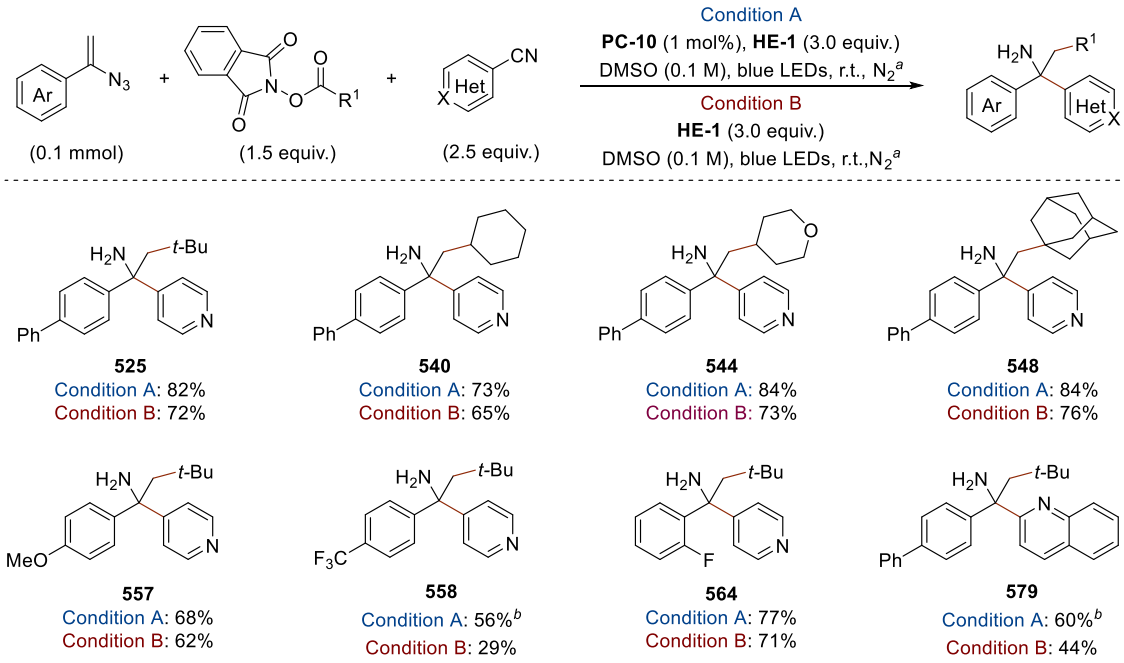

[a]Yields were determined by ^{1}H NMR spectroscopy of the crude reaction mixture with mesitylene as internal standard.
[b]$Ir(ppy)_2(bpy)PF_6$ as photocatalyst.

Scheme 115: Comparison of reactions with and without photocatalyst

4.3.5 UV-Vis Studies and Job's Plot

According to the research precedents, the association of an electron-rich substrate (such as Hantzsch ester **HE-1**) with an electron-accepting molecule (such as *N*-phthalimide) can form an electron donor-acceptor (EDA) complex,[123] which can trigger single-electron-transfer event upon visible-light irradiation to generate radical intermediates.[124] The reaction components was analysed by UV/vis absorption spectroscopy. In line with seminal reports by Chen[125] and Molander,[126] DMSO solution of NHPI ester **524** and Hantzsch ester **HE-1** was found to have a clear bathochromic shift in the visible region, confirming the formation of an EDA complex (Figure 26, purple and black lines). When NHPI ester **524** was mixed with different molar

fraction of Hantzsch ester **HE-1**, the Job's plot with UV/vis absorption experiments showed a 1:1 ratio between **524** and **HE-1** of the most absorbing species (Figure 27).

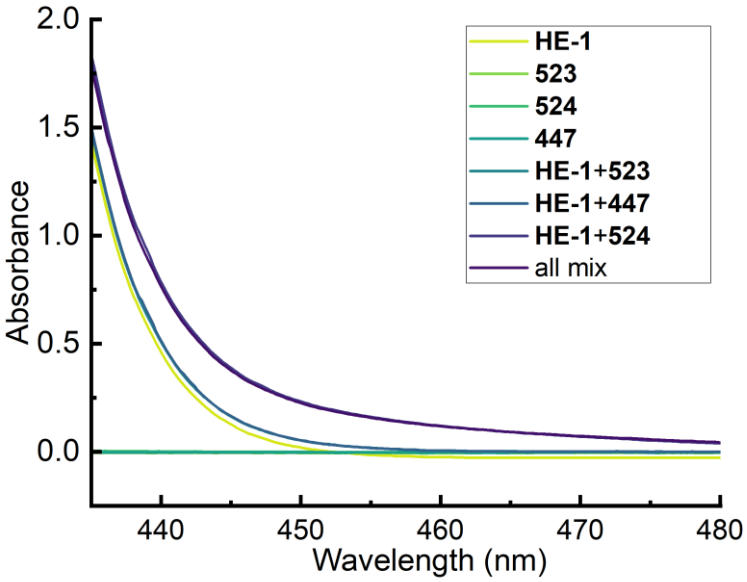

Figure 26: UV-vis studies of reaction components.

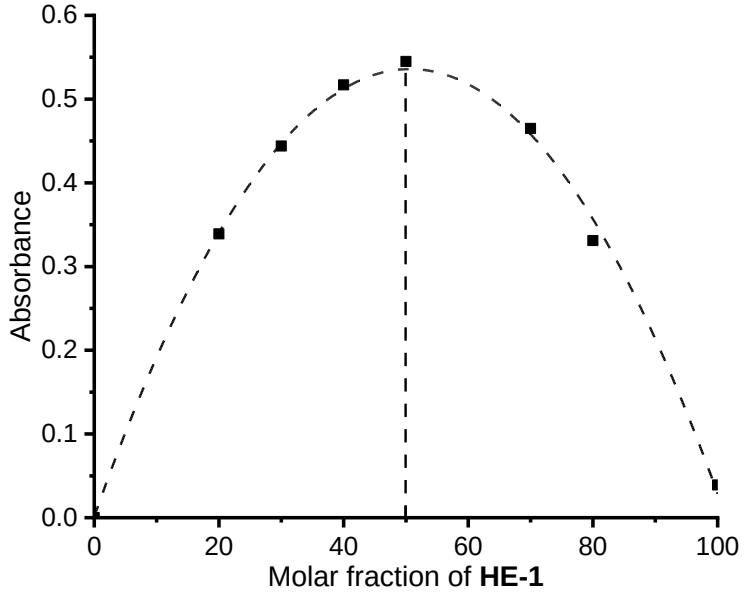

Figure 27: The Job's plot for ratio between Hantzsch ester (HE-1) and NHPI ester 524

4.3.6 Reactions under Different Light Wavelength

It has been reported that Hantzsch ester **HE-1** can directly reach an electronically excited state ***HE-1** upon light absorption and then trigger single-electron transfer events with substrates.[127] Analysis of the UV-vis absorption spectrum of **HE-1** showed that **HE-1** has a maximum absorbance at λ = 376 nm in DMSO (Figure 28). The non-zero absorbance at λ = 410-430 nm indicated that **HE-1** can absorb light emitted by the blue LEDs to reach an excited state ***HE-1**.

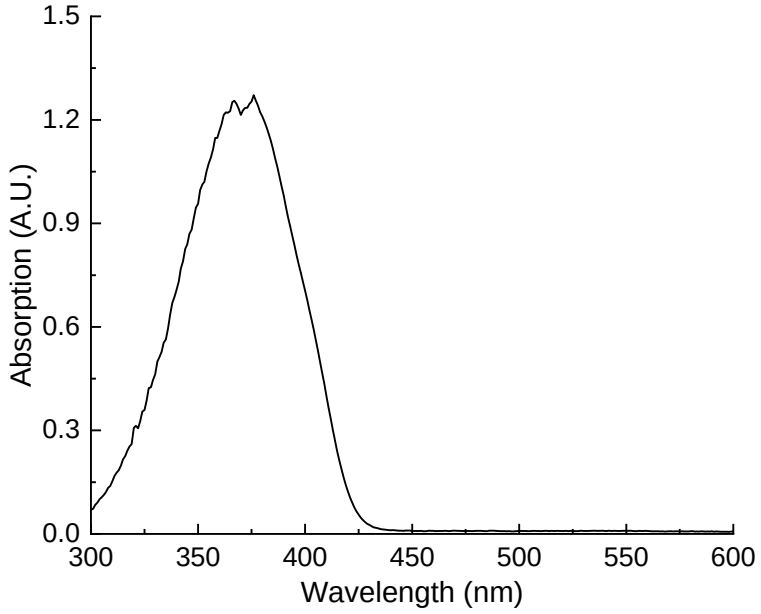

Figure 28: Absorbance of Hantzsch ester HE-1 in DMSO

In order to investigate whether the photoexcited Hantzsch ester ***HE-1** was involved in the reactions, several control experiments with a commercially available laser line filter (CWL = 488 nm, FWHM = 10 nm, see Figure 29) were performed. The excitation of the Hanztsch ester **HE-1** to its photoexcited state ***HE-1** is nearly impossible at λ = 488 nm.

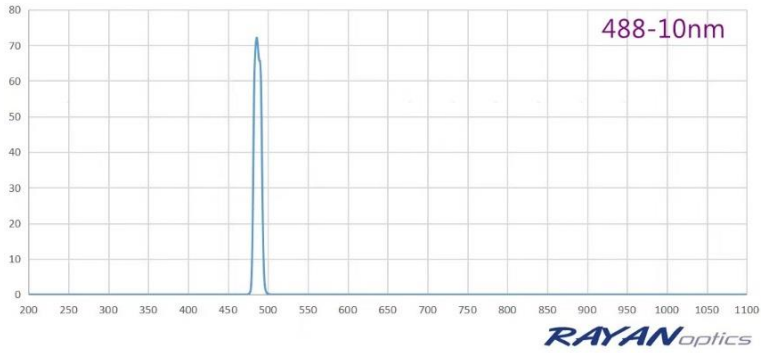

Figure 29: Spectrum of light with a laser line filter (CWL = 488 nm, FWHM = 10 nm)

When the reaction was conducted in the absence of **PC-10**, α-tertiary amine product **525** was formed in 72% yield alongside 5% of the ketone **612**. When the laser line filter was further applied, most of the vinyl azide **523** was recovered and the product **525** was not detected, but **612** was still formed in 21% yield. These results showed that in the absence of a photocatalyst, the photoexcited Hanztsch ester ***HE-1** played a crucial role in the product formation, but it was not necessary in the ketimine intermediate formation step. Furthermore, the reaction can proceed with the laser line filter when sub-stoichiometric amount of **PC-10** was added, the amine product **525** was obtained in 22% yield and **612** was formed in 44% yield (Scheme 116). These results suggested the involvement of a photocatalytic reaction pathway which does not require the participation ***HE-1**.

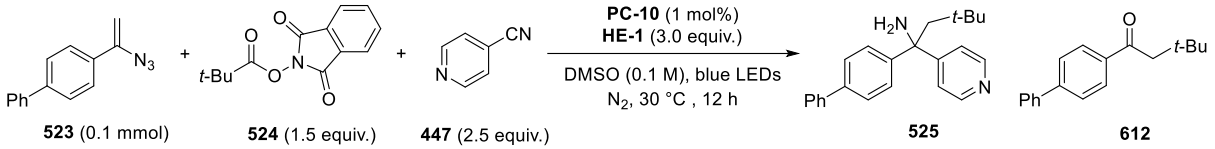

Entry	Laser liner filter (480 ± 10 nm)	1 mol% **PC-10**	Yield of **525**[a]	Yield of **612**[a]
1	no	no	72%	5%
2	with	no	0%	21% (78%[b])
3	no	with	83%	4%
4	with	with	22%	44%

[a]Yields were determined by ^{1}H NMR spectroscopy of the crude reaction mixture with mesitylene as internal standard.
[b]Recovery of vinyl azide.

Scheme 116: Reactions with or without a laser line filter

4.3.7 Light On-Off Experiments

Light on-off experiments were performed using model substrates to see if the reaction yield was determined by photon flux. As show in Scheme 117, the product formation occurred only during the period of constant light irradiation.

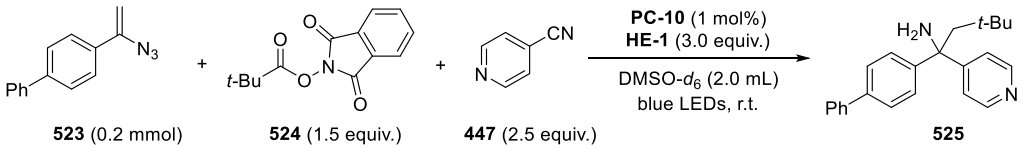

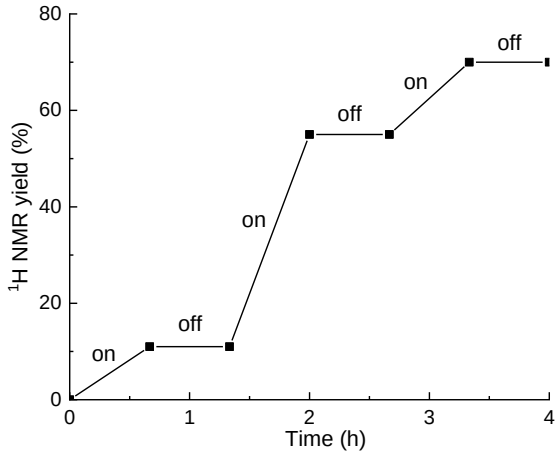

Scheme 117: Light on-off experiments

4.3.8 Quantum Yield Determination

The light on-off experiments showed that no reaction progress was made under the dark conditions. However, typical lifetime of radical chain process can be on the second or sub-second timescale, which means chain processes can terminate faster than the timescale of the analytical measurement used.[128] The quantum yield of the model reaction was calculated.

The blue LED used in the reactions has a wavelength of maximum emission (λ_{max}) at 440 nm. The photon flux of the blue LED was calculated using standard ferrioxalate actinometry to be 5.9932×10^{-9} einstein s^{-1}. The fraction of light absorbed by **PC-10** at $\lambda = 440$ nm was determined by UV/vis spectroscopy to be 0.6107. The standard reaction was performed in a cuvette for 180 min, the yield of primary amine **525** was determined by ^{1}H NMR analysis of the crude reaction mixture to be 49%, which means about 9.8×10^{-5} mol of product was formed. The number of photons absorbed by photocatalyst during a period of 180 min was 3.95×10^{-5} einstein. Based on these data, the quantum yield of the reaction was calculated to be $\Phi = (9.8 - 3.95) \times 10^{-5} = 2.48 > 1$ (see section 5.5.3 for experimental details), which indicated a radical chain process might be involved during the reaction (Scheme 118).

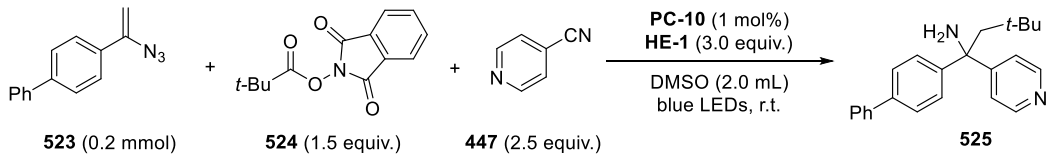

Scheme 118: Quantum yield determination

4.3.9 Proposed Mechanism

Based on the results above, a proposed reaction mechanism was depicted in Scheme 119. Initially, light irradiation of the photocatalyst would generate the excited state $*Ir^{III}$ ($E_{1/2}^{red}[*Ir^{III}/Ir^{II}]$ = +0.97 V vs SCE),[129] which was reductively quenched by Hantzsch ester **HE-1** ($E_{1/2}^{red}$ = +0.79 V vs SCE)[130] to generate Ir^{II} and **HE-1**$^{\bullet+}$. The reduced state Ir^{II} ($E_{1/2}^{red}[Ir^{III}/Ir^{II}]$ = −1.43 V vs SCE)[129] was sufficient to undergo SET with a wide range of NHPI esters **613**, delivering alkyl radical species **614** after decarboxylative fragmentation and the ground state photocatalyst Ir^{III}. Another viable pathway for the generation of **614** involved an intra-complex SET reaction between redox-active NHPI ester **613** and **HE-1** under photoirradiation. Some direct electron transfer between the photoexcited ***HE-1** and NHPI esters **613** to generate **614** can not be ruled out.[126] The radical addition of **614** to vinyl azides **615** would give the iminyl radical species **616** after denitrogenation. A hydrogen atom transfer (HAT) process between **616** and the Hantzsch ester **HE-1** or its radical cation **HE-1**$^{\bullet+}$ gave the ketimine **617** and the HE radical **HE-1**· or pyridinium ion PyH^+.[131,132] The generated HE radical **HE-1**· might initiate a new chain propagation through a SET event with NHPI esters **613**.[132] Further protonation of the **617** afforded iminium species **618**, which could be reduced by Ir^{II} or ***HE-1** ($E_{1/2}^{red}$[***HE-1**/ **HE-1**$^{\bullet+}$] = −2.28 V vs SCE)[133] to yield α-amino alkyl radical species **619**. In the meantime, a proton-coupled electron-transfer reduction of cyanopyridines **620** by Ir^{II} was postulated to give persistent radical species **621**.[101] Alternatively, the single-electron reduction of **620** by photoexcited ***HE-1** follow by protonation to generate **621** was also possible.[134] Finally, the

hetero-radical coupling between α-amino alkyl radical species **619** and persistent radical species **621** led to the formation of α-tertiary primary amines **622** after the elimination of a hydrogen cyanide. As for the synthesis of 1,2-amino alcohols, aryl aldehydes were likely reduced by the photocatalyst Ir^{II} to afford corresponding ketyl anion radicals, which underwent radical cross coupling with α-amino alkyl radical species **619** to afford the products.

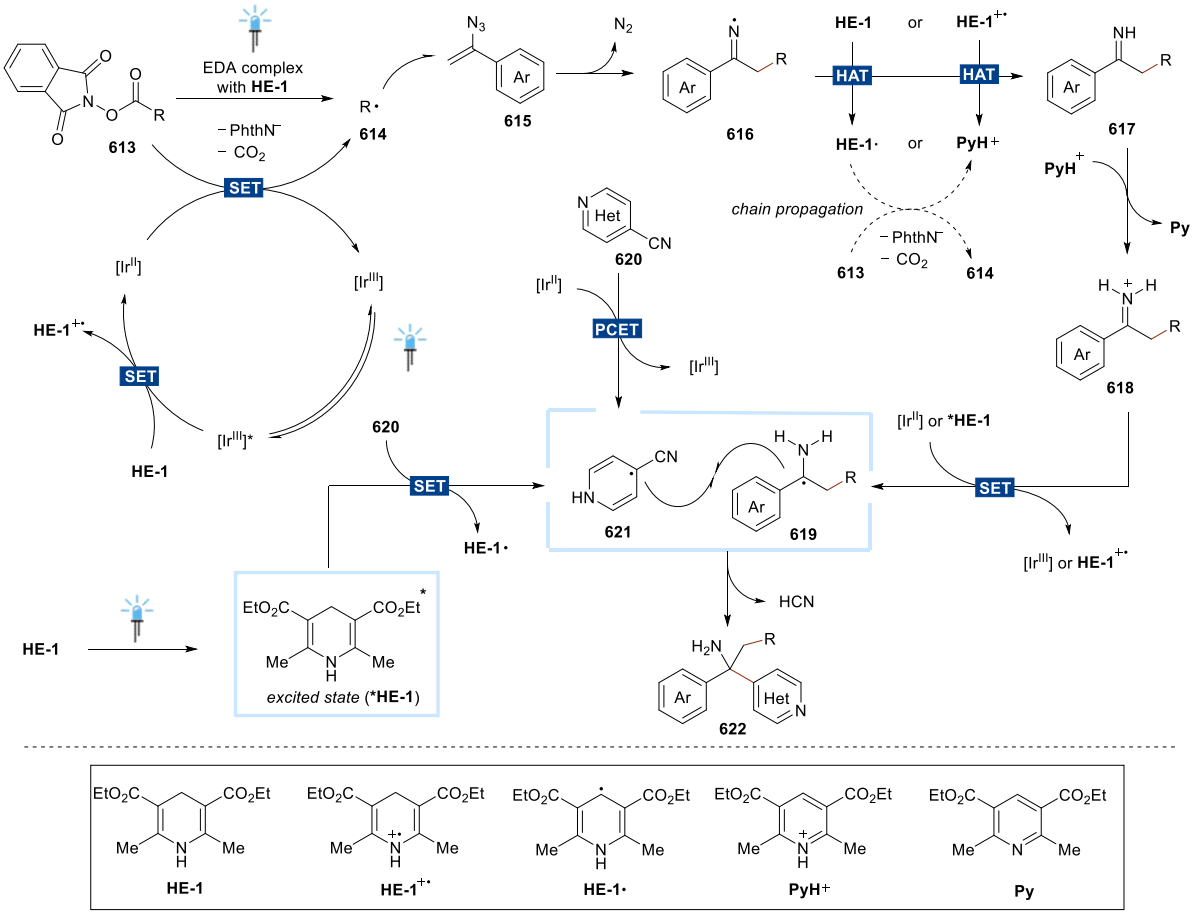

Scheme 119: Proposed mechanism

4.3.10 A Common Radical-Radical Coupling Side-Product

There are several radical species formed during the reaction: the alkyl radical species **614**, the iminyl radical species **616**, the α-amino alkyl radical species **619**, the Hantzsch ester radical species **HE-1·**, and the persitent radical species **621**. Apart from the desired radical coupling pathway as illustrated in Scheme 119, the hetero-radical coupling between Hanztsch ester radical **HE-1·** and radical species **621** was also observed, leading to the formation of **624** after the elimination of a hydrogen cyanide. The oxidation of the intermediate **624** by the excited photocatalyst followed by deprotonation would eventually deliver **623** as the main side-product in the reaction.

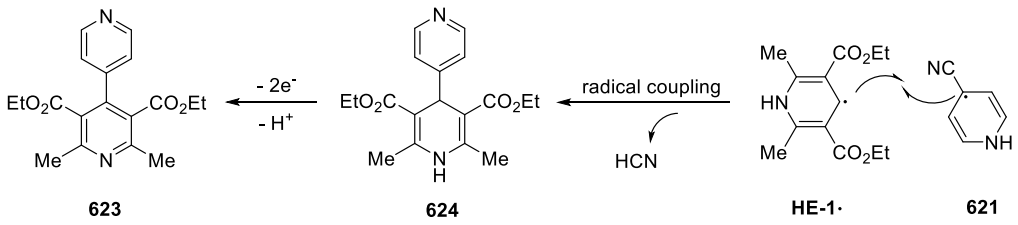

Scheme 120: Possible pathway for the formation of the bipyridine side-product

4.4 Conclusion and Outlook

In summary, the synthesis of α,α,α-alkyldiaryl primary amines from vinyl azides through visible-light induced denitrogenative alkylarylation with redox-active NHPI esters and cyanoarenes was presented. The use of NHPI esters, which were derived from earth abundant alkyl carboxylic acids, as coupling reagent provids rapid access to structurally and functionally diverse α-tertiary primary amines. In addition, the modular synthesis of 2,2-diaryl-1,2,3,4-

tetrahydroquinolines by palladium-catalysed intramolecular C–N coupling of 2-bromo-substituted γ-arylamines, and the synthesis of 1,2-amino alcohols using aryl aldehydes as coupling partners were also demonstrated.

Apart from the photocatalytic cycle, mechanistic studies showed that the product formation was also attributed to a non-catalytic reaction pathway where Hantzsch ester played a dual role to act as a sacrificial reductant (at its photoexcited state) and form electron donor-acceptor complex with NHPI redox-active esters. These two reaction pathways ensure the efficient formation of α-amino alkyl radicals from *in situ* generated ketimine intermediates, as well as the persistent radical species from cyanoarenes, which led to the rapid formation of corresponding α-tertiary primary amines.

Through the course of this research, I have discovered three novel radical-triggered cascade transformations for the synthesis of nitrogen heterocycles, α-arylated carbonyl compounds, and α-tertiary primary amines under visible-light conditions.

The utilisation of the protecting aryl sulfonamide in ynamides for skeleton assembly has been demonstrated in the fragmentary rearrangement cascade reaction of ene-ynamides. While this work provided rapid access to a series of [1,2]-annulated indole motifs, a detailed reaction mechanism remains to be validated. The choice between two aryl groups from the aryl sulfonamide and the aryl ethynyl parts remains empirical, which might require extensive synthetic work to test the reaction feasibility. Future work should aim to have a deeper

understanding of the final C(sp^2)–N bond formation step so as to have a general route for obtaining the desired single regioisomer product.

The continuous utilisation of photocatalyst to engage single electron transfer processes with potassium alkyltrifluoroborates and *in situ* generated *gem*-difluoroalkenes has been realised for the synthesis of α-arylated carbonyl compounds from α-trifluoromethyl alkenes. Upon single electron oxidation of *gem*-difluoroalkene, the radical cation intermediate was trapped by H_2O and converted into acyl fluoride species for subsequent nucleophilic substitution reactions. Future work on identifying suitable carbon, nitrogen, or other types of nucleophiles to trap the radical cation intermediate for further transformations would expand the diversity of defluorinative functionalisation reactions of α-trifluoromethyl alkenes.

Finally, the utilisation of α-aryl vinyl azides as α-tertiary primary amine precursors has been demonstrated under reductive conditions using blue light. The formation of α-amino alkyl radicals was achieved through single electron transfer process between *in situ* generated ketimines and photocatalyst or Hanztsch ester. Work on finding other efficient radical precursors and coupling partners might lead to the synthesis of biologically active molecules.

Chapter 5: Experimental Section

5.1 General Experimental

Commercially available chemicals/reagents were purchased from Chemical Management Platform of Southern University of Science and Technology (major suppliers: Sigma-Aldrich, Bide Pharm, LeYan), and were used without further purification. Solvents were purchased in HPLC quality, and re-distilled according to *Purification of Laboratory Chemicals* (Fifth Edition). All catalysis reactions were carried out under nitrogen atmosphere in oven-dried Schlenk tube. Conversion was monitored by thin layer chromatography (TLC) using Merck TLC silica gel 60 F254. Compounds were visualized by UV light at 254 nm and by dipping the plates in an ethanolic vanillin/sulfuric acid solution or an aqueous potassium permanganate solution followed by heating. Flash column chromatography was performed over silica gel (230 – 400 mesh). NMR spectra were recorded on 400 MHz or 600 MHz Bruker spectrometers. Chemical shifts are given in ppm. The spectra are calibrated to the residual ^{1}H and ^{13}C signals of the solvents. Multiplicities are abbreviated as follows: singlet (s), doublet (d), triplet (t), quartet (q), doublet-doublet (dd), quintet (quint), septet (sept), multiplet (m), and broad (br). High resolution electrospray ionization and electronic impact mass spectrometry was performed on a Thermo Scientific Q Exactive mass spectrometer (mass analyzer type: Orbitrap). A mass accuracy $\leqslant$ 2 ppm was obtained in the peak matching acquisition mode by using a solution containing 2 <l PEG200, 2 <l PPG450, and 1.5 mg NaOAc (all obtained from Sigma‐Aldrich, CH‐Buchs) dissoled in 100 mL MeOH (HPLC Supra grade, Scharlau, E‐Barcelona) as internal standard.

Photochemical reactions were carried with 30 W blue LED (composed of 30 LED units each with 1.0 W). The emission band of the blue LED light source was determined (λ_{max} = 440 nm), using a UVN-SR fiber optic spectrometer. The emission spectrum of the LEDs was shown in Figure 30.

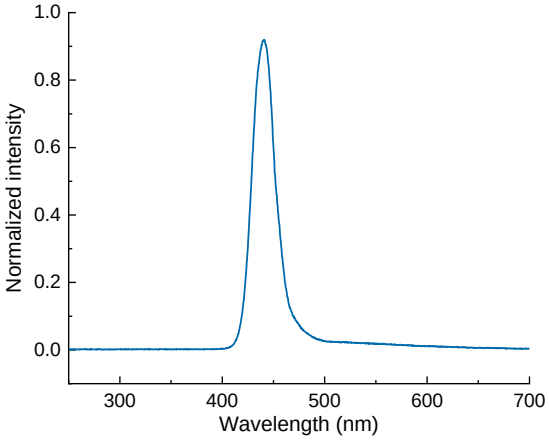

Figure 30: Emission spectrum of the blue LED light source

The reaction set-up is displayed in Figure 31. The distance between the lamp and the sealed reaction tubes was set 3 cm. Two external fans were used, and the ambient temperature of the reaction vessel was measured to be 30 °C during light irradiation.

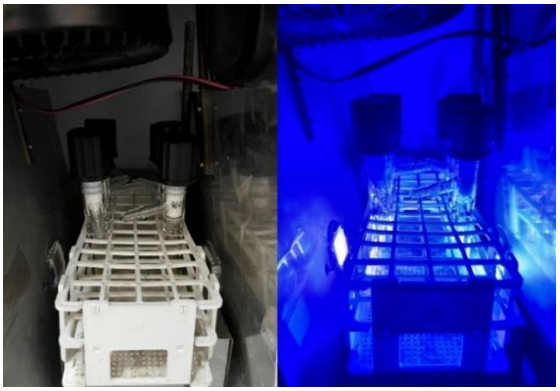

Figure 31: Photochemical reaction set-up

5.2 Precursors for Chapter 2, 3 and 4

5.2.1 Preparation of Alkene-Tethered Ynamides

General Procedure 1 (GP1)

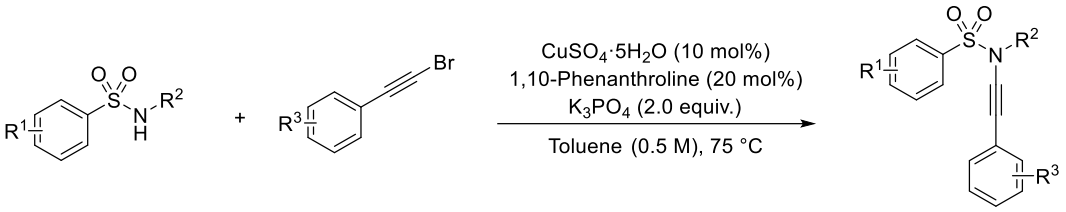

Following the method reported by Hsung and co-workers,[16] $CuSO_4{\cdot}5H_2O$ (10 mol%), 1,10-phenanthroline (20 mol%), K_3PO_4 (2.0 equiv.) and corresponding sulfonamide (if solid, 1.0 equiv.) were added to a Schlenk flask. The Schlenk flask was evacuated and backfilled with N_2 three times. Bromoalkyne (1.2 equiv.), corresponding sulfonamide (if liquid, 1.0 equiv.) and dry toluene (0.5 M) were then added under N_2 atmosphere, and the reaction mixture was allowed to react at 75 °C in an oil-bath until complete consumption of the starting sulfonamide was observed by TLC. The reaction mixture was then cooled to room temperature, filtered through a pad of silica gel, washed with ethyl acetate. The filtrate was concentrated on a rotary evaporator. The crude residue was purified by flash chromatography over silica gel.

General Procedure 2 (GP2)

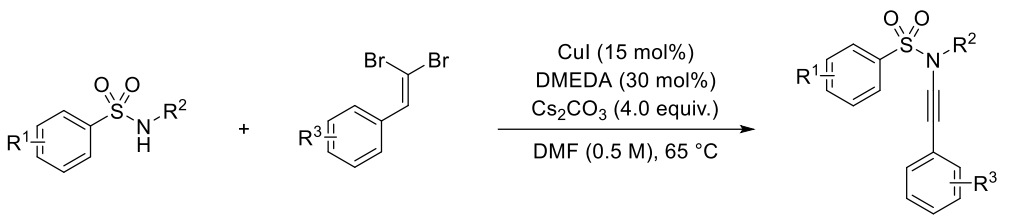

Following the method reported by Evano and co-workers,[17] CuI (15 mol%), Cs_2CO_3 (4.0 equiv.), and corresponding sulfonamide (if solid, 1.0 equiv.) were added to a Schlenk flask. The Schlenk flask was evacuated and backfilled with N_2 three times. 1,1-dibromo-1-alkene (1.2~1.5 equiv.), corresponding sulfonamide (if liquid, 1.0 equiv.), DMEDA (*N*,*N*'-dimethylethylenediamine, 30 mol%) and dry DMF (0.5 M) were then added under N_2 atmosphere, and the reaction mixture was allowed to react at 65 °C in an oil-bath until complete consumption of the starting sulfonamide was observed by TLC. The reaction mixture was then cooled to room temperature, diluted with water, extracted with ethyl acetate. The combined with organic layers were dried over Na_2SO_4, filtered and concentrated on a rotary evaporator. The crude residue was purified by flash chromatography over silica gel.

4-Methyl-N-(3-methylbut-3-en-1-yl)-N-(p-tolylethynyl)benzenesulfonamide **134**

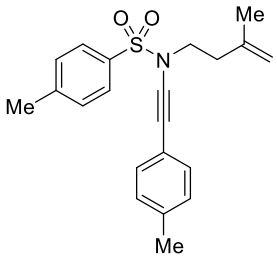

Following the **GP2** using 4-methyl-*N*-(3-methylbut-3-en-1-yl)benzenesulfonamide (1196 mg, 5.0 mmol) and 1-(2,2-dibromovinyl)-4-methylbenzene (1656 mg, 6.0 mmol). Purification by flash column chromatography (5-10% EtOAc in hexane), the product was obtained as colourless oil (1271 mg, 72% yield). ^{1}H NMR (600 MHz, $CDCl_3$) δ 7.87 (d, *J* = 8.1 Hz, 2H), 7.36 (d, *J* = 8.1 Hz, 2H), 7.0 (d, *J* = 8.1 Hz, 2H), 7.12 (d, *J* = 8.1 Hz, 2H), 4.85 – 4.82 (m, 1H), 4.80 –

4.77 (m, 1H), 3.55 (t, *J* = 7.5 Hz, 2H), 2.44 (s, 3H), 2.43 (t, *J* = 7.5 Hz, 2H), 2.34 (s, 3H), 1.77 (s, 3H); ^{13}C NMR (151 MHz, $CDCl_3$) δ 144.6, 141.2, 137.9, 134.5, 131.4 (2C), 129.7 (2C), 129.0 (2C), 127.6 (2C), 119.6, 112.8, 81.4, 70.9, 49.9, 35.8, 22.2, 21.5, 21.3. HRMS ESI $[M+H]^+$ calculated for ($C_{21}H_{23}NO_2S^+$) 354.1522, found 354.1522.

***N-(3-Methylbut-3-en-1-yl)-N-(phenylethynyl)benzenesulfonamide* 625**

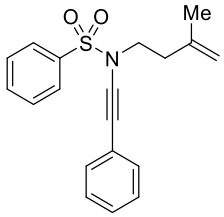

Following the **GP1** using *N*-(3-methylbut-3-en-1-yl)benzenesulfonamide (3377 mg, 15.0 mmol) and (bromoethynyl)benzene (3258 mg, 18.0 mmol). Purification by flash column chromatography (5-10% EtOAc in hexane), the product was obtained as colourless oil (2975 mg, 61% yield). ^{1}H NMR (400 MHz, $CDCl_3$) δ 8.01 – 7.93 (m, 2H), 7.70 – 7.62 (m, 1H), 7.61 – 7.53 (m, 2H), 7.41 – 7.34 (m, 2H), 7.32 – 7.27 (m, 3H), 4.82 – 4.79 (m, 1H), 4.76 – 4.73 (m, 1H), 3.55 (t, *J* = 7.5 Hz, 2H), 2.41 (t, *J* = 7.5 Hz, 2H), 1.75 (s, 3H); ^{13}C NMR (101 MHz, $CDCl_3$) δ 141.3, 137.7, 133.8, 131.5 (2C), 129.3 (2C), 128.4 (2C), 128.0, 127.8 (2C), 122. 9, 113.1, 82.1, 71.1, 50.2, 36.1, 22.4. HRMS ESI $[M+H]^+$ calculated for ($C_{19}H_{20}NO_2S^+$) 326.1209, found 326.1208.

***N-([1,1'-Biphenyl]-4-ylethynyl)-N-(3-methylbut-3-en-1-yl)-[1,1'-biphenyl]-4-sulfonamide* 626**

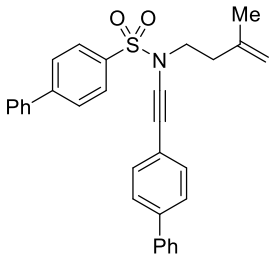

Following the **GP1** using *N*-(3-methylbut-3-en-1-yl)-[1,1'-biphenyl]-4-sulfonamide (1206 mg, 4.0 mmol) and 4-(bromoethynyl)-1,1'-biphenyl (1620 mg, 4.8 mmol). Purification by flash column chromatography (5-10% EtOAc in hexane), the product was obtained as colourless oil (1470 mg, 77% yield). ^{1}H NMR (400 MHz, $CDCl_3$) δ 7.92 (d, *J* = 8.2 Hz, 2H), 7.64 (d, *J* =8.2 Hz, 2H), 7.53 – 7.38 (m, 6H), 7.32 (m, 7H), 7.23 (d, *J* = 7.3 Hz, 1H), 4.71 (d, *J* = 1.2 Hz, 1H), 4.67 (d, *J* = 1.2 Hz, 1H), 3.49 (t, *J* = 7.5 Hz, 2H), 2.34 (t, *J* = 7.5 Hz, 2H), 1.66 (s, 3H); ^{13}C NMR (101 MHz, $CDCl_3$) δ 146.6, 141.3, 140.7, 140.4, 139.1, 136.1, 131.9 (2C), 129.2 (2C), 128.9 (2C), 128.8, 128.3 (2C), 127.8 (2C), 127.7, 127.4 (2C), 127.1 (2C), 127.0 (2C), 121.8, 113.1, 82.8, 71.1, 50.2, 36.1, 22.4. HRMS ESI $[M+H]^+$ calculated for ($C_{31}H_{28}NO_2S^+$) 478.1835, found 478.1834.

4-Methoxy-N-((4-methoxyphenyl)ethynyl)-N-(3-methylbut-3-en-1-yl) benzenesulfonamide 627

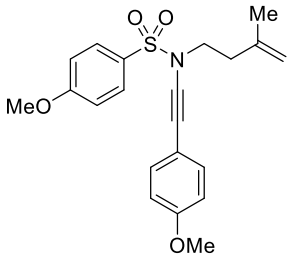

Following the **GP1** using 4-methoxy-*N*-(3-methylbut-3-en-1-yl)benzenesulfonamide (1277 mg, 5.0 mmol) and 1-(bromoethynyl)-4-methoxybenzene (1267 mg, 6.0 mmol). Purification by

flash column chromatography (10% EtOAc in hexane), the product was obtained as pale-yellow solid (1021 mg, 53% yield). ^{1}H NMR (400 MHz, $CDCl_3$) δ 7.88 (d, *J* = 8.9 Hz, 2H), 7.32 (d, *J* = 8.9 Hz, 2H), 7.01 (d, *J* = 9.0 Hz, 2H), 6.82 (d, *J* = 8.9 Hz, 2H), 4.82 – 4.78 (m, 1H), 4.75 – 4.73 (m, 1H), 3.88 (s, 3H), 3.79 (s, 3H), 3.50 (t, *J* = 7.6 Hz, 2H), 2.39 (t, *J* = 7.6 Hz, 2H), 1.75 (s, 3H); ^{13}C NMR (101 MHz, $CDCl_3$) δ 163.7, 159.6, 141.5, 133.4 (2C), 129.9 (2C), 129.2, 114.8, 114.3 (2C), 114.0 (2C), 112.8, 80.9, 70.6, 55.8, 55.4, 50.0, 36.0, 22.4. HRMS ESI $[M+H]^+$ calculated for ($C_{21}H_{24}NO_4S^+$) 386.1421, found 386.1417.

***4-Fluoro-N-((4-fluorophenyl)ethynyl)-N-(3-methylbut-3-en-1-yl)benzenesulfonamide* 628**

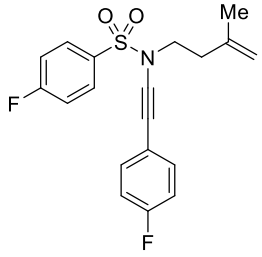

Following the **GP2** using 4-fluoro-*N*-(3-methylbut-3-en-1-yl)benzenesulfonamide (730 mg, 3.0 mmol) and 1-(bromoethynyl)-4-fluorobenzene (1260 mg, 4.5 mmol). Purification by flash column chromatography (5-10% EtOAc in hexane), the product was obtained as colourless oil (791 mg, 73% yield). ^{1}H NMR (400 MHz, $CDCl_3$) δ 7.93 – 7.85 (m, 2H), 7.30 – 7.22 (m, 2H), 7.22 – 7.11 (m, 2H), 6.98 – 6.85 (m, 2H), 4.74 – 4.71 (m, 1H), 4.67 – 4.64 (m, 1H), 3.46 (t, *J* = 7.6 Hz, 2H), 2.32 (t, *J* = 7.6 Hz, 2H), 1.66 (s, 3H); ^{13}C NMR (101 MHz, $CDCl_3$) δ 165.8 (d, $^{1}J_{C\text{-}F}$ = 257.6 Hz), 162.5 (d, $^{1}J_{C\text{-}F}$ = 250.5 Hz), 141.1, 133.69, 133.67 (d, $^{3}J_{C\text{-}F}$ = 8.1 Hz, 2C), 130.5 (d, $^{3}J_{C\text{-}F}$ = 10.1 Hz, 2C), 118.7 (d, $^{4}J_{C\text{-}F}$ = 4.0 Hz), 116.6 (d, $^{2}J_{C\text{-}F}$ = 23.2 Hz, 2C), 115.7 (d, $^{2}J_{C\text{-}F}$ = 22.2 Hz,

2C), 113.2, 81.4, 70.2, 50.1, 36.0, 22.4; ^{19}F NMR (376 MHz, $CDCl_3$) δ -103.20 – -103.30 (m, 1F), -111.01 – -111.10 (m, 1F). HRMS ESI $[M+H]^+$ calculated for ($C_{19}H_{18}NO_2S^+$) 362.1021, found 362.1018.

N-((4-(Tert-Butyl)phenyl)ethynyl)-4-methyl-N-(3-methylbut-3-en-1-yl)benzenesulfonamide

629

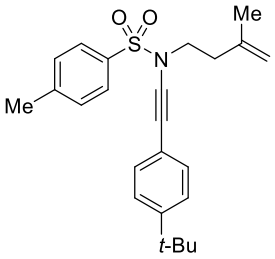

Following the **GP2** using 4-methyl-*N*-(3-methylbut-3-en-1-yl)benzenesulfonamide (1197 mg, 5.0 mmol) and 1-(bromoethynyl)-4-(*tert*-butyl)benzene (1423 mg, 6.0 mmol). Purification by flash column chromatography (5% EtOAc in hexane), the product was obtained as colourless oil (1068 mg, 54% yield). ^{1}H NMR (400 MHz, $CDCl_3$) δ 7.86 (d, *J* = 8.3 Hz, 2H), 7.36 (d, *J* = 8.3 Hz, 2H), 7.34 – 7.32 (m, 4H), 4.82 – 4.80 (m, 1H), 4.76 – 4.74 (m, 1H), 3.53 (t, *J* = 7.4 Hz, 2H), 2.46 (s, 3H), 2.41 (t, *J* = 7.4 Hz, 2H), 1.75 (s, 3H), 1.32 (s, 9H); ^{13}C NMR (101 MHz, $CDCl_3$) δ 151.3, 144.7, 141.4, 134.7, 131.4 (2C), 129.8 (2C), 127.8 (2C), 125.4 (2C), 119.9, 112.9, 81.6, 70.9, 50.1, 36.0, 34.8, 31.3 (3C), 22.4, 21.7. HRMS ESI $[M+H]^+$ calculated for ($C_{24}H_{30}NO_2S^+$) 396.1992, found 396.1989.

N-((3-Methoxyphenyl)ethynyl)-4-methyl-N-(3-methylbut-3-en-1-yl)benzenesulfonamide

630

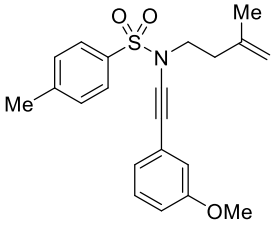

Following the **GP1** using 4-methyl-*N*-(3-methylbut-3-en-1-yl)benzenesulfonamide (1197 mg, 5.0 mmol) and 1-(bromoethynyl)-3-methoxybenzene (1266 mg, 6.0 mmol). Purification by flash column chromatography (10% EtOAc in hexane), the product was obtained as colourless oil (940 mg, 51% yield). ^{1}H NMR (600 MHz, $CDCl_3$) δ 7.85 (d, *J* = 8.3 Hz, 2H), 7.36 (d, *J* = 8.3 Hz, 2H), 7.23 – 7.18 (m, 1H), 6.99 – 6.95 (m, 1H), 6.91 (dd, *J* = 2.6, 1.4 Hz, 1H), 6.86 – 6.83 (m, 1H), 4.82 – 4.80 (m, 1H), 4.78 – 4.73 (m, 1H), 3.79 (s, 3H), 3.53 (t, *J* = 7.4 Hz, 2H), 2.45 (s, 3H), 2.41 (t, *J* = 7.4 Hz, 2H), 1.76 (s, 3H); ^{13}C NMR (151 MHz, $CDCl_3$) δ 159.4, 144.8, 141.2, 134.6, 129.8 (2C), 129.4, 127.7 (2C), 123.93, 123.86, 116.4, 114.2, 113.0, 82.1, 71.0, 55.3, 50.0, 36.0, 22.4, 21.7. HRMS ESI $[M+H]^+$ calculated for ($C_{21}H_{24}NO_3S^+$) 370.1471, found 370.1467.

***N-((4-Fluorophenyl)ethynyl)-4-methyl-N-(3-methylbut-3-en-1-yl)benzenesulfonamide* 631**

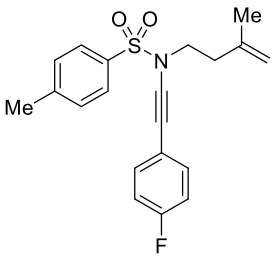

Following the **GP2** using 4-methyl-*N*-(3-methylbut-3-en-1-yl)benzenesulfonamide (957 mg, 4.0 mmol) and 1-(bromoethynyl)-4-fluorobenzene (1680 mg, 6.0 mmol). Purification by flash column chromatography (5-10% EtOAc in hexane), the product was obtained as colourless oil.

^{1}H NMR (600 MHz, $CDCl_3$) δ 7.83 (d, *J* = 8.3 Hz, 2H), 7.38 – 7.32 (m, 4H), 7.01 – 6.96 (m, 2H), 4.82 – 4.79 (m, 1H), 4.75 – 4.73 (m, 1H), 3.52 (t, *J* = 7.5 Hz, 2H), 2.45 (s, 3H), 2.49 (t, *J* = 7.5 Hz, 2H), 1.74 (s, 3H); ^{13}C NMR (151 MHz, $CDCl_3$) δ 162.4 (d, $^{1}J_{C\text{-}F}$ = 249.2 Hz), 144.8, 141.3, 134.7, 133.5 (d, $^{3}J_{C\text{-}F}$ = 8.4Hz, 2C), 129.9 (2C), 127.7 (2C), 119.0 (d, $^{4}J_{C\text{-}F}$ = 3.4 Hz), 115.6 (d, $^{2}J_{C\text{-}F}$ = 21.1 Hz, 2C), 113.0, 81.9, 69.9, 50.0, 36.0, 22.4, 21.7. ^{19}F NMR (565 MHz, $CDCl_3$) δ -111.41– -111.47 (m, 1F). HRMS ESI $[M+H]^+$ calculated for ($C_{20}H_{21}NFO_2S^+$) 358.1272, found 358.1269.

***N-((3-Fluorophenyl)ethynyl)-4-methyl-N-(3-methylbut-3-en-1-yl)benzenesulfonamide* 205**

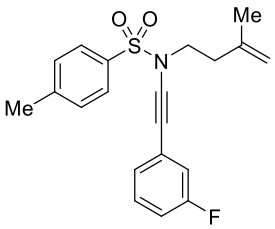

Following the **GP1** using 4-methyl-*N*-(3-methylbut-3-en-1-yl)benzenesulfonamide (718 mg, 3.0 mmol) and 1-(bromoethynyl)-3-fluorobenzene (716 mg, 3.6 mmol). Purification by flash column chromatography (5-10% EtOAc in hexane), the product was obtained as colourless oil (729 mg, 68% yield). ^{1}H NMR (400 MHz, $CDCl_3$) δ 7.86 (d, *J* = 8.3 Hz, 2H), 7.39 (d, *J* = 8.3 Hz, 2H), 7.31 – 7.24 (m, 1H), 7.18 – 7.15 (m, 1H), 7.09 – 7.05 (m, 1H), 7.02 – 6.98 (m, 1H), 4.85 – 4.82 (m, 1H), 4.80 – 4.75 (m, 1H), 3.55 (t, *J* = 7.6 Hz, 2H), 2.47 (s, 3H), 2.41 (t, *J* = 7.6 Hz, 2H), 1.78 (s, 3H); ^{13}C NMR (101 MHz, $CDCl_3$) δ 162.3 (d, $^{1}J_{C\text{-}F}$ = 247.5 Hz), 144.9, 141.1, 134.5, 129.9, 129.9 (2C), 127.6 (2C), 127.0 (d, $^{4}J_{C\text{-}F}$ = 3.0 Hz), 124.8 (d, $^{3}J_{C\text{-}F}$ = 9.6 Hz), 117.8 (d, $^{2}J_{C\text{-}F}$ = 23.3 Hz), 114.9 (d, $^{2}J_{C\text{-}F}$ = 21.2 Hz), 113.0, 83.3, 70.1 (d, $^{3}J_{C\text{-}F}$ = 3.5 Hz), 49.9, 35.9, 22.2, 21.6. ^{19}F

NMR (376 MHz, $CDCl_3$) δ -112.84 – -112.97 (m, 1F). HRMS ESI $[M+H]^+$ calculated for ($C_{20}H_{21}NFO_2S^+$) 358.1272, found 358.1270.

***N-((2-Fluorophenyl)ethynyl)-4-methyl-N-(3-methylbut-3-en-1-yl)benzenesulfonamide* 632**

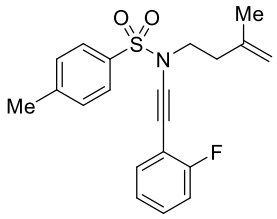

Following the **GP2** using 4-methyl-*N*-(3-methylbut-3-en-1-yl)benzenesulfonamide (718 mg, 3.0 mmol) and 1-(bromoethynyl)-2-fluorobenzene (1260 mg, 4.5 mmol). Purification by flash column chromatography (5-10% EtOAc in hexane), the product was obtained as colourless oil. ^{1}H NMR (600 MHz, $CDCl_3$) δ 7.78 (d, *J* = 8.3 Hz, 2H), 7.30 – 7.24 (m, 3H), 7.18 – 7.13 (m, 1H), 7.01 – 6.92 (m, 2H), 4.72 – 4.70 (m, 1H), 4.67 – 4.66 (s, 1H), 3.45 (t, *J* = 7.5 Hz, 2H), 2.35 (s, 3H), 2.32 (t, *J* = 7.5 Hz, 2H), 1.66 (s, 3H); ^{13}C NMR (151 MHz, $CDCl_3$) δ 162.6 (d, $^1J_{C-F}$ = 250.7 Hz), 144.9, 141.2, 134.6, 133.1, 129.9 (2C), 129.4 (d, $^3J_{C-F}$ = 7.6 Hz), 127.8 (2C), 123.98 (d, $^4J_{C-F}$ = 3.7 Hz), 115.5 (d, $^2J_{C-F}$ = 21.1 Hz), 113.1, 111.6 (d, $^2J_{C-F}$ = 15.1 Hz), 87.1, 64.9, 50.1, 35.9, 22.3, 21.7. ^{19}F NMR (565 MHz, $CDCl_3$) δ -110.24 – -110.37 (m, 1F). HRMS ESI $[M+H]^+$ calculated for ($C_{20}H_{21}NFO_2S^+$) 358.1272, found 358.1269.

***4-(tert-Butyl)-N-((3-fluorophenyl)ethynyl)-N-(3-methylbut-3-en-1-yl)benzenesulfonamide* 633**

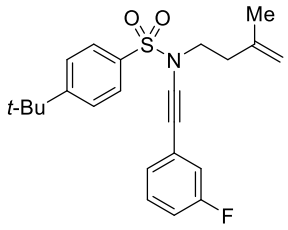

Following the **GP1** using 4-(*tert*-butyl)-*N*-(3-methylbut-3-en-1-yl)benzenesulfonamide (1126 mg, 4.0 mmol) and 1-(bromoethynyl)-3-fluorobenzene (996 mg, 5.0 mmol). Purification by flash column chromatography (5-10% EtOAc in hexane), the product was obtained as colourless oil (1054 mg, 66% yield). ^{1}H NMR (600 MHz, $CDCl_3$) δ 7.86 (d, *J* = 8.6 Hz, 2H), 7.56 (d, *J* = 8.6 Hz, 2H), 7.26 – 7.20 (m, 1H), 7.15 – 7.10 (m, 1H), 7.04 – 7.01 (m, 1H), 6.98 – 6.93 (m, 1H), 4.79 – 4.78 (m, 1H), 4.72 – 4.71 (m, 1H), 3.55 – 3.51 (m, 2H), 2.42 – 2.35 (m, 2H), 1.73 (s, 3H), 1.34 (s, 9H); ^{13}C NMR (151 MHz, $CDCl_3$) δ 162.5 (d, $^{1}J_{C\text{-}F}$ = 246.13 Hz), 157.8, 141.2, 134.7, 130.0 (d, $^{3}J_{C\text{-}F}$ = 9.1 Hz), 127.6 (2C), 127.1 (d, $^{4}J_{C\text{-}F}$ = 3.0 Hz), 126.3 (2C), 125.0 (d, $^{3}J_{C\text{-}F}$ = 9.7 Hz), 117.9 (d, $^{2}J_{C\text{-}F}$ = 22.7 Hz), 115.0 (d, $^{2}J_{C\text{-}F}$ = 21.2 Hz), 113.1, 83.4, 70.3, 50.0, 36.1, 35.4, 31.1 (3C), 22.4; ^{19}F NMR (565 MHz, $CDCl_3$) δ -113.01 – -113.07 (m, 1F). HRMS ESI $[M+H]^+$ calculated for ($C_{23}H_{27}NFO_2S^+$) 400.1741, found 400.1740.

4-(tert-Butyl)-N-((4-chlorophenyl)ethynyl)-N-(3-methylbut-3-en-1-yl)benzenesulfonamide

634

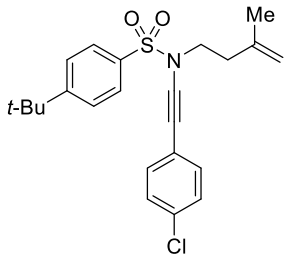

Following the **GP2** using 4-(*tert*-butyl)-*N*-(3-methylbut-3-en-1-yl)benzenesulfonamide (1126 mg, 4.0 mmol) and 1-chloro-4-(2,2-dibromovinyl)benzene (1778 mg, 6.0 mg). Purification by flash column chromatography (5-10% EtOAc in hexane), the product was obtained as colourless oil (898 mg, 54% yield). ^{1}H NMR (600 MHz, $CDCl_3$) δ 7.79 (d, *J* = 8.6 Hz, 2H), 7.49 (d, *J* = 8.6 Hz, 2H), 7.23 – 7.17 (m, 4H), 4.73 – 4.71 (m, 1H), 4.67 – 4.62 (m, 1H), 3.45 (t, *J* = 7.5 Hz, 2H), 2.31 (t, *J* = 7.5 Hz, 2H), 2.33 (s, 3H), 1.28 (s, 9H); ^{13}C NMR (151 MHz, $CDCl_3$) δ 157.8, 141.3, 134.7, 133.8, 132.6 (2C), 128.7 (2C), 127.6 (2C), 126.3 (2C), 121.6, 113.1, 83.3, 70.1, 50.0, 36.1, 35.4, 31.2 (3C), 22.4. HRMS ESI $[M+H]^+$ calculated for ($C_{23}H_{27}NClO_2S^+$) 416.1446, found 416.1443.

***N-((3-Chlorophenyl)ethynyl)-4-methyl-N-(3-methylbut-3-en-1-yl)benzenesulfonamide* 635**

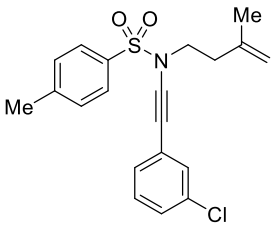

Following the **GP1** using 4-methyl-*N*-(3-methylbut-3-en-1-yl)benzenesulfonamide (957 mg, 4.0 mmol) and 1-(bromoethynyl)-3-chlorobenzene (1034 mg, 4.9 mmol). Purification by flash column chromatography (5-10% EtOAc in hexane), the product was obtained as colourless oil (910 mg, 61% yield). ^{1}H NMR (600 MHz, $CDCl_3$) δ 7.74 (d, *J* = 8.3 Hz, 2H), 7.27 (d, *J* = 8.3 Hz, 2H), 7.24 – 7.22 (m, 1H), 7.17 – 7.09 (m, 3H), 4.73 – 4.69 (m, 1H), 4.67 – 4.62 (m, 1H), 3.43 (t, *J* = 7.7 Hz, 2H), 2.35 (s, 3H), 2.30 (t, *J* = 7.7 Hz, 2H), 1.65 (s, 3H); ^{13}C NMR (151 MHz, CDCl3) δ

144.9, 141.13, 134.6, 134.1, 131.0, 129.9 (2C), 129.6, 129.3, 128.0, 127.7 (2C), 124.7, 113.1, 83.6, 70.0, 50.0, 36.0, 22.4, 21.71. HRMS ESI $[M+H]^+$ calculated for ($C_{20}H_{21}NClO_2S^+$) 374.0976, found 374.0973.

***N-((4-Bromophenyl)ethynyl)-4-methoxy-N-(3-methylbut-3-en-1-yl)benzenesulfonamide* 636**

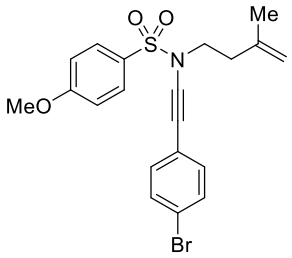

Following the **GP2** using 4-methoxy-*N*-(3-methylbut-3-en-1-yl)benzenesulfonamide (766 mg, 3.0 mmol) and 1-bromo-4-(2,2-dibromovinyl)benzene (1534 mg, 4.5 mmol). Purification by flash column chromatography (10% EtOAc in hexane), the product was obtained as pale-yellow oil (612 mg, 47% yield). ^{1}H NMR (600 MHz, $CDCl_3$) δ 7.87 (d, *J* = 8.9 Hz, 2H), 7.41 (d, *J* = 8.5 Hz, 2H), 7.21 (d, *J* = 8.5 Hz, 2H), 7.01 (d, *J* = 8.9 Hz, 2H), 4.82 – 4.79 (m, 1H), 4.75 – 4.72 (m, 1H), 3.88 (s, 3H), 3.51 (t, *J* = 7.5 Hz, 2H), 2.39 (t, *J* = 7.5 Hz, 2H), 1.74 (s, 3H); ^{13}C NMR (151 MHz, $CDCl_3$) δ 163.9, 141.3, 132.8 (2C), 131.6 (2C), 130.0 (2C), 129.2, 122.1, 121.9, 114.5 (2C), 113.0, 83.6, 70.3, 55.8, 50.0, 36.1, 22.4. HRMS ESI $[M+H]^+$ calculated for ($C_{20}H_{21}NO_3SBr^+$) 434.0420, found 434.0419.

***Methyl 4-(((4-(tert-butyl)-N-(3-methylbut-3-en-1-yl)phenyl) sulfonamido)ethynyl)benzoate* 637**

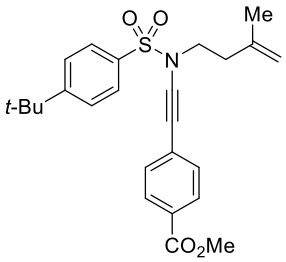

Following the **GP2** using 4-(*tert*-butyl)-*N*-(3-methylbut-3-en-1-yl)benzenesulfonamide (844 mg, 3.0 mmol) and methyl 4-(2,2-dibromovinyl)benzoate (1440 mg, 4.5 mmol). Purification by flash column chromatography (10% EtOAc in hexane), the product was obtained as pale-yellow oil (620 mg, 47% yield). ^{1}H NMR (600 MHz, $CDCl_3$) δ 7.96 (d, *J* = 8.1 Hz, 2H), 7.87 (d, *J* = 8.3 Hz, 2H), 7.57 (d, *J* = 8.3 Hz, 2H), 7.39 (d, *J* = 8.1 Hz, 2H), 4.80 – 4.78 (m, 1H), 4.74 – 4.72 (m, 1H), 3.90 (s, 3H), 3.55 (t, *J* = 7.5 Hz, 2H), 2.41 (t, *J* = 7.5 Hz, 2H), 1.74 (s, 3H), 1.34 (s, 9H); ^{13}C NMR (151 MHz, $CDCl_3$) δ 166.7, 157.9, 141.1, 134.7, 130.6 (2C), 129.6 (2C), 128.8, 128.1, 127.6 (2C), 126.4 (2C), 113.1, 85.7, 71.2, 52.3, 50.0, 36.2, 35.4, 31.1 (3C), 22.4. HRMS ESI $[M+H]^+$ calculated for ($C_{25}H_{30}NO_4S^+$) 440.1890, found 440.1887.

***N-((4-Cyanophenyl)ethynyl)-4-methyl-N-(3-methylbut-3-en-1-yl)benzenesulfonamide* 638**

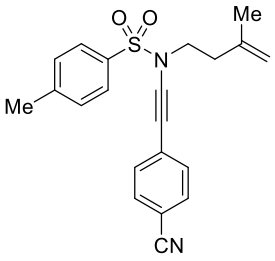

Following the **GP2** using 4-methyl-*N*-(3-methylbut-3-en-1-yl)benzenesulfonamide (718 mg, 3.0 mmol) and 4-(2,2-dibromovinyl)benzonitrile (1291 mg, 4.5 mmol). purification by flash column chromatography (20-30% EtOAc in hexane), the product was obtained as white solid (394 mg, 36% yield). ^{1}H NMR (600 MHz, $CDCl_3$) δ 7.82 (d, *J* = 8.3 Hz, 2H), 7.56 (d, *J* = 8.4 Hz, 2H), 7.40 (d, *J* = 8.4 Hz, 2H), 7.36 (d, *J* = 8.3 Hz, 2H), 4.81 – 4.79 (m, 1H), 4.73 – 4.71 (m, 1H), 3.54 (t, *J* = 7.4 Hz, 2H), 2.44 (s, 3H), 2.38 (t, *J* = 7.4 Hz, 2H), 1.73 (s, 3H); ^{13}C NMR (151 MHz, $CDCl_3$) δ 145.2, 141.0, 134.5, 132.1 (2C), 131.0 (2C), 130.0 (2C), 128.3, 127.7 (2C), 118. 7, 113.2, 110.6, 87.2, 70.7, 49.9, 36.1, 22.3, 21.7. HRMS ESI $[M+H]^+$ calculated for ($C_{21}H_{21}N_2O_2S^+$) 365.1318, found 365.1314.

***N-((4-Cyanophenyl)ethynyl)-4-methoxy-N-(3-methylbut-3-en-1-yl)benzenesulfonamide* 639**

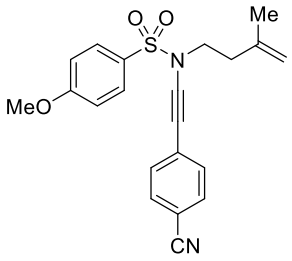

Following the **GP2** using 4-methoxy-*N*-(3-methylbut-3-en-1-yl)benzenesulfonamide (766 mg, 3.0 mmol) and 4-(2,2-dibromovinyl)benzonitrile (1381 mg, 4.5 mmol). Purification by flash column chromatography (20-30% EtOAc in hexane), the product was obtained as white solid (514 mg, 45% yield). ^{1}H NMR (600 MHz, $CDCl_3$) δ 7.87 (d, *J* = 8.9 Hz, 2H), 7.57 (d, *J* = 8.4 Hz, 2H), 7.40 (d, *J* = 8.4 Hz, 2H), 7.02 (d, *J* = 8.9 Hz, 2H), 4.84 – 4.79 (m, 1H), 4.77 – 4.25 (m, 1H), 3.89 (s, 3H), 3.55 (t, *J* = 7.5 Hz, 2H), 2.39 (t, *J* = 7.5 Hz, 2H), 1.75 (s, 3H); ^{13}C NMR (151 MHz, $CDCl_3$)

δ 164.1, 141.1, 132.1 (2C), 131.1 (2C), 130.0 (2C), 129.2, 128.4, 118.8, 114.6 (2C), 113.3, 110.6, 87.4, 70.8, 55.9, 49.9, 36.2, 22.4. HRMS ESI $[M+H]^+$ calculated for ($C_{21}H_{21}N_2O_3S^+$) 381.1267, found 381.1265.

***(1S,3S,5S)-3-Isopropyl-5-methylcyclohexyl4-(((4-methoxy-N-(3-methylbut-3-en-1-yl)phenyl)sulfonamido) ethynyl)benzoate* 640**

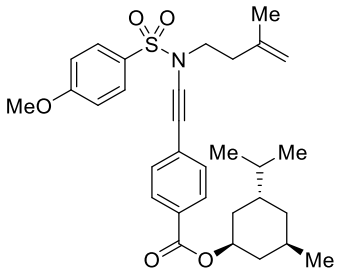

Following the **GP2** using 4-methoxy-*N*-(3-methylbut-3-en-1-yl)benzenesulfonamide (1073 mg, 4.2 mmol) and corresponding *gem*-dibromo alkene (2221 mg, 5.0 mmol). Purification by flash column chromatography (10% EtOAc in hexane), the product was obtained as colourless oil (768 mg, 34% yield). ^{1}H NMR (600 MHz, $CDCl_3$) δ 7.99 – 7.92 (m, 2H), 7.91 – 7.85 (m, 2H), 7.41 – 7.35 (m, 2H), 7.04 – 6.99 (m, 2H), 4.91 (dt, *J* = 10.9, 4.4 Hz, 1H), 4.80 (s, 1H), 4.74 (s, 1H), 3.87 (s, 3H), 3.54 (t, *J* = 7.5 Hz, 2H), 2.40 (t, *J* = 7.5 Hz, 2H), 2.13 – 2.08 (m, 1H), 1.96 – 1.90 (m, 1H), 1.75 (s, 3H), 1.74 – 1.68 (m, 2H), 1.58 – 1.50 (m, 2H), 1.17 – 1.05 (m, 2H), 0.91 (t, *J* = 6.9 Hz, 6H), 0.78 (d, *J* = 7.0 Hz, 3H); ^{13}C NMR (151 MHz, $CDCl_3$) δ 165.6, 163.9, 141.2, 130.6 (2C), 130.0 (2C), 129.5 (2C), 129.5, 129.1, 127.8, 114.5 (2C), 113.1, 85.6, 75.1, 71.2, 55.8, 49.9, 47.3, 41.0, 36.1, 34.4, 31.5, 26.6, 23.7, 22.4, 22.1, 20.8, 16.6. HRMS ESI $[M+H]^+$ calculated for ($C_{31}H_{40}NO_5S^+$) 538.2622, found 538.2631.

***(1S,2S,4R)-1,3,3-Trimethylbicyclo[2.2.1]heptan-2-yl 4-(((4-methoxy-N-(3-methylbut-3-en-1-yl)phenyl) sulfonamide)ethynyl)benzoate* 641**

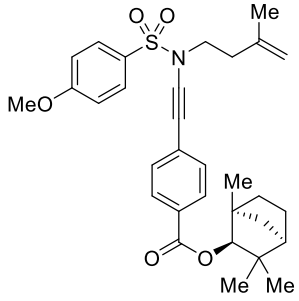

Following the **GP2** using 4-methoxy-*N*-(3-methylbut-3-en-1-yl)benzenesulfonamide (1022 mg, 4.0 mmol) and corresponding *gem*-dibromo alkene (2123 mg, 4.8 mmol). Purification by flash column chromatography (10% DCM in hexane), the product was obtained as colourless oil (960 mg, 45% yield). ^{1}H NMR (600 MHz, CDCl3) δ 1H NMR (600 MHz, $CDCl_3$) δ 8.01 – 7.94 (m, 2H), 7.92 – 7.87 (m, 2H), 7.43 – 7.37 (m, 2H), 7.05 – 7.00 (m, 2H), 4.83 – 4.80 (m, 1H), 4.74 (s, 1H), 4.61 (d, *J* = 2.0 Hz, 1H), 3.88 (s, 3H), 3.55 (t, *J* = 7.5 Hz, 2H), 2.41 (t, *J* = 7.5 Hz, 2H), 1.95 – 1.88 (m, 1H), 1.81 – 1.77 (m, 2H), 1.76 (s, 3H), 1.66 (d, *J* = 10.6 Hz, 1H), 1.55 – 1.47 (m, 1H), 1.25 (d, *J* = 10.4 Hz, 1H), 1.23 – 1.19 (m, 1H), 1.18 (s, 3H), 1.10 (s, 3H), 0.83 (s, 3H); ^{13}C NMR (151 MHz, $CDCl_3$) δ 166.5, 164.0, 141.2, 130.7 (2C), 130.0 (2C), 129.6 (2C), 129.4, 129.2, 127.9, 114.5 (2C), 113.2, 87.0, 85.7, 71.2, 55.9, 50.0, 48.8, 48.5, 41.6, 40.0, 36.2, 29.9, 27.0, 26.0, 22.5, 20.4, 19.6. HRMS ESI $[M+H]^+$ calculated for ($C_{31}H_{38}NO_5S^+$) 536.2465, found 536.2477.

***4-Fluoro-N-((4-methoxyphenyl)ethynyl)-N-(3-methylbut-3-en-1-yl)benzenesulfonamide* 642**

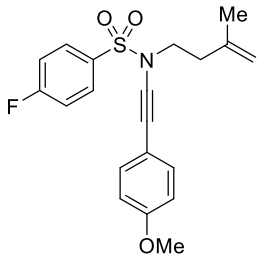

Following the **GP1** using 4-fluoro-*N*-(3-methylbut-3-en-1-yl)benzenesulfonamide (876 mg, 3.6 mmol) and 1-(bromoethynyl)-4-methoxybenzene (908 mg, 4.3 mmol). Purification by flash column chromatography (10% EtOAc in hexane), the product was obtained as colourless oil (860 mg, 64% yield). ^{1}H NMR (600 MHz, $CDCl_3$) δ 7.92 – 7.86 (m, 2H), 7.23 (d, *J* = 8.8 Hz, 2H), 7.19 – 7.13 (m, 2H), 6.75 (d, *J* = 8.8 Hz, 2H), 4.73 – 4.71 (m, 1H), 4.68 – 4.63 (m, 1H), 3.72 (s, 3H), 3.45 (t, *J* = 7.5 Hz, 2H), 2.32 (t, *J* = 7.5 Hz, 2H), 1.66 (s, 3H); ^{13}C NMR (151 MHz, $CDCl_3$) δ 165.8 (d, $^{1}J_{C\text{-}F}$ = 255.19 Hz), 159.8, 141.3, 133.7 (d, $^{4}J_{C\text{-}F}$ = 3.1 Hz), 133.6 (2C), 130.6 (d, $^{3}J_{C\text{-}F}$ = 9.5 Hz, 2C), 116.5 (d, $^{2}J_{C\text{-}F}$ = 22.7 Hz, 2C), 114.5, 114.1 (2C), 113.1, 80.3, 71.0, 55.4, 50.2, 36.0, 22.4; ^{19}F NMR (565 MHz, $CDCl_3$) δ -103.47 – -103.34 (m, 1F). HRMS ESI $[M+H]^+$ calculated for ($C_{20}H_{21}NFO_3S^+$) 374.1221, found 374.1220.

***2-Fluoro-N-((4-methoxyphenyl)ethynyl)-N-(3-methylbut-3-en-1-yl)benzenesulfonamide* 643**

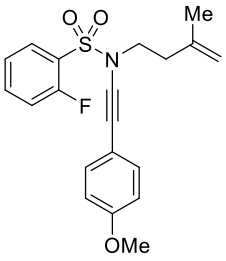

Following the **GP1** using 2-fluoro-*N*-(3-methylbut-3-en-1-yl)benzenesulfonamide (973 mg, 4.0 mmol) and 1-(bromoethynyl)-4-methoxybenzene (1460 mg, 5.0 mmol). Purification by flash

column chromatography (10% EtOAc in hexane), the product was obtained as colourless oil. ^{1}H NMR (400 MHz, $CDCl_3$) δ 7.97 – 7.87 (m, 1H), 7.65 – 7.53 (m, 1H), 7.29 – 7.23 (m, 1H), 7.23 – 7.18 (m, 3H), 6.75 (d, *J* = 8.8 Hz, 2H), 4.80 – 4.77 (m, 1H), 4.76 – 4.74 (m, 1H), 3.74 (s, 3H), 3.67 (t, *J* = 7.5 Hz, 2H), 2.43 (t, *J* = 7.5 Hz, 2H), 1.73 (s, 3H); ^{13}C NMR (101 MHz, $CDCl_3$) δ 159.7, 159.1 (d, $^{1}J_{C\text{-}F}$ = 259.6 Hz), 141.4, 136.0 (d, $^{3}J_{C\text{-}F}$ = 8.5 Hz), 133.5 (2C), 131.7, 126.0 (d, $^{3}J_{C\text{-}F}$ = 14.2 Hz), 124.5 (d, $^{4}J_{C\text{-}F}$ = 3.9 Hz), 117.5 (d, $^{2}J_{C\text{-}F}$ = 21.2 Hz), 114.7, 114.0 (2C), 113.1, 79.6, 71.2, 55.4, 50.5, 36.5, 22.5; ^{19}F NMR (376 MHz, $CDCl_3$) δ -106.78 – -106.87 (m, 1F). HRMS ESI $[M+H]^+$ calculated for ($C_{20}H_{21}NFO_3S^+$) 374.1221, found 374.1216.

***3-Chloro-N-((4-methoxyphenyl)ethynyl)-N-(3-methylbut-3-en-1-yl)benzenesulfonamide* 644**

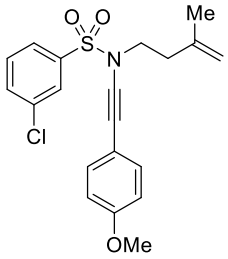

Following the **GP1** using 3-chloro-*N*-(3-methylbut-3-en-1-yl)benzenesulfonamide (1040 mg, 4.0 mmol) and 1-(bromoethynyl)-4-methoxybenzene (1460 mg, 5.0 mmol). Purification by flash column chromatography (10% EtOAc in hexane), the product was obtained as colourless oil. ^{1}H NMR (600 MHz, $CDCl_3$) δ 7.97 – 7.95 (m, 1H), 7.86 – 7.82 (m, 1H), 7.64 – 7.60 (m, 1H), 7.53 – 7.48 (m, 1H), 7.34 (d, *J* = 8.8 Hz, 2H), 6.84 (d, *J* = 8.8 Hz, 2H), 4.82 – 4.79 (m, 1H), 4.78 – 4.74 (m, 1H), 3.79 (s, 3H), 3.55 (t, *J* = 7.5 Hz, 2H), 2.40 (t, *J* = 7.5 Hz, 2H), 1.75 (s, 3H); ^{13}C NMR (151 MHz, $CDCl_3$) δ 159.7, 141.0, 139.0, 135.2, 133.7, 133.6 (2C), 130.5, 127.6, 125.7, 114.2,

114.0 (2C), 113.1, 80.0, 71.1, 55.3, 50.2, 35.9, 22.2. HRMS ESI $[M+H]^+$ calculated for ($C_{20}H_{21}NClO_3S^+$) 390.0925, found 390.0928.

N-((4-Methoxyphenyl)ethynyl)-N-(3-methylbut-3-en-1-yl)-4-(trifluoromethyl) benzenesulfonamide 645

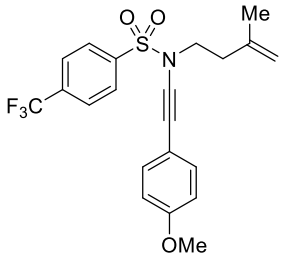

Following the **GP1** using *N*-(3-methylbut-3-en-1-yl)-4-(trifluoromethyl)benzenesulfonamide (880 mg, 3.0 mmol) and 1-(bromoethynyl)-4-methoxybenzene (760 mg, 3.6 mmol). Purification by flash column chromatography (15% DCM in hexane), the product was obtained as white solid (317 mg, 25% yield). ^{1}H NMR (600 MHz, $CDCl_3$) δ 8.09 (d, *J* = 8.2 Hz, 2H), 7.84 (d, *J* = 8.2 Hz, 2H), 7.33 (d, *J* = 8.8 Hz, 2H), 6.84 (d, *J* = 8.8 Hz, 2H), 4.83 – 4.77 (m, 1H), 4.75 – 4.73 (m, 1H), 3.81 (s, 3H), 3.56 (t, *J* = 7.4 Hz, 2H), 2.41 (t, *J* = 7.4 Hz, 2H), 1.75 (s, 3H); ^{13}C NMR (151 MHz, $CDCl_3$) δ 159.9, 141.1, 135.2 (q, $^2J_{C-F}$ = 33.2 Hz, 1C), 133.7 (2C), 128.3 (2C), 126.4 (q, $^3J_{C-F}$ = 3.7 Hz, 2C), 123.3 (q, $^1J_{C-F}$ = 273.2 Hz, 1C), 114.3, 114.2 (2C), 113.2, 79.9, 71.2, 55.4, 50.5, 36.1, 22.4. ^{19}F NMR (565 MHz, $CDCl_3$) δ -63.13 (s, 3F). HRMS ESI $[M+H]^+$ calculated for ($C_{21}H_{21}NF_3O_3S^+$) 424.1189, found 424.1187.

***N-((4-(tert-Butyl)phenyl)ethynyl)-N-(3-methylbut-3-en-1-yl)-4-(trifluoromethyl) benzenesulfonamide* 646**

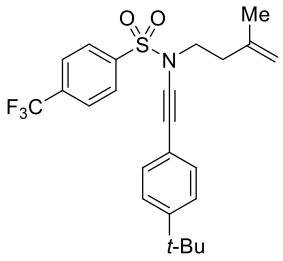

Following the **GP1** using *N*-(3-methylbut-3-en-1-yl)-4-(trifluoromethyl)benzenesulfonamide (1760 mg, 6.0 mmol) and 1-(bromoethynyl)-4-(*tert*-butyl)benzene (1707 mg, 7.2 mmol). Purification by flash column chromatography (5-10% EtOAc in hexane), the product was obtained as yellow oil (1402 mg, 52% yield). ^{1}H NMR (400 MHz, $CDCl_3$) δ 8.10 (d, *J* = 8.2 Hz, 2H), 7.84 (d, *J* = 8.2 Hz, 2H), 7.38 – 7.28 (m, 4H), 4.82 – 4.79 (m, 1H), 4.78 – 4.72 (m, 1H), 3.56 (t, *J* = 7.5 Hz, 2H), 2.40 (t, *J* = 7.5 Hz, 2H), 1.76 (s 3H), 1.32 (s, 9H); ^{13}C NMR (101 MHz, $CDCl_3$) δ 151.8, 141.1 (d, $^{4}J_{C\text{-}F}$ = 0.9 Hz), 141.1, 135.3 (q, $^{2}J_{C\text{-}F}$ = 33.2 Hz), 131.7 (2C), 128.3 (2C), 126.4 (q, $^{3}J_{C\text{-}F}$ = 3.7 Hz, 2C), 125.5 (2C), 123.3 (q, $^{1}J_{C\text{-}F}$ = 274.1 Hz), 119.3, 113.3, 80.6, 71.5, 50.5, 36.1, 34.9, 31.3 (2C), 22.4; ^{19}F NMR (376 MHz, $CDCl_3$) δ -63.14 (s, 3F). HRMS ESI $[M+H]^+$ calculated for ($C_{24}H_{27}NF_3O_2S^+$) 450.1709, found 450.1707.

***N-(But-3-en-1-yl)-N-((4-methoxyphenyl)ethynyl)-4-nitrobenzenesulfonamide* 647**

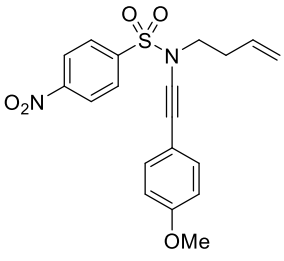

Following the **GP1** using *N*-(3-methylbut-3-en-1-yl)-4-nitrobenzenesulfonamide (770 mg, 3.0 mmol) and 1-(bromoethynyl)-4-methoxybenzene (1314 mg, 4.5 mmol). Purification by flash

column chromatography (20-30% EtOAc in hexane), the product was obtained as yellow solid (383 mg, 33% yield). ^{1}H NMR (600 MHz, $CDCl_3$) δ 8.41 (d, *J* = 8.8 Hz, 2H), 8.13 (d, *J* = 8.8 Hz, 2H), 7.32 (d, *J* = 8.8 Hz, 2H), 6.84 (d, *J* = 8.8 Hz, 2H), 5.77 – 5.68 (m, 1H), 5.14 – 5.13 (m, 1H), 5.08 – 5.05 (m, 1H), 3.82 (s, 3H), 3.52 (t, *J* = 7.2 Hz, 2H), 2.51 – 2.42 (m, 2H); ^{13}C NMR (151 MHz, $CDCl_3$) δ 160.1, 150.7, 143.1, 133.8 (2C), 133.4, 129.1 (2C), 124.5 (2C), 118.3, 114.2 (2C), 114.0, 79.5, 71.6, 55.5, 51.6, 32.4. HRMS ESI $[M+H]^+$ calculated for ($C_{19}H_{19}N_2O_5S^+$) 387.1009, found 387.1020.

3,5-Difluoro-N-((4-methoxyphenyl)ethynyl)-N-(3-methylbut-3-en-1-yl)benzenesulfonamide

648

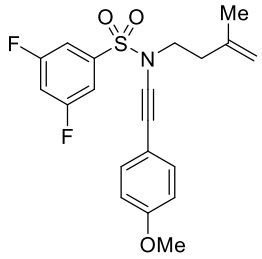

Following the **GP1** using 3,5-difluoro-*N*-(3-methylbut-3-en-1-yl)benzenesulfonamide (1306 mg, 5.0 mmol) and 1-(bromoethynyl)-4-methoxybenzene (1266 mg, 6.0 mmol). Purification by flash column chromatography (10% EtOAc in hexane), the product was obtained as white solid. ^{1}H NMR (600 MHz, $CDCl_3$) δ 7.53 – 7.47 (m, 2H), 7.34 (d, *J* = 8.8 Hz, 2H), 7.14 – 7.09 (m, 1H), 6.85 (d, *J* = 8.8 Hz, 2H), 4.83 – 4.81 (m, 1H), 4.79 – 4.74 (m, 1H), 3.81 (s, 3H), 3.56 (t, *J* = 7.5 Hz, 2H), 2.43 (t, *J* = 7.5 Hz, 2H), 1.76 (s, 3H); ^{13}C NMR (151 MHz, $CDCl_3$) δ 162.9 (d, *J* = 255.3 Hz), 162.8 (d, *J* = 255.3 Hz), 160.0, 141.1, 140.6 (t, *J* = 8.5 Hz), 133.7 (2C), 114.2 (2C), 113.3,

111.38 (d, *J* = 28.7 Hz), 111.35 (d, *J* = 15.5 Hz), 109.4 (d, *J* = 25.0 Hz), 109.3 (d, *J* = 25.0 Hz), 79.6, 71.4, 55.4, 50.6, 36.0, 22.4; ^{19}F NMR (565 MHz, $CDCl_3$) δ -105.26 (dd, *J* = 8.5, 5.6 Hz, 2F). HRMS ESI $[M+H]^+$ calculated for ($C_{20}H_{20}NF_2O_3S^+$) 392.1126, found 392.1123.

N-((3,5-Dimethylphenyl)ethynyl)-3-fluoro-N-(3-methylbut-3-en-1-yl)benzenesulfonamide

649

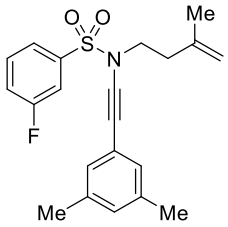

Following the **GP2** using 3-fluoro-*N*-(3-methylbut-3-en-1-yl)benzenesulfonamide (730 mg, 3.0 mmol) and 1-(2,2-dibromovinyl)-3,5-dimethylbenzene (1305 mg, 4.5 mmol). Purification by flash column chromatography (10% EtOAc in hexane), the product was obtained as colourless oil (713 mg, 64% yield). ^{1}H NMR (600 MHz, $CDCl_3$) δ 7.79 – 7.76 (m, 1H), 7.71 – 7.67 (m, 1H), 7.60 – 7.54 (m, 1H), 7.40 – 7.34 (m, 1H), 7.03 (s, 2H), 6.95 (s, 1H), 4.84 – 4.81 (m, 1H), 4.79 – 4.74 (m, 1H), 3.56 (t, *J* = 7.4 Hz, 2H), 2.43 (t, *J* = 7.4 Hz, 2H), 2.30 (s, 6H), 1.77 (s, 3H); ^{13}C NMR (151 MHz, $CDCl_3$) δ 162.4 (d, $^1J_{C\text{-}F}$ = 252.17 Hz), 141.1, 139.5 (d, $^3J_{C\text{-}F}$ = 7.6 Hz), 138.0, 131.1 (d, $^3J_{C\text{-}F}$ = 9.1 Hz), 130.1, 129.3 (2C), 123.5 (d, $^4J_{C\text{-}F}$ = 3.4 Hz), 122.1, 120.9 (d, $^2J_{C\text{-}F}$ = 21.1 Hz), 115.1 (d, $^2J_{C\text{-}F}$ = 25.7 Hz), 113.2, 80.8, 71.7, 50.3, 36.0, 22.4, 21.2 (2C); ^{19}F NMR (565 MHz, $CDCl_3$) δ -109.17 – -109.30 (m, 1F). HRMS ESI $[M+H]^+$ calculated for ($C_{21}H_{23}NFO_2S^+$) 372.1428, found 372.1426.

4-Chloro-N-(3-methylbut-3-en-1-yl)-N-((4-(methylthio)phenyl)ethynyl)benzenesulfonamide

650

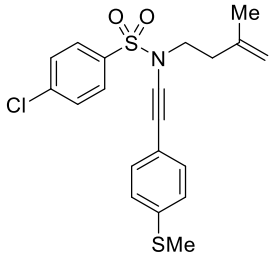

Following the **GP2** using 4-chloro-*N*-(3-methylbut-3-en-1-yl)benzenesulfonamide (1040 mg, 4.0 mmol) and (4-(2,2-dibromovinyl)phenyl)(methyl)sulfane (1480 mg, 4.8 mmol). Purification by flash column chromatography (5-10% EtOAc in hexane), the product was obtained as yellow oil (666 mg, 41% yield). ^{1}H NMR (400 MHz, $CDCl_3$) δ 7.88 (d, *J* = 8.6 Hz, 2H), 7.53 (d, *J* = 8.6 Hz, 2H), 7.28 (d, *J* = 8.5 Hz, 2H), 7.16 (d, *J* = 8.5 Hz, 2H), 4.82 – 4.80 (m, 1H), 4.75 – 4.73 (m, 1H), 3.54 (t, *J* = 7.5 Hz, 2H), 2.47 (s, 3H), 2.40 (t, *J* = 7.5 Hz, 2H), 1.74 (s, 3H); ^{13}C NMR (101 MHz, $CDCl_3$) δ 141.0, 140.2, 139.3, 135.9, 131.9 (2C), 129.4 (2C), 129.0 (2C), 125.9 (2C), 118.6, 113.1, 81.5, 70.9, 50.1, 35.9, 22.3, 15.3. HRMS ESI $[M+H]^+$ calculated for ($C_{20}H_{21}ClNO_2S_2^+$) 406.0697, found 406.0692.

3-Fluoro-N-((4-isopropylphenyl)ethynyl)-N-(3-methylbut-3-en-1-yl)benzenesulfonamide **651**

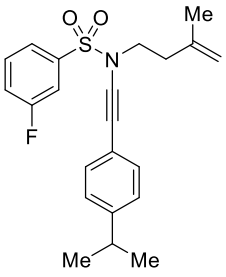

Following the **GP2** using 3-fluoro-*N*-(3-methylbut-3-en-1-yl)benzenesulfonamide (730 mg, 3.0 mmol) and 1-(2,2-dibromovinyl)-4-isopropylbenzene (1368 mg, 4.5 mmol). Purification by flash column chromatography (5-10% EtOAc in hexane), the product was obtained as colourless oil. ^{1}H NMR (600 MHz, $CDCl_3$) δ 7.79 – 7.75 (m, 1H), 7.70 – 7.67 (m, 1H), 7.59 – 7.54 (m, 1H), 7.39 – 7.35 (m, 1H), 7.34 – 7.31 (m, 2H), 7.18 (d, *J* = 8.1 Hz, 2H), 4.83 – 4.80 (m, 1H), 4.76 (s, 1H), 3.56 (t, *J* = 7.4 Hz, 2H), 2.95 – 2.84 (m, 1H), 2.42 (t, *J* = 7.4 Hz, 2H), 1.76 (s, 3H), 1.25 (d, *J* = 7.0 Hz, 6H); ^{13}C NMR (151 MHz, $CDCl_3$) δ 162.5 (d, $^{1}J_{C\text{-}F}$ = 252.2 Hz), 149.4, 141.2, 139.5 (d, $^{3}J_{C\text{-}F}$ = 6.8 Hz), 131.9 (2C), 131.1 (d, $^{3}J_{C\text{-}F}$ = 7.7 Hz), 126.6 (2C), 123.6 (d, $^{4}J_{C\text{-}F}$ = 3.4 Hz), 120.9 (d, $^{2}J_{C\text{-}F}$ = 21.2 Hz), 119.8, 115.1 (d, $^{2}J_{C\text{-}F}$ = 24.7 Hz), 113.2, 80.7, 71.4, 50.4, 36.0, 34.2, 23.9 (2C), 22.4; ^{19}F NMR (565 MHz, $CDCl_3$) δ -109.16 – -109.28 (m, 1F). HRMS ESI $[M+H]^+$ calculated for ($C_{22}H_{25}NFO_2S^+$) 386.1585, found 386.1581.

***N-((4-Methoxyphenyl)ethynyl)-N-(3-methylbut-3-en-1-yl)pyridine-3-sulfonamide* 652**

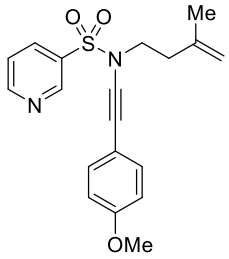

Following the **GP1** using *N*-(3-methylbut-3-en-1-yl)pyridine-3-sulfonamide (838mg, 3.7 mmol) and 1-(bromoethynyl)-4-methoxybenzene (1621 mg, 5.6 mmol). Purification by flash column chromatography (10-15% EtOAc in hexane), the product was obtained as yellow solid (554 mg, 42% yield). ^{1}H NMR (400 MHz, $CDCl_3$) δ 9.15 (d, *J* = 2.2 Hz, 1H), 8.86 (dd, *J* = 4.9, 1.6 Hz, 1H),

8.23 – 8.18 (m, 1H), 7.53 – 7.47 (m, 1H), 7.31 (d, *J* = 8.8 Hz, 2H), 6.82 (d, *J* = 8.8 Hz, 2H), 4.79 – 4.76 (m, 1H), 4.75 – 4.69 (m, 1H), 3.79 (s, 3H), 3.57 (t, *J* = 7.3 Hz, 2H), 2.39 (t, *J* = 7.3 Hz, 2H), 1.73 (s, 3H); ^{13}C NMR (101 MHz, $CDCl_3$) δ 159.9, 154.1, 148.4, 141.0, 135.3, 134.4, 133.7 (2C), 123.8, 114.1, 114.1 (2C), 113.3, 79.6, 71.5, 55.4, 50.3, 36.0, 22.3. HRMS ESI $[M+H]^+$ calculated for ($C_{19}H_{21}N_2O_3S^+$) 357.1267, found 357.1264.

***N-((3-Fluorophenyl)ethynyl)-4-methoxy-N-(3-methylbut-3-en-1-yl)benzenesulfonamide* 653**

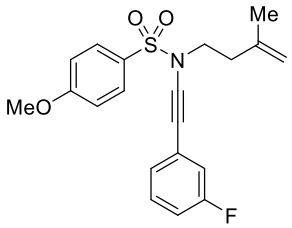

Following the **GP1** using 4-methoxy-*N*-(3-methylbut-3-en-1-yl)benzenesulfonamide (1021 mg, 4.0 mmol) and 1-(bromoethynyl)-3-fluorobenzene (995 mg, 5.0 mmol). Purification by flash column chromatography (10% EtOAc in hexane), the product was obtained as colourless oil (971 mg, 65% yield). ^{1}H NMR (600 MHz, $CDCl_3$) δ 7.78 (d, *J* = 9.0 Hz, 2H), 7.16 – 7.11 (m, 1H), 7.04 – 7.01 (m, 1H), 6.95 – 6.90 (m, 3H), 6.88 – 6.84 (m, 1H), 4.72 – 4.70 (m, 1H), 4.65 – 4.63 (m, 1H), 3.77 (s, 3H), 3.43 (t, *J* = 7.4 Hz, 2H), 2.30 (t, *J* = 7.4 Hz, 2H), 1.63 (s, 3H); ^{13}C NMR (151 MHz, $CDCl_3$) δ 163.9, 162.4 (d, $^1J_{C\text{-}F}$ = 247.6 Hz), 141.2, 130.0, 129.9 (2C), 129.0, 127.0 (d, $^4J_{C\text{-}F}$ = 3.0 Hz), 124.9 (d, $^3J_{C\text{-}F}$ = 9.7 Hz), 117.8 (d, $^2J_{C\text{-}F}$ = 22.8 Hz), 115.0 (d, $^2J_{C\text{-}F}$ = 21.2 Hz), 114.4 (2C), 113.0, 83.5, 70.2, 55.7, 49.8, 36.0, 22.3; ^{19}F NMR (565 MHz, $CDCl_3$) δ -112.98 – -113.04 (m, 1F). HRMS ESI $[M+H]^+$ calculated for ($C_{20}H_{21}NFO_3S^+$) 374.1221, found 374.1219.

***4-Methoxy-N-(3-methylbut-3-en-1-yl)-N-((4-nitrophenyl)ethynyl) benzenesulfonamide* 176**

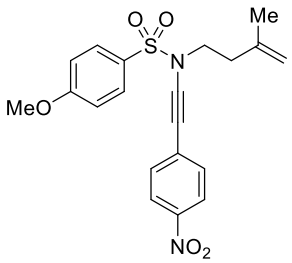

Following the **GP2** using 4-methoxy-*N*-(3-methylbut-3-en-1-yl)benzenesulfonamide (766 mg, 3.0 mmol) and 1-(2,2-dibromovinyl)-4-nitrobenzene (1120 mg, 3.65 mmol). Purification by flash column chromatography (20-30% EtOAc in hexane), the product was obtained as yellow solid (553 mg, 46% yield). ^{1}H NMR (600 MHz, $CDCl_3$) δ 8.16 (d, *J* = 8.8 Hz, 2H), 7.88 (d, *J* = 8.9 Hz, 2H), 7.45 (d, *J* = 8.8 Hz, 2H), 7.03 (d, *J* = 8.9 Hz, 2H), 4.84 – 4.80 (m, 1H), 4.75 – 4.73 (m, 1H), 3.89 (s, 3H), 3.56 (t, *J* = 7.5 Hz, 2H), 2.41 (t, *J* = 7.5 Hz, 2H), 1.76 (s, 3H); ^{13}C NMR (151 MHz, $CDCl_3$) δ 164.2, 146.4, 141.1, 131.0 (2C), 130.6, 130.1 (2C), 129.1, 123.8 (2C), 114.7 (2C), 113.3, 88.6, 71.0, 55.9, 49.9, 36.3, 22.4. HRMS ESI $[M+H]^+$ calculated for ($C_{20}H_{21}N_2O_5S^+$) 401.1166, found 401.1162.

***3-Fluoro-N-((4-methoxyphenyl)ethynyl)-N-(3-methylbut-3-en-1-yl)benzenesulfonamide* 174**

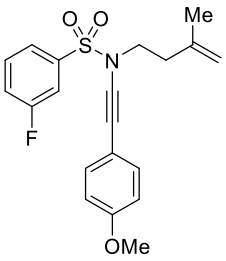

Following the **GP1** using 3-fluoro-*N*-(3-methylbut-3-en-1-yl)benzenesulfonamide (973 mg, 4.0 mmol) and 1-(bromoethynyl)-4-methoxybenzene (1460 mg, 5.0 mmol). Purification by flash column chromatography (10% EtOAc in hexane), the product was obtained as colourless oil (1046 mg, 70% yield). ^{1}H NMR (400 MHz, $CDCl_3$) δ 7.77 – 7.74 (m, 1H), 7.69 – 7.65 (m, 1H), 7.59 – 7.53 (m, 1H), 7.40 – 7.34 (m, 1H), 7.32 (d, *J* = 8.8 Hz, 2H), 6.4 (d, *J* = 8.8 Hz, 2H), 4.82 – 4.79 (m, 1H), 4.78 – 4.73 (m, 1H), 3.81 (s, 3H), 3.54 (t, *J* = 7.5 Hz, 2H), 2.40 (t, *J* = 7.5 Hz, 2H), 1.75 (s, 3H); ^{13}C NMR (101 MHz, $CDCl_3$) δ 162.5 (d, $^{1}J_{C-F}$ = 252.9 Hz), 159.8, 141.2, 139.5 (d, $^{3}J_{C-F}$ = 6.9 Hz), 133.7 (2C), 131.0 (d, $^{3}J_{C-F}$ = 7.8 Hz), 123.6 (d, $^{4}J_{C-F}$ = 3.4 Hz), 120.9 (d, $^{2}J_{C-F}$ = 21.3 Hz), 115.1 (d, $^{2}J_{C-F}$ = 24.7 Hz), 114.4, 114.1 (2C), 113.2, 80.1, 71.1, 55.4, 50.4, 36.0, 22.4; ^{19}F NMR (376 MHz, $CDCl_3$) δ -109.24 – -109.33 (m, 1F). HRMS ESI $[M+H]^+$ calculated for ($C_{20}H_{21}NFO_3S^+$) 374.1221, found 374.1219.

***N-((4-Methoxyphenyl)ethynyl)-N-(3-methylbut-3-en-1-yl)-4-nitrobenzenesulfonamide* 177**

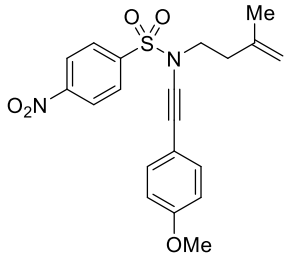

Following the **GP1** *N*-(3-methylbut-3-en-1-yl)-4-nitrobenzenesulfonamide (1081 mg, 4.0 mmol) and 1-(bromoethynyl)-4-methoxybenzene (1013 mg, 4.8 mmol). Purification by flash column chromatography (15% EtOAc in hexane), the product was obtained as yellow solid (833 mg, 52% yield). ^{1}H NMR (600 MHz, $CDCl_3$) δ 8.40 (d, *J* = 8.8 Hz, 2H), 8.14 (d, *J* = 8.8 Hz, 2H), 7.32 (d,

J = 8.7 Hz, 2H), 6.84 (d, *J* = 8.7 Hz, 2H), 4.82 – 4.79 (m, 1H), 4.75 – 4.73 (m, 1H), 3.81 (s, 3H), 3.58 (t, *J* = 7.4 Hz, 2H), 2.41 (t, *J* = 7.4 Hz, 2H), 1.75 (s, 3H); ^{13}C NMR (151 MHz, $CDCl_3$) δ 160.1, 150.7, 143.1, 141.0, 133.8 (2C), 129.0 (2C), 124.5 (2C), 114.2 (2C), 114.0, 113.4, 79.5, 71.5, 55.5, 50.6, 36.1, 22.4. HRMS ESI $[M+H]^+$ calculated for ($C_{20}H_{21}N_2O_5S^+$) 401.1166, found 401.1175.

***4-Methyl-N-(4-methylpent-4-en-1-yl)-N-(p-tolylethynyl) benzenesulfonamide* 654**

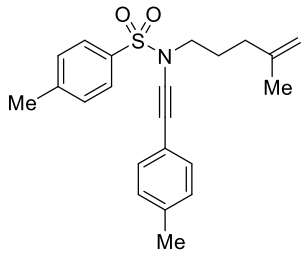

Following the **GP1** using 4-methyl-*N*-(4-methylpent-4-en-1-yl)benzenesulfonamide (507 mg, 2.0 mmol) and 1-(bromoethynyl)-4-methylbenzene (468 mg, 2.4 mmol). Purification by flash column chromatography (5-10% EtOAc in hexane), the product was obtained as colourless oil (456 mg, 62% yield). ^{1}H NMR (600 MHz, $CDCl_3$) δ 7.84 (d, *J* = 7.9 Hz, 2H), 7.35 (d, *J* = 7.9 Hz, 2H), 7.26 (d, *J* = 7.7 Hz, 2H), 7.10 (d, *J* = 7.7 Hz, 2H), 4.75 – 4.73 (m, 1H), 4.70 – 4.68 (m, 1H), 3.39 (t, *J* = 7.2 Hz, 2H), 2.45 (s, 3H), 2.34 (s, 3H), 2.07 (t, *J* = 7.6 Hz, 2H), 1.86 – 1.82 (m, 2H), 1.71 (s, 3H); ^{13}C NMR (151 MHz, $CDCl_3$) δ 144.7, 144.4, 138.1, 134.8, 131.6 (2C), 129.9 (2C), 129.2 (2C), 127.8 (2C), 119.9, 110.8, 81.7, 70.8, 51.4, 34.4, 25.9, 22.5, 21.8, 21.6. HRMS ESI $[M+H]^+$ calculated for ($C_{22}H_{26}NO_2S^+$) 368.1679, found 368.1676.

***N-((3-Fluorophenyl)ethynyl)-4-methyl-N-(pent-4-en-1-yl)benzenesulfonamide* 655**

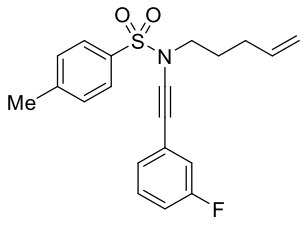

Following the **GP1** using 4-methyl-*N*-(pent-4-en-1-yl)benzenesulfonamide (958 mg, 4.0 mmol) and 1-(bromoethynyl)-3-fluorobenzene (995 mg, 5.0 mmol). Purification by flash column chromatography (5-10% EtOAc in hexane), the product was obtained as colourless oil (872 mg, 61% yield). ^{1}H NMR (600 MHz, $CDCl_3$) δ 7.85 (d, *J* = 8.2 Hz, 2H), 7.39 (d, *J* = 8.2 Hz, 2H), 7.30 – 7.24 (m, 1H), 7.18 – 7.14 (m, 1H), 7.08 – 7.04 (m, 1H), 7.03 – 6.94 (m, 1H), 5.85 – 5.76 (m, 1H), 5.10 – 5.05 (m, 1H), 5.05 – 5.01 (m, 1H), 3.44 (t, *J* = 7.2 Hz, 2H), 2.48 (s, 3H), 2.16 (t, *J* = 7.2 Hz, 2H), 1.87 – 1.80 (m, 2H); ^{13}C NMR (151 MHz, $CDCl_3$) δ 162.5 (d, $^{1}J_{C\text{-}F}$ = 246.13 Hz), 144.9, 137.1, 134.6, 129.95 (d, $^{3}J_{C\text{-}F}$ = 7.6 Hz), 129.94 (2C), 127.7 (2C), 127.1 (d, $^{4}J_{C\text{-}F}$ = 2.9 Hz), 124.9 (d, $^{3}J_{C\text{-}F}$ = 9.1 Hz), 118.0 (d, $^{2}J_{C\text{-}F}$ = 22.7 Hz), 115.8, 115.1 (d, $^{2}J_{C\text{-}F}$ = 21.1 Hz), 83.5, 69.9, 51.1, 30.4, 27.3, 21.8; ^{19}F NMR (565 MHz, $CDCl_3$) δ -113.02 – -113.10 (m, 1F). HRMS ESI $[M+H]^+$ calculated for ($C_{20}H_{21}NFO_2S^+$) 358.1272, found 358.1269.

***3,5-Difluoro-N-((4-methoxyphenyl)ethynyl)-N-(5-methylenenonyl)benzenesulfonamide* 656**

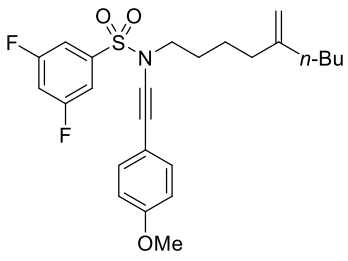

Following the **GP1** using 3,5-difluoro-*N*-(5-methylenenonyl)benzenesulfonamide (1650 mg, 5.0 mmol) and 1-(bromoethynyl)-4-methoxybenzene (1752 mg, 6.0 mmol). Purification by flash column chromatography (5% EtOAc in hexane), the product was obtained as colourless oil (950 mg, 41% yield). ^{1}H NMR (400 MHz, $CDCl_3$) δ 7.54 – 7.43 (m, 2H), 7.33 (d, *J* = 8.4 Hz, 2H), 7.14 – 7.08 (m, 1H), 6.89 – 6.80j (m, 2H), 4.75 – 4.70 (m, 1H), 4.70 – 4.68 (m, 1H), 3.81 (s, 3H), 3.44 (t, *J* = 7.1 Hz, 2H), 2.04 (t, *J* = 7.6 Hz, 2H), 1.98 (t, *J* = 7.6 Hz, 2H), 1.76 – 1.68 (m, 2H), 1.54 – 1.45 (m, 2H), 1.43 – 1.34 (m, 2H), 1.33 – 1.24 (m, 2H), 0.89 (t, *J* = 7.2 Hz, 3H); ^{13}C NMR (101 MHz, $CDCl_3$) δ 163.0 (d, $^{1}J_{C\text{-}F}$ = 256.1 Hz, 1C), 162.8 (d, $^{1}J_{C\text{-}F}$ = 256.1 Hz, 1C), 159.9, 149.3, 140.6 (t, $^{3}J_{C\text{-}F}$ = 8.8 Hz, 1C), 133.7 (2C), 114.24, 114.15 (2C), 111.4 (d, $^{2}J_{C\text{-}F}$ = 28.5 Hz, 1C), 111.3 (d, $^{3}J_{C\text{-}F}$ = 11.4 Hz, 1C), 109.32, 109.27 (t, $^{2}J_{C\text{-}F}$ = 25.0 Hz, 1C), 79.8, 71.1, 55.5, 52.2, 35.7, 35.5, 30.1, 27.6, 24.4, 22.6, 14.1; ^{19}F NMR (565 MHz, $CDCl_3$) δ -106.19 – -106.27 (m, 2F). HRMS ESI $[M+H]^+$ calculated for ($C_{25}H_{30}NF_2O_3S^+$) 462.1909, found 462.1919.

General Procedure 3 (GP3)

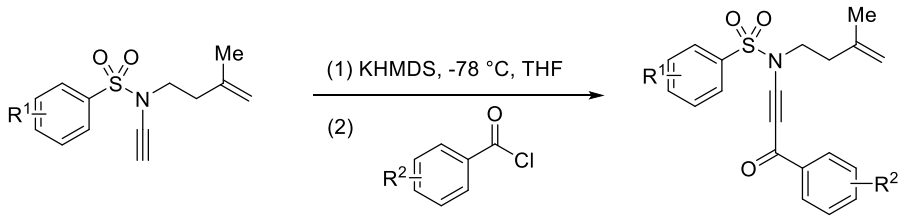

Following the method reported by Hsung and co-workers,[135] to a solution of terminal ynamide (1.0 equiv.) in THF was added Potassium bis(trimethylsilyl)amide (KHMDS, 1.0 M in THF, 1.5 equiv.) at -78 °C. The reaction mixture was stirred at -78 °C for 1 h, then corresponding benzoyl

chloride (1.0 equiv.) was added dropwise. The reaction mixture was stirred for another 0.5 h at -78 °C, and then quenched with sat. aqueous NH_4Cl. This mixture was extracted with ethyl acetate. The organic layers were dried over Na_2SO_4, filtered, and concentrated on a rotary evaporator. The crude residue was purified using silica gel flash chromatography to afford the ynamide.

***4-methoxy-N-(3-methylbut-3-en-1-yl)-N-(3-(4-nitrophenyl)-3-oxoprop-1-yn-1-yl) benzene sulfonamide* 187**

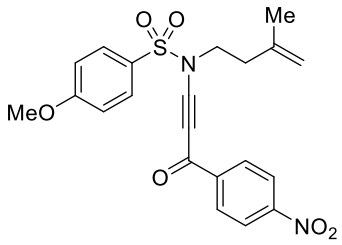

Following the **GP3**, using *N*-ethynyl-4-methoxy-*N*-(3-methylbut-3-en-1-yl) benzene sulfonamide (1196 mg, 4.28 mmol) and 4-nitrobenzoyl chloride (795 mg, 4.28 mmol). Purification by flash column chromatography (10-20% EtOAc in hexane), the product was obtained as a white solid (1136 mg, 62% yield). ^{1}H NMR (600 MHz, $CDCl_3$) δ 8.34 (d, *J* = 8.9 Hz, 2H), 8.32 (d, *J* = 8.9 Hz, 2H), 7.85 (d, *J* = 8.9 Hz, 2H), 7.03 (d, *J* = 8.9 Hz, 2H), 4.82 – 4.79 (m, 1H), 4.72 – 4.69 (m, 1H), 3.88 (s, 3H), 3.60 (t, *J* = 7.5 Hz, 2H), 2.41 (t, *J* = 7.5 Hz, 2H), 1.72 (s, 3H); ^{13}C NMR (151 MHz, $CDCl_3$) δ 174.6, 164.6, 150.7, 141.4, 140.4, 130.1 (2C), 130.1 (2C), 128.4, 123.9 (2C), 115.0 (2C), 113.7, 93.4, 77.8, 56.0, 49.6, 36.1, 22.3. HRMS ESI $[M+H]^+$ calculated for ($C_{21}H_{21}N_2O_6S^+$) 429.1115, found 429.1125.

5.2.2 Preparation of α-Trifluoromethyl Alkenes

General Procedure 4 (GP4)

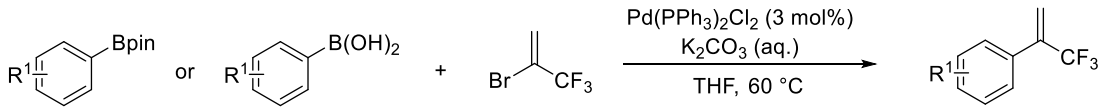

Following the method reported by Gouverneur and co-workers,[136] to a Schlenk flask equipped with stir bar was added corresponding $ArB(OH)_2$ or ArBpin (1.0 equiv.) and $Pd(PPh_3)_2Cl_2$ (3 mol%). The flask was evacuated and filled with N_2 (three times), then degassed aqueous solution of K_2CO_3 (4.0 equiv.) and THF (0.3 M) were added. After addition of 2-bromo-3,3,3-trifluoro-1-propene (2.0 equiv.), the solution was stirred at 60 °C in an oil-bath for 12 h (TLC tracking detection). Upon completion, the solvent was removed under reduced pressure and the residue was purified by column chromatography to afford the corresponding α-trifluoromethyl alkene (hexane/EtOAc). Novel compounds are reported here.

***1-(Allyloxy)-3-(3,3,3-trifluoroprop-1-en-2-yl)benzene* 657**

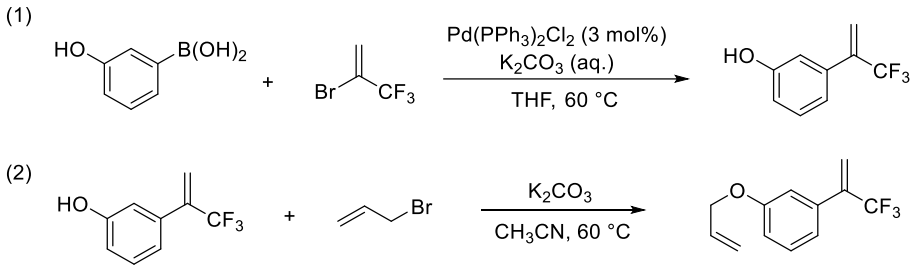

Following the **GP4** using (3-hydroxyphenyl)boronic acid (1103 mg, 8.0 mmol) and 2-bromo-3,3,3-trifluoroprop-1-ene (2379 mg, 13.6 mmol), Purification by flash column chromatography (10% EtOAc in hexane), 3-(3,3,3-trifluoroprop-1-en-2-yl)phenol was obtained as colourless oil

(1705 mg, quant yield). Then to a round bottom flask was added K_2CO_3 (1877 mg, 13.6 mmol) and CH_3CN (40 mL), followed by 3-(3,3,3-trifluoroprop-1-en-2-yl)phenol (1705 mg, 8.0 mmol). After stirring for 5 min, 3-bromoprop-1-ene was added, the resulting reaction mixture was then stirred at 60 °C in an oil-bath for 12 h. The crude product was purified by flash chromatography (hexane), the product was obtained as pale-yellow oil (1351 mg, 74% yield). ^{1}H NMR (400 MHz, $CDCl_3$) δ 7.34 – 7.28 (m, 1H), 7.09 – 7.02 (m, 2H), 6.98 – 6.93 (m, 1H), 6.08 (ddt, *J* = 17.3, 10.6, 5.3 Hz, 1H), 5.97 (q, *J* = 1.4 Hz, 1H), 5.78 (q, *J* = 1.7 Hz, 1H), 5.48 – 5.41 (m, 1H), 5.35 – 5.29 (m, 1H), 4.59 – 4.55 (m, 2H); ^{13}C NMR (101 MHz, $CDCl_3$) 158.7, 138.9 (q, $^2J_{C\text{-}F}$ = 30.2 Hz), 135.1, 133.2, 129.7, 123.4 (q, $^1J_{C\text{-}F}$ = 275.0 Hz), 120.7 (q, $^3J_{C\text{-}F}$ = 5.8 Hz), 120.1, 118.0, 115.2, 114.3, 69.0; ^{19}F NMR (376 MHz, $CDCl_3$) δ -64.73 (s, 3F). HRMS ESI $[M+H]^+$ calculated for ($C_{12}H_{12}OF_3^+$) 229.0835, found 229.0832.

***Trimethyl((4-(3,3,3-trifluoroprop-1-en-2-yl)phenyl)ethynyl)silane* 658**

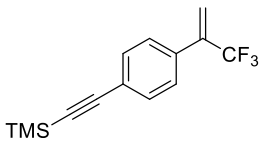

Following the **GP4** using trimethyl((4-(4,4,5,5-tetramethyl-1,3,2-dioxaborolan-2-yl)phenyl)ethynyl)silane (1201 mg, 4.0 mmol) and 2-bromo-3,3,3-trifluoroprop-1-ene (1399 mg, 8.0 mmol). Purification by flash column chromatography (hexane), the product was obtained as colourless oil (719 mg, 67% yield). ^{1}H NMR (400 MHz, $CDCl_3$) δ 7.48 (d, *J* = 8.0 Hz, 2H), 7.40 (d, *J* = 8.0 Hz, 2H), 5.97 (q, *J* = 1.4 Hz, 1H), 5.79 (q, *J* = 1.7 Hz, 1H), 0.27 (s, 9H); ^{13}C

NMR (101 MHz, $CDCl_3$) δ 138.5 (q, $^2J_{C\text{-}F}$ = 30.4 Hz), 133.6, 132.2 (2C), 127.3 (2C), 124.1, 123.3 (q, $^1J_{C\text{-}F}$ = 275.1 Hz), 120.9 (q, $^3J_{C\text{-}F}$ = 5.8 Hz), 104.4, 96.0, 0.1 (3C); ^{19}F NMR (376 MHz, $CDCl_3$) δ -64.63 (s, 3F). HRMS ESI $[M+H]^+$ calculated for ($C_{14}H_{16}F_3Si^+$) 269.0968, found 269.0965.

***Preparation of 7-phenyl-4-(trifluoromethyl)-1,2-dihydronaphthalene* 659**

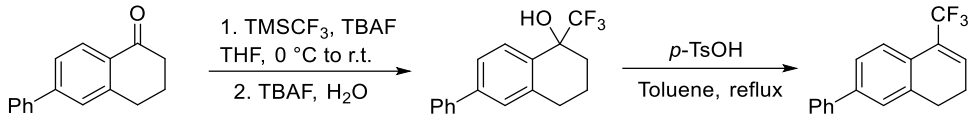

Following the method reported by Monlander and co-workers,[60] to a 250 mL Schlenk flask equipped with a stir bar was added 6-phenyl-3,4-dihydronaphthalen-1(2*H*)-one (1333 mg, 6.0 mmol), THF (60 mL), and $TMSCF_3$ (1109 mg, 7.8 mmol) under N_2. The reaction mixture was cooled to 0 °C in an ice-water bath. After stirring for approximately 10 min, TBAF (0.06 mL, 1 M in THF, 0.06 mmol) was added dropwise via a syringe. After stirring for 10 min, the ice-bath was removed, and the solution was allowed to stir overnight.

To cleave the silyl ether formed by the reaction, H_2O (600 mg, 33 mmol) was added followed by TBAF (0.6 mL, 1 M in THF, 0.6 mmol). When the cleavage was judged to be completed by TLC, the contents of the flask were transferred to a separatory funnel. H_2O and Et_2O were added, and the layers were partitioned. The aqueous layer was extracted with Et_2O. The organic layers were combined, then washed with H_2O and brine. The organic layer was dried over Na_2SO_4, and the solvent was removed under reduced pressure and the residue was purified by column chromatography to afford the alcohol (1420 mg, 81% yield).

To a 250 mL Schlenk flask equipped with a stir bar and fitted with a reflux condenser was added alcohol, *p*-TsOH•H_2O (462 mg, 2.43 mmol), and toluene (30 mL). The flask was heated in an oil-bath to reflux for 24 h. When the reaction was judged to be complete, the reaction mixture was cooled to room temperature and quenched with sat. aq. $NaHCO_3$. The reaction mixture was diluted with EtOAc and the layers were separated. The combined organic layers were washed with brine (150 mL). The organic layer was dried over Na_2SO_4, and the solvent was removed under reduced pressure and the residue was purified by column chromatography (hexane) to afford the product as colourless oil (1030 mg, 78% yield). ^{1}H NMR (600 MHz, $CDCl_3$) δ 7.66 – 7.61 (m, 2H), 7.55 – 7.50 (m, 2H), 7.50 – 7.45 (m, 3H), 7.42 – 7.37 (m, 1H), 6.78 – 6.74 (m, 1H), 2.91 (t, *J* = 8.1 Hz, 2H), 2.51 – 2.45 (m, 2H); ^{13}C NMR (151 MHz, $CDCl_3$) δ 141.1, 140.6, 136.5, 132.3 (q, $^3J_{C\text{-}F}$ = 6.3 Hz), 129.0 (2C), 128.6 (q, $^2J_{C\text{-}F}$ = 29.6 Hz), 127.7, 127.6, 127.1 (2C), 126.9, 125.6, 125.3 (q, $^1J_{C\text{-}F}$ = 273.0 Hz), 124.7, 27.6, 22.7; ^{19}F NMR (565 MHz, $CDCl_3$) δ -63.87 (s, 3F). HRMS ESI $[M\text{-}H]^-$ calculated for ($C_{17}H_{12}F_3^-$) 273.0897, found 273.0891.

5.2.3 Preparation of Potassium Alkyltrifluoroborate Compounds

General Procedure 5 (GP5)

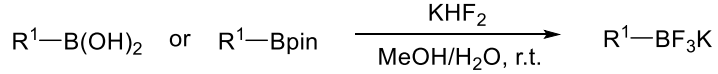

Following the method reported by Molander and co-workers,[137] to a solution of alkyl boronic acid or alkyl pinacol ester (1.0 equiv.) in methanol was added saturated aqueous KHF_2 (6.0 equiv.). The resulting suspension was stirred for 5 h at room temperature and then

concentrated to dryness. The residue was extracted with hot acetone, and the combined filtered extracts were concentrated to approximately 5 mL. Diethyl ether (or dichloromethane) was added and the resultant precipitate was collected and dried to afford the potassium alkyltrifluoroborates as a white solid. Spectra data of alkyltrifluoroborates used in this study were consistent with reported data.

5.2.4 Preparation of Vinyl Azides

General Procedure 6 (GP6)

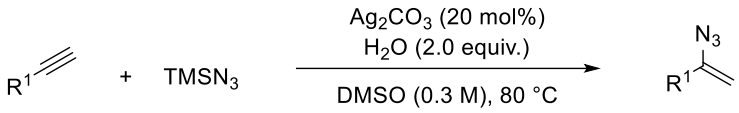

Following the method reported by Bi and co-workers,[108] to a Schlenk flask equipped with a stir bar was added alkyne (if solid, 1.0 equiv.) and Ag_2CO_3 (0.2 equiv.). The flask was evacuated and filled with N_2 (three times), DMSO (0.3 M) and H_2O (2.0 equiv.) were then added. Alkyne (if liquid) was added, followed by the addition of $TMSN_3$ (2.0 equiv.) under N_2. The resulting reaction mixture was stirred at 80 °C in an oil bath until the full consumption of the alkyne (determined by TLC). Upon completion, the reaction mixture was allowed to cool to room temperature and filtered. The filtrate was diluted with diethyl ether and poured into a separatory funnel before being washed with brine. The combined organic phases were dried over Na_2SO_4 and concentrated under reduced pressure after filtration. The crude product was purified by column chromatography to afford the corresponding vinyl azides. Novel compounds are reported here.

***1-(Allyloxy)-4-(1-azidovinyl)benzene* 660**

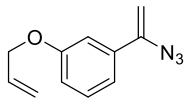

Following **GP6** using 1-(allyloxy)-3-ethynylbenzene (158 mg, 1.0 mmol), $TMSN_3$ (230 mg, 2.0 mmol), H_2O (36 mg, 2.0 mmol), Ag_2CO_3 (56 mg, 0.2 mmol) and DMSO (4.0 mL) for 3 h. Purification by flash chromatography (hexane), the product was obtained as yellow oil (133 mg, 66% yield). ^{1}H NMR (400 MHz, CD_3CN) δ 7.55 (d, *J* = 9.0 Hz, 2H), 6.96 (d, *J* = 9.0 Hz, 2H), 6.09 (ddt, *J* = 17.3, 10.5, 5.3 Hz, 1H), 5.47 – 5.38 (m, 2H), 5.32 – 5.26 (m, 1H), 4.93 (d, *J* = 2.5 Hz, 1H), 4.62 – 4.57 (m, 2H); ^{13}C NMR (101 MHz, CD_3CN) δ 160.4, 145.5, 134.4, 127.9 (2C), 127.8, 118.0, 115. 6 (2C), 97.3, 69.5. HRMS ESI $[M+H-N_2]^+$ calculated for ($C_{11}H_{12}NO^+$) 174.0913, found 174.0915.

***1-(1-Azidovinyl)-3-(trifluoromethoxy)benzene* 661**

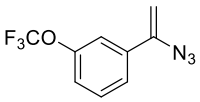

Following **GP6** using 1-ethynyl-3-(trifluoromethoxy)benzene (700 mg, 3.8 mmol), $TMSN_3$ (876 mg, 7.6 mmol), H_2O (137 mg, 7.6 mmol), Ag_2CO_3 (210 mg, 0.76 mmol) and DMSO (10.0 mL) for 3 h. Purification by flash chromatography (hexane), the product was obtained as yellow oil (444 mg, 51% yield). ^{1}H NMR (600 MHz, CD_3CN) δ 7.60 (d, *J* = 8.0 Hz, 1H), 7.52 – 7.44 (m, 2H), 7.30 (d, *J* = 8.3 Hz, 1H), 5.62 (d, *J* = 2.7 Hz, 1H), 5.10 (d, *J* = 2.7 Hz, 1H); ^{13}C NMR (151 MHz, CD_3CN) δ 150.2, 144.5, 137.5, 131.4, 125.3, 122.6, 121.6 (q, $^1J_{C-F}$ = 255.9 Hz), 119.2, 100.6; ^{19}F

NMR (377 MHz, CD_3CN) δ -58.63 (s, 3F). HRMS ESI $[M+H-N_2]^+$ calculated for ($C_9H_7F_3NO^+$) 202.0474, found 202.0473.

***5-(1-Azidovinyl)benzo[b]thiophene* 662**

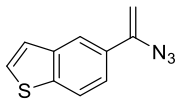

Following **GP6** using 5-ethynylbenzo[*b*]thiophene (872 mg, 5.5 mmol), $TMSN_3$ (1267 mg, 11.0 mmol), H_2O (198 mg, 11.0 mmol), Ag_2CO_3 (152 mg, 0.55 mmol) and DMSO (15 mL) for 3 h. Purification by flash chromatography (hexane), the product was obtained as a yellow solid (460 mg, 40% yield). ^1H NMR (600 MHz, CD_3CN) δ 8.08 (d, *J* = 1.6 Hz, 1H), 7.94 (d, *J* = 8.5 Hz, 1H), 7.63 – 7.58 (m, 2H), 7.42 (d, *J* = 5.4 Hz, 1H), 5.60 (d, *J* = 2.6 Hz, 1H), 5.06 (d, *J* = 2.6 Hz, 1H); ^{13}C NMR (151 MHz, CD_3CN) δ 146.0, 141.3, 140.9, 131.7, 129.0, 125.2, 123.5, 122.7, 121.6, 99.0. HRMS ESI $[M+H]^+$ calculated for ($C_{10}H_8N_3S^+$) 202.0433, found 202.0433.

***2-(1-Azidovinyl)dibenzo[b,d]furan* 663**

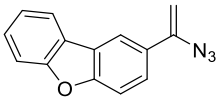

Following **GP6** using 2-ethynyldibenzo[*b*,*d*]furan (961 mg, 5.0 mmol), $TMSN_3$ (1152 mg, 10.0 mmol), H_2O (180 mg, 10 mmol), Ag_2CO_3 (138 mg, 0.5 mmol) and DMSO (15 mL) for 3 h. Purification by flash chromatography (hexane), the product was obtained as a white solid (506 mg, 43% yield). ^1H NMR (600 MHz, CD_3CN) δ 8.23 (d, *J* = 1.8 Hz, 1H), 8.04 (d, *J* = 7.7 Hz, 1H),

7.70 (dd, *J* = 8.6, 1.9 Hz, 1H), 7.59 (d, *J* = 8.3 Hz, 1H), 7.55 (d, *J* = 8.6 Hz, 1H), 7.53 – 7.48 (m, 1H), 7.40 – 7.37 (m, 1H), 5.58 (d, *J* = 2.7 Hz, 1H), 5.03 (d, *J* = 2.7 Hz, 1H); ^{13}C NMR (151 MHz, CD_3CN) δ 157.6, 157. 5, 145.9, 130.5, 128.8, 126.1, 125.3, 124.8, 124.2, 122.1, 119.3, 112.6, 112.5, 98.7. HRMS ESI $[M+H]^+$ calculated for ($C_{14}H_{10}N_3O^+$) 236.0818, found 236.0816.

***tert-Butyl 5-(1-azidovinyl)-1H-indole-1-carboxylate* 664**

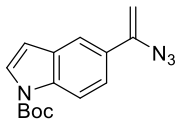

Following **GP6** using *tert*-butyl 5-ethynyl-*1*H-indole-1-carboxylate (748 mg, 3.1 mmol), $TMSN_3$ (714 mg, 6.2 mmol), H_2O (112 mg, 6.2 mmol), Ag_2CO_3 (86 mg, 0.31 mmol) and DMSO (6 mL) for 3 h. Purification by flash chromatography (hexane), the product was obtained as yellow oil (290 mg, 33% yield). ^{1}H NMR (400 MHz, CD_3CN) δ 8.10 (d, *J* = 8.8 Hz, 1H), 7.80 (d, *J* = 1.6 Hz, 1H), 7.65 (d, *J* = 3.7 Hz, 1H), 7.55 (dd, *J* = 8.8, 1.6 Hz, 1H), 6.65 – 6.61 (m, 1H), 5.51 (d, *J* = 2.5 Hz, 1H), 4.99 (d, *J* = 2.5 Hz, 1H), 1.65 (s, 9H); ^{13}C NMR (101 MHz, CD_3CN) δ 150.4, 146.2, 136.5, 131.6, 129.8, 128.1, 122.8, 119.2, 115.9, 108.3, 98.3, 85.1, 28.3 (3C). HRMS ESI $[M+H-N_2]^+$ calculated for ($C_{15}H_{17}N_2O_2^+$) 257.1285, found 257.1281.

***3-(1-Azidovinyl)thiophene* 665**

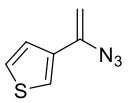

Following **GP6** using 3-ethynylthiophene (541 mg, 5.0 mmol), $TMSN_3$ (1152 mg, 10.0 mmol), H_2O (180 mg, 10 mmol), Ag_2CO_3 (275 mg, 1.0 mmol) and DMSO (15 mL) for 3 h. Purification by flash chromatography (hexane), the product was obtained as yellow oil (325 mg, 43% yield). ^1H NMR (600 MHz, CD_3CN) δ 7.50 (d, *J* = 2.9 Hz, 1H), 7.41 (dd, *J* = 5.1, 2.9 Hz, 1H), 7.31 (d, *J* = 5.1 Hz, 1H), 5.46 (d, *J* = 2.5 Hz, 1H), 4.96 (d, *J* = 2.5 Hz, 1H); ^{13}C NMR (151 MHz, CD_3CN) δ 141.9, 137.5, 128.0, 126.1, 123.9, 98.1. HRMS ESI $[M+H]^+$ calculated for ($C_6H_6N_3S^+$) 152.0277, found 152.0277.

5.2.5 Preparation of *N*-hydroxyphthalimide (NHPI) Esters

General procedure 7 (GP7)

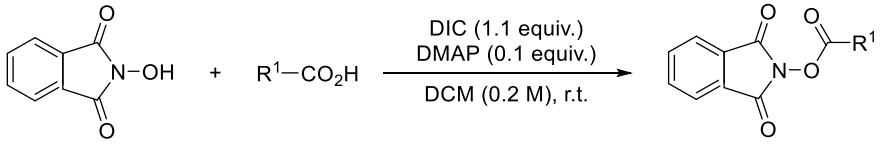

Following the method reported by Baran and co-workers,[138] a round-bottom flask was charged with carboxylic acid (if solid, 1.0 equiv.), *N*-hydroxyphthalimide (1.05 equiv.) and 4-dimethylaminopyridine (DMAP, 0.1 equiv.). Dichloromethane (0.2 M) was then added, and the reaction mixture was stirred vigorously. Carboxylic acid (if liquid, 1.0 equiv.) was added via syringe, followed by the dropwise addition of *N,N'*-diisopropylcarbodiimide (DIC, 1.1 equiv.). The resulting reaction mixture was allowed to stir at room temperature until the full consumption of the carboxylic acid (determined by TLC). Upon completion, the reaction mixture was filtered through a fritted funnel and rinsed with dichloromethane. The solvent

was removed under reduced pressure, and the residue was purified by column chromatography to give the corresponding NHPI redox-active esters.

1,3-Dioxoisoindolin-2-yl-4-oxoadamantane-1-carboxylate **666**

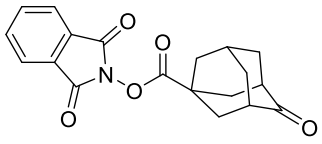

Following **GP7** using oxoadamantane-1-carboxylic acid (971.2 mg, 5.0 mmol), *N*-hydroxyphthalimide (856.4 mg, 5.25), 4-dimethylaminopyridine (61.1 mg, 0.5 mmol), *N,N'*-diisopropylcarbodiimide (694.1 mg, 5.5 mmol) and dichloromethane (25 mL). Purification by flash chromatography (EtOAc : hexane = 1 : 4), the product was obtained as a white solid (1391.3 mg, 82% yield). ^{1}H NMR (400 MHz, $CDCl_3$) δ 7.91 – 7.85 (m, 2H), 7.82 – 7.75 (m, 2H), 2.72 – 2.65 (m, 2H), 2.49 – 2.40 (m, 4H), 2.36 (d, *J* = 2.6 Hz, 2H), 2.31 – 2.25 (m, 1H), 2.13 (d, *J* = 11.4 Hz, 2H), 2.04 (d, *J* = 12.6 Hz, 2H); ^{13}C NMR (101 MHz, $CDCl_3$) δ 215.4, 171.9, 162.0 (2C), 134.9 (2C), 129.1 (2C), 124.1 (2C), 45.6 (2C), 40.2, 39.8 (2C), 38.3 (2C), 37.6, 27.2. HRMS ESI $[M+H]^+$ calculated for ($C_{19}H_{18}NO_5^+$) 340.1179, found 340.1175.

5.2.6 Preparation of Substituted 4-Cyanopyridines

General procedure 8 (GP8)

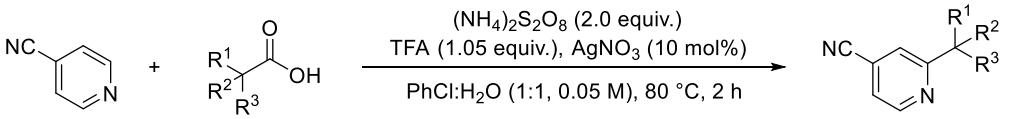

Following the method reported by Hamilton and co-workers,[139] to the solution of 4-cyanopyridine (1.0 equiv.) in PhCl / H_2O (1:1, 0.05 M) was added alkyl carboxylic acid (2.8 equiv.), $(NH_4)_2S_2O_8$ (2.0 equiv.), TFA (1.05 equiv.) and $AgNO_3$ (10 mol%). The resulting heterogeneous mixture was stirred in an oil bath at 50 °C for 2 h (TLC tracking detection). Then the reaction mixture was cooled to 0 °C and NaOH (8 M) was added slowly until pH 9~10. The mixture was filtered through a pad of Celite and extracted with ethyl acetate. The combined organic layers were dried over Na_2SO_4 and concentrated under reduced pressure after filtration. The crude product was purified by flash chromatography on silica gel to afford corresponding cyanopyridines.

***2-Cyclobutylisonicotinonitrile* 667**

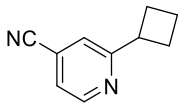

Following **GP8** using 4-cyanopyridine (1041 mg, 10.0 mmol), cyclobutanecarboxylic acid (2803 mg, 28.0 mmol), $(NH_4)_2S_2O_8$ (4564 mg, 20.0 mmol), TFA (1197 mg, 10.5 mmol) and $AgNO_3$ (170 mg, 1.0 mmol) and PhCl / H_2O (1:1, 200 mL). Purification by flash chromatography (EtOAc : hexane = 1 : 10), the product was obtained as yellow oil (855 mg, 54% yield). ^{1}H NMR (400 MHz, $CDCl_3$) δ 8.72 (dd, *J* = 5.0, 0.9 Hz, 1H), 7.36 (s, 1H), 7.31 (dd, *J* = 5.0, 1.5 Hz, 1H), 3.71 (p, *J* = 8.7 Hz, 1H), 2.43 – 2.26 (m, 4H), 2.15 – 2.02 (m, 1H), 1.97 – 1.86 (m, 1H); ^{13}C NMR (101 MHz, $CDCl_3$) δ 166.5, 150.3, 122.9, 122.4, 120.6, 117.0, 41.9, 28.4 (2C), 18.3. HRMS ESI $[M+H]^+$ calculated for ($C_{10}H_{11}N_2^+$) 159.0917, found 159.0916.

***2-(Cyclopent-3-en-1-yl)isonicotinonitrile* 668**

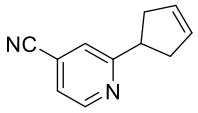

Following **GP8** using 4-cyanopyridine (521 mg, 5.0 mmol), cyclopent-3-ene-1-carboxylic acid (1401 mg, 12.5 mmol), $(NH_4)_2S_2O_8$ (2282 mg, 10.0 mmol), TFA (599 mg, 5.25 mmol) and $AgNO_3$ (85 mg, 0.5 mmol) and PhCl / H_2O (1:1, 100 mL). Purification by flash chromatography (EtOAc : hexane = 1 : 10), the product was obtained as yellow oil (272 mg, 32% yield). ^{1}H NMR (400 MHz, $CDCl_3$) δ 8.73 – 8.67 (m, 1H), 7.42 (s, 1H), 7.33 (dd, *J* = 5.0, 1.4 Hz, 1H), 5.80 – 5.74 (m, 2H), 3.75 – 3.65 (m, 1H), 2.87 (dd, *J* = 14.3, 8.9 Hz, 2H), 2.60 (dd, *J* = 14.3, 8.9 Hz, 2H); ^{13}C NMR (101 MHz, $CDCl_3$) δ 168.1, 150.3, 129.6 (2C), 123.4, 122.5, 120.8, 116.9, 44.9, 40.1 (2C). HRMS ESI $[M+H]^+$ calculated for ($C_{11}H_{11}N_2^+$) 171.0917, found 171.0915.

5.3 Smiles rearrangement products for Chapter 2

5.3.1 Synthesis of [1,2]-Annulated Indoles

General Procedure 9 (GP9)

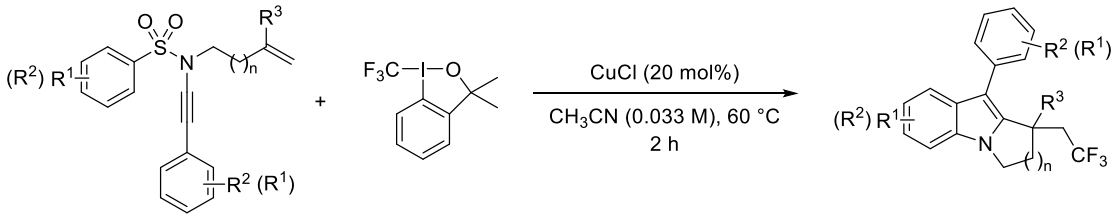

A 10-mL Schlenk tube equipped with a magnetic stir bar was charged with ynamide (0.2 mmol, if solid), CuCl (4 mg, 0.04 mmol, 20 mol%), Togni's reagent (79.2 mg, 0.24 mmol, 1.2 equiv).

The flask was evacuated and backfilled with N_2 for 3 times. CH_3CN (6 mL) or a solution of ynamide (0.2 mmol) in CH_3CN (6 mL) was then added via syringe under N_2. The reaction mixture was then vigorously stirred at 60 °C in an oil-bath for 2 h. Then the reaction mixture was diluted with ethyl acetate and poured into a separatory funnel, washed with brine for three times. The organic layers were dried over Na_2SO_4 and concentrated under reduced pressure after filtration. The crude product was purified by flash chromatography on silica gel to afford the desired product.

1,6-Dimethyl-9-(p-tolyl)-1-(2,2,2-trifluoroethyl)-2,3-dihydro-1H-pyrrolo[1,2-a]indole **140**

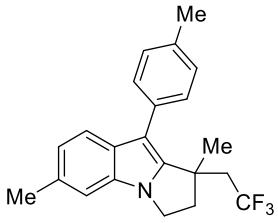

Following **GP9** using ynamide **134** (70.7 mg, 0.20 mmol) and Togni's reagent (79.2 mg, 0.24 mmol). Purification by flash chromatography (3% EtOAc in hexane), the product was obtained as a white solid (45.1 mg, 63% yield). ^{1}H NMR (600 MHz, $CDCl_3$) δ 7.42 (d, *J* = 8.2 Hz, 1H), 7.35 (d, *J* = 8.0 Hz, 2H), 7.27 (d, *J* = 8.0 Hz, 2H), 7.10 (s, 1H), 6.95 (dd, *J* = 8.2, 1.5 Hz, 1H), 4.19 – 4.15 (m, 1H), 4.14 – 4.09 (m, 1H), 2.79 – 2.71 (m, 1H), 2.71 – 2.65 (m, 1H), 2.56 – 2.52 (m, 1H), 2.51 (s, 3H), 2.45 (s, 3H), 2.39 – 2.27 (m, 1H), 1.58 (s, 3H); ^{13}C NMR (151 MHz, $CDCl_3$) δ 144.7, 136.1, 132.3, 131.7, 131.4, 130.1, 130.1 (2C), 129.3 (2C), 126.7 (q, $^1J_{C\text{-}F}$ = 278.82 Hz), 121.3, 119.4, 109.5, 108.7, 42.5, 42.2 (q, $^2J_{C\text{-}F}$ = 27.2 Hz), 42.1, 39.8, 26.1, 21.8, 21.4; ^{19}F NMR (565 MHz,

$CDCl_3$) δ -60.31 (t, *J* = 11.8 Hz, 3F). HRMS ESI $[M+H]^+$ calculated for ($C_{22}H_{23}NF_3^+$) 358.1777, found 358.1773.

1-Methyl-9-phenyl-1-(2,2,2-trifluoroethyl)-2,3-dihydro-1H-pyrrolo[1,2-a]indole **141**

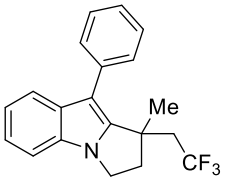

Following **GP9** using ynamide **652** (65.1 mg, 0.20 mmol) and Togni's reagent (79.2 mg, 0.24 mmol). Purification by flash chromatography (3% EtOAc in hexane), the product was obtained as a white solid (32.3 mg, 49% yield). ^{1}H NMR (400 MHz, $CDCl_3$) δ 7.53 – 7.49 (m, 1H), 7.45 – 7.43 (m, 2H), 7.43 – 7.42 (m, 2H), 7.35 – 7.30 (m, 1H), 7.27 – 7.24 (m, 1H), 7.24 – 7.16 (m, 1H), 7.10 – 7.05 (m, 1H), 4.23 – 4.09 (m, 2H), 2.80 – 2.72 (m, 1H), 2.67 – 2.57 (m, 1H), 2.57 – 2.46 (m, 1H), 2.37 – 2.25 (m, 1H), 1.56 (s, 3H); ^{13}C NMR (101 MHz, $CDCl_3$) δ 145.5, 134.6, 132.2, 131.9, 130.4 (2C), 128.6 (2C), 126.7 (q, $^1J_{C\text{-}F}$ = 279.7 Hz), 126.6, 121.6, 119.8, 119.7, 109.5, 109.0, 42.5, 42.3 (q, $^2J_{C\text{-}F}$ = 26.9 Hz), 42.3, 39.9, 26.1; ^{19}F NMR (376 MHz, $CDCl_3$) δ -60.35 (t, *J* = 11.4 Hz, 3F). HRMS ESI $[M+H]^+$ calculated for ($C_{20}H_{19}NF_3^+$) 330.1465, found 330.1462.

9-([1,1'-Biphenyl]-4-yl)-1-methyl-6-phenyl-1-(2,2,2-trifluoroethyl)-2,3-dihydro-1H-pyrrolo[1,2-a]indole **142**

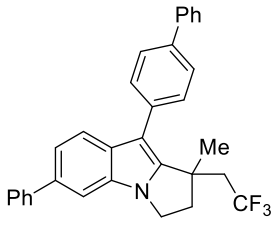

Following **GP9** using ynamide **653** (95.1 mg, 0.20 mmol) and Togni's reagent (79.2 mg, 0.24 mmol). Purification by flash chromatography (3% EtOAc in hexane), the product was obtained as a white solid (62.5 mg, 65% yield). ^{1}H NMR (400 MHz, $CDCl_3$) δ 7.78 – 7.70 (m, 6H), 7.68 (d, *J* = 8.3 Hz, 1H), 7.62 – 7.56 (m, 2H), 7.56 – 7.46 (m, 5H), 7.46 – 7.34 (m, 3H), 4.31 – 4.18 (m, 2H), 2.89 – 2.69 (m, 2H), 2.66 – 2.54 (m, 1H), 2.50 – 2.34 (m, 1H), 1.66 (s, 3H); ^{13}C NMR (101 MHz, $CDCl_3$) δ 146.3, 142.5, 140.9, 139.3, 135.5, 133.6, 132.5, 131.5, 130.6 (2C), 128.9 (2C), 128.8 (2C), 127.5 (2C), 127.4, 127.3 (2C), 127.1 (2C), 126.7, 126.6 (q, $^{1}J_{C\text{-}F}$ = 279.9 Hz), 120.0, 119.8, 108.6, 108.2, 42.5, 42.3, 42.2 (q, $^{2}J_{C\text{-}F}$ = 26.9 Hz), 40.1, 26.2; ^{19}F NMR (376 MHz, $CDCl_3$) δ -60.24 (t, *J* = 11.4 Hz, 3F). HRMS ESI $[M+H]^+$ calculated for ($C_{32}H_{27}NF_3^+$) 482.2091, found 482.2089.

6-Methoxy-9-(4-methoxyphenyl)-1-methyl-1-(2,2,2-trifluoroethyl)-2,3-dihydro-1H-pyrrolo[1,2-a]indole **143**

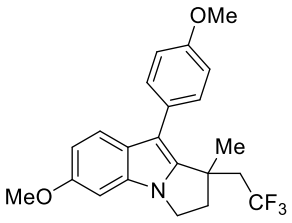

Following **GP9** using ynamide **654** (77.1 mg, 0.20 mmol) and Togni's reagent (79.2 mg, 0.24 mmol), the reaction was conducted at room temperature. Purification by flash chromatography (5-10% EtOAc in hexane), the product was obtained as a white solid (35.0 mg, 45% yield). ^{1}H NMR (600 MHz, $CDCl_3$) δ 7.38 – 7.35 (m, 3H), 7.00 (d, *J* = 8.6 Hz, 2H), 6.79 – 6.75 (m, 2H), 4.16 – 4.06 (m, 2H), 3.89 (s, 6H), 2.77 – 2.72 (m, 1H), 2.66 – 2.58 (m, 1H), 2.57 – 2.47 (m, 1H), 2.36 – 2.26 (m, 1H), 1.56 (s, 3H); ^{13}C NMR (151 MHz, $CDCl_3$) δ 158.4, 156.3, 144.1, 132.3, 131.2 (2C), 126.9, 126.8, 126.7 (q, $^{1}J_{C\text{-}F}$ = 278.9 Hz), 120.37, 114.0 (2C), 109.4, 108.3, 93.2, 55.9, 55.4, 42.5, 42.3 (q, $^{2}J_{C\text{-}F}$ = 26.6 Hz), 42.1, 39.7, 26.2; ^{19}F NMR (565 MHz, $CDCl_3$) δ -60.35 (t, *J* = 11.5 Hz, 3F). HRMS ESI $[M+H]^+$ calculated for ($C_{22}H_{23}NO_2F_3^+$) 390.1676, found 390.1672.

6-Fluoro-9-(4-fluorophenyl)-1-methyl-1-(2,2,2-trifluoroethyl)-2,3-dihydro-1H-pyrrolo[1,2-a]indole **144**

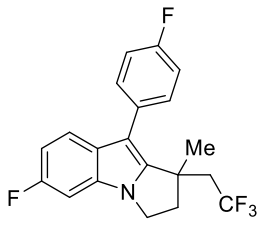

Following **GP9** using ynamide **655** (72.3 mg, 0.20 mmol) and Togni's reagent (79.2 mg, 0.24 mmol). Purification by flash chromatography (3% EtOAc in hexane), the product was obtained as a white solid (51.8 mg, 71% yield). ^{1}H NMR (600 MHz, $CDCl_3$) δ 7.38 – 7.35 (m, 2H), 7.35 – 7.32 (m, 1H), 7.17 – 7.12 (m, 2H), 6.95 (dd, *J* = 9.4, 2.3 Hz, 1H), 6.87 – 6.82 (m, 1H), 4.18 – 4.05

(m, 2H), 2.81 – 2.76 (m, 1H), 2.62 – 2.46 (m, 2H), 2.41 – 2.24 (m, 1H), 1.55 (s, 3H). ^{13}C NMR (151 MHz, $CDCl_3$) δ 162.0 (d, $^1J_{C\text{-}F}$ = 246.0 Hz), 159.8 (d, $^1J_{C\text{-}F}$ = 238.2 Hz), 145.7 (d, $^4J_{C\text{-}F}$ = 3.4 Hz), 131.8 (d, $^3J_{C\text{-}F}$ = 7.6 Hz, 2C), 131.7 (d, $^3J_{C\text{-}F}$ = 13.6 Hz), 130.2 (d, $^4J_{C\text{-}F}$ = 3.0 Hz), 128.9, 126.5 (q, $^1J_{C\text{-}F}$ = 278.8 Hz), 120.2 (d, $^3J_{C\text{-}F}$ = 10.6 Hz), 115.6 (d, $^2J_{C\text{-}F}$ = 21.1Hz, 2C), 108.4 (d, $^2J_{C\text{-}F}$ = 25.7 Hz), 108.0, 96.0 (d, $^2J_{C\text{-}F}$ = 27.2 Hz), 42.4 (q, $^2J_{C\text{-}F}$ = 26.4 Hz), 42.3, 42.3, 39.9, 26.3. ^{19}F NMR (565 MHz, $CDCl_3$) δ -60.50 (t, *J* = 11.3 Hz, 3F), -115.72 – -115.78 (m, 1F), -120.98 – -121.02 (m, 1F). HRMS ESI $[M+H]^+$ calculated for $C_{20}H_{17}NF_5^+$ 366.1276, found 366.1277.

9-(4-(Tert-butyl)phenyl)-1,6-dimethyl-1-(2,2,2-trifluoroethyl)-2,3-dihydro-1H-pyrrolo[1,2-a]indole **145** ***& 6-(Tert-butyl)-1-methyl-9-(p-tolyl)-1-(2,2,2-trifluoroethyl)-2,3-dihydro-1H-pyrrolo[1,2-a]indole*** **146**

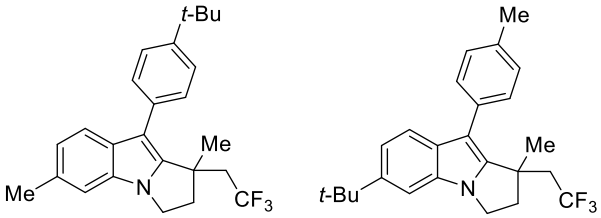

Following **GP9** using ynamide **656** (79.1 mg, 0.20 mmol) and Togni's reagent (79.2 mg, 0.24 mmol). Purification by flash chromatography (2-3% EtOAc in hexane), two regioisomers were obtained as colourless oil (47.9 mg, 60% yield). The ratio (1:1) of two regioisomers was determined by ^{19}F NMR spectroscopy of the crude reaction mixture. ^{1}H NMR (600 MHz, $CDCl_3$) δ 7.38 – 7.33 (m, 4H), 7.30 – 7.26 (m, 2H), 7.25 – 7.22 (m, 2H), 7.18 – 7.13 (m, 3H), 7.09 (dd, *J* = 8.5, 1.8 Hz, 1H), 6.98 (s, 1H), 6.83 (dd, *J* = 8.2, 1.5 Hz, 1H), 4.13 – 3.97 (m, 4H), 2.67 – 2.51

(m, 4H), 2.45 – 2.38 (m, 5H), 2.33 (s, 3H), 2.26 – 2.17 (m, 2H), 1.48 (s, 3H), 1.46 (s, 3H), 1.32 (s, 9H), 1.30 (s, 9H). ^{13}C NMR (151 MHz, $CDCl_3$) δ 149.2, 145.2, 145.2, 144.7, 136.0, 132.3, 131.8, 131.8, 131.7, 131.5, 130.2, 130.2 (2C), 130.0, 129.8 (2C), 129.3 (2C), 126.8 (q, $^1J_{C\text{-}F}$ = 278.9 Hz), 126.7 (q, $^1J_{C\text{-}F}$ = 279.0 Hz), 125.4 (2C), 121.3, 119.6, 119.3, 118.0, 109.5, 108.7, 108.6, 105.7, 42.6 (d, *J* = 6.9 Hz), 42.6, 42.3 (q, $^2J_{C\text{-}F}$ = 26.7 Hz), 42.1 (q, $^3J_{C\text{-}F}$ = 6.2 Hz), 39.8, 34.9, 34.6, 32.0 (3C), 31.5 (3C), 26.0, 26.0, 21.8, 21.4. ^{19}F NMR (565 MHz, $CDCl_3$) δ -60.22 – -60.32 (m, 6F). HRMS ESI $[M+H]^+$ calculated for $C_{25}H_{29}NF_3^+$ 400.2247, found 400.2256.

9-(3-Methoxyphenyl)-1,6-dimethyl-1-(2,2,2-trifluoroethyl)-2,3-dihydro-1H-pyrrolo[1,2-a]indole **147**

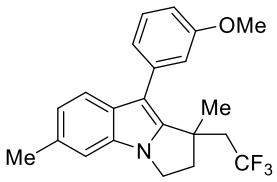

Following **GP9** using ynamide **657** (74.8 mg, 0.20 mmol) and Togni's reagent (79.2 mg, 0.24 mmol). Purification by flash chromatography (5-10% EtOAc in hexane), two regioisomers were obtained as a white solid (40.3 mg, 54% yield). The ratio (2.8:1) of two regioisomers was determined by ^{19}F NMR spectroscopy of the crude reaction mixture. Preparative TLC plates were used for further purification (5% EtOAc in hexane). Major regioisomer: ^{1}H NMR (600 MHz, $CDCl_3$) δ 7.47 (d, *J* = 8.2 Hz, 1H), 7.39 – 7.36 (m, 1H), 7.12 – 7.08 (m, 1H), 7.06 – 7.04 (m, 1H), 7.03 – 7.02 (m, 1H), 6.96 (dd, *J* = 8.2, 1.5 Hz, 1H), 6.92 – 6.89 (m, 1H), 4.20 – 4.09 (m, 2H), 3.87 (s, 3H), 2.80 – 2.66 (m, 2H), 2.56 – 2.47 (m, 4H), 2.40 – 2.30 (m, 1H), 1.60 (s, 3H). ^{13}C NMR (151

MHz, $CDCl_3$) δ 159.7, 144.8, 136.3, 132.3, 131.6, 129.9, 129.5, 126.7 (q, $^1J_{C\text{-}F}$ = 278.8 Hz), 122.7, 121.5, 119.5, 115.7, 112.1, 109.5, 108.7, 55.3, 42.6, 42.2 (q, $^2J_{C\text{-}F}$ = 26.9 Hz), 42.1, 39.8, 26.0, 21.8. ^{19}F NMR (565 MHz, $CDCl_3$) δ -60.32 (t, *J* = 11.4 Hz, 3F). HRMS ESI $[M+H]^+$ calculated for $C_{22}H_{23}NOF_3^+$ 374.1726, found 374.1740.

7-Methoxy-1-methyl-9-(p-tolyl)-1-(2,2,2-trifluoroethyl)-2,3-dihydro-1H-pyrrolo[1,2-a]indole

148

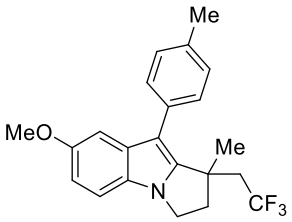

Following **GP9** using ynamide **657** (74.8 mg, 0.20 mmol) and Togni's reagent (79.2 mg, 0.24 mmol). Purification by flash chromatography (5-10% EtOAc in hexane), two regioisomers were obtained as a white solid (40.3 mg, 54% yield). The ratio (2.8:1) of two regioisomers was determined by ^{19}F NMR spectroscopy of the crude reaction mixture. Preparative TLC plates were used for further purification (5% EtOAc in hexane). Minor regioisomer: ^{1}H NMR (600 MHz, $CDCl_3$) δ 7.33 – 7.30 (m, 2H), 7.27 – 7.24 (m, 2H), 7.15 (d, *J* = 8.7 Hz, 1H), 6.95 (d, *J* = 2.4 Hz, 1H), 6.85 (dd, *J* = 8.8, 2.4 Hz, 1H), 4.17 – 4.06 (m, 2H), 3.77 (s, 3H), 2.77 – 2.70 (m, 1H), 2.65 – 2.57 (m, 1H), 2.52 – 2.46 (m, 1H), 2.42 (s, 3H), 2.37 – 2.23 (m, 1H), 1.54 (s, 3H). ^{13}C NMR (151 MHz, $CDCl_3$) δ 154.5, 146.1, 136.2, 132.6, 131.7, 130.2 (2C), 129.4 (2C), 127.2, 126.7 (q, $^1J_{C\text{-}F}$ = 278.8 Hz),111.8, 110.2, 108.6, 101.7, 56.2, 42.5, 42.4, 42.3 (q, $^2J_{C\text{-}F}$ = 26.7 Hz), 40.1, 26.1, 21.4.

^{19}F NMR (565 MHz, $CDCl_3$) δ -60.36 (t, *J* = 11.4 Hz, 3F). HRMS ESI $[M+H]^+$ calculated for $C_{22}H_{23}NOF_3^+$ 374.1726, found 374.1739.

9-(4-Fluorophenyl)-1,6-dimethyl-1-(2,2,2-trifluoroethyl)-2,3-dihydro-1H-pyrrolo[1,2-a]indole **149**

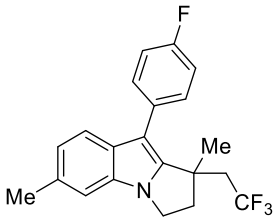

Following **GP9** using ynamide **658** (71.5 mg, 0.20 mmol) and Togni's reagent (79.2 mg, 0.24 mmol). Purification by flash chromatography (3% EtOAc in hexane), two regioisomers were obtained as a white solid (38.3 mg, 53% yield). The ratio (4:1) of two regioisomers was determined by ^{19}F NMR spectroscopy of the crude reaction mixture. The major product **93** was obtained by recrystallization (DCM/Hexane). ^{1}H NMR (600 MHz, $CDCl_3$) δ 7.41 – 7.35 (m, 2H), 7.33 (d, *J* = 8.1 Hz, 1H), 7.17 – 7.10 (m, 2H), 7.08 (s, 1H), 6.93 (dd, *J* = 8.2, 1.5 Hz, 1H), 4.18 – 4.08 (m, 2H), 2.77 – 2.73 (m, 1H), 2.61 – 2.50 (m, 2H), 2.49 (s, 3H), 2.35 – 2.26 (m, 1H), 1.54 (s, 3H). ^{13}C NMR (151 MHz, $CDCl_3$) δ 161.8 (q, $^1J_{C\text{-}F}$ = 246.1 Hz), 144.8, 132.2, 131.8 (d, $^3J_{C\text{-}F}$ = 7.9 Hz, 2C), 131.6, 130.7 (d, $^4J_{C\text{-}F}$ = 3.3 Hz), 130.2, 126.5 (q, $^1J_{C\text{-}F}$ = 278.9 Hz), 121.6, 119.2, 115.5 (d, $^2J_{C\text{-}F}$ = 21.23 Hz, 2C), 109.6, 107.7, 42.4, 42.4 (q, $^2J_{C\text{-}F}$ = 26.8 Hz), 42.1, 39.8, 26.3, 21.8. ^{19}F NMR (565 MHz, $CDCl_3$) δ -60.45 (t, *J* = 11.4 Hz), -116.28 – -116.34 (m, *J* = 14.2, 8.8, 5.6 Hz). HRMS ESI $[M+H]^+$ calculated for $C_{21}H_{20}NF_4^+$ 362.1527, found 362.1523.

9-(3-Fluorophenyl)-1,6-dimethyl-1-(2,2,2-trifluoroethyl)-2,3-dihydro-1H-pyrrolo[1,2-a]indole **151**

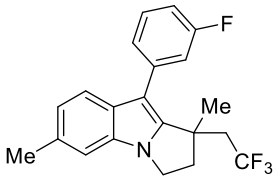

Following **GP9** using ynamide **205** (71.5 mg, 0.20 mmol) and Togni's reagent (79.2 mg, 0.24 mmol). Purification by flash chromatography (3% EtOAc in hexane), the product was obtained as a white solid (46.2 mg, 64% yield). ^{1}H NMR (600 MHz, $CDCl_3$) δ 7.46 – 7.38 (m, 2H), 7.25 – 7.22 (m, 1H), 7.19 – 7.16 (m, 1H), 7.11 (s, 1H), 7.07 – 7.03 (m, 1H), 6.98 (dd, *J* = 8.2, 1.5 Hz, 1H), 4.21 – 4.09 (m, 2H), 2.82 – 2.74 (m, 1H), 2.68 – 2.60 (m, 1H), 2.59 – 2.53 (m, 1H), 2.52 (s, 3H), 2.42 – 2.28 (m, 1H), 1.60 (s, 3H). ^{13}C NMR (151 MHz, $CDCl_3$) δ 163.0 (d, $^{1}J_{C\text{-}F}$ = 246.1 Hz), 144.9, 137.2 (d, $^{3}J_{C\text{-}F}$ = 9.1 Hz), 132.3, 131.8, 129.9 (d, $^{3}J_{C\text{-}F}$ = 9.1 Hz), 129.7, 126.6 (q, $^{1}J_{C\text{-}F}$ = 277.8 Hz), 125.9 (d, $^{4}J_{C\text{-}F}$ = 3.0 Hz), 121.8, 119.2, 116.9 (d, $^{2}J_{C\text{-}F}$ = 21.1 Hz), 113.4 (d, $^{2}J_{C\text{-}F}$ = 21.1 Hz), 109.7, 107.7 (d, $^{4}J_{C\text{-}F}$ = 3.0 Hz), 42.5, 42.3 (q, $^{2}J_{C\text{-}F}$ = 27.2 Hz), 42.1, 39.9, 26.2, 21.8. ^{19}F NMR (376 MHz, $CDCl_3$) δ -60.39 (t, *J* = 11.3 Hz, 3F), -113.23 – -113.32 (m, 1F). HRMS ESI $[M+H]^+$ calculated for $C_{21}H_{20}NF_4^+$ 362.1527, found 362.1525.

9-(2-Fluorophenyl)-1,6-dimethyl-1-(2,2,2-trifluoroethyl)-2,3-dihydro-1H-pyrrolo[1,2-a]indole **152**

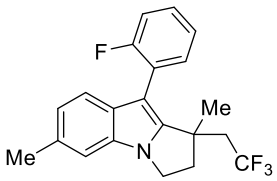

Following **GP9** using ynamide **659** (71.5 mg, 0.20 mmol) and Togni's reagent (79.2 mg, 0.24 mmol). Purification by flash chromatography (3% EtOAc in hexane), the product was obtained as a white solid (47.7 mg, 66% yield). ^{1}H NMR (600 MHz, $CDCl_3$) δ 7.38 – 7.35 (m, 1H), 7.33 – 7.30 (m, 1H), 7.22 (d, *J* = 8.1 Hz, 1H), 7.20 – 7.14 (m, 2H), 7.07 (d, *J* = 1.5 Hz, 1H), 6.91 (dd, *J* = 8.1, 1.5 Hz, 1H), 4.16 – 4.04 (m, 2H), 2.76 – 2.70 (m, 1H), 2.60 – 2.49 (m, 2H), 2.46 (s, 3H), 2.41 – 2.29 (m, 1H), 1.46 (s, 3H). ^{13}C NMR (151 MHz, $CDCl_3$) δ 160.6 (d, $^{1}J_{C\text{-}F}$ = 244.6 Hz), 145.9, 133.2 (d, $^{4}J_{C\text{-}F}$ = 1.5 Hz), 132.4, 131.6, 130.3, 128.9 (d, $^{3}J_{C\text{-}F}$ = 7.6 Hz), 126.6 (q, $^{1}J_{C\text{-}F}$ = 279.4 Hz), 124.0 (d, $^{4}J_{C\text{-}F}$ = 3.0 Hz), 122.1 (d, $^{2}J_{C\text{-}F}$ = 16.6 Hz), 121.5, 119.4, 115.9 (d, $^{2}J_{C\text{-}F}$ = 24.2 Hz), 109.6, 101.4, 42.2, 41.8 (q, $^{2}J_{C\text{-}F}$ = 25.7 Hz), 39.8, 29.8, 24.9, 21.8. ^{19}F NMR (565 MHz, $CDCl_3$) δ -60.40 (t, *J* = 11.9 Hz, 3F), -112.18 – -112.25 (m, 1F). HRMS ESI $[M+H]^+$ calculated for $C_{21}H_{20}NF_4^+$ 362.1527, found 362.1527.

9-(3-Chlorophenyl)-1,6-dimethyl-1-(2,2,2-trifluoroethyl)-2,3-dihydro-1H-pyrrolo[1,2-a]indole **153**

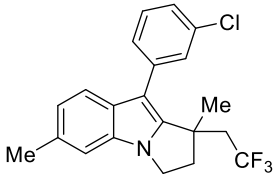

Following **GP9** using ynamide **662** (74.0 mg, 0.20 mmol) and Togni's reagent (79.2 mg, 0.24 mmol). Purification by flash chromatography (3% EtOAc in hexane), the product was obtained as a white solid (48.3 mg, 64% yield). ^{1}H NMR (600 MHz, $CDCl_3$) δ 7.46 – 7.43 (m, 1H), 7.41 – 7.35 (m, 2H), 7.38 – 7.36 (m, 1H), 7.33 – 7.30 (m, 2H), 7.09 (d, *J* = 1.5 Hz, 1H), 6.96 (dd, *J* = 8.2, 1.5 Hz, 1H), 4.19 – 4.09 (m, 2H), 2.80 – 2.73 (m, 1H), 2.66 – 2.56 (m, 1H), 2.56 – 2.50 (m, 1H), 2.50 (s, 3H), 2.37 – 2.28 (m, 1H), 1.57 (s, 3H). ^{13}C NMR (151 MHz, $CDCl_3$) δ 145.1, 136.9, 134.3, 132.2, 131.8, 130.1, 129.7, 129.7, 128.3, 126.2, 126.5 (q, $^{1}J_{C\text{-}F}$ = 278.8 Hz), 121.80, 119.1, 109.6, 107.5, 42.4, 42.3 (q, $^{2}J_{C\text{-}F}$ = 25.7 Hz), 42.1, 39.9, 26.3, 21.8. ^{19}F NMR (565 MHz, $CDCl_3$) δ -60.40 (t, *J* = 11.3 Hz, 3F). HRMS ESI $[M+H]^+$ calculated for $C_{21}H_{20}NOClF_3^+$ 378.1231, found 378.1230.

6-(tert-Butyl)-9-(3-fluorophenyl)-1-methyl-1-(2,2,2-trifluoroethyl)-2,3-dihydro-1H-pyrrolo[1,2-a]indole **154**

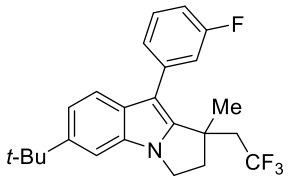

Following **GP9** using ynamide **660** (80.0 mg, 0.20 mmol) and Togni's reagent (79.2 mg, 0.24 mmol). Purification by flash chromatography (1-3% EtOAc in hexane), the product was obtained as colourless oil (47.7 mg, 59% yield). ^{1}H NMR (400 MHz, $CDCl_3$) δ 7.58 – 7.52 (m, 1H), 7.48 – 7.42 (m, 1H), 7.35 – 7.33 (m, 1H), 7.31 – 7.29 (m, 1H), 7.28 – 7.26 (m, 1H), 7.25 – 7.21 (m, 1H), 7.11 – 7.06 (m, 1H), 4.30 – 4.16 (m, 2H), 2.86 – 2.76 (m, 1H), 2.75 – 2.65 (m, 1H), 2.64 – 2.52 (m, 1H), 2.48 – 2.30 (m, 1H), 1.63 (s, 3H), 1.48 (s, 9H). ^{13}C NMR (101 MHz, $CDCl_3$) δ

163.0 (d, $^{1}J_{C\text{-}F}$ = 246.4 Hz), 145.6, 145.4, 137.3 (d, $^{3}J_{C\text{-}F}$ = 8.1 Hz), 131.9, 130.0 (d, $^{3}J_{C\text{-}F}$ = 9.1 Hz), 129.6, 126.61 (q, $^{1}J_{C\text{-}F}$ = 279.8 Hz), 125.9 (d, $^{4}J_{C\text{-}F}$ = 2.0 Hz), 119.0, 118.4, 116.9 (d, $^{2}J_{C\text{-}F}$ = 20.2 Hz), 113.3 (d, $^{2}J_{C\text{-}F}$ = 21.2 Hz), 107.6, 105.8, 42.5 (q, $^{4}J_{C\text{-}F}$ = 1.0 Hz), 42.2 (q, $^{2}J_{C\text{-}F}$ = 26.8 Hz), 42.1, 39.9, 34.9, 31.9 (3C), 26.1. ^{19}F NMR (376 MHz, $CDCl_3$) δ -60.29 (t, *J* = 11.4 Hz, 3F), -113.16 – -113.24 (m, 1F). HRMS ESI $[M+H]^+$ calculated for $C_{24}H_{26}NF_4^+$ 404.1996, found 404.1993.

6-(tert-Butyl)-9-(4-chlorophenyl)-1-methyl-1-(2,2,2-trifluoroethyl)-2,3-dihydro-1H-pyrrolo[1,2-a]indole **155**

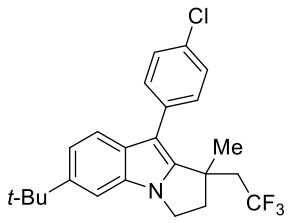

Following **GP9** using ynamide **661** (83.2 mg, 0.20 mmol) and Togni's reagent (79.2 mg, 0.24 mmol). Purification by flash chromatography (1-3% EtOAc in hexane), the product was obtained as colourless oil (52.9 mg, 63% yield). ^{1}H NMR (600 MHz, CDCl3) δ 7.41 – 7.35 (m, 3H), 7.36 – 7.31 (m, 2H), 7.24 (d, *J* = 1.7 Hz, 1H), 7.19 – 7.16 (m, 1H), 4.19 – 4.14 (m, 1H), 4.13 – 4.08 (m, 1H), 2.75 – 2.67 (m, 1H), 2.60 – 2.53 (m, 1H), 2.50 – 2.45 (m, 1H), 2.30 – 2.22 (m, 1H), 1.51 (s, 3H), 1.38 (s, 9H). ^{13}C NMR (151 MHz, $CDCl_3$) δ 145.5, 145.3, 133.4, 132.3, 131.9, 131.4 (2C), 129.7, 128.8 (2C), 126.5 (q, $^{1}J_{C\text{-}F}$ = 279.1 Hz), 118.9, 118.3, 107.4, 105.8, 42.5, 42.3 (q, $^{2}J_{C\text{-}F}$ = 26.8 Hz), 42.1, 39.8, 34.9, 31.9 (3C), 26.1. ^{19}F NMR (565 MHz, $CDCl_3$) δ -60.27 (t, *J* = 11.4 Hz, 3F). HRMS ESI $[M+H]^+$ calculated for $C_{24}H_{26}NClF_3^+$ 420.1701, found 420.1699.

9-(4-Bromophenyl)-6-methoxy-1-methyl-1-(2,2,2-trifluoroethyl)-2,3-dihydro-1H-pyrrolo[1,2-a]indole **156**

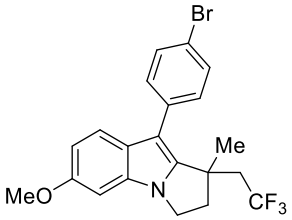

Following **GP9** using ynamide **663** (86.9 mg, 0.20 mmol) and Togni's reagent (79.2 mg, 0.24 mmol). Purification by flash chromatography (3-10% EtOAc in hexane), the product was obtained as a pale-yellow solid (49.8 mg, 57% yield). ^{1}H NMR (600 MHz, $CDCl_3$) δ 7.57 (d, *J* = 8.3 Hz, 2H), 7.35 (d, *J* = 8.7 Hz, 1H), 7.31 (d, *J* = 8.3 Hz, 2H), 6.78 (dd, *J* = 8.7, 2.3 Hz, 1H), 6.76 (d, *J* = 2.2 Hz, 1H), 4.17 – 4.06 (m, 2H), 3.88 (s, 1H), 2.77 – 2.73 (m, 1H), 2.65 – 2.56 (m, 1H), 2.55 – 2.50 (m, 1H), 2.36 – 2.27 (m, 1H), 1.56 (s, 3H). ^{13}C NMR (151 MHz, $CDCl_3$) δ 156.5, 144.3, 133.8, 132.5, 131.8 (2C), 131.7 (2C), 126.6 (q, $^{1}J_{C\text{-}F}$ = 277.8 Hz), 126.2, 120.4, 120.1, 109.8, 107.6, 93.2, 55.9, 42.4, 42.4 (q, $^{2}J_{C\text{-}F}$ = 26.9 Hz), 42.2, 39.8, 26.3. ^{19}F NMR (565 MHz, $CDCl_3$) δ -60.39 (t, *J* = 11.4 Hz, 3F). HRMS ESI $[M+H]^+$ calculated for $C_{21}H_{20}NOBrF_3^+$ 438.0675, found 438.0675.

Methyl 4-(6-(tert-butyl)-1-methyl-1-(2,2,2-trifluoroethyl)-2,3-dihydro-1H-pyrrolo[1,2-a]indol-9-yl)benzoate **157**

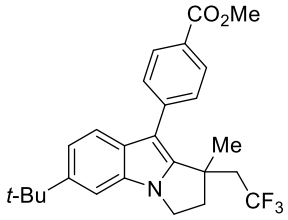

Following **GP9** using ynamide **664** (88.0 mg, 0.20 mmol) and Togni's reagent (79.2 mg, 0.24 mmol). Purification by flash chromatography (3-5% EtOAc in hexane), the product was obtained as a white solid (46.1 mg, 52% yield). ^{1}H NMR (400 MHz, $CDCl_3$) δ 8.03 (d, *J* = 8.4 Hz, 2H), 7.44 (d, *J* = 8.4 Hz, 2H), 7.40 (d, *J* = 8.5 Hz, 1H), 7.19 (d, *J* = 1.7 Hz, 1H), 7.13 (dd, *J* = 8.5, 1.7 Hz, 1H), 4.17 – 4.02 (m, 2H), 3.87 (s, 3H), 2.72 – 2.60 (m, 1H), 2.59 – 2.49 (m, 1H), 2.49 – 2.40 (m, 1H), 2.27 – 2.15 (m, 1H), 1.50 (s, 3H), 1.32 (s, 9H). ^{13}C NMR (101 MHz, $CDCl_3$) δ 167.2, 145.7, 145.7, 140.2, 132.1, 129.9 (2C), 129.9 (2C), 126.5 (q, $^{1}J_{C\text{-}F}$ = 279.8 Hz), 129.3, 128.0, 119.0, 118.5, 107.9, 105.9, 52.2, 42.6, 42.2, 42.2 (q, $^{2}J_{C\text{-}F}$ = 27.3 Hz), 40.0 (d, $^{4}J_{C\text{-}F}$ = 2.0 Hz), 34.9, 31.9 (3C), 26.1. ^{19}F NMR (376 MHz, $CDCl_3$) δ -60.32 (t, *J* = 11.3 Hz, 3F). HRMS ESI $[M+H]^+$ calculated for $C_{26}H_{29}NO_2F_3^+$ 444.2145, found 444.2144.

4-(1,6-Dimethyl-1-(2,2,2-trifluoroethyl)-2,3-dihydro-1H-pyrrolo[1,2-a]indol-9-yl)benzonitrile

158

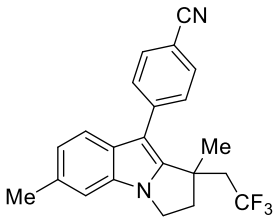

Following **GP9** using ynamide **665** (73.0 mg, 0.20 mmol) and Togni's reagent (79.2 mg, 0.24 mmol). Purification by flash chromatography (5-10% EtOAc in hexane), the product was obtained as a white solid (25.6 mg, 35% yield). ^{1}H NMR (600 MHz, CDCl3) δ 7.73 (d, *J* = 8.0 Hz, 2H), 7.57 (d, *J* = 8.0 Hz, 2H), 7.41 (d, *J* = 8.2 Hz, 1H), 7.12 (d, *J* = 1.5 Hz, 1H), 6.99 (dd, *J* = 8.3, 1.5 Hz, 1H), 4.22 – 4.11 (m, 2H), 2.82 – 2.76 (m, 1H), 2.63 – 2.53 (m, 1H), 2.51 (s, 3H), 2.37 – 2.30 (m, 1H), 1.60 (s, 3H). ^{13}C NMR (151 MHz, $CDCl_3$) δ 145.4, 140.4, 132.5, 132.4 (2C), 132.2, 130.5 (2C), 129.2, 126.4 (q, $^{1}J_{C\text{-}F}$ = 279.4 Hz), 122.2, 119.2, 118.8, 109.8, 109.7, 107.3, 42.5, 42.3 (q, $^{2}J_{C\text{-}F}$ = 27.3 Hz), 42.2, 40.0, 26.3, 21.7. ^{19}F NMR (565 MHz, $CDCl_3$) δ -60.40 (t, *J* = 11.3 Hz, 3F). HRMS ESI $[M+H]^+$ calculated for $C_{22}H_{20}N_2F_3^+$ 369.1574, found 369.1570.

4-(6-Methoxy-1-methyl-1-(2,2,2-trifluoroethyl)-2,3-dihydro-1H-pyrrolo[1,2-a]indol-9-yl)benzonitrile **159**

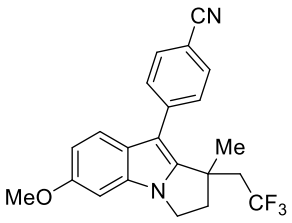

Following **GP9** using ynamide **666** (76.1 mg, 0.20 mmol) and Togni's reagent (79.2 mg, 0.24 mmol). Purification by flash chromatography (8-15% EtOAc in hexane), the product was obtained as a white solid (48.2 mg, 63% yield). ^{1}H NMR (600 MHz, $CDCl_3$) δ 7.73 (d, *J* = 7.9 Hz, 2H), 7.55 (d, *J* = 7.9 Hz, 2H), 7.38 (d, *J* = 8.7 Hz, 1H), 6.80 (dd, *J* = 8.6, 2.3 Hz, 1H), 6.77 (d, *J* = 2.3 Hz, 1H), 4.19 – 4.11 (m, 2H), 3.89 (s, 3H), 2.82 – 2.75 (m, 1H), 2.64 – 2.50 (m, 2H), 2.42 –

2.25 (m, 1H), 1.59 (s, 3H). ^{13}C NMR (151 MHz, $CDCl_3$) δ 156.7, 144.8, 140.2, 132.8, 132.4 (2C), 130.4 (2C), 126.3 (q, $^{1}J_{C\text{-}F}$ = 279.4 Hz), 125.5, 119.9, 119.2, 110.3, 109.8, 107.5, 93.3, 55.9, 42.5, 42.3 (q, $^{2}J_{C\text{-}F}$ = 25.7 Hz), 42.2, 40.0, 26.3. ^{19}F NMR (565 MHz, $CDCl_3$) δ -60.42 (t, *J* = 11.3 Hz, 3F). HRMS ESI $[M+H]^+$ calculated for $C_{22}H_{20}N_2OF_3^+$ 385.1523, found 385.1520.

(1S,3S,5S)-3-Isopropyl-5-methylcyclohexyl 4-(6-methoxy-1-methyl-1-(2,2,2-trifluoroethyl)-2,3-dihydro-1H-pyrrolo[1,2-a]indol-9-yl)benzoate **160**

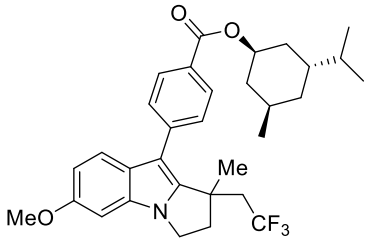

Following **GP9** using ynamide **667** (108.0 mg, 0.20 mmol) and Togni's reagent (79.2 mg, 0.24 mmol). Purification by flash chromatography (3-10% EtOAc in hexane), two inseparable diastereoisomers (1:1, estimated by HPLC) were obtained as colourless oil (60.6 mg, 56% yield). ^{1}H NMR (600 MHz, $CDCl_3$) δ 8.13 (d, *J* = 7.9 Hz, 2H), 7.52 (d, *J* = 7.9 Hz, 2H), 7.42 (d, *J* = 8.7 Hz, 1H), 6.79 (d, *J* = 8.7 Hz, 1H), 6.7 (s, 1H), 4.99 (dt, *J* = 10.9, 4.4 Hz, 1H), 4.18 – 4.09 (m, 1H), 3.89 (s, 3H), 2.81 – 2.74 (m, 1H), 2.70 – 2.60 (m, 1H), 2.59 – 2.50 (m, 1H), 2.37 – 2.27 (m, 1H), 2.24 – 2.14 (m, 1H), 2.08 – 2.03 (m, 1H), 1.80 – 1.72 (m, 2H), 1.66 – 1.55 (m, 5H), 1.21 – 1.11 (m, 2H), 1.00 – 0.92 (m, 8H), 0.85 (dd, *J* = 7.1, 2.4 Hz, 3H). ^{13}C NMR (151 MHz, $CDCl_3$) δ 13C NMR (151 MHz, $CDCl_3$) δ 166.3, 156.6, 144.7, 139.8, 132.71, 129.9 (2C), 129.9 (2C), 128.8, 126.6 (q, $^{1}J_{C\text{-}F}$ = 278.8 Hz), 126.0, 120.3, 110.0, 108.2, 93.3, 74.9, 55.9, 47.5, 42.6, 42.2 (q, $^{2}J_{C\text{-}F}$ = 27.2

Hz, 1C), 42.2, 42.1, 39.9, 34.5, 31.6, 26.6, 26.2, 23.7, 22.1, 20.9, 16.6.^{19}F NMR (565 MHz, $CDCl_3$) δ -60.30 – -60.40 (m, 3F). HRMS ESI $[M+H]^+$ calculated for $C_{32}H_{39}F_3NO_3^+$ 542.2877, found 542.2889.

(1S,2S,4R)-1,3,3-Trimethylbicyclo[2.2.1]heptan-2-yl 4-(6-methoxy-1-methyl-1-(2,2,2-trifluoroethyl)-2,3-dihydro-1H-pyrrolo[1,2-a]indol-9-yl)benzoate **161**

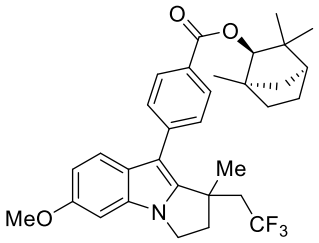

Following **GP9** using ynamide **668** (107.1 mg, 0.20 mmol) and Togni's reagent (79.2 mg, 0.24 mmol). Purification by flash chromatography (3-10% EtOAc in hexane), two inseparable diastereoisomers (1:1, estimated by HPLC) were obtained as colourless oil (58.3 mg, 54% yield). ^{1}H NMR (600 MHz, $CDCl_3$) δ 8.14 (d, *J* = 7.9 Hz, 2H), 7.53 (d, *J* = 7.9 Hz, 2H), 7.43 (d, *J* = 8.7 Hz, 1H), 6.79 (dd, *J* = 8.7, 2.2 Hz, 1H), 6.76 (d, *J* = 2.2 Hz, 1H), 4.67 (d, *J* = 2.2 Hz, 1H), 4.18 – 4.09 (m, 2H), 3.89 (s, 3H), 2.82 – 2.75 (m, 1H), 2.70 – 2.62 (m, 1H), 2.57 – 2.53 (m, 1H), 2.40 – 2.30 (m, 1H), 2.06 – 1.97 (m, 1H), 1.88 – 1.77 (m, 2H), 1.70 (d, *J* = 10.4 Hz, 1H), 1.61 (s, 3H), 1.57 – 1.52 (m, 1H), 1.28 (d, *J* = 10.4 Hz, 1H), 1.25 – 1.20 (m, 4H), 1.16 (d, *J* = 4.9 Hz, 3H), 0.92 (d, *J* = 3.6 Hz, 3H). ^{13}C NMR (151 MHz, $CDCl_3$) δ 167.0, 156.6, 144.6, 139.9, 132.7, 129.9 (2C), 129.9 (2C), 128.6, 126.6 (q, $^1J_{C-F}$ = 278.87 Hz), 126.0, 120.3, 110.0, 108.2, 93.3, 86.8, 55.9, 48.8, 48.6, 42.6, 42.3 (q, $^2J_{C-F}$ = 27.6 Hz, 1H), 42.2, 41.6, 40.0, 40.0, 29.9, 27.1, 26.2, 26.1, 20.5, 19.70. ^{19}F

NMR (565 MHz, $CDCl_3$) δ -60.32 (t, *J* = 11.3 Hz, 3F). HRMS ESI $[M+H]^+$ calculated for $C_{32}H_{37}F_3NO_3^+$ 540.2721, found 540.2731.

9-(4-Fluorophenyl)-6-methoxy-1-methyl-1-(2,2,2-trifluoroethyl)-2,3-dihydro-1H-pyrrolo[1,2-a]indole **162**

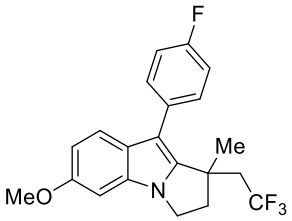

Following **GP9** using ynamide **669** (74.7 mg, 0.20 mmol) and Togni's reagent (79.2 mg, 0.24 mmol). Purification by flash chromatography (3-10% EtOAc in hexane), the product was obtained as a white solid (42.2 mg, 56% yield). ^{1}H NMR (600 MHz, $CDCl_3$) δ 7.42 – 7.37 (m, 2H), 7.34 (dd, *J* = 8.5, 0.9 Hz, 1H), 7.18 – 7.12 (m, 2H), 6.80 – 6.76 (m, 2H), 4.18 – 4.07 (m, 2H), 3.89 (s, 3H), 2.78 – 2.73 (m, 1H), 2.63 – 2.56 (m, 1H), 2.56 – 2.50 (m, 1H), 2.39 – 2.27 (m, 1H), 1.56 (s, 3H). ^{13}C NMR (151 MHz, $CDCl_3$) δ 161.8 (d, $^1J_{C-F}$ = 244.6 Hz), 156.4, 144.2, 132.4, 131.7 (d, $^3J_{C-F}$ = 7.6 Hz, 2C), 130.6 (d, $^4J_{C-F}$ = 3.0 Hz), 126.6, 126.6 (q, $^1J_{C-F}$ = 278.9 Hz), 120.2, 115.5 (d, $^2J_{C-F}$ = 21.1 Hz, 2C), 109.7, 107.8, 93.2, 55.9, 42.43, 42.4 (q, $^2J_{C-F}$ = 26.8 Hz), 42.1, 39.7, 26.2. ^{19}F NMR (565 MHz, $CDCl_3$) δ -60.45 (t, *J* = 17.1 Hz, 3F), -116.19 – -116.28 (m, 1F). HRMS ESI $[M+H]^+$ calculated for $C_{21}H_{20}NOF_4^+$ 378.1476, found 378.1473.

9-(2-Fluorophenyl)-6-methoxy-1-methyl-1-(2,2,2-trifluoroethyl)-2,3-dihydro-1H-pyrrolo[1,2-a]indole **163**

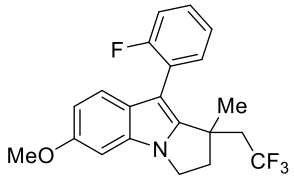

Following **GP9** using ynamide **670** (74.7 mg, 0.20 mmol) and Togni's reagent (79.2 mg, 0.24 mmol). Purification by flash chromatography (3-8% EtOAc in hexane), the product was obtained as a white solid (43.7 mg, 58% yield). ^{1}H NMR (400 MHz, $CDCl_3$) δ 7.44 – 7.33 (m, 2H), 7.29 – 7.16 (m, 3H), 6.80 – 6.76 (m, 2H), 4.21 – 4.08 (m, 2H), 3.89 (s, 3H), 2.82 – 2.74 (m, 1H), 2.63 – 2.44 (m, 2H), 2.44 – 2.31 (m, 1H), 1.51 (s, 3H). ^{13}C NMR (101 MHz, CDCl3) δ 160.6 (d, $^{1}J_{C\text{-}F}$ = 245.4 Hz), 156.4, 145.3, 133.1 (d, $^{4}J_{C\text{-}F}$ = 4.0 Hz), 132.5, 128.91 (d, $^{3}J_{C\text{-}F}$ = 8.1 Hz), 126.7, 126.6 (q, $^{1}J_{C\text{-}F}$ = 279.8 Hz), 124.1 (d, $^{4}J_{C\text{-}F}$ = 4.0 Hz), 122.0 (d, $^{2}J_{C\text{-}F}$ = 16.7 Hz), 120.4, 115.9 (d, $^{2}J_{C\text{-}F}$ = 22.2 Hz), 109.7, 101.5, 93.3, 55.9, 42.2 (2C), 41.8 (q, $^{2}J_{C\text{-}F}$ = 28.3 Hz), 39.7, 25.0. ^{19}F NMR (376 MHz, $CDCl_3$) δ -60.41 (t, *J* = 11.4 Hz, 3F), -112.27 – -112.35 (m, 1F). HRMS ESI $[M+H]^+$ calculated for $C_{21}H_{20}NOF_4^+$ 378.1476, found 378.1476.

9-(3-Chlorophenyl)-6-methoxy-1-methyl-1-(2,2,2-trifluoroethyl)-2,3-dihydro-1H-pyrrolo[1,2-a]indole **164**

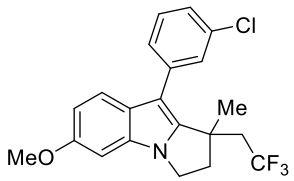

Following **GP9** using ynamide **671** (78.0 mg, 0.20 mmol) and Togni's reagent (79.2 mg, 0.24 mmol). Purification by flash chromatography (3-8% EtOAc in hexane), the product was

obtained as a white solid (44.0 mg, 56% yield). ^{1}H NMR (600 MHz, $CDCl_3$) δ 7.46 – 7.44 (m, 1H), 7.40 – 7.36 (m, 2H), 7.35 – 7.30 (m, 2H), 6.79 (dd, *J* = 8.7, 2.3 Hz, 1H), 6.76 (d, *J* = 2.3 Hz, 1H), 4.18 – 4.08 (m, 2H), 3.89 (s, 3H), 2.80 – 2.74 (m, 1H), 2.67 – 2.57 (m, 1H), 2.57 – 2.50 (m, 1H), 2.39 – 2.30 (m, 1H), 1.58 (s, 3H). ^{13}C NMR (151 MHz, $CDCl_3$) δ 156.5, 144.4, 136.8, 134.4, 132.5, 130.1, 129.8, 128.3, 126.6, 126.5 (q, $^{1}J_{C\text{-}F}$ = 278.9 Hz), 126.2, 120.2, 109.9, 107.6, 93.3, 55.9, 42.4, 42.4 (q, $^{2}J_{C\text{-}F}$ = 26.7 Hz), 42.2, 39.9, 26.3. ^{19}F NMR (565 MHz, $CDCl_3$) δ -60.40 (t, *J* = 11.4 Hz, 3F). HRMS ESI $[M+H]^+$ calculated for $C_{21}H_{20}NClOF_3^+$ 394.1181, found 394.1176.

6-Methoxy-1-methyl-1-(2,2,2-trifluoroethyl)-9-(4-(trifluoromethyl)phenyl)-2,3-dihydro-1H-pyrrolo[1,2-a]indole **165**

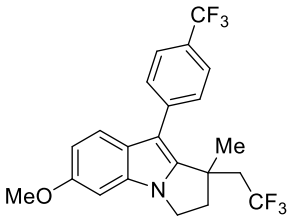

Following **GP9** using ynamide **672** (84.7 mg, 0.20 mmol) and Togni's reagent (79.2 mg, 0.24 mmol). Purification by flash chromatography (3-10% EtOAc in hexane), the product was obtained as a white solid (43.6 mg, 51% yield). ^{1}H NMR (600 MHz, $CDCl_3$) δ 7.72 (d, *J* = 7.9 Hz, 2H), 7.58 (d, *J* = 7.9 Hz, 2H), 7.40 (d, *J* = 8.7 Hz, 1H), 6.82 (dd, *J* = 8.7, 2.3 Hz, 1H), 6.79 (d, *J* = 2.3 Hz, 1H), 4.20 – 4.12 (m, 2H), 3.91 (s, 3H), 2.83 – 2.76 (m, 1H), 2.68 – 2.59 (m, 1H), 2.58 – 2.53 (m, 1H), 2.42 – 2.29 (m, 1H), 1.61 (s, 3H). ^{13}C NMR (151 MHz, $CDCl_3$) δ 156.6, 144.7, 138.9, 132.7, 130.3 (2C), 128.5 (q, $^{2}J_{C\text{-}F}$ = 32.4 Hz), 128.4 (q, $^{1}J_{C\text{-}F}$ = 278.8 Hz), 126.1, 125.6 (q, $^{4}J_{C\text{-}F}$ =

3.7 Hz), 124.5 (q, $^{1}J_{C\text{-}F}$ = 272.0 Hz), 123.8, 120.1, 110.1, 107.7, 93.3, 55.9, 42.5, 42.4 (q, $^{2}J_{C\text{-}F}$ = 26.8 Hz), 42.2, 39.9, 26.3. HRMS ESI $[M+H]^+$ calculated for $C_{22}H_{20}NOF_6^+$ 428.1444, found 428.1442.

9-(3,5-Difluorophenyl)-6-methoxy-1-methyl-1-(2,2,2-trifluoroethyl)-2,3-dihydro-1H-pyrrolo[1,2-a]indole **166**

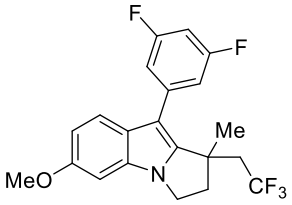

Following **GP9** using ynamide **675** (78.3 mg, 0.20 mmol) and Togni's reagent (79.2 mg, 0.24 mmol). Purification by flash chromatography (5-10% EtOAc in hexane), the product was obtained as a white solid (45.0 mg, 57% yield). ^{1}H NMR (600 MHz, $CDCl_3$) δ 7.40 (d, *J* = 8.7 Hz, 1H), 6.98 – 6.94 (m, 2H), 6.82 – 6.78 (m, 2H), 6.76 (d, *J* = 2.3 Hz, 1H), 4.17 – 4.09 (m, 2H), 3.89 (s, 3H), 2.81 – 2.75 (m, 1H), 2.69 – 2.58 (m, 1H), 2.58 – 2.52 (m, 1H), 2.41 – 2.31 (m, 1H), 1.59 (s, 3H). ^{13}C NMR (151 MHz, $CDCl_3$) δ 163.2 (d, $^{1}J_{C\text{-}F}$ = 248.7 Hz), 163.1 (d, $^{1}J_{C\text{-}F}$ = 235.1 Hz), 156.6, 144.5, 138.4 (t, $^{3}J_{C\text{-}F}$ = 10.1 Hz), 132.6, 126.5 (q, $^{1}J_{C\text{-}F}$ = 278.8 Hz), 125.8, 120.0, 112.8 (d, $^{2}J_{C\text{-}F}$ = 24.5 Hz), 112.8 (d, $^{2}J_{C\text{-}F}$ = 14.4 Hz), 110.2, 107.1 (t, $^{4}J_{C\text{-}F}$ = 2.3 Hz), 101.9 (t, $^{2}J_{C\text{-}F}$ = 25.4 Hz), 93.3, 55.9, 42.5, 42.3, 42.2, 39.9, 26.3. ^{19}F NMR (565 MHz, $CDCl_3$) δ -60.45 (t, *J* = 11.2 Hz, 3F), -110.03 – -110.10 (m, 1F). HRMS ESI $[M+H]^+$ calculated for $C_{21}H_{19}NOF_5^+$ 396.1382, found 396.1380.

6-(tert-Butyl)-1-methyl-1-(2,2,2-trifluoroethyl)-9-(4-(trifluoromethyl)phenyl)-2,3-dihydro-1H-pyrrolo[1,2-a]indole **167**

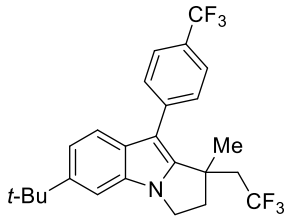

Following **GP9** using ynamide **673** (90.0 mg, 0.20 mmol) and Togni's reagent (79.2 mg, 0.24 mmol). Purification by flash chromatography (3-8% EtOAc in hexane), the product was obtained as a white solid (63.4 mg, 70% yield). ^{1}H NMR (400 MHz, $CDCl_3$) δ 7.72 (d, *J* = 8.0 Hz, 2H), 7.59 (d, *J* = 8.0 Hz, 2H), 7.48 (dd, *J* = 8.5, 0.7 Hz, 1H), 7.31 (dd, *J* = 1.8, 0.7 Hz, 1H), 7.25 (dd, *J* = 8.5, 1.8 Hz, 1H), 4.29 – 4.13 (m, 2H), 2.85 – 2.76 (m, 1H), 2.70 – 2.61 (m, 1H), 2.60 – 2.50 (m, 1H), 2.41 – 2.27 (m, 1H), 1.63 – 1.56 (m, 3H), 1.44 (s, 9H). ^{13}C NMR (101 MHz, $CDCl_3$) δ 145.8, 145.7, 139.0 (d, $^{4}J_{C\text{-}F}$ = 1.2 Hz), 132.1, 130.3 (2C), 129.5, 128.5 (q, $^{2}J_{C\text{-}F}$ = 32.5 Hz), 126.5 (q, $^{1}J_{C\text{-}F}$ = 279.7 Hz), 124.6 (q, $^{1}J_{C\text{-}F}$ = 272.9 Hz), 118.9 (2C), 118.6 (2C), 107.5, 106.0, 42.6, 42.6, 42.4 (q, $^{2}J_{C\text{-}F}$ = 27.0 Hz), 40.0 (q, $^{4}J_{C\text{-}F}$ = 1.8 Hz), 35.0, 31.9 (3C), 26.2. ^{19}F NMR (376 MHz, $CDCl_3$) δ -60.35 (t, *J* = 11.3 Hz, 3F), -62.23 (s, 3F). HRMS ESI $[M+H]^+$ calculated for $C_{25}H_{26}NF_6^+$ 454.1964, found 454.1963.

6-Methoxy-9-(4-nitrophenyl)-1-(2,2,2-trifluoroethyl)-2,3-dihydro-1H-pyrrolo[1,2-a]indole **168**

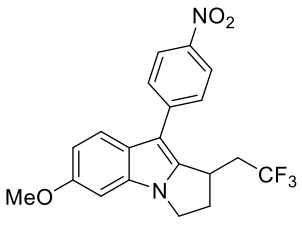

Following **GP9** using ynamide **674** (77.3 mg, 0.20 mmol) and Togni's reagent (79.2 mg, 0.24 mmol). Purification by flash chromatography (8-15% EtOAc in hexane), the product was obtained as a yellow solid (40.6 mg, 52% yield). ^{1}H NMR (600 MHz, $CDCl_3$) δ 8.30 (d, *J* = 8.8 Hz, 2H), 7.72 – 7.64 (m, 3H), 6.87 (dd, *J* = 8.8, 2.3 Hz, 1H), 6.79 (d, *J* = 2.3 Hz, 1H), 4.20 – 4.10 (m, 2H), 4.02 – 3.97 (m, 1H), 3.89 (s, 3 H), 3.07 – 3.01 (m, 1H), 2.63 – 2.47 (m, 2H), 2.15 – 2.05 (m, 1H). ^{13}C NMR (151 MHz, $CDCl_3$) δ 156.7, 145.4, 142.3, 141.9, 133.6, 127.8 (2C), 126.4 (q, $^{1}J_{C\text{-}F}$ = 277.9 Hz), 124.6, 124.5 (2C), 120.2, 110.9, 107.2, 93.9, 55.9, 42.9, 36.9 (q, $^{2}J_{C\text{-}F}$ = 27.7 Hz), 34.4, 32.3. ^{19}F NMR (565 MHz, $CDCl_3$) δ -64.94 (t, *J* = 10.6 Hz, 3F). HRMS ESI $[M+H]^+$ calculated for $C_{20}H_{18}N_2O_3F_3^+$ 391.1265, found 391.1261.

9-(3-Fluorophenyl)-1,5,7-trimethyl-1-(2,2,2-trifluoroethyl)-2,3-dihydro-1H-pyrrolo[1,2-a]indole **169**

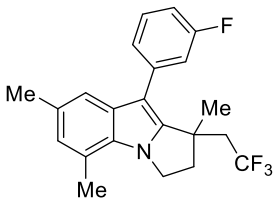

Following **GP9** using ynamide **676** (74.3 mg, 0.20 mmol) and Togni's reagent (79.2 mg, 0.24 mmol). Purification by flash chromatography (3% EtOAc in hexane), the product was obtained

as colourless oil (33.1 mg, 44% yield). ^{1}H NMR (600 MHz, $CDCl_3$) δ 7.43 – 7.38 (m, 1H), 7.21 – 7.18 (m, 1H), 7.16 – 7.13 (m, 1H), 7.08 (s, 1H), 7.08 – 7.03 (m, 1H), 6.80 (s, 1H), 4.53 – 4.48 (m, 1H), 4.44 – 4.40 (m, 1H), 2.77 – 2.73 (m, 1H), 2.67 (s, 3H), 2.63 – 2.54 (m, 1H), 2.53 – 2.46 (m, 1H), 2.37 (s, 3H), 2.35– 2.30 (m, 1H), 1.55 (s, 3H).). ^{13}C NMR (151 MHz, $CDCl_3$) δ 162.9 (d, $^{1}J_{C-F}$ = 246.1 Hz), 146.1, 137.4 (d, $^{3}J_{C-F}$ = 7.6 Hz), 132.6, 129.9 (d, $^{3}J_{C-F}$ = 9.1 Hz), 129.7, 126.6 (q, $^{1}J_{C-F}$ = 277.8 Hz), 126.3 (d, $^{4}J_{C-F}$ = 2.7 Hz), 125.2, 120.5, 117.3 (d, $^{2}J_{C-F}$ = 21.1 Hz), 116.7 (2C), 113.5 (d, $^{2}J_{C-F}$ = 21.1 Hz), 107.6 (d, $^{4}J_{C-F}$ = 2.0 Hz), 45.1, 42.4, 42.4 (q, $^{2}J_{C-F}$ = 26.9 Hz), 39.2, 26.2, 21.4, 18.0. ^{19}F NMR (565 MHz, $CDCl_3$) δ -60.37 (t, *J* = 11.4 Hz, 3F), -113.31 – -113.37 (m, 1F). HRMS ESI $[M+H]^+$ calculated for $C_{22}H_{22}NF_4^+$ 376.1683, found 376.1681.

9-(4-Chlorophenyl)-1-methyl-6-(methylthio)-1-(2,2,2-trifluoroethyl)-2,3-dihydro-1H-pyrrolo[1,2-a]indole **170**

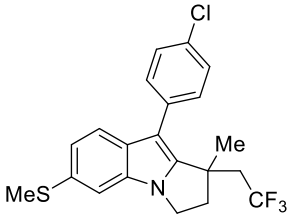

Following **GP9** using ynamide **677** (81.2 mg, 0.20 mmol) and Togni's reagent (79.2 mg, 0.24 mmol). Purification by flash chromatography (3% EtOAc in hexane), the product was obtained as colourless oil (46.6 mg, 57% yield). ^{1}H NMR (400 MHz, $CDCl_3$) δ 7.44 – 7.40 (m, 2H), 7.37 (dd, *J* = 8.4, 0.6 Hz, 1H), 7.36 – 7.32 (m, 2H), 7.25 (dd, *J* = 1.7, 0.6 Hz, 1H), 7.10 (dd, *J* = 8.4, 1.7 Hz, 1H), 4.22 – 4.08 (m, 2H), 2.81 – 2.72 (m, 1H), 2.64 – 2.56 (m, 1H), 2.54 (s, 3H), 2.57 – 2.48

(m, 1H), 2.40 – 2.24 (m, 1H), 1.55 (s, 3H). ^{13}C NMR (101 MHz, $CDCl_3$) δ 145.6, 132.9, 132.6, 132.4, 131.5 (2C), 131.0, 130.5, 128.9 (2C), 126.5 (q, $^{1}J_{C\text{-}F}$ = 279.5 Hz), 121.3, 119.8, 109.7, 107.9, 42.4, 42.3 (q, $^{2}J_{C\text{-}F}$ = 27.4 Hz), 42.3, 39.9, 26.3, 18.3. ^{19}F NMR (376 MHz, $CDCl_3$) δ -60.43 (t, *J* = 11.3 Hz, 3F). HRMS ESI $[M+H]^+$ calculated for $C_{21}H_{20}NClSF_3^+$ 410.0952, found 410.0948.

9-(3-Fluorophenyl)-6-isopropyl-1-methyl-1-(2,2,2-trifluoroethyl)-2,3-dihydro-1H-pyrrolo[1,2-a]indole **171**

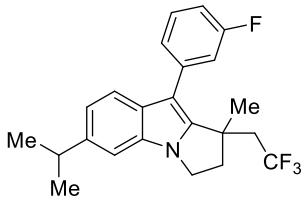

Following **GP9** using ynamide **678** (77.1 mg, 0.20 mmol) and Togni's reagent (79.2 mg, 0.24 mmol). Purification by flash chromatography (3% EtOAc in hexane), the product was obtained as colourless oil (39.0 mg, 50% yield). ^{1}H NMR (600 MHz, $CDCl_3$) δ 7.50 – 7.46 (m, 1H), 7.45 – 7.41 (m, 1H), 7.25 – 7.22 (m, 1H), 7.21 – 7.18 (m, 1H), 7.18 – 7.16 (m, 1H), 7.08 – 7.04 (m, 2H), 4.24 – 4.20 (m, 1H), 4.19 – 4.14 (m, 1H), 3.11 – 3.05 (m, 1H), 2.82 – 2.76 (m, 1H), 2.72 – 2.60 (m, 1H), 2.59 – 2.52 (m, 1H), 2.41 – 2.29 (m, 1H), 1.62 – 1.59 (m, 3H), 1.37 (s, 3H), 1.37 (s, 3H). ^{13}C NMR (151 MHz, $CDCl_3$) δ 163.0 (d, $^{1}J_{C\text{-}F}$ = 244.6 Hz), 145.2, 143.4, 137.3 (d, $^{3}J_{C\text{-}F}$ = 7.6 Hz), 132.1, 130.1, 129.9 (d, $^{3}J_{C\text{-}F}$ = 9.1 Hz), 126.6 (q, $^{1}J_{C\text{-}F}$ = 279.4 Hz), 125.9 (d, $^{4}J_{C\text{-}F}$ = 2.7 Hz), 119.4, 119.3, 116.9 (d, $^{2}J_{C\text{-}F}$ = 19.6 Hz), 113.4 (d, $^{2}J_{C\text{-}F}$ = 21.1 Hz), 107.7 (d, $^{4}J_{C\text{-}F}$ = 2.1 Hz), 106.8, 42.6, 42.3 (q, $^{2}J_{C\text{-}F}$ = 26.8 Hz), 42.2, 39.9, 34.6, 26.2, 24.7 (2C). ^{19}F NMR (565 MHz, $CDCl_3$) δ -

60.35 (t, *J* = 11.4 Hz, 3F), -113.24 – -113.29 (m, 1F). HRMS ESI $[M+H]^+$ calculated for $C_{23}H_{24}NF_4^+$ 390.1840, found 390.1836.

***6-Methoxy-1-methyl-9-(pyridin-3-yl)-1-(2,2,2-trifluoroethyl)-2,3-dihydro-1H-pyrrolo[1,2-a]indole* 172**

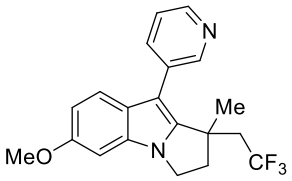

Following **GP9** using ynamide **679** (71.3 mg, 0.20 mmol) and Togni's reagent (79.2 mg, 0.24 mmol). Purification by flash chromatography (3-10% EtOAc in hexane), the product was obtained as a yellow solid (30.9 mg, 43% yield). ^{1}H NMR (400 MHz, $CDCl_3$) δ 8.73 (s, 1H), 8.60 (d, *J* = 5.0 Hz, 1H), 7.85 – 7.80 (m, 1H), 7.45 (dd, *J* = 7.9, 5.0 Hz, 1H), 7.33 (dd, *J* = 8.5, 0.8 Hz, 1H), 6.81 – 6.74 (m, 2H), 4.20 – 4.08 (m, 2H), 3.88 (s, 3H), 2.82 – 2.74 (m, 1H), 2.61 – 2.46 (m, 2H), 2.42 – 2.27 (m, 1H), 1.57 (s, 3H). ^{13}C NMR (101 MHz, $CDCl_3$) δ 156.7, 149.9, 146.9, 145.1, 138.2, 132.7, 131.6, 126.4 (q, $^1J_{C\text{-}F}$ = 279.8 Hz), 126.1, 123.9, 119.7, 110.2, 104.5, 93.4, 55.9, 42.5 (q, $^2J_{C\text{-}F}$ = 27.0 Hz), 42.3, 42.3, 40.0 (d, $^4J_{C\text{-}F}$ = 1.8 Hz), 26.6. ^{19}F NMR (376 MHz, $CDCl_3$) δ -60.47 (t, *J* = 11.2 Hz, 3F). HRMS ESI $[M+H]^+$ calculated for $C_{20}H_{20}N_2OF_3^+$ 361.1523, found 361.1519.

***9-(3-Fluorophenyl)-6-methoxy-1-methyl-1-(2,2,2-trifluoroethyl)-2,3-dihydro-1H-pyrrolo[1,2-a]indole* 175**

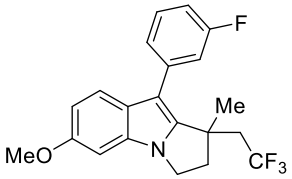

Following **GP9** using ynamide **680** (74.7 mg, 0.20 mmol) and Togni's reagent (79.2 mg, 0.24 mmol). Purification by flash chromatography (3-5% EtOAc in hexane), the product was obtained as a white solid (42.4 mg, 56% yield). ^{1}H NMR (400 MHz, $CDCl_3$) δ 7.45 – 7.36 (m, 2H), 7.24 – 7.20 (m, 1H), 7.18 – 7.13 (m, 1H), 7.10 – 6.99 (m, 1H), 6.79 (dd, *J* = 8.6, 2.3 Hz, 1H), 6.77 – 6.75 (m, 1H), 4.19 – 4.06 (m, 2H), 3.89 (s, 3H), 2.82 – 2.73 (m, 1H), 2.70 – 2.59 (m, 1H), 2.57 – 2.50 (m, 1H), 2.42 – 2.27 (m, 1H), 1.62 – 1.53 (m, 3H). ^{13}C NMR (101 MHz, $CDCl_3$) δ 163.0 (d, $^{1}J_{C\text{-}F}$ = 247.5 Hz), 156.5, 144.4, 137.2 (d, $^{3}J_{C\text{-}F}$ = 8.1 Hz), 132.5, 130.0 (d, $^{3}J_{C\text{-}F}$ = 8.1 Hz), 126.6 (q, $^{1}J_{C\text{-}F}$ = 279.8 Hz), 126.2, 125.9 (d, $^{4}J_{C\text{-}F}$ = 3.0 Hz), 120.2, 116.9 (d, $^{2}J_{C\text{-}F}$ = 21.1 Hz), 113.4 (d, $^{2}J_{C\text{-}F}$ = 21.2 Hz), 109.9, 107.9 (d, $^{4}J_{C\text{-}F}$ = 2.0 Hz), 93.3, 55.9, 42.5 (d, $^{4}J_{C\text{-}F}$ = 1.0 Hz), 42.3 (q, $^{2}J_{C\text{-}F}$ = 27.4 Hz), 42.2, 39.9, 26.2. ^{19}F NMR (376 MHz, $CDCl_3$) δ -60.41 (t, *J* = 11.4 Hz, 3F), -113.19 – -113.27 (m, 1F). HRMS ESI $[M+H]^+$ calculated for $C_{21}H_{20}NOF_4^+$ 378.1476, found 378.1482.

6-Methoxy-1-methyl-9-(4-nitrophenyl)-1-(2,2,2-trifluoroethyl)-2,3-dihydro-1H-pyrrolo[1,2-a]indole **178**

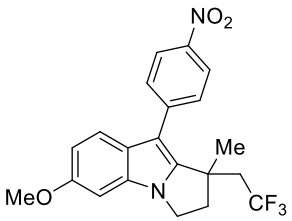

Following **GP9** using ynamide **176** (80.1 mg, 0.20 mmol) and Togni's reagent (79.2 mg, 0.24 mmol). Purification by flash chromatography (8-15% EtOAc in hexane), the product was obtained as a yellow solid (50.2 mg, 62% yield). ^{1}H NMR (400 MHz, $CDCl_3$) δ 8.31 (d, *J* = 8.8 Hz, 2H), 7.60 (d, *J* = 8.8 Hz, 2H), 7.41 (d, *J* = 8.7 Hz, 1H), 6.82 (dd, *J* = 8.7, 2.3 Hz, 1H), 6.78 (d, *J* = 2.3 Hz, 1H), 4.22 – 4.10 (m, 2H), 3.89 (s, 3H), 2.84 – 2.75 (m, 1H), 2.68 – 2.52 (m, 1H), 2.43 – 2.30 (m, 1H), 1.62 (s, 3H). ^{13}C NMR (101 MHz, $CDCl_3$) δ 156.8, 146.1, 145.2, 142.5, 132.9, 130.2 (2C), 126.4 (q, $^{1}J_{C\text{-}F}$ = 279.8 Hz), 125.5, 124.0 (2C), 120.0, 110.5, 107.3, 93.5, 55.9, 42.6, 42.3 (q, $^{2}J_{C\text{-}F}$ = 27.3 Hz), 42.3, 40.2, 26.4. ^{19}F NMR (376 MHz, $CDCl_3$) δ -60.42 (t, *J* = 11.3 Hz, 3F). HRMS ESI $[M+H]^+$ calculated for $C_{21}H_{20}N_2O_3F_3^+$ 405.1420, found 405.1420.

***3,9-Dimethyl-10-(p-tolyl)-9-(2,2,2-trifluoroethyl)-6,7,8,9-tetrahydropyrido[1,2-a]indole* 179**

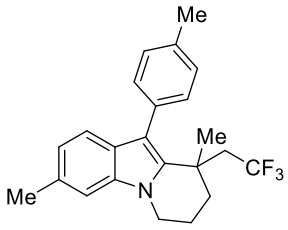

Following **GP9** using ynamide **681** (73.5 mg, 0.20 mmol) and Togni's reagent (79.2 mg, 0.24 mmol). Purification by flash chromatography (3% EtOAc in hexane), the product was obtained as colourless oil (53.4 mg, 72% yield). ^{1}H NMR (400 MHz, $CDCl_3$) δ 7.24 – 7.18 (m, 4H), 7.07 (s, 1H), 7.04 (d, *J* = 8.0 Hz, 1H), 6.86 (d, *J* = 8.0 Hz, 1H), 4.14 – 4.06 (m, 1H), 4.05 – 3.96 (m, 1H), 2.60 – 2.29 (m, 8H), 2.17 – 2.02 (m, 3H), 1.85 – 1.75 (m, 1H), 1.41 (s, 3H). ^{13}C NMR (151 MHz, $CDCl_3$) δ 137.6, 136.6, 135.2, 133.5, 131.5, 131.4 (2C), 129.1 (2C), 127.6, 126.5 (q, $^{1}J_{C\text{-}F}$ = 279.35

Hz), 121.6, 118.8, 113.5, 108.8, 43.5 (q, $^{2}J_{C\text{-}F}$ = 25.9 Hz), 42.6, 34.8, 33.8, 29.0, 21.9, 21.4, 19.5. ^{19}F NMR (565 MHz, $CDCl_3$) δ -59.03 (t, *J* = 11.5 Hz, 3F). HRMS ESI $[M+H]^+$ calculated for $C_{23}H_{25}NF_3^+$ 372.1934, found 372.1931.

10-(3-Fluorophenyl)-3-methyl-9-(2,2,2-trifluoroethyl)-6,7,8,9-tetrahydropyrido[1,2-a]indole

180

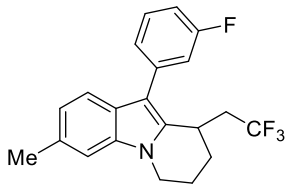

Following **GP9** using ynamide **682** (71.5 mg, 0.20 mmol) and Togni's reagent (79.2 mg, 0.24 mmol). Purification by flash chromatography (3% EtOAc in hexane), the product was obtained as colourless oil (29.4 mg, 42% yield). ^{1}H NMR (600 MHz, $CDCl_3$) δ 7.51 (d, *J* = 8.1 Hz, 1H), 7.44 – 7.40 (m, 1H), 7.27 – 7.23 (m, 1H), 7.23 – 7.19 (m, 1H), 7.16 – 7.13 (m, 1H), 7.05 – 6.99 (m, 2H), 4.22 – 4.17 (m, 1H), 4.04 – 3.97 (m, 1H), 3.95 – 3.88 (m, 1H), 2.52 (s, 3H), 2.30 – 2.23 (m, 2H), 2.21 – 2.14 (m, 2H), 2.12 – 1.99 (m, 2H). ^{13}C NMR (151 MHz, $CDCl_3$) δ 163.3 (d, $^{1}J_{C\text{-}F}$ = 246.1 Hz), 137.5 (d, $^{3}J_{C\text{-}F}$ = 9.1 Hz), 136.3, 133.5, 131.8, 130.3 (d, $^{3}J_{C\text{-}F}$ = 7.6 Hz), 126.4 (q, $^{1}J_{C\text{-}F}$ = 277.8 Hz), 125.1 (d, $^{4}J_{C\text{-}F}$ = 3.0 Hz), 125.1, 122.4, 118.5, 116.2 (d, $^{2}J_{C\text{-}F}$ = 19.6 Hz), 113.3 (d, $^{2}J_{C\text{-}F}$ = 21.1 Hz), 112.1 (d, $^{4}J_{C\text{-}F}$ = 2.0Hz), 109.1, 42.5, 37.6 (q, $^{2}J_{C\text{-}F}$ = 27.2 Hz), 27.4, 25.5, 21.9, 19.6. ^{19}F NMR (565 MHz, $CDCl_3$) δ -63.81 (t, *J* = 11.9 Hz, 3F), -113.15 – -113.24 (m, 1F). HRMS ESI $[M+H]^+$ calculated for $C_{21}H_{20}NF_4^+$ 362.1527, found 362.1525.

10-Butyl-11-(3,5-difluorophenyl)-3-methoxy-10-(2,2,2-trifluoroethyl)-7,8,9,10-tetrahydro-6H-azepino[1,2-a]indole **181**

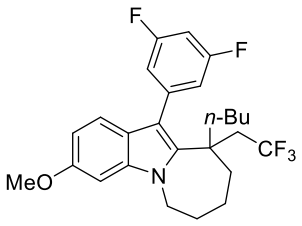

Following **GP9** using ynamide **683** (92.3 mg, 0.20 mmol) and Togni's reagent (79.2 mg, 0.24 mmol). Purification by flash chromatography (3% EtOAc in hexane), the product was obtained as colourless oil (34.1 mg, 37% yield). ^{1}H NMR (600 MHz, $CDCl_3$) δ 6.91 (d, *J* = 8.6 Hz, 1H), 6.89 – 6.85 (m, 2H), 6.84 – 6.80 (m, 1H), 6.78 (d, *J* = 2.2 Hz, 1H), 6.70 (dd, *J* = 8.6, 2.2 Hz, 1H), 4.38 – 4.33 (m, 1H), 4.25 – 4.19 (m, 1H), 3.87 (s, 3H), 2.64 – 2.47 (m, 2H), 2.08 – 2.03 (m, 1H), 2.01 – 1.96 (m, 1H), 1.95 – 1.87 (m, 2H), 1.87 – 1.82 (m, 2H), 1.78 – 1.70 (m, 2H), 1.22 – 1.15 (m, 2H), 1.10 – 1.01 (m, 1H), 0.97 – 0.90 (m, 1H), 0.78 (t, *J* = 7.3 Hz, 3H). ^{13}C NMR (151 MHz, $CDCl_3$) δ 162.8 (d, *J* = 248.6 Hz), 162.7 (d, $^{1}J_{C\text{-}F}$ = 248.7 Hz), 156.9, 141.4 (t, $^{3}J_{C\text{-}F}$ = 10.0 Hz), 138.3, 136.6, 126.6 (q, $^{1}J_{C\text{-}F}$ = 279.5 Hz), 123.8, 119.7, 114.6 (d, $^{2}J_{C\text{-}F}$ = 21.1 Hz), 114.4 (d, $^{2}J_{C\text{-}F}$ = 22.7 Hz), 114.2 (t, $^{4}J_{C\text{-}F}$ = 2.4 Hz), 109.5, 102.5 (t, $^{2}J_{C\text{-}F}$ = 25.3 Hz), 92.9, 56.0, 43.9, 42.4 (q, $^{2}J_{C\text{-}F}$ = 25.2 Hz), 42.2, 40.3, 35.3, 27.7, 26.7, 23.0, 22.8, 14.0. ^{19}F NMR (565 MHz, $CDCl_3$) δ -58.43 (t, *J* = 10.7 Hz, 3F), -110.43 – -110.50 (m, 1F), -110.94 – -110.02 (m, 1F). HRMS ESI $[M+H]^+$ calculated for $C_{26}H_{29}F_5NO^+$ 466.2164, found 466.2172.

General procedure 10 (GP10)

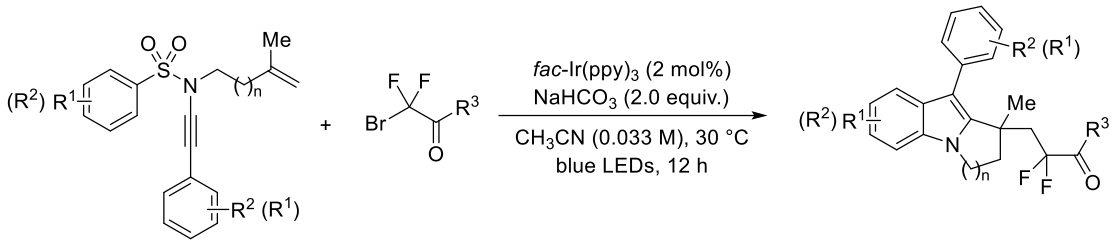

A 10-mL Schlenk tube equipped with a magnetic stir bar was charged with *fac*-Ir(ppy)$_3$ (1.3 mg, 2 mol%), ynamide (0.2 mmol, if solid), $NaHCO_3$ (16.8 mg, 0.4 mmol, 2.0 equiv.), corresponding radical precursor (0.24 mmol, 1.2 equiv., if solid). The flask was evacuated and backfilled with N_2 for 3 times. CH_3CN (6 mL) or a solution of ynamide (0.2 mmol) in CH_3CN (6 mL), corresponding radical precursor (0.24 mmol, 1.2 equiv) were then added via syringe under N_2. The reaction mixture was then vigorously stirred under blue LED light (30 W) at room temperature (two fans were used to cool down the reaction mixture) for 12 h. After the reaction was completed, the mixture was diluted with ethyl acetate and poured into a separatory funnel, washed with brine for three times. The organic layers were dried over Na_2SO_4 and concentrated under reduced pressure after filtration. The crude product was purified by flash chromatography on silica gel to afford the desired product.

3-(1,6-Dimethyl-9-(p-tolyl)-2,3-dihydro-1H-pyrrolo[1,2-a]indol-1-yl)-2,2-difluoro-N-propylpropanamide **182**

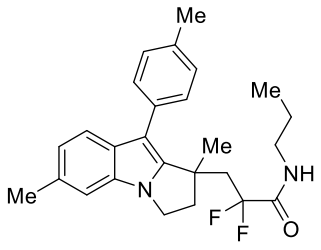

Following **GP10** using ynamide **134** (70.7 mg, 0.20 mmol) and 2-bromo-2,2-difluoro-*N*-propylacetamide (55.2 mg, 0.24 mmol). Purification by flash chromatography (3-10% EtOAc in hexane), the product was obtained as a white solid (41.8 mg, 51% yield). ^{1}H NMR (400 MHz, $CDCl_3$) δ 7.43 (d, *J* = 8.2 Hz, 1H), 7.38 (d, *J* = 8.1 Hz, 2H), 7.26 (d, *J* = 8.1 Hz, 2H), 7.08 (d, *J* = 1.5 Hz, 1H), 6.93 (dd, *J* = 8.2, 1.5 Hz, 1H), 6.17 (br s, 1H), 4.20 – 4.03 (m, 2H), 3.25 – 3.15 (m, 1H), 3.15 – 3.05 (m, 1H), 2.86 – 2.77 (m, 1H), 2.74 – 2.58 (m, 1H), 2.57 – 2.45 (m, 5H), 2.43 (s, 3H), 1.55 (s, 3H), 1.48 (p, *J* = 7.2 Hz, 2H), 0.90 (t, *J* = 7.4 Hz, 3H). ^{13}C NMR (101 MHz, $CDCl_3$) δ 164.4 (t, $^{2}J_{C\text{-}F}$ = 28.4 Hz), 145.2, 135.7, 132.3, 132.0, 131.2, 130.2, 130.2 (2C), 129.2 (2C), 121.2, 119.4, 118.3 (t, $^{1}J_{C\text{-}F}$ = 255.4 Hz), 109.4, 108.6, 42.6, 42.1, 41.9 (t, $^{2}J_{C\text{-}F}$ = 21.9 Hz), 41.3, 40.3, 26.9, 22.4, 21.8, 21.3, 11.3. ^{19}F NMR (376 MHz, $CDCl_3$) δ -101.0 – -105.3 (m, 2F). HRMS ESI $[M+H]^+$ calculated for $C_{26}H_{31}F_2N_2O^+$ 425.2399, found 425.2404.

3-(1,6-Dimethyl-9-(p-tolyl)-2,3-dihydro-1H-pyrrolo[1,2-a]indol-1-yl)-2,2-difluoro-N-Phenylpropanamide **183**

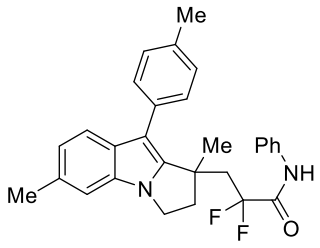

Following **GP10** using ynamide **134** (70.7 mg, 0.20 mmol) and 2-bromo-2,2-difluoro-*N*-phenylacetamide (60.0 mg, 0.24 mmol). Purification by flash chromatography (3-10% EtOAc in hexane), the product was obtained as a white solid (39.1 mg, 44% yield). ^{1}H NMR (400 MHz,

$CDCl_3$) δ 7.66 (br s, 1H), 7.33 (d, *J* = 8.2 Hz, 2H), 7.29 (d, *J* = 8.1 Hz, 1H), 7.28 – 7.20 (m, 4H), 7.13 (d, *J* = 8.2 Hz, 2H), 7.10 – 7.04 (m, 1H), 6.96 (d, *J* = 1.5 Hz, 1H), 6.81 (dd, *J* = 8.1, 1.5 Hz, 2H), 4.09 – 3.92 (m, 2H), 2.77 – 2.71 (m, 1H), 2.64 (dt, *J* = 22.9, 13.7 Hz, 1H), 2.56 – 2.42 (m, 1H), 2.39 (s, 3H), 2.28 (s, 3H), 1.48 (s, 3H). ^{13}C NMR (101 MHz, $CDCl_3$) δ 162.1 (t, $^2J_{C-F}$ = 28.7 Hz), 144.9, 135.9, 135.8, 132.3, 131.9, 131.3, 130.2, 130.2 (2C), 129.3 (2C), 129.2 (2C), 125.7, 121.3, 120.4 (2C), 119.4, 118.2 (t, $^1J_{C-F}$ = 256.6 Hz), 109.5, 108.7, 42.7, 42.1, 41.7 (t, $^2J_{C-F}$ = 21.8 Hz), 40.3, 27.2, 21.8, 21.3. ^{19}F NMR (376 MHz, $CDCl_3$) δ -100.3 – -104.1 (m, 2F). HRMS ESI $[M+H]^+$ calculated for $C_{29}H_{29}F_2N_2O^+$ 459.2243, found 459.2249.

3-(1,6-Dimethyl-9-(p-tolyl)-2,3-dihydro-1H-pyrrolo[1,2-a]indol-1-yl)-2,2-difluoro-1-(piperidin-1-yl)propan-1-one **184**

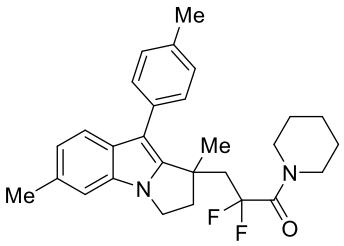

Following **GP10** using ynamide **134** (70.7 mg, 0.20 mmol) and 2-bromo-2,2-difluoro-1-(piperidin-1-yl)ethan-1-one (58.1 mg, 0.24 mmol). Purification by flash chromatography (3-8% EtOAc in hexane), the product was obtained as colourless oil (40.5 mg, 46% yield). ^1H NMR (600 MHz, $CDCl_3$) δ 7.42 (d, *J* = 8.1 Hz, 1H), 7.37 (d, *J* = 8.0 Hz, 2H), 7.24 (d, *J* = 8.0 Hz, 2H), 7.09 (d, *J* = 1.3 Hz, 1H), 6.93 (dd, *J* = 8.1, 1.3 Hz, 1H), 4.18 – 4.13 (m, 1H), 4.12 – 4.07 (m, 1H), 3.58 – 3.53 (m, 1H), 3.52 (t, *J* = 5.7 Hz, 1H), 3.49 – 3.44 (m, 2H), 2.84 – 2.78 (m, 1H), 2.77 – 2.66 (m,

1H), 2.58 – 2.52 (m, 1H), 2.50 (s, 3H), 2.49 – 2.43 (m, 1H), 2.42 (s, 3H), 1.67 – 1.63 (m, 2H), 1.61 – 1.54 (m, 5H), 1.53 – 1.44 (m, 2H). ^{13}C NMR (151 MHz, $CDCl_3$) δ 162.2 (t, $^{2}J_{C\text{-}F}$ = 28.6 Hz), 146.0, 135.7, 132.2, 132.1, 131.1, 130.2 (2C), 129.1 (2C), 121.2, 121.2, 119.5 (t, $^{1}J_{C\text{-}F}$ = 254.8 Hz), 119.3, 109.5, 108.4, 47.0 (t, $^{3}J_{C\text{-}F}$ = 6.1 Hz), 44.6, 43.0, 42.6 (t, $^{2}J_{C\text{-}F}$ = 21.5 Hz), 42.2, 40.7, 26.7, 26.5, 25.7, 24.5, 21.8, 21.3. ^{19}F NMR (565 MHz, $CDCl_3$) δ -96.2 – -98.0 (m, 2F). HRMS ESI $[M+H]^+$ calculated for $C_{28}H_{33}F_2N_2O^+$ 451.2556, found 451.2561.

Ethyl 3-(9-(3,5-difluorophenyl)-6-methoxy-1-methyl-2,3-dihydro-1H-pyrrolo[1,2-a]indol-1-yl)-2,2-difluoropropanoate **185**

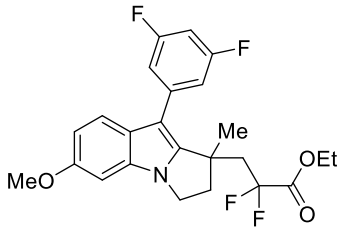

Following **GP10** using ynamide **675** (78.4 mg, 0.20 mmol) and ethyl 2-bromo-2,2-difluoroacetate (48.7 mg, 0.24 mmol). Purification by flash chromatography (3-8% EtOAc in hexane), the product was obtained as colourless oil (48.4 mg, 54% yield). ^{1}H NMR (400 MHz, $CDCl_3$) δ 7.39 (d, *J* = 8.6 Hz, 1H), 7.02 – 6.94 (m, 2H), 6.81 – 6.78 (m, 1H), 6.77 – 6.75 (m, 1H), 6.74 (d, *J* = 2.3 Hz, 1H), 4.20 – 4.13 (m, 1H), 4.11 – 3.99 (m, 3H), 3.88 (s, 3H), 2.85 – 2.77 (m, 1H), 2.71 – 2.58 (m, 1H), 2.57 – 2.38 (m, 2H), 1.51 (s, 3H), 1.21 (t, *J* = 7.1 Hz, 3H). ^{13}C NMR (101 MHz, $CDCl_3$) δ 164.0 (t, $^{2}J_{C\text{-}F}$ = 32.7 Hz), 163.2 (d, $^{1}J_{C\text{-}F}$ = 248.7 Hz), 163.0 (d, $^{1}J_{C\text{-}F}$ = 248.7 Hz), 156.6, 144.6, 138.5 (t, $^{3}J_{C\text{-}F}$ = 10.3 Hz), 132.6, 125.7, 120.0, 116.1 (t, $^{1}J_{C\text{-}F}$ = 252.9 Hz), 112.8 (d,

$^{3}J_{C\text{-}F}$ = 11.4 Hz, 1C), 112.7 (d, $^{2}J_{C\text{-}F}$ = 24.8 Hz), 110.2, 107.1 (t, $^{4}J_{C\text{-}F}$ = 2.6 Hz), 101.7 (t, $^{2}J_{C\text{-}F}$ = 25.5 Hz), 93.3, 63.3, 55.9, 43.5 (t, $^{2}J_{C\text{-}F}$ = 22.3 Hz), 42.7, 42.3, 40.4 (t, $^{4}J_{C\text{-}F}$ = 2.4 Hz), 26.9, 13.8. ^{19}F NMR (376 MHz, $CDCl_3$) δ -100.2 – -103.6 (m, 2F), -110.3 – -110.5 (m, 2F). HRMS ESI $[M+H]^+$ calculated for $C_{24}H_{24}F_4NO_3^+$ 450.1687, found 450.1683.

Ethyl 3-(6-(tert-butyl)-9-(3-fluorophenyl)-1-methyl-2,3-dihydro-1H-pyrrolo[1,2-a]indol-1-yl)-2,2-difluoropropanoate **186**

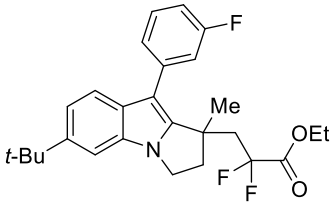

Following **GP10** using ynamide **660** (80.0 mg, 0.20 mmol) and ethyl 2-bromo-2,2-difluoroacetate (48.7 mg, 0.24 mmol). Purification by flash chromatography (3-8% EtOAc in hexane), the product was obtained as colourless oil (50.1 mg, 55% yield). ^{1}H NMR (400 MHz, $CDCl_3$) δ 7.48 (d, *J* = 8.5 Hz, 1H), 7.43 – 7.32 (m, 1H), 7.28 – 7.24 (m, 2H), 7.24 – 7.17 (m, 2H), 7.06 – 6.99 (m, 1H), 4.25 – 4.18 (m, 1H), 4.17 – 4.10 (m, 2H), 4.08 – 4.00 (m, 1H), 2.85 – 2.77 (m, 1H), 2.74 – 2.59 (m, 1H), 2.58 – 2.50 (m, 1H), 2.50 – 2.35 (m, 1H), 1.53 (s, 3H), 1.42 (s, 9H), 1.22 (t, *J* = 7.2 Hz, 3H). ^{13}C NMR (101 MHz, $CDCl_3$) δ 164.1 (t, $^{2}J_{C\text{-}F}$ = 32.7 Hz, 1C), 163.0 (d, $^{1}J_{C\text{-}F}$ = 246.5 Hz), 145.6, 145.5, 137.4 (d, $^{3}J_{C\text{-}F}$ = 8.4 Hz), 132.0, 129.8 (d, $^{3}J_{C\text{-}F}$ = 8.7 Hz), 129.6, 126.0 (d, $^{4}J_{C\text{-}F}$ = 2.7 Hz), 118.9, 118.3, 116.9 (d, $^{2}J_{C\text{-}F}$ = 21.0 Hz), 116.2 (t, $^{1}J_{C\text{-}F}$ = 252.7 Hz), 113.1 (d, $^{2}J_{C\text{-}F}$ = 21.1 Hz), 107.6 (d, $^{4}J_{C\text{-}F}$ = 2.2 Hz), 105.9, 63.2, 43.2 (t, $^{2}J_{C\text{-}F}$ = 22.1 Hz), 42.8, 42.3, 40.4,

35.0, 32.0 (3C), 26.6, 13.8. ^{19}F NMR (376 MHz, $CDCl_3$) δ -100.4 – -103.5 (m, 2F), -113.4 – -113.6 (m, F). HRMS ESI $[M+H]^+$ calculated for $C_{27}H_{31}F_3NO_2^+$ 458.2302, found 458.2310.

(6-Methoxy-1-methyl-1-(2,2,2-trifluoroethyl)-2,3-dihydro-1H-pyrrolo[1,2-a]indol-9-yl)(4-nitrophenyl)methanone **188**

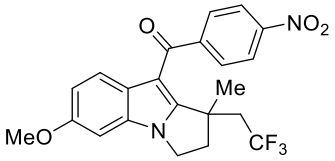

Following **GP10** using ynamide **187** (85.7 mg, 0.20 mmol), Togni's reagent (79.2 mg, 0.24 mmol) and photocatalyst $Ir(ppy)_2(dtbbpy)PF_6$, and without $NaHCO_3$. Purification by flash chromatography (10% EtOAc in hexane), the product was obtained as a yellow solid (43.9 mg, 51% yield). ^{1}H NMR (600 MHz, $CDCl_3$) δ 8.32 (d, *J* = 8.7 Hz, 2H), 7.86 (d, *J* = 8.7 Hz, 2H), 6.77 (m, 1H), 6.67 (d, *J* = 2.3 Hz, 1H), 6.62 – 6.59 (m, 1H), 4.28 – 4.16 (m, 2H), 3.84 (s, 3H), 3.13 – 3.02 (m, 2H), 3.01 – 2.96 (m, 1H), 2.65 – 2.59 (m, 1H), 1.68 (s, 3H). ^{13}C NMR (101 MHz, $CDCl_3$) δ 189.5, 157.1, 156.7, 149.4, 147.1, 132.9, 129.7 (2C), 126.8 (q, $^1J_{C\text{-}F}$ = 279.5 Hz) 124.5, 123.8 (2C), 121.8, 111.7, 107.9, 94.3, 55.8, 43.6, 41.7 (q, $^4J_{C\text{-}F}$ = 2.0 Hz), 40.5 (q, $^2J_{C\text{-}F}$ = 26.9 Hz), 40.5, 25.1. ^{19}F NMR (565 MHz, $CDCl_3$) δ -60.71 (t, *J* = 11.1 Hz, 3F). HRMS ESI $[M+H]^+$ calculated for $C_{22}H_{20}F_3N_2O_4^+$ 433.1370, found 433.1376.

Gram-scale synthesis of product 144

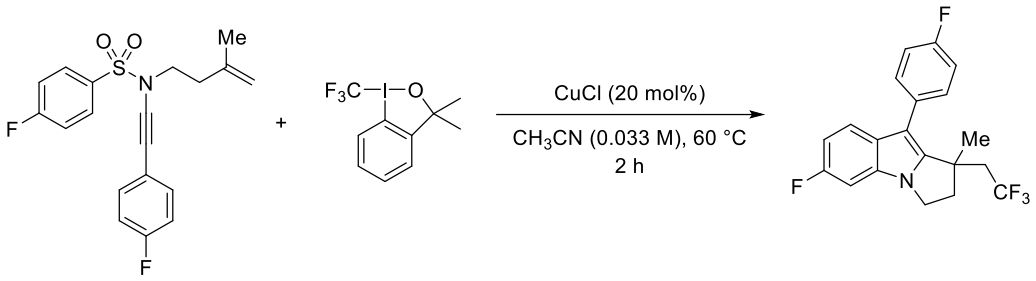

To a flame-dried Schlenk flask charged with a stir bar was added Togni's reagent (2.37 g, 7.2 mmol, 1.2 equiv) and CuCl (119 mg, 1.2 mmol, 20 mol%) under N_2 atmosphere. The flask was evacuated and backfilled with N_2 for 3 times. A solution of ynamide **655** (2.16 g, 6 mmol, 1.0 equiv) in CH_3CN (180 mL) was then added. The resulting reaction mixture was stirred at 60 °C in an oil-bath for about 2 hours (as judged by TLC analysis), the mixture was cooled down to room temperature, diluted with ethyl acetate and poured into a separatory funnel, washed with brine for three times. The organic layer was dried over Na_2SO_4 and concentrated under reduced pressure after filtration. The crude product was purified by flash chromatography on silica gel to afford the desired product **144** as a white solid (1.12 g, 51% yield).

5.4 Defluorinative products for Chapter 3

5.4.1 Synthesis of α-Arylated Carbonyl Compounds

General procedure 11 (GP11) for the synthesis of α-arylated carboxylic acids

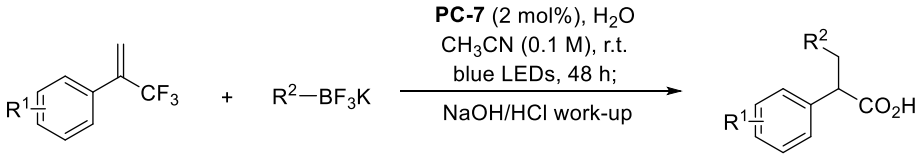

A 10-mL Schlenk tube equipped with a magnetic stir bar was charged with corresponding α-trifluoromethyl alkene (0.1 mmol, if solid), potassium alkyltrifluoroborate (0.15 mmol), **PC-7** (1.2-3.0 mg, 0.002-0.005 mmol). The flask was evacuated and backfilled with N_2 3 times. CH_3CN (1.0 mL) or a solution of α-trifluoromethyl alkene (0.1 mmol, if liquid) in CH_3CN (1.0 mL) was then added via syringe followed by the addition of H_2O (30-100 µL) under N_2. The reaction mixture was then vigorously stirred under blue LED light (30 W, λ_{max} = 440 nm) at 30 °C (two fans were used to cool down the reaction mixture) for 16-48 h. After the reaction was completed, 1.0 mL of aq. NaOH (0.2 M) was added to the reaction mixture at room temperature, the resulting solution was stirred for 2 min at room temperature before acidified by HCl solution (2 N). The reaction mixture was then diluted with ethyl acetate, poured into a separatory funnel, before being washed with brine. The combined organic layers were dried over Na_2SO_4 and concentrated under reduced pressure after filtration. The crude product was purified by flash chromatography on silica gel to afford the desired product.

2-([1,1'-Biphenyl]-4-yl)-3-cyclohexylpropanoic acid **321**

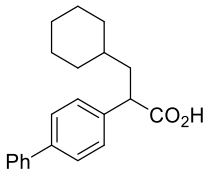

Following **GP11** using α-trifluoromethyl alkene **232** (24.8 mg, 0.10 mmol), potassium cyclohexyltrifluoroborate **320** (28.5 mg, 0.15 mmol) and H_2O (30 µL) for 16 h. Purification by flash chromatography (EtOAc : Hexane : AcOH = 15 : 100 : 2), the product was obtained as a

white solid (24.7 mg, 80% yield). ^{1}H NMR (400 MHz, $CDCl_3$) δ 7.61 – 7.53 (m, 4H), 7.46 – 7.37 (m, 4H), 7.37 – 7.31 (m, 1H), 3.76 (t, *J* = 7.8 Hz, 1H), 2.02 (dt, *J* = 13.7, 7.8 Hz, 1H), 1.83 – 1.71 (m, 3H), 1.71 – 1.57 (m, 3H), 1.30 – 1.10 (m, 4H), 0.99 – 0.85 (m, 2H); ^{13}C NMR (101 MHz, $CDCl_3$) δ 180.0, 140.9, 140.5, 138.0, 128.9 (2C), 128.6 (2C), 127.5 (2C), 127.4, 127.2 (2C), 48.4, 40.8, 35.3, 33.4, 33.1, 26.6, 26.21, 26.18. HRMS ESI $[M-H]^-$ calculated for ($C_{21}H_{23}O_3^-$) 307.1698, found 307.1695.

***3-Cyclohexyl-2-(4-methoxyphenyl)propanoic acid* 322**

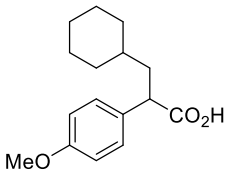

Following **GP11** using corresponding α-trifluoromethyl alkene (20.2 mg, 0.10 mmol), potassium cyclohexyltrifluoroborate **320** (28.5 mg, 0.15 mmol) and H_2O (50 µL) for 48 h. Purification by flash chromatography (EtOAc : Hexane : AcOH = 15 : 100 : 2), the product was obtained as a white solid (21.8 mg, 84% yield). ^{1}H NMR (600 MHz, $CDCl_3$) δ 7.24 (d, *J* = 8.7 Hz, 2H), 6.86 (d, *J* = 8.7 Hz, 2H), 3.79 (s, 3H), 3.64 (t, *J* = 7.8 Hz, 1H), 1.93 (dt, *J* = 13.7, 7.8 Hz, 1H), 1.76 – 1.68 (m, 2H), 1.68 – 1.57 (m, 4H), 1.21 – 1.09 (m, 4H), 0.95 – 0.85 (m, 2H); ^{13}C NMR (151 MHz, $CDCl_3$) δ 180.8, 159.0, 130.9, 129.2 (2C), 114.2 (2C), 55.4, 47.9, 40.7, 35.2, 33.5, 33.0, 26.6, 26.22, 26.17. HRMS ESI $[M-H]^-$ calculated for ($C_{16}H_{21}O_3^-$) 261.1496, found 261.1488.

2-(4-(*tert*-Butyl)phenyl)-3-cyclohexylpropanoic acid 323

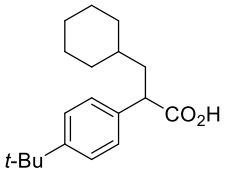

Following **GP11** using corresponding α-trifluoromethyl alkene (22.8 mg, 0.10 mmol), potassium cyclohexyltrifluoroborate **320** (28.5 mg, 0.15 mmol) and H_2O (30 µL) for 36 h. Purification by flash chromatography (EtOAc : Hexane : AcOH = 10 : 100 : 2), the product was obtained as a white solid (24.1 mg, 84% yield). ^{1}H NMR (400 MHz, $CDCl_3$) δ 7.36 (d, *J* = 8.4 Hz, 2H), 7.28 (d, *J* = 8.4 Hz, 2H), 3.70 (dd, *J* = 8.5, 6.9 Hz, 1H), 2.01 (ddd, *J* = 13.8, 8.5, 6.9 Hz, 1H), 1.81 – 1.73 (m, 2H), 1.73 – 1.63 (m, 4H), 1.34 (s, 9H), 1.27 – 1.15 (m, 4H), 0.99 – 0.87 (m, 2H); ^{13}C NMR (101 MHz, $CDCl_3$) δ 180.8, 150.3, 135.9, 127.8 (2C), 125.7 (2C), 48.4, 40.81, 35.3, 34.6, 33.3, 33.2, 31.5 (3C), 26.6, 26.19, 26.17. HRMS ESI $[M-H]^-$ calculated for ($C_{19}H_{27}O_2^+$) 287.2017, found 287.2008.

***3-Cyclohexyl-2-(4-fluorophenyl)propanoic acid* 324**

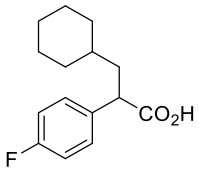

Following **GP11** using corresponding α-trifluoromethyl alkene (19.0 mg, 0.10 mmol), potassium cyclohexyltrifluoroborate **320** (28.5 mg, 0.15 mmol) and H_2O (30 µL) for 48 h. Purification by flash chromatography (EtOAc : Hexane : AcOH = 10 : 100 : 2), the product was obtained as a white solid (15.1 mg, 60% yield). ^{1}H NMR (400 MHz, $CDCl_3$) δ 7.30 – 7.23 (m, 2H), 7.03 – 6.95 (m, 2H), 3.66 (t, *J* = 7.8 Hz, 1H), 1.92 (dt, *J* = 13.8, 7.8 Hz, 1H), 1.74 – 1.56 (m, 6H),

1.17 – 1.05 (m, 4H), 0.97 – 0.79 (m, 2H); ^{13}C NMR (101 MHz, $CDCl_3$) δ 180.4, 162.3 (d, $^{1}J_{C\text{-}F}$ = 246.4 Hz), 134.5 (d, $^{4}J_{C\text{-}F}$ = 3.2 Hz), 129.8 (d, $^{3}J_{C\text{-}F}$ = 8.0 Hz, 2C), 115.6 (d, $^{2}J_{C\text{-}F}$= 22.2 Hz, 2C), 48.0, 40.8, 35.2, 33.4, 33.0, 26.6, 26.20, 26.15; ^{19}F NMR (376 MHz, $CDCl_3$) δ -115.16 – -115.25 (m, 1F). HRMS ESI $[M\text{-}H]^-$ calculated for ($C_{15}H_{18}O_2F^-$) 249.1296, found 249.1286.

***3-Cyclohexyl-2-(4-(trimethylsilyl)phenyl)propanoic acid* 325**

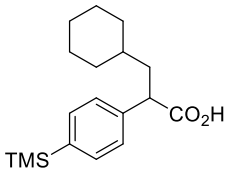

Following **GP11** using corresponding α-trifluoromethyl alkene (24.4 mg, 0.10 mmol), potassium cyclohexyltrifluoroborate **320** (28.5 mg, 0.15 mmol) and H_2O (30 µL) for 48 h. Purification by flash chromatography (EtOAc : Hexane : AcOH = 12 : 100 : 2), the product was obtained as a white solid (15.6 mg, 51% yield). ^{1}H NMR (400 MHz, $CDCl_3$) δ 7.47 (d, *J* = 8.0 Hz, 2H), 7.30 (d, *J* = 8.0, 2H), 3.68 (dd, *J* = 8.5, 6.9 Hz, 1H), 1.98 (ddd, *J* = 13.8, 8.5, 6.9 Hz, 1H), 1.79 – 1.70 (m, 2H), 1.70 – 1.58 (m, 4H), 1.25 – 1.12 (m, 4H), 0.99 – 0.82 (m, 2H), 0.26 (s, 9H); ^{13}C NMR (101 MHz, $CDCl_3$) δ 180.3, 139.6, 139.5, 133.8 (2C), 127.6 (2C), 48.8, 40.7, 35.3, 33.3, 33.2, 26.6, 26.19, 26.16, -1.0 (3C). HRMS ESI $[M+Na]^+$ calculated for ($C_{18}H_{27}O_2SiNa^+$) 327.1751, found 327.1745.

***2-(4-Acetamidophenyl)-3-cyclohexylpropanoic acid* 326**

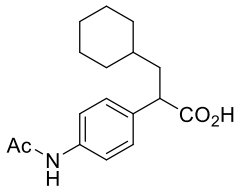

Following **GP11** using corresponding α-trifluoromethyl alkene (22.9 mg, 0.10 mmol), potassium cyclohexyltrifluoroborate **320** (28.5 mg, 0.15 mmol) and H_2O (30 µL) for 48 h. Purification by flash chromatography (EtOAc : Hexane : AcOH = 30 : 100 : 2), the product was obtained as a white solid (14.2 mg, 49% yield). ^{1}H NMR (600 MHz, $CDCl_3$) δ 7.77 (br s, 1H), 7.40 (d, *J* = 8.0 Hz, 2H), 7.22 (d, *J* = 8.0 Hz, 2H), 3.65 (t, *J* = 7.8 Hz, 1H), 2.12 (s, 3H), 1.92 (dt, *J* = 14.4, 7.8 Hz, 1H), 1.75 – 1.60 (m, 6H), 1.17 – 1.10 (m, 4H), 0.93 – 0.85 (m, 2H); ^{13}C NMR (151 MHz, $CDCl_3$) δ 179.4, 169.2, 137.0, 135.1, 128.7 (2C), 120.5 (2C), 48.3, 40.6, 35.2, 33.4, 33.0, 26.6, 26.20, 26.16, 24.5. HRMS ESI $[M+H]^+$ calculated for ($C_{17}H_{24}O_3N^+$) 290.1751, found 290.1747.

***3-Cyclohexyl-2-(4-ethynylphenyl)propanoic acid* 327**

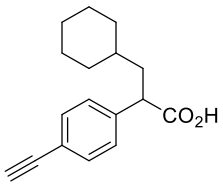

Following **GP11** using α-trifluoromethyl alkene **685** (26.8 mg, 0.10 mmol), potassium cyclohexyltrifluoroborate **320** (28.5 mg, 0.15 mmol), H_2O (50 µL) and **PC-7** (5 mol%) for 48 h. Purification by flash chromatography (EtOAc : Hexane : AcOH = 12 : 100 : 2), the product was obtained as a white solid (17.3 mg, 68% yield). ^{1}H NMR (600 MHz, $CDCl_3$) δ 7.44 (d, *J* = 8.1 Hz, 2H), 7.27 (d, *J* = 8.1 Hz, 2H), 3.69 (t, *J* = 7.8 Hz, 1H), 3.06 (s, 1H), 1.95 (dt, *J* = 13.7, 7.8 Hz, 1H),

1.74 – 1.58 (m, 6H), 1.20 – 1.09 (m, 4H), 0.94 – 0.85 (m, 2H); ^{13}C NMR (151 MHz, $CDCl_3$) δ 179.6, 139.6, 132.6 (2C), 128.3 (2C), 121.4, 83.5, 77.5, 48.7, 40.6, 35.2, 33.4, 33.0, 26.6, 26.2, 26.1. HRMS ESI $[M+Na]^+$ calculated for ($C_{17}H_{20}O_2Na^+$) 279.1356, found 279.1351.

***3-Cyclohexyl-2-(3-methoxyphenyl)propanoic acid* 328**

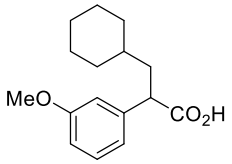

Following **GP11** using corresponding α-trifluoromethyl alkene (20.2 mg, 0.10 mmol), potassium cyclohexyltrifluoroborate **320** (28.5 mg, 0.15 mmol) and H_2O (30 µL) for 48 h. Purification by flash chromatography (EtOAc : Hexane : AcOH = 15 : 100 : 2), the product was obtained as a white solid (18.5 mg, 71% yield). ^{1}H NMR (600 MHz, $CDCl_3$) δ 7.25 – 7.21 (m, 1H), 6.91 (dd, *J* = 7.7, 1.5 Hz, 1H), 6.89 – 6.87 (m, 1H), 6.81 (dd, *J* = 8.2, 2.6 Hz, 1H), 3.80 (s, 3H), 3.67 (t, *J* = 7.7 Hz, 1H), 1.95 (dt, *J* = 13.3, 7.7 Hz, 1H), 1.77 – 1.71 (m, 2H), 1.68 – 1.63 (m, 3H), 1.64 – 1.58 (m, 1H), 1.22 – 1.13 (m, 4H), 0.94 – 0.87 (m, 2H); ^{13}C NMR (151 MHz, $CDCl_3$) δ 180.4, 159.9, 140.4, 129.7, 120.6, 114.0, 112.8, 55.4, 48.8, 40.7, 35.2, 33.4, 33.1, 26.6, 26.20, 26.16. HRMS ESI $[M-H]^-$ calculated for ($C_{16}H_{21}O_3^-$) 261.1496, found 261.1487.

***2-(3-(Allyloxy)phenyl)-3-cyclohexylpropanoic acid* 329**

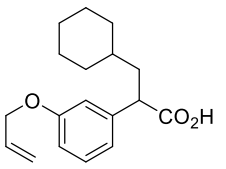

Following **GP11** using α-trifluoromethyl alkene **684** (22.8 mg, 0.10 mmol), potassium cyclohexyltrifluoroborate **320** (28.5 mg, 0.15 mmol), H_2O (50 μL) and **PC-7** (5 mol%) for 48 h. Purification by flash chromatography (EtOAc : Hexane : AcOH = 12 : 100 : 2), the product was obtained as a white solid (14.7 mg, 54% yield). ^{1}H NMR (400 MHz, $CDCl_3$) δ 7.25 – 7.19 (m, 1H), 6.93 – 6.87 (m, 2H), 6.84 – 6.79 (m, 1H), 6.05 (ddt, *J* = 17.3, 10.5, 5.3 Hz, 1H), 5.45 – 5.37 (m, 1H), 5.31 – 5.25 (m, 1H), 4.55 – 4.51 (m, 2H), 3.66 (t, *J* = 7.8 Hz, 1H), 1.94 (dt, *J* = 13.7, 7.8 Hz, 1H), 1.77 – 1.57 (m, 6H), 1.23 – 1.07 (m, 4H), 0.96 – 0.83 (m, 2H); ^{13}C NMR (101 MHz, $CDCl_3$) δ 179.8, 158.9, 140.4, 133.4, 129.7, 120.8, 117.9, 114.8, 113.6, 68.9, 48.7, 40.7, 35.2, 33.4, 33.1, 26.6, 26.20, 26.17. HRMS ESI $[M+H]^+$ calculated for ($C_{18}H_{25}O_3^+$) 289.1798, found 289.1792.

3-Cyclohexyl-2-(3,5-dimethylphenyl)propanoic acid **330**

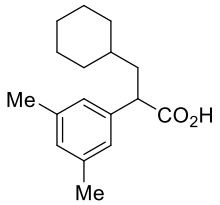

Following **GP11** using corresponding α-trifluoromethyl alkene (20.0 mg, 0.10 mmol), potassium cyclohexyltrifluoroborate **320** (28.5 mg, 0.15 mmol) and H_2O (30 μL) for 36 h. Purification by flash chromatography (EtOAc : Hexane : AcOH = 12 : 100 : 2), the product was obtained as a white solid (16.2 mg, 62% yield). ^{1}H NMR (600 MHz, $CDCl_3$) δ 6.93 (s, 2H), 6.91 (s, 1H), 3.62 (t, *J* = 7.7 Hz, 1H), 2.30 (s, 6H), 1.97 (dt, *J* = 13.1, 7.7 Hz, 1H), 1.78 – 1.70 (m, 2H), 1.69 – 1.65 (m, 2H), 1.63 – 1.58 (m, 2H), 1.24 – 1.09 (m, 4H), 0.95 – 0.86 (m, 2H); ^{13}C NMR (151 MHz, $CDCl_3$) δ 180.6, 138.9, 138.3 (2C), 129.2, 125.9 (2C), 48.7, 40.7, 35.3, 33.3, 33.2,

26.6, 26.20, 26.19, 21.4 (2C). HRMS ESI [M-H]$^-$ calculated for ($C_{17}H_{23}O_2^-$) 259.1704, found 259.1695.

***3-Cyclohexyl-2-(naphthalen-2-yl)propanoic acid* 331**

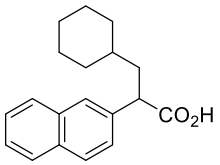

Following **GP11** using corresponding α-trifluoromethyl alkene (22.2 mg, 0.10 mmol), potassium cyclohexyltrifluoroborate **320** (28.5 mg, 0.15 mmol) and H_2O (30 µL) for 36 h. Purification by flash chromatography (EtOAc : Hexane : AcOH = 12 : 100 : 2), the product was obtained as a white solid (23.5 mg, 83% yield). ^{1}H NMR (400 MHz, $CDCl_3$) δ 9.02 (br s, 1H), 7.83 – 7.71 (m, 4H), 7.47 – 7.43 (m, 3H), 3.83 (t, *J* = 7.7 Hz, 1H), 2.01 (dt, *J* = 14.5, 7.7 Hz, 1H), 1.83 – 1.73 (m, 2H), 1.72 – 1.57 (m, 4H), 1.24 – 1.03 (m, 4H), 0.97 – 0.85 (m, 2H); ^{13}C NMR (101 MHz, $CDCl_3$) δ 180.5, 136.6, 133.5, 132.8, 128.4, 128.0, 127.7, 127.2, 126.21, 126.17, 125.9, 49.2, 40.7, 35.2, 33.6, 32.9, 26.6, 26.2, 26.1. HRMS ESI [M-H]$^-$ calculated for ($C_{19}H_{21}O_2^-$) 281.1547, found 281.1538.

***2-(Benzo[b]thiophen-2-yl)-3-cyclohexylpropanoic acid* 332**

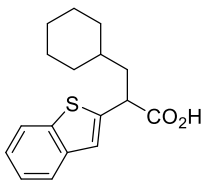

Following **GP11** using corresponding α-trifluoromethyl alkene (22.8 mg, 0.10 mmol), potassium cyclohexyltrifluoroborate **320** (28.5 mg, 0.15 mmol) and H_2O (30 µL) for 48 h. Purification by flash chromatography (EtOAc : Hexane : AcOH = 15 : 100 : 2), the product was obtained as a white solid (17.6 mg, 61% yield). ^{1}H NMR (400 MHz, $CDCl_3$) δ 7.78 (dd, *J* = 7.7, 1.5 Hz, 1H), 7.71 (dd, *J* = 7.7, 1.5Hz, 1H), 7.36 – 7.27 (m, 2H), 7.21 (s, 1H), 4.08 (t, *J* = 7.8 Hz, 1H), 2.02 (dt, *J* = 14.5, 7.8 Hz, 1H), 1.87 – 1.83 (m, 1H), 1.80 – 1.72 (m, 2H), 1.71 – 1.65 (m, 2H), 1.65 – 1.56 (m, 1H), 1.35 – 1.25 (m, 1H), 1.20 – 1.10 (m, 3H), 1.01 – 0.87 (m, 2H); ^{13}C NMR (101 MHz, $CDCl_3$) δ 179.2, 142.0, 139.63, 139.55, 124.4, 124.3, 123.5, 122.6, 122.4, 44.9, 41.4, 35.2, 33.4, 32.9, 26.5, 26.2, 26.1. HRMS ESI $[M-H]^-$ calculated for ($C_{17}H_{10}O_2S^-$) 287.1111, found 287.1102.

3-Cyclohexyl-2-(dibenzo[b,d]furan-4-yl)propanoic acid **333**

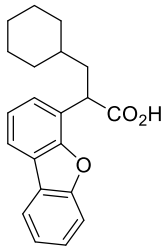

Following **GP11** using corresponding α-trifluoromethyl alkene (26.2 mg, 0.10 mmol), potassium cyclohexyltrifluoroborate **320** (28.5 mg, 0.15 mmol) and H_2O (30 µL) for 48 h. Purification by flash chromatography (EtOAc : Hexane : AcOH = 12 : 100 : 2), the product was obtained as a white solid (28.9 mg, 90% yield). ^{1}H NMR (400 MHz, $CDCl_3$) δ 7.95 (dd, *J* = 7.7, 1.3 Hz, 1H), 7.86 (dd, *J* = 7.7, 1.3 Hz, 1H), 7.60 (d, *J* = 8.2 Hz, 1H), 7.48 – 7.43 (m, 2H), 7.38 –

7.29 (m, 2H), 4.48 (t, *J* = 7.7 Hz, 1H), 2.17 – 2.06 (m, 1H), 1.97 – 1.83 (m, 2H), 1.82 – 1.71 (m, 1H), 1.71 – 1.63 (m, 2H), 1.63 – 1.55 (m, 1H), 1.31 – 1.18 (m, 2H), 1.16 – 1.12 (m, 2H), 1.02 – 0.92 (m, 2H); ^{13}C NMR (101 MHz, $CDCl_3$) δ 180.1, 156.2, 154.4, 127.3, 126.1, 124.5, 124.4, 123.2, 123.0, 122.9, 120.8, 119.7, 112.0, 42.2, 39.9, 35.4, 33.9, 33.0, 26.6, 26.2, 26.1. HRMS ESI $[M+Na]^+$ calculated for ($C_{21}H_{22}O_3Na^+$) 345.1461, found 345.1458.

3-Cyclohexyl-2-(6-methoxypyridin-3-yl)propanoic acid **334**

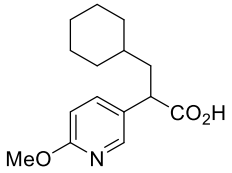

Following **GP11** using corresponding α-trifluoromethyl alkene (20.3 mg, 0.10 mmol), potassium cyclohexyltrifluoroborate **320** (28.5 mg, 0.15 mmol) and H_2O (30 μL) for 48 h. Purification by flash chromatography (EtOAc : Hexane : AcOH = 25 : 100 : 2), the product was obtained as a white solid (10.5 mg, 40% yield). ^{1}H NMR (600 MHz, $CDCl_3$) δ ^{1}H NMR (600 MHz, $CDCl_3$) δ 8.07 (d, *J* = 2.5 Hz, 1H), 7.60 (dd, *J* = 8.6, 2.5 Hz, 1H), 6.73 (d, *J* = 8.6 Hz, 1H), 3.92 (s, 3H), 3.65 (t, *J* = 7.8 Hz, 1H), 1.93 (dt, *J* = 13.8, 7.8 Hz, 1H), 1.72 – 1.58 (m, 6H), 1.17 – 1.09 (m, 4H), 0.96 – 0.85 (m, 2H); ^{13}C NMR (151 MHz, $CDCl_3$) δ 179.0, 163.6, 146.3, 138.5, 127.5, 111.1, 53.8, 45.4, 40.6, 35.1, 33.5, 32.8, 26.6, 26.2, 26.1. HRMS ESI $[M+H]^+$ calculated for ($C_{15}H_{22}O_3N^+$) 264.1594, found 264.1591.

2-(Methoxymethyl)-6-phenyl-1,2,3,4-tetrahydronaphthalene-1-carboxylic acid **335**

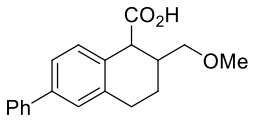

Following **GP11** using α-trifluoromethyl alkene **686** (54.9 mg, 0.20 mmol), potassium methoxymethyltrifluoroborate **336** (45.6 mg, 0.3 mmol), H_2O (60 µL) for 48 h. Purification by flash chromatography (EtOAc : Hexane : AcOH = 15 : 100 : 1), the product was obtained as a white solid (38.9 mg, 57% yield), dr = 1 : 1. ^{1}H NMR (400 MHz, $CDCl_3$) δ 9.98 (br s, 1H), 7.78 (d, *J* = 7.7 Hz, 2H), 7.47 – 7.39 (m, 3H), 7.38 – 7.32 (m, 3H), 4.02 (d, *J* = 5.4 Hz, 0.5H), 3.78 (d, *J* = 7.5 Hz, 0.5H), 3.62 – 3.56 (m, 0.5H), 3.55 – 3.46 (m, 1H), 3.45 – 3.43 (m, 0.5H), 3.40 (s, 1.5H), 3.38 (s, 1.5H), 3.08 – 2.98 (m, 0.5H), 2.97 – 2.82 (m, 1.5H), 2.66 – 2.57 (m, 0.5H), 2.36 – 2.27 (m, 0.5H), 2.19 – 2.06 (m, 1H), 1.89 – 1.81 (m, 0.5H), 1.64 – 1.53 (m, 0.5H); ^{13}C NMR (101 MHz, $CDCl_3$) δ 180.8, 179.1, 141.0, 140.9, 140.4, 140.1, 137.6, 137. 5, 132.1, 131.4, 130.1, 129.5, 128.8, 128.3, 128.0, 127.3, 127.19, 127.17, 125.2, 124.9, 75.8, 75.0, 59.07, 59.05, 48.1, 45.9, 37.4, 37.2, 28.8, 28.1, 24.1, 21.6. HRMS ESI $[M+Na]^+$ calculated for ($C_{19}H_{20}O_3Na^+$) 319.1305, found 319.1300.

2-([1,1'-Biphenyl]-4-yl)-3-cyclopentylpropanoic acid **337**

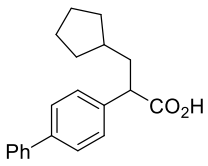

Following **GP11** using α-trifluoromethyl alkene **232** (24.8 mg, 0.10 mmol), potassium cyclopentyltrifluoroborate (26.4 mg, 0.15 mmol) and H_2O (30 µL) for 48 h. Purification by flash

chromatography (EtOAc : Hexane : AcOH = 15 : 100 : 2), the product was obtained as a white solid (21.5 mg, 73% yield). ^{1}H NMR (600 MHz, $CDCl_3$) δ 7.61 – 7.54 (m, 4H), 7.46 – 7.40 (m, 4H), 7.37 – 7.32 (m, 1H), 3.67 (t, *J* = 7.7 Hz, 1H), 2.13 (dt, *J* = 13.4, 7.7 Hz, 1H), 1.88 (ddd, *J* = 13.4, 7.8, 6.8 Hz, 1H), 1.84 – 1.70 (m, 3H), 1.65 – 1.57 (m, 2H), 1.54 – 1.45 (m, 2H), 1.17 – 1.08 (m, 2H); ^{13}C NMR (151 MHz, $CDCl_3$) δ 180.5, 140.9, 140.5, 137.8, 128.9 (2C), 128.7 (2C), 127.5 (2C), 127.4, 127.2 (2C), 50.6, 39.6, 37.9, 32.8, 32.5, 25.22, 25.20. HRMS ESI $[M-H]^-$ calculated for ($C_{20}H_{21}O_2^-$) 293.1547, found 293.1539.

2-([1,1'-Biphenyl]-4-yl)-3-cycloheptylpropanoic acid **338**

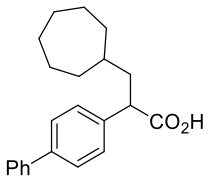

Following **GP11** using α-trifluoromethyl alkene **232** (24.8 mg, 0.10 mmol), potassium cycloheptyltrifluoroborate (30.6 mg, 0.15 mmol) and H_2O (30 µL) for 48 h. Purification by flash chromatography (EtOAc : Hexane : AcOH = 15 : 100 : 2), the product was obtained as a white solid (18.3 mg, 57% yield). ^{1}H NMR (600 MHz, $CDCl_3$) δ 7.59 (d, *J* = 7.7 Hz, 2H), 7.56 (d, *J* = 8.0 Hz, 2H), 7.46 (d, *J* = 7.7 Hz, 2H), 7.41 (d, *J* = 8.0 Hz, 2H), 7.37 – 7.32 (m, 1H), 3.73 (t, *J* = 7.7 Hz, 1H), 2.05 (dt, *J* = 14.5, 7.7 Hz, 1H), 1.79 – 1.70 (m, 3H), 1.65 – 1.57 (m, 2H), 1.58 – 1.51 (m, *J* = 5.6 Hz, 2H), 1.48 – 1.43 (m, 3H), 1.43 – 1.35 (m, 2H), 1.30 – 1.19 (m, 2H); ^{13}C NMR (151 MHz, $CDCl_3$) δ 180.5, 140.8, 140.5, 137.9, 128.9 (2C), 128.7 (2C), 127.5 (2C), 127.4, 127.2 (2C), 49.1,

41.2, 36.7, 34.6, 34.2, 28.7 (2C), 26.2, 26.1. HRMS ESI [M-H]$^-$ calculated for ($C_{22}H_{25}O_2^-$) 321.1860, found 321.1850.

2-([1,1'-Biphenyl]-4-yl)-3-(4,4-difluorocyclohexyl)propanoic acid **339**

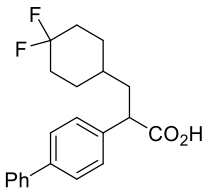

Following **GP11** using α-trifluoromethyl alkene **232** (24.8 mg, 0.10 mmol), potassium 4,4-difluorocycloheptyltrifluoroborate (33.9 mg, 0.15 mmol) and H_2O (30 µL) for 48 h. Purification by flash chromatography (EtOAc : Hexane : AcOH = 15 : 100 : 2), the product was obtained as a white solid (27.5 mg, 80% yield). ^{1}H NMR (600 MHz, $CDCl_3$) δ 7.60 – 7.54 (m, 4H), 7.46 – 7.42 (m, 2H), 7.39 (d, *J* = 7.8 Hz, 2H), 7.37 – 7.33 (m, 1H), 3.72 (t, *J* = 7.8 Hz, 1H), 2.11 – 2.00 (m, 3H), 1.85 – 1.75 (m, 3H), 1.69 – 1.57 (m, 2H), 1.35 – 1.25 (m, 3H); ^{13}C NMR (151 MHz, $CDCl_3$) δ 179.6, 140.8, 140.6, 137.2, 129.0 (2C), 128.5 (2C), 127.7 (2C), 127.6, 127.2 (2C), 123.6 (t, $^1J_{C\text{-}F}$ = 239.9 Hz), 48.7, 39.0 (d, $^4J_{C\text{-}F}$ = 1.2 Hz), 33.43, 33.40 (t, $^2J_{C\text{-}F}$ = 22.8 Hz), 33.39 (t, $^2J_{C\text{-}F}$ = 22.8 Hz), 29.1 (d, $^3J_{C\text{-}F}$ = 9.4 Hz), 28.8 (d, $^3J_{C\text{-}F}$ = 9.4 Hz); ^{19}F NMR (376 MHz, $CDCl_3$) δ -91.81 (d, *J* = 233.6 Hz), -101.98 (d, *J* = 267.8 Hz). HRMS ESI [M+Na]$^+$ calculated for ($C_{21}H_{22}F_2O_2Na^+$) 367.1480, found 367.1477.

2-([1,1'-Biphenyl]-4-yl)-3-(1-(tert-butoxycarbonyl)piperidin-4-yl)propanoic acid **340**

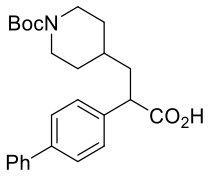

Following **GP11** using α-trifluoromethyl alkene **232** (24.8 mg, 0.10 mmol), potassium (*tert*-butoxycarbonyl)piperdinyltrifluoroborate (43.7 mg, 0.15 mmol) and H_2O (100 µL) for 48 h. Purification by flash chromatography (EtOAc : Hexane : AcOH = 20 : 100 : 2), the product was obtained as a white solid (17.4 mg, 43% yield). ^{1}H NMR (600 MHz, $CDCl_3$) δ 7.59 – 7.54 (m, 4H), 7.45 – 7.41 (m, 2H), 7.39 (d, *J* = 7.7 Hz, 2H), 7.37 – 7.32 (m, 1H), 4.09 – 4.02 (m, 2H), 3.74 (t, *J* = 7.7 Hz, 1H), 2.68 – 2.58 (m, 2H), 2.06 (dd, *J* = 14.4, 7.3 Hz, 1H), 1.77 (dt, *J* = 14.4, 7.3 Hz, 1H), 1.69 (t, *J* = 14.4 Hz, 2H), 1.45 (s, 9H), 1.42 – 1.38 (m, 1H), 1.18 – 1.09 (m, 2H); ^{13}C NMR (151 MHz, $CDCl_3$) δ 179.4, 155.0, 140.7, 140.6, 137.5, 128.9 (2C), 128.5 (2C), 127.6 (2C), 127.5, 127.2 (2C), 79.6, 48.3, 43.9, 39.8, 33.7, 32.2, 31.9, 28.6 (3C), 20.9. HRMS ESI $[M-H]^-$ calculated for ($C_{25}H_{30}O_4N^-$) 408.2180, found 408.2166.

***2-([1,1'-Biphenyl]-4-yl)-3-(tetrahydro-2H-pyran-4-yl)propanoic acid* 341**

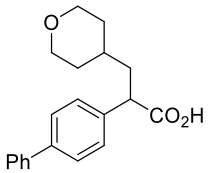

Following **GP11** using α-trifluoromethyl alkene **232** (24.8 mg, 0.10 mmol), potassium tetrahydropyranyltrifluoroborate (28.8 mg, 0.15 mmol) and H_2O (30 µL) for 48 h. Purification by flash chromatography (EtOAc : Hexane : AcOH = 15 : 100 : 2), the product was obtained as a white solid (25.7 mg, 83% yield). ^{1}H NMR (400 MHz, $CDCl_3$) δ 7.61 – 7.54 (m, 4H), 7.47 – 7.41

(m, 2H), 7.40 (d, *J* = 7.7 Hz, 2H), 7.38 – 7.32 (m, 1H), 3.99 – 3.91 (m, 2H), 3.75 (t, *J* = 7.8 Hz, 1H), 3.38 – 3.27 (m, 2H), 2.12 – 2.02 (m, 1H), 1.84 – 1.74 (m, 1H), 1.70 – 1.58 (m, 2H), 1.57 – 1.43 (m, 1H), 1.39 – 1.28 (m, 2H); ^{13}C NMR (101 MHz, $CDCl_3$) δ 179.5, 140.7, 137.5, 128.9 (2C), 128.6 (2C), 127.6 (2C), 127.5, 127.2 (2C), 67.89, 67.85, 48.0, 40.1, 33.0, 32.8, 32.6. HRMS ESI $[M-H]^-$ calculated for ($C_{20}H_{21}O_3^-$) 309.1496, found 309.1487.

***2-([1,1'-Biphenyl]-4-yl)-4-ethylhexanoic acid* 342**

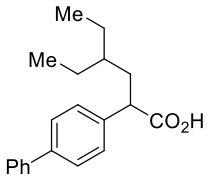

Following **GP11** using α-trifluoromethyl alkene **232** (24.8 mg, 0.10 mmol), potassium pentan-3-yltrifluoroborate (26.7 mg, 0.15 mmol) and H_2O (30 µL) for 48 h. Purification by flash chromatography (EtOAc : Hexane : AcOH = 15 : 100 : 2), the product was obtained as a white solid (25.7 mg, 83% yield). ^{1}H NMR (400 MHz, $CDCl_3$) δ 7.63 – 7.53 (m, 4H), 7.48 – 7.40 (m, 4H), 7.39 – 7.32 (m, 1H), 3.73 (t, *J* = 7.8 Hz, 1H), 2.11 – 2.02 (m, 1H), 1.84 – 1.74 (m, 1H), 1.42 – 1.29 (m, 4H), 1.24 – 1.16 (m, 1H), 0.87 (t, *J* = 7.4, 3H), 0.84 (t, *J* = 7.4, 3H); ^{13}C NMR (101 MHz, $CDCl_3$) δ 180.6, 140.8, 140.5, 137.9, 128.9 (2C), 128.7 (2C), 127.5 (2C), 127.4, 127.2 (2C), 49.1, 37.8, 36.6, 25.2, 25.0, 10.6, 10.4. HRMS ESI $[M+Na]^+$ calculated for ($C_{20}H_{24}O_2Na^+$) 319.1669, found 319.1663.

***2-([1,1'-Biphenyl]-4-yl)-4,4-dimethylpentanoic acid* 343**

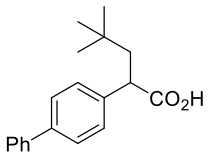

Following **GP11** using α-trifluoromethyl alkene **232** (24.8 mg, 0.10 mmol), potassium *tert*-butyltrifluoroborate (24.6 mg, 0.15 mmol), H_2O (50 µL) and **PC-7** (5 mol%) for 48 h. Purification by flash chromatography (EtOAc : Hexane : AcOH = 15 : 100 : 2), the product was obtained as a white solid (21.1 mg, 75% yield). ^{1}H NMR (600 MHz, $CDCl_3$) δ 7.57 (d, *J* = 7.4 Hz, 2H), 7.54 (d, *J* = 8.2 Hz, 2H), 7.45 – 7.40 (m, 4H), 7.37 – 7.32 (m, 1H), 3.72 (dd, *J* = 8.7, 4.3 Hz, 1H), 2.32 (dd, *J* = 14.0, 8.7 Hz, 1H), 1.68 (dd, *J* = 14.0, 4.3 Hz, 1H), 0.94 (s, 9H); ^{13}C NMR (151 MHz, $CDCl_3$) δ 181.0, 140.8, 140.4, 139.4, 128.9 (2C), 128.5 (2C), 127.6 (2C), 127.4, 127.2 (2C), 47.9, 47.0, 31.3, 29.6 (3C). HRMS ESI $[M-H]^-$ calculated for ($C_{19}H_{21}O_2^-$) 281.1547, found 281.1546.

***2-([1,1'-Biphenyl]-4-yl)-4,4,5-trimethylhexanoic acid* 344**

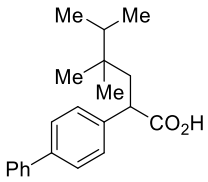

Following **GP11** using α-trifluoromethyl alkene **232** (24.8 mg, 0.10 mmol), potassium 2,3-dimethylbutan-2-yltrifluoroborate (24.6 mg, 0.15 mmol), H_2O (50 µL) and **PC-7** (5 mol%) for 48 h. Purification by flash chromatography (EtOAc : Hexane : AcOH = 15 : 100 : 2), the product was obtained as a white solid (25.3 mg, 82% yield). ^{1}H NMR (400 MHz, $CDCl_3$) δ 7.58 (d, *J* = 7.8 Hz, 2H), 7.55 (d, *J* = 8.3 Hz, 2H), 7.46 – 7.40 (m, 4H), 7.38 – 7.31 (m, 1H), 3.73 (dd, *J* = 8.6, 4.0

Hz, 1H), 2.34 (dd, *J* = 14.2, 8.6 Hz, 1H), 1.70 (dd, *J* = 14.2, 4.0 Hz, 1H), 1.60 – 1.51 (m, 1H), 0.88 (d, *J* = 6.8 Hz, 3H), 0.85 (s, 3H), 0.84 – 0.80 (m, 6H); ^{13}C NMR (101 MHz, $CDCl_3$) δ 181.1, 140.8, 140.4, 139.7, 128.9 (2C), 128.5 (2C), 127.5 (2C), 127.4, 127.2 (2C), 47.3, 43.3, 36.2, 36.0, 24.4, 23.9, 17.60, 17.55. HRMS ESI $[M+Na]^+$ calculated for ($C_{21}H_{26}O_2Na^+$) 333.1825, found 333.1819.

2-([1,1'-Biphenyl]-4-yl)-3-(adamantan-1-yl)propanoic acid **345**

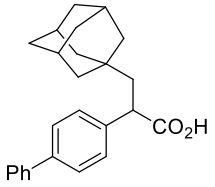

Following **GP11** using α-trifluoromethyl alkene **232** (24.8 mg, 0.10 mmol), potassium adamantan-1-yltrifluoroborate (36.3 mg, 0.15 mmol), H_2O (50 µL) and **PC-7** (5 mol%) for 48 h. Purification by flash chromatography (EtOAc : Hexane : AcOH = 15 : 100 : 2), the product was obtained as a white solid (21.1 mg, 68% yield). ^{1}H NMR (600 MHz, $CDCl_3$) δ 7.57 (d, *J* = 7.6 Hz, 2H), 7.54 (d, *J* = 7.6 Hz, 2H), 7.45 – 7.39 (m, 4H), 7.36 – 7.32 (m, 2H), 3.78 (dd, *J* = 8.8, 4.0 Hz, 1H), 2.19 (dd, *J* = 14.1, 8.8 Hz, 1H), 1.94 (s, 3H), 1.69 (d, *J* = 12.4 Hz, 3H), 1.62 (d, *J* = 12.4 Hz, 3H), 1.57 – 1.50 (m, 4H), 1.47 (d, *J* = 12.4 Hz, 3H); ^{13}C NMR (151 MHz, $CDCl_3$) δ 180.9, 140.8, 140.3, 139.7, 128.9 (2C), 128.5 (2C), 127.5 (2C), 127.4, 127.2 (2C), 47.8, 45.9, 42.4 (2C), 37.1 (2C), 33.1, 28.7 (3C). HRMS ESI $[M-H]^-$ calculated for ($C_{25}H_{27}O_2^-$) 359.2017, found 359.2004.

2-([1,1'-Biphenyl]-4-yl)-4,4-dimethyl-6-oxoheptanoic acid **346**

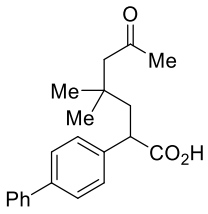

Following **GP11** using α-trifluoromethyl alkene **232** (24.8 mg, 0.10 mmol), corresponding potassium alkyltrifluoroborate (30.9 mg, 0.15 mmol), H_2O (50 µL) and **PC-7** (5 mol%) for 48 h. Purification by flash chromatography (EtOAc : Hexane : AcOH = 15 : 100 : 2), the product was obtained as a white solid (20.4 mg, 63% yield). ^{1}H NMR (400 MHz, $CDCl_3$) δ 7.58 – 7.50 (m, 4H), 7.45 – 7.37 (m, 4H), 7.37 – 7.30 (m, 1H), 3.71 (dd, *J* = 8.0, 5.0 Hz, 1H), 2.39 – 2.35 (m, 1H), 2.35 – 2.31 (m, 2H), 2.02 (s, 3H), 1.94 (dd, *J* = 14.2, 5.0 Hz, 1H), 1.04 (s, 3H), 1.02 (s, 3H); ^{13}C NMR (101 MHz, $CDCl_3$) δ 208.4, 179.9, 140.9, 140.6, 138.9, 128.9 (2C), 128.6 (2C), 127.6 (2C), 127.5, 127.2 (2C), 53.8, 47.5, 44.6, 34.0, 32.3, 27.6, 27.5. HRMS ESI $[M+Na]^+$ calculated for ($C_{21}H_{24}O_3Na^+$) 347.1618, found 347.1611.

***2-([1,1'-Biphenyl]-4-yl)-4-methoxybutanoic acid* 347**

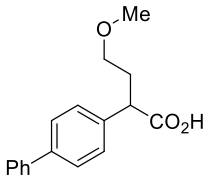

Following **GP11** using α-trifluoromethyl alkene **232** (24.8 mg, 0.10 mmol), potassium methoxymethyltrifluoroborate (22.8 mg, 0.15 mmol) and H_2O (30 µL) for 48 h. Purification by flash chromatography (EtOAc : Hexane : AcOH = 15 : 100 : 2), the product was obtained as a white solid (14.2 mg, 57% yield). ^{1}H NMR (600 MHz, $CDCl_3$) δ 7.59 – 7.54 (m, 4H), 7.45 – 7.41

(m, 2H), 7.40 (d, *J* = 8.3 Hz, 2H), 7.37 – 7.32 (m, 1H), 3.85 (t, *J* = 7.6 Hz, 1H), 3.44 – 3.39 (m, 1H), 3.34 – 3.29 (m, 1H), 3.31 (s, 3H), 2.46 – 2.37 (m, 1H), 2.07 – 2.00 (m, 1H); ^{13}C NMR (151 MHz, $CDCl_3$) δ 179.4, 140.8, 140.6, 137.3, 128.9 (2C), 128.7 (2C), 127.6 (2C), 127.5, 127.2 (2C), 70.0, 58.8, 47.7, 33.0. HRMS ESI $[M-H]^-$ calculated for ($C_{17}H_{17}O_3^-$) 269.1183, found 269.1174.

***2-([1,1'-Biphenyl]-4-yl)-4-((3-methylbut-3-en-1-yl)oxy)butanoic acid* 348**

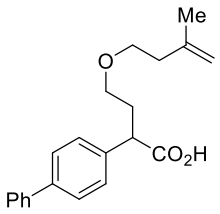

Following **GP11** using α-trifluoromethyl alkene **232** (24.8 mg, 0.10 mmol), corresponding potassium alkyltrifluoroborate (30.9 mg, 0.15 mmol) and H_2O (30 µL) for 48 h. Purification by flash chromatography (EtOAc : Hexane : AcOH = 15 : 100 : 2), the product was obtained as a white solid (17.1 mg, 53% yield). ^{1}H NMR (400 MHz, $CDCl_3$) δ 7.59 – 7.53 (m, 4H), 7.46 – 7.42 (m, 2H), 7.39 (d, *J* = 8.4 Hz, 2H), 7.37 – 7.31 (m, 1H), 4.81 – 4.76 (m, 1H), 4.74 – 4.70 (m, 1H), 3.86 (t, *J* = 7.6 Hz, 1H), 3.54 – 3.43 (m, 3H), 3.37 – 3.32 (m, 1H), 2.51 – 2.34 (m, 1H), 2.28 (t, *J* = 6.9 Hz, 2H), 2.07 – 1.96 (m, 1H), 1.74 (s, 3H); ^{13}C NMR (101 MHz, $CDCl_3$) δ 179.5, 142.9, 140.8, 140.6, 137.3, 128.9 (2C), 128.7 (2C), 127.6 (2C), 127.5, 127.2 (2C), 111.7, 69.5, 68.0, 47.8, 37.8, 33.0, 22.9. HRMS ESI $[M+Na]^+$ calculated for ($C_{21}H_{24}O_3Na^+$) 347.1618, found 347.1611.

***2-([1,1'-Biphenyl]-4-yl)-4-(((1R,2S,5R)-2-isopropyl-5-methylcyclohexyl)oxy)butanoic acid* 349**

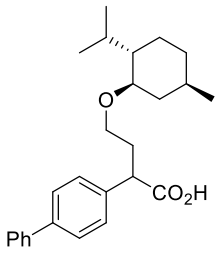

Following **GP11** using α-trifluoromethyl alkene **232** (24.8 mg, 0.10 mmol), corresponding potassium alkyltrifluoroborate (41.4 mg, 0.15 mmol), H_2O (50 µL) and **PC-7** (5 mol%) for 48 h. Purification by flash chromatography (EtOAc : Hexane : AcOH = 15 : 100 : 2), the product was obtained as colourless oil (24.2 mg, 61% yield), dr = 1:1. ^{1}H NMR (400 MHz, $CDCl_3$) δ 7.60 – 7.52 (m, 4H), 7.47 – 7.37 (m, 4H), 7.36 – 7.32 (m, 1H), 3.90 (t, *J* = 7.5 Hz, 1H), 3.64 (dt, *J* = 10.2, 5.9 Hz, 0.5H), 3.62 – 3.55 (m, 0.5H), 3.32 (ddd, *J* = 9.5, 6.7, 5.0 Hz, 0.5H), 3.18 (td, *J* = 8.7, 4.8 Hz, 0.5H), 3.04 – 2.91 (m, 1H), 2.46 – 2.33 (m, 1H), 2.30 – 2.18 (m, 1H), 2.14 – 1.97 (m, 2H), 1.67 – 1.56 (m, 2H), 1.38 – 1.14 (m, 2H), 1.02 – 0.86 (m, 7.5H), 0.86 – 0.80 (m, 1.5H), 0.76 (t, *J* = 6.5 Hz, 3H); ^{13}C NMR (101 MHz, $CDCl_3$) δ 179.6, 140.8, 140.5, 137.5, 128.9 (2C), 128.8, 128.7, 127.5 (2C), 127.4, 127.2 (2C), 79.5, 65.6, 48.4, 47.8, 40.5, 34.7, 33.6, 31.6, 25.8, 23.5, 22.5, 21.2, 16.4. HRMS ESI $[M+Na]^+$ calculated for ($C_{26}H_{34}O_3Na^+$) 417.2400, found 417.2393.

General procedure 12 (GP12) for the synthesis of α-arylated amides

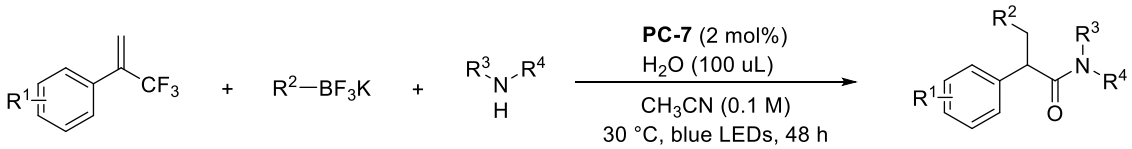

A 10-mL Schlenk tube equipped with a magnetic stir bar was charged with corresponding α-trifluoromethyl alkene (0.1 mmol, if solid), potassium alkyltrifluoroborate (0.15 mmol), *N*-

nucleophile (0.15 mmol, if solid), **PC-7** (1.2-3.0 mg, 0.002-0.005 mmol). The flask was evacuated and backfilled with N_2 3 times. CH_3CN (1.0 mL) or a solution of α-trifluoromethyl alkene (0.1 mmol, if liquid) in CH_3CN (1.0 mL) was then added via syringe followed by the addition of H_2O (100 μL) and *N*-nucleophile (0.15 mmol, if liquid) under N_2. The reaction mixture was then vigorously stirred under blue LED light (30 W, λ_{max} = 440 nm) at 30 °C (two fans were used to cool down the reaction mixture) for 48 h. After the reaction was completed, the reaction mixture was then diluted with ethyl acetate, poured into a separatory funnel, before being washed with brine. The combined organic layers were dried over Na_2SO_4 and concentrated under reduced pressure after filtration. The crude product was purified by flash chromatography on silica gel to afford the desired product.

2-([1,1'-Biphenyl]-4-yl)-N,3-dicyclohexylpropanamide **354**

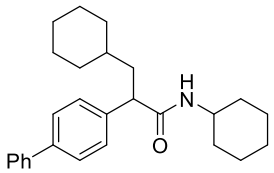

Following **GP12** using α-trifluoromethyl alkene **232** (24.8 mg, 0.10 mmol), potassium cyclohexyltrifluoroborate **320** (28.5 mg, 0.15 mmol) and cyclohexanamine **353** (14.9 mg, 0.15 mmol). Purification by flash chromatography (EtOAc : Hexane : Et_3N = 15 : 100 : 1), the product was obtained as a white foam (28.0 mg, 72% yield). ^{1}H NMR (600 MHz, $CDCl_3$) δ 7.59 (d, *J* = 7.6 Hz, 2H), 7.55 (d, *J* = 8.1 Hz, 2H), 7.44 (d, *J* = 7.6 Hz, 2H), 7.37 (d, *J* = 8.1 Hz, 2H), 7.35 – 7.32 (m, 1H), 5.33 (d, *J* = 8.2 Hz, 1H), 3.75 (m, 1H), 3.46 (t, *J* = 7.7 Hz, 1H), 2.06 (dt, *J* = 14.4, 7.7 Hz, 1H),

1.89 (m, 1H), 1.78 (m, 3H), 1.74 – 1.64 (m, 4H), 1.60 (m, 3H), 1.40 – 1.24 (m, 2H), 1.24 – 1.13 (m, 4H), 1.13 – 1.05 (m, 2H), 0.97 (m, 3H); ^{13}C NMR (151 MHz, $CDCl_3$) δ 172.8, 140.8, 139.9, 139.9, 128.9 (2C), 128.4 (2C), 127.5 (2C), 127.4, 127.1 (2C), 50.4, 48.3, 41.1, 35.4, 33.7, 33.2, 33.1, 33.0, 26.7, 26.3, 26.2, 25.6, 24.91, 24.86. HRMS ESI $[M+H]^+$ calculated for ($C_{27}H_{36}ON^+$) 390.2791, found 390.2786.

2-([1,1'-Biphenyl]-4-yl)-N-butyl-3-cyclohexylpropanamide **355**

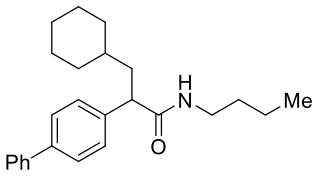

Following **GP12** using α-trifluoromethyl alkene **232** (24.8 mg, 0.10 mmol), potassium cyclohexyltrifluoroborate **320** (28.5 mg, 0.15 mmol) and butan-1-amine (11.0 mg, 0.15 mmol). Purification by flash chromatography (EtOAc : Hexane : Et_3N = 15 : 100 : 1), the product was obtained as a white solid (26.9 mg, 74% yield). ^{1}H NMR (400 MHz, $CDCl_3$) δ 7.61 – 7.57 (m, 2H), 7.55 (d, *J* = 7.9 Hz, 2H), 7.46 – 7.40 (m, 2H), 7.37 (d, *J* = 7.9 Hz, 2H), 7.36 – 7.31 (m, 1H), 5.52 (t, *J* = 5.8 Hz, 1H), 3.51 (t, *J* = 7.7 Hz, 1H), 3.30 –3.11 (m, 2H), 2.08 (dt, *J* = 14.4, 7.7 Hz, 1H), 1.85 – 1.58 (m, 7H), 1.46 – 1.35 (m, 2H), 1.31 – 1.21 (m, 2H), 1.19 – 1.09 (m, 3H), 1.01 – 0.90 (m, 2H), 0.87 (t, *J* = 7.3 Hz, 3H); ^{13}C NMR (101 MHz, $CDCl_3$) δ 173.8, 140.8, 140.0, 139.7, 128.9 (2C), 128.5 (2C), 127.5 (2C), 127.4, 127.1 (2C), 50.3, 40.91, 39.5, 35.2, 33.7, 33.0, 31.7, 26.7, 26.3, 26.2, 20.1, 13.8. HRMS ESI $[M+H]^+$ calculated for ($C_{25}H_{34}ON^+$) 364.2635, found 364.2630.

2-([1,1'-Biphenyl]-4-yl)-3-cyclohexyl-N-isobutylpropanamide **356**

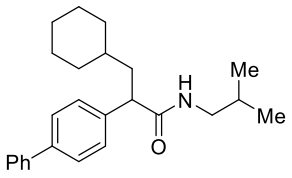

Following **GP12** using α-trifluoromethyl alkene **232** (24.8 mg, 0.10 mmol), potassium cyclohexyltrifluoroborate **320** (28.5 mg, 0.15 mmol) and 2-methylpropan-1-amine (11.0 mg, 0.15 mmol). Purification by flash chromatography (EtOAc : Hexane : Et_3N = 15 : 100 : 1), the product was obtained as a white solid (23.8 mg, 65% yield). ^{1}H NMR (600 MHz, $CDCl_3$) δ 7.60 (d, *J* = 7.8 Hz, 2H), 7.56 (d, *J* = 7.8 Hz, 2H), 7.46 – 7.42 (m, 2H), 7.38 (d, *J* = 7.8 Hz, 2H), 7.36 – 7.32 (m, 1H), 5.53 (t, *J* = 6.1 Hz, 1H), 3.53 (t, *J* = 7.7 Hz, 1H), 3.09 – 2.98 (m, 2H), 2.09 (dt, *J* = 14.3, 7.3 Hz, 1H), 1.81 – 1.59 (m, 7H), 1.24 – 1.10 (m, 4H), 1.00 – 0.89 (m, 2H), 0.82 (s, 3H), 0.81 (s, 3H); ^{13}C NMR (151 MHz, $CDCl_3$) δ 173.8, 140.8, 140.1, 139.7, 128.9 (2C), 128.5 (2C), 127.6 (2C), 127.4, 127.1 (2C), 50.4, 47.0, 40.9, 35.3, 33.7, 33.0, 28.6, 26.7, 26.3, 26.2, 20.1 (2C). HRMS ESI $[M+H]^+$ calculated for ($C_{25}H_{34}ON^+$) 364.2635, found 364.2630.

***2-([1,1'-Biphenyl]-4-yl)-3-cyclohexyl-N-neopentylpropanamide* 357**

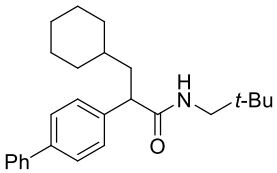

Following **GP12** using α-trifluoromethyl alkene **232** (24.8 mg, 0.10 mmol), potassium cyclohexyltrifluoroborate **320** (28.5 mg, 0.15 mmol) and 2,2-dimethylpropan-1-amine (12.1 mg, 0.15 mmol). Purification by flash chromatography (EtOAc : Hexane : Et_3N = 15 : 100 : 1), the product was obtained as a white solid (28.6 mg, 75% yield). ^{1}H NMR (400 MHz, $CDCl_3$) δ

7.61 – 7.55 (m, 4H), 7.46 – 7.41 (m, 2H), 7.41 – 7.37 (m, 2H), 7.37 – 7.31 (m, 1H), 5.51 (t, *J* = 6.4 Hz, 1H), 3.56 (t, *J* = 7.8 Hz, 1H), 3.06 – 2.96 (m, 2H), 2.10 (dt, *J* = 13.7, 7.8 Hz, 1H), 1.78 – 1.64 (m, 5H), 1.64 – 1.57 (m, 1H), 1.25 – 1.09 (m, 4H), 1.03 – 0.89 (m, 2H), 0.80 (s, 9H); ^{13}C NMR (101 MHz, $CDCl_3$) δ 173.8, 140.7, 140.1, 139.7, 128.9 (2C), 128.5 (2C), 127.6 (2C), 127.4, 127.1 (2C), 50.6, 50.5, 40.7, 35.3, 33.7, 33.0, 32.1, 27.2 (3C), 26.7, 26.3, 26.2. HRMS ESI $[M+H]^+$ calculated for ($C_{26}H_{36}ON^+$) 378.2791, found 378.2786.

2-([1,1'-Biphenyl]-4-yl)-3-cyclohexyl-N-(2-methylallyl)propenamide **358**

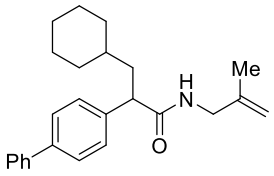

Following **GP12** using α-trifluoromethyl alkene **232** (24.8 mg, 0.10 mmol), potassium cyclohexyltrifluoroborate **320** (28.5 mg, 0.15 mmol) and 2-methylprop-2-en-1-amine (10.7 mg, 0.15 mmol). Purification by flash chromatography (EtOAc : Hexane : Et_3N = 10 : 100 : 1), the product was obtained as a white solid (20.1 mg, 56% yield). ^{1}H NMR (400 MHz, $CDCl_3$) δ 7.62 – 7.54 (m, 4H), 7.47 – 7.41 (m, 2H), 7.41 – 7.37 (m, 2H), 7.37 – 7.31 (m, 1H), 5.61 (t, *J* = 6.1 Hz, 1H), 4.77 – 4.72 (m, 1H), 4.68 – 4.64 (m, 1H), 3.84 – 3.69 (m, 2H), 3.57 (t, *J* = 7.7 Hz, 1H), 2.11 (dt, *J* = 13.7, 7.7 Hz, 1H), 1.84 – 1.54 (m, 9H), 1.27 – 1.05 (m, 4H), 1.01 – 0.86 (m, 2H); ^{13}C NMR (101 MHz, $CDCl_3$) δ 173.7, 142.2, 140.7, 140.1, 139.5, 128.9 (2C), 128.5 (2C), 127.6 (2C), 127.4, 127.1 (2C), 110.7, 50.3, 45.1, 40.8, 35.2, 33.7, 33.0, 26.7, 26.3, 26.2, 20.4. HRMS ESI $[M+H]^+$ calculated for ($C_{25}H_{31}ON^+$) 362.2478, found 362.2473.

***2-([1,1'-Biphenyl]-4-yl)-3-cyclohexyl-N-(prop-2-yn-1-yl)propenamide* 359**

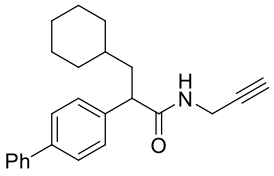

Following **GP12** using α-trifluoromethyl alkene **232** (24.8 mg, 0.10 mmol), potassium cyclohexyltrifluoroborate **320** (28.5 mg, 0.15 mmol) and prop-2-yn-1-amine (8.3 mg, 0.15 mmol). Purification by flash chromatography (EtOAc : Hexane : Et_3N = 15 : 100 : 1), the product was obtained as a white solid (18.2 mg, 53% yield). ^{1}H NMR (400 MHz, $CDCl_3$) δ 7.61 – 7.53 (m, 4H), 7.47 – 7.40 (m, 2H), 7.39 – 7.30 (m, 3H), 5.68 (t, *J* = 5.4 Hz, 1H), 4.07 (ddd, *J* = 17.8, 5.4, 2.5 Hz, 1H), 3.94 (ddd, *J* = 17.8, 5.4, 2.5 Hz, 1H), 3.54 (dd, *J* = 8.3, 7.1 Hz, 1H), 2.18 (t, *J* = 2.5 Hz, 1H), 2.13 – 2.00 (m, 1H), 1.82 – 1.57 (m, 7H), 1.23 – 1.08 (m, 4H), 1.01 – 0.86 (m, 2H); ^{13}C NMR (101 MHz, $CDCl_3$) δ 173.5, 140.7, 140.3, 139.0, 128.9 (2C), 128.5 (2C), 127.7 (2C), 127.5, 127.1 (2C), 79.6, 71.7, 50.0, 40.8, 35.1, 33.8, 32.9, 29.5, 26.6, 26.3, 26.2. HRMS ESI $[M+H]^+$ calculated for ($C_{24}H_{27}ON^+$) 346.2165, found 346.2159.

***2-([1,1'-biphenyl]-4-yl)-3-cyclohexyl-N-(2,2,2-trifluoroethyl)propenamide* 360**

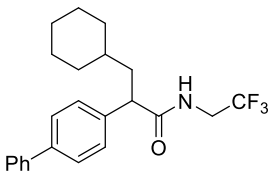

Following **GP12** using α-trifluoromethyl alkene **232** (24.8 mg, 0.10 mmol), potassium cyclohexyltrifluoroborate **320** (28.5 mg, 0.15 mmol) and 2,2,2-trifluoroethan-1-amine (14.9 mg, 0.15 mmol). Purification by flash chromatography (EtOAc : Hexane : Et_3N = 8 : 100 : 1), the

product was obtained as a white solid (28.1 mg, 72% yield). ^{1}H NMR (400 MHz, $CDCl_3$) δ 7.63 – 7.56 (m, 4H), 7.47 – 7.41 (m, 2H), 7.40 – 7.30 (m, 3H), 5.81 (t, *J* = 6.6 Hz, 1H), 4.05 – 3.90 (m, 1H), 3.83 – 3.68 (m, 1H), 3.61 (t, *J* = 7.7 Hz, 1H), 2.08 (dt, *J* = 13.8, 7.7 Hz, 1H), 1.81 – 1.57 (m, 6H), 1.24 – 1.09 (m, 4H), 1.03 – 0.85 (m, 2H); ^{13}C NMR (101 MHz, $CDCl_3$) δ 174.2, 140.6, 138.6, 129.0 (2C), 128.5 (2C), 127.8 (2C), 127.5, 127.1 (2C), 124.2 (q, $^{1}J_{C\text{-}F}$ = 279.7 Hz) , 50.0, 40.8, 40.8 (q, $^{2}J_{C\text{-}F}$ = 34.8 Hz), 35.1, 33.7, 32.9, 26.6, 26.24, 26.17; ^{19}F NMR (376 MHz, $CDCl_3$) δ -72.53 (t, *J* = 9.1 Hz, 3F). HRMS ESI $[M+H]^+$ calculated for ($C_{23}H_{27}ONF_3^+$) 390.2039, found 390.2032.

2-([1,1'-Biphenyl]-4-yl)-3-cyclohexyl-N-phenethylpropanamide **361**

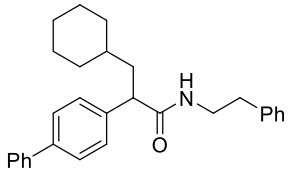

Following **GP12** using α-trifluoromethyl alkene **232** (24.8 mg, 0.10 mmol), potassium cyclohexyltrifluoroborate **320** (28.5 mg, 0.15 mmol) and 2-phenylethan-1-amine (18.2 mg, 0.15 mmol). Purification by flash chromatography (EtOAc : Hexane : Et_3N = 15 : 100 : 1), the product was obtained as a white solid (23.1 mg, 56% yield). ^{1}H NMR (600 MHz, $CDCl_3$) δ 7.60 (d, *J* = 7.6 Hz, 2H), 7.55 (d, *J* = 7.8 Hz, 2H), 7.47 – 7.43 (m, 2H), 7.38 – 7.34 (m, 1H), 7.31 (d, *J* = 7.8 Hz, 2H), 7.23 – 7.15 (m, 3H), 7.01 (d, *J* = 7.4 Hz, 2H), 5.46 (t, *J* = 6.0 Hz, 1H), 3.54 – 2.40 (m, 3H), 2.73 (t, *J* = 6.8 Hz, 2H), 2.07 (dt, *J* = 14.2, 7.3 Hz, 1H), 1.78 – 1.59 (m, 6H), 1.22 – 1.09 (m, 4H), 1.00 – 0.86 (m, 2H); ^{13}C NMR (151 MHz, $CDCl_3$) δ 173.8, 140.8, 140.1, 139.5, 139.0, 128.9 (2C), 128.9 (2C), 128.7 (2C), 128.5 (2C), 127.6 (2C), 127.4, 127.1 (2C), 126.5, 50.3, 40.8, 40.6,

35.7, 35.2, 33.7, 32.9, 26.7, 26.3, 26.2. HRMS ESI $[M+H]^+$ calculated for ($C_{29}H_{33}ON^+$) 412.2635, found 412.2630.

***2-([1,1'-biphenyl]-4-yl)-N-(2-cyanoethyl)-3-cyclohexylpropanamide* 362**

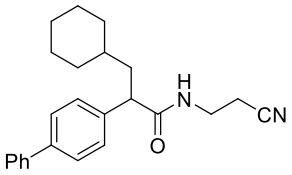

Following **GP12** using α-trifluoromethyl alkene **232** (24.8 mg, 0.10 mmol), potassium cyclohexyltrifluoroborate **320** (28.5 mg, 0.15 mmol) and 3-aminopropanenitrile (10.5 mg, 0.15 mmol). Purification by flash chromatography (EtOAc : Hexane : Et_3N = 25 : 100 : 1), the product was obtained as a white solid (24.0 mg, 67% yield). ^{1}H NMR (400 MHz, $CDCl_3$) δ ^{1}H NMR (400 MHz, $CDCl_3$) δ 7.62 – 7.54 (m, 4H), 7.47 – 7.40 (m, 2H), 7.40 – 7.29 (m, 3H), 6.07 (t, *J* = 6.2 Hz, 1H), 3.57 (t, *J* = 7.7 Hz, 1H), 3.53 – 3.43 (m, 1H), 3.43 – 3.34 (m, 1H), 2.68 – 2.49 (m, 2H), 2.05 (dt, *J* = 14.3, 7.7 Hz, 1H), 1.86 – 1.64 (m, 5H), 1.64 – 1.55 (m, 1H), 1.24 – 1.04 (m, 4H), 1.01 – 0.87 (m, 2H); ^{13}C NMR (101 MHz, $CDCl_3$) δ 174.7, 140.6, 140.4, 138.8, 128.9 (2C), 128.5 (2C), 127.7 (2C), 127.5, 127.1 (2C), 118.2, 50.0, 40.7, 35.9, 35.2, 33.72, 32.9, 26.6, 26.23, 26.15, 18.4. HRMS ESI $[M+H]^+$ calculated for ($C_{24}H_{29}ON_2^+$) 361.2274, found 361.2267.

***2-([1,1'-biphenyl]-4-yl)-3-cyclohexyl-N-(2-hydroxyethyl)propenamide* 363**

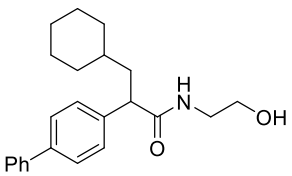

Following **GP12** using α-trifluoromethyl alkene **232** (24.8 mg, 0.10 mmol), potassium cyclohexyltrifluoroborate **320** (28.5 mg, 0.15 mmol) and 2-aminoethan-1-ol (9.2 mg, 0.15 mmol). Purification by flash chromatography (EtOAc : Hexane : Et_3N = 25 : 100 : 1), the product was obtained as a white solid (25.2 mg, 72% yield). ^{1}H NMR (400 MHz, $CDCl_3$) δ 7.61 – 7.52 (m, 4H), 7.46 – 7.40 (m, 2H), 7.39 – 7.30 (m, 3H), 6.14 (t, *J* = 5.7 Hz, 1H), 3.64 (t, *J* = 5.0 Hz, 2H), 3.56 (t, *J* = 7.7 Hz, 1H), 3.44 – 3.27 (m, 2H), 2.51 (br s, 1H), 2.04 (dt, *J* = 14.4, 7.7 Hz, 1H), 1.82 – 1.63 (m, 5H), 1.63 – 1.54 (m, 1H), 1.21 – 1.08 (m, 4H), 1.00 – 0.85 (m, 2H); ^{13}C NMR (101 MHz, $CDCl_3$) δ 175.4, 140.7, 140.2, 139.3, 128.9 (2C), 128.5 (2C), 127.6 (2C), 127.4, 127.1 (2C), 62.5, 50.1, 42.8, 40.9, 35.2, 33.8, 32.9, 26.6, 26.3, 26.2. HRMS ESI $[M+H]^+$ calculated for ($C_{23}H_{30}O_2N^+$) 352.2271, found 352.2266.

N,N'-(Ethane-1,2-diyl)bis(2-([1,1'-biphenyl]-4-yl)-3-cyclohexylpropanamide) 364

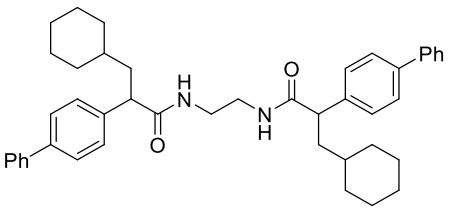

Following **GP12** using α-trifluoromethyl alkene **232** (24.8 mg, 0.10 mmol), potassium cyclohexyltrifluoroborate **320** (28.5 mg, 0.15 mmol) and ethane-1,2-diamine (9.0 mg, 0.15 mmol). Purification by flash chromatography (DCM : MeOH : Et_3N = 50 : 1 : 1), the product was obtained as a white solid (24.5 mg, 75% yield). ^{1}H NMR (400 MHz, $CDCl_3$) δ 7.59 – 7.46 (m, 8H), 7.46 – 7.36 (m, 4H), 7.36 – 7.24 (m, 6H), 6.32 – 6.19 (m, 2H), 3.47 (q, *J* = 7.4 Hz, 2H), 3.33 – 3.15 (m, 4H), 1.97 (dq, *J* = 14.8, 7.6 Hz, 2H), 1.80 – 1.54 (m, 14H), 1.19 – 1.02 (m, 8H), 0.99 –

0.81 (m, 4H); ^{13}C NMR (101 MHz, $CDCl_3$) δ 175.3 (2C), 140.7, 140.7, 140.11, 140.08, 139.3, 139.3, 128.91 (2C), 128.90 (2C), 128.49 (2C), 128.47 (2C), 127.58 (2C), 127.57 (2C), 127.43, 127.41, 127.09 (2C), 127.08 (2C), 50.1 (2C), 40.8, 40.6, 40.4, 40.3, 35.2, 35.1, 33.82, 33.81, 32.9, 32.8, 26.63, 26.61, 26.3 (2C), 26.18, 26.15. HRMS ESI $[M+H]^+$ calculated for ($C_{44}H_{53}O_2N_2^+$) 641.4102, found 641.4096.

2-([1,1'-Biphenyl]-4-yl)-3-cyclohexyl-N,N-dimethylpropanamide **365**

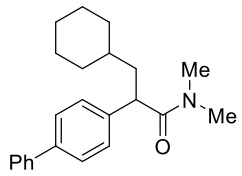

Following **GP12** using α-trifluoromethyl alkene **232** (24.8 mg, 0.10 mmol), potassium cyclohexyltrifluoroborate **320** (28.5 mg, 0.15 mmol) and dimethylamine (6.8 mg, 0.15 mmol). Purification by flash chromatography (EtOAc : Hexane : Et_3N = 12 : 100 : 1), the product was obtained as a white solid (16.7 mg, 50% yield). ^{1}H NMR (400 MHz, $CDCl_3$) δ 7.60 – 7.55 (m, 2H), 7.55 – 7.50 (m, 2H), 7.45 – 7.39 (m, 2H), 7.38 – 7.30 (m, 3H), 3.92 (dd, *J* = 8.1, 6.6 Hz, 1H), 3.00 (s, 3H), 2.96 (s, 3H), 2.06 (ddd, *J* = 13.7, 8.1, 6.6 Hz, 1H), 1.86 – 1.75 (m, 1H), 1.73 – 1.54 (m, 5H), 1.28 – 1.09 (m, 4H), 1.00 – 0.85 (m, 2H); ^{13}C NMR (101 MHz, $CDCl_3$) δ 173.4, 140.9, 139.8, 139.7, 128.9 (2C), 128.4 (2C), 127.5 (2C), 127.3, 127.1 (2C), 45.3 (2C), 42.9, 37.4, 36.1, 35.3, 33.5, 26.7, 26.31, 26.26. HRMS ESI $[M+H]^+$ calculated for ($C_{23}H_{30}ON^+$) 336.2322, found 336.2315.

2-([1,1'-Biphenyl]-4-yl)-3-cyclohexyl-1-morpholinopropan-1-one **366**

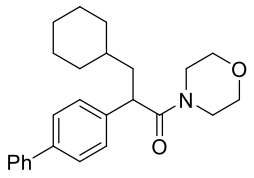

Following **GP12** using α-trifluoromethyl alkene **232** (24.8 mg, 0.10 mmol), potassium cyclohexyltrifluoroborate **320** (28.5 mg, 0.15 mmol) and morpholine (13.1 mg, 0.15 mmol). Purification by flash chromatography (EtOAc : Hexane : Et_3N = 10 : 100 : 1), the product was obtained as a white solid (31.3 mg, 83% yield). ^{1}H NMR (600 MHz, $CDCl_3$) δ 7.58 (d, *J* = 7.7 Hz, 2H), 7.55 (d, *J* = 7.7 Hz, 2H), 7.45 – 7.40 (m, 2H), 7.35 – 7.29 (m, 3H), 3.88 (t, *J* = 7.3 Hz, 1H), 3.79 – 3.72 (m, 1H), 3.69 – 3.62 (m, 1H), 3.57 – 3.48 (m, 4H), 3.47 – 3.40 (m, 1H), 3.23 – 3.17 (m, 1H), 2.08 (dt, *J* = 14.2, 7.3 Hz, 1H), 1.85 – 1.78 (m, 1H), 1.72 – 1.65 (m, 3H), 1.65 – 1.58 (m, 2H), 1.30 – 1.10 (m, 4H), 0.99 – 0.88 (m, 2H); ^{13}C NMR (151 MHz, $CDCl_3$) δ 171.9, 140.6, 139.8, 139.6, 128.8 (2C), 128.2 (2C), 127.6 (2C), 127.4, 127.0 (2C), 66.9, 66.5, 46.2, 45.0, 42.6, 42.5, 35.2, 33.49, 33.47, 26.6, 26.24, 26.20. HRMS ESI $[M+H]^+$ calculated for ($C_{25}H_{32}O_2N^+$) 378.2428, found 378.2420.

2-([1,1'-Biphenyl]-4-yl)-1-(azepan-1-yl)-3-cyclohexylpropan-1-one **367**

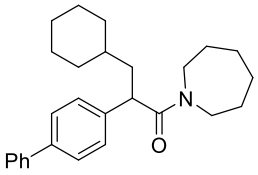

Following **GP12** using α-trifluoromethyl alkene **232** (24.8 mg, 0.10 mmol), potassium cyclohexyltrifluoroborate **320** (28.5 mg, 0.15 mmol) and azepane (14.9 mg, 0.15 mmol). Purification by flash chromatography (EtOAc : Hexane : Et_3N = 10 : 100 : 1), the product was

obtained as a white solid (29.0 mg, 75% yield). ^{1}H NMR (400 MHz, $CDCl_3$) δ 7.62 – 7.56 (m, 2H), 7.56 – 7.50 (m, 2H), 7.46 – 7.35 (m, 4H), 7.35 – 7.29 (m, 1H), 3.91 (dd, *J* = 8.1, 6.6 Hz, 1H), 3.73 – 3.64 (m, 1H), 3.63 – 3.55 (m, 1H), 3.41 – 3.27 (m, 2H), 2.06 (ddd, *J* = 14.2, 8.1, 6.6 Hz, 1H), 1.89 – 1.78 (m, 1H), 1.76 – 1.45 (m, 12H), 1.42 – 1.31 (m, 1H), 1.27 – 1.10 (m, 4H), 1.00 – 0.86 (m, 2H); ^{13}C NMR (101 MHz, $CDCl_3$) δ 172.8, 140.9, 140.3, 139.6, 128.8 (2C), 128.5 (2C), 127.4 (2C), 127.3, 127.1 (2C), 47.9, 46.6, 45.4, 43.2, 35.5, 33.63, 33.58, 29.4, 27.7, 27.1, 26.7, 26.6, 26.33, 26.28. HRMS ESI $[M+H]^+$ calculated for ($C_{27}H_{36}ON^+$) 390.2791, found 390.2784.

2-([1,1'-Biphenyl]-4-yl)-3-cyclohexyl-1-(piperidin-1-yl)propan-1-one **368**

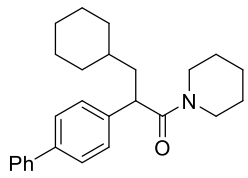

Following **GP12** using α-trifluoromethyl alkene **232** (24.8 mg, 0.10 mmol), potassium cyclohexyltrifluoroborate **320** (28.5 mg, 0.15 mmol) and piperidine (12.8 mg, 0.15 mmol). Purification by flash chromatography (EtOAc : Hexane : Et_3N = 10 : 100 : 1), the product was obtained as a white solid (29.2 mg, 78% yield). ^{1}H NMR (400 MHz, $CDCl_3$) δ 7.61 – 7.56 (m, 2H), 7.56 – 7.50 (m, 2H), 7.45 – 7.39 (m, 2H), 7.38 – 7.29 (m, 3H), 3.94 (dd, *J* = 8.1, 6.6 Hz, 1H), 3.72 – 3.60 (m, 1H), 3.54 – 3.35 (m, 3H), 2.08 (ddd, *J* = 14.2, 8.1, 6.6 Hz, 1H), 1.92 – 1.76 (m, 1H), 1.74 – 1.34 (m, 10H), 1.32 – 1.03 (m, 2H), 0.99 – 0.86 (m, 2H); ^{13}C NMR (101 MHz, $CDCl_3$) δ 171.4, 140.8, 140.3, 139.5, 128.8 (2C), 128.3 (2C), 127.4 (2C), 127.3, 127.1 (2C), 46.8, 44.9 (2C),

43.3, 42.8, 35.3, 33.5 (2C), 26.7, 26.30, 26.25, 25.7, 24.7. HRMS ESI $[M+H]^+$ calculated for ($C_{26}H_{34}ON^+$) 376.2635, found 376.2628.

***2-([1,1'-Biphenyl]-4-yl)-3-cyclohexyl-1-(1,4-dioxa-8-azaspiro[4.5]decan-8-yl)propan-1-one* 369**

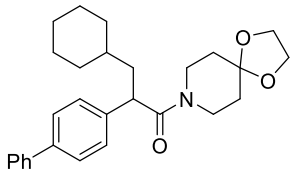

Following **GP12** using α-trifluoromethyl alkene **232** (24.8 mg, 0.10 mmol), potassium cyclohexyltrifluoroborate **320** (28.5 mg, 0.15 mmol) and 1,4-dioxa-8-azaspiro[4.5]decane (21.5 mg, 0.15 mmol). Purification by flash chromatography (EtOAc : Hexane : Et_3N = 15 : 100 : 1), the product was obtained as a white solid (38.7 mg, 90% yield). ^1H NMR (400 MHz, $CDCl_3$) δ 7.59 – 7.55 (m, 2H), 7.55 – 7.50 (m, 2H), 7.44 – 7.38 (m, 2H), 7.35 – 7.28 (m, 3H), 3.97 – 3.38 (m, 6H), 3.62 – 3.48 (m, 3H), 2.12 – 2.02 (m, 1H), 1.90 – 1.74 (m, 1H), 1.72 – 1.44 (m, 8H), 1.29 – 1.07 (m, 5H), 0.98 – 0.84 (m, 2H); ^{13}C NMR (101 MHz, $CDCl_3$) δ 171.5, 140.7, 140.0, 139.7, 128.8 (2C), 128.2 (2C), 127.5 (2C), 127.3, 127.1 (2C), 107.1, 64.5 (2C), 45.1, 43.6, 42.7, 40.3, 35.3, 35.2, 34.8, 33.53, 33.51, 26.7, 26.3, 26.2. HRMS ESI $[M+H]^+$ calculated for ($C_{28}H_{36}ON^+$) 434.2690, found 434.2681.

***Ethyl 1-(2-([1,1'-biphenyl]-4-yl)-3-cyclohexylpropanoyl)piperidine-4-carboxylate* 370**

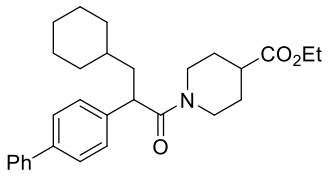

Following **GP12** using α-trifluoromethyl alkene **232** (24.8 mg, 0.10 mmol), potassium cyclohexyltrifluoroborate **320** (28.5 mg, 0.15 mmol) and ethyl piperidine-4-carboxylate (23.6 mg, 0.15 mmol). Purification by flash chromatography (EtOAc : Hexane : Et_3N = 10 : 100 : 1), the product was obtained as a white solid (35.7 mg, 80% yield), dr = 1:1. ^{1}H NMR (400 MHz, $CDCl_3$) δ 7.62 – 7.56 (m, 2H), 7.55 – 7.48 (m, 2H), 7.45 – 7.37 (m, 2H), 7.36 – 7.27 (m, 3H), 4.43 (dd, *J* = 58.5, 13.5 Hz, 1H), 4.14 (q, *J* = 7.1 Hz, 1H), 4.04 (q, *J* = 7.1 Hz, 1H), 3.98 – 3.85 (m, 2H), 3.16 – 2.92 (m, 1H), 2.92 – 2.74 (m, 1H), 2.50 – 2.37 (m, 1H), 2.13 – 2.00 (m, 1H), 1.94 – 1.73 (m, 3H), 1.73 – 1.43 (m, 7H), 1.32 – 1.07 (m, 7H), 1.04 – 0.82 (m, 2H); ^{13}C NMR (101 MHz, $CDCl_3$) δ 174.4, 171.7, 140.8, 140.0, 139.7, 128.8 (2C), 128.3 (2C), 127.6 (2C), 127.3, 127.1 (2C), 60.7, 45.2, 45.0, 42.7, 41.6, 41.2, 35.3, 33.5, 28.5, 28.1, 27.7, 26.7, 26.3, 26.2, 14.3; the other isomer: ^{13}C NMR (101 MHz, $CDCl_3$) δ 174.1, 171.6, 140.8, 139.9, 139.7, 128.8 (2C), 128.2 (2C), 127.5 (2C), 127.3, 127.1 (2C), 60.6, 45.0, 44.9, 42.7, 41.5, 40.9, 35.2, 33.5, 28.5, 28.1, 27.7, 26.7, 26.3, 26.2, 14.2. HRMS ESI $[M+H]^+$ calculated for ($C_{29}H_{38}O_3N^+$) 448.2846, found 448.2838.

1-(2-([1,1'-Biphenyl]-4-yl)-3-cyclohexylpropanoyl)piperidine-4-carboxylic acid **371**

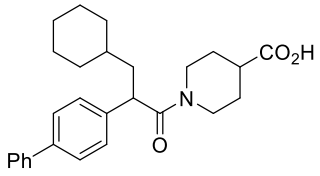

Following **GP12** using α-trifluoromethyl alkene **232** (24.8 mg, 0.10 mmol), potassium cyclohexyltrifluoroborate **320** (28.5 mg, 0.15 mmol) and ethyl piperidine-4-carboxylic acid (19.4 mg, 0.15 mmol). Purification by flash chromatography (EtOAc : Hexane = 1 : 4), the product was obtained as a white solid (26.8 mg, 64% yield), dr = 1:1. ^{1}H NMR (400 MHz, $CDCl_3$) δ 7.58 (d, *J* = 7.7 Hz, 2H), 7.53 (d, *J* = 8.1 Hz, 2H), 7.45 – 7.38 (m, 2H), 7.36 – 7.28 (m, 3H), 4.54 – 4.26 (m, 1H), 3.98 – 3.85 (m, 2H), 3.18 – 2.96 (m, 1H), 2.96 – 2.76 (m, 1H), 2.54 – 2.40 (m, 1H), 2.10 – 1.99 (m, 1H), 1.95 – 1.85 (m, 1H), 1.84 – 1.75 (m, 1H), 1.74 – 1.40 (m, 8H), 1.29 – 1.08 (m, 4H), 1.03 – 0.83 (m, 2H); ^{13}C NMR (151 MHz, $CDCl_3$) δ 179.5, 171.9, 140.8, 139.9, 139.7, 128.9 (2C), 128.3 (2C), 127.6 (2C), 127.4, 127.1 (2C), 45.2, 45.0, 42.7, 41.6, 40.8, 35.3, 33.6, 33.5, 28.2, 27.9, 26.7, 26.3, 26.2; the other isomer: ^{13}C NMR (151 MHz, $CDCl_3$) δ 179.4, 171.8, 140.8, 139.9, 139.7, 128.9 (2C), 128.2 (2C), 127.6 (2C), 127.4, 127.1 (2C), 45.0, 44.8, 42.7, 41.5, 40.6, 35.2, 33.54, 33.47, 27.8, 27.5, 26.7, 26.3, 26.2. HRMS ESI $[M+H]^+$ calculated for ($C_{27}H_{34}O_3N^+$) 420.2533, found 420.2525.

***2-([1,1'-Biphenyl]-4-yl)-3-cyclohexyl-1-(4-(pyrimidin-2-yl)piperazin-1-yl)propan-1-one* 372**

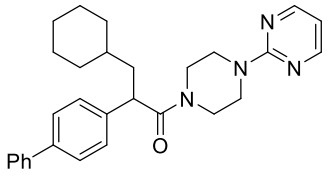

Following **GP12** using α-trifluoromethyl alkene **232** (24.8 mg, 0.10 mmol), potassium cyclohexyltrifluoroborate **320** (28.5 mg, 0.15 mmol) and 2-(piperazin-1-yl)pyrimidine (24.6 mg, 0.15 mmol). Purification by flash chromatography (EtOAc : Hexane : Et_3N = 10 : 100 : 1), the

product was obtained as a white solid (24.9 mg, 55% yield). ^{1}H NMR (400 MHz, $CDCl_3$) δ 8.28 (d, *J* = 4.8 Hz, 2H), 7.61 – 7.51 (m, 4H), 7.46 – 7.38 (m, 2H), 7.38 – 7.29 (m, 3H), 6.49 (t, *J* = 4.8 Hz, 1H), 3.99 – 3.79 (m, 4H), 3.63 – 3.50 (m, 4H), 3.28 – 3.17 (m, 1H), 2.10 (ddd, *J* = 14.3, 7.9, 6.7 Hz, 1H), 1.88 – 1.78 (m, 1H), 1.74 – 1.57 (m, 5H), 1.32 – 1.07 (m, 4H), 1.00 – 0.87 (m, 2H); ^{13}C NMR (101 MHz, $CDCl_3$) δ 172.0, 161.5, 157.8 (2C), 140.7, 139.8, 128.9 (2C), 128.3 (2C), 127.6 (2C), 127.4, 127.1 (2C), 110.4, 45.5, 45.3, 43.7 (2C), 42.7, 42.0, 35.3, 33.6, 33.5, 26.7, 26.3, 26.2. HRMS ESI $[M+H]^+$ calculated for ($C_{29}H_{35}ON_4^+$) 455.2805, found 455.2803.

***2-([1,1'-biphenyl]-4-yl)-N-(4-(tert-butyl)phenyl)-3-cyclohexylpropanamide* 373**

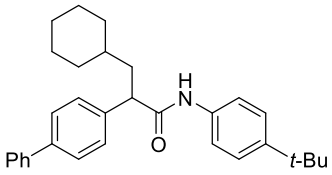

Following **GP12** using α-trifluoromethyl alkene **232** (24.8 mg, 0.10 mmol), potassium cyclohexyltrifluoroborate **320** (28.5 mg, 0.15 mmol) and 4-(*tert*-butyl)aniline (22.4 mg, 0.15 mmol), 5 mol% of **PC-7** was used. Purification by flash chromatography (EtOAc : Hexane : Et_3N = 4 : 100 : 1), the product was obtained as a white solid (32.9 mg, 75% yield). ^{1}H NMR (600 MHz, $CDCl_3$) δ 7.57 – 7.52 (m, 4H), 7.42 – 7.38 (m, 4H), 7.37 – 7.34 (m, 2H), 7.33 – 7.29 (m, 1H), 7.27 – 7.21 (m, 2H), 3.66 (t, *J* = 7.6 Hz, 1H), 2.14 (dt, *J* = 14.3, 7.6 Hz, 1H), 1.81 – 1.68 (m, 3H), 1.68 – 1.60 (m, 2H), 1.60 – 1.54 (m, 1H), 1.26 – 1.20 (m, 10H), 1.16 – 1.08 (m, 3H), 0.99 – 0.87 (m, 2H); ^{13}C NMR (151 MHz, $CDCl_3$) δ 171.9, 147.3, 140.7, 140.3, 139.2, 135.5, 128.9 (2C), 128.5 (2C), 127.8 (2C), 127.5, 127.1 (2C), 125.8 (2C), 119.7 (2C), 51.4, 41.0, 35.3, 34.4, 33.7, 33.0,

31.5 (3C), 26.6, 26.3, 26.2. HRMS ESI $[M+H]^+$ calculated for ($C_{31}H_{38}ON^+$) 440.2948, found 440.2940.

***2-([1,1'-Biphenyl]-4-yl)-3-cyclohexyl-N-(4-(trifluoromethyl)phenyl)propenamide* 374**

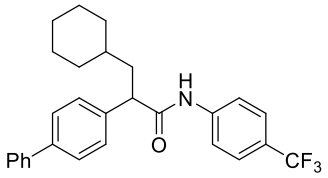

Following **GP12** using α-trifluoromethyl alkene **232** (24.8 mg, 0.10 mmol), potassium cyclohexyltrifluoroborate **320** (28.5 mg, 0.15 mmol) and 4-(trifluoromethyl)aniline (24.2 mg, 0.15 mmol), 5 mol% of **PC-7** was used. Purification by flash chromatography (EtOAc : Hexane : Et_3N = 4 : 100 : 1), the product was obtained as a white solid (23.1 mg, 51% yield). ^{1}H NMR (600 MHz, $CDCl_3$) δ 7.63 – 7.56 (m, 6H), 7.53 (d, *J* = 8.4 Hz, 2H), 7.47 – 7.39 (m, 4H), 7.37 – 7.35 (m, 1H), 7.29 (br s, 1H), 3.70 (t, *J* = 7.6 Hz, 1H), 2.16 (dt, *J* = 14.4, 7.4 Hz, 1H), 1.84 – 1.76 (m, 2H), 1.76 – 1.65 (m, 3H), 1.64 – 1.60 (m, 1H), 1.30 – 1.09 (m, 4H), 1.05 – 0.86 (m, 2H); ^{13}C NMR (151 MHz, $CDCl_3$) δ 172.3, 141.1, 140.7, 140.5, 138.6, 129.0 (2C), 128.5 (2C), 128.0 (2C), 127.6, 127.2 (2C), 126.3 (q, $^3J_{C\text{-}F}$ = 3.8 Hz, 2C), 124.2 (q, $^1J_{C\text{-}F}$ = 271.6 Hz), 119.4, 51.3, 40.8, 35.2, 33.8, 32.9, 26.6, 26.3, 26.2; ^{19}F NMR (565 MHz, $CDCl_3$) δ -62.12 (s, 3F). HRMS ESI $[M+H]^+$ calculated for ($C_{28}H_{29}ONF_3^+$) 452.2196, found 452.2188.

***2-([1,1'-Biphenyl]-4-yl)-3-cyclohexyl-N-(2,4-dimethylphenyl)propenamide* 375**

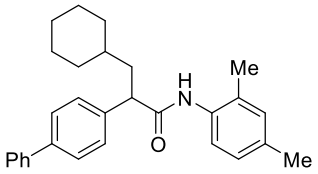

Following **GP12** using α-trifluoromethyl alkene **232** (24.8 mg, 0.10 mmol), potassium cyclohexyltrifluoroborate **320** (28.5 mg, 0.15 mmol) and 2,4-dimethylaniline (18.2 mg, 0.15 mmol), 5 mol% of **PC-7** was used. Purification by flash chromatography (EtOAc : Hexane : Et_3N = 5 : 100 : 1), the product was obtained as a white solid (27.2 mg, 66% yield). ^{1}H NMR (600 MHz, $CDCl_3$) δ 7.66 – 7.57 (m, 5H), 7.48 – 7.41 (m, 4H), 7.39 – 7.34 (m, 1H), 7.00 – 6.88 (m, 3H), 3.75 (t, *J* = 7.8 Hz, 1H), 2.26 (s, 3H), 2.20 (dt, *J* = 14.5, 7.8 Hz, 1H), 1.95 (s, 3H), 1.87 – 1.79 (m, 2H), 1.78 – 1.74 (m, 1H), 1.73 – 1.67 (m, 2H), 1.66 – 1.60 (m, 1H), 1.35 – 1.25 (m, 1H), 1.23 – 1.13 (m, 3H), 1.05 – 0.93 (m, 2H); ^{13}C NMR (151 MHz, $CDCl_3$) δ 172.1, 140.7, 140.4, 139.3, 134.8, 133.2, 131.1, 129.0, 129.0 (2C), 128.7 (2C), 127.8 (2C), 127.5, 127.3, 127.1 (2C), 123.0, 51.0, 40.4, 35.3, 33.9, 32.9, 26.7, 26.3, 26.2, 20.9, 17.4. HRMS ESI $[M+H]^+$ calculated for ($C_{29}H_{34}ON^+$) 412.2635, found 412.2628.

***2-([1,1'-Biphenyl]-4-yl)-N-butyl-4-(2-(trimethylsilyl)ethoxy)butanamide* 376**

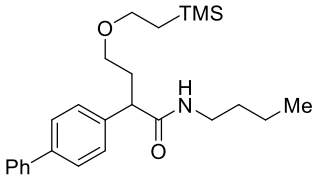

Following **GP12** using α-trifluoromethyl alkene **232** (24.8 mg, 0.10 mmol), corresponding potassium alkyltrifluoroborate (35.7 mg, 0.15 mmol) and butan-1-amine (11.0 mg, 0.15 mmol).

Purification by flash chromatography (EtOAc : Hexane : Et_3N = 10 : 100 : 1), the product was obtained as colourless oil (19.7 mg, 48% yield). ^1H NMR (600 MHz, $CDCl_3$) δ 7.58 (d, *J* = 8.1 Hz, 2H), 7.57 – 7.53 (m, 2H), 7.45 – 7.41 (m, 2H), 7.41 – 7.37 (m, 2H), 7.36 – 7.32 (m, 1H), 5.57 (br s, 1H), 3.64 – 3.59 (m, 1H), 3.46 (t, *J* = 8.0 Hz, 2H), 3.43 – 3.39 (m, 1H), 3.34 – 3.29 (m, 1H), 3.28 – 3.23 (m, 1H), 3.20 – 3.14 (m, 1H), 2.46 – 2.39 (m, 1H), 2.06 – 1.99 (m, 1H), 1.46 – 1.39 (m, 2H), 1.31 – 1.23 (m, 2H), 0.93 (t, *J* = 8.0 Hz, 2H), 0.88 (t, *J* = 7.4Hz, 3H), 0.02 (s, 9H); ^{13}C NMR (151 MHz, $CDCl_3$) δ 173.3, 140.8, 140.2, 139.2, 128.9 (2C), 128.6 (2C), 127.5 (2C), 127.4, 127.1 (2C), 68.1, 67.7, 49.4, 39.5, 33.6, 31.8, 20.1, 18.4, 13.8, -1.2 (3C). HRMS ESI $[M+H]^+$ calculated for ($C_{25}H_{37}O_2NSi^+$) 412.2666, found 412.2658.

***N-butyl-2-(dibenzo[b,d]furan-4-yl)-4,4-dimethyl-6-oxoheptanamide* 377**

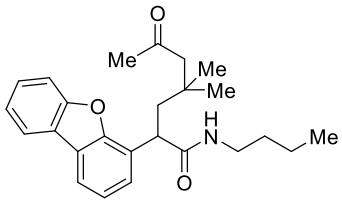

Following **GP12** using corresponding α-trifluoromethyl alkene (26.3 mg, 0.10 mmol), corresponding potassium alkyltrifluoroborate (30.9 mg, 0.15 mmol) and butan-1-amine (11.0 mg, 0.15 mmol). Purification by flash chromatography (EtOAc : Hexane : Et_3N = 10 : 100 : 1), the product was obtained as colourless oil (25.2 mg, 64% yield). ^1H NMR (600 MHz, $CDCl_3$) δ 7.95 (ddd, *J* = 7.7, 1.3, 0.6 Hz, 1H), 7.82 (dd, *J* = 7.7, 1.3 Hz, 1H), 7.61 – 7.58 (m, 1H), 7.50 – 7.45 (m, 2H), 7.38 – 7.33 (m, 1H), 7.33 – 7.30 (m, 1H), 5.86 (t, *J* = 5.8 Hz, 1H), 4.18 (t, *J* = 6.7 Hz, 1H), 3.22 – 3.16 (m, 1H), 3.16 – 3.07 (m, 1H), 2.57 (dd, *J* = 14.2, 6.7 Hz, 1H), 2.44 – 2.29 (m, 2H),

2.03 – 1.98 (m, 4H), 1.40 – 1.29 (m, 2H), 1.20 – 1.14 (m, 2H), 1.03 (s, 3H), 1.01 (s, 3H), 0.78 (t, *J* = 7.4 Hz, 3H); ^{13}C NMR (151 MHz, $CDCl_3$) δ 208.9, 173.0, 156.0, 153.7, 127.4, 126.3, 125.7, 124.6, 124.2, 123.6, 123.1, 121.0, 119.3, 111.8, 53.8, 43.7, 42.5, 39.6, 34.1, 32.4, 31.5, 27.6, 27.5, 20.0, 13.7. HRMS ESI $[M+H]^+$ calculated for ($C_{25}H_{31}O_3N^+$) 394.2377, found 394.2374.

2-([1,1'-Biphenyl]-4-yl)-3-cycloheptyl-1-morpholinopropan-1-one **378**

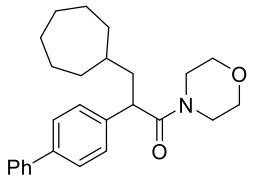

Following **GP12** using α-trifluoromethyl alkene **232** (24.8 mg, 0.10 mmol), potassium cycloheptyltrifluoroborate (30.6 mg, 0.15 mmol) and morpholine (13.1 mg, 0.15 mmol). Purification by flash chromatography (EtOAc : Hexane : Et_3N = 10 : 100 : 1), the product was obtained as a white solid (28.9 mg, 74% yield). ^{1}H NMR (400 MHz, $CDCl_3$) δ 7.61 – 7.51 (m, 4H), 7.46 – 7.39 (m, 2H), 7.36 – 7.28 (m, 3H), 3.84 (t, *J* = 7.3 Hz, 1H), 3.79 – 3.71 (m, 1H), 3.70 – 3.61 (m, 1H), 3.60 – 3.47 (m, 4H), 3.46 – 3.38 (m, 1H), 3.26 – 3.15 (m, 1H), 2.09 (dt, *J* = 14.1, 7.3 Hz, 1H), 1.83 – 1.75 (m, 1H), 1.72 – 1.59 (m, 3H), 1.59 – 1.46 (m, 4H), 1.46 – 1.31 (m, 4H), 1.29 – 1.16 (m, 2H); ^{13}C NMR (101 MHz, $CDCl_3$) δ 172.0, 140.7, 139.8, 139.6, 128.9 (2C), 128.3 (2C), 127.6 (2C), 127.4, 127.1 (2C), 67.0, 66.6, 46.2, 45.7, 43.0, 42.6, 36.6, 34.7, 34.6, 28.70, 28.69, 26.33, 26.27. HRMS ESI $[M+H]^+$ calculated for ($C_{26}H_{34}O_2N^+$) 392.2584, found 392.2582.

2-([1,1'-Biphenyl]-4-yl)-4,4,5-trimethyl-1-morpholinohexan-1-one **379**

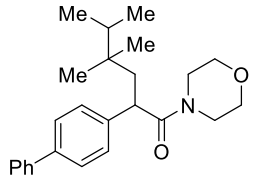

Following **GP12** using α-trifluoromethyl alkene **232** (24.8 mg, 0.10 mmol), corresponding potassium alkyltrifluoroborate (24.6 mg, 0.15 mmol) and morpholine (13.1 mg, 0.15 mmol). Purification by flash chromatography (EtOAc : Hexane : Et_3N = 10 : 100 : 1), the product was obtained as a white solid (32.8 mg, 87% yield). ^1H NMR (400 MHz, $CDCl_3$) δ 7.57 (d, *J* = 7.4 Hz, 2H), 7.53 (d, *J* = 8.0 Hz, 2H), 7.42 (t, *J* = 7.4 Hz, 2H), 7.37 – 7.30 (m, 3H), 3.87 (dd, *J* = 8.5, 3.0 Hz, 1H), 3.76 – 3.68 (m, 1H), 3.68 – 3.47 (m, 6H), 3.34 – 3.25 (m, 1H), 2.60 (dd, *J* = 14.1, 8.5 Hz, 1H), 1.58 – 1.44 (m, 2H), 0.90 – 0.82 (m, 9H), 0.78 (s, 3H); ^{13}C NMR (101 MHz, $CDCl_3$) δ 172.4, 141.1, 140.7, 139.7, 128.9 (2C), 128.1 (2C), 127.6 (2C), 127.4, 127.1 (2C), 66.9, 66.6, 46.3, 43.9, 43.2, 42.8, 36.7, 35.9, 24.8, 23.9, 17.7, 17.6. HRMS ESI $[M+H]^+$ calculated for ($C_{25}H_{34}O_2N^+$) 380.2584, found 380.2582.

3-Cyclohexyl-2-(4-ethynylphenyl)-1-morpholinopropan-1-one **380**

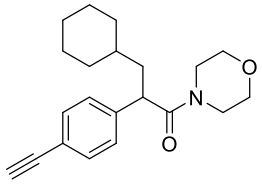

Following **GP12** using α-trifluoromethyl alkene **685** (26.8 mg, 0.10 mmol), potassium cyclohexyltrifluoroborate **320** (28.5 mg, 0.15 mmol) and morpholine (13.1 mg, 0.15 mmol). Purification by flash chromatography (EtOAc : Hexane : Et_3N = 10 : 100 : 1), the desilylation

product was obtained as a white solid (13.9 mg, 43% yield). ^{1}H NMR (400 MHz, $CDCl_3$) δ 7.44 (d, *J* = 8.2 Hz, 2H), 7.20 (d, *J* = 8.2 Hz, 2H), 3.82 (t, *J* = 7.3 Hz, 1H), 3.78 – 3.70 (m, 1H), 3.69 – 3.59 (m, 1H), 3.57 – 3.30 (m, 5H), 3.20 – 3.11 (m, 1H), 3.06 (s, 1H), 2.01 (dt, *J* = 14.3, 7.3 Hz, 1H), 1.81 – 1.72 (m, 1H), 1.70 – 1.59 (m, 4H), 1.58 – 1.50 (m, 1H), 1.23 – 1.06 (m, 4H), 0.96 – 0.82 (m, 2H); ^{13}C NMR (151 MHz, $CDCl_3$) δ 171.5, 141.5, 132.8 (2C), 127.9 (2C), 12`0.8, 83.4, 77.5, 66.9, 66.5, 46.2, 45.3, 42.6, 42.5, 35.2, 33.5, 33.4, 26.6, 26.3, 26.2. HRMS ESI $[M+H]^+$ calculated for ($C_{21}H_{28}O_2N^+$) 326.2115, found 326.2112.

N-butyl-3-cyclohexyl-2-((8R,9S,13S,14S)-13-methyl-17-oxo-7,8,9,11,12,13,14,15,16,17-decahydro -6H-cyclopenta[a]phenanthren-3-yl)propenamide **381**

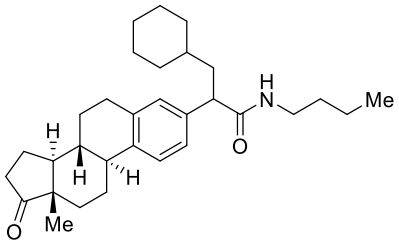

Following **GP12** using corresponding α-trifluoromethyl alkene (34.8 mg, 0.10 mmol), potassium cyclohexyltrifluoroborate **320** (28.5 mg, 0.15 mmol) and butan-1-amine (11.0 mg, 0.15 mmol). Purification by flash chromatography (EtOAc : Hexane : Et_3N = 15 : 100 : 1), the product was obtained as colourless oil (31.2 mg, 67% yield), dr = 1:1. ^{1}H NMR (600 MHz, $CDCl_3$) δ 7.22 (d, *J* = 8.0 Hz, 1H), 7.07 – 7.02 (m, 1H), 7.01 (d, *J* = 4.3 Hz, 1H), 5.43 (t, *J* = 5.9 Hz, 1H), 3.38 (t, *J* = 7.7 Hz, 1H), 3.22 (dq, *J* = 13.6, 6.9 Hz, 1H), 3.12 (dp, *J* = 15.1, 8.0, 7.4 Hz, 1H), 2.89 (dd, *J* = 9.5, 4.1 Hz, 2H), 2.50 (dd, *J* = 19.0, 8.8 Hz, 1H), 2.40 (dd, *J* = 12.9, 4.2 Hz, 1H), 2.28 (td,

J = 11.1, 3.9 Hz, 1H), 2.14 (dt, *J* = 18.5, 8.9 Hz, 1H), 2.09 – 2.04 (m, 0H), 2.04 (s, 1H), 1.96 (d, *J* = 11.9 Hz, 1H), 1.84 (s, 1H), 1.74 (d, *J* = 12.9 Hz, 1H), 1.69 (d, *J* = 13.4 Hz, 0H), 1.67 – 1.63 (m, 1H), 1.59 (dt, *J* = 14.1, 7.8 Hz, 2H), 1.51 (qd, *J* = 13.3, 5.7 Hz, 3H), 1.47 – 1.43 (m, 1H), 1.40 (p, *J* = 7.1 Hz, 3H), 1.25 (h, *J* = 7.5 Hz, 3H), 1.19 – 1.09 (m, 4H), 0.93 (t, *J* = 6.5 Hz, 1H), 0.91 (s, 4H), 0.87 (t, *J* = 7.4 Hz, 4H); ^{13}C NMR (151 MHz, $CDCl_3$) δ 221.0, 173.9, 138.6, 138.2, 137.0, 128.5, 125.8, 125.4, 50.7, 50.1, 48.1, 46.0, 44.5, 41.0, 39.4, 38.2, 36.0, 35.3, 33.6, 33.1, 31.7, 29.5, 26.7, 26.6, 26.3, 25.8, 21.7, 20.1, 14.0, 13.9, 8.8. HRMS ESI $[M+H]^+$ calculated for ($C_{31}H_{46}O_2N^+$) 464.3523, found 464.3521.

***2-([1,1'-Biphenyl]-4-yl)-3-cyclohexyl-N-(((1R,4aS,10aR)-7-isopropyl-1,4a-dimethyl-1,2,3,4,4a,9,10,10a-octahydrophenanthren-1-yl)methyl)propanamide* 382**

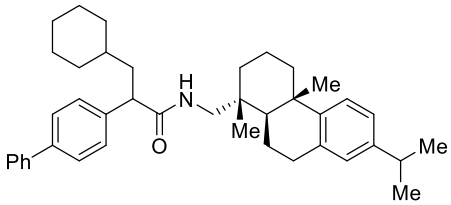

Following **GP12** using α-trifluoromethyl alkene **232** (24.8 mg, 0.10 mmol), potassium cyclohexyltrifluoroborate **320** (28.5 mg, 0.15 mmol) and (+)-dehydroabietylamine (42.8 mg, 0.15 mmol). Purification by flash chromatography (EtOAc : Hexane : Et_3N = 12 : 100 : 1), the product was obtained as colourless oil (36.5 mg, 62% yield), dr = 1:1. ^{1}H NMR (600 MHz, $CDCl_3$) δ 7.48 (d, *J* = 7.7 Hz, 1H), 7.45 (d, *J* = 7.9 Hz, 1H), 7.43 – 7.37 (m, 3H), 7.32 (q, *J* = 7.5 Hz, 2H), 7.26 (q, *J* = 9.7, 8.9 Hz, 2H), 7.04 (dd, *J* = 30.6, 8.1 Hz, 1H), 6.90 (dd, *J* = 21.5, 8.3 Hz, 1H), 6.83 (d, *J* = 7.3 Hz, 1H), 5.42 (dt, *J* = 13.8, 6.7 Hz, 1H), 3.49 (dt, *J* = 14.5, 7.9 Hz, 1H), 3.27 (td, *J* = 14.9,

6.7 Hz, 1H), 2.92 – 2.62 (m, 4H), 2.16 (dd, *J* = 30.6, 12.8 Hz, 1H), 2.10 – 2.02 (m, 1H), 1.86 – 1.77 (m, 1H), 1.76 – 1.59 (m, 7H), 1.59 – 1.46 (m, 3H), 1.26 – 1.15 (m, 10H), 1.13 (d, *J* = 11.8 Hz, 3H), 1.11 – 0.95 (m, 6H), 0.92 – 0.86 (m, 2H), 0.83 (d, *J* = 10.0 Hz, 3H); ^{13}C NMR (151 MHz, $CDCl_3$) δ 173.7, 147.2, 145.6, 140.8, 140.2, 139.8, 134.9, 128.8 (2C), 128.3 (2C), 127.6 (2C), 127.4, 127.2 (2C), 127.0, 124.3, 123.8, 50.6, 49.7, 44.9, 40.6, 38.5, 37.5, 36.2, 35.3, 33.7, 33.5, 33.1, 30.4, 26.7, 26.2, 26.1, 25.4, 24.2, 24.1 (2C), 19.1, 19.0, 18.7. HRMS ESI $[M+H]^+$ calculated for ($C_{41}H_{54}ON^+$) 576.4200, found 576.4192.

2-([1,1'-Biphenyl]-4-yl)-3-cyclohexylpropanamide **383**

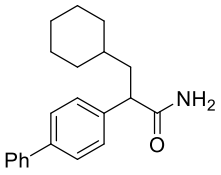

Following **GP12** using α-trifluoromethyl alkene **232** (24.8 mg, 0.10 mmol), potassium cyclohexyltrifluoroborate **320** (28.5 mg, 0.15 mmol) and ammonium acetate (15.4 mg, 0.2 mmol). Purification by flash chromatography (EtOAc : Hexane : Et_3N = 30 : 70 : 1), the product was obtained as a white solid (21.3 mg, 70% yield). ^{1}H NMR (600 MHz, $CDCl_3$) δ 7.57 (dd, *J* = 10.5, 7.8 Hz, 4H), 7.44 (t, *J* = 7.5 Hz, 2H), 7.37 (d, *J* = 7.9 Hz, 2H), 7.34 (t, *J* = 7.4 Hz, 1H), 5.71 (s, 1H), 5.49 (s, 1H), 3.59 (t, *J* = 7.7 Hz, 1H), 2.05 (dt, *J* = 14.4, 7.4 Hz, 1H), 1.82 – 1.59 (m, 6H), 1.25 – 1.10 (m, 4H), 1.00 – 0.87 (m, 2H); ^{13}C NMR (151 MHz, $CDCl_3$) δ 176.5, 140.7, 140.3, 139.3, 128.9 (2C), 128.5 (2C), 127.7 (2C), 127.5, 127.1 (2C), 49.6, 40.6, 35.1, 33.8, 32.9, 26.6, 26.3, 26.2. HRMS ESI $[M+H]^+$ calculated for ($C_{21}H_{26}ON^+$) 308.2009, found 308.2005.

2-([1,1'-Biphenyl]-4-yl)-3-(adamantan-1-yl)propanamide **384**

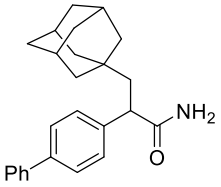

Following **GP12** using α-trifluoromethyl alkene **232** (24.8 mg, 0.10 mmol), corresponding potassium alkyltrifluoroborate (36.3 mg, 0.15 mmol) and ammonium acetate (15.4 mg, 0.2 mmol). Purification by flash chromatography (EtOAc : Hexane : Et_3N = 30 : 70 : 1), the product was obtained as a white solid (26.2 mg, 73% yield). ^{1}H NMR (400 MHz, $CDCl_3$) δ 7.57 (d, *J* = 7.8 Hz, 2H), 7.55 (d, *J* = 7.8 Hz, 2H), 7.46 – 7.41 (m, 2H), 7.39 (d, *J* = 8.0 Hz, 2H), 7.36 – 7.31 (m, 1H), 5.52 (br s, 2H), 3.59 (dd, *J* = 7.3, 5.1 Hz, 1H), 2.26 (dd, *J* = 14.2, 7.3 Hz, 1H), 1.93 (q, *J* = 3.6 Hz, 4H), 1.68 (d, *J* = 12.4 Hz, 3H), 1.60 (d, *J* = 12.4 Hz, 3H), 1.56 – 1.43 (m, 7H); ^{13}C NMR (151 MHz, $CDCl_3$) δ 176.6, 141.3, 140.7, 140.1, 128.9 (2C), 128.3 (2C), 127.7 (2C), 127.4, 127.1 (2C), 47.4, 47.2, 42.6 (2C), 37.1 (2C), 33.1, 28.7 (2C). HRMS ESI $[M+H]^+$ calculated for ($C_{25}H_{30}ON^+$) 360.2322, found 360.2319.

2-([1,1'-Biphenyl]-4-yl)-4-((3-methylbut-3-en-1-yl)oxy)butanamide **385**

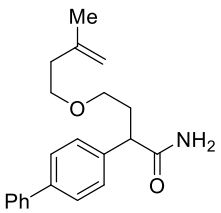

Following **GP12** using α-trifluoromethyl alkene **232** (24.8 mg, 0.10 mmol), corresponding potassium alkyltrifluoroborate (30.9 mg, 0.15 mmol) and ammonium acetate (15.4 mg, 0.2

mmol). Purification by flash chromatography (EtOAc : Hexane : Et_3N = 30 : 70 : 1), the product was obtained as a white solid (16.0 mg, 53% yield). ^{1}H NMR (400 MHz, $CDCl_3$) δ 7.60 – 7.53 (m, 4H), 7.46 – 7.41 (m, 2H), 7.41 – 7.37 (m, 2H), 7.37 – 7.31 (m, 1H), 5.66 (br s, 2H), 4.82 – 4.78 (m, 1H), 4.78 – 4.67 (m, 1H), 3.72 (t, *J* = 7.5 Hz, 1H), 3.55 – 3.44 (m, 3H), 3.39 – 3.30 (m, 1H), 2.48 – 2.38 (m, 1H), 2.29 (t, *J* = 6.8 Hz, 2H), 2.13 – 1.89 (m, 1H), 1.76 (s, 3H); ^{13}C NMR (101 MHz, $CDCl_3$) δ 175.9, 143.1, 140.7, 140.4, 138.7, 128.9 (2C), 128.6 (2C), 127.6 (2C), 127.5, 127.1 (2C), 111.6, 69.3, 68.1, 48.6, 37.9, 33.2, 22.9. HRMS ESI $[M+H]^+$ calculated for ($C_{21}H_{26}O_2N^+$) 324.1958, found 324.1956.

2-([1,1'-Biphenyl]-4-yl)-4,4-dimethyl-6-oxoheptanamide **386**

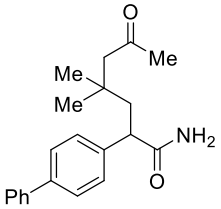

Following **GP12** using α-trifluoromethyl alkene **232** (24.8 mg, 0.10 mmol), corresponding alkyltrifluoroborate (30.9 mg, 0.15 mmol) and ammonium acetate (15.4 mg, 0.2 mmol). Purification by flash chromatography (EtOAc : Hexane : Et_3N = 30 : 70 : 1), the product was obtained as a white solid (24.2 mg, 75% yield). ^{1}H NMR (400 MHz, $CDCl_3$) δ 7.58 – 7.51 (m, 4H), 7.45 – 7.40 (m, 2H), 7.38 (d, *J* = 8.1 Hz, 2H), 7.36 – 7.31 (m, 1H), 5.79 (br s, 1H), 5.72 (br s, 1H), 3.59 (t, *J* = 6.4 Hz, 1H), 2.41 (dd, *J* = 14.3, 6.0 Hz, 1H), 2.40 – 2.27 (m, 2H), 2.03 (s, 3H), 1.90 (dd, *J* = 14.3, 6.0 Hz, 1H), 1.01 (s, 6H); ^{13}C NMR (101 MHz, $CDCl_3$) δ 209.1, 176.5, 140.7, 140.4, 140.3

128.9 (2C), 128.5 (2C), 127.7 (2C), 127.5, 127.1 (2C), 53.8, 48.7, 44.4, 34.1, 32.4, 27.9, 27.8. HRMS ESI $[M+H]^+$ calculated for ($C_{21}H_{26}O_2N^+$) 324.1958, found 324.1956.

***3-Cyclohexyl-2-(naphthalen-2-yl)propenamide* 387**

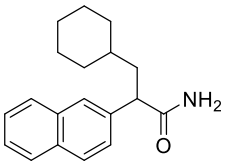

Following **GP12** using corresponding α-trifluoromethyl alkene (22.2 mg, 0.10 mmol), potassium cyclohexyltrifluoroborate **320** (28.5 mg, 0.15 mmol) and ammonium acetate (15.4 mg, 0.2 mmol). Purification by flash chromatography (EtOAc : Hexane : Et_3N = 30 : 70 : 1), the product was obtained as a white solid (19.4 mg, 69% yield). ^{1}H NMR (600 MHz, $CDCl_3$) δ 7.85 – 7.80 (m, 3H), 7.74 (s, 1H), 7.51 – 7.45 (m, 2H), 7.44 (d, *J* = 8.5 Hz, 1H), 5.64 (br s, 1H), 5.46 (br s, 1H), 3.71 (t, *J* = 7.7 Hz, 1H), 2.09 (dt, *J* = 14.4, 7.7 Hz, 1H), 1.85 – 1.77 (m, 2H), 1.70 – 1.62 (m, 3H), 1.61 – 1.56 (m, 1H), 1.21 – 1.05 (m, 4H), 1.00 – 0.87 (m, 2H); ^{13}C NMR (151 MHz, $CDCl_3$) δ 176.4, 137.7, 133.6, 132.8, 128.9, 127.9, 127.8, 127.0, 126.4, 126.1, 126.0, 50.0, 40.4, 35.1, 33.9, 32.8, 26.6, 26.3, 26.2. HRMS ESI $[M+H]^+$ calculated for ($C_{19}H_{24}ON^+$) 282.1852, found 282.1849.

***2-(4-(tert-Butyl)phenyl)-3-cyclopentylpropanamide* 388**

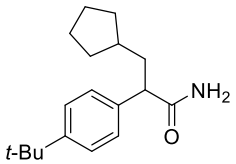

Following **GP12** using corresponding α-trifluoromethyl alkene (22.8 mg, 0.10 mmol), potassium cyclopentyltrifluoroborate **395** (26.4 mg, 0.15 mmol) and ammonium acetate (15.4 mg, 0.2 mmol). Purification by flash chromatography (EtOAc : Hexane : Et_3N = 30 : 70 : 1), the product was obtained as a white solid (17.1 mg, 62% yield). ^1H NMR (600 MHz, $CDCl_3$) δ 7.36 – 7.31 (m, 2H), 7.25 – 7.20 (m, 2H), 5.58 (br s, 1H), 5.39 (br s, 1H), 3.41 (t, *J* = 7.7 Hz, 1H), 2.11 (dt, *J* = 14.1, 7.7 Hz, 1H), 1.87 – 1.80 (m, 1H), 1.78 – 1.72 (m, 1H), 1.71 – 1.63 (m, 1H), 1.61 – 1.55 (m, 1H), 1.50 – 1.41 (m, 1H), 1.31 (s, 9H), 1.16 – 1.08 (m, 2H); ^{13}C NMR (151 MHz, $CDCl_3$) δ 176.7, 150.3, 137.1, 127.7 (2C), 125.9 (2C), 51.6, 39.3, 37.7, 34.6, 33.0, 32.3, 31.5 (3C), 25.3, 25.2. HRMS ESI $[M+H]^+$ calculated for ($C_{18}H_{28}ON^+$) 274.2165, found 274.2161.

2-(Benzo[b]thiophen-2-yl)-3-cyclohexylpropanamide **389**

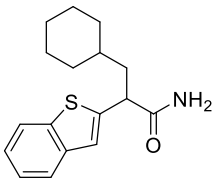

Following **GP12** using corresponding α-trifluoromethyl alkene (22.8 mg, 0.10 mmol), potassium cyclohexyltrifluoroborate **320** (28.5 mg, 0.15 mmol) and ammonium acetate (15.4 mg, 0.2 mmol). Purification by flash chromatography (EtOAc : Hexane : Et_3N = 30 : 70 : 1), the product was obtained as a white solid (14.9 mg, 52% yield). ^1H NMR (400 MHz, $CDCl_3$) δ 7.82 – 7.75 (m, 1H), 7.71 (dd, *J* = 7.4, 1.6 Hz, 1H), 7.38 – 7.27 (m, 2H), 7.19 (s, 1H), 5.83 (br s, 1H), 5.73 (br s, 1H), 3.92 (dd, *J* = 9.2, 6.3 Hz, 1H), 2.10 – 2.01 (m, 1H), 1.88 – 1.77 (m, 2H), 1.75 – 1.56 (m, 4H), 1.33 – 1.22 (m, 1H), 1.22 – 1.06 (m, 3H), 1.03 – 0.86 (m, 2H); ^{13}C NMR (101 MHz,

$CDCl_3$) δ 175.1, 143.8, 139.7, 139.6, 124.6, 124.4, 123.4, 122.4 (2C), 46.0, 41.3, 35.1, 33.7, 32.6, 26.6, 26.2, 26.1. HRMS ESI $[M+H]^+$ calculated for ($C_{17}H_{22}ONS^+$) 288.1417, found 288.1414.

***3-Cyclohexyl-2-(dibenzo[b,d]furan-4-yl)propanamide* 390**

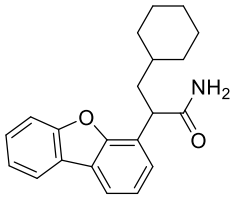

Following **GP12** using corresponding α-trifluoromethyl alkene (26.2 mg, 0.10 mmol), potassium cyclohexyltrifluoroborate **320** (28.5 mg, 0.15 mmol) and ammonium acetate (15.4 mg, 0.2 mmol). Purification by flash chromatography (EtOAc : Hexane : Et_3N = 30 : 70 : 1), the product was obtained as a white solid (23.6 mg, 73% yield). ^{1}H NMR (600 MHz, $CDCl_3$) δ 7.95 (d, *J* = 7.6 Hz, 1H), 7.85 (d, *J* = 7.6 Hz, 1H), 7.59 (d, *J* = 8.2 Hz, 1H), 7.50 – 7.43 (m, 2H), 7.38 – 7.31 (m, 2H), 5.75 (d, *J* = 8.9 Hz, 2H), 4.28 (t, *J* = 7.7 Hz, 1H), 2.19 (dt, *J* = 14.4, 7.7 Hz, 1H), 1.91 (dt, *J* = 14.4, 7.2 Hz, 1H), 1.83 (d, *J* = 12.9 Hz, 1H), 1.75 (d, *J* = 12.9 Hz, 1H), 1.68 – 1.62 (m, 2H), 1.61 – 1.56 (m, 1H), 1.28 – 1.19 (m, 1H), 1.18 – 1.06 (m, 3H), 1.02 – 0.91 (m, 2H); ^{13}C NMR (101 MHz, $CDCl_3$) δ 175.7, 156.0, 154.2, 127.4, 126.0, 124.6, 124.3, 124.2, 123.6, 123.1, 120.9, 119.6, 111.9, 43.3, 38.9, 35.4, 33.7, 33.0, 26.6, 26.3, 26.2 HRMS ESI $[M+H]^+$ calculated for ($C_{21}H_{24}O_2N^+$) 322.1802, found 322.1797.

General procedure 13 (GP13) for the synthesis of α-arylated ester

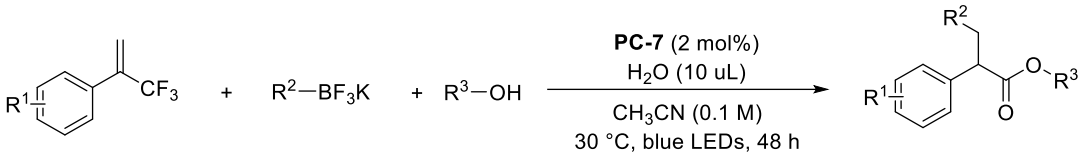

A 10-mL Schlenk tube equipped with a magnetic stir bar was charged with corresponding α-trifluoromethyl alkene (0.1 mmol, if solid), alkyltrifluoroborate (0.15 mmol), **PC-7** (1.2 mg, 0.002 mmol). The flask was evacuated and backfilled with N_2 3 times. CH_3CN (1.0 mL) or a solution of α-trifluoromethyl alkene (0.1 mmol, if liquid) in CH_3CN (1.0 mL) was then added via syringe followed by the addition of H_2O (10 μL) and alcohol (0.50 mmol), under N_2. The reaction mixture was then vigorously stirred under blue LED light (30 W, λ_{max} = 440 nm) at 30 °C (two fans were used to cool down the reaction mixture) for 48 h. After the reaction was completed, the reaction mixture was then diluted with ethyl acetate, poured into a separatory funnel, before being washed with brine. The combined organic layers were dried over Na_2SO_4 and concentrated under reduced pressure after filtration. The crude product was purified by flash chromatography on silica gel to afford the desired product.

***Methyl 2-([1,1'-biphenyl]-4-yl)-4,4-dimethylpentanoate* 351**

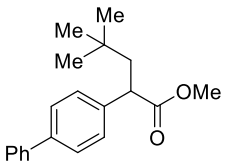

Following **GP13** usingα-trifluoromethyl alkene **232** (24.8 mg, 0.10 mmol), potassium *tert*-butyltrifluoroborate (24.6 mg, 0.15 mmol) and methanol (16.0 mg, 0.50 mmol). Purification by flash chromatography (EtOAc : Hexane = 5 : 95), the product was obtained as colourless oil

(18.1 mg, 61% yield). ^{1}H NMR (400 MHz, $CDCl_3$) δ 7.58 (d, *J* = 7.3 Hz, 2H), 7.54 (d, *J* = 8.2 Hz, 2H), 7.44 (d, *J* = 7.3 Hz, 2H), 7.41 (d, *J* = 8.2 Hz, 2H), 7.36 – 7.31 (m, 1H), 3.72 (dd, *J* = 9.3, 3.8 Hz, 1H), 3.67 (s, 3H), 2.36 (dd, *J* = 14.0, 9.3 Hz, 1H), 1.63 (dd, *J* = 14.0, 3.8 Hz, 1H), 0.93 (s, 9H); ^{13}C NMR (101 MHz, $CDCl_3$) δ 175.4, 140. 9, 140.14, 140.08, 128.9 (2C), 128.3 (2C), 127.5 (2C), 127.4, 127.2 (2C), 52.2, 47.9, 47.6, 31.2, 29.5 (3C). HRMS ESI $[M+H]^+$ calculated for ($C_{20}H_{25}O_2^+$) 297.1849, found 297.1843.

***Cyclohexyl 2-([1,1'-biphenyl]-4-yl)-4,4-dimethylpentanoate* 352**

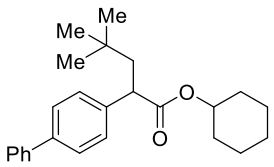

Following **GP13** usingα-trifluoromethyl alkene **232** (24.8 mg, 0.10 mmol), potassium *tert*-butyltrifluoroborate (24.6 mg, 0.15 mmol) and cyclohexanol (50.1 mg, 0.50 mmol). Purification by flash chromatography (EtOAc : Hexane = 5 : 95), the product was obtained as colourless oil (21.2 mg, 58% yield). ^{1}H NMR (600 MHz, $CDCl_3$) δ 7.59 (d, *J* = 7.3 Hz, 2H), 7.54 (d, *J* = 7.3 Hz, 2H), 7.45 – 7.39 (m, 4H), 7.36 – 7.31 (m, 1H), 4.79 – 4.70 (m, 1H), 3.68 (d, *J* = 9.1 Hz, 1H), 2.37 (dd, *J* = 14.0, 9.1 Hz, 1H), 1.85 (dd, *J* = 14.0, 5.3 Hz, 1H), 1.75 – 1.69 (m, 2H), 1.68 – 1.57 (m, 2H), 1.55 – 1.48 (m, 1H), 1.48 – 1.40 (m, 1H), 1.39 – 1.24 (m, 4H), 0.95 (s, 9H); ^{13}C NMR (151 MHz, $CDCl_3$) δ 174.3, 141.0, 140.6, 139.9, 128.9 (2C), 128.3 (2C), 127.4 (2C), 127.3, 127.2 (2C), 73.0, 48.4, 47.4, 31.52, 31.45, 31.2, 29.6 (3C), 25.5, 23.82, 23.75. HRMS ESI $[M+H]^+$ calculated for ($C_{25}H_{33}O_2^+$) 365.2475, found 365.2475.

5.4.2 Product Transformations

Scale-up reaction

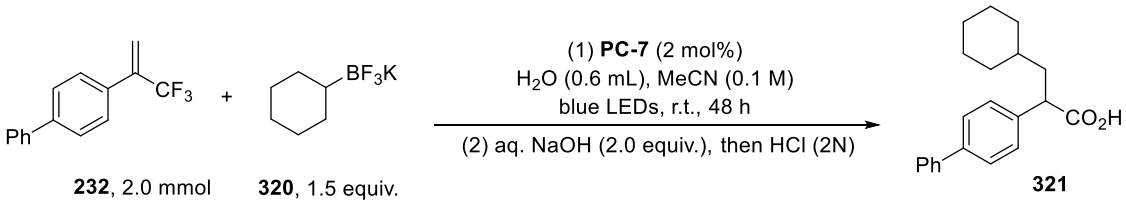

232, 2.0 mmol **320**, 1.5 equiv. **321**

A 100 mL Schlenk tube equipped with a magnetic stir bar was charged with α-trifluoromethyl alkene **232** (496.5 mg, 2.0 mmol), potassium cyclohexyltrifluoroborate **320** (570.2 mg, 3.0 mmol,), **PC-7** (23 mg, 2 mol%). The flask was evacuated and backfilled with N_2 3 times. CH_3CN (20 mL) and H_2O (0.6 mL) were then added via syringe under N_2. The reaction mixture was then vigorously stirred under blue LED light (30 W, λ_{max} = 440 nm) at 30 °C (two fans were used to cool down the reaction mixture) for 48 h. After the reaction was completed, 8.0 mL of aq. NaOH (0.5 M) was added to the reaction mixture at room temperature, the resulting solution was stirred for 5 min at room temperature before acidified by HCl solution (2 N). The reaction mixture was then diluted with ethyl acetate, poured into a separatory funnel, before being washed with brine. The combined organic layers were dried over Na_2SO_4 and concentrated under reduced pressure after filtration. The crude product was purified by flash chromatography on silica gel to afford **321** as a white solid (506 mg, 82% yield).

Synthesis of β-arylated alcohol 391

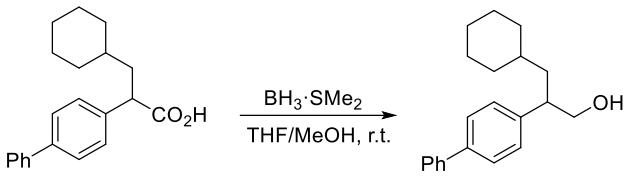

To a solution of **321** (61.7 mg, 0.2 mmol, 1.0 equiv.) in of THF (2.0 mL) was slowly added $BH_3{\cdot}SMe_2$ (0.2 mL, 10 M, 2.0 mmol) at 0 °C under N_2. The solution was stirred at 0 °C for 3 h and then at room temperature overnight. Then the reaction solution was cooled to 0 °C and of H_2O (4 mL) was slowly added. The organic layer was extracted with of EtOAc for three times and washed with brine. The organic layers were dried over Na_2SO_4, filtered and evaporated. The crude reaction mixture was purified by flash chromatography (EtOAc : Hexane = 1 : 10) to give the reduced product **391** as a white solid (60.0 mg, quant.). ^{1}H NMR (600 MHz, $CDCl_3$) δ 7.62 (d, *J* = 7.6 Hz, 2H), 7.58 (d, *J* = 7.7 Hz, 2H), 7.46 (t, *J* = 7.6 Hz, 2H), 7.38 – 7.33 (m, 1H), 7.30 (d, *J* = 7.7 Hz, 2H), 3.78 – 3.74 (m, 1H), 3.73 – 3.68 (m, 1H), 3.03 – 2.95 (m, 1H), 1.87 – 1.81 (m, 1H), 1.72 – 1.61 (m, 4H), 1.60 – 1.48 (m, 3H), 1.23 – 1.10 (m, 4H), 0.99 – 0.85 (m, 2H); 13C NMR (151 MHz, CDCl3) δ 141.9, 141.0, 139.6, 128.9 (2C), 128.6 (2C), 127.4 (2C), 127.2, 127.1 (2C), 68.1, 45.3, 39.9 34.8, 34.3, 32.9, 26.7, 26.3, 26.2. HRMS ESI $[M+Na]^+$ calculated for ($C_{21}H_{26}ONa^+$) 317.1876, found 317.1870.

Synthesis of α-arylated nitrile 392

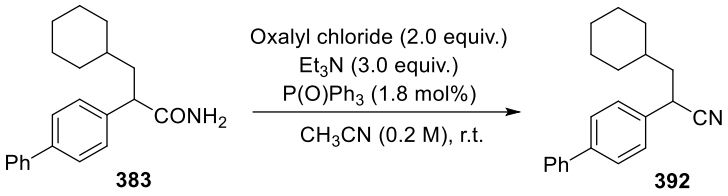

Following the method reported by Malkov and co-workers,[85] Ph_3PO (0.5 mg, 0.0018 mmol,) and amide **383** (30.7 mg, 0.1 mmol) were dissolved in 0.5 mL of anhydrous acetonitrile in a 5 mL vial equipped with a magnetic stirring bar, followed by addition of Et_3N (30.4 mg, 0.3 mmol). The resulting solution was treated dropwise with oxalyl chloride (25.4 mg, 0.2 mmol), the reaction mixture was stirred for 10 min at room temperature. After the reaction was complete, the solution was concentrated and purified by flash chromatography (EtOAc : hexane = 1 : 10), **392** was obtained as a yellow solid (20.6 mg, 71%). ^{1}H NMR (400 MHz, $CDCl_3$) δ 7.62 – 7.54 (m, 4H), 7.48 – 7.42 (m, 2H), 7.42 – 7.33 (m, 3H), 3.89 (dd, *J* = 10.0, 6.2 Hz, 1H), 1.97 – 1.89 (m, 1H), 1.89 – 1.81 (m, 1H), 1.80 – 1.62 (m, 5H), 1.63 – 1.50 (m, 1H), 1.35 – 1.25 (m, 2H), 1.25 – 1.12 (m, 1H), 1.05 – 0.89 (m, 2H); ^{13}C NMR (151 MHz, $CDCl_3$) δ 141.1, 140.4, 135.6, 129.0 (2C), 127.9 (2C), 127.8 (2C), 127.7, 127.2 (2C), 121.2, 43.8, 35.5, 34.6, 33.4, 32.5, 26.5, 26.1, 26.0. HRMS ESI $[M+Na]^+$ calculated for ($C_{21}H_{23}NNa^+$) 312.1723, found 312.1717.

Synthesis of a quinazoline derivative 394

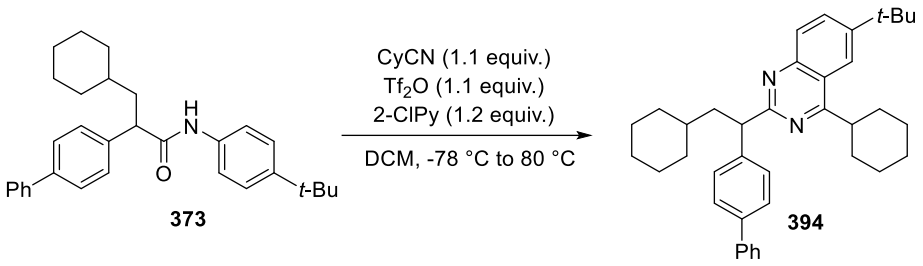

Following the method reported by Hill and co-workers,[140] trifluoromethanesulfonic anhydride (31.0 mg, 0.11 mmol) was added via syringe over 1 min to a stirred mixture of amide **289** (44 mg, 0.1 mmol) and 2-chloropyridine (13.6 mg, 0.12 mmol) in dichloromethane (0.5 mL) at – 78 °C. After 5 min, the reaction vessel was placed in an ice-water bath and allowed to warm to 0 °C, before cyclohexanecarbonitrile **309** (12.1 mg, 0.11 mmol) was added via syringe. The resulting solution was allowed to warm to room temperature for 5 minutes before the reaction vessel was heated to 80 °C. After 16 h, the reaction vessel was allowed to cool to room temperature. Dichloromethane (5 mL) was added to dilute the mixture and the layers were separated. The organic layer was washed with brine (2 mL), dried over Na_2SO_4, filtered and evaporated. The residue was purified by flash column chromatography (EtOAc : hexanes = 1 : 15) to give the product **310** as colourless oil (29.2 mg, 55%). ^{1}H NMR (400 MHz, $CDCl_3$) δ 8.02 (d, *J* = 2.1 Hz, 1H), 7.98 (d, *J* = 8.9 Hz, 1H), 7.92 (dd, *J* = 8.9, 2.1 Hz, 1H), 7.73 – 7.67 (m, 2H), 7.60 – 7.56 (m, 2H), 7.55 – 7.50 (m, 2H), 7.45 – 7.38 (m, 2H), 7.35 – 7.27 (m, 1H), 4.53 (dd, *J* = 9.0, 6.5 Hz, 1H), 3.55 (tt, *J* = 11.0, 3.5 Hz, 1H), 2.48 (ddd, *J* = 13.5, 9.0, 6.5 Hz, 1H), 2.08 (dd, *J* = 13.5, 6.5 Hz, 1H), 2.04 – 1.84 (m, 9H), 1.78 (d, *J* = 13.0 Hz, 1H), 1.72 – 1.51 (m, 4H), 1.45 (s,

9H), 1.22 – 0.96 (m, 6H); ^{13}C NMR (151 MHz, $CDCl_3$) δ 174.6, 167.2, 149.4, 149.0, 143.3, 141.3, 139.1, 131.9, 128.9 (2C), 128.8 (2C), 128.6, 127.1 (2C), 127.0, 127.0 (2C), 121.1, 118.7, 52.5, 43.6, 41.5, 35.8, 35.2, 33.8, 33.5, 32.3, 32.1, 31.3 (3C), 29.6, 26.8, 26.7, 26.6, 26.4, 26.3. HRMS ESI $[M+H]^+$ calculated for ($C_{38}H_{47}N_2^+$) 531.3734, found 531.3726.

Synthesis of a glucokinase activator 397

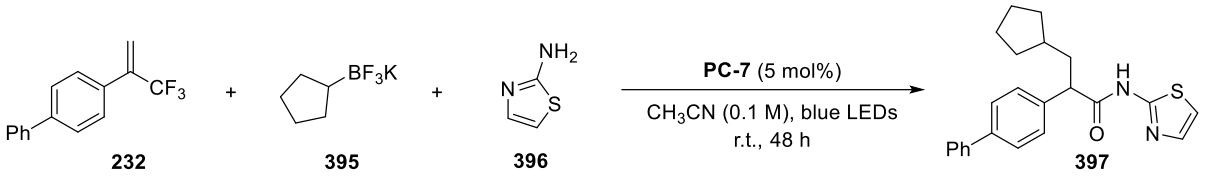

232 395 396 397

Following **GP12** using corresponding α-trifluoromethyl alkene **232** (24.8 mg, 0.10 mmol), potassium cyclopentyltrifluoroborate **395** (26.4 mg, 0.15 mmol) and thiazol-2-amine **396** (15.0 mg, 0.15 mmol), 5 mol% of **PC-7** was used. Purification by flash chromatography (EtOAc : Hexane : Et_3N = 15 : 100 : 1), the product **397** was obtained as a white solid (18.1 mg, 48% yield). ^{1}H NMR (400 MHz, $CDCl_3$) δ 7.53 – 7.37 (m, 6H), 7.37 – 7.29 (m, 4H), 7.28 – 7.22 (m, 1H), 6.96 (d, *J* = 3.6 Hz, 1H), 3.71 (t, *J* = 7.6 Hz, 1H), 2.22 (dt, *J* = 13.9, 7.6 Hz, 1H), 1.92 – 1.83 (m, 1H), 1.76 – 1.60 (m, 3H), 1.56 – 1.50 (m, 2H), 1.44 – 1.38 (m, 2H), 1.12 – 1.00 (m, 2H); ^{13}C NMR (151 MHz, $CDCl_3$) δ 172.0, 159.9, 140.73, 140.65, 137.7, 135.9, 128.9 (2C), 128.4 (2C), 127.8 (2C), 127.5, 127.2 (2C), 114.0, 52.0, 39.8, 37.9, 32.9, 32.6, 25.3, 25.2. HRMS ESI $[M+H]^+$ calculated for ($C_{23}H_{25}N_2OS^+$) 377.1682, found 377.1680.

5.5 Products for Chapter 4

5.5.1 Synthesis of α-Tertiary Amines

General procedure 14 (GP14)

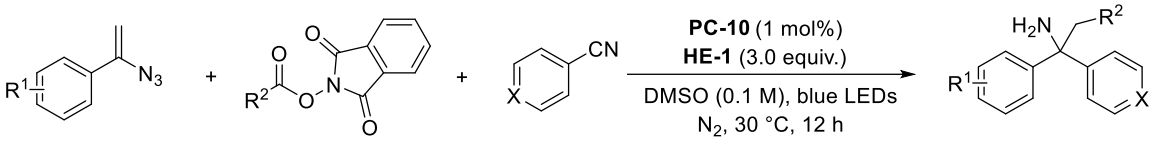

A 10-mL Schlenk tube equipped with a magnetic stir bar was charged with corresponding vinyl azide (if solid, 0.20 mmol), NHPI ester (0.30 mmol), cyanoarene (if solid, 0.50 mmol), Hantzsch ester **HE-1** (152.0 mg, 0.6 mmol) and **PC-10** (2.0 mg, 0.002 mmol). The flask was evacuated and backfilled with N_2 3 times. DMSO (2.0 mL, 0.1 M) was then added via syringe followed by the addition of vinyl azide (if liquid), or cyanoarene (if liquid) under N_2. The reaction mixture was then vigorously stirred under blue LED light (30 W, λ_{max} = 440 nm) at 30 °C (two fans were used to cool down the reaction mixture) for 12 h. After the reaction was completed, the reaction mixture was diluted with ethyl acetate and poured into a separatory funnel, washed with brine. The combined organic layers were dried over Na_2SO_4 and concentrated under reduced pressure after filtration. The crude product was purified by flash chromatography on silica gel to afford corresponding primary amine product.

***1-([1,1'-Biphenyl]-4-yl)-3,3-dimethyl-1-(pyridin-4-yl)butan-1-amine* 525**

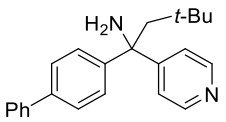

Following **GP14** using vinyl azide **523** (44.3 mg, 0.20 mmol), NHPI ester **524** (74.2 mg, 0.30 mmol) and 4-cyanopyridine **447** (52.1 mg, 0.50 mmol). Purification by flash chromatography (CH_2Cl_2 : Hexane : Et_3N = 50 : 50 : 1), the product was obtained as a white solid (48.2 mg, 73% yield). ^{1}H NMR (600 MHz, DMSO-d_6) δ 8.43 (d, *J* = 5.9 Hz, 2H), 7.63 (d, *J* = 7.7 Hz, 2H), 7.56 (d, *J* = 8.4 Hz, 2H), 7.52 (d, *J* = 8.4 Hz, 2H), 7.48 (d, *J* = 5.9 Hz, 2H), 7.45 – 7.41 (m, 2H), 7.35 – 7.31 (m, 1H), 2.36 (br s, 2H), 2.35 (d, *J* = 14.3 Hz, 1H), 2.32 (d, *J* = 14.3 Hz, 1H), 0.81 (s, 9H); ^{13}C NMR (151 MHz, DMSO-d_6) δ 159.6 (2C), 149.1, 149.0 (2C), 139.8, 137.7, 128.9 (2C), 127.3, 127.0 (2C), 126. 6 (2C), 126.1 (2C), 121.7, 60.5, 51.7, 31.9 (4C). HRMS ESI $[M+H]^+$ calculated for ($C_{23}H_{27}N_2^+$) 331.2169, found 331.2173.

***1-([1,1'-Biphenyl]-4-yl)-3-(4-(tert-butyl)phenyl)-1-(pyridin-4-yl)propan-1-amine* 526**

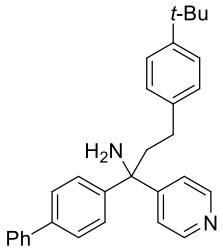

Following **GP14** using vinyl azide **523** (44.3 mg, 0.20 mmol), corresponding NHPI ester (101.2 mg, 0.30 mmol) and 4-cyanopyridine **447** (52.1 mg, 0.50 mmol). Purification by flash chromatography (CH_2Cl_2 : Hexane : Et_3N = 40 : 60 : 1), the product was obtained as a white solid (54.6 mg, 65% yield). ^{1}H NMR (400 MHz, $CDCl_3$) δ 8.56 (d, *J* = 5.8 Hz, 2H), 7.61 – 7.54 (m, 4H), 7.48 – 7.41 (m, 4H), 7.39 (d, *J* = 5.8 Hz, 2H), 7.37 – 7.34 (m, 1H), 7.32 (d, *J* = 8.4 Hz, 2H), 7.10 (d, *J* = 8.4 Hz, 2H), 2.65 – 2.43 (m, 4H), 2.01 (br s, 2H), 1.32 (s, 9H); ^{13}C NMR (101 MHz,

$CDCl_3$) δ 157.2 (2C), 150.0, 149.0, 145.9 (2C), 140.5, 139.9, 138.8, 128.9 (2C), 128.1 (2C), 127.5, 127.3 (2C), 127.1 (2C), 127.0 (2C), 125.5 (2C), 121.8, 60.9, 44.0, 34.5, 31.5 (3C), 29.9. HRMS ESI $[M+H]^+$ calculated for ($C_{30}H_{33}N_2^+$) 421.2638, found 421.2641.

1-([1,1'-Biphenyl]-4-yl)-3-(4-(methylthio)phenyl)-1-(pyridin-4-yl)propan-1-amine **527**

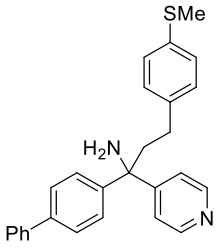

Following **GP14** using vinyl azide **523** (44.3 mg, 0.20 mmol), corresponding NHPI ester (98.2 mg, 0.30 mmol) and 4-cyanopyridine **447** (52.1 mg, 0.50 mmol). Purification by flash chromatography (CH_2Cl_2 : Hexane : Et_3N = 40 : 60 : 1), the product was obtained as a white solid (41.0 mg, 50% yield). ^{1}H NMR (400 MHz, $CDCl_3$) δ 8.55 (d, *J* = 5.2 Hz, 2H), 7.61 – 7.53 (m, 4H), 7.46 – 7.40 (m, 4H), 7.39 – 7.31 (m, 3H), 7.19 (d, *J* = 8.2 Hz, 2H), 7.07 (d, *J* = 8.2 Hz, 2H), 2.61 – 2.47 (m, 4H), 2.46 (s, 3H), 2.05 (br s, 2H); ^{13}C NMR (101 MHz, $CDCl_3$) δ 157.0 (2C), 150.0, 145.7 (2C), 140.4, 140.1, 139.0, 135.8, 129.0 (2C), 128.9 (2C), 127.6, 127.4 (2C), 127.3 (2C), 127.1 (2C), 126.9 (2C), 121.8, 61.0, 43.9, 30.0, 16.4. HRMS ESI $[M+H]^+$ calculated for ($C_{27}H_{27}N_2S^+$) 411.1889, found 411.1884.

1-([1,1'-Biphenyl]-4-yl)-3-(4-(((tert-butyldimethylsilyl)oxy)methyl)phenyl)-1-(pyridin-4-yl) propan-1-amine **528**

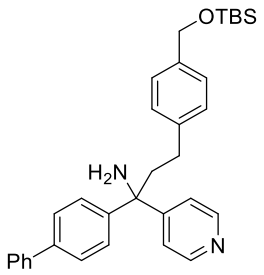

Following **GP14** using vinyl azide **523** (44.3 mg, 0.20 mmol), corresponding NHPI ester (127.7 mg, 0.30 mmol) and 4-cyanopyridine **447** (52.1 mg, 0.50 mmol). Purification by flash chromatography (CH_2Cl_2 : Hexane : Et_3N = 40 : 60 : 1), the product was obtained as colourless oil (69.2 mg, 68% yield). ^{1}H NMR (600 MHz, CD_3CN) δ 8.23 (d, *J* = 6.1 Hz, 2H), 7.37 (d, *J* = 7.9 Hz, 2H), 7.34 (d, *J* = 8.6 Hz, 2H), 7.28 (d, *J* = 8.6 Hz, 2H), 7.21 – 7.16 (m, 4H), 7.12 – 7.08 (m, 1H), 6.98 (d, *J* = 8.0 Hz, 2H), 6.90 (d, *J* = 8.0 Hz, 2H), 4.44 (s, 2H), 2.32 – 2.14 (m, 4H), 1.94 (br s, 2H), 0.68 (s, 9H), -0.16 (s, 6H); ^{13}C NMR (151 MHz, CD_3CN) δ 158.7 (2C), 150.6, 147.9 (2C), 142.2, 141.3, 140.1, 140.0, 129.9 (2C), 129.2 (2C), 128.4, 128.0 (2C), 127.8 (2C), 127.7 (2C), 127.5 (2C), 122.6, 65.5, 61.4, 44.6, 30.8, 26.3 (3C), 19.0, -5.06 (2C). HRMS ESI $[M+H]^+$ calculated for ($C_{33}H_{41}N_2OSi^+$) 509.2983, found 509.2982.

1-([1,1'-Biphenyl]-4-yl)-1-(pyridin-4-yl)-3-(4-(trifluoromethyl)phenyl)propan-1-amine **529**

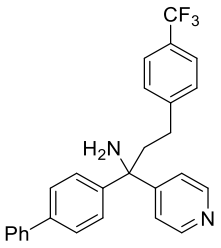

Following **GP14** using vinyl azide **523** (44.3 mg, 0.20 mmol), corresponding NHPI ester (104.8 mg, 0.30 mmol) and 4-cyanopyridine **447** (52.1 mg, 0.50 mmol). Purification by flash chromatography (CH_2Cl_2 : Hexane : Et_3N = 40 : 60 : 1), the product was obtained as a white solid (56.2 mg, 65% yield). ^{1}H NMR (400 MHz, DMSO-d_6) δ 8.49 (d, *J* = 6.2 Hz, 2H), 7.66 – 7.59 (m, 6H), 7.58 – 7.55 (m, 2H), 7.51 (d, *J* = 6.2 Hz, 2H), 7.47 – 7.40 (m, 4H), 7.36 – 7.31 (m, 1H), 2.67 (br s, 2H), 2.64 – 2.46 (m, 4H); ^{13}C NMR (151 MHz, DMSO-d_6) δ 157.6 (2C), 149.4, 147.4 (2C), 146.9, 139.8, 138.1, 129.1 (2C), 128.9 (2C), 127.3, 127.0 (2C), 126.6 (2C), 126.3 (2C), 126.5 (q, $^2J_{C\text{-}F}$ = 31.6 Hz, 1C), 125.1 (q, $^4J_{C\text{-}F}$ = 3.5 Hz, 2C), 124.5 (q, $^1J_{C\text{-}F}$ = 271.8 Hz), 121.7, 60.1, 42.6, 29.9; ^{19}F NMR (565 MHz, DMSO-d_6) δ -60.7 (s, 3F). HRMS ESI $[M+H]^+$ calculated for ($C_{27}H_{24}F_3N_2^+$) 433.1886, found 433.1889.

1-([1,1'-Biphenyl]-4-yl)-3-(4-fluorophenyl)-1-(pyridin-4-yl)propan-1-amine **530**

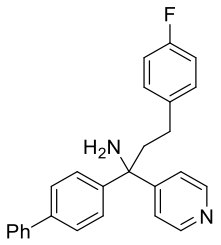

Following **GP14** using vinyl azide **523** (44.3 mg, 0.20 mmol), corresponding NHPI ester (89.8 mg, 0.30 mmol) and 4-cyanopyridine **447** (52.1 mg, 0.50 mmol). Purification by flash chromatography (CH_2Cl_2 : Hexane : Et_3N = 50 : 50 : 1), the product was obtained as colourless oil (52.0 mg, 67% yield). ^{1}H NMR (400 MHz, CD_3CN) δ 8.50 (d, *J* = 5.6 Hz, 2H) 7.65 – 7.61 (m, 2H), 7.61 – 7.58 (m, 2H), 7.55 – 7.49 (m, 2H), 7.47 – 7.41 (m, 4H), 7.39 – 7.33 (m, 1H), 7.22 –

7.15 (m, 2H), 7.06 – 6.98 (m, 2H), 2.59 – 2.42 (m, 4H), 2.15 (br s, 2H); ^{13}C NMR (151 MHz, CD_3CN) δ 162.1 (d, $^{1}J_{C\text{-}F}$ = 241.6 Hz), 158.6 (2C), 150.6, 147.9 (2C), 141.2, 140.0, 139.5 (d, $^{4}J_{C\text{-}F}$ = 3.0 Hz), 131.0 (d, $^{3}J_{C\text{-}F}$ = 9.1 Hz, 2C), 129.9 (2C), 128.4, 128.0 (2C), 127.8 (2C), 127.7 (2C), 122.6, 115.9 (d, $^{2}J_{C\text{-}F}$ = 21.1 Hz, 2C), 61.3, 44.5, 30.3; ^{19}F NMR (377 MHz, CD_3CN) δ -119.2 – -119.3 (m, 1F). HRMS ESI $[M+H]^+$ calculated for ($C_{26}H_{24}FN_2^+$) 383.1918, found 383.1919.

1-([1,1'-Biphenyl]-4-yl)-3-(3-methoxyphenyl)-1-(pyridin-4-yl)propan-1-amine **531**

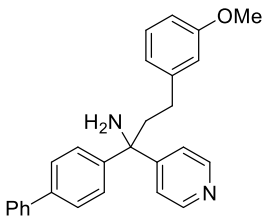

Following **GP14** using vinyl azide **523** (44.3 mg, 0.20 mmol), corresponding NHPI ester (93.4 mg, 0.30 mmol) and 4-cyanopyridine **447** (52.1 mg, 0.50 mmol). Purification by flash chromatography (CH_2Cl_2 : Hexane : Et_3N = 50 : 50 : 1), the product was obtained as a white solid (55.2 mg, 70% yield). ^{1}H NMR (600 MHz, CD_3CN) δ 8.47 (d, *J* = 5.5 Hz, 2H), 7.61 (d, *J* = 7.7 Hz, 2H), 7.57 (d, *J* = 8.3 Hz, 2H), 7.51 (d, *J* = 8.3 Hz, 2H), 7.45 – 7.40 (m, 4H), 7.36 – 7.31 (m, 1H), 7.20 – 7.15 (m, 1H), 6.78 – 6.70 (m, 3H), 3.74 (s, 3H), 2.59 – 2.37 (m, 4H), 2.16 (br s, 2H).; ^{13}C NMR (151 MHz, CD_3CN) δ 160.8, 158.7 (2C), 150.6, 148.0 (2C), 145.2, 141.3, 139.99, 130.4, 129.9 (2C), 128.4, 128.0 (2C), 127.8 (2C), 127.7 (2C), 122.6, 121.7, 115.1, 112.1, 61.3, 55.7, 44.4, 31.2. HRMS ESI $[M+H]^+$ calculated for ($C_{27}H_{27}N_2O^+$) 395.2118, found 395.2120.

1-([1,1'-Biphenyl]-4-yl)-3-(naphthalen-2-yl)-1-(pyridin-4-yl)propan-1-amine **532**

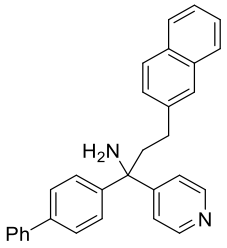

Following **GP14** using vinyl azide **523** (44.3 mg, 0.20 mmol), corresponding NHPI ester (99.4 mg, 0.30 mmol) and 4-cyanopyridine **447** (52.1 mg, 0.50 mmol). Purification by flash chromatography (CH_2Cl_2 : Hexane : Et_3N = 50 : 50 : 1), the product was obtained as a white solid (52.2 mg, 63% yield). ^{1}H NMR (600 MHz, DMSO-d_6) δ 8.50 (d, *J* = 4.9 Hz, 2H), 7.87 – 7.80 (m, 3H), 7.69 (s, 1H), 7.64 (d, *J* = 7.7 Hz, 2H), 7.63 – 7.57 (m, 4H), 7.53 (d, *J* = 4.9 Hz, 2H), 7.48 – 7.41 (m, 4H), 7.39 (d, *J* = 8.4 Hz, 1H), 7.36 – 7.31 (m, 1H), 2.74 – 2.54 (m, 6H); ^{13}C NMR (151 MHz, DMSO-d_6) δ 157.8 (2C), 149.4, 147.1 (2C), 140.0, 139.8, 138.0, 133.2, 131.5, 128.9 (2C), 127.7, 127.5, 127.4, 127.3, 127.2, 127.0 (2C), 126.7 (2C), 126.3 (2C), 125.92, 125.90, 125.1, 121.7, 60.2, 42.9, 30.2. HRMS ESI $[M+H]^+$ calculated for ($C_{30}H_{27}N_2^+$) 415.2169, found 415.2168.

1-([1,1'-Biphenyl]-4-yl)-1-(pyridin-4-yl)-3-(thiophen-3-yl)propan-1-amine **533**

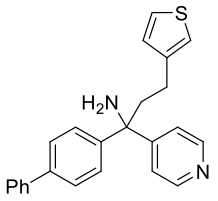

Following **GP14** using vinyl azide **523** (44.3 mg, 0.20 mmol), corresponding NHPI ester (86.2 mg, 0.30 mmol) and 4-cyanopyridine **447** (52.1 mg, 0.50 mmol). Purification by flash chromatography (CH_2Cl_2 : Hexane : Et_3N = 50 : 50 : 1), the product was obtained as yellow oil

(46.6 mg, 63% yield). ^{1}H NMR (600 MHz, $CDCl_3$) δ 8.55 (d, *J* = 5.8 Hz, 2H), 7.61 – 7.52 (m, 4H), 7.47 – 7.40 (m, 4H), 7.38 – 7.32 (m, 3H), 7.26 – 7.22 (m, 1H), 6.97 – 6.88 (m, 2H), 2.68 – 2.50 (m, 4H), 1.86 (br s, 2H); ^{13}C NMR (101 MHz, CD_3CN) δ 158. 7 (2C), 150.6, 147.9 (2C), 143.6, 141.3, 140.0, 129.9 (2C), 129.4, 128.4, 128.0 (2C), 127.8 (2C), 127.7 (2C), 126.5, 122.6, 121.0, 61.3, 43.1, 25.6. HRMS ESI $[M+H]^+$ calculated for ($C_{24}H_{23}N_2S^+$) 371.1576, found 371.1578.

***1-([1,1'-Biphenyl]-4-yl)-4,4-dimethyl-1-(pyridin-4-yl)pentan-1-amine* 532**

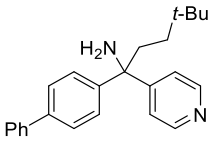

Following **GP14** using vinyl azide **523** (44.3 mg, 0.20 mmol), corresponding NHPI ester (78.4 mg, 0.30 mmol) and 4-cyanopyridine **447** (52.1 mg, 0.50 mmol). Purification by flash chromatography (CH_2Cl_2 : Hexane : Et_3N = 40 : 60 : 1), the product was obtained as yellow oil (44.8 mg, 61% yield). ^{1}H NMR (400 MHz, DMSO-d_6) δ 8.46 (d, *J* = 6.2 Hz, 2H), 7.63 (d, *J* = 7.1 Hz, 2H), 7.58 (d, *J* = 8.6 Hz, 2H), 7.51 (d, *J* = 8.6 Hz, 2H), 7.47 – 7.39 (m, 4H), 7.36 – 7.30 (m, 1H), 2.42 (br s, 2H), 2.22 – 2.09 (m, 2H), 1.17 – 0.97 (m, 2H), 0.85 (s, 9H); ^{13}C NMR (101 MHz, DMSO-d_6) δ 158.0 (2C), 149.2, 147.4 (2C), 139.8, 137.9, 128.9 (2C), 127.3, 127.0 (2C), 126.5 (2C), 126.2 (2C), 121.7, 60.0, 37.2, 36.0, 29.9, 29.3 (3C). HRMS ESI $[M+H]^+$ calculated for ($C_{24}H_{29}N_2^+$) 345.2325, found 345.2327.

***1-([1,1'-Biphenyl]-4-yl)-6-chloro-1-(pyridin-4-yl)hexan-1-amine* 535**

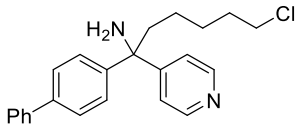

Following **GP14** using vinyl azide **523** (44.3 mg, 0.20 mmol), corresponding NHPI ester (84.5 mg, 0.30 mmol) and 4-cyanopyridine **447** (52.1 mg, 0.50 mmol). Purification by flash chromatography (CH_2Cl_2 : Hexane : Et_3N = 40 : 60 : 1), the product was obtained as colourless oil (38.1 mg, 58% yield). ^{1}H NMR (600 MHz, $CDCl_3$) δ 8.53 (d, *J* = 4.9 Hz, 2H), 7.57 (d, *J* = 7.7 Hz, 2H), 7.54 (d, *J* = 7.8 Hz, 2H), 7.45 – 7.41 (m, 2H), 7.39 (d, *J* = 7.8 Hz, 2H), 7.36 – 7.29 (m, 3H), 3.48 (t, *J* = 6.5 Hz, 2H), 2.28 – 2.18 (m, 2H), 2.01 (br s, 2H), 1.77 – 1.69 (m, 2H), 1.51 – 1.43 (m, 2H), 1.34 – 1.25 (m, 1H), 1.23 – 1.16 (m, 1H); ^{13}C NMR (151 MHz, $CDCl_3$) δ 157.4 (2C), 149.9, 146.2 (2C), 140.5, 139.8, 128.9 (2C), 127.5, 127.2 (2C), 127.1 (2C), 126.9 (2C), 121.8, 60.7, 45.0, 41.8, 32.5, 27.4, 23.4. HRMS ESI $[M+H]^+$ calculated for ($C_{23}H_{26}ClN_2^+$) 365.1779, found 365.1781.

7-([1,1'-biphenyl]-4-yl)-7-amino-7-(pyridin-4-yl)heptan-2-one **536**

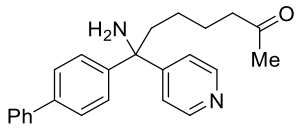

Following **GP14** using vinyl azide **523** (44.3 mg, 0.20 mmol), corresponding NHPI ester (82.6 mg, 0.30 mmol) and 4-cyanopyridine **447** (52.1 mg, 0.50 mmol). Purification by flash chromatography (CH_2Cl_2 : Et_3N = 100 : 1), the product was obtained as colourless oil (30.1 mg, 42% yield). ^{1}H NMR (600 MHz, CD_3CN) δ 8.45 (d, *J* = 5.0 Hz, 2H), 7.62 (d, *J* = 7.8 Hz, 2H), 7.57 (d, *J* = 8.2 Hz, 2H), 7.48 (d, *J* = 7.8 Hz, 2H), 7.45 – 7.42 (m, 2H), 7.38 (d, *J* = 5.0 Hz, 2H), 7.36 – 7.33 (m, 1H), 2.39 (t, *J* = 7.3 Hz, 2H), 2.26 – 2.17 (m, 4H), 2.02 (s, 3H), 1.53 (p, *J* = 7.4 Hz, 2H),

1.25 – 1.10 (m, 2H); ^{13}C NMR (101 MHz, CD_3CN) δ 209.6, 158.9 (2C), 150.5, 148.1 (2C), 141.3, 140.0, 129.9 (2C), 128.4, 128.0 (2C), 127.8 (2C), 127.6 (2C), 122.6, 61.3, 43.8, 42.2, 30.0, 24.8, 24.3. HRMS ESI $[M+H]^+$ calculated for ($C_{24}H_{27}N_2O^+$) 359.2118, found 359.2118.

***tert-Butyl 3-(3-([1,1'-biphenyl]-4-yl)-3-amino-3-(pyridin-4-yl)propyl) azetidine-1-carboxylate* 537**

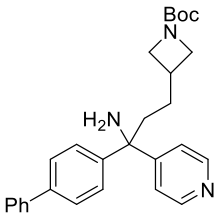

Following **GP14** using vinyl azide **523** (44.3 mg, 0.20 mmol), corresponding NHPI ester (108.1 mg, 0.30 mmol) and 4-cyanopyridine **447** (52.1 mg, 0.50 mmol). Purification by flash chromatography (CH_2Cl_2 : Et_3N = 100 : 1), the product was obtained as yellow oil (62.0 mg, 70% yield). ^{1}H NMR (400 MHz, CD_3CN) δ 8.47 (d, *J* = 6.2 Hz, 2H), 7.64 – 7.60 (m, 2H), 7.58 (d, *J* = 8.6 Hz, 2H), 7.49 (d, *J* = 8.6 Hz, 2H), 7.46 – 7.41 (m, 2H), 7.39 (d, *J* = 6.2 Hz, 2H), 7.37 – 7.32 (m, 1H), 3.95 – 3.85 (m, 2H), 3.44 – 3.34 (m, 2H), 2.51 – 2.43 (m, 1H), 2.30 (br s, 2H), 2.19 – 2.12 (m, 2H), 1.53 – 1.41 (m, 2H), 1.37 (s, 9H); ^{13}C NMR (151 MHz, CD_3CN) δ 158.8, 157.3 (2C), 150.6, 148.1 (2C), 141.3, 140.0, 129.9 (2C), 128.4, 127.9 (2C), 127.8 (2C), 127.7 (2C), 122.6, 79.7 (2C), 61.0, 54.7, 39.5, 29.9, 29.6, 28.6 (3C). HRMS ESI $[M+H]^+$ calculated for ($C_{28}H_{34}N_3O_2^+$) 444.2646, found 444.2649.

***1-([1,1'-Biphenyl]-4-yl)-2-cyclobutyl-1-(pyridin-4-yl)ethan-1-amine* 538**

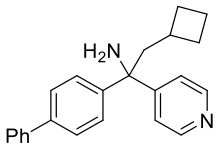

Following **GP14** using vinyl azide **523** (44.3 mg, 0.20 mmol), corresponding NHPI ester (73.6 mg, 0.30 mmol) and 4-cyanopyridine **447** (52.1 mg, 0.50 mmol). Purification by flash chromatography (CH_2Cl_2 : Et_3N = 100 : 1), the product was obtained as yellow oil (42.0 mg, 64% yield). ^{1}H NMR (400 MHz, CD_3CN) δ 8.37 (d, *J* = 6.2 Hz, 2H), 7.54 (d, *J* = 7.1 Hz, 2H), 7.48 (d, *J* = 8.5 Hz, 2H), 7.40 – 7.32 (m, 4H), 7.30 – 7.22 (m, 3H), 2.31 – 2.20 (m, 3H), 1.93 (br s, 2H), 1.78 – 1.48 (m, 6H); ^{13}C NMR (101 MHz, CD_3CN) δ 159.1 (2C), 150.4, 148.5 (2C), 141.3, 139.9, 129.9 (2C), 128.4, 128.0 (2C), 127.8 (2C), 127.5 (2C), 122.7, 61.5, 49.5, 33.3, 30.9, 30.8, 20.1. HRMS ESI $[M+H]^+$ calculated for ($C_{23}H_{25}N_2^+$) 329.2012, found 329.2009.

1-([1,1'-Biphenyl]-4-yl)-2-cyclopentyl-1-(pyridin-4-yl)ethan-1-amine **539**

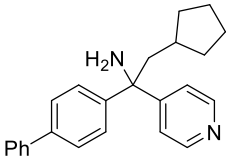

Following **GP14** using vinyl azide **523** (44.3 mg, 0.20 mmol), corresponding NHPI ester (77.8 mg, 0.30 mmol) and 4-cyanopyridine **447** (52.1 mg, 0.50 mmol). Purification by flash chromatography (CH_2Cl_2 : Hexane : Et_3N = 50 : 50 : 1), the product was obtained as yellow oil (50.6 mg, 74% yield). ^{1}H NMR (400 MHz, CD_3CN) δ 8.45 (d, *J* = 5.2 Hz, 2H), 7.62 (d, *J* = 7.7 Hz, 2H), 7.57 (d, *J* = 8.4 Hz, 2H), 7.49 (d, *J* = 8.4 Hz, 2H), 7.46 – 7.42 (m, 2H), 7.40 (d, *J* = 5.2 Hz, 2H), 7.36 – 7.32 (m, 1H), 2.42 – 2.32 (m, 2H), 2.13 (br s, 2H), 1.77 – 1.70 (m, 1H), 1.65 – 1.50 (m,

4H), 1.42 – 1.31 (m, 2H), 1.12 – 1.02 (m, 2H); ^{13}C NMR (151 MHz, CD_3CN) δ 159.5 (2C), 150.4, 148.9 (2C), 141.3, 139.8, 129.9 (2C), 128.4, 128.1 (2C), 127.8 (2C), 127.5 (2C), 122.8, 61.6, 48.4, 37.3, 35.3, 35.2, 25.5, 25.4. HRMS ESI $[M+H]^+$ calculated for ($C_{24}H_{27}N_2^+$) 343.2169, found 343.2172.

***1-([1,1'-Biphenyl]-4-yl)-2-cyclohexyl-1-(pyridin-4-yl)ethan-1-amine* 540**

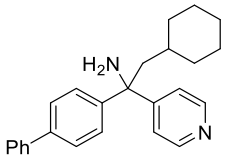

Following **GP14** using vinyl azide **523** (44.3 mg, 0.20 mmol), corresponding NHPI ester (82.0 mg, 0.30 mmol) and 4-cyanopyridine **447** (52.1 mg, 0.50 mmol). Purification by flash chromatography (CH_2Cl_2 : Hexane : Et_3N = 40 : 60 : 1), the product was obtained as yellow oil (46.3 mg, 65% yield). ^{1}H NMR (600 MHz, DMSO-d_6) δ 8.45 (d, *J* = 6.1 Hz, 2H), 7.64 (d, *J* = 7.5 Hz, 2H), 7.58 (d, *J* = 8.4 Hz, 2H), 7.50 (d, *J* = 8.4 Hz, 2H), 7.47 – 7.42 (m, 4H), 7.36 – 7.32 (m, 1H), 2.36 (br s, 2H), 2.12 (d, *J* = 4.9 Hz, 2H), 1.56 – 1.42 (m, 6H), 1.09 – 1.01 (m, 3H), 0.95 – 0.84 (m, 2H); ^{13}C NMR (151 MHz, DMSO-d_6) δ 158.6 (2C), 149.2, 148.1 (2C), 139.8, 137.8, 128.9 (2C), 127.3, 126.9 (2C), 126.5 (2C), 126.1 (2C), 121.7, 60.3, 48.1, 34.8, 34.7, 33.0, 25.91, 25.89, 25.8. HRMS ESI $[M+H]^+$ calculated for ($C_{25}H_{29}N_2^+$) 357.2325, found 357.2325.

***Methyl 4-(2-([1,1'-biphenyl]-4-yl)-2-amino-2-(pyridin-4-yl)ethyl)cyclohexane-1-carboxylate* 541**

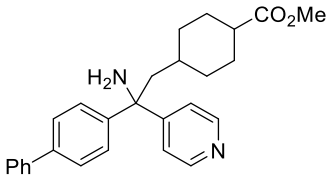

Following **GP14** using vinyl azide **523** (44.3 mg, 0.20 mmol), corresponding NHPI ester (99.4 mg, 0.30 mmol) and 4-cyanopyridine **447** (52.1 mg, 0.50 mmol). Purification by flash chromatography (CH_2Cl_2 : Et_3N = 100 : 1), the product was obtained as a white solid (59.6 mg, 72% yield), dr = 1:1.5. ^{1}H NMR (600 MHz, CD_3CN) δ 8.43 (d, *J* = 6.0 Hz, 2H), 7.60 (d, *J* = 7.2 Hz, 2H), 7.55 (d, *J* = 8.6 Hz, 2H), 7.46 (dd, *J* = 8.6, 2.2 Hz, 1H), 7.44 – 7.40 (m, 2H), 7.38 – 7.36 (m, 2H), 7.35 – 7.31 (m, 1H), 3.60 (s, 1.8H), 3.55 (s, 1.2H), 2.40 – 2.10 (m, 5H), 1.81 – 1.74 (m, 2H), 1.62 – 1.41 (m, 2H), 1.39 – 1.31 (m, 2H), 1.25 – 1.14 (m, 2H), 1.05 – 0.89 (m, 1H). ^{13}C NMR (151 MHz, CD_3CN) δ 176.5, 159.4 (2C), 150.4, 148.7 (2C), 141.2, 139.8, 129.9 (2C), 128.4, 128.0 (2C), 127.7 (2C), 127.48 (2C), 122.70, 61.7, 51.89, 43.5, 41.0, 34.9, 34.0, 32.22, 30.0, 26.8; the other isomer: 177.0, 159.5 (2C), 150.4, 148.8 (2C), 141.2, 139.8, 129.9 (2C), 128.4, 127.9 (2C), 127.7 (2C), 127.49 (2C), 122.65, 61.5, 51.86, 49.1, 47.0, 34.8, 34.0, 32.19, 29.9, 26.8. HRMS ESI $[M+H]^+$ calculated for ($C_{27}H_{31}N_2O_2^+$) 415.2380, found 415.2373.

***1-([1,1'-Biphenyl]-4-yl)-2-(4,4-difluorocyclohexyl)-1-(pyridin-4-yl)ethan-1-amine* 542**

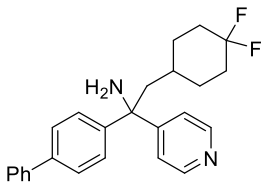

Following **GP14** using vinyl azide **523** (44.3 mg, 0.20 mmol), corresponding NHPI ester (92.8 mg, 0.30 mmol) and 4-cyanopyridine **447** (52.1 mg, 0.50 mmol). Purification by flash chromatography (CH_2Cl_2 : Hexane : Et_3N = 30 : 70 : 1), the product was obtained as colourless oil (57.3 mg, 73% yield). ^{1}H NMR (600 MHz, DMSO-d_6) δ 8.46 (d, *J* = 5.9 Hz, 2H), 7.64 (d, *J* = 7.7 Hz, 2H), 7.59 (d, *J* = 8.3 Hz, 2H), 7.52 (d, *J* = 8.3 Hz, 2H), 7.47 (d, *J* = 5.9 Hz, 2H), 7.46 – 7.52 (m, 2H), 7.36 – 7.32 (m, 1H), 2.51 (br s, 2H), 2.27 – 2.16 (m, 2H), 1.93 – 1.82 (m, 2H), 1.68 – 1.51 (m, 5H), 1.27 – 1.13 (m, 2H); ^{13}C NMR (151 MHz, DMSO-d_6) δ 158.4 (2C), 149.2, 147.7 (2C), 139.7, 137.9, 128.9 (2C), 127.3, 126.9 (2C), 126.5 (2C), 126.2 (2C), 124.1 (t, $^1J_{C\text{-}F}$ = 240.0 Hz), 121.7, 60.3, 45.8, 32.8 (dd, $^2J_{C\text{-}F}$ = 23.6, 23.2 Hz, 2C), 30.9, 30.2 (dd, $^3J_{C\text{-}F}$ = 8.5, 3.0 Hz, 2C); ^{19}F NMR (377 MHz, DMSO-d_6) δ -90.0 (d, *J* = 222.3 Hz, 1F), -98.9 (d, *J* = 232.5 Hz, 1F). HRMS ESI $[M+H]^+$ calculated for ($C_{25}H_{27}F_2N_2^+$) 393.2137, found 393.2136.

4-(2-([1,1'-Biphenyl]-4-yl)-2-amino-2-(pyridin-4-yl)ethyl)cyclohexan-1-one **543**

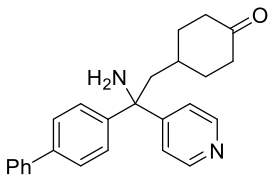

Following **GP14** using vinyl azide **523** (44.3 mg, 0.20 mmol), corresponding NHPI ester (86.2 mg, 0.30 mmol) and 4-cyanopyridine **447** (52.1 mg, 0.50 mmol). Purification by flash chromatography (CH_2Cl_2 : Hexane : Et_3N = 50 : 50 : 1), the product was obtained as colourless oil (51.1 mg, 69% yield). ^{1}H NMR (600 MHz, CD_3CN) δ 8.47 (d, *J* = 6.1 Hz, 2H), 7.62 (d, *J* = 7.9 Hz, 2H), 7.58 (d, *J* = 8.4 Hz, 2H), 7.50 (d, *J* = 8.4 Hz, 2H), 7.46 – 7.42 (m, 2H), 7.41 (d, *J* = 6.1 Hz,

2H), 7.37 – 7.33 (m, 1H), 2.33 – 2.25 (m, 2H), 2.23 – 2.08 (m, 6H), 1.89 – 1.76 (m, 3H), 1.46 – 1.36 (m, 2H); ^{13}C NMR (151 MHz, CD_3CN) δ 211.9, 159.3 (2C), 150.5, 148.6 (2C), 141.2, 139.9, 129.9 (2C), 128.4, 128.0 (2C), 127.8 (2C), 127.6 (2C), 122.7, 61.6, 47.0 (2C), 41.3, 35.3 (2C), 32.8. HRMS ESI $[M+H]^+$ calculated for ($C_{25}H_{27}N_2O^+$) 371.2118, found 371.2115.

***1-([1,1'-Biphenyl]-4-yl)-1-(pyridin-4-yl)-2-(tetrahydro-2H-pyran-4-yl)ethan-1-amine* 544**

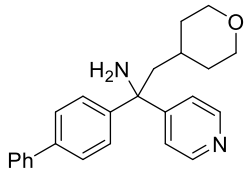

Following **GP14** using vinyl azide **523** (44.3 mg, 0.20 mmol), corresponding NHPI ester (82.6 mg, 0.30 mmol) and 4-cyanopyridine **447** (52.1 mg, 0.50 mmol). Purification by flash chromatography (CH_2Cl_2 : Hexane : Et_3N = 50 : 50 : 1), the product was obtained as a white solid (53.8 mg, 75% yield). ^{1}H NMR (600 MHz, DMSO-d_6) δ 8.45 (d, *J* = 6.0 Hz, 2H), 7.64 (d, *J* = 7.3 Hz, 2H), 7.58 (d, *J* = 8.3 Hz, 2H), 7.51 (d, *J* = 8.3 Hz, 2H), 7.47 – 7.42 (m, 4H), 7.37 – 7.32 (m, 1H), 3.67 (d, *J* = 11.7 Hz, 2H), 3.15 – 3.09 (m, 2H), 2.43 (br s, 2H), 2.18 (d, *J* = 5.1 Hz, 2H), 1.70 – 1.60 (m, 1H), 1.41 – 1.31 (m, 2H), 1.23 – 1.12 (m, 2H); ^{13}C NMR (151 MHz, DMSO-d_6) δ 158.5 (2C), 149.2, 147.9 (2C), 139.7, 137.8, 128.9 (2C), 127.3, 126.9 (2C), 126.5 (2C), 126.1 (2C), 121.7, 67.03, 67.00, 60.2, 47.5, 34.55, 34.54, 30.6. HRMS ESI $[M+H]^+$ calculated for ($C_{24}H_{27}N_2O^+$) 359.2118, found 359.2118.

***tert-Butyl 4-(2-([1,1'-biphenyl]-4-yl)-2-amino-2-(pyridin-4-yl)ethyl)piperidine-1-carboxylate* 545**

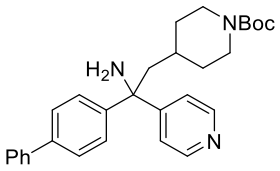

Following **GP14** using vinyl azide **523** (44.3 mg, 0.20 mmol), corresponding NHPI ester (112.3 mg, 0.30 mmol) and 4-cyanopyridine **447** (52.1 mg, 0.50 mmol). Purification by flash chromatography (CH_2Cl_2 : Et_3N = 100 : 1), the product was obtained as a white solid (73.2 mg, 80% yield). ^{1}H NMR (400 MHz, $CDCl_3$) δ 8.52 (d, *J* = 5.2 Hz, 2H), 7.59 – 7.55 (m, 2H), 7.53 (d, *J* = 8.4 Hz, 2H), 7.44 – 7.39 (m, 2H), 7.37 (d, *J* = 8.4 Hz, 2H), 7.35 – 7.29 (m, 3H), 4.00 – 3.82 (m, 2H), 2.62 – 2.47 (m, 2H), 2.21 – 2.16 (m, 2H), 2.12 (br s, 2H), 1.56 – 1.44 (m, 3H), 1.41 (s, 9H), 1.18 – 1.06 (m, 2H); ^{13}C NMR (101 MHz, $CDCl_3$) δ 157.9 (2C), 154.8, 149.8, 146.6 (2C), 140.4, 139.8, 128.9 (2C), 127.5, 127.1 (2C), 127.0 (2C), 126.8 (2C), 121.8, 79.30, 60.9, 48.0, 44.0, 34.1 (2C), 32.1 (2C), 28.5 (3C). HRMS ESI $[M+H]^+$ calculated for ($C_{29}H_{36}N_3O_2^+$) 458.2802, found 458.2805.

***1-([1,1'-Biphenyl]-4-yl)-3-ethyl-1-(pyridin-4-yl)pentan-1-amine* 546**

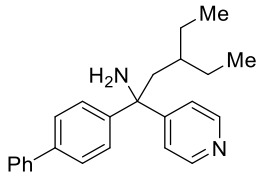

Following **GP14** using vinyl azide **523** (44.3 mg, 0.20 mmol), corresponding NHPI ester (78.4 mg, 0.30 mmol) and 4-cyanopyridine **447** (52.1 mg, 0.50 mmol). Purification by flash chromatography (CH_2Cl_2 : Hexane : Et_3N = 30 : 70 : 1), the product was obtained as colourless

oil (57.8 mg, 84% yield). ^{1}H NMR (600 MHz, $CDCl_3$) δ 8.52 (d, *J* = 4.9 Hz, 2H), 7.58 (d, *J* = 8.0 Hz, 2H), 7.53 (d, *J* = 8.3 Hz, 2H), 7.46 – 7.38 (m, 4H), 7.35 – 7.31 (m, 3H), 2.18 (d, *J* = 4.8 Hz, 2H), 1.94 (br s, 2H), 1.34 – 1.30 (m, 1H), 1.25 – 1.19 (m, 2H), 1.17 – 1.10 (m, 2H), 0.75 (t, *J* = 7.4 Hz, 3H), 0.71 (t, *J* = 7.4 Hz, 3H); ^{13}C NMR (151 MHz, $CDCl_3$) δ 158.2 (2C), 149.7, 147.2 (2C), 140.6, 139.7, 128.9 (2C), 127.4, 127.09 (2C), 127.06 (2C), 127.0 (2C), 122.1, 61.1, 44.9, 35.7, 26.9, 26.8, 10.59, 10.56. HRMS ESI $[M+H]^+$ calculated for ($C_{24}H_{29}N_2^+$) 345.2325, found 345.2328.

***1-([1,1'-Biphenyl]-4-yl)-2-(1-methylcyclohexyl)-1-(pyridin-4-yl)ethan-1-amine* 547**

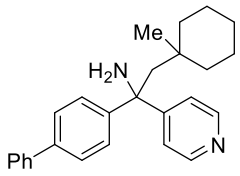

Following **GP14** using vinyl azide **523** (44.3 mg, 0.20 mmol), corresponding NHPI ester (86.2 mg, 0.30 mmol) and 4-cyanopyridine **447** (52.1 mg, 0.50 mmol). Purification by flash chromatography (CH_2Cl_2 : Hexane : Et_3N = 30 : 70 : 1), the product was obtained as colourless oil (59.6 mg, 80% yield). ^{1}H NMR (600 MHz, CD_3CN) δ 8.42 (d, *J* = 6.2 Hz, 2H), 7.60 (d, *J* = 7.3 Hz, 2H), 7.53 (d, *J* = 8.5 Hz, 2H), 7.50 (d, *J* = 8.5 Hz, 2H), 7.44 – 7.39 (m, 4H), 7.35 – 7.31 (m, 1H), 2.38 (s, 2H), 2.03 (br s, 2H), 1.43 – 1.15 (m, 10H), 0.76 (s, 3H); ^{13}C NMR (151 MHz, CD_3CN) δ 160.8 (2C), 150.3, 150.2 (2C), 141.2, 139.5, 129.8 (2C), 128.3, 127.9 (2C), 127.7 (2C), 127.3 (2C), 122.6, 61.7, 53.0, 40.90, 40.87, 35.5, 27.1, 25.8, 22.69, 22.68. HRMS ESI $[M+H]^+$ calculated for ($C_{26}H_{31}N_2^+$) 371.2482, found 371.2479.

***1-([1,1'-Biphenyl]-4-yl)-2-(adamantan-1-yl)-1-(pyridin-4-yl)ethan-1-amine* 548**

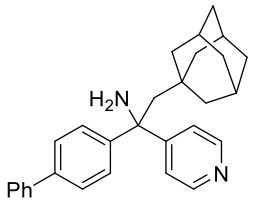

Following **GP14** using vinyl azide **523** (44.3 mg, 0.20 mmol), corresponding NHPI ester (97.6 mg, 0.30 mmol) and 4-cyanopyridine **447** (52.1 mg, 0.50 mmol). Purification by flash chromatography (CH_2Cl_2 : Hexane : Et_3N = 50 : 50 : 1), the product was obtained as a white solid (62.1 mg, 76% yield). ^{1}H NMR (400 MHz, DMSO-d_6) δ 8.43 (d, *J* = 6.1 Hz, 2H), 7.63 (d, *J* = 7.2 Hz, 2H), 7.56 (d, *J* = 8.6 Hz, 2H), 7.51 (d, *J* = 8.6 Hz, 2H), 7.47 (d, *J* = 6.1 Hz, 2H), 7.46 – 7.40 (m, 2H), 7.36 – 7.30 (m, 1H), 2.40 (br s, 2H), 2.21 (d, *J* = 14.6 Hz, 1H), 2.17 (d, *J* = 14.6 Hz, 1H), 1.78 – 1.71 (m, 3H), 1.58 – 1.42 (m, 12H); ^{13}C NMR (151 MHz, DMSO-d_6) δ 159.4 (2C), 149.12 (2C), 149.05, 139.7, 137.6, 128.9 (2C), 127.3, 126.8 (2C), 126.5 (2C), 126.0 (2C), 121.6, 60.4, 53.5, 43.7 (3C), 36.4 (3C), 34.1, 28.2 (3C). HRMS ESI $[M+H]^+$ calculated for ($C_{29}H_{33}N_2^+$) 409.2638, found 409.2639.

5-(2-([1,1'-Biphenyl]-4-yl)-2-amino-2-(pyridin-4-yl)ethyl)adamantan-2-one **549**

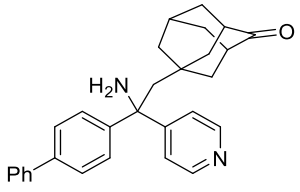

Following **GP14** using vinyl azide **523** (44.3 mg, 0.20 mmol), corresponding NHPI ester (101.8 mg, 0.30 mmol) and 4-cyanopyridine **447** (52.1 mg, 0.50 mmol). Purification by flash chromatography (EtOAc : Et_3N = 100 : 1), the product was obtained as colourless oil (38.9 mg,

46% yield). ^{1}H NMR (600 MHz, CD_3CN) δ 8.24 (d, *J* = 5.9 Hz, 2H), 7.42 (d, *J* = 7.4 Hz, 2H), 7.37 (d, *J* = 8.4 Hz, 2H), 7.28 (d, *J* = 8.4 Hz, 2H), 7.26 – 7.22 (m, 2H), 7.20 (d, *J* = 5.9 Hz, 2H), 7.17 – 7.13 (m, 1H), 2.13 (s, 2H), 2.09 – 2.06 (m, 2H), 2.01 (br s, 2H), 1.78 – 1.47 (m, 11H); ^{13}C NMR (151 MHz, CD_3CN) δ 218.0, 160.4 (2C), 150.4, 149.5 (2C), 141.1, 139.7, 129.9 (2C), 128.4, 127.8 (2C), 127.7 (2C), 127.4 (2C), 122.5, 61.5, 52.5, 47.7, 47.6, 45.9, 45.8, 43.5, 39.0 (2C), 35.2, 29.0. HRMS ESI $[M+H]^+$ calculated for ($C_{29}H_{31}N_2O^+$) 423.2431, found 423.2428.

***Methyl 4-(2-([1,1'-biphenyl]-4-yl)-2-amino-2-(pyridin-4-yl)ethyl)bicyclo[2.2.2] octane-1-carboxylate* 550**

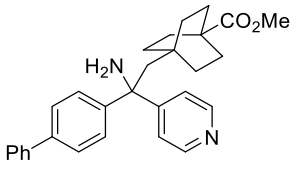

Following **GP14** using vinyl azide **523** (44.3 mg, 0.20 mmol), corresponding NHPI ester (107.2 mg, 0.30 mmol) and 4-cyanopyridine **447** (52.1 mg, 0.50 mmol). Purification by flash chromatography (CH_2Cl_2 : Hexane : Et_3N = 50 : 50 : 1), the product was obtained as a white solid (69.6 mg, 79% yield). ^{1}H NMR (400 MHz, $CDCl_3$) δ 8.49 (d, *J* = 4.9 Hz, 2H), 7.56 (d, *J* = 7.2 Hz, 2H), 7.51 (d, *J* = 8.5 Hz, 2H), 7.44 – 7.35 (m, 4H), 7.28 – 7.21 (m, 3H), 3.57 (s, 3H), 2.29 (s, 2H), 2.12 (br s, 2H), 1.69 – 1.58 (m, 6H), 1.43 – 1.33 (m, 6H); ^{13}C NMR (101 MHz, $CDCl_3$) δ 178.3, 159.0 (2C), 149.6, 147.8 (2C), 140.3, 139.4, 128.8 (2C), 127.4, 127.0 (2C), 126.8 (2C), 126.7 (2C), 121.7, 60.8, 51.61, 51.57, 38.3, 32.3, 32.2 (3C), 28.5 (3C). HRMS ESI $[M+H]^+$ calculated for ($C_{29}H_{33}N_2O_2^+$) 441.2537, found 441.2537.

***1-([1,1'-Biphenyl]-4-yl)-3,3,3-trifluoro-1-(pyridin-4-yl)propan-1-amine* 551**

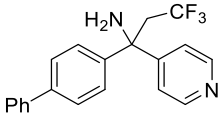

Following **GP14** using vinyl azide **523** (44.3 mg, 0.20 mmol), Togni's reagent **54** (99.0 mg, 0.30 mmol) and 4-cyanopyridine **447** (52.1 mg, 0.50 mmol), photocatalyst **PC-11** (1.8 mg, 0.002 mmol) was used instead of **PC-10**. Purification by flash chromatography (CH_2Cl_2 : Hexane : Et_3N = 40 : 60 : 1), the product was obtained as colourless oil (30.1 mg, 44% yield). ^{1}H NMR (600 MHz, CD_3CN) δ 8.61 (d, *J* = 5.1 Hz, 2H), 7.73 (d, *J* = 7.4 Hz, 2H), 7.71 (d, *J* = 8.5 Hz, 2H), 7.64 (d, *J* = 8.5 Hz, 2H), 7.57 – 7.52 (m, 4H), 7.49– 7.44 (m, 1H), 3.50 – 3.41 (m, 2H), 2.38 (br s, 2H); ^{13}C NMR (151 MHz, CD_3CN) δ 157.0 (2C), 150.7, 146.5 (2C), 141.0, 140. 6, 129.9 (2C), 128.6, 127.84 (2C), 127.79 (2C), 127.64 (q, $^1J_{C\text{-}F}$ = 277.8 Hz), 127.57 (2C), 122.2, 59.2, 44.8 (q, $^2J_{C\text{-}F}$ = 24.2 Hz); ^{19}F NMR (565 MHz, CD_3CN) δ -58.42 (t, *J* = 10.8 Hz, 3F). HRMS ESI $[M+H]^+$ calculated for ($C_{20}H_{18}F_3N_2^+$) 343.1417, found 343.1413.

***1-([1,1'-Biphenyl]-4-yl)-2-phenyl-1-(pyridin-4-yl)ethan-1-amine* 552**

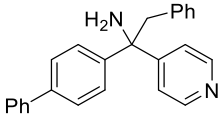

Following **GP14** using vinyl azide **523** (44.3 mg, 0.20 mmol), diphenyliodonium salt **585** (129.1 mg, 0.30 mmol) and 4-cyanopyridine **447** (52.1 mg, 0.50 mmol), photocatalyst **PC-11** (1.8 mg, 0.002 mmol) was used instead of **PC-10**. Purification by flash chromatography (CH_2Cl_2 : Hexane : Et_3N = 50 : 50 : 1), the product was obtained as a white solid (22.4 mg, 32% yield). ^{1}H

NMR (400 MHz, $CDCl_3$) δ 8.52 (d, *J* = 5.4 Hz, 2H), 7.60 (d, *J* = 7.3 Hz, 2H), 7.56 (d, *J* = 8.4 Hz, 2H), 7.48 – 7.40 (m, 4H), 7.38 – 7.33 (m, 1H), 7.30 (d, *J* = 6.7 Hz, 2H), 7.22 – 7.10 (m, 3H), 6.78 (d, *J* = 6.7 Hz, 2H), 3.62 (d, *J* = 12.9 Hz, 1H), 3.57 (d, *J* = 12.9 Hz, 1H), 1.99 (br s, 2H); ^{13}C NMR (101 MHz, $CDCl_3$) δ 156.8 (2C), 149.7, 145.8 (2C), 140.5, 139.9, 135.9, 130.9 (2C), 128.9 (2C), 128.1 (2C), 127.5, 127.3 (2C), 127.11 (2C), 127.05 (2C), 126.9, 122.2, 61.0, 48.4. HRMS ESI $[M+H]^+$ calculated for ($C_{25}H_{23}N_2^+$) 351.1856, found 351.1852.

3,3-Dimethyl-1-phenyl-1-(pyridine-4-yl)butan-1-amine **554**

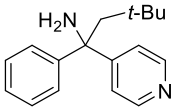

Following **GP14** using corresponding vinyl azide (29.0 mg, 0.20 mmol), NHPI ester **524** (74.2 mg, 0.30 mmol) and 4-cyanopyridine **447** (52.1 mg, 0.50 mmol). Purification by flash chromatography (CH_2Cl_2 : Hexane : Et_3N = 30 : 70 : 1), the product was obtained as colourless oil (39.6 mg, 78% yield). ^{1}H NMR (400 MHz, CD_3CN) δ 8.42 (d, *J* = 6.2 Hz, 2H), 7.46 – 7.42 (m, 2H), 7.39 (d, *J* = 6.2 Hz, 2H), 7.30 – 7.24 (m, 2H), 7.20 – 7.15 (m, 1H), 2.37 (s, 2H), 2.04 (br s, 2H), 0.82 (s, 9H); ^{13}C NMR (101 MHz, CD_3CN) δ 160.8 (2C), 150.4 (2C), 150.3, 128.9 (2C), 127.4 (2C), 127.2, 122.6, 61.8, 53.0, 32.6, 32.2 (3C). HRMS ESI $[M+H]^+$ calculated for ($C_{17}H_{23}N_2^+$) 255.1856, found 255.1851.

3,3-Dimethyl-1-(pyridine-4-yl)-1-(p-tolyl)butan-1-amine **555**

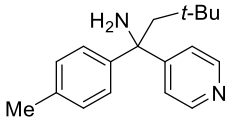

Following **GP14** using corresponding vinyl azide (31.8 mg, 0.20 mmol), NHPI ester **524** (74.2 mg, 0.30 mmol) and 4-cyanopyridine **447** (52.1 mg, 0.50 mmol). Purification by flash chromatography (CH_2Cl_2 : Hexane : Et_3N = 30 : 70 : 1), the product was obtained as colourless oil (35.1 mg, 64% yield). ^1H NMR (400 MHz, CD_3CN) δ 8.41 (d, *J* = 6.2 Hz, 2H), 7.38 (d, *J* = 6.2 Hz, 2H), 7.30 (d, *J* = 8.3 Hz, 2H), 7.09 (d, *J* = 8.3 Hz, 2H), 2.35 (s, 2H), 2.27 (s, 3H), 2.06 (br s, 2H), 0.82 (s, 9H); ^{13}C NMR (101 MHz, CD_3CN) δ 160.9 (2C), 150.2, 147.6 (2C), 136.7, 129.5 (2C), 127.2 (2C), 122.6, 61.6, 53.0, 32.7, 32.3 (3C), 20.9. HRMS ESI $[M+H]^+$ calculated for ($C_{18}H_{25}N_2^+$) 269.2012, found 269.2009.

1-(4-(tert-Butyl)phenyl)-3,3-dimethyl-1-(pyridine-4-yl)butan-1-amine **556**

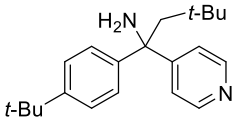

Following **GP14** using corresponding vinyl azide (40.3 mg, 0.20 mmol), NHPI ester **524** (74.2 mg, 0.30 mmol) and 4-cyanopyridine **447** (52.1 mg, 0.50 mmol). Purification by flash chromatography (CH_2Cl_2 : Hexane : Et_3N = 30 : 70 : 1), the product was obtained as colourless oil (43.5 mg, 70% yield). ^1H NMR (400 MHz, CD_3CN) δ 8.41 (d, *J* = 6.2 Hz, 2H), 7.41 (d, *J* = 6.2 Hz, 2H), 7.37 – 7.23 (m, 4H), 2.40 (d, *J* = 14.5 Hz, 1H), 2.33 (d, *J* = 14.5 Hz, 1H), 2.00 (br s, 2H), 1.26 (s, 9H), 0.82 (s, 9H); ^{13}C NMR (101 MHz, CD_3CN) δ 160.5 (2C), 150.2, 150.0 (2C), 148.0,

126.8 (2C), 125.8 (2C), 122.7, 61.5, 53.1, 34.9, 32.7, 32.3 (3C), 31.6 (3C). HRMS ESI $[M+H]^+$ calculated for ($C_{21}H_{31}N_2^+$) 311.2482, found 311.2485.

1-(4-Methoxyphenyl)-3,3-dimethyl-1-(pyridine-4-yl)butan-1-amine **557**

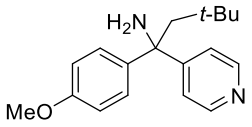

Following **GP14** using corresponding vinyl azide (35.0 mg, 0.20 mmol), NHPI ester **524** (74.2 mg, 0.30 mmol) and 4-cyanopyridine **447** (52.1 mg, 0.50 mmol). Purification by flash chromatography (CH_2Cl_2 : Hexane : Et_3N = 30 : 70 : 1), the product was obtained as yellow oil (35.6 mg, 62% yield). ^1H NMR (600 MHz, CD_3CN) δ 8.35 (d, *J* = 5.4 Hz, 2H), 7.32 (d, *J* = 5.4 Hz, 2H), 7.27 (d, *J* = 8.6 Hz, 2H), 6.76 (d, *J* = 8.6 Hz, 2H), 3.68 (s, 3H), 2.27 (s, 2H), 1.88 (br s, 2H), 0.76 (s, 9H); ^{13}C NMR (151 MHz, CD_3CN) δ 161.0 (2C), 159.0, 150.3, 142.5 (2C), 128.5 (2C), 122.6 (2C), 114.1, 61.4, 55.8, 53.2, 32.6, 32.2 (3C). HRMS ESI $[M+H]^+$ calculated for ($C_{18}H_{25}N_2O^+$) 285.1961, found 285.1958.

3,3-Dimethyl-1-(pyridine-4-yl)-1-(4-(trifluoromethyl)phenyl)butan-1-amine **558**

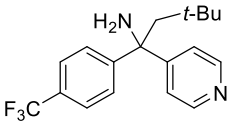

Following **GP14** using corresponding vinyl azide (31.8 mg, 0.20 mmol), NHPI ester **524** (74.2 mg, 0.30 mmol) and 4-cyanopyridine **447** (52.1 mg, 0.50 mmol), **PC-11** was used as photocatalyst. Purification by flash chromatography (CH_2Cl_2 : Hexane : Et_3N = 30 : 70 : 1), the

product was obtained as yellow oil (35.6 mg, 62% yield). ^{1}H NMR (600 MHz, CD_3CN) δ 8.44 (d, *J* = 5.8 Hz, 2H), 7.64 (d, *J* = 8.2 Hz, 2H), 7.59 (d, *J* = 8.2 Hz, 2H), 7.37 (d, *J* = 5.8 Hz, 2H), 2.41 (d, *J* = 14.4 Hz, 1H), 2.38 (d, *J* = 14.4 Hz, 1H), 2.12 (br s, 2H), 0.82 (s, 9H); ^{13}C NMR (151 MHz, CD_3CN) δ 160.1 (2C), 154.8 (2C), 150.5, 128.7 (q, $^{2}J_{C\text{-}F}$ = 32.1 Hz) , 128.3 (2C), 125.8 (q, $^{3}J_{C\text{-}F}$ = 3.8 Hz, 2C), 125.5 (q, $^{1}J_{C\text{-}F}$ = 271.2 Hz), 122.5, 62.0, 52.8, 32.7, 32.2 (3C); ^{19}F NMR (565 MHz, CD_3CN) δ -62.81 (s, 3F). HRMS ESI $[M+H]^+$ calculated for ($C_{18}H_{22}F_3N_2^+$) 323.1730, found 323.1726.

1-(3-Methoxyphenyl)-3,3-dimethyl-1-(pyridine-4-yl)butan-1-amine **559**

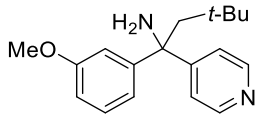

Following **GP14** using corresponding vinyl azide (35.0 mg, 0.20 mmol), NHPI ester **524** (74.2 mg, 0.30 mmol) and 4-cyanopyridine **447** (52.1 mg, 0.50 mmol). Purification by flash chromatography (CH_2Cl_2 : Hexane : Et_3N = 40 : 60 : 1), the product was obtained as colourless oil (38.6 mg, 68% yield). ^{1}H NMR (400 MHz, CD_3CN) δ 8.25 (d, *J* = 6.1 Hz, 2H), 7.23 (d, *J* = 6.1 Hz, 2H), 7.05 – 7.00 (m, 1H), 6.86 – 6.84 (m, 1H), 6.81 (d, *J* = 8.1 Hz, 1H), 6.58 (dd, *J* = 8.1, 2.5 Hz, 1H), 3.57 (s, 3H), 2.22 (d, *J* = 14.5 Hz, 1H), 2.17 (d, *J* = 14.5 Hz, 1H), 1.94 (br s, 2H), 0.66 (s, 9H); ^{13}C NMR (101 MHz, CD_3CN) δ 160.3, 160.0 (2C), 151.7 (2C), 149.9, 129.5, 122.1, 119.5, 113.3, 111.5, 61.4, 55.4, 52.4, 32.2, 31.8 (3C). HRMS ESI $[M+H]^+$ calculated for ($C_{18}H_{25}N_2O^+$) 285.1961, found 285.1958.

1-(3-Fluorophenyl)-3,3-dimethyl-1-(pyridine-4-yl)butan-1-amine **560**

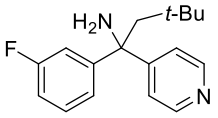

Following **GP14** using corresponding vinyl azide (32.6 mg, 0.20 mmol), NHPI ester **524** (74.2 mg, 0.30 mmol) and 4-cyanopyridine **447** (52.1 mg, 0.50 mmol). Purification by flash chromatography (CH_2Cl_2 : Hexane : Et_3N = 30 : 70 : 1), the product was obtained as yellow oil (48.1 mg, 78% yield). ^{1}H NMR (400 MHz, CD_3CN) δ 8.43 (d, *J* = 6.2 Hz, 2H), 7.38 (d, *J* = 6.2 Hz, 2H), 7.31 – 7.16 (m, 3H), 6.97 – 6.88 (m, 1H), 2.36 (s, 2H), 2.04 (br s, 2H), 0.82 (s, 9H); ^{13}C NMR (101 MHz, CD_3CN) δ 163.6 (d, $^1J_{C\text{-}F}$ = 243.7 Hz), 160.2 (2C), 153.5 (d, $^3J_{C\text{-}F}$ = 6.4 Hz), 150.4 (2C), 130.6 (d, $^3J_{C\text{-}F}$ = 8.2 Hz), 123.6 (d, $^4J_{C\text{-}F}$ = 2.7 Hz), 122.5, 114.4 (d, $^2J_{C\text{-}F}$ = 22.9 Hz), 113.8 (d, $^2J_{C\text{-}F}$ = 21.4 Hz), 67.5, 52.9, 32.7, 32.2 (3C); ^{19}F NMR (377 MHz, CD_3CN) δ -114.79 – -114.91 (m, 1F). HRMS ESI $[M+H]^+$ calculated for ($C_{17}H_{22}FN_2^+$) 273.1762, found 273.1757.

1-(3-Chlorophenyl)-3,3-dimethyl-1-(pyridine-4-yl)butan-1-amine **561**

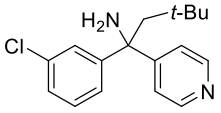

Following **GP14** using corresponding vinyl azide (35.9 mg, 0.20 mmol), NHPI ester **524** (74.2 mg, 0.30 mmol) and 4-cyanopyridine **447** (52.1 mg, 0.50 mmol). Purification by flash chromatography (CH_2Cl_2 : Hexane : Et_3N = 30 : 70 : 1), the product was obtained as colourless oil (40.4 mg, 70% yield). ^{1}H NMR (400 MHz, CD_3CN) δ 8.43 (d, *J* = 6.2 Hz, 2H), 7.52 – 7.50 (m, 1H), 7.37 (d, *J* = 6.2 Hz, 2H), 7.36 – 7.32 (m, 1H), 7.27 – 7.22 (m, 1H), 7.21 – 7.18 (m, 1H), 2.35 (s, 2H), 2.06 (br s, 2H), 0.82 (s, 9H); ^{13}C NMR (101 MHz, CD_3CN) δ 160.1 (2C), 152.8 (2C), 150.4,

134.4, 130.5, 127.5, 127.2, 126.2, 122.5, 61.8, 52.8, 32.7, 32.2 (3C). HRMS ESI $[M+H]^+$ calculated for ($C_{17}H_{22}ClN_2^+$) 289.1466, found 289.1463.

1-(3-Bromophenyl)-3,3-dimethyl-1-(pyridine-4-yl)butan-1-amine **562**

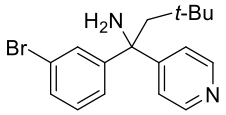

Following **GP14** using corresponding vinyl azide (44.8 mg, 0.20 mmol), NHPI ester **524** (74.2 mg, 0.30 mmol) and 4-cyanopyridine **447** (52.1 mg, 0.50 mmol). Purification by flash chromatography (CH_2Cl_2 : Hexane : Et_3N = 50 : 50 : 1), the product was obtained as yellow oil (44.5 mg, 67% yield). ^{1}H NMR (400 MHz, CD_3CN) δ 8.44 (d, *J* = 5.4 Hz, 2H), 7.67 – 7.64 (m, 1H), 7.43 – 7.31 (m, 4H), 7.22 – 7.16 (m, 1H), 2.35 (s, 2H), 2.15 (br s, 2H), 0.82 (s, 9H); ^{13}C NMR (101 MHz, CD_3CN) δ 160.1 (2C), 153.1 (2C), 150.4, 130.8, 130.5, 130.2, 126.6, 122.8, 122.5, 61.8, 52.8, 32.7, 32.2 (3C). HRMS ESI $[M+H]^+$ calculated for ($C_{17}H_{22}BrN_2^+$) 333.0961, found 333.0956.

3,3-Dimethyl-1-(pyridine-4-yl)-1-(3-(trifluoromethoxy)phenyl)butan-1-amine **563**

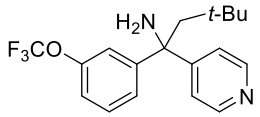

Following **GP14** using vinyl azide **688** (45.8 mg, 0.20 mmol), NHPI ester **524** (74.2 mg, 0.30 mmol) and 4-cyanopyridine **447** (52.1 mg, 0.50 mmol). Purification by flash chromatography (CH_2Cl_2 : Hexane : Et_3N = 30 : 70 : 1), the product was obtained as yellow oil (45.3 mg, 67% yield). ^{1}H NMR (600 MHz, CD_3CN) δ 8.43 (d, *J* = 6.2 Hz, 2H), 7.44 (s, 1H), 7.42 – 7.40 (m, 1H),

7.38 – 7.33 (m, 3H), 7.14 – 7.10 (m, 1H), 2.37 (d, *J* = 14.5 Hz, 1H), 2.34 (d, *J* = 14.5 Hz, 1H), 2.10 (br s, 2H), 0.81 (s, 9H); ^{13}C NMR (151 MHz, CD_3CN) δ 160.2 (2C), 152.9 (2C), 150.5, 149.8, 130.5, 126.7, 122.4, 121.8 (q, $^{1}J_{C\text{-}F}$ = 255.3 Hz), 120.5, 119.7, 61.7, 52.8, 32.6, 32.1 (3C); ^{19}F NMR (565 MHz, CD_3CN) δ -58.5 (s, 3F). HRMS ESI $[M+H]^+$ calculated for ($C_{18}H_{22}F_3N_2O^+$) 339.1679, found 339.1673.

1-(4-(Allyloxy)phenyl)-3,3-dimethyl-1-(pyridine-4-yl)butan-1-amine **564**

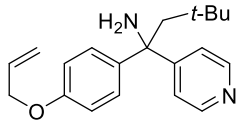

Following **GP14** using vinyl azide **687** (40.2 mg, 0.20 mmol), NHPI ester **524** (74.2 mg, 0.30 mmol) and 4-cyanopyridine **447** (52.1 mg, 0.50 mmol). Purification by flash chromatography (CH_2Cl_2 : Hexane : Et_3N = 30 : 70 : 1), the product was obtained as yellow oil (36.0 mg, 58% yield). ^{1}H NMR (400 MHz, CD_3CN) δ 8.41 (d, *J* = 6.2 Hz, 2H), 7.38 (d, *J* = 6.2 Hz, 2H), 7.32 (d, *J* = 8.9 Hz, 2H), 6.82 (d, *J* = 8.9 Hz, 2H), 6.04 (ddt, *J* = 17.3, 10.6, 5.3 Hz, 1H), 5.37 (dd, *J* = 17.3, 1.7 Hz, 1H), 5.23 (dd, *J* = 10.6, 1.7 Hz, 1H), 4.50 (dt, *J* = 5.3, 1.7 Hz, 2H), 2.35 (d, *J* = 14.4 Hz, 1H), 2.31 (d, *J* = 14.4 Hz, 1H), 2.06 (br s, 2H), 0.81 (s, 9H); ^{13}C NMR (101 MHz, CD_3CN) δ 161.0 (2C), 157.9 (2C), 150.3, 142.7, 134. 8, 128.5 (2C), 122.6, 117.8, 114.9 (2C), 69.4, 61.4, 53.2, 32.6, 32.2 (3C). HRMS ESI $[M+H]^+$ calculated for ($C_{20}H_{27}N_2O^+$) 311.2118, found 311.2114.

(4-(1-Amino-3,3-dimethyl-1-(pyridin-4-yl)butyl)phenyl)methanol **565**

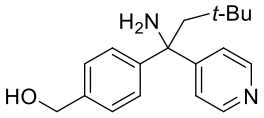

Following **GP14** using corresponding vinyl azide (35.0 mg, 0.20 mmol), NHPI ester **524** (74.2 mg, 0.30 mmol) and 4-cyanopyridine **447** (52.1 mg, 0.50 mmol). Purification by flash chromatography (EtOAc : Hexane : Et_3N = 70 : 30 : 1), the product was obtained as yellow oil (34.8 mg, 61% yield). ^1H NMR (600 MHz, CD_3CN) δ 8.39 (d, *J* = 4.5 Hz, 2H), 7.43 – 7.31 (m, 4H), 7.23 (d, *J* = 8.1 Hz, 2H), 4.52 (s, 2H), 2.48 (br s, 2H), 2.37 (s, 2H), 1.81 (s, 1H), 0.82 (s, 9H); ^{13}C NMR (151 MHz, CD_3CN) δ 160.8 (2C), 150.1, 149.1 (2C), 141.2, 127.4 (2C), 127.3 (2C), 122.7, 64.3, 61.8, 53.0, 32.7, 32.2 (3C). HRMS ESI $[M+H]^+$ calculated for ($C_{18}H_{25}N_2O^+$) 285.1961, found 285.1957.

1-(2-Fluorophenyl)-3,3-dimethyl-1-(pyridine-4-yl)butan-1-amine **566**

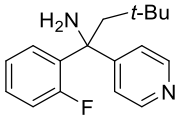

Following **GP14** using corresponding vinyl azide (32.6 mg, 0.20 mmol), NHPI ester **524** (74.2 mg, 0.30 mmol) and 4-cyanopyridine **447** (52.1 mg, 0.50 mmol). Purification by flash chromatography (CH_2Cl_2 : Hexane : Et_3N = 50 : 50 : 1), the product was obtained as colourless oil (41.3 mg, 76% yield). ^1H NMR (400 MHz, $CDCl_3$) δ 8.49 (d, *J* = 6.2 Hz, 2H), 7.82 – 7.76 (m, 1H), 7.31 – 7.27 (m, 1H), 7.24 (d, *J* = 6.2 Hz, 2H), 7.22 (dd, *J* = 7.6, 1.3 Hz, 1H), 6.91 (ddd, *J* = 12.1, 7.6, 1.3 Hz, 1H), 2.55 (d, *J* = 14.3 Hz, 1H), 2.22 (d, *J* = 14.3 Hz, 1H), 1.97 (br s, 2H), 0.82 (s, 9H); ^{13}C NMR (101 MHz, $CDCl_3$) δ 160.7 (d, $^1J_{C\text{-}F}$ = 248.5 Hz), 159.4 (2C), 149.7 (2C), 134.8 (d,

$^{2}J_{C\text{-}F}$ = 11.1 Hz), 129.3 (d, $^{2}J_{C\text{-}F}$ = 9.1 Hz), 127.7 (d, $^{3}J_{C\text{-}F}$ = 4.0 Hz), 124.0 (d, $^{4}J_{C\text{-}F}$ = 3.0 Hz), 120.8, 116.3 (d, $^{2}J_{C\text{-}F}$ = 23.2 Hz), 59.6 (d, $^{3}J_{C\text{-}F}$ = 1.0 Hz), 50.7 (d, $^{4}J_{C\text{-}F}$ = 2.0 Hz), 32.1, 31.5 (3C); ^{19}F NMR (376 MHz, $CDCl_3$) δ -108.9 – -109.0 (m, 1F). HRMS ESI $[M+H]^+$ calculated for ($C_{17}H_{22}FN_2^+$) 273.1762, found 273.1757.

1-(2-Methoxyphenyl)-3,3-dimethyl-1-(pyridine-4-yl)butan-1-amine **567**

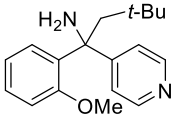

Following **GP14** using corresponding vinyl azide (35.0 mg, 0.20 mmol), NHPI ester **524** (74.2 mg, 0.30 mmol) and 4-cyanopyridine **447** (52.1 mg, 0.50 mmol). Purification by flash chromatography (CH_2Cl_2 : Hexane : Et_3N = 30 : 70 : 1), the product was obtained as colourless oil (23.8 mg, 31% yield). ^{1}H NMR (600 MHz, CD_3CN) δ 8.35 (d, *J* = 5.9 Hz, 2H), 7.79 (d, *J* = 7.8 Hz, 1H), 7.28 – 7.24 (m, 1H), 7.20 (d, *J* = 5.9 Hz, 2H), 7.03 – 6.99 (m, 1H), 6.82 (d, *J* = 8.1 Hz, 1H), 3.36 (s, 3H), 2.58 (d, *J* = 14.0 Hz, 1H), 2.16 (d, *J* = 14.0 Hz, 1H), 2.12 (br s, 2H), 0.76 (s, 9H); ^{13}C NMR (151 MHz, CD_3CN) δ 162.0, 158.2 (2C), 149.9, 137.8 (2C), 129.3, 127.8, 121.9, 121.2, 113.2, 60.6, 55.4, 50.6, 32.6, 31.8 (3C). HRMS ESI $[M+H]^+$ calculated for ($C_{18}H_{25}N_2O^+$) 285.1961, found 285.1958.

1-(Benzo[d][1,3]dioxol-5-yl)-3,3-dimethyl-1-(pyridine-4-yl)butan-1-amine **568**

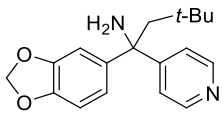

Following **GP14** using corresponding vinyl azide (37.8 mg, 0.20 mmol), NHPI ester **524** (74.2 mg, 0.30 mmol) and 4-cyanopyridine **447** (52.1 mg, 0.50 mmol). Purification by flash chromatography (CH_2Cl_2 : Hexane : Et_3N = 40 : 60 : 1), the product was obtained as colourless oil (32.9 mg, 55% yield). ^{1}H NMR (600 MHz, CD_3CN) δ 8.42 (d, *J* = 5.7 Hz, 2H), 7.37 (d, *J* = 5.7 Hz, 2H), 6.94 – 6.91 (m, 2H), 6.73 (d, *J* = 8.7 Hz, 1H), 5.89 (s, 2H), 2.31 (s, 2H), 2.10 (br s, 2H), 0.82 (s, 9H); ^{13}C NMR (151 MHz, CD_3CN) δ 160.9 (2C), 150.3 (2C), 148.4, 146.8, 144.5, 122.5, 120.5, 108.4, 108.2, 102.2, 61.7, 53.1, 32.6, 32.2 (3C). HRMS ESI $[M+H]^+$ calculated for ($C_{18}H_{23}N_2O_2^+$) 299.1754, found 299.1751.

3,3-Dimethyl-1-(naphthalen-2-yl)-1-(pyridine-4-yl)butan-1-amine **569**

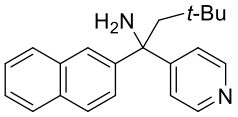

Following **GP14** using corresponding vinyl azide (39.0 mg, 0.20 mmol), NHPI ester **524** (74.2 mg, 0.30 mmol) and 4-cyanopyridine **447** (52.1 mg, 0.50 mmol). Purification by flash chromatography (CH_2Cl_2 : Hexane : Et_3N = 40 : 60 : 1), the product was obtained as colourless oil (39.5 mg, 65% yield). ^{1}H NMR (400 MHz, CD_3CN) δ 8.42 (d, *J* = 6.2 Hz, 2H), 8.10 (d, *J* = 1.6 Hz, 1H), 7.87 (d, *J* = 7.6 Hz, 1H), 7.80 (d, *J* = 8.7 Hz, 1H), 7.72 (d, *J* = 8.7 Hz, 1H), 7.52 – 7.43 (m, 2H), 7.40 (d, *J* = 6.2 Hz, 2H), 7.36 (dd, *J* = 8.7, 2.0 Hz, 1H), 2.51 (d, *J* = 14.4 Hz, 1H), 2.45 (d, *J* = 14.4 Hz, 1H), 2.16 (br s, 2H), 0.83 (s, 9H); ^{13}C NMR (101 MHz, CD_3CN) δ 160.6 (2C), 150.4, 147.7 (2C), 134.0, 132.9, 129.1, 128.4, 128.2, 127.1, 127.0, 126.9, 125.0, 122.7, 62.0, 52.7, 32.7, 32.2 (3C). HRMS ESI $[M+H]^+$ calculated for ($C_{21}H_{25}N_2^+$) 305.2012, found 305.2010.

***1-(Benzo[b]thiophen-5-yl)-3,3-dimethyl-1-(pyridine-4-yl)butan-1-amine* 570**

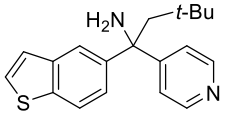

Following **GP14** using vinyl azide **689** (40.3 mg, 0.20 mmol), NHPI ester **524** (74.2 mg, 0.30 mmol) and 4-cyanopyridine **447** (52.1 mg, 0.50 mmol). Purification by flash chromatography (CH_2Cl_2 : Hexane : Et_3N = 30 : 70 : 1), the product was obtained as yellow oil (38.9 mg, 62% yield). ^{1}H NMR (400 MHz, CD_3CN) δ 8.41 (d, *J* = 6.2 Hz, 2H), 8.05 (d, *J* = 1.9 Hz, 1H), 7.78 (d, *J* = 8.6 Hz, 1H), 7.53 (d, *J* = 5.4 Hz, 1H), 7.39 (d, *J* = 6.2 Hz, 2H), 7.35 (d, *J* = 5.4 Hz, 1H), 7.31 (dd, *J* = 8.6, 1.9 Hz, 1H), 2.46 (d, *J* = 14.4 Hz, 1H), 2.42 (d, *J* = 14.4 Hz, 1H), 2.15 (br s, 2H), 0.82 (s, 9H); ^{13}C NMR (101 MHz, CD_3CN) δ 161.0 (2C), 150.3, 146.8 (2C), 140.6, 138.4, 128.1, 125.2, 125.0, 122.8, 122.6, 121.9, 61.9, 53.1, 32.7, 32.2 (3C). HRMS ESI $[M+H]^+$ calculated for ($C_{19}H_{23}N_2S^+$) 311.1576, found 311.1572.

***1-(Dibenzo[b,d]furan-2-yl)-3,3-dimethyl-1-(pyridine-4-yl)butan-1-amine* 571**

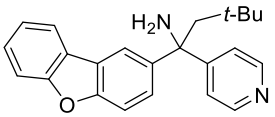

Following **GP14** using vinyl azide **690** (47.1 mg, 0.20 mmol), NHPI ester **524** (74.2 mg, 0.30 mmol) and 4-cyanopyridine **447** (52.1 mg, 0.50 mmol). Purification by flash chromatography (CH_2Cl_2 : Hexane : Et_3N = 30 : 70 : 1), the product was obtained as yellow oil (43.3 mg, 63% yield). ^{1}H NMR (600 MHz, CD_3CN) δ 8.42 (d, *J* = 6.2 Hz, 2H), 8.23 (dd, *J* = 1.7, 0.8 Hz, 1H), 8.02 (d, *J* = 8.2 Hz, 1H), 7.57 (d, *J* = 8.2 Hz, 1H), 7.49 – 7.44 (m, 3H), 7.41 (d, *J* = 6.2 Hz, 2H), 7.37 –

7.33 (m, 1H), 2.47 (d, *J* = 14.2 Hz, 1H), 2.44 (d, *J* = 14.2 Hz, 1H), 2.16 (br s, 2H), 0.81 (s, 9H); ^{13}C NMR (151 MHz, CD_3CN) δ 161.1, 157.4 (2C), 155.5 (2C), 150.3, 145.3, 128.3, 127.6, 125.1, 124.4, 123.9, 122.6, 121.8, 119.6, 112.5, 111.7, 61.9, 53.3, 32.7, 32.2 (3C). HRMS ESI $[M+H]^+$ calculated for ($C_{23}H_{25}N_2O^+$) 345.1961, found 345.1958.

***tert-Butyl 5-(1-amino-3,3-dimethyl-1-(pyridine-4-yl)butyl)-1H-indole-1-carboxylate* 572**

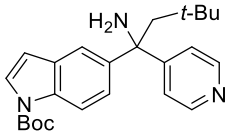

Following **GP14** using vinyl azide **691** (56.9 mg, 0.20 mmol), NHPI ester **524** (74.2 mg, 0.30 mmol) and 4-cyanopyridine **447** (52.1 mg, 0.50 mmol). Purification by flash chromatography (CH_2Cl_2 : Hexane : Et_3N = 40 : 60 : 1), the product was obtained as colourless oil (48.0 mg, 61% yield). ^{1}H NMR (400 MHz, CD_3CN) δ 8.40 (d, *J* = 6.2 Hz, 2H), 7.96 (d, *J* = 8.8 Hz, 1H), 7.74 (d, *J* = 1.9 Hz, 1H), 7.59 (d, *J* = 3.7 Hz, 1H), 7.37 (d, *J* = 6.2 Hz, 2H), 7.27 (dd, *J* = 8.8, 1.9 Hz, 1H), 6.57 (d, *J* = 3.7 Hz, 1H), 2.43 (d, *J* = 14.4 Hz, 1H), 2.38 (d, *J* = 14.4 Hz, 1H), 1.99 (br s, 2H), 1.61 (s, 9H), 0.80 (s, 9H); ^{13}C NMR (101 MHz, CD_3CN) δ 161.3 (2C), 150.6, 150.3 (2C), 144.8, 134.4, 131.2, 127.4, 124.5, 122.6, 119.4, 115.3, 108.3, 84.7, 61.8, 53.2, 32.7, 32.2 (3C), 28.3 (3C). HRMS ESI $[M+H]^+$ calculated for ($C_{24}H_{32}N_3O_2^+$) 394.2489, found. 394.2484.

***3,3-Dimethyl-1-(pyridine-4-yl)-1-(thiophen-3-yl)butan-1-amine* 573**

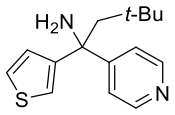

Following **GP14** using vinyl azide **692** (30.2 mg, 0.20 mmol), NHPI ester **524** (74.2 mg, 0.30 mmol) and 4-cyanopyridine **447** (52.1 mg, 0.50 mmol). Purification by flash chromatography (CH_2Cl_2 : Hexane : Et_3N = 50 : 50 : 1), the product was obtained as yellow oil (30.2 mg, 58% yield). ^{1}H NMR (600 MHz, CD_3CN) δ 8.43 (d, *J* = 6.1 Hz, 2H), 7.44 (d, *J* = 6.1 Hz, 2H), 7.27 (dd, *J* = 5.1, 3.0 Hz, 1H), 7.24 – 7.22 (m, 1H), 6.94 (dd, *J* = 5.1, 1.1 Hz, 1H), 2.35 (d, *J* = 14.5 Hz, 1H), 2.27 (d, *J* = 14.5 Hz, 1H), 2.04 (br s, 2H), 0.83 (s, 9H); ^{13}C NMR (151 MHz, CD_3CN) δ 159.2 (2C), 153.2 (2C), 150.3, 128.1, 126.6, 122.5, 120.7, 60. 8, 53.8, 32.7, 32.1 (3C). HRMS ESI $[M+H]^+$ calculated for ($C_{15}H_{21}N_2S^+$) 261.1420, found 261.1418.

1-([1,1'-Biphenyl]-4-yl)-1-(2-(tert-butyl)pyridine-4-yl)-3,3-dimethylbutan-1-amine **574**

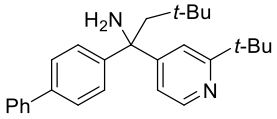

Following **GP14** using vinyl azide **523** (44.3 mg, 0.20 mmol), NHPI ester **524** (74.2 mg, 0.30 mmol) and 2-(*tert*-butyl)isonicotinonitrile (80.1 mg, 0.50 mmol), $Ir(ppy)_2(bpy)PF_6$ was used as photocatalyst. Purification by flash chromatography (CH_2Cl_2 : Hexane : Et_3N = 15 : 85 : 1), the product was obtained as colourless oil (54.0 mg, 70% yield). ^{1}H NMR (400 MHz, CD_3CN) δ 8.34 (d, *J* = 5.3 Hz, 1H), 7.60 (d, *J* = 7.1 Hz, 2H), 7.58 – 7.56 (m, 1H), 7.56 – 7.48 (m, 4H), 7.45 – 7.39 (m, 2H), 7.36 – 7.30 (m, 1H), 7.19 (dd, *J* = 5.3, 1.8 Hz, 1H), 2.43 (d, *J* = 14.4 Hz, 1H), 2.38 (d, *J* = 14.4 Hz, 1H), 2.06 (br s, 2H), 1.31 (s, 9H), 0.85 (s, 9H); ^{13}C NMR (101 MHz, CD_3CN) δ 169.6, 160.3, 150.3, 148.9, 141.3, 139.5, 129.8 (2C), 128.3, 127.8 (2C), 127.7 (2C), 127.3 (2C), 120.1,

117.9, 62.0, 53.2, 38.2, 32.7, 32.3 (3C), 30.5 (3C). HRMS ESI $[M+H]^+$ calculated for ($C_{27}H_{35}N_2^+$) 387.2795, found 387.2788.

1-([1,1'-Biphenyl]-4-yl)-1-(2-cyclobutylpyridin-4-yl)-3,3-dimethylbutan-1-amine **575**

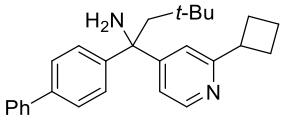

Following **GP14** using vinyl azide **523** (44.3 mg, 0.20 mmol), NHPI ester **524** (74.2 mg, 0.30 mmol) and 2-cyclobutylisonicotinonitrile (79.1 mg, 0.50 mmol), $Ir(ppy)_2(bpy)PF_6$ was used as photocatalyst. Purification by flash chromatography (CH_2Cl_2 : Hexane : Et_3N = 15 : 85 : 1), the product was obtained as colourless oil (57.3 mg, 74% yield). ^{1}H NMR (400 MHz, CD_3CN) δ 8.36 (d, *J* = 5.3 Hz, 1H), 7.60 (d, *J* = 7.2 Hz, 2H), 7.56 – 7.47 (m, 4H), 7.44 – 7.39 (m, 2H), 7.36 – 7.30 (m, 2H), 7.20 (dd, *J* = 5.3, 1.9 Hz, 1H), 3.64 – 3.56 (m, 1H), 2.39 (s, 2H), 2.32 – 2.18 (m, 4H), 2.08 (br s, 2H), 2.05 – 1.98 (m, 1H), 1.88 – 1.79 (m, 1H), 0.84 (s, 9H); ^{13}C NMR (101 MHz, CD_3CN) δ 165.0, 160.7, 150.0, 149.7, 141.3, 139.5, 129.8 (2C), 128.3, 127.9 (2C), 127.7 (2C), 127.3 (2C), 120.2, 119.8, 61.8, 53.1, 43.1, 32.7, 32.3 (3C), 29.2, 29.1, 18.8. HRMS ESI $[M+H]^+$ calculated for ($C_{27}H_{33}N_2^+$) 385.2638, found 385.2633.

1-([1,1'-Biphenyl]-4-yl)-1-(2-(cyclopent-3-en-1-yl)pyridine-4-yl)-3,3-dimethylbutan-1-amine **576**

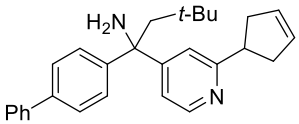

Following **GP14** using vinyl azide **523** (44.3 mg, 0.20 mmol), NHPI ester **524** (74.2 mg, 0.30 mmol) and 2-(cyclopent-3-en-1-yl)isonicotinonitrile (85.1 mg, 0.50 mmol), $Ir(ppy)_2(bpy)PF_6$ was used as photocatalyst. Purification by flash chromatography (CH_2Cl_2 : Hexane : Et_3N = 15 : 85 : 1), the product was obtained as colourless oil (57.8 mg, 73% yield). ^1H NMR (400 MHz, CD_3CN) δ 8.33 (d, *J* = 5.3 Hz, 1H), 7.60 (d, *J* = 7.2 Hz, 2H), 7.56 – 7.48 (m, 4H), 7.45 – 7.38 (m, 3H), 7.35 – 7.30 (m, 1H), 7.20 (dd, *J* = 5.3, 1.9 Hz, 1H), 5.75 – 5.69 (m, 2H), 3.59 (tt, *J* = 9.3, 7.3 Hz, 1H), 2.78 – 2.66 (m, 2H), 2.63 – 2.49 (m, 2H), 2.40 (d, *J* = 14.4 Hz, 1H), 2.36 (d, *J* = 14.4 Hz, 1H), 2.02 (br s, 2H), 0.84 (s, 9H); ^{13}C NMR (101 MHz, CD_3CN) δ 166.2, 160.7, 150.1, 149.5, 141.3, 139.5, 130.44, 130.40, 129.8 (2C), 128.3, 127.9 (2C), 127.7 (2C), 127.3 (2C), 120.6, 120.3, 61.8, 53.1, 46.1, 40.64, 40.57, 32.7, 32.3 (3C). HRMS ESI $[M+H]^+$ calculated for ($C_{28}H_{33}N_2^+$) 397.2638, found 397.2634.

***1-([1,1'-Biphenyl]-4-yl)-1-(2,6-dimethylpyridin-4-yl)-3,3-dimethylbutan-1-amine* 577**

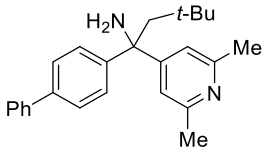

Following **GP14** using vinyl azide **523** (44.3 mg, 0.20 mmol), NHPI ester **524** (74.2 mg, 0.30 mmol) and 2,6-dimethylisonicotinonitrile (66.1 mg, 0.50 mmol), $Ir(ppy)_2(bpy)PF_6$ was used as photocatalyst. Purification by flash chromatography (CH_2Cl_2 : Hexane : Et_3N = 50 : 50 : 1), the product was obtained as yellow oil (48.8 mg, 68% yield). ^1H NMR (600 MHz, CD_3CN) δ 7.60 (d, *J* = 7.4 Hz, 2H), 7.53 (d, *J* = 8.5 Hz, 2H), 7.50 (d, *J* = 8.5 Hz, 2H), 7.44 – 7.40 (m, 2H), 7.35 – 7.31

(m, 1H), 7.12 (s, 2H), 2.38 (s, 6H), 2.37 (s, 2H), 1.98 (br s, 2H), 0.85 (s, 9H); ^{13}C NMR (151 MHz, CD_3CN) δ 161.3 (2C), 158.1 (2C), 150.0, 141.3, 139.5, 129.8 (2C), 128.3, 127. 9 (2C), 127.7 (2C), 127.3 (2C), 118.9, 61.6, 53.0, 32.7, 32.3 (3C), 24.6 (2C). HRMS ESI $[M+H]^+$ calculated for ($C_{25}H_{31}N_2^+$) 359.2482, found 359.2478.

1-([1,1'-Biphenyl]-4-yl)-1-(5-fluoropyridin-2-yl)-3,3-dimethylbutan-1-amine **578**

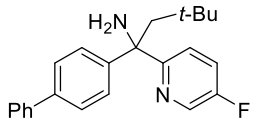

Following **GP14** using vinyl azide **523** (44.3 mg, 0.20 mmol), NHPI ester **524** (74.2 mg, 0.30 mmol) and 5-fluoropicolinonitrile (61.1 mg, 0.50 mmol), $Ir(ppy)_2(bpy)PF_6$ was used as photocatalyst. Purification by flash chromatography (CH_2Cl_2 : Hexane : Et_3N = 10 : 90 : 1), the product was obtained as yellow oil (31.6 mg, 31% yield). ^{1}H NMR (600 MHz, CD_3CN) δ 8.36 (d, *J* = 3.0 Hz, 1H), 7.67 (dd, *J* = 8.9, 4.4 Hz, 1H), 7.60 (d, *J* = 8.2 Hz, 2H), 7.57 (d, *J* = 8.2 Hz, 2H), 7.52 (d, *J* = 8.4 Hz, 2H), 7.45 – 7.40 (m, 3H), 7.35 – 7.31 (m, 1H), 2.58 (d, *J* = 14.4 Hz, 1H), 2.39 (d, *J* = 14.4 Hz, 1H), 2.20 (br s, 2H), 0.84 (s, 9H); ^{13}C NMR (151 MHz, CD_3CN) δ 165.3 (d, $^4J_{C\text{-}F}$ = 3.4 Hz), 159.4 (d, $^1J_{C\text{-}F}$ = 252.5 Hz), 150.08, 141.43, 139.36, 136.72 (d, $^2J_{C\text{-}F}$ = 23.4 Hz), 129.83 (2C), 128.24, 127.89 (2C), 127.72 (2C), 127.20 (2C), 123.9 (d, $^2J_{C\text{-}F}$ = 18.2 Hz), 122.63 (d, $^3J_{C\text{-}F}$ = 4.0 Hz), 63.5, 53.4, 32.6, 32.2 (3C); ^{19}F NMR (565 MHz, CD_3CN) δ -133.3 (dd, *J* = 8.7, 4.4 Hz, 1F). HRMS ESI $[M+Na]^+$ calculated for ($C_{23}H_{25}FN_2Na^+$) 371.1894, found 371.1891.

1-([1,1'-Biphenyl]-4-yl)-3,3-dimethyl-1-(pyridine342-2-yl)butan-1-amine **579**

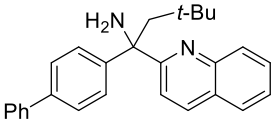

Following **GP14** using vinyl azide **523** (44.3 mg, 0.20 mmol), NHPI ester **524** (74.2 mg, 0.30 mmol) and quinoline-2-carbonitrile (77.1 mg, 0.50 mmol), $Ir(ppy)_2(bpy)PF_6$ was used as photocatalyst. Purification by flash chromatography (CH_2Cl_2 : Hexane : Et_3N = 5 : 95 : 1), the product was obtained as colourless oil (40.3 mg, 53% yield). ^1H NMR (600 MHz, CD_3CN) δ 8.10 (d, *J* = 8.5 Hz, 1H), 8.01 (d, *J* = 8.5 Hz, 1H), 7.82 (d, *J* = 8.0 Hz, 1H), 7.74 – 7.68 (m, 1H), 7.62 – 7.58 (m, 3H), 7.58 – 7.55 (m, 2H), 7.54 – 7.49 (m, 3H), 7.42 – 7.38 (m, 2H), 7.33 – 7.29 (m, 1H), 2.74 (d, *J* = 14.5 Hz, 1H), 2.53 (d, *J* = 14.5 Hz, 1H), 2.34 (br s, 2H), 0.85 (s, 9H); ^{13}C NMR (151 MHz, CD_3CN) δ 168.6, 150.2, 147.5, 141.4, 139.4, 136.9, 130.4, 129.9, 129.8 (2C), 128.5, 128.2, 128.0 (2C), 127.7 (2C), 127.5, 127.3 (2C), 127.2, 120.9, 64.2, 52.9, 32.6, 32.2 (3C). HRMS ESI $[M+H]^+$ calculated for ($C_{27}H_{29}N_2^+$) 381.2325, found 381.2320.

1-([1,1'-Biphenyl]-4-yl)-3,3-dimethyl-1-(pyrimidin-2-yl)butan-1-amine **580**

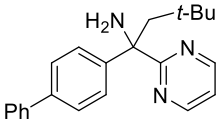

Following **GP14** using vinyl azide **523** (44.3 mg, 0.20 mmol), NHPI ester **524** (74.2 mg, 0.30 mmol) and pyrimidine-2-carbonitrile (52.6 mg, 0.50 mmol), $Ir(ppy)_2(bpy)PF_6$ was used as photocatalyst. Purification by flash chromatography (CH_2Cl_2 : Hexane : Et_3N = 5 : 95 : 1), the product was obtained as yellow solid (25.2 mg, 38% yield). ^1H NMR (600 MHz, $CDCl_3$) δ 8.71 (d, *J* = 4.8 Hz, 2H), 7.67 (d, *J* = 8.4 Hz, 2H), 7.56 (d, *J* = 7.4 Hz, 2H), 7.51 (d, *J* = 8.4 Hz, 2H), 7.42

– 7.37 (m, 2H), 7.33 – 7.28 (m, 1H), 7.09 – 7.06 (m, 1H), 2.73 (d, *J* = 14.6 Hz, 1H), 2.70 (br s, 2H), 2.54 (d, *J* = 14.6 Hz, 1H), 0.88 (s, 9H); ^{13}C NMR (151 MHz, $CDCl_3$) δ 175.1 (2C), 156.7, 147.4, 140.9, 139.2, 128.8 (2C), 127.2, 127.1 (2C), 126.8 (2C), 126.6 (2C), 118.5, 64.2, 52.5, 32.0, 31.8 (3C). HRMS ESI $[M+H]^+$ calculated for ($C_{22}H_{26}N_3^+$) 332.2121, found 332.2116.

1-([1,1'-Biphenyl]-4-yl)-1-(pyridin-4-yl)nonadecan-1-amine **581**

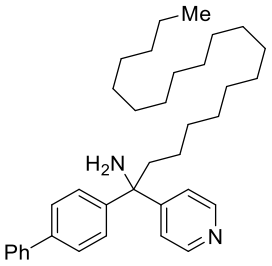

Following **GP14** using vinyl azide **523** (44.3 mg, 0.20 mmol), corresponding NHPI ester (128.9 mg, 0.30 mmol) and 4-cyanopyridine **447** (52.2 mg, 0.50 mmol). Purification by flash chromatography (CH_2Cl_2 : Hexane : Et_3N = 40 : 60 : 1), the product was obtained as a white solid (72.7 mg, 71% yield). ^{1}H NMR (400 MHz, $CDCl_3$) δ 8.53 (d, *J* = 5.1 Hz, 2H), 7.58 (d, *J* = 8.0 Hz, 2H), 7.54 (d, *J* = 8.0 Hz, 2H), 7.46 – 7.38 (m, 4H), 7.37 – 7.30 (m, 3H), 2.25 – 2.17 (m, 2H), 1.83 (br s, 2H), 1.35 – 1.14 (m, 32H), 0.88 (t, *J* = 6.5 Hz, 3H); ^{13}C NMR (101 MHz, $CDCl_3$) δ 157.7 (2C), 149.9, 148.5 (2C), 146.6, 140.6, 139.7, 128.9 (2C), 127.5, 127.1 (2C), 127.0 (2C), 121.9 (2C), 60.7, 42.2, 32.1, 30.2, 29.9 – 29.8 (m, 7C), 29.79, 29.75, 29.7, 29.6, 29.5, 24.1, 22.8, 14.3. HRMS ESI $[M+H]^+$ calculated for ($C_{36}H_{53}N_2^+$) 513.4203, found 513.4210.

(10Z,13Z)-1-([1,1'-Biphenyl]-4-yl)-1-(pyridine-4-yl)nonadeca-10,13-dien-1-amine **582**

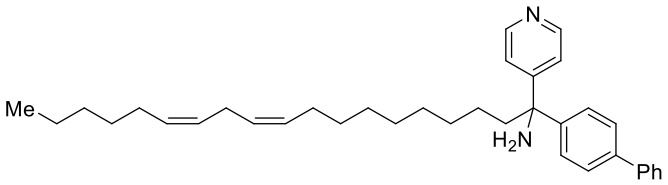

Following **GP14** using vinyl azide **523** (44.3 mg, 0.20 mmol), corresponding NHPI ester (127.7 mg, 0.30 mmol) and 4-cyanopyridine **447** (52.2 mg, 0.50 mmol). Purification by flash chromatography (CH_2Cl_2 : Hexane : Et_3N = 40 : 60 : 1), the product was obtained as a white solid (66.1 mg, 65% yield). ^{1}H NMR (600 MHz, $CDCl_3$) δ 8.53 (d, *J* = 5.5 Hz, 2H), 7.58 (d, *J* = 8.2 Hz, 2H), 7.54 (d, *J* = 8.2 Hz, 2H), 7.45 – 7.39 (m, 4H), 7.35 – 7.30 (m, 3H), 5.42 – 5.30 (m, 4H), 2.78 (t, *J* = 6.7 Hz, 2H), 2.26 – 2.17 (m, 2H), 2.08 – 2.02 (m, 4H), 1.93 (br s, 2H), 1.39 – 1.25 (m, 18H), 1.19 – 1.13 (m, 1H), 0.89 (t, *J* = 6.7 Hz, 3H); ^{13}C NMR (151 MHz, $CDCl_3$) δ 157.6 (2C), 149.8, 146.4 (2C), 140.6, 139.7, 130.3, 130.2, 128.9 (2C), 128.1, 128.0, 127.4, 127.1 (2C), 127.08 (2C), 126.9 (2C), 121.8, 60.7, 42.1, 31.6, 30.1, 29.7, 29.58, 29.55, 29.4, 29.3, 27.30, 27.29, 25.7, 24.0, 22.7, 14.2. HRMS ESI $[M+H]^+$ calculated for ($C_{36}H_{50}N_2^+$) 509.3890, found 509.3894.

***1-([1,1'-Biphenyl]-4-yl)-6-(2,5-dimethylphenoxy)-3,3-dimethyl-1-(pyridine-4-yl)hexan-1-amine* 583**

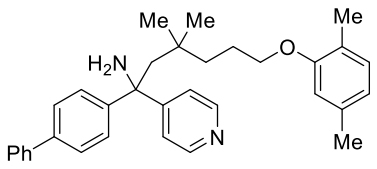

Following **GP14** using vinyl azide **523** (44.3 mg, 0.20 mmol), corresponding NHPI ester (118.6 mg, 0.30 mmol) and 4-cyanopyridine **447** (52.2 mg, 0.50 mmol). Purification by flash

chromatography (CH_2Cl_2 : Hexane : Et_3N = 50 : 50 : 1), the product was obtained as colourless oil (70.0 mg, 73% yield). ^{1}H NMR (600 MHz, DMSO-d_6) δ 8.44 (d, *J* = 6.2 Hz, 2H), 7.61 (d, *J* = 7.3 Hz, 2H), 7.56 (d, *J* = 8.6 Hz, 2H), 7.53 (d, *J* = 8.6 Hz, 2H), 7.48 (d, *J* = 6.2 Hz, 2H), 7.45 – 7.40 (m, 2H), 7.35 – 7.31 (m, 1H), 6.98 (d, *J* = 7.5 Hz, 1H), 6.65 (s, 1H), 6.62 (d, *J* = 7.5 Hz, 1H), 3.81 – 3.74 (m, 2H), 2.39 (br s, 2H), 2.38 (d, *J* = 14.5 Hz, 1H), 2.35 (d, *J* = 14.5 Hz, 1H), 2.23 (s, 3H), 2.10 (s, 3H), 1.72 – 1.64 (m, 2H), 1.36 – 1.29 (m, 2H), 0.81 (s, 3H), 0.79 (s, 3H); ^{13}C NMR (151 MHz, DMSO-d_6) δ 159.7 (2C), 156.6, 149.1, 148.7 (2C), 139.8, 137.7, 136.0, 130.0, 128.8 (2C), 127.2, 126.9 (2C), 126.5 (2C), 126.0 (2C), 122.5, 121.6, 120.4, 112.0, 68.0, 60.5, 49.4, 40.6, 34.0, 29.0, 28.9, 23.8, 21.0, 15.6. HRMS ESI $[M+H]^+$ calculated for ($C_{33}H_{39}N_2O^+$) 479.3057, found 479.3060.

***tert-Butyl ((1-(3-([1,1'-biphenyl]-4-yl)-3-amino-3-(pyridine-4-yl)propyl)cyclohexyl)methyl) carbamate* 584**

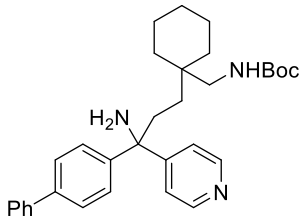

Following **GP14** using vinyl azide **523** (44.3 mg, 0.20 mmol), corresponding NHPI ester (124.9 mg, 0.30 mmol) and 4-cyanopyridine **447** (52.2 mg, 0.50 mmol). Purification by flash chromatography (CH_2Cl_2 : Hexane : Et_3N = 50 : 50 : 1), the product was obtained as yellow oil (55.1 mg, 55% yield). ^{1}H NMR (400 MHz, $CDCl_3$) δ 8.53 (d, *J* = 5.8 Hz, 2H), 7.57 (d, *J* = 7.2 Hz, 2H), 7.54 (d, *J* = 8.4 Hz, 2H), 7.45 – 7.38 (m, 4H), 7.36 – 7.29 (m, 3H), 4.53 (t, *J* = 6.6 Hz, 1H),

3.05 (d, *J* = 6.6 Hz, 2H), 2.27 – 2.14 (m, 2H), 1.91 (br s, 2H), 1.42 (s, 9H), 1.39 – 1.05 (m, 12H); ^{13}C NMR (101 MHz, $CDCl_3$) δ 157.7 (2C), 156.4, 149.9 (2C), 146.6, 140.6, 139.7, 128.9 (2C), 127.4, 127.2 (2C), 127.1 (2C), 126.9 (2C), 121.8, 79.2, 60.5, 46.7, 45.9, 36.3, 34.8, 33.9, 33.8, 28.6 (3C), 28.2, 26.2, 21.5. HRMS ESI $[M+H]^+$ calculated for ($C_{32}H_{42}N_3O_2^+$) 500.3272, found 500.3275.

4-(6-([1,1'-Biphenyl]-4-yl)-6-amino-6-(pyridin-4-yl)hexyl)tetrahydro-1H-thieno[3,4-d]imidazol-2(3H)-one **585**

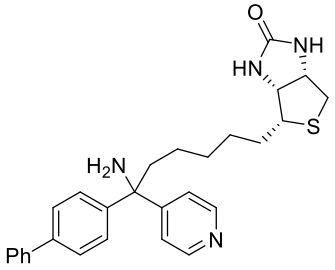

Following **GP14** using vinyl azide **523** (44.3 mg, 0.20 mmol), corresponding NHPI ester (116.7 mg, 0.30 mmol) and 4-cyanopyridine **447** (52.2 mg, 0.50 mmol). Purification by flash chromatography (EtOAc : MeOH : Et_3N = 95 : 5 : 1 to 85 : 15 : 1), the product was obtained as a white solid (57.6 mg, 61% yield), dr = 1:1. ^{1}H NMR (400 MHz, $CDCl_3$) δ 8.49 (d, *J* = 6.0 Hz, 2H), 7.54 (d, *J* = 7.4 Hz, 2H), 7.51 (d, *J* = 8.4 Hz, 2H), 7.43 – 7.34 (m, 4H), 7.33 – 7.27 (m, 3H), 6.26 (d, *J* = 5.7 Hz, 1H), 6.02 (s, 1H), 4.42 – 4.31 (m, 1H), 4.24 – 4.15 (m, 1H), 3.45 – 2.85 (m, 4H), 2.80 (dd, *J* = 12.7, 4.9 Hz, 1H), 2.64 (d, *J* = 12.7 Hz, 1H), 2.27 – 2.10 (m, 2H), 1.71 – 1.47 (m, 2H), 1.43 – 1.05 (m, 5H); ^{13}C NMR (101 MHz, $CDCl_3$) δ 164.1, 156.9, 149.8, 145.7, 145.6, 140.4, 139.72, 139.69, 128.8, 127.4, 127.07, 127.05, 126.99, 126.95, 126.94, 121.8, 62.1, 60.98, 60.95,

60.1, 55.8, 45.9, 41.58, 41.55, 40.6, 29.9, 28.8, 28.5, 23.6, 8.8. HRMS ESI $[M+H]^+$ calculated for ($C_{28}H_{33}N_4OS^+$) 473.2370, found 473.2372.

6-([1,1'-Biphenyl]-4-yl)-6-amino-6-(pyridine-4-yl)hexan-2-yl)-10,13-dimethyldodecahydro-3H-cyclopenta[a]phenanthrene-3,7,12(2H,4H)-trione **586**

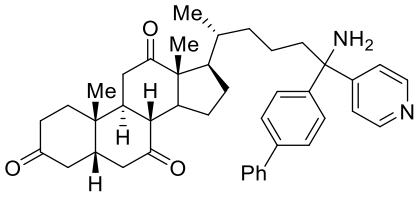

Following **GP14** using vinyl azide **523** (44.3 mg, 0.20 mmol), corresponding NHPI ester (164.3 mg, 0.30 mmol) and 4-cyanopyridine **447** (52.2 mg, 0.50 mmol). Purification by flash chromatography (CH_2Cl_2 : Et_3N = 100 : 1), the product was obtained as a yellow solid (89.5 mg, 71% yield), dr = 1:1. ^{1}H NMR (600 MHz, CD_3CN) δ 8.47 (d, *J* = 5.5 Hz, 2H), 7.66 – 7.61 (m, 2H), 7.61 – 7.56 (m, 2H), 7.53 – 7.48 (m, 2H), 7.47 – 7.42 (m, 2H), 7.42 – 7.39 (m, 2H), 7.38 – 7.33 (m, 1H), 3.01 (t, *J* = 11.9 Hz, 1H), 2.94 (dd, *J* = 12.5, 5.6 Hz, 1H), 2.85 (t, *J* = 14.4 Hz, 1H), 2.45 – 2.37 (m, 1H), 2.33 – 2.10 (m, 8H), 2.09 – 2.02 (m, 3H), 2.01 – 1.99 (m, 1H), 1.95 – 1.89 (m, 3H), 1.88 – 1.85 (m, 1H), 1.77 – 1.70 (m, 1H), 1.60 – 1.52 (m, 1H), 1.51 – 1.45 (m, 1H), 1.39 – 1.24 (m, 6H), 1.19 – 1.08 (m, 2H), 1.03 (d, *J* = 4.0 Hz, 3H), 0.75 (d, *J* = 6.7 Hz, 3H); ^{13}C NMR (151 MHz, CD_3CN) δ 213.2, 210.4, 210.2, 159.1, 159.0, 150.48, 150.46, 148.3, 148.2, 141.2, 139.73, 139.71, 129.9, 128.3, 128.0, 127.7, 127.5, 122.6, 61.3, 57.7, 52.8, 49.5, 47.4, 46.79, 46.77, 45.9, 45.6, 43.4, 42.9, 39.4, 37.2, 36.8, 36.7, 36.65, 36.61, 35.7, 28.6, 25.8, 21.9, 21.52, 21.47, 19.6, 12.2. HRMS ESI $[M+H]^+$ calculated for ($C_{42}H_{51}N_2O_3^+$) 631.3894, found 631.3900.

1-([1,1'-Biphenyl]-4-yl)-3-(2-bromophenyl)-1-(pyridine-4-yl)propan-1-amine **587**

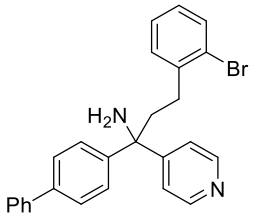

Following **GP14** using vinyl azide **523** (44.3 mg, 0.20 mmol), corresponding NHPI ester (108.0 mg, 0.30 mmol) and 4-cyanopyridine **447** (52.2 mg, 0.50 mmol). Purification by flash chromatography (CH_2Cl_2 : Hexane : Et_3N = 40 : 60 : 1), the product was obtained as a yellow solid (54.8 mg, 62% yield). ^{1}H NMR (400 MHz, CD_3CN) δ 8.47 (d, *J* = 6.1 Hz, 2H), 7.61 (d, *J* = 7.4 Hz, 2H), 7.58 (d, *J* = 8.5 Hz, 2H), 7.55 – 7.49 (m, 3H), 7.46 – 7.40 (m, 4H), 7.37 – 7.31 (m, 1H), 7.30 – 7.23 (m, 2H), 7.13 – 7.05 (m, 1H), 2.72 – 2.56 (m, 2H), 2.55 – 2.41 (m, 2H), 2.17 (br s, 2H); ^{13}C NMR (151 MHz, CD_3CN) δ 158.5 (2C), 150.6, 147.8 (2C), 142.7, 141.3, 140.0, 133.6, 131.7, 129.9, 128.90 (2C), 128.85, 128.4, 128.0 (2C), 127.8 (2C), 127.7 (2C), 124.9, 122.7, 61.3, 42.7, 31.7. HRMS ESI $[M+H]^+$ calculated for ($C_{26}H_{24}BrN_2^+$) 443.1117, found 443.1120.

1-([1,1'-Biphenyl]-4-yl)-3-(2-bromo-4-fluorophenyl)-1-(pyridine-4-yl)propan-1-amine **588**

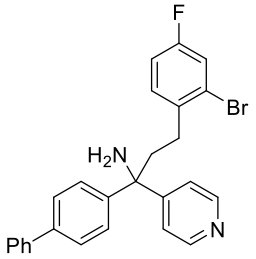

Following **GP14** using vinyl azide **523** (44.3 mg, 0.20 mmol), corresponding NHPI ester (113.4 mg, 0.30 mmol) and 4-cyanopyridine **447** (52.2 mg, 0.50 mmol). Purification by flash

chromatography (CH_2Cl_2 : Hexane : Et_3N = 40 : 60 : 1), the product was obtained as a yellow solid (58.9 mg, 64% yield). ^1H NMR (400 MHz, $CDCl_3$) δ 8.58 (d, *J* = 5.0 Hz, 2H), 7.61 – 7.53 (m, 4H), 7.47 – 7.41 (m, 4H), 7.39 (d, *J* = 5.0 Hz, 2H), 7.37 – 7.31 (m, 1H), 7.29 – 7.24 (m, 1H), 7.13 – 7.07 (m, 1H), 6.98 – 6.90 (m, 1H), 2.74 – 2.64 (m, 1H), 2.63 – 2.54 (m, 1H), 2.53 – 2.40 (m, 2H), 1.96 (br s, 2H); ^{13}C NMR (151 MHz, $CDCl_3$) δ 161.0 (d, $^1J_{C\text{-}F}$ = 249.2 Hz), 157.2 (2C), 150.0, 146.0 (2C), 140.5, 140.0, 137.3 (d, $^4J_{C\text{-}F}$ = 3.0 Hz), 131.2 (d, $^3J_{C\text{-}F}$ = 9.1 Hz), 128.9 (2C), 127.6, 127.3 (2C), 127.1 (2C), 126.9 (2C), 124.1 (d, $^3J_{C\text{-}F}$ = 9.1 Hz), 121.9, 120.2 (d, $^2J_{C\text{-}F}$ = 24.2 Hz), 114.9 (d, $^2J_{C\text{-}F}$ = 21.1 Hz), 60.6, 42.4, 30.5; ^{19}F NMR (377 MHz, $CDCl_3$) δ -114.68 – -114.85 (m, 1F). HRMS ESI $[M+H]^+$ calculated for ($C_{26}H_{23}BrFN_2^+$) 461.1023, found 461.1020.

1-([1,1'-Biphenyl]-4-yl)-3-(2-bromo-5-chlorophenyl)-1-(pyridine-4-yl)propan-1-amine **589**

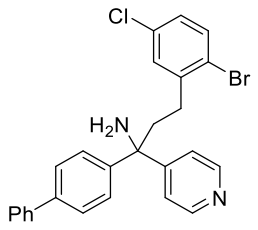

Following **GP14** using vinyl azide **523** (44.3 mg, 0.20 mmol), corresponding NHPI ester (118.4 mg, 0.30 mmol) and 4-cyanopyridine **447** (52.2 mg, 0.50 mmol). Purification by flash chromatography (CH_2Cl_2 : Hexane : Et_3N = 50 : 50 : 1), the product was obtained as a white solid (59.0 mg, 62% yield). ^1H NMR (600 MHz, $CDCl_3$) δ 8.57 (d, *J* = 5.7 Hz, 2H), 7.58 (d, *J* = 7.6 Hz, 2H), 7.56 (d, *J* = 8.4 Hz, 2H), 7.46 – 7.41 (m, 5H), 7.38 (d, *J* = 5.7 Hz, 2H), 7.36 – 7.32 (m, 1H), 7.14 (d, *J* = 2.3 Hz, 1H), 7.04 (dd, *J* = 8.4, 2.3 Hz, 1H), 2.72 – 2.64 (m, 1H), 2.61 – 2.55 (m,

1H), 2.52 – 2.45 (m, 2H), 1.94 (br s, 2H); ^{13}C NMR (151 MHz, $CDCl_3$) δ 157.1 (2C), 150.0, 145.9 (2C), 143.2, 140.5, 140.0, 134.0, 133.5, 130.4, 128.9 (2C), 128.0, 127.5, 127.3 (2C), 127.1 (2C), 126.9 (2C), 122.2, 121.8, 60.6, 42.0, 31.2. HRMS ESI $[M+H]^+$ calculated for ($C_{26}H_{23}BrClN_2^+$) 477.0728, found 477.0724.

3-(2-Bromophenyl)-1-phenyl-1-(pyridine-4-yl)propan-1-amine **590**

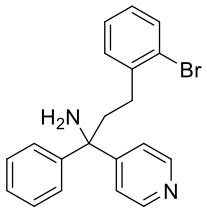

Following **GP14** using corresponding vinyl azide (29.0 mg, 0.20 mmol), corresponding NHPI ester (108.0 mg, 0.30 mmol) and 4-cyanopyridine **447** (52.2 mg, 0.50 mmol). Purification by flash chromatography (CH_2Cl_2 : Hexane : Et_3N = 50 : 50 : 1), the product was obtained as yellow oil (35.1 mg, 48% yield). ^{1}H NMR (400 MHz, CD_3CN) δ 8.46 (d, *J* = 6.2 Hz, 2H), 7.52 (d, *J* = 8.3 Hz, 1H), 7.45 (d, *J* = 8.0 Hz, 2H), 7.39 (d, *J* = 6.2 Hz, 2H), 7.35 – 7.29 (m, 2H), 7.28 – 7.19 (m, 3H), 7.12 – 7.06 (m, 1H), 2.68 – 2.53 (m, 2H), 2.51 – 2.40 (m, 2H), 2.14 (br s, 2H); ^{13}C NMR (101 MHz, CD_3CN) δ 158.7 (2C), 150.5, 148.5 (2C), 142.7, 133.6, 131.7, 129.2 (2C), 128.9, 128.8, 127.6, 127.4 (2C), 124.8, 122.7, 61.4, 42.7, 31.7. HRMS ESI $[M+H]^+$ calculated for ($C_{20}H_{20}BrN_2^+$) 367.0804, found 367.0800.

3-(2-Bromophenyl)-1-(pyridine-4-yl)-1-(3-(trifluoromethoxy)phenyl)propan-1-amine **591**

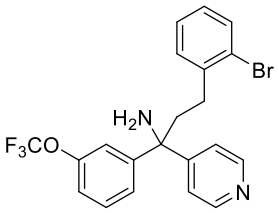

Following **GP14** using corresponding vinyl azide (45.8 mg, 0.20 mmol), corresponding NHPI ester (108.0 mg, 0.30 mmol) and 4-cyanopyridine **447** (52.2 mg, 0.50 mmol). Purification by flash chromatography (CH_2Cl_2 : Hexane : Et_3N = 50 : 50 : 1), the product was obtained as yellow oil (45.0 mg, 50% yield). ^{1}H NMR (400 MHz, CD_3CN) δ 8.48 (d, *J* = 6.2 Hz, 2H), 7.54 – 7.50 (m, 1H), 7.45 – 7.37 (m, 5H), 7.30 – 7.23 (m, 2H), 7.17 (d, *J* = 7.2 Hz, 1H), 7.12 – 7.06 (m, 1H), 2.64 – 2.57 (m, 2H), 2.48 – 2.42 (m, 2H), 2.18 (br s, 2H); ^{13}C NMR (101 MHz, CD_3CN) δ 157. 9 (2C), 151.3, 150.7, 145.0, 142.5 (2C), 133.6, 131.7, 130.9, 129.0, 128.9, 126.6, 124.8, 122.5, 121.5 (q, $^1J_{C\text{-}F}$ = 256.5 Hz) 120.4, 120.1, 61.4, 42.5, 31.6; ^{19}F NMR (377 MHz, CD_3CN) δ -58.42 (s, 3F). HRMS ESI $[M+H]^+$ calculated for ($C_{21}H_{19}BrF_3N_2O^+$) 451.0627, found 451.0623.

1-([1,1'-Biphenyl]-4-yl)-3-(2-bromophenyl)-1-(2-cyclobutylpyridin-4-yl)propan-1-amine **592**

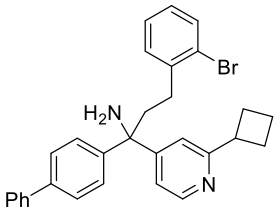

Following **GP14** using vinyl azide **523** (44.3 mg, 0.20 mmol), corresponding NHPI ester (108.0 mg, 0.30 mmol) and 2-cyclobutylisonicotinonitrile (79.1 mg, 0.50 mmol). Purification by flash chromatography (CH_2Cl_2 : Hexane : Et_3N = 30 : 70 : 1), the product was obtained as yellow oil (62.5 mg, 63% yield). ^{1}H NMR (600 MHz, CD_3CN) δ 8.43 (d, *J* = 5.3 Hz, 1H), 7.62 (d, *J* = 7.6 Hz,

2H), 7.59 (d, *J* = 8.4 Hz, 2H), 7.55 – 7.51 (m, 3H), 7.47 – 7.42 (m, 2H), 7.37 – 7.34 (m, 1H), 7.34 – 7.33 (m, 1H), 7.30 – 7.27 (m, 2H), 7.24 (dd, *J* = 5.3, 1.7 Hz, 1H), 7.13 – 7.07 (m, 1H), 3.63 (dt, *J* = 17.4, 8.6 Hz, 1H), 2.73 – 2.58 (m, 2H), 2.52 – 2.46 (m, 2H), 2.35 – 2.23 (m, 4H), 2.19 (br s, 2H), 2.07 – 2.00 (m, 1H), 1.90 – 1.81 (m, 1H); ^{13}C NMR (151 MHz, CD_3CN) δ 165.3, 158.6, 145.0, 148.0, 142.8, 141.3, 139.9, 133.6, 131.7, 129.9 (2C), 128.9, 128.8, 128.4, 128.0 (2C), 127.8 (2C), 127.6 (2C), 124.9, 120.2, 119.8, 61.3, 43.1, 42. 8, 31.8, 29.2, 29.1, 18.8. HRMS ESI $[M+H]^+$ calculated for ($C_{30}H_{30}BrN_2^+$) 497.1587, found 497.1583.

5.5.2 Synthesis of 1,2,3,4-Tetrahydroquinolines.

General procedure 15 (GP15)

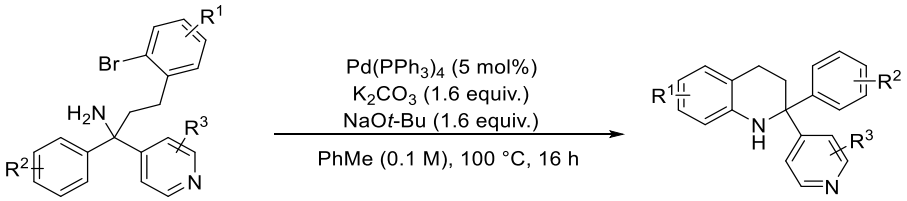

Following the method reported by Zhao and co-workers,[141] a 10-mL Schlenk tube equipped with a magnetic stir bar was charged with α-tertiary primary amine (1.0 equiv.), K_2CO_3 (1.6 equiv.), NaO*t*Bu (1.6 equiv.), $Pd(PPh_3)_4$ (5 mol%). The flask was evacuated and backfilled with N_2 3 times. Toluene (0.1 M) was then added via syringe under N_2. The reaction mixture was then vigorously stirred in an oil bath at 100 °C for 16 h. After the reaction was completed, the reaction mixture was cooled to room temperature, diluted with ethyl acetate, and poured into a separatory funnel, washed with brine. The combined organic layers were dried over Na_2SO_4

and concentrated under reduced pressure after filtration. The crude product was purified by flash chromatography on silica gel to afford the corresponding 1,2,3,4-tetrahydroquinolines.

***2-([1,1'-Biphenyl]-4-yl)-2-(pyridine-4-yl)-1,2,3,4-tetrahydroquinoline* 593**

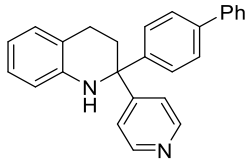

Following **GP15** using α-tertiary amine **587** (44.2 mg, 0.1 mmol), K_2CO_3 (22.1 mg, 0.16 mmol), NaO*t*Bu (15.4 mg, 0.16 mmol), $Pd(PPh_3)_4$ (5.8 mg, 0.005 mmol) and toluene (1.0 mL). Purification by flash chromatography (EtOAc : Hexane : Et_3N = 30 : 70 : 1), the product was obtained as yellow oil (35.5 mg, 98% yield). ^{1}H NMR (400 MHz, $CDCl_3$) δ 8.55 (d, *J* = 6.0 Hz, 2H), 7.63 – 7.53 (m, 4H), 7.49 – 7.42 (m, 2H), 7.41 – 7.33 (m, 3H), 7.31 (d, *J* = 6.0 Hz, 2H), 7.11 – 7.04 (m, 1H), 6.96 (d, *J* = 7.5 Hz, 1H), 6.73 – 6.63 (m, 2H), 4.48 (br s, 1H), 2.73 – 2.63 (m, 1H), 2.61 – 2.52 (m, 2H), 2.51 – 2.40 (m, 1H); ^{13}C NMR (101 MHz, $CDCl_3$) δ 156.2 (2C), 149.9, 144.5 (2C), 143.1, 140.5, 140.4, 129.4, 128.9 (2C), 127.6, 127.5 (2C), 127.29, 127.27 (2C), 127.1 (2C), 122.4, 120.3, 117.7, 114.1, 61.6, 32.4, 24.2. HRMS ESI $[M+H]^+$ calculated for ($C_{26}H_{23}N_2^+$) 363.1856, found 363.1851.

***2-([1,1'-Biphenyl]-4-yl)-7-fluoro-2-(pyridine-4-yl)-1,2,3,4-tetrahydroquinoline* 594**

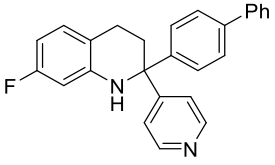

Following **GP15** using α-tertiary amine **588** (46.0 mg, 0.1 mmol), K_2CO_3 (22.1 mg, 0.16 mmol), NaO*t*Bu (15.4 mg, 0.16 mmol), $Pd(PPh_3)_4$ (5.8 mg, 0.005 mmol) and toluene (1.0 mL). Purification by flash chromatography (EtOAc : Hexane : Et_3N = 30 : 70 : 1), the product was obtained as yellow oil (26.6 mg, 70% yield). ^{1}H NMR (400 MHz, $CDCl_3$) δ 8.55 (d, *J* = 6.4 Hz, 2H), 7.61 – 7.53 (m, 4H), 7.48 – 7.41 (m, 2H), 7.39 – 7.33 (m, 3H), 7.27 (d, *J* = 6.4 Hz, 2H), 6.91 – 6.80 (m, 1H), 6.41 – 6.32 (m, 2H), 4.56 (br s, 1H), 2.65 – 2.51 (m, 3H), 2.47 – 2.32 (m, 1H); ^{13}C NMR (101 MHz, $CDCl_3$) δ 162.4 (d, $^1J_{C\text{-}F}$ = 242.4 Hz), 155.6 (2C), 150.2, 144.2 (d, $^3J_{C\text{-}F}$ = 11.1 Hz), 144.1 (2C), 140.7, 140.3, 130.4 (d, $^3J_{C\text{-}F}$ = 10.1 Hz), 129.0 (2C), 127.7, 127.5 (2C), 127.3 (2C), 127.2 (2C), 122.2, 115.9 (d, $^4J_{C\text{-}F}$ = 2.0 Hz), 104.3 (d, $^2J_{C\text{-}F}$ = 21.2 Hz), 100.5 (d, $^2J_{C\text{-}F}$ = 25.3 Hz), 61.5, 32.5, 23.7; ^{19}F NMR (376 MHz, $CDCl_3$) δ -115.95 – -116.10 (m, 1F). HRMS ESI $[M+H]^+$ calculated for ($C_{26}H_{22}FN_2^+$) 381.1762, found 381.1758.

2-([1,1'-Biphenyl]-4-yl)-6-chloro-2-(pyridine-4-yl)-1,2,3,4-tetrahydroquinoline **595**

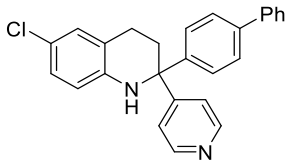

Following **GP15** using α-tertiary amine **589** (47.6 mg, 0.1 mmol), K_2CO_3 (22.1 mg, 0.16 mmol), NaO*t*Bu (15.4 mg, 0.16 mmol), $Pd(PPh_3)_4$ (5.8 mg, 0.005 mmol) and toluene (1.0 mL). Purification by flash chromatography (EtOAc : Hexane : Et_3N = 30 : 70 : 1), the product was obtained as colourless oil (29.7 mg, 75% yield). ^{1}H NMR (600 MHz, $CDCl_3$) δ 8.55 (d, *J* = 5.5 Hz, 2H), 7.59 – 7.54 (m, 4H), 7.46 – 7.41 (m, 2H), 7.38 – 7.32 (m, 3H), 7.28 – 7.22 (m, 2H), 7.01 (dd,

J = 8.5, 2.0 Hz, 1H), 6.92 (s, 1H), 6.59 (d, *J* = 8.5 Hz, 1H), 4.45 (br s, 1H), 2.64 – 2.57 (m, 1H), 2.57 – 2.51 (m, 2H), 2.47 – 2.38 (m, 1H); ^{13}C NMR (151 MHz, $CDCl_3$) δ 155.6 (2C), 150.2, 144.1 (2C), 141.7, 140.7, 140.4, 129.1, 129.0 (2C), 127.7, 127.6 (2C), 127.22 (2C), 127.16 (2C), 122.2 (2C), 121.9, 115.2 (2C), 61.6, 32.1, 24.2. HRMS ESI $[M+H]^+$ calculated for ($C_{26}H_{22}ClN_2^+$) 397.1466, found 397.1463.

2-Phenyl-2-(pyridine-4-yl)-1,2,3,4-tetrahydroquinoline **596**

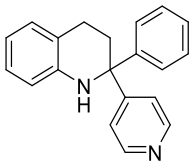

Following **GP15** using α-tertiary amine **590** (54.9 mg, 0.15 mmol), K_2CO_3 (33.2 mg, 0.24 mmol), NaO*t*Bu (23.1 mg, 0.24 mmol), $Pd(PPh_3)_4$ (8.7 mg, 0.0075 mmol) and toluene (1.5 mL). Purification by flash chromatography (EtOAc : Hexane : Et_3N = 30 : 70 : 1), the product was obtained as yellow oil (33.9 mg, 79% yield). ^{1}H NMR (600 MHz, $CDCl_3$) δ 8.52 (d, *J* = 6.0 Hz, 2H), 7.36 – 7.31 (m, 4H), 7.30 – 7.27 (m, 1H), 7.25 (d, *J* = 7.2 Hz, 2H), 7.08 – 7.03 (m, 1H), 6.93 (d, *J* = 7.2 Hz, 1H), 6.69 – 6.64 (m, 2H), 4.43 (br s, 1H), 2.64 – 2.58 (m, 1H), 2.57 – 2.52 (m, 2H), 2.47 – 2.41 (m, 1H); ^{13}C NMR (151 MHz, $CDCl_3$) δ 156.1 (2C), 150.0, 145.6 (2C), 143.1, 129.4, 128.8 (2C), 127.6, 127.3, 126.8 (2C), 122.3, 120.3, 117.6, 114.1, 61.7, 32.4, 24.2. HRMS ESI $[M+H]^+$ calculated for ($C_{20}H_{19}N_2^+$) 287.1543, found 287.1539.

2-(Pyridin-4-yl)-2-(3-(trifluoromethoxy)phenyl)-1,2,3,4-tetrahydroquinoline **597**

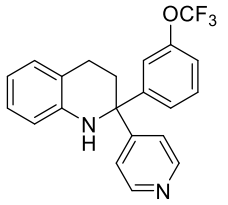

Following **GP15** using α-tertiary amine **591** (67.5 mg, 0.15 mmol), K_2CO_3 (33.2 mg, 0.24 mmol), NaO*t*Bu (23.1 mg, 0.24 mmol), $Pd(PPh_3)_4$ (8.7 mg, 0.0075 mmol) and toluene (1.5 mL). Purification by flash chromatography (EtOAc : Hexane : Et_3N = 30 : 70 : 1), the product was obtained as yellow oil (42.2 mg, 76% yield). ^{1}H NMR (600 MHz, $CDCl_3$) δ 8.57 (d, *J* = 6.0 Hz, 2H), 7.41 – 7.35 (m, 1H), 7.29 – 7.24 (m, 3H), 7.23 (s, 1H), 7.18 (d, *J* = 8.1 Hz, 1H), 7.11 – 7.07 (m, 1H), 6.96 (d, *J* = 7.5 Hz, 1H), 6.73 – 6.68 (m, 2H), 4.46 (br s, 1H), 2.65 – 2.58 (m, 1H), 2.58 – 2.53 (m, 2H), 2.53 – 2.47 (m, 1H); ^{13}C NMR (151 MHz, $CDCl_3$) δ 155.1 (2C), 150.3, 149.6, 148.1, 142.7 (2C), 130.2, 129.4, 127.4, 125.4, 122.1, 120.5 (q, $^1J_{C\text{-}F}$ = 256.7 Hz) 120.2, 119.9, 119.8, 118.0, 114.2, 61.6, 32.6, 24.1; ^{19}F NMR (565 MHz, $CDCl_3$) δ -57.75 (s, 3F). HRMS ESI $[M+H]^+$ calculated for ($C_{21}H_{18}F_3N_2O^+$) 371.1366, found 371.1362.

2-([1,1'-Biphenyl]-4-yl)-2-(2-cyclobutylpyridin-4-yl)-1,2,3,4-tetrahydroquinoline **598**

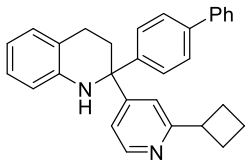

Following **GP15** using α-tertiary amine **592** (59.5 mg, 0.12 mmol), K_2CO_3 (26.5 mg, 0.192 mmol), NaO*t*Bu (18.5 mg, 0.192 mmol), $Pd(PPh_3)_4$ (5.8 mg, 0.006 mmol) and toluene (1.2 mL). Purification by flash chromatography (EtOAc : Hexane : Et_3N = 30 : 70 : 1), the product was

obtained as colourless oil (31.4 mg, 62% yield). ^{1}H NMR (600 MHz, $CDCl_3$) δ 8.51 (d, *J* = 5.2 Hz, 1H), 7.61 – 7.54 (m, 4H), 7.47 – 7.42 (m, 2H), 7.38 (d, *J* = 8.3 Hz, 2H), 7.37 – 7.34 (m, 1H), 7.16 (s, 1H), 7.10 – 7.04 (m, 2H), 6.95 (d, *J* = 7.4 Hz, 1H), 6.70 – 6.64 (m, 2H), 4.42 (br s, 1H), 3.64 (dt, *J* = 17.5, 8.8 Hz, 1H), 2.67 – 2.46 (m, 4H), 2.36 – 2.26 (m, 4H), 2.08 – 1.99 (m, 1H), 1.92 – 1.85 (m, 1H); ^{13}C NMR (151 MHz, $CDCl_3$) δ 165.1, 156.0, 149.6, 144.7, 143.2, 140.5, 140.3, 129.4, 128.9 (2C), 127.6, 127.38 (2C), 127.35 (2C), 127.3, 127.1 (2C), 120.5, 119.7, 119.4, 117.6, 114.0, 61.6, 42.3, 32.6, 28.7, 28.5, 24.3, 18.3. HRMS ESI $[M+H]^+$ calculated for ($C_{30}H_{29}N_2^+$) 417.2325, found 417.2321.

5.5.3 Synthesis of 1,2-Amino Alcohols

General procedure 16 (GP16)

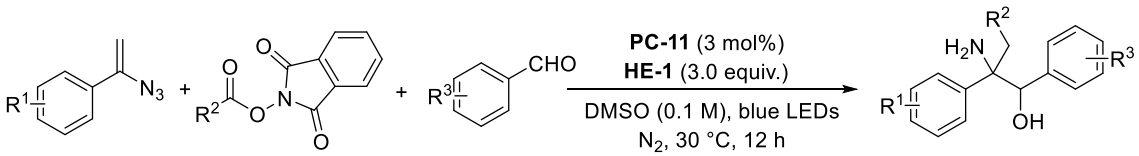

A 10-mL Schlenk tube equipped with a magnetic stir bar was charged with vinyl azide (if solid, 0.2 mmol, 1.0 equiv.), NHPI ester (if solid, 0.24 mmol, 1.2 equiv.), aryl aldehyde (if solid, 0.4 mmol, 2.0 equiv.), Hantzsch ester **HE-1** (0.6 mmol, 152.0 mg, 3.0 equiv.), and **PC-11** (2.1 mg, 3 mol%). The flask was evacuated and backfilled with N_2 3 times. DMSO (2.0 mL, 0.1 M) was then added via syringe followed by the addition of vinyl azide, NHPI ester, aryl aldehyde (if liquid) under N_2. The reaction mixture was then vigorously stirred under blue LED light (30 W, λ_{max} = 440 nm) at 30 °C (two fans were used to cool down the reaction mixture) for 12 h. After

the reaction was completed, the reaction mixture was diluted with ethyl acetate and poured into a separatory funnel, washed with brine. The combined organic layers were dried over Na_2SO_4 and concentrated under reduced pressure after filtration. The crude product was purified by flash chromatography on silica gel to afford corresponding 1,2-amino alcohol product.

***Methyl 4-(2-([1,1'-biphenyl]-4-yl)-2-amino-1-hydroxy-4,4-dimethylpentyl)benzoate* 600**

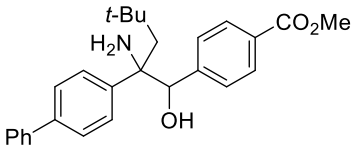

Following the **GP16** using vinyl azide **523** (44.3 mg, 0.20 mmol), NHPI ester **524** (74.2 mg, 0.30 mmol) and methyl 4-formylbenzoate (65.7 mg, 0.40 mmol). Purification by flash column chromatography (EtOAc : Hexane : Et_3N = 20 : 80 : 1), the product (62.7 mg) was obtained in 75% yield as a white solid as a 1:1 mixture of diastereoisomers. Diastereoisomer 1: ^{1}H NMR (400 MHz, $CDCl_3$) δ 8.02 (d, *J* = 8.3 Hz, 2H), 7.64 (d, *J* = 7.2 Hz, 2H), 7.63 – 7.60 (m, 4H), 7.48 – 7.43 (m, 2H), 7.40 (d, *J* = 8.3 Hz, 2H), 7.38 – 7.33 (m, 1H), 4.84 (s, 1H), 3.93 (s, 3H), 2.03 (d, *J* = 14.6 Hz, 1H), 1.76 (br s, 2H), 1.25 (d, *J* = 14.6 Hz, 1H), 0.67 (s, 9H); ^{13}C NMR (101 MHz, $CDCl_3$) δ 167.2, 145.1, 143.1, 140.6, 139.6, 129.7, 129.0, 128.9, 128.5, 127.6, 127.5, 127.1, 126.9, 82.31, 62.8, 52.3, 50.6, 32.04, 31.96. Diastereoisomer 2: ^{1}H NMR (400 MHz, $CDCl_3$) δ 7.73 (d, *J* = 8.4 Hz, 2H), 7.60 (d, *J* = 7.2 Hz, 2H), 7.47 – 7.39 (m, 4H), 7.36 – 7.31 (m, 1H), 7.18 (d, *J* = 8.4 Hz, 2H), 6.93 (d, *J* = 8.3 Hz, 2H), 4.76 (s, 1H), 3.85 (s, 3H), 2.23 (d, *J* = 14.9 Hz, 1H), 2.18 (d, *J* = 14.9

Hz, 1H), 1.65 (br s, 2H), 0.80 (s, 9H); ^{13}C NMR (101 MHz, $CDCl_3$) δ 167.2, 145.4, 142.3, 140.5, 139.3, 128.93, 128.89, 128.5, 127.8, 127.6, 127.3, 127.0, 126.2, 81.4, 63.4, 52.1, 50.1, 32.4, 32.1. HRMS ESI $[M+H]^+$ calculated for ($C_{27}H_{31}NO_3$) 418.2377, found 418.2371.

2-([1,1'-Biphenyl]-4-yl)-2-amino-4,4-dimethyl-1-(4-(methylsulfonyl)phenyl)pentan-1-ol **601**

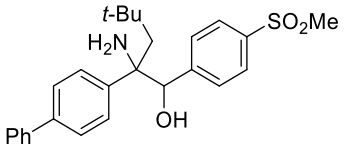

Following the **GP16** using vinyl azide **523** (44.3 mg, 0.20 mmol), NHPI ester **524** (74.2 mg, 0.30 mmol) and 4-(methylsulfonyl)benzaldehyde (73.7 mg, 0.40 mmol). Purification by flash column chromatography (EtOAc : Hexane : Et_3N = 50 : 50 : 1 to 100 : 0: 1), the product (62.8 mg) was obtained in 72% yield as a grey solid as a 1:1 mixture of diastereoisomers. ^{1}H NMR (400 MHz, DMSO-d_6) δ 7.83 (d, *J* = 8.0 Hz, 1H), 7.71 (d, *J* = 7.8 Hz, 2H), 7.66 (d, *J* = 7.8 Hz, 1H), 7.63 – 7.55 (m, 3H), 7.53 (d, *J* = 8.1 Hz, 1H), 7.49 – 7.41 (m, 2H), 7.41 – 7.30 (m, 2H), 7.14 (d, *J* = 8.1 Hz, 1H), 5.86 (s, 0.5H), 5.48 (s, 0.5H), 4.86 (s, 0.5H), 4.84 (s, 0.5H), 3.20 (s, 1.5H), 3.09 (s, 1.5H), 2.26 (d, *J* = 14.7 Hz, 0.5H), 2.19 (d, *J* = 14.7 Hz, 0.5H), 2.11 (d, *J* = 14.7 Hz, 0.5H), 1.64 (br s, 2H), 1.13 (d, *J* = 14.7 Hz, 0.5H), 0.76 (s, 4.5H), 0.64 (s, 4.5H); ^{13}C NMR (101 MHz, DMSO-d_6) δ 148.7, 147.8, 145.2, 143.9, 140.0, 139.7, 139.2, 138.6, 137.20, 137.16, 129.4, 128.9, 128.8, 128.0, 127.5, 127.2, 127.1, 126.4, 126.3, 125.6, 125.2, 125.1, 80.9, 80.1, 62.6, 61.9, 50.5, 49.7, 43.6, 43.5, 32.0, 31.9, 31.62, 31.58. HRMS ESI $[M+H]^+$ calculated for ($C_{26}H_{32}NO_3S^+$) 438.2097, found 438.2092.

***4-(2-([1,1'-Biphenyl]-4-yl)-2-amino-1-hydroxy-4,4-dimethylpentyl)benzonitrile* 602**

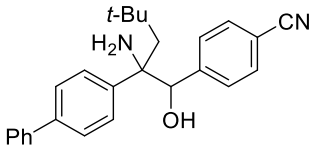

Following the **GP16** using vinyl azide **523** (44.3 mg, 0.20 mmol), NHPI ester **524** (74.2 mg, 0.30 mmol) and 4-formylbenzonitrile (52.4 mg, 0.40 mmol). Purification by flash column chromatography (EtOAc:Hexane:Et_3N = 30:70:1), the product (62.5 mg) was obtained in 81% yield as a white solid as a 1:1 mixture of diastereoisomers. ^{1}H NMR (400 MHz, $CDCl_3$) δ 7.66 – 7.56 (m, 5H), 7.49 – 7.39 (m, 4H), 7.39 – 7.30 (m, 2H), 7.16 (d, *J* = 8.4 Hz, 1H), 6.95 (d, *J* = 8.4 Hz, 1H), 4.79 (s, 0.5H), 4.71 (s, 0.5H), 2.22 (d, *J* = 14.8 Hz, 0.5H), 2.16 (d, *J* = 14.8 Hz, 0.5H), 2.02 (d, *J* = 14.5 Hz, 0.5H), 1.61 (br s, 2H), 1.25 (d, *J* = 14.5 Hz, 0.5H), 0.81 (s, 4.5H), 0.69 (s, 4.5H); ^{13}C NMR (101 MHz, $CDCl_3$) δ 145.7, 145.5, 142.8, 141.9, 140.4, 140.3, 139.7, 139.4, 131.4, 130.9, 129.2, 128.9, 128.5, 127.52, 127.50, 127.48, 127.2, 127.0, 126.9, 126.8, 126.2, 119.0, 118.9, 111.6, 110.8, 82.1, 81.1, 63.3, 62.7, 50.3, 50.0, 32.3, 32.0, 31.93, 31.90. HRMS ESI $[M+H]^+$ calculated for ($C_{26}H_{29}N_2O^+$) 385.2274, found 385.2269.

***1,2-Di([1,1'-biphenyl]-4-yl)-2-amino-4,4-dimethylpentan-1-ol* 603**

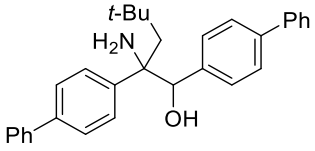

Following the **GP16** using vinyl azide **523** (44.3 mg, 0.20 mmol), NHPI ester **524** (74.2 mg, 0.30 mmol) and [1,1'-biphenyl]-4-carbaldehyde (72.9 mg, 0.40 mmol). Purification by flash column

chromatography (EtOAc : Hexane : Et_3N = 10 : 90 : 1 to 15 : 85 : 1), the product (53.1 mg) was obtained in 61% yield as a white solid as a 1:1 mixture of diastereoisomers. Diastereoisomer 1: ^1H NMR (400 MHz, $CDCl_3$) δ 7.71 – 7.67 (m, 3H), 7.66 – 7.62 (m, 5H), 7.61 (d, *J* = 8.2 Hz, 2H), 7.49 – 7.44 (m, 4H), 7.41 (d, *J* = 8.2 Hz, 2H), 7.39 – 7.33 (m, 2H), 4.88 (s, 1H), 2.09 (d, *J* = 14.6 Hz, 1H), 1.78 (br s, 2H), 1.37 (d, *J* = 14.6 Hz, 1H), 0.71 (s, 9H); ^{13}C NMR (101 MHz, $CDCl_3$) δ 143.5, 140.8, 140.73, 140.68, 139.4, 139.0, 128.93, 128.90, 128.89, 127.7, 127.5, 127.4, 127.2, 127.1, 126.8, 126.6, 82. 5, 62.8, 50.9, 32.1, 32.0. Diastereoisomer 2: ^1H NMR (400 MHz, $CDCl_3$) δ 7.62 (d, *J* = 7.2 Hz, 2H), 7.52 (d, *J* = 7.2 Hz, 2H), 7.48 (d, *J* = 8.4 Hz, 2H), 7.46 – 7.40 (m, 3H), 7.38 (d, *J* = 7.8 Hz, 2H), 7.36 – 7.30 (m, 3H), 7.26 (d, *J* = 8.4 Hz, 2H), 6.94 (d, *J* = 8.2 Hz, 2H), 4.79 (s, 1H), 2.32 – 2.16 (m, 3H), 0.83 (s, 9H); ^{13}C NMR (101 MHz, $CDCl_3$) δ 142.8, 140.8, 140.7, 139.9, 139.1, 139.0, 128.9, 128.8, 128.2, 127.6, 127.31, 127.29, 127.04, 126.99, 126.1, 125.9, 81.7, 63.3, 50.1, 32.4, 32.0. HRMS ESI $[M+H]^+$ calculated for ($C_{31}H_{34}NO^+$) 436.2635, found 436.2628.

***2-([1,1'-Biphenyl]-4-yl)-2-amino-1-(4-iodophenyl)-4,4-dimethylpentan-1-ol* 604**

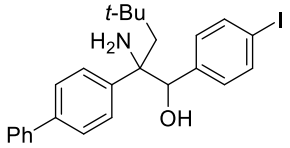

Following the **GP16** using vinyl azide **523** (44.3 mg, 0.20 mmol), NHPI ester **524** (74.2 mg, 0.30 mmol) and 4-iodobenzaldehyde (92.8 mg, 0.40 mmol). Purification by flash column chromatography (EtOAc : Hexane : Et_3N = 10 : 90 : 1 to 15 : 85 : 1), the product (49.5 mg) was obtained in 51% yield as a white solid as a 1:1 mixture of diastereoisomers. Diastereoisomer

1: ^{1}H NMR (400 MHz, $CDCl_3$) δ 7.67 (d, *J* = 8.2 Hz, 2H), 7.64 (d, *J* = 7.4 Hz, 2H), 7.62 – 7.58 (m, 4H), 7.48 – 7.42 (m, 2H), 7.38 – 7.32 (m, 1H), 7.06 (d, *J* = 8.2 Hz, 2H), 4.75 (s, 1H), 2.00 (d, *J* = 14.6 Hz, 1H), 1.86 (br s, 2H), 1.30 (d, *J* = 14.6 Hz, 1H), 0.68 (s, 9H); ^{13}C NMR (101 MHz, $CDCl_3$) δ 143.0, 140.6, 139.6, 139.5, 136.9, 130.4, 128.9, 127.6, 127.5, 127.1, 126.9, 93.7, 82.1, 62.7, 50.4, 32.1, 32.0. Diastereoisomer 2: ^{1}H NMR (400 MHz, $CDCl_3$) δ 7.60 (d, *J* = 7.2 Hz, 2H), 7.47 (d, *J* = 8.4 Hz, 2H), 7.46 – 7.41 (m, 2H), 7.39 (d, *J* = 8.4 Hz, 2H), 7.36 – 7.31 (m, 1H), 7.19 (d, *J* = 8.4 Hz, 2H), 6.60 (d, *J* = 8.4 Hz, 2H), 4.68 (s, 1H), 2.20 (d, *J* = 14.9 Hz, 1H), 2.14 (d, *J* = 14.9 Hz, 1H), 1.79 (br s, 2H), 0.80 (s, 9H); ^{13}C NMR (101 MHz, $CDCl_3$) δ 142.0, 140.5, 139.7, 139.3, 136.3, 129.8, 128.9, 127.5, 127.4, 127.0, 126.2, 93.1, 81.2, 63.3, 50.0, 32.4, 32.0. HRMS ESI $[M+H]^+$ calculated for ($C_{25}H_{29}INO^+$) 486.1288, found 486.1284.

***2-([1,1'-Biphenyl]-4-yl)-2-amino-4,4-dimethyl-1-(4-((trimethylsilyl)ethynyl)phenyl) pentan-1-ol* 605**

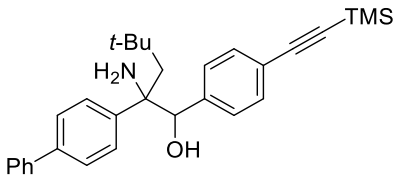

Following the **GP16** using vinyl azide **523** (44.3 mg, 0.20 mmol), NHPI ester **524** (74.2 mg, 0.30 mmol) and 4-((trimethylsilyl)ethynyl)benzaldehyde (80.9 mg, 0.40 mmol). Purification by flash column chromatography (EtOAc : Hexane : Et_3N = 15 : 85 : 1 to 20 : 80 : 1), the product (67.1 mg) was obtained in 71% yield as a white solid as a 1:1 mixture of diastereoisomers. Diastereoisomer 1: ^{1}H NMR (600 MHz, $CDCl_3$) δ 7.64 (d, *J* = 7.0 Hz, 2H), 7.63 – 7.58 (m, 4H),

7.48 – 7.42 (m, 4H), 7.37 – 7.33 (m, 1H), 7.27 (d, *J* = 7.2 Hz, 2H), 4.78 (s, 1H), 1.99 (d, *J* = 14.5 Hz, 1H), 1.55 (br s, 2H), 1.24 (d, *J* = 14.5 Hz, 1H), 0.66 (s, 9H), 0.27 (s, 9H); ^{13}C NMR (151 MHz, $CDCl_3$) δ 143.3, 140.7, 140.4, 139.5, 131.5, 128.9, 128.3, 127.6, 127.4, 127.1, 126.9, 122.6, 105.0, 94.7, 82.4, 62.7, 50.7, 32.1, 32.0, 0.1. Diastereoisomer 2: ^{1}H NMR (600 MHz, $CDCl_3$) δ 7.61 (d, *J* = 7.7 Hz, 2H), 7.48 – 7.40 (m, 4H), 7.36 – 7.31 (m, 1H), 7.21 – 7.14 (m, 4H), 6.79 (d, *J* = 7.7 Hz, 2H), 4.70 (s, 1H), 2.20 (d, *J* = 14.9 Hz, 1H), 2.15 (d, *J* = 14.9 Hz, 1H), 1.65 (br s, 2H), 0.80 (s, 9H), 0.22 (s, 9H); ^{13}C NMR (151 MHz, $CDCl_3$) δ 142.4, 140.62, 140.59, 139.1, 130.9, 128.9, 127.7, 127.42, 127.35, 127.0, 126.1, 121.8, 105.2, 94.2, 81.5, 63.3, 50.1, 32.4, 32.0, 0.1. HRMS ESI $[M+H]^+$ calculated for ($C_{30}H_{38}NOSi^+$) 456.2717, found 456.2712.

2-([1,1'-Biphenyl]-4-yl)-2-amino-4,4-dimethyl-1-(3-(trifluoromethoxy)phenyl)pentan-1-ol

606

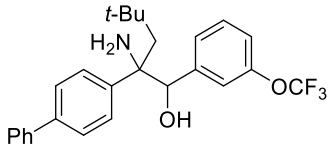

Following the **GP16** using vinyl azide **523** (44.3 mg, 0.20 mmol), NHPI ester **524** (74.2 mg, 0.30 mmol) and 3-(trifluoromethoxy)benzaldehyde (76.0 mg, 0.40 mmol). Purification by flash column chromatography (EtOAc : Hexane : Et_3N = 15 : 85 : 1 to 20 : 80 : 1), the product (59.8 mg) was obtained in 67% yield as a white solid as a 1:1 mixture of diastereoisomers. ^{1}H NMR (400 MHz, $CDCl_3$) δ 7.75 – 7.72 (m, 1H), 7.71– 7.70 (m, 2H), 7.69 – 7.65 (m, 1H), 7.57 – 7.49 (m, 3H), 7.49 – 7.40 (m, 1.5H), 7.38 – 7.33 (m, 0.5H), 7.30 – 7.24 (m, 2H), 7.21 – 7.15 (m, 0.5H),

7.06 (d, *J* = 8.2 Hz, 0.5H), 6.92 (d, *J* = 7.7 Hz, 0.5H), 6.81 (s, 0.5H), 4.89 (s, 0.5H), 4.80 (s, 0.5H), 2.31 (d, *J* = 14.8 Hz, 0.5H), 2.25 (d, *J* = 14.8 Hz, 0.5H), 2.12 (d, *J* = 14.5 Hz, 0.5H), 1.67 (br s, 2H), 1.38 (d, *J* = 14.5 Hz, 0.5H), 0.90 (s, 4.5H), 0.78 (s, 4.5H); ^{13}C NMR (101 MHz, $CDCl_3$) δ 148.8, 148.5, 143.08, 142.6, 142.4, 142.2, 140.7, 140.6, 139.6, 139.5, 129.1, 128.9, 128.8, 128.5, 127.6, 127.4, 127.3, 127.2, 127.1, 127.0, 126.9, 126.8, 126.3, 126.1, 121.3,120.7 (q, $^1J_{C\text{-}F}$ = 258.6 Hz), 120.6, 120.5 (q, $^1J_{C\text{-}F}$ = 257.6 Hz), 120.4, 119.7, 82.0, 81.1, 63.2, 62.6, 50.6, 50.1, 32.3, 32.01, 31.95, 31.9; ^{19}F NMR (377 MHz, $CDCl_3$) δ 57.70 (s), 57.71 (s). HRMS ESI $[M+H]^+$ calculated for ($C_{26}H_{29}F_3NO_2^+$) 444.2145, found 444.2137.

2-([1,1'-Biphenyl]-4-yl)-2-amino-1-(2-bromophenyl)-4,4-dimethylpentan-1-ol **607**

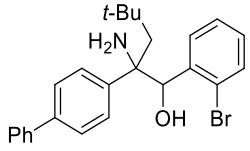

Following the **GP16** using vinyl azide **523** (44.3 mg, 0.20 mmol), NHPI ester **524** (74.2 mg, 0.30 mmol) and 2-bromobenzaldehyde (74.0 mg, 0.40 mmol). Purification by flash column chromatography (EtOAc : Hexane : Et_3N = 20 : 80 : 1), the product (69.3 mg) was obtained in 79% yield as a white solid as a 1.2:1 mixture of diastereoisomers. Diastereoisomer 1: ^{1}H NMR (400 MHz, $CDCl_3$) δ 7.71 (d, *J* = 8.4 Hz, 2H), 7.68 – 7.62 (m, 4H), 7.61 (dd, *J* = 8.0, 1.0 Hz, 1H), 7.51 (dd, *J* = 7.8, 1.6 Hz, 1H), 7.49 – 7.43 (m, 2H), 7.39 – 7.32 (m, 2H), 7.22 – 7.16 (m, 1H), 5.41 (s, 1H), 2.68 (br s, 1H), 2.47 (d, *J* = 14.7 Hz, 1H), 1.66 (br s, 2H), 1.13 (d, *J* = 14.7 Hz, 1H), 0.68 (s, 9H); ^{13}C NMR (151 MHz, $CDCl_3$) δ 144.2, 140.8, 139.9, 139.4, 132.9, 129.34, 129.27, 128.9,

127.44, 127.39, 127.34, 127.1, 126.8, 125.4, 79.6, 64.01, 50.04, 32.09, 32.05. Diastereoisomer 2: ^{1}H NMR (400 MHz, $CDCl_3$) δ 7.61 (d, *J* = 7.2 Hz, 2H), 7.47 – 7.39 (m, 5H), 7.37 – 7.31 (m, 1H), 7.29 (d, *J* = 8.4 Hz, 2H), 7.10 – 6.97 (m, 2H), 6.89 (dd, *J* = 7.6, 1.7 Hz, 1H), 5.12 (s, 1H), 2.29 (d, *J* = 15.1 Hz, 1H), 2.22 (d, *J* = 15.1 Hz, 1H), 1.87 (br s, 2H), 0.86 (s, 9H); ^{13}C NMR (151 MHz, $CDCl_3$) δ 140.7, 140.6, 139.6, 139.2, 132.6, 130.8, 129.0, 128.8, 128.2, 127.3, 127.0, 126.5, 125.6, 124.6, 79.4, 64.4, 49.7, 32.7, 32.0. HRMS ESI $[M+H]^+$ calculated for ($C_{25}H_{29}BrNO^+$) 438.1427, found 438.1421.

2-([1,1'-Biphenyl]-4-yl)-2-amino-1-(4-chloro-3-methoxyphenyl)-4,4-dimethylpentan-1-ol

608

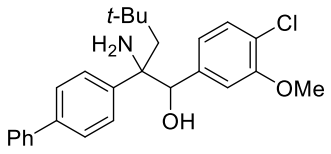

Following the **GP16** using vinyl azide **523** (44.3 mg, 0.20 mmol), NHPI ester **524** (74.2 mg, 0.30 mmol) and 4-chloro-3-methoxybenzaldehyde (68.2 mg, 0.40 mmol). Purification by flash column chromatography (EtOAc : Hexane : Et_3N = 15 : 85 : 1), the product (57.0 mg) was obtained in 67% yield as a white solid as a 1:1 mixture of diastereoisomers. ^{1}H NMR (400 MHz, $CDCl_3$) δ 7.65 – 7.54 (m, 4.5H), 7.49 – 7.40 (m, 3H), 7.38 – 7.33 (m, 1H), 7.31 (d, *J* = 8.1 Hz, 0.5H), 7.22 (d, *J* = 8.3 Hz, 0.5H), 7.15 (d, *J* = 8.1 Hz, 1H), 6.84 (dd, *J* = 8.1, 1.7 Hz, 0.5H), 6.73 – 6.71 (m, 0.5H), 6.65 (dd, *J* = 8.1, 1.7 Hz, 0.5H), 6.07 (d, *J* = 1.7 Hz, 0.5H), 4.73 (s, 0.5H), 4.70 (s, 0.5H), 3.79 (s, 1.5H), 3.42 (s, 1.5H), 2.36 – 2.04 (m, 3.5H), 1.43 (d, *J* = 14.6 Hz, 0.5H), 0.82 (s,

4.5H), 0.72 (s, 4.5H); ^{13}C NMR (151 MHz, $CDCl_3$) δ 154.4, 153.7, 140.6, 140.5, 140.0, 139.9, 139.6, 139.5, 129.3, 129.0, 128.94, 128.90, 127.74, 127.70, 127.48, 127.47, 127.1, 127.0, 126.7, 126.2, 121.9, 121.6, 121.2, 120.22, 112.11, 112.06, 82.5, 81.1, 63.4, 62.7, 56.2, 55.8, 50.2, 49.8, 32.4, 32.2, 32.0, 31.9. HRMS ESI $[M+H]^+$ calculated for ($C_{26}H_{31}NO_2Cl^+$) 424.2038, found 424.2031.

2-([1,1'-Biphenyl]-4-yl)-2-amino-4,4-dimethyl-1-(thiophen-2-yl)pentan-1-ol **609**

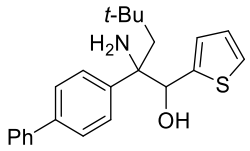

Following the **GP16** using vinyl azide **523** (44.3 mg, 0.20 mmol), NHPI ester **524** (74.2 mg, 0.30 mmol) and thiophene-2-carbaldehyde (44.9 mg, 0.40 mmol). Purification by flash column chromatography (EtOAc : Hexane : Et_3N = 20 : 80 : 1), the product (42.8 mg) was obtained in 59% yield as a white solid as a 1:1 mixture of diastereoisomers. ^{1}H NMR (600 MHz, $CDCl_3$) δ 7.69 (d, *J* = 7.5 Hz, 1H), 7.67 – 7.62 (m, 3H), 7.54 (d, *J* = 7.5 Hz, 1H), 7.48 – 7.42 (m, 2H), 7.38 – 7.30 (m, 2.5H), 7.06 – 7.01 (m, 1.5H), 6.73 (s, 0.5H), 6.34 (s, 0.5H), 5.13 (s, 0.5H), 5.06 (s, 0.5H), 2.29 (d, *J* = 14.8 Hz, 0.5H), 2.14 (d, *J* = 14.8 Hz, 0.5H), 2.00 (d, *J* = 14.7 Hz, 0.5H), 1.75 (br s, 2H), 1.42 (d, *J* = 14.7 Hz, 0.5H), 0.80 (s, 4.5H), 0.71 (s, 4.5H); ^{13}C NMR (151 MHz, $CDCl_3$) δ 144.4, 143.6, 143.4, 143.1, 140.7, 140.6, 139.5, 139.3, 128.88, 128.87, 127.6, 127.37, 127.36, 127.2, 127.1, 127.0, 126.9, 126.5, 126.3, 126.2, 125.5, 125.1, 124.5, 79.57, 78.51, 63.3, 62.4, 50.9,

50.6, 32.07, 32.05, 31.98, 31.95. HRMS ESI $[M+H]^+$ calculated for ($C_{23}H_{28}NOS^+$) 366.1886, found 366.1889.

5.5.4 Further Transformation

Gram-scale synthesis of product 550

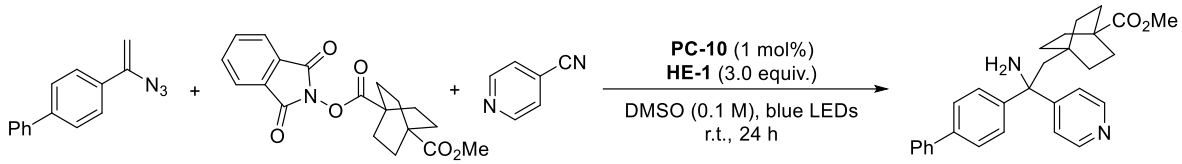

A 100-mL Schlenk tube equipped with a magnetic stir bar was charged with corresponding NHPI ester (2.14 g, 6.0 mmol), vinyl azide **523** (885 mg, 4.0 mmol), 4-cyanopyridine **447** (1.04 g, 10 mol), Hantzsch ester **HE-1** (3.04 g, 12 mmol) and **PC-10** (40 mg, 0.04 mmol). The flask was evacuated and backfilled with N_2 3 times. DMSO (40 mL, 0.1 M) was then added via syringe under N_2. The reaction mixture was then vigorously stirred under blue LED light (30 W, λ_{max} = 440 nm) at room temperature (two fans were used to cool down the reaction mixture) for 24 h. After the reaction was completed, the reaction mixture was diluted with ethyl acetate and poured into a separatory funnel, washed with brine. The combined organic layers were dried over Na_2SO_4 and concentrated under reduced pressure after filtration. The crude product was purified by flash chromatography on silica gel (eluent: EtOAc : Hexane : Et_3N = 50 : 50 : 1) to afford product **550** in 66% yield (white solid, 1.16 g).

Synthesis of 2*H*-azirine 610 from vinyl azide 523

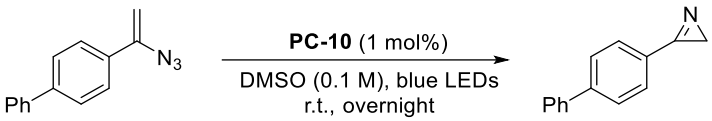

A 10-mL Schlenk tube equipped with a magnetic stir bar was charged with vinyl azide **523** (22.1 mg, 0.1 mmol), **PC-10** (1.0 mg, 0.001 mmol). The flask was evacuated and backfilled with N_2 3 times. DMSO (1.0 mL) was then added via syringe under N_2. The reaction mixture was then vigorously stirred under blue LED light (30 W, λ_{max} = 440 nm) at room temperature (two fans were used to cool down the reaction mixture) overnight. After the reaction was completed, the reaction mixture was diluted with ethyl acetate and poured into a separatory funnel, washed with brine. The combined organic layers were dried over Na_2SO_4 and concentrated under reduced pressure after filtration. The crude product was purified by flash chromatography on silica gel (eluent: hexane) to afford 2*H*-azirine **610** in 71% yield (white solid, 13.7 mg). ^{1}H NMR (400 MHz, $CDCl_3$) δ 7.98 (d, *J* = 8.4 Hz, 2H), 7.79 (d, *J* = 8.4 Hz, 2H), 7.66 (d, *J* = 7.1 Hz, 2H), 7.49 (d, *J* = 7.1 Hz, 2H), 7.45 – 7.39 (m, 1H), 1.82 (s, 2H); ^{13}C NMR (101 MHz, $CDCl_3$) δ 165.6, 145.9, 134.0, 130.2 (2C), 129.2 (2C), 128.5, 127.9 (2C), 127.4 (2C), 124.4, 19.85. HRMS ESI $[M+H]^+$ calculated for ($C_{14}H_{12}N$) 194.0964, found 194.0963. The experimental data are in accordance with the literature report.[142]

5.5.5 Determination of Light Intensity and Quantum Yield

Determination of the photon flux of the blue LEDs

The photon flux of the blue LED light was determined by standard ferrioxalate actinometry.[143,144] A 0.15 M solution of ferrioxalate was prepared by dissolving 2.21 g of potassium ferrioxalate hydrate in 30 mL of 0.05 M H_2SO_4. A buffered solution of phenanthroline was prepared by dissolving 50 mg of 1,10-phenanthroline and 11.25 g of sodium acetate in 50 mL of 0.5 M H_2SO_4. Both solutions were stored in the dark. To determine the photon flux of the blue LED light, 2.0 mL of the ferrioxalate solution was placed in a cuvette (two sides of the cuvette were coated with black electrical tape to ensure a minimum pathway of the light of 1 cm) and irradiated for 30 seconds with a blue LED lamp. After irradiation, 0.35 mL of the 1,10-phenanthroline solution was added to the cuvette immediately. The solution was mixed and then allowed to rest for 1 h to allow the ferrous ions to completely coordinate to the phenanthroline. The absorbance of the solution was measured at 510 nm. A non-irradiated sample was also prepared and the absorbance at 510 nm measured. Conversion was calculated using eq 1:

$$\text{mol } Fe^{2+} = \frac{V \cdot \Delta A}{l \cdot \varepsilon}$$

Where V is the total volume (0.00235 L) of the solution after addition of phenanthroline, ΔA is the difference in the absorbance at 510 nm between the irradiated and non-irradiated

solutions, l is the path length (1.0 cm), and ε is the molar absorptivity at 510 nm (11,100 L mol^{-1} cm^{-1}). The photon flux can be calculated using eq 2:

$$\text{photon flux} = \frac{\text{mol } Fe^{2+}}{\Phi \cdot t \cdot f}$$

Where Φ is the quantum yield for the ferrioxalate actinometer (1.01 for a 0.15 M solution at λ = 440 nm), t is the time (30 s), and f is the fraction of light absorbed at λ = 440 nm (0.99690, *vide infra*). The photon flux was calculated (average of three experiments) to be 5.9932 × 10^{-9} einstein s^{-1}.

$$\text{mol } Fe^{2+} = \frac{0.00235 \text{ L} \cdot 0.85509}{1.0 \text{ cm} \cdot 11{,}100 \text{ L mol}^{-1} \text{ cm}^{-1}} = 1.8103 \times 10^{-7} \text{ mol}$$

$$\text{photon flux} = \frac{1.8103 \times 10^{-7} \text{ mol}}{1.01 \cdot 30 \text{ s} \cdot 0.99690} = 5.9932 \times 10^{-9} \text{ einstein s}^{-1}$$

Quantum yield determination of the standard reaction

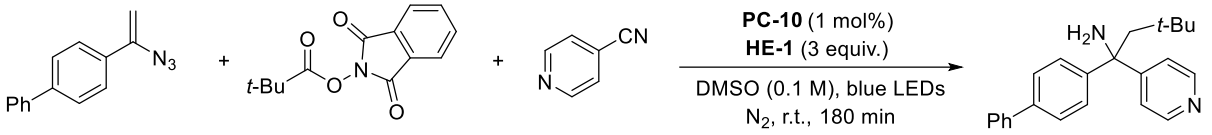

In a glovebox, a cuvette was charged with vinyl azide **523** (44.3 mg, 0.2 mmol), NHPI ester **524** (74.1 mg, 0.3 mmol), 4-cyanopyridine **447** (52.1 mg, 0.5 mmol), Hantzsch ester **HE-1** (151.9 mg, 0.6 mmol), **PC-10** (2.0 mg, 0.002 mmol) and DMSO (2.0 mL, 0.1 M). The cuvette was then capped with a stopper, and two sides of the cuvette were coated with black electrical tape to ensure a minimum pathway of the light of 1 cm. The distance between the cuvette and the light was set to 3 cm. The sample was stirred and irradiated for 10800 s (180 min). After

irradiation, the reaction mixture was diluted with ethyl acetate and poured into a separatory funnel, washed with brine. The combined organic layers were dried over Na_2SO_4 and concentrated under reduced pressure. The yield of product formed was determined by ^1H NMR analysis of the crude reaction mixture with mesitylene as an internal standard. The reaction yield was 49% (9.8×10^{-5} mol) for 180 min. The quantum yield was determined using eq 3:

$$\Phi = \frac{\text{mol product}}{\text{flux} \cdot t \cdot f}$$

Where t is the time (10800 s) and f is the fraction of light absorbed by **PC-1** ($Ir(dFMeppy)_2(dtbbpy)PF_6$) at λ = 440 nm, where $f = 1 - 10^{-A}$ (for a 1.0×10^{-3} M solution in DMSO, this was determined by UV/vis spectroscopy to be 0.61017, Figure 32).

$$\Phi = \frac{9.8 \times 10^{-5}\ \text{mol}}{5.9932 \times 10^{-9}\ \text{einstein}\ s^{-1} \cdot 10800\ s \cdot 0.61017} = 2.48$$

$\Phi > 1$ would mean the chain propagation;

$\Phi < 1$ would mean closed photocatalytic pathway.

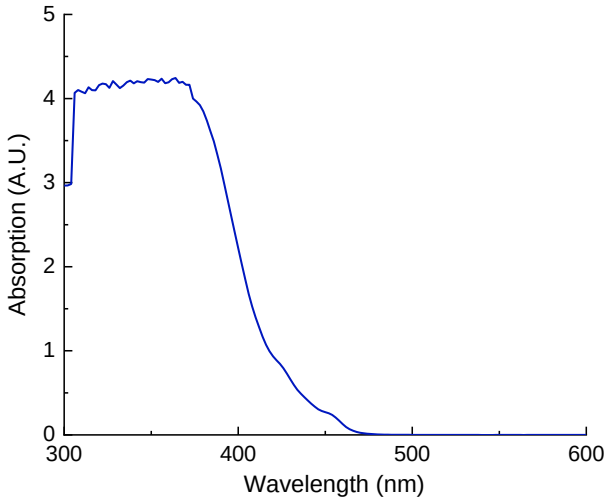

Figure 32: Absorbance of a 1.0×10^{-3} M solution of $Ir(dFMeppy)_2(dtbbpy)PF_6$ in DMSO

Conclusion: Although the light on-off experiments showed that the product formation occured only during periods of constant irradiation. Typical lifetime of radical chain process can be on the second or sub-second timescale, which means chain processes can terminate faster than the timescale of the analytical measurement used. The quantum yield measurement ($\Phi > 1$) indicated that a radical chain process was involved during the reaction.[128]

6 Appendix

For all relevant spectra and DFT calculation details for "Chapter 2: A Radical-Triggered Fragmentary Rearrangement Cascade of Ene-Ynamides to Construct [1,2]-Annulated Indoles" please see the supplementary information of our published paper "A Radical-Initiated Fragmentary Rearrangement Cascade of Ene-Ynamides to [1,2]-Annulated Indoles via Site-Selective Cyclization".[145]

Link to the paper: https://doi.org/10.1021/acs.orglett.1c02519

For all relevant spectra for "Chapter 3: Photoredox Catalysed Triple C–F Bond Cleavage of α-Trifluoromethyl Alkenes to Access α-Arylated Carbonyl Compounds" please see the supplementary information of our published paper "Modular synthesis of a-arylated carboxylic acids, esters and amides *via* photocatalyzed triple C–F bond cleavage of methyltrifluorides".[146]

Link to the paper: https://doi.org/10.1039/D2SC01905A

6.1 Crystal Data and Structure Refinement

6.1.1 Crystal data and structure refinement for compound 126

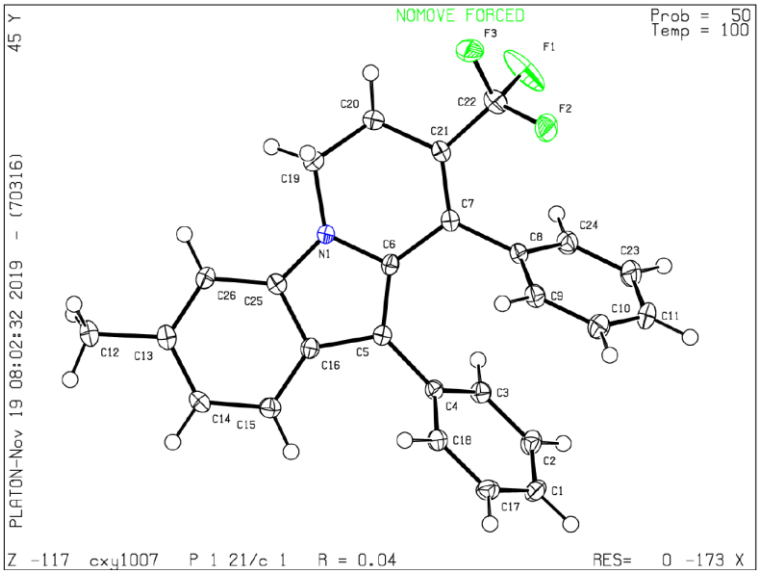

Table 6 Crystal data and structure refinement for compound 126.

Identification code	cxy1007
Empirical formula	$C_{26}H_{20}F_3N$
Formula weight	403.43
Temperature/K	100
Crystal system	monoclinic
Space group	$P2_1/c$
a/Å	15.0390(6)
b/Å	12.9170(5)
c/Å	10.3145(4)
α/°	90
β/°	99.2940(10)

γ/°	90
Volume/Å^3	1977.38(13)
Z	4
ρ_{calc}g/cm^3	1.355
μ/mm^{-1}	0.098
F(000)	840.0
Crystal size/mm^3	0.32 × 0.3 × 0.24
Radiation	MoKα (λ = 0.71073)
2Θ range for data collection/°	4.18 to 56.652
Index ranges	-19 ≤ h ≤ 20, -16 ≤ k ≤ 17, -12 ≤ l ≤ 13
Reflections collected	23642
Independent reflections	4904 [R_{int} = 0.0528, R_{sigma} = 0.0416]
Data/restraints/parameters	4904/0/273
Goodness-of-fit on F^2	1.027
Final R indexes [I>=2σ (I)]	R_1 = 0.0439, wR_2 = 0.0986
Final R indexes [all data]	R_1 = 0.0650, wR_2 = 0.1084
Largest diff. peak/hole / e Å^{-3}	0.29/-0.28

Table 7 Fractional Atomic Coordinates (× 10^4) and Equivalent Isotropic Displacement Parameters (Å^2 × 10^3) for compound 75. U_{eq} is defined as 1/3 of of the trace of the orthogonalised U_{IJ} tensor.

Atom	*x*	*y*	*z*	U(eq)
F1	8880.8(9)	6315.4(9)	7217.9(12)	53.2(4)
F2	8924.6(6)	6422.8(7)	5159.5(11)	33.4(3)

F3	10038.6(6)	5790.1(8)	6446.1(10)	32.1(2)
N1	8441.3(7)	2655.4(9)	5523.1(11)	14.9(2)
C1	4913.6(9)	4117.1(12)	1485.4(15)	20.9(3)
C2	5001.3(9)	4263.7(12)	2829.8(15)	20.5(3)
C3	5727.8(9)	3843.6(11)	3664.0(14)	17.4(3)
C4	6384.3(9)	3280.2(11)	3157.3(14)	14.9(3)
C5	7188.1(9)	2866.9(11)	4010.6(13)	14.1(3)
C6	7844.5(9)	3381.8(11)	4877.4(13)	14.5(3)
C7	8053.2(9)	4481.0(11)	5100.2(13)	14.7(3)
C8	7469.1(9)	5261.9(11)	4303.7(14)	16.1(3)
C9	7406.1(10)	5321.3(11)	2944.2(14)	19.1(3)
C10	6841.8(11)	6042.1(12)	2238.5(15)	24.5(3)
C11	6330.8(11)	6704.1(13)	2878.4(17)	28.0(4)
C12	8612.4(11)	-1201.9(12)	5127.8(16)	23.9(3)
C13	8215.3(10)	-147.6(11)	4769.6(14)	18.3(3)
C14	7429.2(9)	-53.2(11)	3824.4(14)	18.3(3)
C15	7029.2(9)	892.6(11)	3486.3(14)	17.5(3)
C16	7419.5(9)	1788.3(11)	4097.4(13)	14.7(3)
C17	5544.6(10)	3525.7(12)	974.3(14)	19.6(3)
C18	6271.8(9)	3105.8(11)	1805.2(14)	17.0(3)
C19	9289.4(10)	2911.5(12)	6348.4(15)	20.9(3)
C20	9208.7(10)	3948.1(12)	6994.8(15)	21.3(3)
C21	8754.2(9)	4738.9(11)	6031.9(14)	16.6(3)

C22	9126.9(10)	5810.1(12)	6203.0(15)	22.3(3)
C23	6391.1(11)	6651.3(12)	4229.8(16)	26.2(3)
C24	6957.5(10)	5933.6(12)	4936.7(15)	20.7(3)
C25	8204.7(9)	1687.3(11)	5047.1(13)	15.1(3)
C26	8609.3(9)	732.5(11)	5382.5(14)	17.4(3)

Table 8 Anisotropic Displacement Parameters ($Å^2 \times 10^3$) for compound 75. The Anisotropic displacement factor exponent takes the form: $-2\pi^2[h^2a^{*2}U_{11}+2hka^*b^*U_{12}+\cdots]$.

Atom	U_{11}	U_{22}	U_{33}	U_{23}	U_{13}	U_{12}
F1	78.1(9)	32.1(6)	61.0(8)	-28.3(6)	46.0(7)	-26.1(6)
F2	27.1(5)	19.1(5)	50.6(6)	12.7(4)	-3.7(4)	-5.8(4)
F3	23.0(5)	27.5(5)	42.1(6)	3.9(4)	-6.3(4)	-9.2(4)
N1	15.7(5)	12.4(6)	15.5(6)	0.7(4)	-0.3(4)	0.7(4)
C1	15.5(6)	20.7(8)	24.5(7)	5.6(6)	-2.4(6)	0.5(6)
C2	15.9(6)	19.9(7)	26.1(8)	3.0(6)	4.6(6)	3.2(6)
C3	18.0(6)	16.9(7)	17.3(7)	0.3(6)	3.3(5)	0.3(5)
C4	14.3(6)	12.7(6)	17.3(7)	1.9(5)	1.5(5)	-1.1(5)
C5	14.5(6)	14.3(7)	13.9(6)	0.8(5)	3.3(5)	0.9(5)
C6	16.1(6)	14.2(7)	13.6(6)	2.1(5)	3.4(5)	2.5(5)
C7	16.7(6)	13.6(7)	14.8(6)	0.9(5)	5.2(5)	1.1(5)
C8	17.3(6)	12.2(7)	18.6(7)	0.5(5)	2.2(5)	-0.5(5)
C9	23.1(7)	16.0(7)	18.6(7)	0.6(6)	4.4(6)	0.3(6)
C10	32.1(8)	20.9(8)	19.0(7)	5.3(6)	-0.9(6)	0.8(6)
C11	31.2(8)	18.5(8)	31.1(9)	5.2(7)	-4.6(7)	7.0(6)

C12	28.6(8)	14.0(7)	28.4(8)	0.6(6)	2.7(6)	2.9(6)
C13	22.6(7)	14.0(7)	19.5(7)	1.4(5)	6.7(6)	2.3(5)
C14	20.1(7)	14.5(7)	20.5(7)	-3.1(6)	4.4(6)	-2.4(5)
C15	17.1(6)	18.0(7)	17.2(7)	-0.1(6)	2.3(5)	-1.0(5)
C16	14.6(6)	14.8(7)	15.3(6)	0.9(5)	3.7(5)	1.5(5)
C17	20.8(7)	21.2(8)	16.0(7)	0.8(6)	0.2(5)	-2.9(6)
C18	17.3(6)	16.2(7)	17.7(7)	-0.4(5)	3.7(5)	1.1(5)
C19	19.2(7)	17.5(7)	23.4(7)	1.0(6)	-4.0(6)	0.5(6)
C20	23.2(7)	17.5(7)	21.0(7)	-1.2(6)	-3.3(6)	-1.2(6)
C21	19.0(6)	13.0(7)	18.0(7)	-1.0(5)	3.9(5)	0.0(5)
C22	24.0(7)	18.7(8)	24.9(8)	-2.0(6)	6.0(6)	-3.2(6)
C23	28.3(8)	20.0(8)	29.6(8)	-4.1(7)	2.1(7)	8.0(6)
C24	24.4(7)	18.2(7)	19.3(7)	-1.5(6)	2.7(6)	2.4(6)
C25	16.6(6)	14.6(7)	14.8(6)	-0.5(5)	4.6(5)	-0.6(5)
C26	17.3(6)	16.9(7)	17.7(7)	2.9(6)	1.8(5)	2.4(5)

Table 9 Bond Lengths for compound 75.

Atom	Atom	Length/Å	Atom	Atom	Length/Å
F1	C22	1.3357(18)	C8	C9	1.392(2)
F2	C22	1.3310(18)	C8	C24	1.390(2)
F3	C22	1.3537(17)	C9	C10	1.385(2)
N1	C6	1.3916(17)	C10	C11	1.386(2)
N1	C19	1.4527(17)	C11	C23	1.384(2)

N1	C25	1.3693(18)	C12	C13	1.509(2)
C1	C2	1.385(2)	C13	C14	1.411(2)
C1	C17	1.387(2)	C13	C26	1.386(2)
C2	C3	1.387(2)	C14	C15	1.381(2)
C3	C4	1.3944(19)	C15	C16	1.400(2)
C4	C5	1.4756(18)	C16	C25	1.4133(19)
C4	C18	1.3957(19)	C17	C18	1.386(2)
C5	C6	1.3896(19)	C19	C20	1.509(2)
C5	C16	1.4354(19)	C20	C21	1.509(2)
C6	C7	1.4642(19)	C21	C22	1.493(2)
C7	C8	1.4937(19)	C23	C24	1.384(2)
C7	C21	1.3486(19)	C25	C26	1.394(2)

Table 10 Bond Angles for compound 75.

Atom	Atom	Atom	Angle/°	Atom	Atom	Atom	Angle/°
C6	N1	C19	124.36(12)	C26	C13	C14	119.54(13)
C25	N1	C6	109.51(11)	C15	C14	C13	122.21(13)
C25	N1	C19	124.80(12)	C14	C15	C16	118.90(13)
C2	C1	C17	119.72(13)	C15	C16	C5	133.96(13)
C1	C2	C3	120.38(13)	C15	C16	C25	118.58(12)
C2	C3	C4	120.40(13)	C25	C16	C5	107.44(12)
C3	C4	C5	121.78(12)	C18	C17	C1	120.02(13)
C3	C4	C18	118.68(12)	C17	C18	C4	120.72(13)

C18	C4	C5	119.54(12)	N1	C19	C20	109.58(12)
C6	C5	C4	129.72(13)	C21	C20	C19	111.71(12)
C6	C5	C16	106.54(12)	C7	C21	C20	121.37(13)
C16	C5	C4	123.73(12)	C7	C21	C22	123.28(13)
N1	C6	C7	118.25(12)	C22	C21	C20	115.35(12)
C5	C6	N1	108.75(12)	F1	C22	F3	105.35(13)
C5	C6	C7	132.62(12)	F1	C22	C21	113.54(12)
C6	C7	C8	118.45(12)	F2	C22	F1	106.68(13)
C21	C7	C6	118.33(12)	F2	C22	F3	104.69(12)
C21	C7	C8	123.21(13)	F2	C22	C21	115.03(13)
C9	C8	C7	121.97(13)	F3	C22	C21	110.73(12)
C24	C8	C7	118.95(13)	C11	C23	C24	119.88(15)
C24	C8	C9	119.06(13)	C23	C24	C8	120.71(14)
C10	C9	C8	120.18(14)	N1	C25	C16	107.69(12)
C9	C10	C11	120.29(15)	N1	C25	C26	129.89(13)
C23	C11	C10	119.87(14)	C26	C25	C16	122.41(13)
C14	C13	C12	120.10(13)	C13	C26	C25	118.36(13)
C26	C13	C12	120.35(13)				

Table 11 Torsion Angles for compound 75.

A	**B**	**C**	**D**	**Angle/°**	**A**	**B**	**C**	**D**	**Angle/°**
N1	C6	C7	C8	173.61(12)	C8	C7	C21	C22	-11.6(2)
N1	C6	C7	C21	-7.57(19)	C8	C9	C10	C11	-0.5(2)

N1 C19 C20 C21 -45.19(17)	C9 C8 C24 C23 0.1(2)
N1 C25 C26 C13 178.20(14)	C9 C10 C11 C23 0.6(2)
C1 C2 C3 C4 0.8(2)	C10 C11 C23 C24 -0.4(2)
C1 C17 C18 C4 -0.7(2)	C11 C23 C24 C8 0.0(2)
C2 C1 C17 C18 -1.6(2)	C12 C13 C14 C15 178.49(14)
C2 C3 C4 C5 176.93(13)	C12 C13 C26 C25 -178.23(13)
C2 C3 C4 C18 -3.1(2)	C13 C14 C15 C16 0.3(2)
C3 C4 C5 C6 -57.1(2)	C14 C13 C26 C25 0.6(2)
C3 C4 C5 C16 121.55(15)	C14 C15 C16 C5 -178.75(14)
C3 C4 C18 C17 3.0(2)	C14 C15 C16 C25 -0.6(2)
C4 C5 C6 N1 176.42(13)	C15 C16 C25 N1 -178.40(12)
C4 C5 C6 C7 -11.0(3)	C15 C16 C25 C26 0.9(2)
C4 C5 C16 C15 0.8(2)	C16 C5 C6 N1 -2.42(15)
C4 C5 C16 C25 -177.57(12)	C16 C5 C6 C7 170.16(14)
C5 C4 C18 C17 -176.99(13)	C16 C25 C26 C13 -0.9(2)
C5 C6 C7 C8 1.6(2)	C17 C1 C2 C3 1.6(2)
C5 C6 C7 C21 -179.59(14)	C18 C4 C5 C6 122.94(16)
C5 C16 C25 N1 0.24(15)	C18 C4 C5 C16 -58.40(19)
C5 C16 C25 C26 179.50(13)	C19 N1 C6 C5 170.00(12)
C6 N1 C19 C20 30.88(19)	C19 N1 C6 C7 -3.81(19)
C6 N1 C25 C16 -1.75(15)	C19 N1 C25 C16 -169.03(12)
C6 N1 C25 C26 179.06(14)	C19 N1 C25 C26 11.8(2)
C6 C5 C16 C15 179.68(15)	C19 C20 C21 C7 38.93(19)

C6	C5	C16	C25	1.35(15)	C19	C20	C21	C22	-141.90(13)
C6	C7	C8	C9	-63.32(18)	C20	C21	C22	F1	-75.85(17)
C6	C7	C8	C24	115.17(15)	C20	C21	C22	F2	160.86(13)
C6	C7	C21	C20	-11.2(2)	C20	C21	C22	F3	42.43(17)
C6	C7	C21	C22	169.67(13)	C21	C7	C8	C9	117.92(16)
C7	C8	C9	C10	178.61(14)	C21	C7	C8	C24	-63.59(19)
C7	C8	C24	C23	-178.41(14)	C24	C8	C9	C10	0.1(2)
C7	C21	C22	F1	103.31(17)	C25	N1	C6	C5	2.65(15)
C7	C21	C22	F2	-20.0(2)	C25	N1	C6	C7	-171.16(12)
C7	C21	C22	F3	-138.42(14)	C25	N1	C19	C20	-163.68(13)
C8	C7	C21	C20	167.54(13)	C26	C13	C14	C15	-0.3(2)

Table 12 Hydrogen Atom Coordinates (Å×10^4) and Isotropic Displacement Parameters (Å^2 ×10^3) for compound 75.

Atom	*x*	*y*	*z*	U(eq)
H1	4423.33	4420.18	915.58	25
H2	4561.56	4654.32	3183.04	25
H3	5778.22	3940.37	4586.05	21
H9	7751.19	4866.02	2499.47	23
H10	6804.77	6083.05	1311.71	29
H11	5940.02	7193.21	2390.21	34
H12A	9254.76	-1197.96	5058.87	36
H12B	8301.18	-1721.43	4526.34	36
H12C	8539.28	-1371.25	6030.7	36

H14	7166.09	-660.44	3406.56	22
H15	6498.13	934.7	2849.73	21
H17	5478.53	3408.41	54.51	24
H18	6698.15	2694.93	1450.46	20
H19A	9776.81	2937.44	5808.66	25
H19B	9443.58	2371.62	7028.89	25
H20A	8857.11	3865.96	7721.18	26
H20B	9817.11	4199.08	7374.58	26
H23	6044.31	7106.7	4671.65	31
H24	6997.04	5899.61	5864.27	25
H26	9141.94	685.94	6015.51	21

6.1.2 Crystal data and structure refinement for compound 144

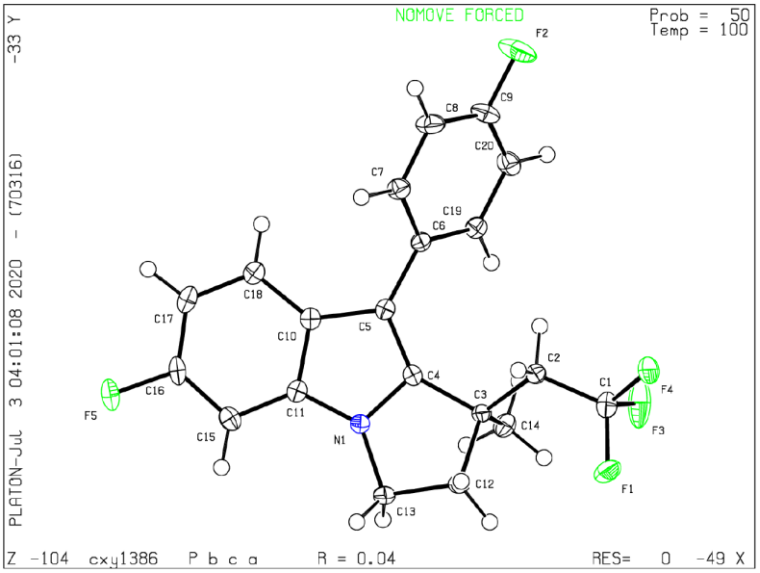

Table 13 Crystal data and structure refinement for compound 144.

Identification code	cxy1386

Empirical formula	$C_{20}H_{16}NF_5$
Formula weight	365.34
Temperature/K	100.0
Crystal system	orthorhombic
Space group	Pbca
a/Å	16.2053(8)
b/Å	11.4051(5)
c/Å	17.4590(8)
α/°	90
β/°	90
γ/°	90
Volume/Å^3	3226.8(3)
Z	8
ρ_{calc}g/cm^3	1.504
μ/mm^{-1}	0.128
F(000)	1504.0
Crystal size/mm^3	0.36 × 0.29 × 0.24
Radiation	MoKα (λ = 0.71073)
2Θ range for data collection/°	4.666 to 55.132
Index ranges	-20 ≤ h ≤ 21, -14 ≤ k ≤ 13, -21 ≤ l ≤ 22
Reflections collected	53244
Independent reflections	3713 [R_{int} = 0.0960, R_{sigma} = 0.0401]
Data/restraints/parameters	3713/0/237

Goodness-of-fit on F^2	1.050
Final R indexes [I>=2σ (I)]	R_1 = 0.0411, wR_2 = 0.0961
Final R indexes [all data]	R_1 = 0.0627, wR_2 = 0.1040
Largest diff. peak/hole / e $Å^{-3}$	0.29/-0.26

Table 14 Fractional Atomic Coordinates ($\times 10^4$) and Equivalent Isotropic Displacement Parameters ($Å^2 \times 10^3$) for compound 88. U_{eq} is defined as 1/3 of of the trace of the orthogonalised U_{IJ} tensor.

Atom	*x*	*y*	*z*	U(eq)
F1	1675.1(7)	3824.4(11)	6395.3(6)	35.9(3)
F2	6379.3(7)	6011.2(10)	7791.9(7)	40.5(3)
F3	2794.6(9)	2840.8(10)	6525.8(7)	48.1(4)
F4	2401.8(6)	3992.7(9)	7418.4(5)	26.9(3)
F5	3979.0(7)	9644.4(9)	2893.3(6)	27.7(3)
N1	3127.6(8)	6414.3(12)	4508.4(7)	15.1(3)
C1	2450.6(11)	3893.3(15)	6651.0(9)	21.5(4)
C2	2931.4(10)	4883.0(14)	6307.9(9)	15.5(3)
C3	2960.4(10)	4926.1(13)	5426.8(8)	14.1(3)
C4	3484.6(10)	5948.8(13)	5157.4(8)	13.7(3)
C5	4191.8(10)	6556.5(13)	5335.7(8)	14.1(3)
C6	4764.9(9)	6391.1(14)	5980.8(9)	14.6(3)
C7	5039.0(10)	7362.7(15)	6398.0(9)	19.0(4)
C8	5589.1(11)	7245.6(16)	7004.0(10)	24.9(4)

C9	5855.1(11)	6135.5(17)	7190.3(10)	24.7(4)
C10	4268.4(10)	7453.8(14)	4750.5(9)	15.0(3)
C11	3593.2(10)	7326.3(13)	4239.4(9)	15.1(3)
C12	2115.2(10)	5259.8(14)	5057.0(9)	17.1(3)
C13	2341.7(10)	5874.3(14)	4300.9(9)	17.8(3)
C14	3285.0(11)	3780.1(14)	5067.4(9)	19.6(4)
C15	3478.1(10)	8048.4(14)	3601.4(9)	18.3(3)
C16	4068.4(11)	8897.4(14)	3498.8(9)	19.5(4)
C17	4746.0(11)	9053.7(15)	3971.8(10)	21.0(4)
C18	4852.4(10)	8332.4(14)	4602.1(9)	17.9(3)
C19	5067.1(10)	5285.7(14)	6188.0(9)	16.4(3)
C20	5608.0(10)	5152.5(15)	6798.5(9)	21.0(4)

Table 15 Anisotropic Displacement Parameters ($Å^2 \times 10^3$) for compound 88. The Anisotropic displacement factor exponent takes the form: $-2\pi^2[h^2a^{*2}U_{11}+2hka^*b^*U_{12}+\cdots]$.

Atom	U_{11}	U_{22}	U_{33}	U_{23}	U_{13}	U_{12}
F1	29.2(6)	50.0(7)	28.5(6)	7.0(5)	-3.5(5)	-23.1(5)
F2	40.4(7)	41.0(7)	40.1(7)	-5.8(5)	-26.2(6)	11.2(6)
F3	79.0(10)	17.3(5)	47.9(7)	9.8(5)	27.5(7)	10.5(6)
F4	29.1(6)	33.8(6)	17.7(5)	7.4(4)	2.4(4)	-5.1(5)
F5	35.8(6)	24.6(5)	22.8(5)	11.7(4)	3.2(4)	1.5(5)
N1	15.9(7)	15.0(6)	14.3(6)	0.2(5)	-1.2(5)	-1.3(5)
C1	25.4(9)	18.8(8)	20.3(8)	1.6(7)	3.4(7)	-0.8(7)
C2	14.1(8)	16.5(8)	16.0(7)	0.4(6)	0.3(6)	-0.3(6)

C3	13.0(8)	15.4(7)	14.0(7)	0.0(6)	-0.6(6)	-0.8(6)
C4	15.0(8)	13.6(7)	12.4(7)	-0.9(6)	1.7(6)	2.7(6)
C5	15.8(8)	11.7(7)	14.8(7)	-2.2(6)	2.3(6)	0.9(6)
C6	10.4(7)	17.1(7)	16.1(7)	0.6(6)	2.1(6)	0.5(6)
C7	16.6(8)	16.6(8)	23.9(8)	-0.8(7)	-1.8(7)	1.5(6)
C8	21.8(9)	23.2(9)	29.8(9)	-6.0(8)	-8.5(7)	-1.3(7)
C9	18.3(9)	32.9(10)	22.7(8)	-1.0(7)	-8.5(7)	4.3(8)
C10	15.3(8)	14.1(7)	15.5(7)	-1.5(6)	3.0(6)	3.0(6)
C11	17.1(8)	12.9(7)	15.4(7)	-2.5(6)	3.6(6)	1.2(6)
C12	15.3(8)	18.8(8)	17.1(7)	-0.8(6)	-1.6(6)	-1.7(6)
C13	18.5(9)	18.1(8)	16.9(7)	-0.9(6)	-4.1(6)	-3.1(7)
C14	21.1(9)	17.0(8)	20.8(8)	-2.0(6)	2.8(7)	-2.0(7)
C15	21.5(9)	18.6(8)	14.7(7)	-0.7(6)	1.2(6)	3.8(7)
C16	27.5(9)	14.6(8)	16.2(8)	5.0(6)	6.2(7)	4.1(7)
C17	21.3(9)	15.5(8)	26.0(9)	2.4(7)	6.6(7)	-2.1(7)
C18	16.4(8)	15.9(8)	21.3(8)	-0.5(6)	2.0(6)	0.6(6)
C19	14.2(8)	16.8(8)	18.2(7)	-0.7(6)	2.0(6)	1.1(6)
C20	17.8(9)	22.3(9)	23.0(8)	2.5(7)	-0.4(7)	6.6(7)

Table 16 Bond Lengths for compound 88.

Atom	Atom	Length/Å	Atom	Atom	Length/Å
F1	C1	1.336(2)	C5	C10	1.452(2)
F2	C9	1.3583(19)	C6	C7	1.398(2)

F3	C1	1.341(2)	C6	C19	1.400(2)
F4	C1	1.3470(19)	C7	C8	1.390(2)
F5	C16	1.3654(18)	C8	C9	1.376(3)
N1	C4	1.3785(19)	C9	C20	1.373(2)
N1	C11	1.368(2)	C10	C11	1.419(2)
N1	C13	1.460(2)	C10	C18	1.402(2)
C1	C2	1.497(2)	C11	C15	1.398(2)
C2	C3	1.540(2)	C12	C13	1.539(2)
C3	C4	1.518(2)	C15	C16	1.373(2)
C3	C12	1.561(2)	C16	C17	1.385(2)
C3	C14	1.542(2)	C17	C18	1.385(2)
C4	C5	1.375(2)	C19	C20	1.388(2)
C5	C6	1.472(2)			

Table 17 Bond Angles for compound 88.

Atom	Atom	Atom	Angle/°	Atom	Atom	Atom	Angle/°
C4	N1	C13	114.05(13)	C7	C6	C19	117.89(14)
C11	N1	C4	110.09(13)	C19	C6	C5	122.27(14)
C11	N1	C13	135.76(13)	C8	C7	C6	121.60(16)
F1	C1	F3	106.49(15)	C9	C8	C7	117.97(16)
F1	C1	F4	106.39(14)	F2	C9	C8	118.33(16)
F1	C1	C2	113.60(14)	F2	C9	C20	118.85(16)
F3	C1	F4	105.18(13)	C20	C9	C8	122.82(15)

F3	C1	C2	113.16(14)	C11	C10	C5	107.72(14)
F4	C1	C2	111.42(14)	C18	C10	C5	133.75(15)
C1	C2	C3	116.09(13)	C18	C10	C11	118.52(14)
C2	C3	C12	113.21(13)	N1	C11	C10	106.69(13)
C2	C3	C14	112.94(13)	N1	C11	C15	130.39(15)
C4	C3	C2	110.57(12)	C15	C11	C10	122.92(15)
C4	C3	C12	100.11(12)	C13	C12	C3	104.86(12)
C4	C3	C14	109.53(12)	N1	C13	C12	100.79(12)
C14	C3	C12	109.73(13)	C16	C15	C11	115.25(15)
N1	C4	C3	108.41(13)	F5	C16	C15	117.85(15)
C5	C4	N1	109.98(13)	F5	C16	C17	117.73(15)
C5	C4	C3	141.60(14)	C15	C16	C17	124.42(15)
C4	C5	C6	129.39(14)	C18	C17	C16	119.73(15)
C4	C5	C10	105.50(13)	C17	C18	C10	119.16(16)
C10	C5	C6	125.10(14)	C20	C19	C6	121.18(15)
C7	C6	C5	119.82(14)	C9	C20	C19	118.51(15)

Table 18 Torsion Angles for compound 88.

A	**B**	**C**	**D**	**Angle/°**	**A**	**B**	**C**	**D**	**Angle/°**
F1	C1	C2	C3	-54.38(19)	C6	C5	C10	C18	2.2(3)
F2	C9	C20	C19	179.51(15)	C6	C7	C8	C9	-0.6(3)
F3	C1	C2	C3	67.2(2)	C6	C19	C20	C9	-1.2(2)
F4	C1	C2	C3	-174.51(14)	C7	C6	C19	C20	1.4(2)

F5	C16	C17	C18	178.64(14)	C7	C8	C9	F2	-178.66(16)
N1	C4	C5	C6	178.79(15)	C7	C8	C9	C20	0.8(3)
N1	C4	C5	C10	-0.11(17)	C8	C9	C20	C19	0.1(3)
N1	C11	C15	C16	179.55(15)	C10	C5	C6	C7	44.6(2)
C1	C2	C3	C4	-178.48(13)	C10	C5	C6	C19	-133.92(17)
C1	C2	C3	C12	70.12(18)	C10	C11	C15	C16	0.1(2)
C1	C2	C3	C14	-55.36(19)	C11	N1	C4	C3	-178.81(12)
C2	C3	C4	N1	-143.02(13)	C11	N1	C4	C5	0.70(17)
C2	C3	C4	C5	37.7(3)	C11	N1	C13	C12	-158.59(17)
C2	C3	C12	C13	151.10(13)	C11	C10	C18	C17	0.9(2)
C3	C4	C5	C6	-2.0(3)	C11	C15	C16	F5	-178.70(14)
C3	C4	C5	C10	179.13(18)	C11	C15	C16	C17	0.8(2)
C3	C12	C13	N1	-31.11(15)	C12	C3	C4	N1	-23.39(15)
C4	N1	C11	C10	-0.99(17)	C12	C3	C4	C5	157.4(2)
C4	N1	C11	C15	179.53(16)	C13	N1	C4	C3	4.26(17)
C4	N1	C13	C12	17.27(17)	C13	N1	C4	C5	-176.23(13)
C4	C3	C12	C13	33.41(14)	C13	N1	C11	C10	175.00(16)
C4	C5	C6	C7	-134.09(17)	C13	N1	C11	C15	-4.5(3)
C4	C5	C6	C19	47.4(2)	C14	C3	C4	N1	91.89(15)
C4	C5	C10	C11	-0.48(17)	C14	C3	C4	C5	-87.4(2)
C4	C5	C10	C18	-178.79(17)	C14	C3	C12	C13	-81.72(15)
C5	C6	C7	C8	-179.09(15)	C15	C16	C17	C18	-0.8(3)
C5	C6	C19	C20	179.94(15)	C16	C17	C18	C10	-0.1(2)

C5	C10	C11	N1	0.90(17)
C5	C10	C11	C15	-179.57(14)
C5	C10	C18	C17	179.07(16)
C6	C5	C10	C11	-179.45(14)
C18	C10	C11	N1	179.50(13)
C18	C10	C11	C15	-1.0(2)
C19	C6	C7	C8	-0.5(2)

Table 19 Hydrogen Atom Coordinates (Å×10^4) and Isotropic Displacement Parameters (Å^2 ×10^3) for compound 88.

Atom	*x*	*y*	*z*	U(eq)
H2A	3504.87	4838.06	6501.14	19
H2B	2692.87	5629.23	6494.66	19
H7	4844.57	8121.18	6263.84	23
H8	5775.7	7911.46	7281.28	30
H12A	1779.3	4550.54	4958.87	20
H12B	1800.69	5793.92	5395.58	20
H13A	2407.28	5305.37	3876.99	21
H13B	1925.37	6469.77	4156.39	21
H14A	3359.82	3890.81	4515.16	29
H14B	2886.56	3148.46	5157.09	29
H14C	3814.83	3572.97	5301.75	29
H15	3023.64	7958.05	3262.75	22
H17	5136.08	9653.25	3864.12	25
H18	5315.11	8431.39	4929.92	21
H19	4899.05	4614.72	5905.82	20
H20	5802.77	4398.21	6941.94	25

6.1.3 Crystal data and structure refinement for compound 155

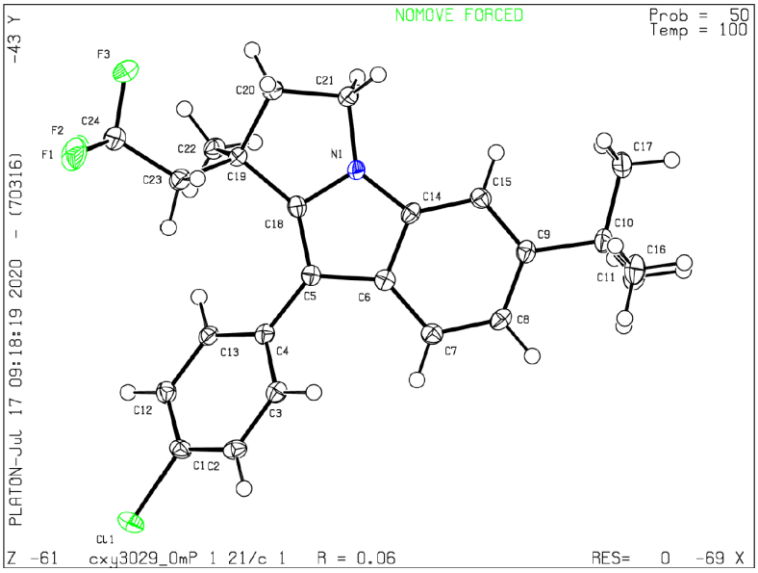

Table 20 Crystal data and structure refinement for compound 155.

Identification code	cxy3029_0m
Empirical formula	$C_{24}H_{25}ClF_3N$
Formula weight	419.90
Temperature/K	100.0
Crystal system	monoclinic
Space group	$P2_1/c$
a/Å	5.9225(3)
b/Å	14.7827(8)
c/Å	23.7371(12)
α/°	90
β/°	90.671(2)
γ/°	90
Volume/Å^3	2078.05(19)

Z	4
ρ_{calc}g/cm^3	1.342
μ/mm^{-1}	1.940
F(000)	880.0
Crystal size/mm^3	0.35 × 0.31 × 0.29
Radiation	CuKα (λ = 1.54178)
2Θ range for data collection/°	7.044 to 144.442
Index ranges	-7 ≤ h ≤ 7, -18 ≤ k ≤ 18, -29 ≤ l ≤ 29
Reflections collected	53982
Independent reflections	4089 [R_{int} = 0.0397, R_{sigma} = 0.0202]
Data/restraints/parameters	4089/0/267
Goodness-of-fit on F^2	1.243
Final R indexes [I>=2σ (I)]	R_1 = 0.0562, wR_2 = 0.1306
Final R indexes [all data]	R_1 = 0.0569, wR_2 = 0.1308
Largest diff. peak/hole / e Å^{-3}	0.31/-0.31

Table 21 Fractional Atomic Coordinates (× 10^4) and Equivalent Isotropic Displacement Parameters (Å^2 × 10^3) for compound 99. U_{eq} is defined as 1/3 of of the trace of the orthogonalised U_{IJ} tensor.

Atom	*x*	*y*	*z*	U(eq)
Cl1	-3224.4(11)	219.1(4)	1532.3(3)	23.42(18)
F1	1197(3)	4815.9(14)	570.7(8)	37.3(5)
F2	3806(3)	3866.7(12)	362.8(7)	32.1(4)
F3	4706(3)	5175.2(12)	691.6(7)	34.6(4)

N1	6430(4)	3855.8(14)	2584.7(8)	15.3(4)
C1	-1309(4)	1023.4(17)	1780.2(11)	17.6(5)
C2	-1664(4)	1429.3(17)	2297.3(11)	18.0(5)
C3	-57(4)	2032.6(17)	2508.3(11)	16.8(5)
C4	1918(4)	2234.1(16)	2212.3(10)	14.8(5)
C5	3642(4)	2839.2(17)	2455.4(10)	14.6(5)
C6	4415(4)	2816.0(17)	3039.0(10)	15.4(5)
C7	3875(4)	2295.3(17)	3514.9(11)	17.3(5)
C8	5069(4)	2427.3(18)	4011.0(11)	18.5(5)
C9	6832(4)	3071.8(17)	4063.4(10)	16.9(5)
C10	8059(5)	3170.3(19)	4634.8(10)	19.5(5)
C11	9069(5)	2261(2)	4815.6(12)	24.9(6)
C12	603(4)	1212.8(17)	1469.4(11)	17.7(5)
C13	2198(4)	1812.7(17)	1687.4(10)	16.0(5)
C14	6175(4)	3452.9(17)	3098.6(10)	15.1(5)
C15	7388(4)	3589.2(17)	3602.2(10)	16.8(5)
C16	6346(5)	3491(2)	5076.3(11)	26.6(6)
C17	9983(5)	3863(2)	4610.4(12)	25.0(6)
C18	4952(4)	3488.4(17)	2200.1(10)	15.4(5)
C19	5360(4)	3926.3(17)	1629.4(10)	15.9(5)
C20	6641(4)	4800.6(18)	1812.8(11)	18.6(5)
C21	7866(4)	4567.9(18)	2369.3(10)	18.5(5)
C22	6941(4)	3328.1(18)	1274.8(11)	17.9(5)

C23	3095(4)	4130.6(18)	1331.7(11)	18.8(5)
C24	3219(5)	4500(2)	740.8(12)	23.8(6)

Table 22 Anisotropic Displacement Parameters ($Å^2 \times 10^3$) for compound 99. The Anisotropic displacement factor exponent takes the form: $-2\pi^2[h^2a^{*2}U_{11}+2hka^*b^*U_{12}+\cdots]$.

Atom	U_{11}	U_{22}	U_{33}	U_{23}	U_{13}	U_{12}
Cl1	21.2(3)	18.8(3)	30.3(4)	-3.2(3)	-2.0(2)	-5.6(2)
F1	33.1(10)	46.3(11)	32.1(10)	14.9(8)	-10.3(8)	5.7(8)
F2	42.2(10)	37.2(10)	16.9(8)	-0.8(7)	-3.0(7)	-3.0(8)
F3	44.2(11)	32.3(10)	27.0(9)	13.2(7)	-6.0(8)	-15.5(8)
N1	18.9(10)	15.3(10)	11.6(10)	-0.8(8)	-0.3(8)	-2.0(8)
C1	18.2(12)	11.3(12)	23.2(13)	2.4(10)	-4.4(10)	-1.4(9)
C2	16.3(12)	15.3(12)	22.5(13)	4.1(10)	1.5(10)	0.9(10)
C3	19.1(12)	14.3(12)	16.9(12)	1.1(9)	0.7(9)	3.0(10)
C4	18.3(12)	10.0(11)	15.9(12)	1.5(9)	-1.1(9)	3.4(9)
C5	15.8(12)	13.7(11)	14.2(11)	-1.8(9)	0.9(9)	2.3(9)
C6	17.0(12)	13.1(12)	16.3(12)	-1.6(9)	1.2(9)	3.0(9)
C7	20.2(12)	12.8(12)	18.8(12)	-1.3(10)	0.7(10)	0.5(9)
C8	23.4(13)	15.9(12)	16.4(12)	3.3(10)	2.8(10)	1.2(10)
C9	21.3(12)	15.1(12)	14.3(12)	-1.7(9)	-0.2(10)	2.9(10)
C10	23.6(13)	22.6(13)	12.3(12)	-0.8(10)	-1.6(10)	0.3(11)
C11	26.8(14)	27.2(15)	20.5(13)	4.0(11)	-3.4(11)	-0.2(12)
C12	21.1(13)	16.1(12)	15.7(12)	-1.2(10)	-1.5(10)	1.1(10)
C13	18.5(12)	15.0(12)	14.6(11)	2.8(9)	0.6(9)	-0.3(10)

C14	18.9(12)	14.0(12)	12.4(11)	0.6(9)	3.3(9)	3.1(9)
C15	19.1(12)	14.6(12)	16.8(12)	-2.2(10)	0.4(9)	-0.9(10)
C16	32.5(15)	31.2(16)	16.0(13)	-3.7(11)	-1.3(11)	3.2(12)
C17	31.2(15)	25.4(14)	18.3(13)	1.2(11)	-7.3(11)	-3.2(12)
C18	16.7(12)	15.4(12)	14.1(12)	-3.0(9)	-0.2(9)	2.2(9)
C19	18.2(12)	15.9(12)	13.7(11)	1.9(9)	0.1(9)	-2.0(10)
C20	22.1(13)	16.6(13)	17.0(12)	1.3(10)	0.4(10)	-3.2(10)
C21	23.2(13)	17.7(13)	14.6(12)	0.8(10)	0.5(10)	-3.8(10)
C22	19.5(12)	17.8(13)	16.3(12)	-0.6(10)	3.3(10)	0.0(10)
C23	19.5(13)	19.4(13)	17.7(12)	3.2(10)	0.3(10)	-0.3(10)
C24	24.5(14)	24.8(14)	21.8(14)	4.9(11)	-3.7(11)	-2.5(11)

Table 23 Bond Lengths for compound 99.

Atom	Atom	Length/Å	Atom	Atom	Length/Å
Cl1	C1	1.741(3)	C6	C14	1.410(4)
F1	C24	1.343(3)	C7	C8	1.380(4)
F2	C24	1.345(3)	C8	C9	1.418(4)
F3	C24	1.337(3)	C9	C10	1.538(3)
N1	C14	1.367(3)	C9	C15	1.379(4)
N1	C18	1.370(3)	C10	C11	1.530(4)
N1	C21	1.450(3)	C10	C16	1.542(4)
C1	C2	1.385(4)	C10	C17	1.533(4)
C1	C12	1.387(4)	C12	C13	1.391(4)

C2	C3	1.393(4)	C14	C15	1.402(3)
C3	C4	1.404(4)	C18	C19	1.523(3)
C4	C5	1.470(3)	C19	C20	1.558(3)
C4	C13	1.405(3)	C19	C22	1.544(3)
C5	C6	1.454(3)	C19	C23	1.539(3)
C5	C18	1.379(4)	C20	C21	1.539(3)
C6	C7	1.407(4)	C23	C24	1.508(4)

Table 24 Bond Angles for compound 99.

Atom	Atom	Atom	Angle/°	Atom	Atom	Atom	Angle/°
C14	N1	C18	110.2(2)	C17	C10	C9	111.9(2)
C14	N1	C21	134.6(2)	C17	C10	C16	108.4(2)
C18	N1	C21	115.2(2)	C1	C12	C13	119.1(2)
C2	C1	Cl1	119.4(2)	C12	C13	C4	121.7(2)
C2	C1	C12	121.2(2)	N1	C14	C6	106.9(2)
C12	C1	Cl1	119.4(2)	N1	C14	C15	129.6(2)
C1	C2	C3	119.1(2)	C15	C14	C6	123.5(2)
C2	C3	C4	121.7(2)	C9	C15	C14	118.2(2)
C3	C4	C5	120.8(2)	N1	C18	C5	110.0(2)
C3	C4	C13	117.2(2)	N1	C18	C19	108.5(2)
C13	C4	C5	122.0(2)	C5	C18	C19	141.5(2)
C6	C5	C4	124.7(2)	C18	C19	C20	100.72(19)
C18	C5	C4	130.0(2)	C18	C19	C22	110.2(2)

C18	C5	C6	105.2(2)	C18	C19	C23	110.2(2)
C7	C6	C5	134.9(2)	C22	C19	C20	109.3(2)
C7	C6	C14	117.4(2)	C23	C19	C20	112.6(2)
C14	C6	C5	107.7(2)	C23	C19	C22	113.1(2)
C8	C7	C6	119.2(2)	C21	C20	C19	106.1(2)
C7	C8	C9	122.6(2)	N1	C21	C20	101.1(2)
C8	C9	C10	118.7(2)	C24	C23	C19	116.5(2)
C15	C9	C8	119.1(2)	F1	C24	F2	106.1(2)
C15	C9	C10	122.2(2)	F1	C24	C23	110.6(2)
C9	C10	C16	108.7(2)	F2	C24	C23	112.6(2)
C11	C10	C9	110.1(2)	F3	C24	F1	107.4(2)
C11	C10	C16	109.7(2)	F3	C24	F2	106.6(2)
C11	C10	C17	108.0(2)	F3	C24	C23	113.0(2)

Table 25 Torsion Angles for compound 99.

A	**B**	**C**	**D**	**Angle/°**	**A**	**B**	**C**	**D**	**Angle/°**
Cl1	C1	C2	C3	176.26(19)	C8	C9	C10	C16	-63.0(3)
Cl1	C1	C12	C13	-175.89(19)	C8	C9	C10	C17	177.4(2)
N1	C14	C15	C9	-178.2(2)	C8	C9	C15	C14	0.0(4)
N1	C18	C19	C20	-19.3(3)	C10	C9	C15	C14	-179.9(2)
N1	C18	C19	C22	96.1(2)	C12	C1	C2	C3	-0.5(4)
N1	C18	C19	C23	-138.4(2)	C13	C4	C5	C6	-135.1(3)
C1	C2	C3	C4	-0.5(4)	C13	C4	C5	C18	40.5(4)

C1	C12	C13	C4	-0.3(4)	C14	N1	C18	C5	1.1(3)
C2	C1	C12	C13	0.9(4)	C14	N1	C18	C19	-177.6(2)
C2	C3	C4	C5	-177.1(2)	C14	N1	C21	C20	-164.2(3)
C2	C3	C4	C13	1.0(4)	C14	C6	C7	C8	0.0(4)
C3	C4	C5	C6	42.9(4)	C15	C9	C10	C11	-122.8(3)
C3	C4	C5	C18	-141.5(3)	C15	C9	C10	C16	117.0(3)
C3	C4	C13	C12	-0.6(4)	C15	C9	C10	C17	-2.7(4)
C4	C5	C6	C7	-0.6(4)	C18	N1	C14	C6	-1.5(3)
C4	C5	C6	C14	175.9(2)	C18	N1	C14	C15	177.0(3)
C4	C5	C18	N1	-176.6(2)	C18	N1	C21	C20	15.2(3)
C4	C5	C18	C19	1.5(5)	C18	C5	C6	C7	-177.1(3)
C5	C4	C13	C12	177.4(2)	C18	C5	C6	C14	-0.6(3)
C5	C6	C7	C8	176.3(3)	C18	C19	C20	C21	28.2(2)
C5	C6	C14	N1	1.2(3)	C18	C19	C23	C24	-175.4(2)
C5	C6	C14	C15	-177.4(2)	C19	C20	C21	N1	-26.7(3)
C5	C18	C19	C20	162.6(3)	C19	C23	C24	F1	-167.7(2)
C5	C18	C19	C22	-82.0(4)	C19	C23	C24	F2	73.7(3)
C5	C18	C19	C23	43.5(4)	C19	C23	C24	F3	-47.2(3)
C6	C5	C18	N1	-0.3(3)	C20	C19	C23	C24	73.1(3)
C6	C5	C18	C19	177.7(3)	C21	N1	C14	C6	178.0(3)
C6	C7	C8	C9	0.1(4)	C21	N1	C14	C15	-3.6(5)
C6	C14	C15	C9	0.1(4)	C21	N1	C18	C5	-178.4(2)
C7	C6	C14	N1	178.5(2)	C21	N1	C18	C19	2.9(3)

C7	C6	C14	C15	-0.1(4)	C22	C19	C20	C21	-87.8(2)
C7	C8	C9	C10	179.8(2)	C22	C19	C23	C24	-51.5(3)
C7	C8	C9	C15	-0.1(4)	C23	C19	C20	C21	145.5(2)
C8	C9	C10	C11	57.2(3)					

Table 26 Hydrogen Atom Coordinates (Å×10^4) and Isotropic Displacement Parameters (Å^2 ×10^3) for compound 99.

Atom	*x*	*y*	*z*	U(eq)
H2	-2985.58	1298.34	2505.24	22
H3	-304.94	2315.03	2861.7	20
H7	2701.34	1857.79	3495	21
H8	4694.55	2072.03	4330.09	22
H11A	10168.29	2062.97	4536.02	37
H11B	7862.21	1810.42	4843.58	37
H11C	9822.79	2328.15	5182.96	37
H12	819.5	936.65	1112.72	21
H13	3511.06	1940.75	1475.57	19
H15	8562.05	4026.23	3624.95	20
H16A	5129	3045.4	5106.67	40
H16B	5711.14	4075.43	4960.21	40
H16C	7108.72	3557.17	5442.61	40
H17A	10727.54	3903.16	4980.43	38
H17B	9368.48	4456.33	4506.48	38
H17C	11081.82	3672.28	4328.75	38

H20A 7739.89	4980.66	1522.41	22
H20B 5565.91	5304.71	1868.81	22
H21A 9419.41	4347.99	2303.25	22
H21B 7921.62	5093.9	2627.22	22
H22A 8225.99	3131.47	1508.23	27
H22B 7491.65	3676.31	953.06	27
H22C 6109.54	2797.06	1138.25	27
H23A 2197.89	3565.62	1320.22	23
H23B 2258.69	4570.61	1564.5	23

6.1.4 Crystal data and structure refinement for compound 162

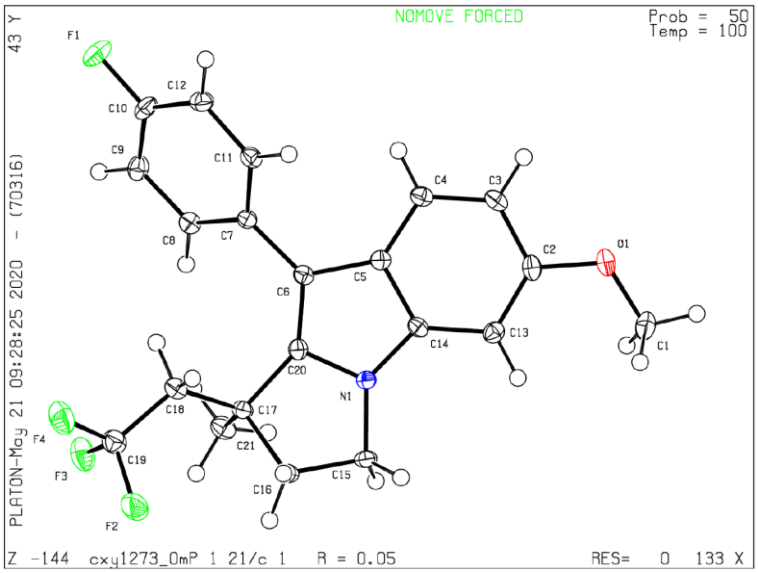

Table 27 Crystal data and structure refinement for compound 162.

Identification code	cxy1273_0m
Empirical formula	$C_{21}H_{19}F_4NO$
Formula weight	377.37

Temperature/K	100.0
Crystal system	monoclinic
Space group	$P2_1/c$
a/Å	9.8850(4)
b/Å	15.8544(7)
c/Å	11.3937(6)
α/°	90
β/°	106.016(2)
γ/°	90
Volume/Å^3	1716.32(14)
Z	4
ρ_{calc}g/cm^3	1.460
μ/mm^{-1}	0.119
F(000)	784.0
Crystal size/mm^3	0.35 × 0.34 × 0.29
Radiation	MoKα (λ = 0.71073)
2Θ range for data collection/°	4.52 to 54.976
Index ranges	-12 ≤ h ≤ 12, -20 ≤ k ≤ 20, -13 ≤ l ≤ 14
Reflections collected	16025
Independent reflections	3927 [R_{int} = 0.0678, R_{sigma} = 0.0519]
Data/restraints/parameters	3927/0/247
Goodness-of-fit on F^2	1.041
Final R indexes [I>=2σ (I)]	R_1 = 0.0481, wR_2 = 0.1192

Final R indexes [all data] $R_1 = 0.0744$, $wR_2 = 0.1292$

Largest diff. peak/hole / e $Å^{-3}$ 0.59/-0.34

Table 28 Fractional Atomic Coordinates ($\times 10^4$) and Equivalent Isotropic Displacement Parameters ($Å^2 \times 10^3$) for compound 106. U_{eq} is defined as 1/3 of of the trace of the orthogonalised U_{IJ} tensor.

Atom	*x*	*y*	*z*	U(eq)
F1	10075.6(13)	6567.2(8)	5423.4(12)	27.6(3)
F2	7557.2(16)	1532.5(9)	6547.1(13)	39.4(4)
F3	7789.9(14)	2601.8(9)	7731.1(11)	30.9(3)
F4	9432.7(13)	2291.5(9)	6908.3(12)	32.7(3)
O1	1193.7(15)	4339.5(10)	-608.6(12)	23.2(3)
N1	4099.4(16)	3208.9(10)	3316.0(14)	14.2(3)
C1	-3(2)	3830.1(15)	-649(2)	27.7(5)
C2	2303.8(19)	4286.4(13)	427.7(16)	17.2(4)
C3	3306(2)	4933.1(13)	533.1(17)	17.3(4)
C4	4473(2)	4977.2(12)	1528.0(16)	15.8(4)
C5	4675.0(19)	4366.9(12)	2450.4(16)	13.7(4)
C6	5726.4(19)	4244.0(12)	3610.3(16)	13.2(4)
C7	6915.9(19)	4817.9(12)	4113.0(16)	13.4(4)
C8	7269(2)	5088.2(13)	5333.4(17)	15.9(4)
C9	8347(2)	5665.1(13)	5784.4(17)	18.2(4)
C10	9047.4(19)	5986.9(13)	4993.7(18)	18.0(4)
C11	7683(2)	5153.2(12)	3358.0(16)	15.9(4)

C12	8739(2)	5744.5(13)	3785.0(17)	18.0(4)
C13	2459.8(19)	3662.9(13)	1306.1(16)	15.8(4)
C14	3663.7(19)	3712.8(12)	2306.8(16)	13.6(4)
C15	3647(2)	2408.1(12)	3713.7(17)	16.4(4)
C16	5013(2)	2117.9(13)	4652.9(17)	18.2(4)
C17	5771.3(19)	2945.3(12)	5198.5(16)	14.8(4)
C18	7381(2)	2878.6(13)	5610.0(17)	18.6(4)
C19	8027(2)	2328.4(14)	6694.4(18)	21.0(4)
C20	5319.5(19)	3525.1(12)	4098.8(16)	13.9(4)
C21	5153(2)	3260.7(13)	6229.8(17)	19.9(4)

Table 29 Anisotropic Displacement Parameters ($Å^2 \times 10^3$) for compound 106. The Anisotropic displacement factor exponent takes the form: $-2\pi^2[h^2a^{*2}U_{11}+2hka^*b^*U_{12}+\cdots]$.

Atom	U_{11}	U_{22}	U_{33}	U_{23}	U_{13}	U_{12}
F1	23.8(6)	25.9(7)	32.7(7)	-8.2(6)	7.1(5)	-12.7(5)
F2	53.0(9)	17.9(7)	34.4(8)	5.6(6)	-9.8(7)	-4.4(7)
F3	31.3(7)	43.0(9)	16.3(6)	0.3(6)	2.9(5)	3.2(6)
F4	25.1(6)	41.7(9)	28.5(7)	8.1(6)	2.9(5)	8.6(6)
O1	22.2(7)	27.6(8)	15.1(6)	2.5(6)	-2.8(6)	-1.0(6)
N1	15.4(7)	13.6(8)	13.2(7)	0.6(6)	3.5(6)	-2.4(6)
C1	19.5(10)	29.0(12)	27.5(11)	1.3(9)	-5.5(8)	-2.9(9)
C2	16.4(9)	21.1(10)	12.6(8)	-1.7(7)	1.7(7)	2.5(8)
C3	22.2(9)	15.7(10)	14.3(8)	3.8(7)	5.7(7)	2.3(8)
C4	19.6(9)	13.8(9)	14.8(8)	0.2(7)	6.4(7)	0.0(8)

C5	15.3(8)	13.3(9)	13.1(8)	-1.1(7)	5.1(7)	-0.2(7)
C6	16.6(8)	12.8(9)	11.0(8)	-0.8(7)	5.1(7)	0.4(7)
C7	13.7(8)	10.0(9)	15.6(8)	0.7(7)	2.7(7)	1.5(7)
C8	17.4(9)	15.6(10)	15.3(9)	-0.1(7)	5.4(7)	1.1(7)
C9	17.7(9)	18.0(10)	17.4(9)	-4.9(7)	2.3(7)	0.9(8)
C10	14.3(8)	13.5(9)	24.8(10)	-5.1(8)	2.8(7)	-2.8(8)
C11	19.5(9)	14.9(10)	13.3(8)	0.6(7)	4.7(7)	1.1(7)
C12	17.7(9)	16.7(10)	20.7(9)	2.3(7)	7.3(8)	-1.5(8)
C13	16.4(8)	16.3(9)	15.1(8)	-2.3(7)	5.0(7)	-1.7(7)
C14	16.7(8)	13.3(9)	11.7(8)	0.7(7)	5.3(7)	2.1(7)
C15	19.3(9)	13.7(9)	16.6(8)	1.1(7)	5.6(7)	-5.2(8)
C16	23.1(9)	14.5(9)	17.3(9)	2.4(7)	6.2(8)	-2.2(8)
C17	17.3(9)	12.8(9)	14.4(8)	2.1(7)	4.7(7)	-1.2(7)
C18	20.0(9)	18.9(10)	16.7(9)	3.7(8)	4.6(7)	-0.3(8)
C19	23.9(10)	18.7(10)	20.1(9)	0.9(8)	5.4(8)	0.8(8)
C20	14.7(8)	14.8(9)	12.0(8)	-1.6(7)	3.6(7)	0.4(7)
C21	24.4(10)	19.5(10)	17.2(9)	1.4(8)	8.0(8)	1.6(8)

Table 30 Bond Lengths for compound 106.

Atom	Atom	Length/Å	Atom	Atom	Length/Å
F1	C10	1.358(2)	C6	C7	1.472(3)
F2	C19	1.339(3)	C6	C20	1.376(3)
F3	C19	1.338(2)	C7	C8	1.404(2)

F4	C19	1.344(2)	C7	C11	1.399(2)
O1	C1	1.423(3)	C8	C9	1.391(3)
O1	C2	1.375(2)	C9	C10	1.377(3)
N1	C14	1.368(2)	C10	C12	1.380(3)
N1	C15	1.459(2)	C11	C12	1.388(3)
N1	C20	1.381(2)	C13	C14	1.405(3)
C2	C3	1.408(3)	C15	C16	1.544(3)
C2	C13	1.385(3)	C16	C17	1.553(3)
C3	C4	1.378(3)	C17	C18	1.534(3)
C4	C5	1.402(3)	C17	C20	1.518(3)
C5	C6	1.451(2)	C17	C21	1.550(3)
C5	C14	1.418(3)	C18	C19	1.503(3)

Table 31 Bond Angles for compound 106.

Atom	Atom	Atom	Angle/°	Atom	Atom	Atom	Angle/°
C2	O1	C1	116.90(16)	C10	C12	C11	118.38(17)
C14	N1	C15	135.76(16)	C2	C13	C14	116.54(18)
C14	N1	C20	110.31(15)	N1	C14	C5	106.35(16)
C20	N1	C15	113.78(15)	N1	C14	C13	130.45(18)
O1	C2	C3	113.88(17)	C13	C14	C5	123.17(17)
O1	C2	C13	124.59(18)	N1	C15	C16	100.94(15)
C13	C2	C3	121.52(17)	C15	C16	C17	105.01(16)
C4	C3	C2	121.11(18)	C18	C17	C16	114.17(16)

C3	C4	C5	119.72(18)	C18	C17	C21	112.57(16)
C4	C5	C6	133.91(18)	C20	C17	C16	100.46(14)
C4	C5	C14	117.91(17)	C20	C17	C18	109.77(15)
C14	C5	C6	108.16(16)	C20	C17	C21	110.04(15)
C5	C6	C7	124.45(16)	C21	C17	C16	109.17(15)
C20	C6	C5	105.29(16)	C19	C18	C17	117.43(16)
C20	C6	C7	130.22(17)	F2	C19	F4	106.68(18)
C8	C7	C6	121.84(16)	F2	C19	C18	112.95(17)
C11	C7	C6	120.39(16)	F3	C19	F2	106.08(17)
C11	C7	C8	117.66(17)	F3	C19	F4	106.14(16)
C9	C8	C7	121.49(17)	F3	C19	C18	113.55(17)
C10	C9	C8	118.32(18)	F4	C19	C18	110.94(16)
F1	C10	C9	118.46(17)	N1	C20	C17	108.59(15)
F1	C10	C12	119.04(17)	C6	C20	N1	109.88(16)
C9	C10	C12	122.50(18)	C6	C20	C17	141.52(17)
C12	C11	C7	121.61(17)				

Table 32 Torsion Angles for compound 106.

A	B	C	D	Angle/°	A	B	C	D	Angle/°
F1	C10	C12	C11	-179.79(17)	C11	C7	C8	C9	-0.3(3)
O1	C2	C3	C4	179.08(17)	C13	C2	C3	C4	-1.1(3)
O1	C2	C13	C14	-179.84(17)	C14	N1	C15	C16	157.5(2)
N1	C15	C16	C17	30.72(17)	C14	N1	C20	C6	-0.8(2)

C1	O1	C2	C3	-166.37(17)	C14	N1	C20	C17	-179.57(15)
C1	O1	C2	C13	13.8(3)	C14	C5	C6	C7	-177.05(16)
C2	C3	C4	C5	0.4(3)	C14	C5	C6	C20	0.8(2)
C2	C13	C14	N1	178.90(18)	C15	N1	C14	C5	-173.78(19)
C2	C13	C14	C5	1.1(3)	C15	N1	C14	C13	8.2(3)
C3	C2	C13	C14	0.3(3)	C15	N1	C20	C6	175.46(15)
C3	C4	C5	C6	-177.34(19)	C15	N1	C20	C17	-3.4(2)
C3	C4	C5	C14	1.0(3)	C15	C16	C17	C18	-149.87(15)
C4	C5	C6	C7	1.4(3)	C15	C16	C17	C20	-32.49(17)
C4	C5	C6	C20	179.26(19)	C15	C16	C17	C21	83.17(17)
C4	C5	C14	N1	180.00(16)	C16	C17	C18	C19	-68.2(2)
C4	C5	C14	C13	-1.8(3)	C16	C17	C20	N1	22.40(18)
C5	C6	C7	C8	133.50(19)	C16	C17	C20	C6	-155.8(2)
C5	C6	C7	C11	-42.6(3)	C17	C18	C19	F2	56.8(2)
C5	C6	C20	N1	-0.1(2)	C17	C18	C19	F3	-64.0(2)
C5	C6	C20	C17	178.1(2)	C17	C18	C19	F4	176.52(17)
C6	C5	C14	N1	-1.3(2)	C18	C17	C20	N1	142.98(16)
C6	C5	C14	C13	176.96(17)	C18	C17	C20	C6	-35.2(3)
C6	C7	C8	C9	-176.54(18)	C20	N1	C14	C5	1.3(2)
C6	C7	C11	C12	175.04(18)	C20	N1	C14	C13	-176.81(18)
C7	C6	C20	N1	177.65(17)	C20	N1	C15	C16	-17.46(19)
C7	C6	C20	C17	-4.2(4)	C20	C6	C7	C8	-43.8(3)
C7	C8	C9	C10	1.6(3)	C20	C6	C7	C11	140.1(2)

C7	C11	C12	C10	1.4(3)	C20	C17	C18	C19	179.96(17)
C8	C7	C11	C12	-1.2(3)	C21	C17	C18	C19	57.0(2)
C8	C9	C10	F1	178.29(17)	C21	C17	C20	N1	-92.61(18)
C8	C9	C10	C12	-1.4(3)	C21	C17	C20	C6	89.2(3)
C9	C10	C12	C11	-0.1(3)					

Table 33 Hydrogen Atom Coordinates (Å×10^4) and Isotropic Displacement Parameters (Å^2 ×10^3) for compound 106.

Atom	*x*	*y*	*z*	U(eq)
H1A	237.66	3234.95	-708.3	42
H1B	-774.11	3985.87	-1361.76	42
H1C	-296.63	3918.57	96.23	42
H3	3176.21	5346.13	-92.3	21
H4	5137.08	5419.33	1588.56	19
H8	6759.76	4871.99	5863.1	19
H9	8593.26	5833.02	6616.96	22
H11	7475.97	4971.5	2532.84	19
H12	9238.31	5976.96	3258.26	22
H13	1787.56	3224.11	1235.71	19
H15A	3347.82	2004.31	3027.97	20
H15B	2871.05	2487.37	4097.58	20
H16A	5605.87	1784.84	4250.55	22
H16B	4796.77	1768.81	5298.5	22
H18A	7696.83	2667.32	4911.38	22

H18B 7767.46	3454.62	5796.18	22
H21A 5652.67	3770.84	6598.46	30
H21B 5262.78	2821.48	6854.39	30
H21C 4151.01	3389.17	5888.78	30

6.1.5 Crystal data and structure refinement for compound 188

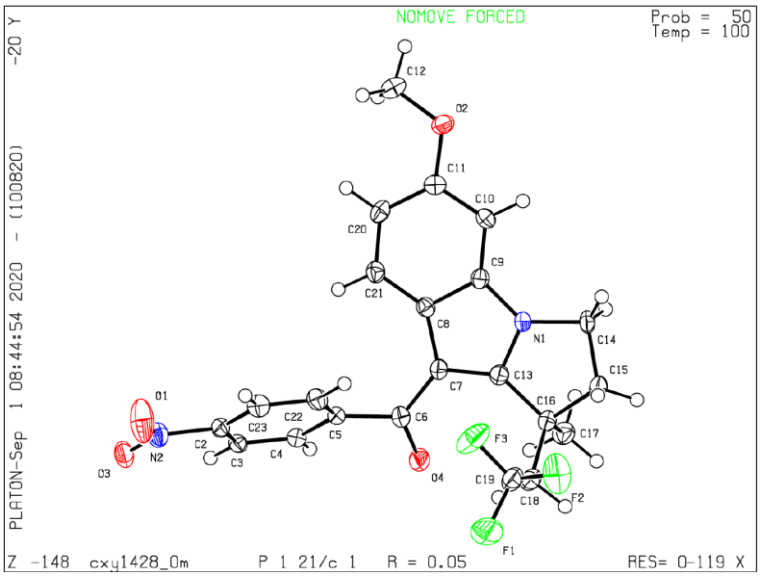

Table 34 Crystal data and structure refinement for compound 188.

Identification code	cxy1428_0m
Empirical formula	$C_{22}H_{19}F_3N_2O_4$
Formula weight	432.39
Temperature/K	100
Crystal system	monoclinic
Space group	$P2_1/c$
a/Å	9.4606(4)
b/Å	15.9489(8)

c/Å	13.2571(6)
α/°	90
β/°	104.405(2)
γ/°	90
Volume/Å^3	1937.43(16)
Z	4
ρ_{calc}g/cm^3	1.482
μ/mm^{-1}	0.122
F(000)	896.0
Crystal size/mm^3	0.34 × 0.29 × 0.08
Radiation	MoKα (λ = 0.71073)
2Θ range for data collection/°	4.446 to 56.702
Index ranges	-12 ≤ h ≤ 12, -21 ≤ k ≤ 21, -14 ≤ l ≤ 17
Reflections collected	28293
Independent reflections	4816 [R_{int} = 0.0602, R_{sigma} = 0.0471]
Data/restraints/parameters	4816/0/283
Goodness-of-fit on F^2	1.032
Final R indexes [I>=2σ (I)]	R_1 = 0.0538, wR_2 = 0.1241
Final R indexes [all data]	R_1 = 0.0900, wR_2 = 0.1418
Largest diff. peak/hole / e Å^{-3}	0.58/-0.40

Table 35 Fractional Atomic Coordinates ($\times 10^4$) and Equivalent Isotropic Displacement Parameters ($Å^2 \times 10^3$) for compound 132. U_{eq} is defined as 1/3 of of the trace of the orthogonalised U_{IJ} tensor.

Atom	*x*	*y*	*z*	U(eq)
F1	370.7(16)	3447.4(11)	4417.5(11)	50.6(4)
F2	-39.6(18)	4198.9(11)	5642.1(13)	54.8(5)
F3	2078.1(15)	4194.3(10)	5343.2(12)	50.4(4)
O1	7693(2)	4033.9(12)	2188.8(16)	55.8(6)
O2	8463.4(15)	5772.9(9)	9293.3(12)	26.0(3)
O3	8380.7(18)	2745.8(10)	2312.8(12)	34.7(4)
O4	4298.7(18)	2156.9(10)	5815.6(13)	33.8(4)
N1	4174.1(17)	4083.8(10)	7960.0(13)	20.0(4)
N2	7770(2)	3344.2(12)	2595.4(14)	29.1(4)
C2	7096(2)	3227.0(13)	3471.4(15)	21.6(4)
C3	7186(2)	2445.0(12)	3933.8(15)	20.2(4)
C4	6530(2)	2331.7(13)	4743.8(15)	20.7(4)
C5	5821(2)	2998.5(12)	5090.1(15)	20.0(4)
C6	4973(2)	2824.9(13)	5887.7(16)	23.5(4)
C7	4935(2)	3441.6(13)	6684.8(16)	21.2(4)
C8	6025(2)	4057.9(12)	7178.4(15)	19.2(4)
C9	5522(2)	4430.3(12)	7993.6(15)	19.2(4)
C10	6312(2)	5010.2(12)	8685.5(15)	19.8(4)
C11	7686(2)	5218.6(12)	8567.4(15)	21.5(4)
C12	9947(2)	5919.0(14)	9280.6(18)	29.6(5)

Table 35 Fractional Atomic Coordinates ($\times 10^4$) and Equivalent Isotropic Displacement Parameters ($Å^2 \times 10^3$) for compound 132. U_{eq} is defined as 1/3 of of the trace of the orthogonalised U_{IJ} tensor.

Atom	*x*	*y*	*z*	U(eq)
C13	3833(2)	3492.9(12)	7203.7(15)	20.8(4)
C14	3137(2)	4134.9(13)	8616.2(16)	22.6(4)
C15	1781(2)	3749.6(14)	7879.9(17)	27.6(5)
C16	2376(2)	3103.8(13)	7203.6(15)	22.2(4)
C17	2631(2)	2250.7(14)	7761.6(17)	27.3(5)
C18	1369(2)	2966.4(14)	6115.0(17)	26.7(5)
C19	968(2)	3705.5(16)	5407.8(17)	31.0(5)
C20	8213(2)	4870.6(13)	7761.0(16)	23.7(4)
C21	7398(2)	4297.7(13)	7072.4(16)	22.5(4)
C22	5769(2)	3779.9(13)	4617.7(16)	24.9(4)
C23	6398(2)	3901.4(13)	3790.6(16)	25.4(5)

Table 36 Anisotropic Displacement Parameters ($Å^2 \times 10^3$) for compound 132. The Anisotropic displacement factor exponent takes the form: $-2\pi^2[h^2a^{*2}U_{11}+2hka^*b^*U_{12}+\cdots]$.

Atom	U_{11}	U_{22}	U_{33}	U_{23}	U_{13}	U_{12}
F1	41.2(8)	72.2(11)	30.4(8)	4.9(7)	-6.0(6)	-6.1(8)
F2	56.3(10)	61.9(11)	50.8(10)	20.3(8)	21.8(8)	26.6(8)
F3	31.5(8)	62.9(10)	49.7(9)	27.9(8)	-3.0(6)	-14.8(7)
O1	81.2(15)	46.0(11)	56.0(12)	28.6(10)	46.8(11)	19.3(10)
O2	20.8(7)	26.5(8)	29.9(8)	-4.8(6)	4.6(6)	-4.1(6)
O3	42.1(9)	36.4(9)	32.7(9)	-6.6(7)	22.9(7)	-5.3(7)

Table 36 Anisotropic Displacement Parameters ($Å^2 \times 10^3$) for compound 132. The Anisotropic displacement factor exponent takes the form: $-2\pi^2[h^2a^{*2}U_{11}+2hka^*b^*U_{12}+\cdots]$.

Atom	U_{11}	U_{22}	U_{33}	U_{23}	U_{13}	U_{12}
O4	39.2(9)	30.2(9)	38.9(9)	-11.3(7)	22.5(7)	-13.6(7)
N1	17.9(8)	23.5(9)	20.3(8)	-2.9(7)	8.1(6)	0.0(7)
N2	31.1(10)	34.6(11)	24.3(9)	2.1(8)	12.1(8)	-1.2(8)
C2	19.5(10)	28.5(11)	16.8(9)	-0.4(8)	4.6(7)	-2.3(8)
C3	17.9(9)	23.3(10)	19.3(10)	-4.6(8)	4.5(7)	0.6(8)
C4	20.3(10)	22.2(10)	19.5(10)	-2.0(8)	4.8(8)	-1.7(8)
C5	18.5(9)	24.0(10)	18.1(10)	-4.1(8)	5.7(7)	-2.8(8)
C6	22.9(10)	26.1(11)	23.3(10)	-3.4(8)	9.3(8)	-0.7(8)
C7	19.7(9)	23.4(10)	22.7(10)	-2.1(8)	9.2(8)	-0.7(8)
C8	19.4(9)	19.2(9)	19.3(9)	-0.3(8)	5.4(7)	2.4(8)
C9	18.1(9)	19.7(9)	20.4(10)	1.8(8)	6.0(7)	2.3(7)
C10	22.8(10)	18.6(10)	18.1(9)	-0.6(7)	5.3(8)	2.2(8)
C11	22.0(10)	18.6(9)	22.2(10)	0.8(8)	2.3(8)	0.7(8)
C12	22.0(10)	28.3(11)	36.1(12)	0.0(9)	2.9(9)	-4.9(9)
C13	19.6(9)	22.6(10)	20.5(10)	0.8(8)	5.6(7)	0.2(8)
C14	22.5(10)	26.4(11)	23.0(10)	-1.2(8)	13.7(8)	1.3(8)
C15	22.7(10)	32.4(12)	31.4(12)	-3.4(9)	13.9(9)	-1.6(9)
C16	19.4(10)	25.9(10)	22.4(10)	-0.4(8)	7.5(8)	-1.2(8)
C17	27.7(11)	26.6(11)	27.9(11)	1.5(9)	7.5(9)	-2.3(9)
C18	20.7(10)	31.5(12)	28.3(11)	0.8(9)	6.9(8)	-4.5(9)
C19	20.9(10)	43.8(14)	28.1(12)	3.7(10)	6.0(9)	-4.6(10)

Table 36 Anisotropic Displacement Parameters ($Å^2 \times 10^3$) for compound 132. The Anisotropic displacement factor exponent takes the form: $-2\pi^2[h^2a^{*2}U_{11}+2hka^*b^*U_{12}+\cdots]$.

Atom	U_{11}	U_{22}	U_{33}	U_{23}	U_{13}	U_{12}
C20	17.1(9)	23.8(10)	31.3(11)	2.3(9)	8.5(8)	0.6(8)
C21	22.3(10)	23.0(10)	24.1(10)	-1.1(8)	9.2(8)	2.0(8)
C22	25.4(10)	22.9(10)	27.5(11)	-4.8(9)	8.7(8)	2.9(8)
C23	27.9(11)	23.2(11)	24.4(11)	4.2(8)	5.0(8)	0.7(8)

Table 37 Bond Lengths for compound 132.

Atom	Atom	Length/Å	Atom	Atom	Length/Å
F1	C19	1.358(3)	C5	C22	1.390(3)
F2	C19	1.331(3)	C6	C7	1.451(3)
F3	C19	1.327(3)	C7	C8	1.457(3)
O1	N2	1.219(2)	C7	C13	1.387(3)
O2	C11	1.377(2)	C8	C9	1.415(3)
O2	C12	1.427(2)	C8	C21	1.395(3)
O3	N2	1.222(2)	C9	C10	1.384(3)
O4	C6	1.233(3)	C10	C11	1.387(3)
N1	C9	1.380(2)	C11	C20	1.402(3)
N1	C13	1.355(3)	C13	C16	1.512(3)
N1	C14	1.467(2)	C14	C15	1.534(3)
N2	C2	1.469(3)	C15	C16	1.560(3)
C2	C3	1.383(3)	C16	C17	1.539(3)
C2	C23	1.382(3)	C16	C18	1.534(3)

Table 37 Bond Lengths for compound 132.

Atom	Atom	Length/Å	Atom	Atom	Length/Å
C3	C4	1.379(3)	C18	C19	1.495(3)
C4	C5	1.395(3)	C20	C21	1.383(3)
C5	C6	1.503(3)	C22	C23	1.385(3)

Table 38 Bond Angles for compound 132.

Atom	Atom	Atom	Angle/°	Atom	Atom	Atom	Angle/°
C11	O2	C12	116.92(16)	C9	C10	C11	116.88(18)
C9	N1	C14	135.04(17)	O2	C11	C10	115.32(18)
C13	N1	C9	110.50(16)	O2	C11	C20	123.88(18)
C13	N1	C14	113.97(16)	C10	C11	C20	120.81(18)
O1	N2	O3	123.38(19)	N1	C13	C7	109.77(17)
O1	N2	C2	118.30(19)	N1	C13	C16	109.55(17)
O3	N2	C2	118.31(18)	C7	C13	C16	140.67(19)
C3	C2	N2	118.31(18)	N1	C14	C15	100.21(15)
C23	C2	N2	118.51(19)	C14	C15	C16	105.44(16)
C23	C2	C3	123.18(19)	C13	C16	C15	100.86(16)
C4	C3	C2	118.27(18)	C13	C16	C17	109.21(16)
C3	C4	C5	120.19(19)	C13	C16	C18	114.31(17)
C4	C5	C6	118.40(18)	C17	C16	C15	110.08(17)
C22	C5	C4	120.05(18)	C18	C16	C15	113.99(17)
C22	C5	C6	121.15(18)	C18	C16	C17	108.19(17)

Table 38 Bond Angles for compound 132.

Atom	Atom	Atom	Angle/°	Atom	Atom	Atom	Angle/°
O4	C6	C5	117.45(18)	C19	C18	C16	118.58(18)
O4	C6	C7	122.38(19)	F1	C19	C18	110.3(2)
C7	C6	C5	120.14(18)	F2	C19	F1	104.76(18)
C6	C7	C8	129.89(18)	F2	C19	C18	113.85(19)
C13	C7	C6	124.04(18)	F3	C19	F1	105.16(18)
C13	C7	C8	105.82(17)	F3	C19	F2	107.0(2)
C9	C8	C7	106.96(17)	F3	C19	C18	114.97(18)
C21	C8	C7	135.47(18)	C21	C20	C11	121.30(18)
C21	C8	C9	117.40(18)	C20	C21	C8	119.66(19)
N1	C9	C8	106.88(17)	C23	C22	C5	120.56(19)
N1	C9	C10	129.17(18)	C2	C23	C22	117.74(19)
C10	C9	C8	123.92(18)				

Table 39 Torsion Angles for compound 132.

A	B	C	D	Angle/°	A	B	C	D	Angle/°
O1	N2	C2	C3	-179.9(2)	C8	C7	C13	C16	-179.9(2)
O1	N2	C2	C23	0.4(3)	C8	C9	C10	C11	-1.1(3)
O2	C11	C20	C21	178.09(18)	C9	N1	C13	C7	-1.6(2)
O3	N2	C2	C3	0.0(3)	C9	N1	C13	C16	178.26(16)
O3	N2	C2	C23	-179.68(19)	C9	N1	C14	C15	166.1(2)

Table 39 Torsion Angles for compound 132.

A	B	C	D	Angle/°	A	B	C	D	Angle/°
O4	C6	C7	C8	151.4(2)	C9	C8	C21	C20	0.8(3)
O4	C6	C7	C13	-22.0(3)	C9	C10	C11	O2	-177.63(17)
N1	C9	C10	C11	176.75(19)	C9	C10	C11	C20	1.8(3)
N1	C13	C16	C15	15.0(2)	C10	C11	C20	C21	-1.3(3)
N1	C13	C16	C17	-100.96(19)	C11	C20	C21	C8	-0.1(3)
N1	C13	C16	C18	137.70(18)	C12	O2	C11	C10	172.14(17)
N1	C14	C15	C16	30.8(2)	C12	O2	C11	C20	-7.3(3)
N2	C2	C3	C4	-178.88(17)	C13	N1	C9	C8	2.6(2)
N2	C2	C23	C22	-179.95(18)	C13	N1	C9	C10	-175.5(2)
C2	C3	C4	C5	-1.0(3)	C13	N1	C14	C15	-22.8(2)
C3	C2	C23	C22	0.4(3)	C13	C7	C8	C9	1.6(2)
C3	C4	C5	C6	172.98(18)	C13	C7	C8	C21	176.5(2)
C3	C4	C5	C22	0.1(3)	C13	C16	C18	C19	-57.4(3)
C4	C5	C6	O4	-37.3(3)	C14	N1	C9	C8	173.9(2)
C4	C5	C6	C7	144.49(19)	C14	N1	C9	C10	-4.2(4)
C4	C5	C22	C23	1.1(3)	C14	N1	C13	C7	-174.88(17)
C5	C6	C7	C8	-30.4(3)	C14	N1	C13	C16	5.0(2)
C5	C6	C7	C13	156.1(2)	C14	C15	C16	C13	-28.4(2)
C5	C22	C23	C2	-1.3(3)	C14	C15	C16	C17	86.9(2)
C6	C5	C22	C23	-171.58(18)	C14	C15	C16	C18	-151.35(17)
C6	C7	C8	C9	-172.8(2)	C15	C16	C18	C19	57.9(2)

Table 39 Torsion Angles for compound 132.

A	B	C	D	Angle/°	A	B	C	D	Angle/°
C6	C7	C8	C21	2.1(4)	C16	C18	C19	F1	165.83(18)
C6	C7	C13	N1	174.75(18)	C16	C18	C19	F2	-76.7(2)
C6	C7	C13	C16	-5.1(4)	C16	C18	C19	F3	47.2(3)
C7	C8	C9	N1	-2.5(2)	C17	C16	C18	C19	-179.28(18)
C7	C8	C9	C10	175.68(18)	C21	C8	C9	N1	-178.48(17)
C7	C8	C21	C20	-173.6(2)	C21	C8	C9	C10	-0.3(3)
C7	C13	C16	C15	-165.2(3)	C22	C5	C6	O4	135.5(2)
C7	C13	C16	C17	78.9(3)	C22	C5	C6	C7	-42.7(3)
C7	C13	C16	C18	-42.5(4)	C23	C2	C3	C4	0.8(3)
C8	C7	C13	N1	0.0(2)					

Table 40 Hydrogen Atom Coordinates (Å×10^4) and Isotropic Displacement Parameters (Å^2 ×10^3) for compound 132.

Atom	*x*	*y*	*z*	U(eq)
H3	7685.37	1997.54	3699.41	24
H4	6562.29	1797.97	5066.92	25
H10	5932.33	5254.12	9216.66	24
H12A	10465.65	5382.56	9331.41	44
H12B	10413.63	6275.27	9872.19	44
H12C	9982.04	6199.47	8629.42	44
H14A	2964.01	4722.09	8795.95	27

Table 40 Hydrogen Atom Coordinates (Å×10^4) and Isotropic Displacement Parameters (Å^2 ×10^3) for compound 132.

Atom	*x*	*y*	*z*	U(eq)
H14B	3466.96	3802.47	9262.71	27
H15A	1194.22	4187.28	7435.43	33
H15B	1163.96	3466.86	8280.14	33
H17A	3106.89	1868.34	7369.99	41
H17B	1692.27	2013.68	7804.85	41
H17C	3256.35	2326.92	8465.25	41
H18A	1838.34	2546.93	5753.53	32
H18B	452.42	2713.06	6204.08	32
H20	9148.14	5031.46	7686.1	28
H21	7771.97	4068.55	6529.88	27
H22	5299.45	4234.43	4864.32	30
H23	6350.8	4430.15	3453.89	31

6.1.6 Crystal data and structure refinement for compound 189

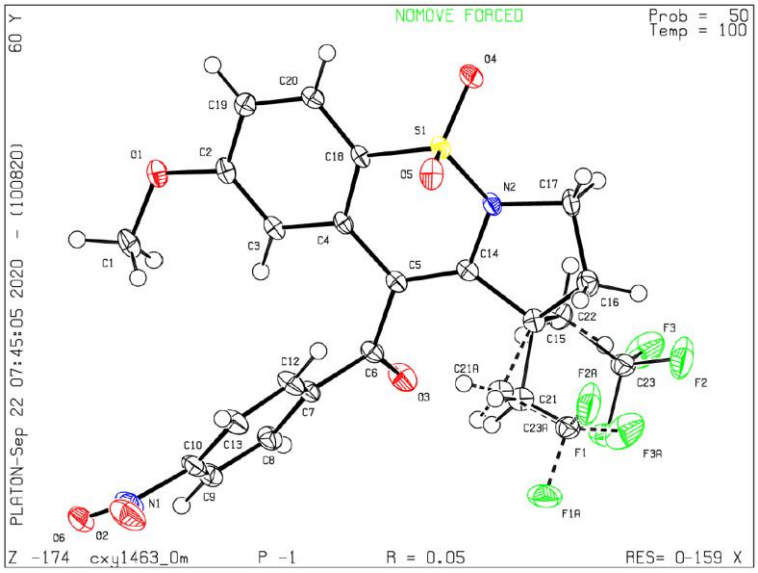

Table 41 Crystal data and structure refinement for compound 189.

Identification code	cxy1463_0m
Empirical formula	$C_{22}H_{19}F_3N_2O_6S$
Formula weight	496.45
Temperature/K	100
Crystal system	triclinic
Space group	P-1
a/Å	7.3756(3)
b/Å	12.0877(6)
c/Å	13.0747(6)
α/°	108.314(2)
β/°	105.9730(10)
γ/°	97.148(2)
Volume/Å^3	1035.10(8)

Z	2
ρ_{calc}g/cm^3	1.593
μ/mm^{-1}	0.229
F(000)	512.0
Crystal size/mm^3	0.38 × 0.36 × 0.15
Radiation	MoKα (λ = 0.71073)
2Θ range for data collection/°	5.768 to 56.88
Index ranges	-9 ≤ h ≤ 9, -16 ≤ k ≤ 16, -17 ≤ l ≤ 17
Reflections collected	15506
Independent reflections	5200 [R_{int} = 0.0306, R_{sigma} = 0.0331]
Data/restraints/parameters	5200/5/327
Goodness-of-fit on F^2	1.058
Final R indexes [I>=2σ (I)]	R_1 = 0.0486, wR_2 = 0.1202
Final R indexes [all data]	R_1 = 0.0585, wR_2 = 0.1262
Largest diff. peak/hole / e Å^{-3}	0.66/-0.49

Table 42 Fractional Atomic Coordinates (× 10^4) and Equivalent Isotropic Displacement Parameters (Å^2 × 10^3) for compound 133. U_{eq} is defined as 1/3 of of the trace of the orthogonalised U_{IJ} tensor.

Atom	*x*	*y*	*z*	U(eq)
S1	6093.8(6)	5431.1(4)	2327.6(4)	15.11(13)
F1	-2457(2)	984.9(13)	-370.4(17)	44.7(5)
F2	-2437(2)	2367.0(18)	-1051.5(15)	46.4(5)
F3	-3699(2)	2444.5(16)	249.2(16)	46.0(5)

O1	8451(2)	4563.8(13)	6588.1(12)	21.0(3)
O2	9878(3)	-1108.4(16)	3120.2(19)	40.6(5)
O3	1767(2)	1608.5(14)	2463.0(14)	26.0(3)
O4	5980(2)	6649.0(13)	2499.7(13)	23.5(3)
O5	7356(2)	4976.7(14)	1723.4(12)	22.6(3)
O6	8715(3)	-1245.5(15)	4448.5(16)	37.1(4)
N2	3875(2)	4588.8(14)	1647.8(14)	15.9(3)
C1	8025(3)	3374(2)	6589.3(19)	24.9(4)
C2	7749(3)	4716.3(18)	5580.5(16)	16.1(4)
C3	6366(3)	3852.9(17)	4615.5(16)	15.6(4)
C4	5750(3)	4045.1(16)	3579.9(16)	14.0(3)
C5	4208(3)	3163.3(16)	2574.8(16)	14.5(3)
C6	3476(3)	1975.3(17)	2624.1(17)	16.8(4)
C7	4877(3)	1220.0(17)	2879.4(17)	17.0(4)
C8	4406(3)	392.0(18)	3360.5(18)	20.6(4)
C9	5683(3)	-309.3(19)	3624.3(19)	23.9(4)
C10	7367(3)	-189.0(18)	3356(2)	23.7(4)
N1	8762(3)	-906.0(17)	3660.5(19)	30.5(4)
C12	6593(3)	1322.4(18)	2624.3(19)	22.0(4)
C13	7841(3)	591.9(19)	2839(2)	24.5(4)
C14	3307(3)	3462.0(16)	1675.2(16)	14.7(4)
C15	1596(3)	2740.9(18)	564.6(16)	17.4(4)
C16	1883(3)	3440.3(19)	-206.8(18)	21.8(4)

C17	2703(3)	4734.6(19)	602.1(17)	20.5(4)
C18	6577(3)	5161.1(16)	3588.7(16)	14.0(3)
C19	8501(3)	5830.5(17)	5569.1(16)	17.0(4)
C20	7912(3)	6052.3(17)	4572.2(16)	15.9(4)
C21	1664(4)	1430(2)	-2(2)	21.1(5)
C22	-291(3)	2861.7(19)	854.9(17)	20.5(4)
C23	-2198(3)	2162(2)	-87(2)	21.7(4)
F1A	1200(30)	-127(14)	-1260(20)	44.7(5)
C23A	1140(30)	1033(17)	-987(18)	21.7(4)
F2A	2140(30)	1450(20)	-1551(17)	46.4(5)
F3A	-740(20)	1070(19)	-1371(19)	46.0(5)
C21A	2120(60)	1520(20)	290(20)	21.1(5)

Table 43 Anisotropic Displacement Parameters ($Å^2 \times 10^3$) for compound 133. The Anisotropic displacement factor exponent takes the form: $-2\pi^2[h^2a^{*2}U_{11}+2hka^*b^*U_{12}+\cdots]$.

Atom	U_{11}	U_{22}	U_{33}	U_{23}	U_{13}	U_{12}
S1	14.2(2)	16.5(2)	18.0(2)	10.77(17)	5.48(17)	3.14(16)
F1	25.2(8)	17.8(7)	70.9(12)	9.6(7)	-4.9(8)	0.1(6)
F2	27.4(8)	64.3(12)	40.6(9)	32.0(9)	-7.5(7)	-4.9(8)
F3	14.7(7)	50.5(11)	54.7(11)	0.6(8)	7.5(7)	3.1(7)
O1	23.2(7)	25.5(7)	18.5(7)	13.4(6)	6.2(6)	7.7(6)
O2	29.5(9)	30.1(9)	70.9(14)	25.3(9)	18.4(9)	16.0(7)
O3	18.0(7)	27.3(8)	41.3(9)	20.6(7)	13.2(7)	5.8(6)
O4	26.6(8)	18.0(7)	26.5(8)	13.9(6)	4.1(6)	2.5(6)

O5	16.9(7)	35.2(8)	21.5(7)	14.9(6)	9.5(6)	7.2(6)
O6	34.7(9)	21.1(8)	46.2(10)	19.0(8)	-5.9(8)	0.4(7)
N2	13.6(7)	16.9(8)	19.9(8)	11.7(6)	4.0(6)	3.5(6)
C1	31.2(11)	27.5(11)	24.7(10)	18.6(9)	10.0(9)	11.5(9)
C2	15.6(8)	23.2(9)	17.3(9)	11.7(7)	9.5(7)	10.5(7)
C3	15.7(8)	17.9(9)	20.8(9)	12.2(7)	9.7(7)	8.0(7)
C4	12.5(8)	16.6(9)	18.2(9)	9.7(7)	7.6(7)	6.9(7)
C5	13.3(8)	15.4(8)	19.3(9)	9.2(7)	8.1(7)	4.9(7)
C6	17.5(9)	16.1(9)	21.1(9)	9.8(7)	8.9(7)	4.7(7)
C7	17.8(9)	15.1(9)	20.9(9)	9.6(7)	7.1(7)	4.3(7)
C8	19.8(9)	19.3(9)	25.8(10)	12.7(8)	8.3(8)	2.3(7)
C9	25.7(10)	18.2(10)	28.4(11)	14.0(8)	5.1(8)	1.6(8)
C10	21.3(10)	14.9(9)	34.6(11)	12.1(8)	4.6(9)	5.8(7)
N1	25.0(9)	16.6(9)	47.2(12)	16.4(8)	3.2(9)	2.8(7)
C12	22.3(10)	18.4(9)	34.0(11)	15.7(8)	14.2(9)	8.0(8)
C13	22.5(10)	20.2(10)	38.2(12)	15.4(9)	14.3(9)	8.7(8)
C14	12.2(8)	15.2(8)	20.4(9)	8.8(7)	7.9(7)	4.2(6)
C15	15.8(9)	19.8(9)	18.7(9)	8.7(7)	7.0(7)	4.1(7)
C16	21.9(10)	25.0(10)	20.7(9)	12.7(8)	5.9(8)	4.8(8)
C17	18.0(9)	25.0(10)	21.0(9)	14.9(8)	2.3(7)	6.1(8)
C18	14.0(8)	16.4(9)	17.2(8)	10.5(7)	7.4(7)	6.6(7)
C19	14.6(8)	19.5(9)	18.0(9)	6.1(7)	6.9(7)	6.0(7)
C20	14.5(8)	15.6(9)	21.5(9)	8.6(7)	9.2(7)	5.8(7)

C21	22.0(16)	18.3(10)	22.0(13)	5.9(9)	7.9(10)	3.7(9)
C22	13.2(9)	25.3(10)	21.2(9)	7.3(8)	5.2(7)	2.8(7)
C23	16.4(10)	17.3(10)	27.9(11)	7.3(9)	3.8(9)	3.1(8)
F1A	25.2(8)	17.8(7)	70.9(12)	9.6(7)	-4.9(8)	0.1(6)
C23A	16.4(10)	17.3(10)	27.9(11)	7.3(9)	3.8(9)	3.1(8)
F2A	27.4(8)	64.3(12)	40.6(9)	32.0(9)	-7.5(7)	-4.9(8)
F3A	14.7(7)	50.5(11)	54.7(11)	0.6(8)	7.5(7)	3.1(7)
C21A	22.0(16)	18.3(10)	22.0(13)	5.9(9)	7.9(10)	3.7(9)

Table 44 Bond Lengths for compound 133.

Atom	Atom	Length/Å	Atom	Atom	Length/Å
S1	O4	1.4345(15)	C6	C7	1.500(3)
S1	O5	1.4327(15)	C7	C8	1.396(3)
S1	N2	1.6493(16)	C7	C12	1.395(3)
S1	C18	1.7310(18)	C8	C9	1.389(3)
F1	C23	1.326(3)	C9	C10	1.383(3)
F2	C23	1.330(3)	C10	N1	1.477(3)
F3	C23	1.343(3)	C10	C13	1.386(3)
O1	C1	1.434(3)	C12	C13	1.386(3)
O1	C2	1.356(2)	C14	C15	1.544(3)
O2	N1	1.224(3)	C15	C16	1.545(3)
O3	C6	1.218(2)	C15	C21	1.537(3)
O6	N1	1.230(3)	C15	C22	1.552(3)

N2	C14	1.389(2)	C15	C21A	1.532(18)
N2	C17	1.479(2)	C16	C17	1.518(3)
C2	C3	1.386(3)	C18	C20	1.397(3)
C2	C19	1.398(3)	C19	C20	1.377(3)
C3	C4	1.407(2)	C22	C23	1.519(3)
C4	C5	1.467(3)	F1A	C23A	1.344(17)
C4	C18	1.405(3)	C23A	F2A	1.337(17)
C5	C6	1.497(3)	C23A	F3A	1.345(17)
C5	C14	1.361(3)	C23A	C21A	1.512(19)

Table 45 Bond Angles for compound 133.

Atom	Atom	Atom	Angle/°	Atom	Atom	Atom	Angle/°
O4	S1	N2	107.42(9)	C10	C13	C12	117.83(19)
O4	S1	C18	112.03(9)	N2	C14	C15	107.31(15)
O5	S1	O4	116.37(9)	C5	C14	N2	121.44(17)
O5	S1	N2	109.54(9)	C5	C14	C15	131.24(17)
O5	S1	C18	110.56(9)	C14	C15	C16	101.12(15)
N2	S1	C18	99.50(8)	C14	C15	C22	106.88(15)
C2	O1	C1	117.55(16)	C16	C15	C22	111.40(16)
C14	N2	S1	123.23(13)	C21	C15	C14	114.59(16)
C14	N2	C17	112.94(15)	C21	C15	C16	109.51(18)
C17	N2	S1	118.43(13)	C21	C15	C22	112.77(18)
O1	C2	C3	123.80(17)	C21A	C15	C14	99.4(11)

O1	C2	C19	115.38(17)	C21A	C15	C16	116.6(15)
C3	C2	C19	120.81(17)	C21A	C15	C22	118.5(18)
C2	C3	C4	121.20(17)	C17	C16	C15	104.84(16)
C3	C4	C5	121.40(17)	N2	C17	C16	101.44(15)
C18	C4	C3	116.49(17)	C4	C18	S1	119.97(14)
C18	C4	C5	121.92(16)	C20	C18	S1	117.38(14)
C4	C5	C6	118.22(16)	C20	C18	C4	122.46(17)
C14	C5	C4	120.93(17)	C20	C19	C2	119.36(18)
C14	C5	C6	120.40(17)	C19	C20	C18	119.58(17)
O3	C6	C5	121.51(17)	C23	C22	C15	117.22(17)
O3	C6	C7	119.23(17)	F1	C23	F2	106.4(2)
C5	C6	C7	119.26(16)	F1	C23	F3	105.59(19)
C8	C7	C6	118.29(17)	F1	C23	C22	113.50(18)
C12	C7	C6	121.12(17)	F2	C23	F3	106.05(19)
C12	C7	C8	120.58(18)	F2	C23	C22	114.23(18)
C9	C8	C7	119.85(19)	F3	C23	C22	110.49(18)
C10	C9	C8	118.05(19)	F1A	C23A	F3A	107.2(18)
C9	C10	N1	118.57(19)	F1A	C23A	C21A	101.4(17)
C9	C10	C13	123.47(19)	F2A	C23A	F1A	106(2)
C13	C10	N1	117.95(19)	F2A	C23A	F3A	110.6(19)
O2	N1	O6	125.2(2)	F2A	C23A	C21A	114(2)
O2	N1	C10	117.9(2)	F3A	C23A	C21A	117(2)
O6	N1	C10	116.9(2)	C23A	C21A	C15	98.4(15)

C13	C12	C7	120.12(18)

Table 46 Torsion Angles for compound 133.

A	B	C	D	Angle/°	A	B	C	D	Angle/°
S1	N2	C14	C5	26.9(3)	C5	C14	C15	C21A	-40.1(17)
S1	N2	C14	C15	-153.50(13)	C6	C5	C14	N2	175.51(16)
S1	N2	C17	C16	133.72(14)	C6	C5	C14	C15	-3.9(3)
S1	C18	C20	C19	-173.09(14)	C6	C7	C8	C9	-179.01(18)
O1	C2	C3	C4	-177.41(16)	C6	C7	C12	C13	-178.2(2)
O1	C2	C19	C20	178.18(16)	C7	C8	C9	C10	-2.4(3)
O3	C6	C7	C8	-24.8(3)	C7	C12	C13	C10	-2.9(3)
O3	C6	C7	C12	154.0(2)	C8	C7	C12	C13	0.5(3)
O4	S1	N2	C14	-157.18(15)	C8	C9	C10	N1	178.37(19)
O4	S1	N2	C17	50.63(17)	C8	C9	C10	C13	0.0(3)
O4	S1	C18	C4	144.89(15)	C9	C10	N1	O2	156.5(2)
O4	S1	C18	C20	-39.84(17)	C9	C10	N1	O6	-24.0(3)
O5	S1	N2	C14	75.56(17)	C9	C10	C13	C12	2.7(3)
O5	S1	N2	C17	-76.62(16)	N1	C10	C13	C12	-175.7(2)
O5	S1	C18	C4	-83.53(16)	C12	C7	C8	C9	2.2(3)
O5	S1	C18	C20	91.74(16)	C13	C10	N1	O2	-25.0(3)
N2	S1	C18	C4	31.61(16)	C13	C10	N1	O6	154.4(2)
N2	S1	C18	C20	-153.11(15)	C14	N2	C17	C16	-21.2(2)
N2	C14	C15	C16	20.74(19)	C14	C5	C6	O3	-49.2(3)

N2	C14	C15	C21	138.40(19)	C14	C5	C6	C7	130.90(19)
N2	C14	C15	C22	-95.88(18)	C14	C15	C16	C17	-33.44(19)
N2	C14	C15	C21A	140.4(17)	C14	C15	C22	C23	-176.25(17)
C1	O1	C2	C3	12.6(3)	C14	C15	C21A	C23A	-153(2)
C1	O1	C2	C19	-168.12(17)	C15	C16	C17	N2	33.42(19)
C2	C3	C4	C5	-176.47(17)	C15	C22	C23	F1	67.8(3)
C2	C3	C4	C18	-1.4(3)	C15	C22	C23	F2	-54.4(3)
C2	C19	C20	C18	-0.1(3)	C15	C22	C23	F3	-173.86(18)
C3	C2	C19	C20	-2.5(3)	C16	C15	C22	C23	74.1(2)
C3	C4	C5	C6	-8.0(3)	C16	C15	C21A	C23A	-46(3)
C3	C4	C5	C14	164.41(17)	C17	N2	C14	C5	-179.52(17)
C3	C4	C18	S1	173.77(13)	C17	N2	C14	C15	0.0(2)
C3	C4	C18	C20	-1.2(3)	C18	S1	N2	C14	-40.36(17)
C4	C5	C6	O3	123.2(2)	C18	S1	N2	C17	167.45(15)
C4	C5	C6	C7	-56.7(2)	C18	C4	C5	C6	177.27(16)
C4	C5	C14	N2	3.3(3)	C18	C4	C5	C14	-10.3(3)
C4	C5	C14	C15	-176.15(17)	C19	C2	C3	C4	3.4(3)
C4	C18	C20	C19	2.1(3)	C21	C15	C16	C17	-154.74(17)
C5	C4	C18	S1	-11.2(2)	C21	C15	C22	C23	-49.5(2)
C5	C4	C18	C20	173.75(17)	C22	C15	C16	C17	79.81(19)
C5	C6	C7	C8	155.07(18)	C22	C15	C21A	C23A	92(2)
C5	C6	C7	C12	-26.1(3)	F1A	C23A	C21A	C15	-168(2)
C5	C14	C15	C16	-159.8(2)	F2A	C23A	C21A	C15	79(3)

C5	C14	C15	C21	-42.1(3)	F3A	C23A	C21A C15 -52(3)
C5	C14	C15	C22	83.6(2)	C21A	C15	C16 C17 -139.9(15)

Table 47 Hydrogen Atom Coordinates (Å×10^4) and Isotropic Displacement Parameters (Å^2 ×10^3) for compound 133.

Atom	*x*	*y*	*z*	U(eq)
H1A	8308.62	2816.97	5957.48	37
H1B	6651.31	3139.5	6495.75	37
H1C	8823.97	3353.16	7315.46	37
H3	5822.97	3118.1	4654.13	19
H8	3214.32	308.22	3507.1	25
H9	5408.75	-855.53	3978.77	29
H12	6905.74	1893.64	2303.12	26
H13	8984.81	625.73	2637.72	29
H16A	2798.57	3148.25	-599.61	26
H16B	633.77	3354.9	-788.78	26
H17A	3517.28	5186.28	309.83	25
H17B	1661.43	5143.43	736.62	25
H19	9410.76	6429.12	6242.53	20
H20	8410.21	6806.47	4553.3	19
H21A	2973.69	1394.24	-23.82	32
H21B	737.84	1096.37	-782.98	32
H21C	1324.08	964.99	438.98	32
H22A	-355.91	2489.38	1414.22	31

H22B	-1416.11	2460.66	157.96	31
H22C	-291.34	3711.4	1175.98	31
H21D	3538.72	1594.24	509.96	25
H21E	1567.69	1027.08	663.19	25

Table 48 Atomic Occupancy for compound 133.

Atom	*Occupancy*	Atom	*Occupancy*	Atom	*Occupancy*
F1	0.9218(18)	F2	0.9218(18)	F3	0.9218(18)
C21	0.9218(18)	H21A	0.9218(18)	H21B	0.9218(18)
H21C	0.9218(18)	H22B	0.0782(18)	C23	0.9218(18)
F1A	0.0782(18)	C23A	0.0782(18)	F2A	0.0782(18)
F3A	0.0782(18)	C21A	0.0782(18)	H21D	0.0782(18)
H21E	0.0782(18)				

6.1.7 Crystal data and structure refinement for compound 548

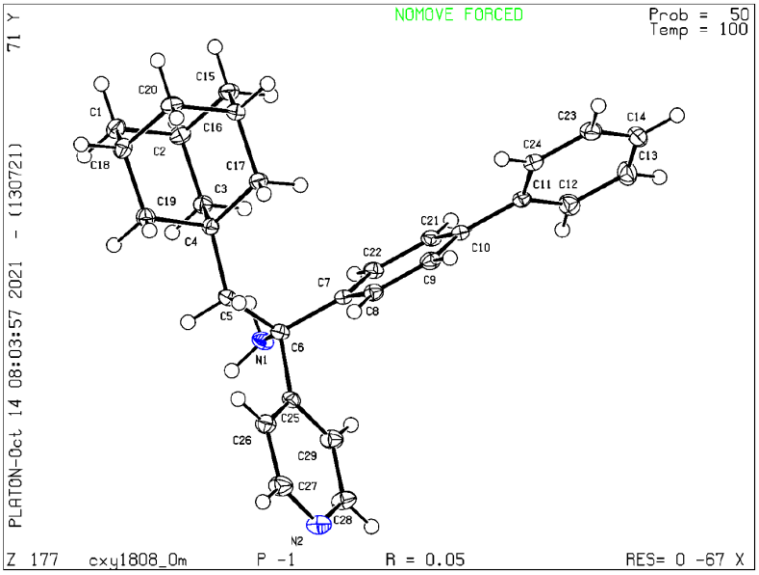

Table 49 Crystal data and structure refinement for compound 548.

Identification code	cxy1808_0m
Empirical formula	$C_{29}H_{32}N_2$
Formula weight	408.56
Temperature/K	100
Crystal system	triclinic
Space group	P-1
a/Å	6.3234(6)
b/Å	11.6046(11)
c/Å	14.9005(14)
α/°	92.793(3)
β/°	97.327(3)
γ/°	96.263(3)
Volume/Å^3	1075.83(18)
Z	2
ρ_{calc}g/cm^3	1.261
μ/mm^{-1}	0.073
F(000)	440.0
Crystal size/mm^3	0.36 × 0.31 × 0.22
Radiation	MoKα (λ = 0.71073)
2Θ range for data collection/°	4.348 to 55.184
Index ranges	-8 ≤ h ≤ 8, -15 ≤ k ≤ 15, -19 ≤ l ≤ 18
Reflections collected	18323

Independent reflections	4970 [R_{int} = 0.0611, R_{sigma} = 0.0585]
Data/restraints/parameters	4970/0/281
Goodness-of-fit on F^2	1.035
Final R indexes [I>=2σ (I)]	R_1 = 0.0456, wR_2 = 0.1007
Final R indexes [all data]	R_1 = 0.0842, wR_2 = 0.1135
Largest diff. peak/hole / e Å^{-3}	0.32/-0.26

Table 50 Fractional Atomic Coordinates (× 10^4) and Equivalent Isotropic Displacement Parameters (Å^2 × 10^3) for compound 456. U_{eq} is defined as 1/3 of the trace of the orthogonalised U_{IJ} tensor.

Atom	*x*	*y*	*z*	U(eq)
N1	-648.9(19)	1471.5(11)	5532.7(8)	17.6(3)
N2	3015(2)	4139.4(12)	3591.3(8)	22.6(3)
C1	2693(2)	-1760.6(13)	7789.0(10)	18.5(3)
C2	1151(2)	-856.2(13)	7936.5(9)	17.2(3)
C3	963(2)	-87.1(13)	7122.7(9)	15.7(3)
C4	3163(2)	546.3(12)	6995.5(9)	13.6(3)
C5	3205(2)	1262.9(12)	6141.8(9)	14.7(3)
C6	1507(2)	2090.1(12)	5856.9(9)	14.6(3)
C7	1362(2)	2990.5(12)	6630.1(8)	13.9(3)
C8	3142(2)	3798.1(12)	6938.2(9)	15.3(3)
C9	3073(2)	4613.5(13)	7639.9(9)	16.5(3)
C10	1219(2)	4661.1(12)	8054.5(9)	14.9(3)
C11	1148(2)	5543.8(12)	8802.3(9)	16.4(3)

Table 50 Fractional Atomic Coordinates ($\times 10^4$) and Equivalent Isotropic Displacement Parameters ($Å^2 \times 10^3$) for compound 456. U_{eq} is defined as 1/3 of the trace of the orthogonalised U_{IJ} tensor.

Atom	*x*	*y*	*z*	U(eq)
C12	-670(3)	6099.9(13)	8866.0(10)	21.0(3)
C13	-694(3)	6937.2(14)	9567.1(10)	24.7(4)
C14	1103(3)	7223.1(14)	10207.0(10)	25.1(4)
C15	2031(2)	-90.2(13)	8801.4(9)	18.1(3)
C16	4245(2)	524.1(13)	8696.8(9)	16.3(3)
C17	4047(2)	1289.2(12)	7882.8(9)	15.3(3)
C18	4903(2)	-1147.0(13)	7686.4(9)	18.3(3)
C19	4692(2)	-386.6(13)	6877.0(9)	16.8(3)
C20	5782(2)	-375.6(13)	8549.0(9)	18.4(3)
C21	-570(2)	3870.6(13)	7733.1(9)	15.9(3)
C22	-495(2)	3046.5(13)	7026.2(9)	15.6(3)
C23	2918(3)	6680.9(13)	10150.0(10)	24.1(4)
C24	2957(3)	5849.8(13)	9448.2(9)	19.2(3)
C25	2129(2)	2786.7(12)	5054.8(9)	15.5(3)
C26	4071(3)	2806.3(13)	4713.0(9)	19.1(3)
C27	4431(3)	3490.2(14)	3990.8(10)	23.2(4)
C28	1154(3)	4120.8(14)	3932.2(10)	22.3(3)
C29	654(3)	3472.7(14)	4648.1(9)	19.6(3)

Table 51 Anisotropic Displacement Parameters ($Å^2 \times 10^3$) for compound 456. The Anisotropic displacement factor exponent takes the form: $-2\pi^2[h^2a^{*2}U_{11}+2hka^*b^*U_{12}+\cdots]$.

Atom	U_{11}	U_{22}	U_{33}	U_{23}	U_{13}	U_{12}
N1	18.4(7)	20.1(7)	12.6(5)	-0.7(5)	0.6(5)	-3.0(5)
N2	23.1(7)	27.0(7)	18.2(6)	5.8(5)	3.1(5)	2.7(6)
C1	21.9(8)	14.7(7)	18.9(7)	2.9(6)	2.0(6)	1.6(6)
C2	15.6(8)	17.5(7)	18.5(7)	4.6(6)	2.3(6)	-0.1(6)
C3	15.0(7)	17.0(7)	15.0(6)	1.5(6)	1.4(5)	2.1(6)
C4	14.7(7)	13.4(7)	12.4(6)	0.9(5)	1.2(5)	1.4(6)
C5	16.0(7)	16.2(7)	11.6(6)	-0.1(5)	2.4(5)	0.7(6)
C6	15.8(7)	16.0(7)	11.5(6)	0.9(5)	1.5(5)	0.2(6)
C7	16.7(7)	14.8(7)	10.4(6)	3.1(5)	0.5(5)	3.1(6)
C8	14.8(7)	17.1(7)	14.6(6)	3.6(5)	3.3(5)	1.9(6)
C9	16.7(8)	17.0(7)	14.7(6)	2.4(6)	-1.3(5)	0.1(6)
C10	19.5(8)	14.6(7)	11.0(6)	3.0(5)	1.5(5)	3.8(6)
C11	23.5(8)	13.0(7)	13.1(6)	3.5(5)	4.9(6)	0.1(6)
C12	22.0(8)	20.7(8)	20.2(7)	0.5(6)	5.3(6)	-0.1(6)
C13	30.6(10)	19.6(8)	26.7(8)	0.7(6)	13.6(7)	4.3(7)
C14	42.5(11)	16.7(8)	16.8(7)	-0.8(6)	9.6(7)	0.2(7)
C15	20.8(8)	19.8(8)	14.9(6)	4.5(6)	4.4(6)	4.3(6)
C16	18.6(8)	17.7(8)	12.3(6)	1.0(5)	0.5(5)	2.8(6)
C17	17.2(7)	14.6(7)	13.8(6)	1.8(5)	1.4(5)	0.4(6)
C18	18.6(8)	17.0(8)	20.0(7)	2.4(6)	2.1(6)	5.2(6)
C19	16.4(8)	18.5(8)	16.0(6)	1.4(6)	2.8(5)	3.9(6)

Table 51 Anisotropic Displacement Parameters ($Å^2 \times 10^3$) for compound 456. The Anisotropic displacement factor exponent takes the form: $-2\pi^2[h^2a^{*2}U_{11}+2hka^*b^*U_{12}+\cdots]$.

Atom	U_{11}	U_{22}	U_{33}	U_{23}	U_{13}	U_{12}
C20	17.2(8)	21.6(8)	16.1(7)	4.4(6)	-0.2(6)	2.5(6)
C21	18.0(8)	18.2(8)	12.7(6)	4.2(5)	5.1(5)	2.2(6)
C22	16.4(8)	16.9(7)	12.8(6)	1.6(5)	0.6(5)	-0.4(6)
C23	37.6(10)	18.7(8)	14.3(7)	1.7(6)	-1.1(6)	0.3(7)
C24	26.6(9)	16.6(8)	14.8(6)	4.0(6)	1.2(6)	4.2(6)
C25	19.3(8)	15.3(7)	10.9(6)	-0.8(5)	0.3(5)	0.1(6)
C26	20.7(8)	21.7(8)	16.2(7)	2.8(6)	4.0(6)	5.8(6)
C27	22.6(9)	29.8(9)	19.5(7)	5.4(6)	7.8(6)	4.9(7)
C28	21.3(8)	26.7(9)	19.7(7)	8.4(6)	0.8(6)	4.6(7)
C29	17.4(8)	24.5(8)	17.6(7)	4.0(6)	3.5(6)	3.0(6)

Table 52 Bond Lengths for compound 456.

Atom	Atom	Length/Å	Atom	Atom	Length/Å
N1	C6	1.4807(18)	C10	C11	1.4848(19)
N2	C27	1.334(2)	C10	C21	1.394(2)
N2	C28	1.339(2)	C11	C12	1.390(2)
C1	C2	1.535(2)	C11	C24	1.399(2)
C1	C18	1.527(2)	C12	C13	1.394(2)
C2	C3	1.5405(19)	C13	C14	1.386(2)
C2	C15	1.5356(19)	C14	C23	1.378(2)
C3	C4	1.540(2)	C15	C16	1.530(2)

Table 52 Bond Lengths for compound 456.

Atom	Atom	Length/Å	Atom	Atom	Length/Å
C4	C5	1.5547(18)	C16	C17	1.5381(19)
C4	C17	1.5488(18)	C16	C20	1.529(2)
C4	C19	1.5463(19)	C18	C19	1.5296(19)
C5	C6	1.550(2)	C18	C20	1.5359(19)
C6	C7	1.5356(19)	C21	C22	1.3966(19)
C6	C25	1.5430(19)	C23	C24	1.392(2)
C7	C8	1.397(2)	C25	C26	1.386(2)
C7	C22	1.386(2)	C25	C29	1.391(2)
C8	C9	1.3838(19)	C26	C27	1.395(2)
C9	C10	1.398(2)	C28	C29	1.384(2)

Table 53 Bond Angles for compound 456.

Atom	Atom	Atom	Angle/°	Atom	Atom	Atom	Angle/°
C27	N2	C28	115.88(13)	C12	C11	C10	121.38(13)
C18	C1	C2	109.72(12)	C12	C11	C24	118.75(13)
C1	C2	C3	109.78(11)	C24	C11	C10	119.86(14)
C1	C2	C15	109.16(12)	C11	C12	C13	120.47(15)
C15	C2	C3	109.16(12)	C14	C13	C12	120.10(16)
C4	C3	C2	111.21(11)	C23	C14	C13	120.00(14)
C3	C4	C5	115.77(11)	C16	C15	C2	109.28(11)
C3	C4	C17	107.68(11)	C15	C16	C17	109.46(12)

Table 53 Bond Angles for compound 456.

Atom	Atom	Atom	Angle/°	Atom	Atom	Atom	Angle/°
C3	C4	C19	107.63(12)	C20	C16	C15	109.82(12)
C17	C4	C5	112.39(11)	C20	C16	C17	109.77(11)
C19	C4	C5	105.37(11)	C16	C17	C4	110.88(11)
C19	C4	C17	107.62(11)	C1	C18	C19	109.06(12)
C6	C5	C4	122.88(12)	C1	C18	C20	109.48(12)
N1	C6	C5	113.25(12)	C19	C18	C20	109.14(12)
N1	C6	C7	109.90(11)	C18	C19	C4	112.11(11)
N1	C6	C25	105.07(11)	C16	C20	C18	109.34(12)
C7	C6	C5	111.30(11)	C10	C21	C22	120.79(14)
C7	C6	C25	106.21(11)	C7	C22	C21	120.84(13)
C25	C6	C5	110.69(11)	C14	C23	C24	120.15(15)
C8	C7	C6	119.30(13)	C23	C24	C11	120.52(15)
C22	C7	C6	122.24(13)	C26	C25	C6	125.25(13)
C22	C7	C8	118.44(13)	C26	C25	C29	116.73(13)
C9	C8	C7	120.77(14)	C29	C25	C6	118.01(13)
C8	C9	C10	121.11(14)	C25	C26	C27	119.20(14)
C9	C10	C11	120.88(13)	N2	C27	C26	124.37(15)
C21	C10	C9	118.02(13)	N2	C28	C29	123.88(15)
C21	C10	C11	121.09(13)	C28	C29	C25	119.94(15)

Table 54 Torsion Angles for compound 456.

A	B	C	D	Angle/°	A	B	C	D	Angle/°
N1	C6	C7	C8	-169.85(12)	C8	C9	C10	C21	-0.7(2)
N1	C6	C7	C22	8.94(18)	C9	C10	C11	C12	140.44(15)
N1	C6	C25	C26	-131.23(14)	C9	C10	C11	C24	-38.00(19)
N1	C6	C25	C29	50.20(16)	C9	C10	C21	C22	0.9(2)
N2	C28	C29	C25	-0.1(2)	C10	C11	C12	C13	-179.17(14)
C1	C2	C3	C4	-59.31(15)	C10	C11	C24	C23	179.62(13)
C1	C2	C15	C16	59.96(15)	C10	C21	C22	C7	0.3(2)
C1	C18	C19	C4	59.94(15)	C11	C10	C21	C22	179.65(13)
C1	C18	C20	C16	-59.69(15)	C11	C12	C13	C14	0.1(2)
C2	C1	C18	C19	-59.35(15)	C12	C11	C24	C23	1.1(2)
C2	C1	C18	C20	60.00(15)	C12	C13	C14	C23	0.1(2)
C2	C3	C4	C5	174.74(11)	C13	C14	C23	C24	0.3(2)
C2	C3	C4	C17	-58.55(14)	C14	C23	C24	C11	-1.0(2)
C2	C3	C4	C19	57.21(14)	C15	C2	C3	C4	60.31(15)
C2	C15	C16	C17	60.30(15)	C15	C16	C17	C4	-60.35(15)
C2	C15	C16	C20	-60.28(14)	C15	C16	C20	C18	59.99(14)
C3	C2	C15	C16	-60.03(15)	C17	C4	C5	C6	-78.47(16)
C3	C4	C5	C6	45.84(18)	C17	C4	C19	C18	57.71(15)
C3	C4	C17	C16	58.42(15)	C17	C16	C20	C18	-60.40(15)
C3	C4	C19	C18	-58.10(14)	C18	C1	C2	C3	59.47(15)
C4	C5	C6	N1	-69.20(16)	C18	C1	C2	C15	-60.14(15)

Table 54 Torsion Angles for compound 456.

A	B	C	D	Angle/°	A	B	C	D	Angle/°
C4	C5	C6	C7	55.22(17)	C19	C4	C5	C6	164.61(12)
C4	C5	C6	C25	173.10(12)	C19	C4	C17	C16	-57.35(15)
C5	C4	C17	C16	-172.92(12)	C19	C18	C20	C16	59.62(15)
C5	C4	C19	C18	177.82(12)	C20	C16	C17	C4	60.25(16)
C5	C6	C7	C8	63.86(16)	C20	C18	C19	C4	-59.62(16)
C5	C6	C7	C22	-117.35(14)	C21	C10	C11	C12	-38.3(2)
C5	C6	C25	C26	-8.63(18)	C21	C10	C11	C24	143.26(14)
C5	C6	C25	C29	172.80(12)	C22	C7	C8	C9	1.8(2)
C6	C7	C8	C9	-179.33(12)	C24	C11	C12	C13	-0.7(2)
C6	C7	C22	C21	179.52(12)	C25	C6	C7	C8	-56.69(16)
C6	C25	C26	C27	-179.07(13)	C25	C6	C7	C22	122.09(14)
C6	C25	C29	C28	179.37(13)	C25	C26	C27	N2	-0.3(2)
C7	C6	C25	C26	112.32(15)	C26	C25	C29	C28	0.7(2)
C7	C6	C25	C29	-66.25(16)	C27	N2	C28	C29	-0.6(2)
C7	C8	C9	C10	-0.6(2)	C28	N2	C27	C26	0.8(2)
C8	C7	C22	C21	-1.7(2)	C29	C25	C26	C27	-0.5(2)
C8	C9	C10	C11	-179.51(13)					

Table 55 Hydrogen Atom Coordinates (Å×10^4) and Isotropic Displacement Parameters (Å^2 ×10^3) for compound 456.

Atom	*x*	*y*	*z*	U(eq)
H1A	-626.65	1094.95	4984.38	21
H1B	-1008.35	946.05	5937.68	21
H1C	2811.59	-2255.26	8311.8	22
H1D	2127.97	-2265.57	7236.94	22
H2	-295.67	-1260.06	8001.88	21
H3A	365.21	-575.53	6565.84	19
H3B	-38.23	491.93	7220.66	19
H5A	4622.72	1737.15	6212.22	18
H5B	3177.32	698.58	5619.07	18
H8	4415.1	3787.38	6662.72	18
H9	4305.34	5149.91	7843.35	20
H12	-1905.86	5908.13	8428.7	25
H13	-1944.74	7312.42	9606.35	30
H14	1083.82	7793.02	10684.78	30
H15A	1041.54	492.4	8905.92	22
H15B	2145.64	-575.27	9330.05	22
H16	4816.28	1023.87	9259.64	20
H17A	5473.91	1699.99	7823.15	18
H17B	3072.84	1880.2	7987.16	18
H18	5904.23	-1736.35	7585.29	22
H19A	4144.06	-884.54	6319.47	20

Table 55 Hydrogen Atom Coordinates (Å×10^4) and Isotropic Displacement Parameters (Å^2 ×10^3) for compound 456.

Atom	*x*	*y*	*z*	U(eq)
H19B	6127.82	0.43	6802.19	20
H20A	5928.91	-859.92	9077.34	22
H20B	7218.02	22.01	8487.04	22
H21	-1855.15	3892.66	7998.07	19
H22	-1733.18	2517.67	6814.01	19
H23	4146.81	6874.52	10590.68	29
H24	4220.55	5487.54	9407.42	23
H26	5142.58	2359.51	4967.49	23
H27	5774.84	3493.69	3768.85	28
H28	114.31	4579.74	3667.06	27
H29	-694.3	3496.37	4861.47	24

7 References

1. Hoffmann, N., Photochemical Reactions as Key Steps in Organic Synthesis. *Chem. Rev.* **2008**, *108*, 1052–1103.
2. Narayanam, J. M.; Stephenson, C. R. J., Visible Light Photoredox Catalysis: Applications in Organic Synthesis. *Chem. Soc. Rev.* **2011**, *40*, 102–113.
3. Prier, C. K.; Rankic, D. A.; MacMillan, D. W. C., Visible Light Photoredox Catalysis with Transition Metal Complexes: Applications in Organic Synthesis. *Chem. Rev.* **2013**, *113*, 5322–5363.
4. Romero, N. A.; Nicewicz, D. A., Organic Photoredox Catalysis. *Chem. Rev.* **2016**, *116*, 10075–10166.
5. Lowry, M. S.; Bernhard, S., Synthetically Tailored Excited States: Phosphorescent, Cyclometalated Iridium(III) Complexes and Their Applications. *Chem. Eur. J.* **2006**, *12*, 7970–7977.
6. Takeda, H.; Ishitani, O., Development of Efficient Photocatalytic Systems for CO_2 Reduction Using Mononuclear and Multinuclear Metal Complexes Based on Mechanistic Studies. *Coord. Chem. Rev.* **2010**, *254*, 346–354.
7. Kalyanasundaram, K.; Grätzel, M., Applications of Functionalized Transition Metal Complexes in Photonic and Optoelectronic Devices. *Coord. Chem. Rev.* **1998**, *177*, 347–414.
8. Nicewicz, D. A.; MacMillan, D. W. C., Merging Photoredox Catalysis with Organocatalysis: The Direct Asymmetric Alkylation of Aldehydes. *Science* **2008**, *322*, 77–80.
9. Ischay, M. A.; Anzovino, M. E.; Du, J.; Yoon, T. P., Efficient Visible Light Photocatalysis of [2+2] Enone Cycloadditions. *J. Am. Chem. Soc.* **2008**, *130*, 12886–12887.
10. Narayanam, J. M. R.; Tucker, J. W.; Stephenson, C. R. J., Electron-Transfer Photoredox Catalysis: Development of a Tin-Free Reductive Dehalogenation Reaction. *J. Am. Chem. Soc.* **2009**, *131*, 8756–8757.
11. Twilton, J.; Le, C.; Zhang, P.; Megan, H. S.; Ryan, W. E.; MacMillan, D. W. C., The Merger of Transition Metal and Photocatalysis. *Nat. Rev. Chem.* **2017**, *1*, 0052.
12. Arias-Rotondo, D. M.; McCusker, J. M., The Photophysics of Photoredox Catalysis: A Roadmap for Catalyst Design. *Chem. Soc. Rev.* **2016**, *45*, 5803–5820.
13. Dexter, D. L., A Theory of Sensitized Luminescence in Solids. *J. Chem. Phys.* **1953**, *21*, 836–850.
14. Evano, G.; Coste, A.; Jouvin, K., Ynamides: Versatile Tools in Organic Synthesis. *Angew. Chem. Int. Ed.* **2010**, *49*, 2840–2859.
15. Feldman, F. S.; Bruendl, M. M.; Schildknegt, K.; Bohnstedt, A. C., Inter- and Intramolecular Addition/Cyclizations of Sulfonamide Anions with Alkynyliodonium Triflates. Synthesis of Dihydropyrrole, Pyrrole, Indole, and Tosylenamide Heterocycles. *J. Org. Chem.* **1996**, *61*, 5440–5452.
16. Zhang, Y.; Hsung, R. P.; Tracey, M. R.; Kurtz, K. C. M.; Vera, E. L., Copper Sulfate-Pentahydrate-1,10-Phenanthroline Catalyzed Amidations of Alkynyl Bromides. Synthesis of Heteroaromatic Amine Substituted Ynamides. *Org. Lett.* **2004**, *6*, 1151–1154.
17. Coste, A.; Karthikeyan, G.; Couty, F.; Evano, G., Copper-Mediated Coupling of 1,1-Dibromo-1-alkenes with Nitrogen Nucleophiles: A General Method for the Synthesis of Ynamides. *Angew. Chem. Int. Ed.* **2009**, *48*, 4381–4385.

18. Hamada, T.; Ye, X.; Stahl, S. S., Copper-Catalyzed Aerobic Oxidative Amidation of Terminal Alkynes: Efficient Synthesis of Ynamides. *J. Am. Chem. Soc.* **2008**, *130*, 833–835.
19. Dekorver, K. A.; Li, H.; Lohse, A. G.; Hayashi, R.; Lu, Z.; Zhang, Y.; Hsung, R. P., Ynamides: A Modern Functional Group for the New Millennium. *Chem. Rev.* **2010**, *110*, 5064–5106.
20. Shu, C.; Li, L.; Tan, T.-D.; Yuan, D.-Q.; Ye, L.-W., Ring Strain Strategy for the Control of Regioselectivity. Gold-Catalyzed Anti-Markovnikov Cycloisomerization Initiated Tandem Reactions of Alkynes. *Sci. Bull.* **2017**, *62*, 352–357.
21. Marion, F.; Courillon, C.; Malacria, M., Radical Cyclization Cascade Involving Ynamides: An Original Access to Nitrogen-Containing Heterocycles. *Org. Lett.* **2003**, *5*, 5095–5097.
22. Baguia, H.; Deldaele, C.; Romero, E.; Michelet, B.; Evano, G., Copper-Catalyzed Photoinduced Radical Domino Cyclization of Ynamides and Cyanamides: A Unified Entry to Rosettacin, Luotonin A, and Deoxyvasicinone. *Synthesis* **2018**, *50*, 3022–3030.
23. Dutta, S.; Mallick, R. K.; Prasad, R.; Gandon, V.; Sahoo, A. K., Alkyne Versus Ynamide Reactivity: Regioselective Radical Cyclization of Yne-Ynamides. *Angew. Chem. Int. Ed.* **2019**, *58*, 2289–2294.
24. Dutta, S.; Prabagar, B.; Vanjari, R.; Gandon, V.; Sahoo, A. K., An Unconventional Sulfur-to-Selenium-to-Carbon Radical Transfer: Chemo-and Regioselective Cyclization of Yne-Ynamides. *Green Chem.* **2020**, *22*, 1113–1118.
25. Wang, Z.-S.; Chen, Y.-B.; Zhang, H.-W.; Sun, Z.; Ye, L.-W., Ynamide Smiles Rearrangement Triggered by Visible-Light-Mediated Regioselective Ketyl–Ynamide Coupling: Rapid Access to Functionalized Indoles and Isoquinolines. *J. Am. Chem. Soc.* **2020**, *142*, 3636–3644.
26. Wang, Z.-S.; Chen, Y.-B.; Wang, K.; Xu, Z.; Ye, L.-W., One-pot Synthesis of 2-Hydroxymethylindoles *via* Photoredox-catalyzed Ketyl–Ynamide Coupling/1,3-Allylic Alcohol Transposition. *Green Chem.* **2020**, *22*, 4483–4488.
27. Zhou, B.; Tan, T.-D.; Zhu, X.-Q.; Shang, M.; Ye, L.-W., Reversal of Regioselectivity in Ynamide Chemistry. *ACS Catal.* **2019**, *9*, 6393–6406.
28. Sato, A.; Yorimitsu, H.; Oshima, K., Regio- and Stereoselective Radical Additions of Thiols to Ynamides. *Synlett* **2009**, *1*, 28–31.
29. Banerjee, B.; Litvinov, D. N.; Kang, J.; Bettale, J. D.; Castle, S. L., Stereoselective Additions of Thiyl Radicals to Terminal Ynamides. *Org. Lett.* **2010**, *12*, 2650–2652.
30. Romain, E.; Fopp, C.; Chemla, F.; Ferreira, F.; Jackowski, O.; Oestreich, M.; Perez-Luna, A., *Trans* -Selective Radical Silylzincation of Ynamides. *Angew. Chem. Int. Ed.* **2014**, *53*, 11333–11337.
31. Cassé, M.; Nisole, C.; Dossmann, H.; Gimbert, Y.; Fourquez, J.-M.; Haberkorn, L.; Ollvier, C.; Fensterbank, L., Trifluoromethyl Radical Triggered Radical Cyclization of *N*-Benzoyl Ynamides Leading to Isoindolinones. *Sci. China Chem.* **2019**, *62*, 1542–1546.
32. Dwadnia, N.; Lingua, H.; Mouysset, D.; Mimoun, L.; Siri, D.; Bertrand, M. P.; Feray, L., Intermolecular Addition of Carbon-Centered Radicals to Ynamides. A Regio- and Stereoselective Route to Persubstituted α-Iodo-enamides. *J. Org. Chem.* **2020**, *85*, 4114–4121.
33. Snape, T. J., A Truce on the Smiles Rearrangement: Revisiting an Old Reaction–The Truce-Smiles Rearrangement. *Chem. Soc. Rev.* **2008**, *37*, 2452–2458.
34. Holden, C. M.; Greaney, M. F., Modern Aspects of the Smiles Rearrangement. *Chem. Eur. J.* **2017**,

23, 8992–9008.

35. Bernasconi, C. F., De Rossi, R. H., Gehriger, C. L., Intermediates in Nucleophilic Aromatic Substitution. X. Synthesis of N-methyl-.beta.-Aminoethyl Nitroaryl Ethers via an Unusual Smiles Rearrangement. *J. Org. Chem.* **1973**, *38*, 2838–2842.
36. Kitching, M. O., Hurst, T. E., Snieckus, V., Copper-Catalyzed Cross-Coupling Interrupted by an Opportunistic Smiles Rearrangement: An Efficient Domino Approach to Dibenzoxazepinones. *Angew. Chem. Int. Ed.* **2012**, *51*, 2925–2929.
37. Truce, W. E., Ray Jr., W. J., Norman, O. L., Eickemeyer, D. B., Rearrangement of Aryl Sulfones. I. The Metalation and Rearrangement of Mesityl Phenyl Sulfone. *J. Am. Chem. Soc.* **1958**, *80*, 3625–3629.
38. Holden, C. M., Sohel, S. M. A., Greaney, M. F., Metal Free Bi(hetero)aryl Synthesis: A Benzyne Truce-Smiles Rearrangement. *Angew. Chem. Int. Ed.* **2016**, *55*, 2450–2453.
39. Rabet, P. T. G., Boyd, S., Greaney, M. F., Metal-Free Intermolecular Aminoarylation of Alkynes. *Angew. Chem. Int. Ed.* **2017**, *56*, 4183–4186.
40. Allart-Simon, I., Gérard, S., Sapi, J., Radical Smiles Rearrangement: An Update. *Molecules* **2016**, *21*, 878–888.
41. Motherwell, W. B., Pennell, A. M. K., A Novel Route to Biaryls *via* Intramolecular Free Radical *ipso* Substitution Reactions. *J. Chem. Soc. Chem. Commun.* **1991**, 877–879.
42. Kong, W.; Casimiro, M.; Merino, E.; Nevado, C., Copper-Catalyzed One-Pot Trifluoromethylation/Aryl Migration/Desulfonylation and C(sp^2)–N Bond Formation of Conjugated Tosyl Amides. *J. Am. Chem. Soc.* **2013**, *135*, 14480–14483.
43. Kong, W., Merino, E., Nevado, C., Arylphosphonylation and Arylazidation of Activated Alkenes. *Angew. Chem. Int. Ed.* **2014**, *53*, 5078–5082.
44. Futentes, N., Kong, W., Fernández-Sánchez, L., Merino, E., Nevado, C., Cyclization Cascades *via N*-Amidyl Radicals toward Highly Functionalized Heterocyclic Scaffolds. *J. Am. Chem. Soc.* **2015**, *137*, 964–973.
45. Hervieu, C., Kirillova, M. S., Suárez, T., Müller, M., Merino, E., Nevado, C., Asymmetric, Visible Light-Mediated Radical Sulfinyl-Smiles Rearrangement to Access All-Carbon Quaternary Stereocentres. *Nat. Chem.* **2021**, *13*, 327–334.
46. Monos, T. M., McAtee, R. C., Stephenson, C. R. J., Arylsulfonylacetamides as Bifunctional Reagents for Alkene Aminoarylation. *Science* **2018**, *361*, 1369–1373.
47. Zheng, G.; Li, Y.; Han, J.; Xiong, T.; Zhang, Q., Radical Cascade Reaction of Alkynes with *N*-Fluoroarylsulfonimides and Alcohols. *Nat. Commun.* **2015**, *6*, 7011–7019..
48. Pratley, C.; Fenner, S.; Murphy, J. A., Nitrogen-Centered Radicals in Functionalization of sp^2 Systems: Generation, Reactivity, and Applications in Synthesis. *Chem. Rev.* **2022**, *122*, 8181–8260.
49. Klumpp, D. A.; Zhang, Y.; O'Connor, M. J.; Esteves, P. M.; de Mlmeide, L. S., Aza-Nazarov Reaction and the Role of Superelectrophiles. *Org. Lett.* **2007**, *9*, 3085–3088.
50. Di Grandi, M. J., Nazarov-Like Cyclization Reactions. *Org. Biomol. Chem.* **2014**, *12*, 5331–5345.
51. Purser, S.; Moore, P. R.; Swallow, S.; Gouverneur, V., Fluorine in Medicinal Chemistry. *Chem. Soc. Rev.* **2008**, *37*, 320–330.
52. Müller, K.; Faeh, C.; Diederich, F., Fluorine in Pharmaceuticals: Looking Beyond Intuition. *Science*

2007, *317*, 1881–1886.

53. Clayden, J., Fluorinated Compounds Present Opportunities for Drug Discovery. *Nature* **2019**, *573*, 37–38.
54. Young, C. J., Mabury, S. A., Atmospheric Perfluorinated Acid Precursors: Chemistry, Occurrence, and Impacts. *Rev. Environ. Contam. Toxicol.* **2010**, *208*, 1–109.
55. Tian, F.; Yan, G.; Yu, J., Recent Advances in the Synthesis and Applications of α-(Trifluoromethyl)styrenes in Organic Synthesis. *Chem. Commun.* **2019**, *55*, 13486–13505.
56. Bégué, J.-P., Bonnet-Delpon, D., Rock, M. H., A Concise Synthesis of Functionalised *gem*-Difluoroalkenes, *via* the Addition of Organolithium Reagents to α-Trifluoromethylstyrene. *Tetrahedron Lett.* **1995**, *36*, 5003–5006.
57. Li, S.; Shu, W., Recent Advances in Radical Enabled Selective C_{sp}^3–F Bond Activation of Multifluorinated Compounds. *Chem. Commun.* **2022**, *58*, 1066–1077.
58. Yan, G.; Qiu, K.; Guo, M., Recent Advance in the C–F Bond Functionalization of Trifluoromethyl-Containing Compounds. *Org. Chem. Front.* **2021**, *8*, 3915–3942.
59. Xiao, T.; Li, L.; Zhou, L., Synthesis of Functionalized *gem*-Difluoroalkenes via a Photocatalytic Decarboxylative/Defluorinative Reaction. *J. Org. Chem.* **2016**, *81*, 7908–7916.
60. Lang, S. B.; Wiles, R. J.; Kelly, C. B.; Molander, G. A., Photoredox Generation of Carbon-Centered Radicals Enables the Construction of 1,1-Difluoroalkene Carbonyl Mimics. *Angew. Chem. Int. Ed.* **2017**, *56*, 15073–15077.
61. Wu, L.-H.; Cheng, J.-K.; Shen, L.; Shen, Z.-L.; Loh, T.-P., Visible Light-Mediated Trifluoromethylation of Fluorinated Alkenes via C−F Bond Cleavage. *Adv. Synth. Catal.* **2018**, *360*, 3894–3899.
62. Xia, P.-J.; Ye, Z.-P.; Hu, Y.-Z.; Song, D.; Xiang, H.-Y.; Chen, X.-Q.; Yang, H., Photocatalytic, Phosphoranyl Radical-Mediated N–O Cleavage of Strained Cycloketone Oximes. *Org. Lett.* **2019**, *21*, 2658–2662.
63. Anand, D.; Sun, Z.; Zhou, L., Visible-Light-Mediated β-C–H *gem*-Difluoroallylation of Aldehydes and Cyclic Ketones through C–F Bond Cleavage of 1-Trifluoromethyl Alkenes. *Org. Lett.* **2020**, *22*, 2371–2375.
64. Guo, Y.-Q.; Wang, R.; Song, H.; Liu, Y.; Wang, Q., Visible-Light-Induced Deoxygenation/Defluorination Protocol for Synthesis of γ,γ-Difluoroallylic Ketones. *Org. Lett.* **2020**, *22*, 709–713.
65. Guo, Y.-Q.; Wu, Y.; Wang, R.; Song, H.; Liu, Y.; Wang, Q., Photoredox/Hydrogen Atom Transfer Cocatalyzed C–H Difluoroallylation of Amides, Ethers, and Alkyl Aldehydes. *Org. Lett.* **2021**, *23*, 2353–2358.
66. Yue, W.-J.; Day, C. S.; Martin, R., Site-Selective Defluorinative sp^3 C–H Alkylation of Secondary Amides. *J. Am. Chem. Soc.* **2021**, *143*, 6395–6400.
67. Xia, P.-J.; Song, D.; Ye, Z.-P.; Hu, Y.-Z.; Xiao, J.-A.; Xiang, H.-Y.; Chen, X.-Q.; Yang, H., Photoinduced Single-Electron Transfer as an Enabling Principle in the Radical Borylation of Alkenes with NHC–Borane. *Angew. Chem. Int. Ed.* **2020**, *59*, 6706–6710.
68. Xu, W.; Jiang, H.; Heng, J.; Ong, H.-W.; Wu, J., Visible-Light-Induced Selective Defluoroborylation of Polyfluoroarenes, *gem*-Difluoroalkenes, and Trifluoromethylalkenes. *Angew. Chem. Int. Ed.*

2020, *59*, 4009–4016.

69. Qi, J.; Zhang, F.-L.; Jin, J.-K.; Zhao, Q.; Li, B.; Liu, L.-X.; Wang, Y.-F., New Radical Borylation Pathways for Organoboron Synthesis Enabled by Photoredox Catalysis. *Angew. Chem. Int. Ed.* **2020**, *59*, 12876–12884.
70. Li, L.; Xiao, T.; Chen, H.; Zhou, L., Visible-Light-Mediated Two-Fold Unsymmetrical C(sp^3)−H Functionalization and Double C−F Substitution. *Chem. – Eur. J.* **2017**, *23*, 2249–2254.
71. Chen, H., He, Y., Zhou, L., A Photocatalytic Decarboxylative/Defluorinative [4+3] Annulation of *O*-Hydroxyphenylacetic Acids and Trifluoromethyl Alkenes: Synthesis of Fluorinated Dihydrobenzoxepines. *Org. Chem. Front.* **2018**, *5*, 3240–3244.
72. Shen, T. Y., Perspectives in Nonsteroidal Anti-inflammatory Agents. *Angew. Chem. Int. Ed.* **1972**, *11*, 460–472.
73. Culkin, D. A., Hartwig, J. F., Palladium-Catalyzed α-Arylation of Carbonyl Compounds and Nitriles. *Acc. Chem. Res.* **2003**, *36*, 234–245.
74. Johansson, C. C. C., Colacot, T. J., Metal-Catalyzed α-Arylation of Carbonyl and Related Molecules: Novel Trends in C–C Bond Formation by C–H Bond Functionalization. *Angew. Chem. Int. Ed.* **2010**, *49*, 676–707.
75. Moradi, W. A., Buchwald, S. L., Palladium-Catalyzed α-Arylation of Esters. *J. Am. Chem. Soc.* **2001**, *123*, 7996–8002.
76. Bala, T., Prasad, B. L. V., Sastry, M., Kahaly, M. U., Waghmare, U. V., Interaction of Different Metal Ions with Carboxylic Acid Group: A Quantitative Study. *J. Phys. Chem. A* **2007**, *111*, 6183–6190.
77. Morita, Y., Yamamoto, T., Nagai, H., Shimizu, Y., Kanai, M., Chemoselective Boron-Catalyzed Nucleophilic Activation of Carboxylic Acids for Mannich-Type Reactions. *J. Am. Chem. Soc.* **2015**, *137*, 7075–7078.
78. Ruiz-Castillo, P., Buchwald, S. L., Applications of Palladium-Catalyzed C–N Cross-Coupling Reactions. *Chem. Rev.* **2016**, *116*, 12564–12649.
79. He, Z.-T., Hartwig, J. F., Palladium-Catalyzed α-Arylation of Carboxylic Acids and Secondary Amides via a Traceless Protecting Strategy. *J. Am. Chem. Soc.* **2019**, *141*, 11749–11753.
80. Vasquez, A. M., Gurak, J. A., Joe, C. L., Cherney, E. C., Engle, K. M., Catalytic α-Hydroarylation of Acrylates and Acrylamides via an Interrupted Hydrodehalogenation Reaction. *J. Am. Chem. Soc.* **2020**, *142*, 10477–10484.
81. Bellina, F., Rossi, R., Transition Metal-Catalyzed Direct Arylation of Substrates with Activated sp^3-Hybridized C–H Bonds and Some of Their Synthetic Equivalents with Aryl Halides and Pseudohalides. *Chem. Rev.* **2010**, *110*, 1082–1146.
82. Liu, H.; Ge, L.; Wang, D.-X.; Chen, N.; Feng, C., Photoredox-Coupled F-Nucleophilic Addition: Allylation of *gem*-Difluoroalkenes. *Angew. Chem. Int. Ed.* **2019**, *58*, 3918–3922.
83. Margrey, K. A.; Nicewicz, D. A., A General Approach to Catalytic Alkene Anti-Markovnikov Hydrofunctionalization Reactions via Acridinium Photoredox Catalysis. *Acc. Chem. Res.* **2016**, *49*, 1997–2006.
84. Adenier, A.; Chehimi, M. M.; Gallardo, I.; Pinson, J.; Vilà, N., Electrochemical Oxidation of Aliphatic Amines and Their Attachment to Carbon and Metal Surfaces. *Langmuir* **2004**, *20*, 8243–8253.

85. Shipilovskikh, S. A.; Vaganov, V. Y.; Denisova, E. I.; Rubtsov, A. E.; Malkov, A. V., Dehydration of Amides to Nitriles under Conditions of a Catalytic Appel Reaction. *Org. Lett.* **2018**, *20*, 728–731.
86. Wang, B.; Zhao, X.; Liu, Q.; Cao, S., Direct Defluorinative Amidation–Hydrolysis Reaction of *gem*-Difluoroalkenes with *N*,*N*-Dimethylformamide, and Primary and Secondary Amines. *Org. Biomol. Chem.* **2018**, *16*, 8546–8552.
87. Vitaku, E.; Smith, D. T.; Njardarson, J. T., Analysis of the Structural Diversity, Substitution Patterns, and Frequency of Nitrogen Heterocycles among U.S. FDA Approved Pharmaceuticals. *J. Med. Chem.* **2014**, *57*, 10257–10274.
88. Clayden, J.; Donnard, M.; Lefrane, J.; Tetlow, D. J., Quaternary Centres Bearing Nitrogen (α-Tertiary Amines) as Products of Molecular Rearrangements. *Chem. Commun.* **2011**, *47*, 4624–4639.
89. Hager, A.; Vrielink, H.; Hager, D.; Lefrane, J.; Trauner, D., Synthetic Approaches Towards Alkaloids Bearing α-Tertiary Amines. *Nat. Prod. Rep.* **2016**, *33*, 491–522.
90. Michaudel, Q., Thevenet, D., Baran, P. S., Intermolecular Ritter-Type C–H Amination of Unactivated sp^3 Carbons. *J. Am. Chem. Soc.* **2012**, *134*, 2547–2550.
91. Gui, J.; Pan, C.-M.; Jin, Y.; Qin, T.; Lo, J. C.; Lee, B. J.; Spergel, S. H.; Mertzman, M. E.; Pitts, W. J.; La Cruz, T. E.; Schmidt, M. A.; Darvatkar, N.; Natarajan, S. R.; Baran, P. S., Practical Olefin Hydroamination with Nitroarenes. *Science* **2015**, *348*, 886–891.
92. Robak, N. T.; Herbage, M. A.; Ellman, J. A., Synthesis and Applications of *tert*-Butanesulfinamide. *Chem. Rev.* **2010**, *110*, 3600–3740.
93. Liu, G.; Cogan, D. A.; Ellman, J. A., Catalytic Asymmetric Synthesis of *tert*-Butanesulfinamide. Application to the Asymmetric Synthesis of Amines. *J. Am. Chem. Soc.* **1997**, *119*, 9913–9914.
94. Vasu, D.; Futentes de Arriba, A. L.; Leitch, J. A.; De Gombert, A.; Dixon, D. J., Primary α-Tertiary Amine Synthesis *via* α-C–H Functionalization. *Chem. Sci.* **2019**, *10*, 3401–3407.
95. Ye, J.; Kalvet, I.; Schoenebeck, F.; Rovis, T., Direct α-Alkylation of Primary Aliphatic Amines Enabled by CO_2 and Electrostatics. *Nat. Chem.* **2018**, *10*, 1037–1041.
96. Ryder, A. S. H.; Cunningham, W. B.; Ballantyne, G.; Mules, T.; Kinsella, A. G.; Turner-Dore, J.; Alder, C. M.; Edwards, L. J.; McKay, B. S. J.; Grayson, M. N.; Cresswell, A. J., Photocatalytic α-Tertiary Amine Synthesis via C−H Alkylation of Unmasked Primary Amines. *Angew. Chem. Int. Ed.* **2020**, *59*, 14986–14991.
97. Askey, H. E.; Grayson, J. D.; Tibbetts, J. D.; Turner-Dore, J. C.; Holmes, J. M.; Kociok-Kohn, G. Wrigley, G. L.; Cresswell, A. J., Photocatalytic Hydroaminoalkylation of Styrenes with Unprotected Primary Alkylamines. *J. Am. Chem. Soc.* **2021**, *143*, 15936–15945.
98. Li, H.; Chiba, S., Synthesis of α-Tertiary Amines by Polysulfide Anions Photocatalysis *via* Single-Electron Transfer and Hydrogen Atom Transfer in Relays. *Chem. Catal.* **2022**, *2*, 1128–1142.
99. Leitch, J. A.; Rossolini, T.; Rogova, T.; Maitland, A. P.; Dixon, D. J., α-Amino Radicals via Photocatalytic Single-Electron Reduction of Imine Derivatives. *ACS. Catal.* **2020**, *10*, 2009–2025.
100. Lehnherr, D.; Lam, Y.-H.; Nicastri, M. C.; Liu, J.; Newman, J. A.; Regalado, E. L.; DiRocco, D. A.; Rovis, T., Electrochemical Synthesis of Hindered Primary and Secondary Amines *via* Proton-Coupled Electron Transfer. *J. Am. Chem. Soc.* **2020**, *142*, 468–478.
101. Nicastri, M. C.; Lehnherr, D.; Lam, Y.-H.; DiRocco, D. A.; Rovis, T., Synthesis of Sterically Hindered

Primary Amines by Concurrent Tandem Photoredox Catalysis. *J. Am. Chem. Soc.* **2020**, *142*, 987–998.

102. Rong, J.; Seeberger, P. H.; Gilmore, K., Chemoselective Photoredox Synthesis of Unprotected Primary Amines Using Ammonia. *Org. Lett.* **2018**, *20*, 4081–4085.
103. Blackwell, J. H.; Harris, G. R.; Smith, M. A.; Gaunt, M. J., Modular Photocatalytic Synthesis of α-Trialkyl-α-Tertiary Amines. *J. Am. Chem. Soc.* **2021**, *143*, 15946–15959.
104. Forster, M. O.; Newman, S. H., CCLXIII.—The triazo-group. Part XV. Triazoethylene (vinylazoimide) and the triazoethyl halides. *J. Chem. Soc. Trans.* **1910**, *97*, 2570–2579.
105. Smolinsky, G.; Pryde, G. A. *The Azido Group*, John Wiley, **1971**, ch. 10, pp. 555–585.
106. Fu, J.; Zanoni, G.; Anderson, E. A.; Bi, X., α-Substituted Vinyl Azides: An Emerging Functionalized Alkene. *Chem. Soc. Rev.* **2017**, *46*, 7208–7228.
107. Liu, Z.; Liu, J.; Zhang, L.; Liao, P.; Song, J. Bi, X., Silver(I)-Catalyzed Hydroazidation of Ethynyl Carbinols: Synthesis of 2-Azidoallyl Alcohols. *Angew. Chem. Int. Ed.* **2014**, *53*, 5305–5309.
108. Liu, Z.; Liao, P.; Bi, X., General Silver-Catalyzed Hydroazidation of Terminal Alkynes by Combining TMS-N_3 and H_2O: Synthesis of Vinyl Azides. *Org. Lett.* **2014**, *16*, 3668–3671.
109. Suzuki, A.; Tabata, M.; Ueda, M., A Facile Reaction of Trialkylboranes with α-Azidostyrene. A Convenient and General Synthesis of Alkyl Aryl Ketones *via* Hydroboration. *Tetrahedron Lett.* **1975**, *16*, 2195–2198.
110. Montevecchi, P. C.; Navacchia, M. L.; Spagnolo, P., Generation of Iminyl Radicals through Sulfanyl Radical Addition to Vinyl Azides. *J. Org. Chem.* **1997**, *62*, 5846–5848.
111. Tang, P.; Zhang, C.; Chen, E.; Chen, B.; Chen, W.; Yu, Y., Mn^{III}-Catalyzed Phosphorylation of Vinyl Azides: The Synthesis of β-Keto Phosphine Oxides. *Tetrahedron Lett.* **2017**, *58*, 2157–2161.
112. Chen, W.; Liu, X.; Chen, E.; Chen, B.; Shao, J.; Yu, Y., KI-Mediated Radical Multi-Functionalization of Vinyl Azides: A One-Pot and Efficient Approach to β-Keto Sulfones and α-Halo-β-keto Sulfones. *Org. Chem. Front.* **2017**, *4*, 1162–1166.
113. Wu, S.-W.; Liu, F., Synthesis of α-Fluoroketones from Vinyl Azides and Mechanism Interrogation. *Org. Lett.* **2016**, *18*, 3642–3645.
114. Qin, H.-T.; Wu, S.-W.; Liu, J.-L.; Liu, F., Photoredox-Catalysed Redox-Neutral Trifluoromethylation of Vinyl Azides for the Synthesis of α-Trifluoromethylated Ketones. *Chem. Commun.* **2017**, *53*, 1696–1699.
115. Shu, W.; Lorente, A.; Gómez-Bengoa, E.; Nevado, C., Expeditious Diastereoselective Synthesis of Elaborated Ketones *via* Remote Csp^3–H Functionalization. *Nat. Commun.* **2017**, *8*, 13832–13839.
116. Wang, Y.-F.; Toh, K. K.; Ng, E. P. J.; Chiba, S., Mn(III)-Mediated Formal [3+3]-Annulation of Vinyl Azides and Cyclopropanols: A Divergent Synthesis of Azaheterocycles. *J. Am. Chem. Soc.* **2011**, *133*, 6411–6421.
117. Wang, Q.; Huang, J.; Zhou, L., Synthesis of Quinolines by Visible-Light Induced Radical Reaction of Vinyl Azides and α-Carbonyl Benzyl Bromides. *Adv. Synth. Catal.* **2015**, *357*, 2479–2484.
118. Ning, Y.; Ji, Q.; Liao, P.; Anderson, E. A.; Bi, X., Silver-Catalyzed Stereoselective Aminosulfonylation of Alkynes. *Angew. Chem. Int. Ed.* **2017**, *56*, 13805–13808.
119. Ning, Y.; Zhao, X.-F.; Wu, Y.-B.; Bi, X., Radical Enamination of Vinyl Azides: Direct Synthesis of *N*-

Unprotected Enamines. *Org. Lett.* **2017**, *19*, 6240–6243.
120. Muthukrishnan, I.; Sridharan, V. Menéndez, J. C., Progress in the Chemistry of Tetrahydroquinolines. *Chem. Rev.* **2019**, *119*, 5057–5191.
121. Péter, A., Agasti, S., Knowles, O., Pye, E., Menéndez, J. C., Recent Advances in the Chemistry of Ketyl Radicals. *Chem. Soc. Rev.* **2021**, *50*, 5349–5365.
122. L'abbé, G., Reactions of Vinyl Azides. *Angew. Chem. Int. Ed.***1975**, *14*, 775–782.
123. Foster, R., Electron Donor-Acceptor Complexes. *J. Phys. Chem.* **1980**, *84*, 2135–2141.
124. Rosokha, S. V.; Kochi, J. K., Fresh Look at Electron-Transfer Mechanisms *via* the Donor/Acceptor Bindings in the Critical Encounter Complex. *Acc. Chem. Res.* **2008**, *41*, 641–653.
125. Zhang, J.; Li, Y.; Xu, R.; Chen, Y., Donor–Acceptor Complex Enables Alkoxyl Radical Generation for Metal-Free C(sp^3)–C(sp^3) Cleavage and Allylation/Alkenylation. *Angew. Chem. Int. Ed.* **2017**, *56*, 12619–12623.
126. Kammer, L. M.; Badir, S. O.; Hu, R.-M.; Molander, G. A., Photoactive Electron Donor–Acceptor Complex Platform for Ni-Mediated C(sp^3)–C(sp^2) Bond Formation. *Chem. Sci.* **2021**, *12*, 5450–5457.
127. Buzzetti, L., Prieto, A., Roy, S. R., Melchiorre, P., Radical-Based C–C Bond-Forming Processes Enabled by the Photoexcitation of 4-Alkyl-1,4-dihydropyridines. *Angew. Chem. Int. Ed.* **2017**, *56*, 15039–15043.
128. Cismesia, M. A.; Yoon, T. P., Characterizing Chain Processes in Visible Light Photoredox Catalysis. *Chem. Sci.* **2015**, *6*, 5426–5434.
129. Ladouceur, S.; Fortin, D.; Zysman-Colman, E., Enhanced Luminescent Iridium(III) Complexes Bearing Aryltriazole Cyclometallated Ligands. *Inorg. Chem.* **2011**, *50*, 11514–11526.
130. Cao, K.; Tan, S. M.; Lee, R.; Yang, S.; Jia, H.; Zhao, X.; Qiao, B.; Jiang, Z., Catalytic Enantioselective Addition of Prochiral Radicals to Vinylpyridines. *J. Am. Chem. Soc.* **2019**, *141*, 5437–5443.
131. Trowbridge, A.; Reich, D.; Gaunt, M. J., Multicomponent Synthesis of Tertiary Alkylamines by Photocatalytic Olefin-Hydroaminoalkylation. *Nature* **2018**, *561*, 522–527.
132. Pratsch, G.; Lackner, G. L.; Overman, L. E., Constructing Quaternary Carbons from *N*-(acyloxy)phthalimide Precursors of Tertiary Radicals using Visible-Light Photocatalysis. *J. Org. Chem.* **2015**, *80*, 6025–6036.
133. Jung, J.; Kim, J.; Park, G.; You, Y.; Cho, E. J., Selective Debromination and α-Bromo Ketones using Hantzsch Ester as Photoreductants. *Adv. Synth. Catal.* **2016**, *358*, 74–80.
134. Chen, D.; Long, T.; Zhu, S.; Yang, J.; Chu, L., Metal-Free, Intermolecular Carbopyridylation of Alkenes via Visible-Light-Induced Reductive Radical Coupling. *Chem. Sci.* **2018**, *9*, 9012–9017.
135. Al-Rashid, Z. F.; Johnson, W. L.; Hsung, R. P.; Wei, Y.; Yao, R.-Y.; Liu, R.; Zhao, K., Synthesis of α-Keto-Imides via Oxidation of Ynamides. *J. Org. Chem.* **2008**, *73*, 8780–8784.
136. Walkowiak, J.; Campo, T. M.; Ameduri, B.; Gouverneur, V., Syntheses of Mono-, Di, and Trifluorinated Styrenic Monomers. *Synthesis* **2010**, *11*, 1883–1890.
137. Matsui, J. K.; Primer, D. N.; Molander, G. A., Metal-Free C–H Alkylation of Heteroarenes with Alkyltrifluoroborates: A General Protocol for 1°, 2° and 3° Alkylation. *Chem. Sci.* **2017**, *8*, 3512–3522.
138. Qin, T.; Cornella, J.; Li, C.; Malins, L. R.; Edwards, J. T.; Kawamura, S.; Mazwell, B. D.; Eastage,

M. D.; Baran, P. S., A General Alkyl-Alkyl Cross-Coupling Enabled by Redox-Active Esters and Alkylzinc Reagents. *Science* **2016**, *352*, 801–805.

139. Becerril, J.; Hamilton, A., Helix Mimetics as Inhibitors of the Interaction of the Estrogen Receptor with Coactivator Peptides. *Angew. Chem. Int. Ed.* **2007**, ***46***, 4471–4473.
140. Movassaghi, M.; Hill, M. D., Single-Step Synthesis of Pyrimidine Derivatives. *J. Am. Chem. Soc.* **2006**, *128*, 14254–14255.
141. Ding, L.; Chen, J.; Hu, Y.; Xu, J.; Gong, X.; Xu, D.; Zhao, B.; Li, H., Aminative Umpolung of Aldehydes to α-Amino Anion Equivalents for Pd-Catalyzed Allylation: An Efficient Synthesis of Homoallylic Amines. *Org. Lett.* **2014**, *16*, 720–723.
142. Ikuo, N.; Akito, I.; Kazuki, Y.; Setsuo, T.; Kazuaki, I.; Hiroshi, T., Laser Flash Photolysis of 3-(4-Biphenylyl)-2*H*-azirine. Direct Detection of Nitrile Ylide. *Chem. Lett.* **1989**, 1615–1618.
143. Kuhn, H. J.; Braslavsky, S. E.; Schmidt, R., Chemical Actinometry (IUPAC Technical Report). *Pure Appl. Chem.* **2004**, *76*, 2105–2146.
144. Montalti, M.; Credi, A.; Prodi, L.; Gandofi, M. T., Chemical Actinometry. *Handbook of photochemistry*, 3re ed, Taylor & Francis group, LLC. Boca Raton, FL, **2016**, 601–616.
145. Li, S.; Wang, Y.; Wu, Z.; Shi, W.; Lei, Y.; Davies, P. D.; Shu, W., A Radical-Initiated Fragmentary Rearrangement Cascade of Ene-Ynamides to [1,2]-Annulated Indoles via Site-Selective Cyclization. *Org. Lett.* **2021**, *23*, 7209–7214.
146. Li, S.; Davies, P. W.; Shu, W., Modular Synthesis of α-Arylated Carboxylic Acids, Esters and Amides *via* Photocatalyzed Triple C–F Bond Cleavage of Methyltrifluorides. *Chem. Sci.* **2022**, *13*, 6636–6641.